

Introduction To Space Shuttle Rendezvous Guidance, Navigation, and Control

Mission Operations Directorate
Flight Design and Dynamics Division

Fourth Edition
November 2009



National Aeronautics and
Space Administration

Lyndon B. Johnson Space Center
Houston, Texas

This page intentionally left blank.

Introduction To Space Shuttle Rendezvous Guidance, Navigation, and Control

Fourth Edition
November 2009

Prepared By:

Original Signed By:

John L. Goodman
Flight Design and Dynamics
United Space Alliance

Approved By:

Original Signed By:

Stephen R. Walker
Lead, Rendezvous Guidance and Procedures Group
Flight Design and Dynamics Division
Mission Operations Directorate

Approved By:

Original Signed By:

Edward P. González
Lead, Orbit Flight Dynamics Group
Flight Design and Dynamics Division
Mission Operations Directorate

This page intentionally left blank.

Table of Contents

1.0 Preface for the 4th Edition	11
1.1 Preface for the 3rd Edition	12
1.2 Preface for the 1st And 2nd Editions	14
2.0 Introduction	17
3.0 Coordinate Systems	19
3.1 LVLH Axes	20
3.2 Planes Formed By LVLH Axes	22
3.3 Views of Relative Motion	24
3.4 Rectilinear and Curvilinear Coordinates	28
3.5 Relative Motion Projected Into the Local Vertical Plane	30
3.6 Relative Motion Projected Into the Local Horizontal Plane	34
3.7 Coordinate Frame Summary	35
4.0 Launch Windows and Constraints	37
4.1 Phase Window	38
4.2 Planar Window	43
4.3 Composite Launch Window	52
4.4 Other Constraints	54
5.0 Ascent, OMS-2, and the Ground Targeted Phase	57
5.1 Ascent	58
5.2 OMS-2 Burn	63
5.3 Ground Targeted Phase	68

5.4	Plane Change Burn (NPC)	70
5.5	Phasing Burn (NC)	71
5.6	Altitude Burn (NH)	72
5.7	Coelliptic Burn (NSR)	73
5.8	Circularization Burn (CIRC)	74
5.9	Ground Targeted Burn Summary	75
5.10	Ground Targeted Phase In LVLH Coordinates	76
5.11	Classical Ground-Up Rendezvous	77
5.12	Rendezvous From Above or Below	78
5.13	Control Box Rendezvous	79
5.14	Hybrid or Modified Control Box Rendezvous	81
5.15	Summary of Ground-Targeted Phase Profiles	82
5.16	Designing a Ground-Up Rendezvous Profile	83
6.0	Day of Rendezvous and Separations	87
6.1	Day of Rendezvous Phase In LVLH Coordinates	89
6.2	Day of Rendezvous Events Covered	90
6.3	Final Ground Targeted Burn	91
6.4	Nominal Star Tracker Passes	95
6.5	Corrective Combination Burn (NCC)	97
6.6	Radar Data Incorporation	98
6.7	Transition Initiation Burn (Ti)	100
6.8	Midcourse Correction-1 Burn (MC-1)	102
6.9	Out-of-Plane Velocity Null	103

6.10	Midcourse Correction-2 Burn (MC-2)	104
6.11	Midcourse Correction-3 Burn (MC-3)	105
6.12	Midcourse Correction-4 Burn (MC-4)	106
6.13	Radar Failure	107
6.14	Rendezvous Breakout	109
6.15	Final Approach	110
6.16	Rbar Pitch Maneuver (RPM)	113
6.17	Fly-Arounds and Separations	114
6.18	Summary of Day of Rendezvous Events	115
7.0	Rendezvous Profile Evolution And Scenarios	117
7.1	Gemini	118
7.2	Apollo	122
7.3	Shuttle Baseline Stable Orbit Rendezvous (BSOR)	126
7.4	+Rbar Approach (BSOR)	139
7.5	Optimized Rbar Targeted Rendezvous (ORBT)	141
7.6	Ground Up Rendezvous	143
7.7	Deploy/Retrieve	144
7.8	Deploy/Ground-Up Rendezvous	145
7.9	Contingency Rendezvous	146
7.10	Ground-Up Double Rendezvous	147
7.11	Ground-Up Triple Rendezvous	148

8.0	On-Board Rendezvous Targeting And Guidance	151
8.1	Lambert Targeting	152
8.2	Display Inputs	155
8.3	Target Sets	157
8.4	Display Outputs	159
8.5	Elevation Angle Option	161
8.6	MC-2 Time of Ignition (TIG) Slip	163
8.7	Elevation Angle Tolerance	164
8.8	Targeting With TIG In The Past	165
8.9	Base Time	167
8.10	Prediction Match	168
8.11	Orbiter State	173
8.12	Lambert Targeting Summary	174
8.13	A Closer Look at the Precision Velocity Required Computation	175
8.14	A Closer Look at the Lambert Algorithm	195
8.15	Guided and Unguided Burns	212
8.16	PEG 7 (External ΔV)	220
8.17	Lambert Cyclic Guidance	223
8.18	Targeting And Guidance Alarms	233
8.19	Illegal Entries On The ORBIT TGT Display	245

9.0 Rendezvous Navigation	253
9.1 State Vector Propagation	254
9.2 State Updates and Sensor Measurement Residuals	260
9.3 Kalman Filtering Overview	273
9.4 Covariance Matrix Position Diagonals	278
9.5 Ratios and Residual Edit Criteria	283
9.6 More On Kalman Gain	288
9.7 Measurement Partials	297
9.8 On-Board Navigation Derived Relative State Data	309
9.9 Inertial State Vector Errors In UVW Coordinates	320
9.10 Inertial State Vector Errors In LVLH Coordinates	329
9.11 Relative State Vector Errors In LVLH Coordinates	333
9.12 Relative State Vector Errors In Line-of-Sight (LOS) Coordinates	341
9.13 Position Updates in LVR and LOS Coordinates	346
9.14 State Vector Management	348
9.15 Rendezvous Navigation Summary	363
9.16 GPS	366
9.17 Differential and Relative GPS	367
9.18 GPS Resynch	369
9.19 GPS Ground Filter	371

10.0 Flight Control During On-board Targeted Phase	373
10.1 Target ID and -Z Body Axis	374
10.2 -Y Star Tracker and Rendezvous	375
10.3 Ti Burn Position Miss Due to Vernier Jets	376
10.4 Flight Control During Burns	377
10.5 0/0/0 LVLH Attitudes	379
11.0 Integrated GN&C During Rendezvous	381
11.1 Integrated GN&C During Orbit Coast	382
11.2 Integrated GN&C For OMS Burns	391
11.3 Integrated GN&C During +X RCS Burns	395
11.4 Integrated GN&C During Multi-Axis RCS Burns	397
12.0 Glossary	399
13.0 Bibliography	405
13.1 JSC Documents	406
13.2 NASA Publications	408
13.3 Conference and Journal Papers	409
14.0 Background On This Document	415

1.0 Preface for the 4th Edition

The Rendezvous Intro continues to be used for training and reference purposes almost 17 years after it was first published. While this document does not address Orion rendezvous, some Orion personnel are using it as a reference for rendezvous GNC and trajectory concepts.

This edition contains corrections that have been identified since the 3rd edition was published in 2000. In addition, new material has been added that was developed by the author in the 1990s and early part of the first decade of the 21st century. While some of this material is perhaps too detailed for an introduction, it is of value and the author wanted to make it available to JSC personnel. The sections on Lambert targeting guidance have been significantly expanded.

New text on a previously existing page is indicated in **bold** and with a change bar. New pages have a change bar on the right side of the page. Assistance with updates and reviews were provided by personnel listed below.

Greg Bartz	Orbit Flight Design (USA)	Nicholas O'Dosey	Rendezvous Guidance and Procedures Office (Barrios)
Ray Bigonesse	Rendezvous Guidance and Procedures Office (USA)	Carolyn Propst	Navigation (USA)
Alan Fox	Crew Training (USA)	Mark Schrock	Orbit Flight Design (USA)
Jorge Frank	Crew Training (USA)	Susan Snyder	Orbit Flight Design (USA)
Deidre Gilmore	Orbit Flight Design (USA)	Jeff Tuxhorn	Crew Training (USA)
Edward P. González	Orbit Flight Dynamics (NASA)	Stephen R. Walker	Rendezvous Guidance and Procedures Office (NASA)
Dr. Leonard Kramer	Navigation (then USA, now Boeing)	Brian Yarbrough	Orbit Flight Design (USA)
Jessica LoPresti-Bellock	Orbit Flight Design (USA)	Patrick Zimmerman	Navigation (USA)

Changes are listed on the next page. Comments, corrections, and suggestions are welcome.

John L. Goodman

USA Flight Design and Dynamics

(b) (6)

(b) (6)

November 2009

New or Updated Material:

4.0 Launch Windows and Constraints

Beta angle, page 55

5.0 Ascent, OMS-2, and the Ground Targeted Phase

GPS Ground Filter, page 68

Ground targeted burn names, page 69

Out-of-plane burn components, page 70

NSR factored in to NC, page 71

NSR factored in to NH, page 72

Meeting lighting constraints without NSR, page 73

New section on Designing a Ground-Up Rendezvous Profile, pages 83-85

6.0 Day of Rendezvous and Separations

Max radar range for measurements, page 98

Ti and orbital noon, page 100

Prox Ops covariance uplink, page 102

+Rbar ISS approaches, page 110

TORVA, page 112

R Bar Pitch Maneuver, page 113

Fly-arounds and separation, page 114

8.0 On-Board Rendezvous Targeting and Guidance

MC-2 TIG -3 min. limit, page 163

Timer count up for TIG in the past, page 165

New Precision Velocity Required section, pages 175-194

New Lambert algorithm section, pages 195-211

OI-30 MNVR EXEC Display Changes, pages 221-222, 230-232, 239, 243

Expanded Lambert Guidance Section, pages 223-228

OI-32 Lambert Guidance improvement, page 232

9.0 Rendezvous Navigation

Drag coefficient computation, page 256

OI-32 IMU Align display change, page 257

Orbiter and target KFACTOR uplink, page 259

H and V star tracker axes, page 263

Kalman filter states, page 277

Rndz, Prox Ops, and COAS covariance values, page 282

Kalman filter bias states, page 286

Kalman filter underweighting, page 300

Range measurement partial, page 301

State vector uplinks, page 349

SHUTTLE_FILTER_FLAG change, page 360

GPS updates, pages 366-368

GPS Ground Filter, page 371

10.0 Flight Control During On-Board Targeted Phase

-Y Star Tracker attitude, page 375

Burn in target track, page 377

0/0/0 attitude for LVLH (+X, -X and -Z sense), page 379

11.0 Integrated GN&C During Rendezvous

Burn in target track, page 397

12.0 Glossary

Glossary updates, pages 400-402

13.0 Bibliography

New bibliography, pages 405-413

14.0 Background On This Document

New pages 415-419

Deleted Material:

8.0 On-Board Rendezvous Targeting and Guidance

10+ day TIG procedure for ORBIT TGT display

9.0 Rendezvous Navigation

GPC Processing of GPS state vectors

1.1 Preface for the 3rd Edition

Since the initial publication in January of 1993, a number of changes have been introduced into the rendezvous phase. As a result, in May of 1999, the Rendezvous Guidance and Procedures Office inquired about the possibility of an updated edition of the book.

The primary change addressed by this updated edition is ORBT, or Optimized R-Bar Targeting. The REL NAV displays have been updated to reflect GPS parameters that were introduced on OI-27. Most ORBIT TGT displays have been changed to reflect the OI-29 "SPEC 34 10 Day Limit" CR. A new chapter on measurement partials in rendezvous navigation has been added. This is based on a presentation I gave to the SAIL IGN&C Forum on November 29, 1995. A chapter concerning rendezvous profile development from Gemini through Shuttle ORBT is also included. Much of the new GPS chapter is based on an April 5, 1996, memo I wrote entitled "OPS 8, OPS 2, GPS And You." Some of the new material on Lambert Targeting and Guidance was originally developed in 1993 for the On-Orbit Translational Guidance book. That book, along with a proposed book on Powered Explicit Guidance (PEG), was never completed.

A list of individuals who provided me with advice and editorial comments is on the following page.

The author welcomes any comments and corrections.

The fourth edition, to be published later in 2000, will contain additional material on Lambert Targeting, Lambert Cyclic Guidance and the MNVR EXEC display.

John L. Goodman

(b) (6)

February 9, 2000

Note: Revision A (May 17, 2000) contains corrections of errors and graphics clean-up.

Unless stated otherwise, individuals are with United Space Alliance.

Milt Contella	Flight Design
Scott Dunham	NASA Rendezvous GPO
Malise Fletcher	NASA Rendezvous GPO
Jorge Frank	Crew Training
Dawn Gabriel	Flight Design Manager
Chris Hickey	Flight Software
John Hutchins	Navigation
Jim Impastato	Boeing Reusable Space Systems/Huntington Beach, Integrated GN&C
Michael Jenkins	Rendezvous Flight Design
Michele Kocen	Navigation
Raymundo Moreno	Rendezvous Flight Design
Larry Roberts	Flight Software
Sean O'Rouke	Rendezvous GPO
Mark Schrock	Prox Ops Flight Design
Tom Snyder	Rendezvous Flight Design
Jeannette Spehar	NASA Rendezvous GPO
Farhad Teymurian	Rendezvous Flight Design
Stacey Valverde	Flight Software
Steve Walker	Rendezvous GPO
Brian Yarborough	Rendezvous Flight Design
William L. Yeakey	FSW Integration
Patrick Zimmerman	Navigation

1.2 Preface for the 1st And 2nd Editions

This document was originally designed to meet rendezvous training needs within the Level 8 GN&C FSW testing group. Most of the material was taken from classes held for Level 8 analysts in the spring of 1991. The text (including style and content) was developed in response to lessons learned over the past 5.5 years while training entry level engineers to perform rendezvous GN&C verification and effectively interface with other elements of the shuttle program. It is intended to allow engineering and management personnel to quickly come up to speed through the development of a “visual rendezvous vocabulary.”

This work was not intended to be a comprehensive introduction to all aspects of rendezvous/proximity operations and crew procedures. Readers should refer questions regarding mission-specific design aspects, flight rules, crew procedures, and overall rendezvous policy to the appropriate personnel in operations, flight design, or crew training. Sources listed in the Bibliography may also be used for further information.

Areas that are of importance to Level 8 analysts (day of rendezvous trajectory, Lambert guidance, on-board navigation, state vector management and state errors) are emphasized. The ground targeted phase is not tested by Level 8, but it is dealt with since Level 8 personnel frequently encounter discussions of that part of the rendezvous in meetings and in flight-specific documents.

Subjects that do not figure prominently in Level 8 analysis (such as proximity operations) are defined but not developed. Some aspects of rendezvous were not covered, since they are adequately dealt with in previously existing texts.

Rendezvous is treated as an integrated whole, rather than as a large number of details that are not tied together. Long, tedious explanations and discussions of mathematical theories behind orbital mechanics often lead to confusion rather than enlightenment, and are therefore avoided.

Over the years, I have found that the traditional, two-dimensional “R_BAR V_BAR” LVLH plot often initially confuses new engineers. For the sake of clarity, many pages in this document employ a “three-dimensional” view that clearly shows all three axes of the LVLH frame.

I would like to thank the following individuals for their help in reviewing this document:

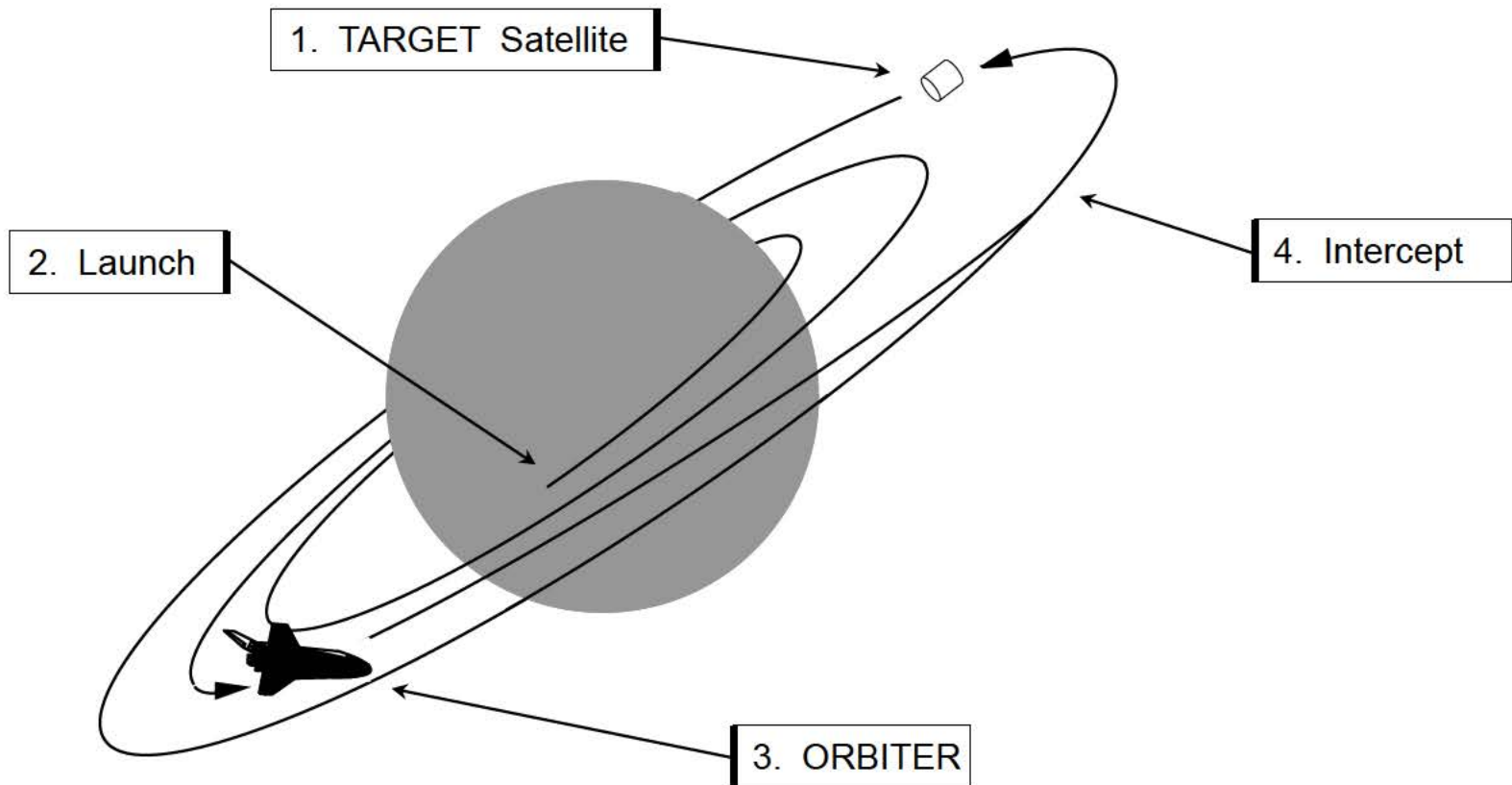
Robert Solis	(Omniplan Engineering Support)
John Hutchins	(Intermetrics Incorporated)
Gene Brownd	(RSOC, Navigation Analysis, R16E)
Dan Sawin	(RSOC, Rendezvous Analysis and Operations, R16C)
Michele Kocen	(RSOC, On-Board Navigation, R16E)
Todd Miller	(RSOC, Rendezvous Guidance and Procedures Officer, DM43)
Val Murdoc	(RSOC, Ground Navigation, R16E)
Bill Roberts	(RSOC, Rendezvous Analysis and Operations, R16C)
Gail Hennington	(RSOC, Rendezvous Crew Training, DG67)
Bob Mahoney	(RSOC, Rendezvous Crew Training, DG67)
Rosemarie Ideler	(RSOC, Flight Software Production/Verification, R18A)
Alan Fox	(RSOC, Rendezvous Crew Training, DG67)
Bill Atkins	(RSOC, Rendezvous Analysis and Operations, R16C)
Alison Smythe	(ARS Graphica)

Errors that remain in this work are my own. Corrections should be referred to myself or the Level 8 Orbit Verification supervisor.

John L. Goodman
RSOC Level 8 GN&C
January, 1993

2.0 Introduction

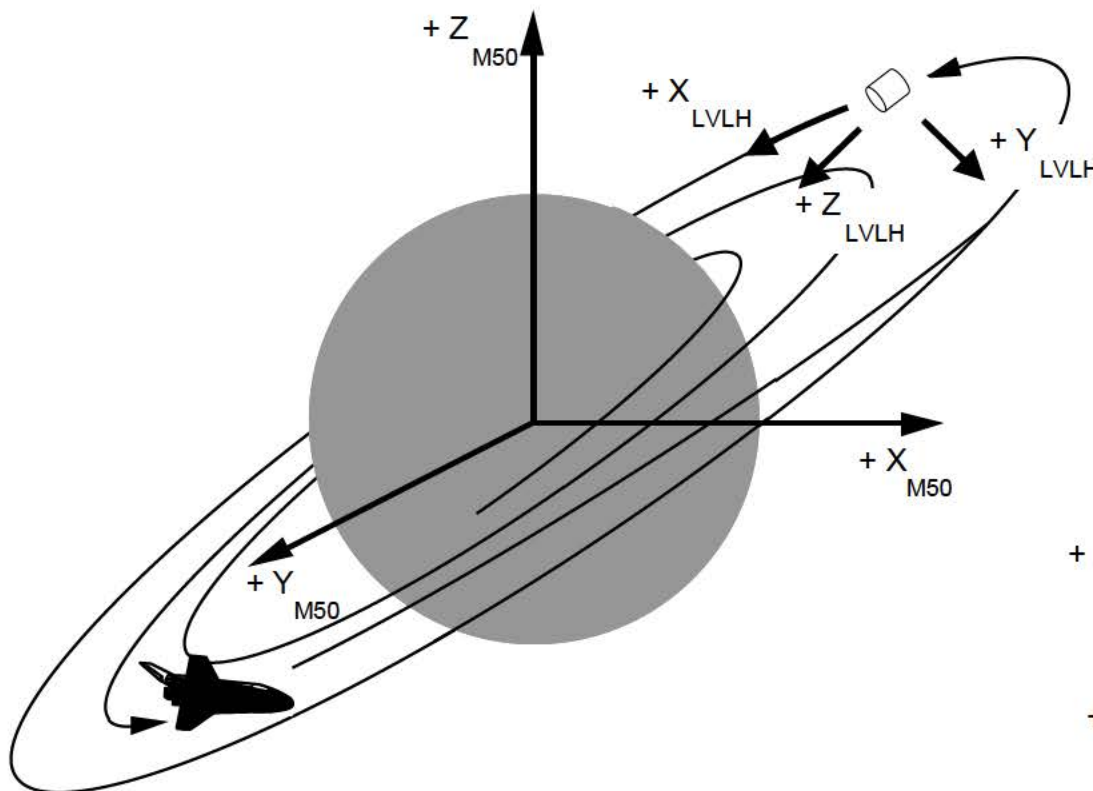
Some missions require that the ORBITER meet, or rendezvous with, a satellite in orbit. If this satellite, or "TARGET," is in orbit prior to the launch of the shuttle, the rendezvous is called a "ground-up rendezvous."



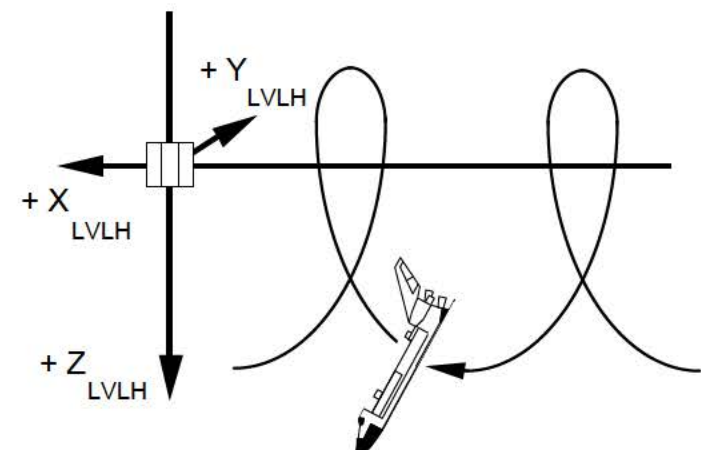
This page intentionally left blank.

3.0 Coordinate Systems

There are two ways of viewing ORBITER motion during rendezvous. The first uses an Earth-centered, inertial system such as M50. The second method involves a relative coordinate system centered on the TARGET. ORBITER motion is plotted as it would appear relative to the TARGET. This system is referred to as “Local Vertical Local Horizontal Rotating Curvilinear coordinates” (also called Local Vertical Curvilinear (LVC), but most commonly known as simply, “LVLH”).



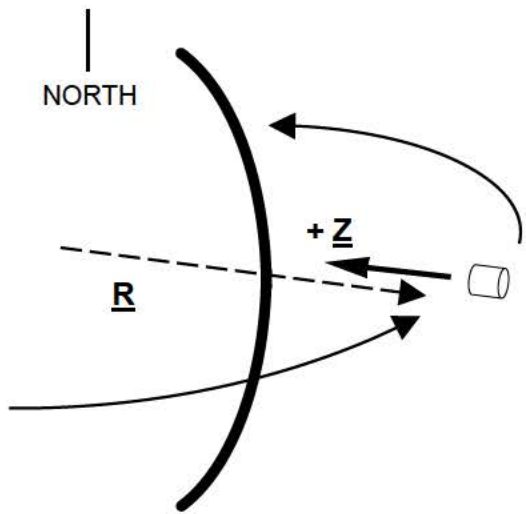
Inertial Coordinates: M50



Relative Coordinates: LVLH

3.1 LVLH Axes

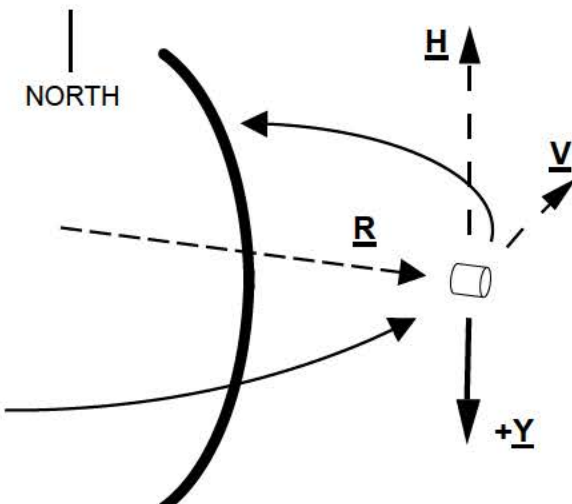
The LVLH frame has its origin on the target and the origin moves with the target. Each of the three axes is defined so that motion can be easily visualized.



The LOCAL VERTICAL axis is pointed at the center of the Earth and is positive in that direction. " \underline{R} " is the position vector of the TARGET.

$$+Z = -\underline{R}$$

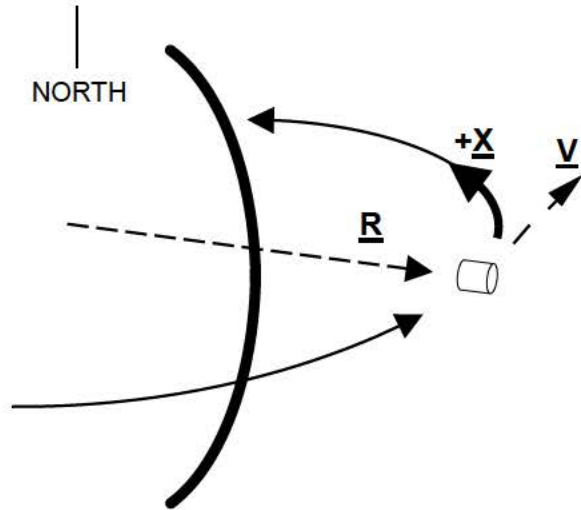
$+Z$ is also called the "R Bar" since it is parallel to the TARGET's position vector.



The OUT-OF-PLANE axis is positive in a southerly direction. It is opposite the angular momentum vector (\underline{H}). " \underline{V} " is the velocity vector of the TARGET.

$$+Y = -(\underline{R} \times \underline{V})$$

$+Y$ is also called the "- H Bar."



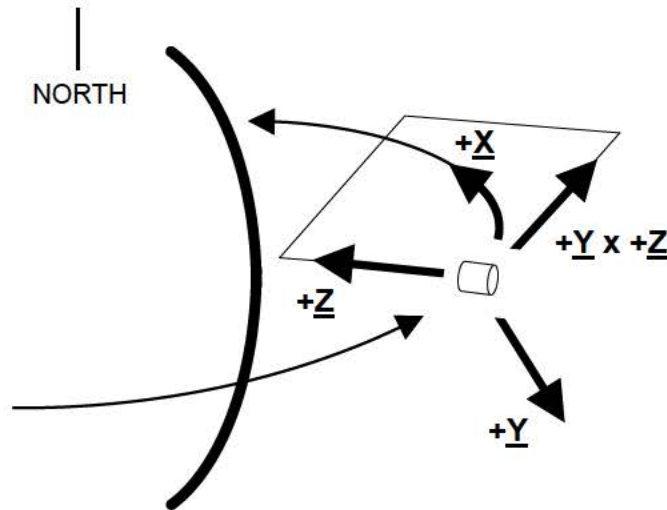
DOWN-TRACK axis is an arc of a circle, and for circular orbits it is superimposed on the orbital path. It is positive in the direction of motion.

$$+\underline{X} = -(\underline{R} \times \underline{V}) \times (-\underline{R})$$

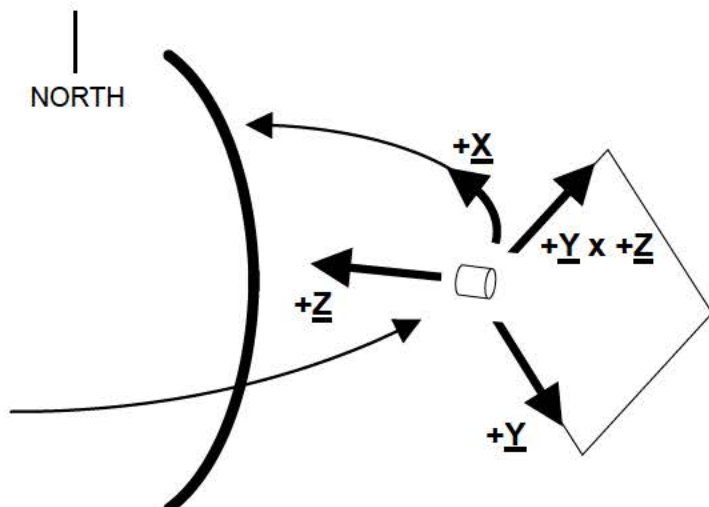
The curved X axis makes the system curvilinear. +X is also commonly called the “V Bar”, since it points in the direction of the velocity vector when close to the TARGET, assuming a circular orbit.

3.2 Planes Formed By LVLH Axes

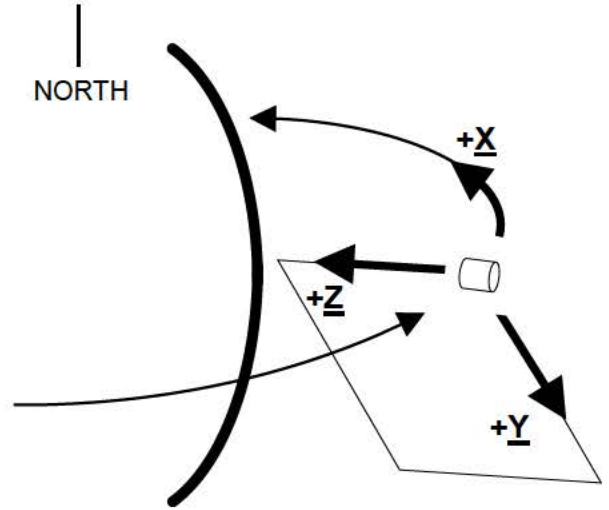
Three important planes are formed by the X, Y and Z axes.



The LOCAL VERTICAL plane is formed by the Z and the cross product of the Y and Z axes.



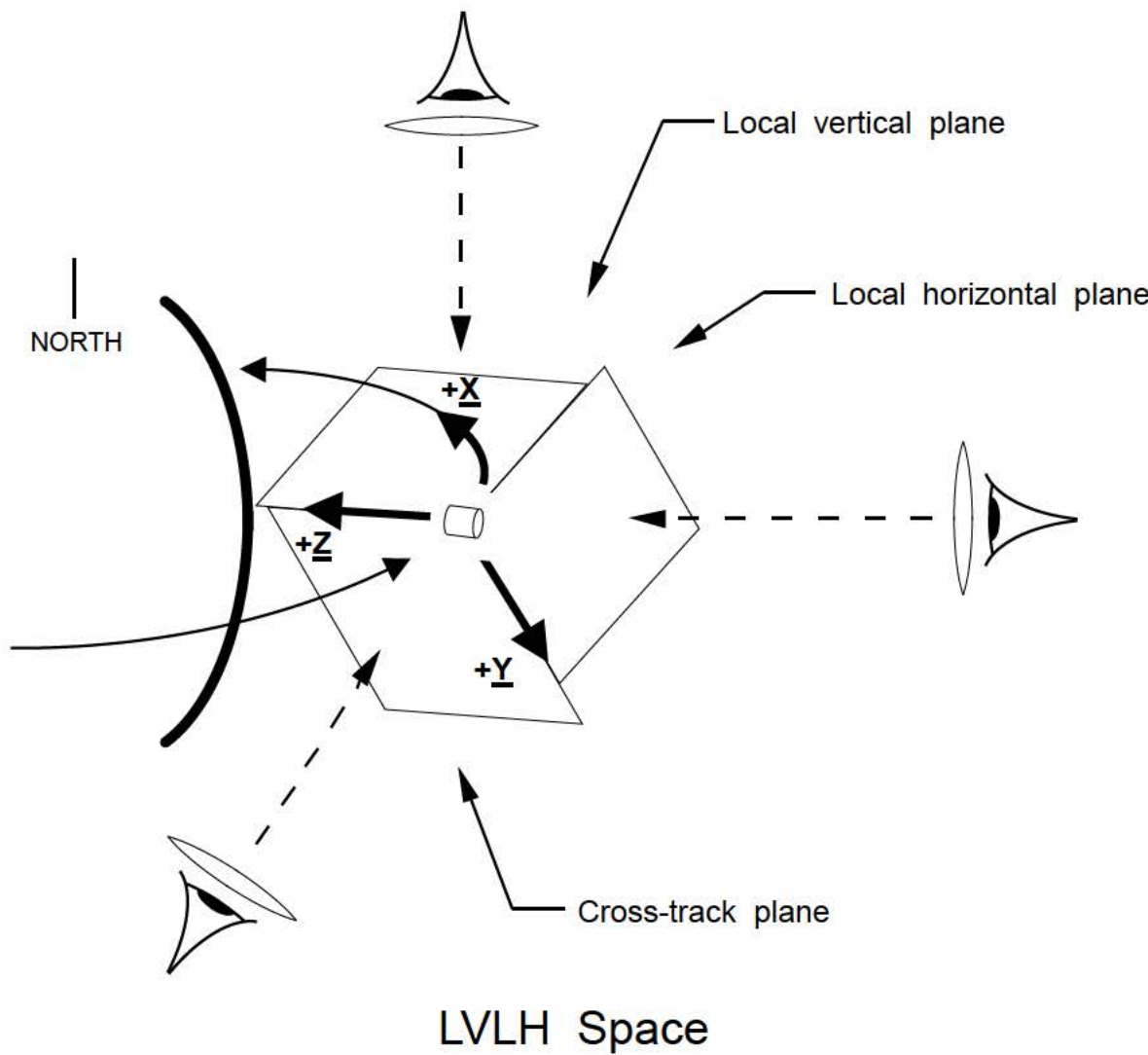
The LOCAL HORIZONTAL plane is formed by the Y axis and the cross product of the Y and Z axes.

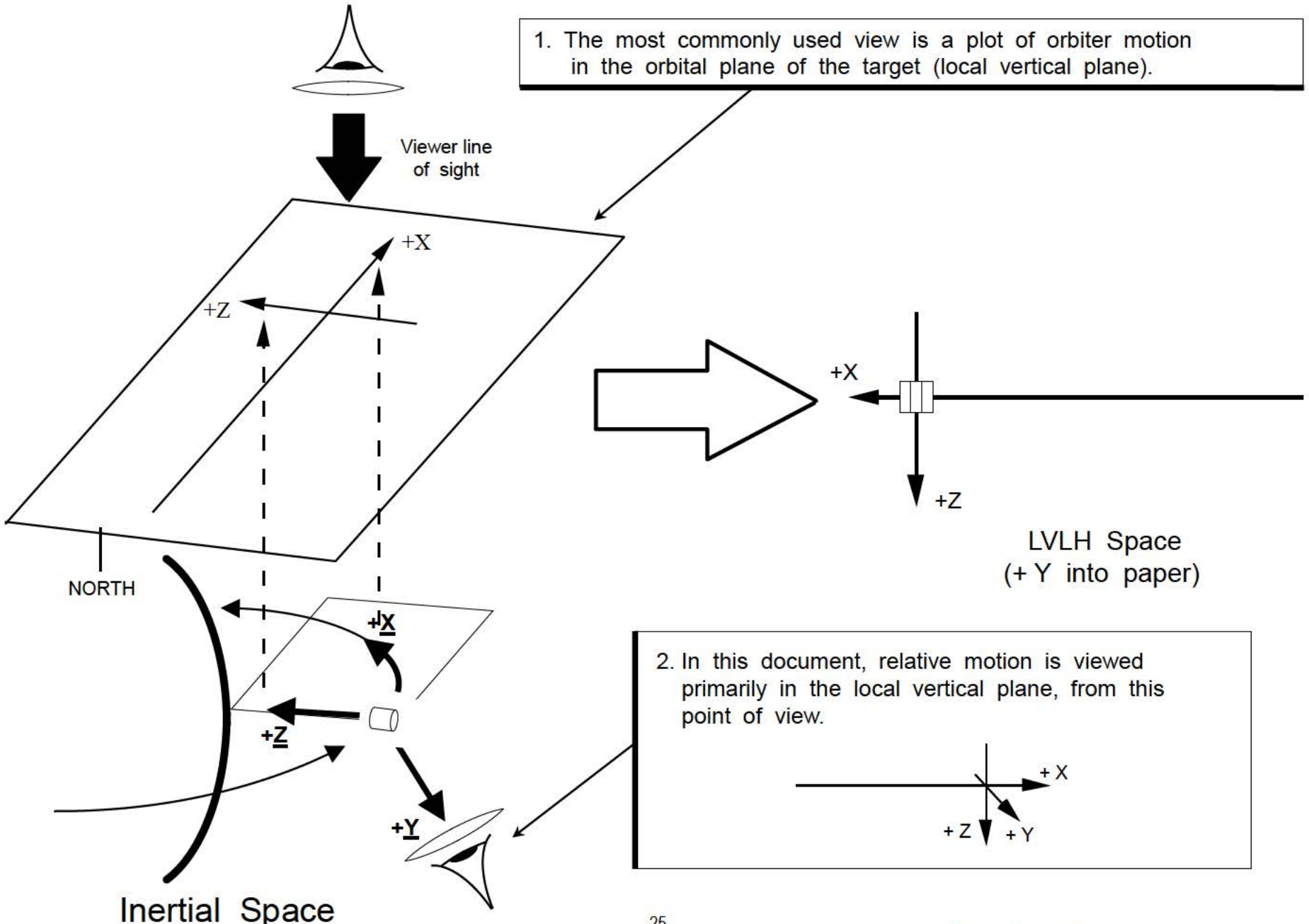


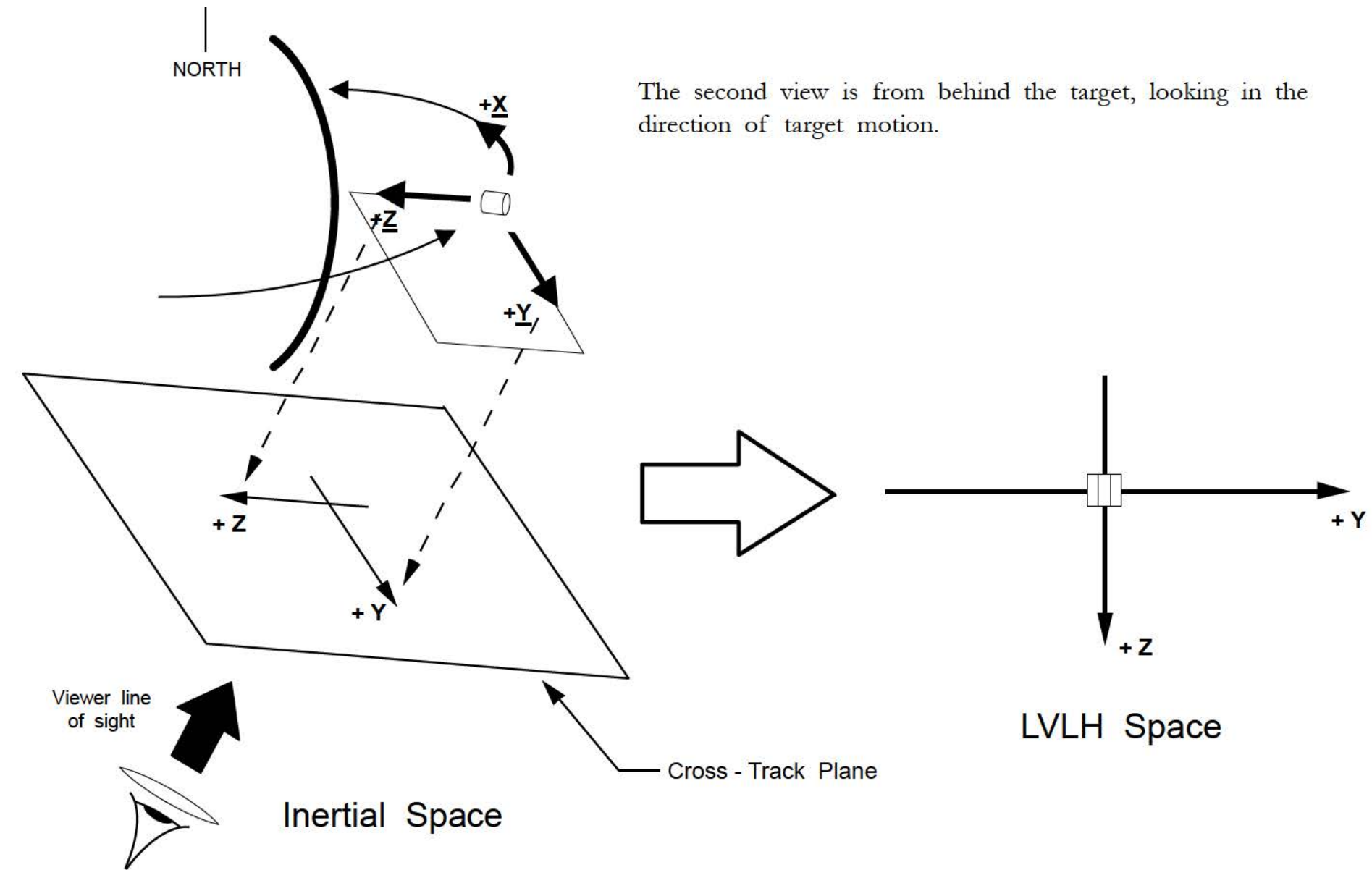
The CROSS-TRACK plane is formed by the Y and Z axes.

3.3 Views of Relative Motion

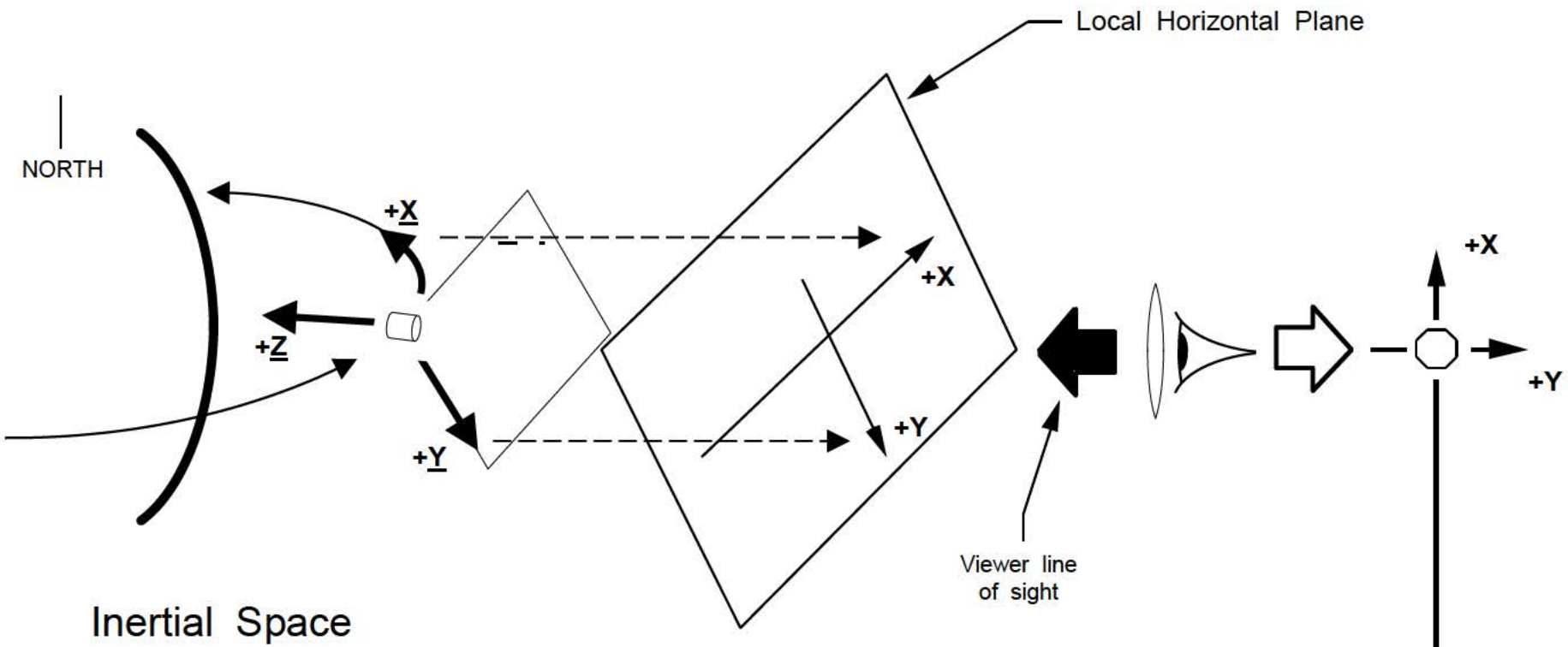
There are three ways of plotting motion in LVLH space. Each view is based on projecting orbiter motion into one of the previously defined planes.







The third view is from along the local vertical, looking down to the Earth.



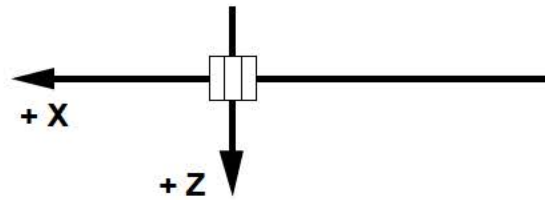
LVLH Space

3.4 Rectilinear and Curvilinear Coordinates

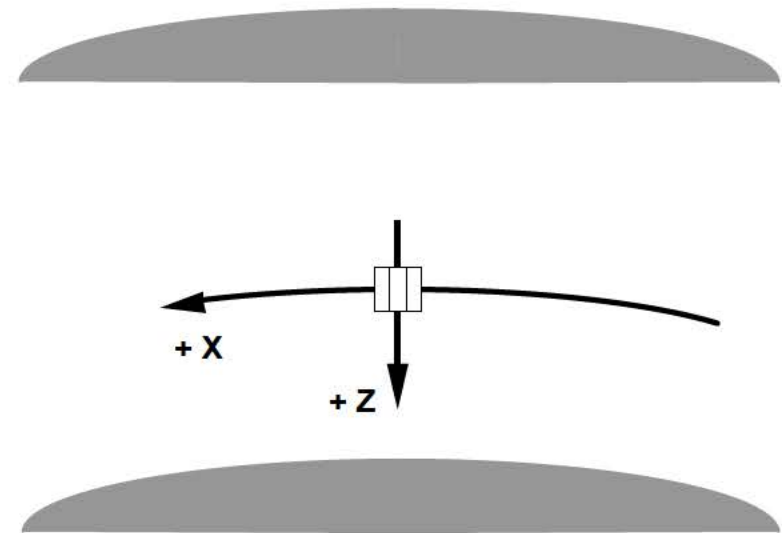
Technically speaking, the term LVLH refers to a system with rectilinear, or straight, axes. However, the term LVLH is commonly used for a system with a curvilinear X axis. In this document, and in the Shuttle Program in general, LVLH and LVC are used interchangeably. On pages where a rectilinear system is used, it will be specified as LVR (Local Vertical Rectilinear).

The LVC and LVR systems are approximately equivalent within about 20 nautical miles of the origin.

Local Vertical Rectilinear
Coordinates (LVR)



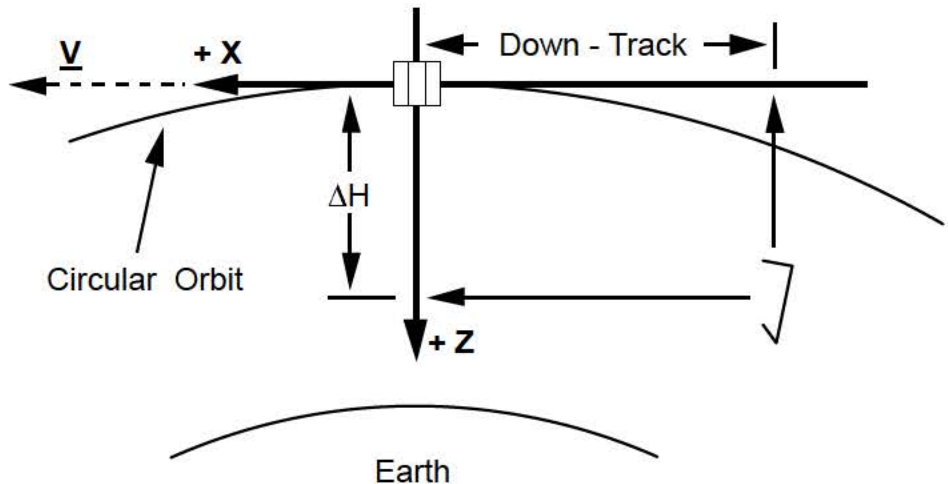
Local Vertical Curvilinear
Coordinates (LVC)



Each system measures relative altitude (also called “delta height” or “ ΔH ”) and down-track differently.

Local Vertical Rectilinear Coordinates (LVR)

For a circular orbit, the +X axis is parallel to the velocity vector.

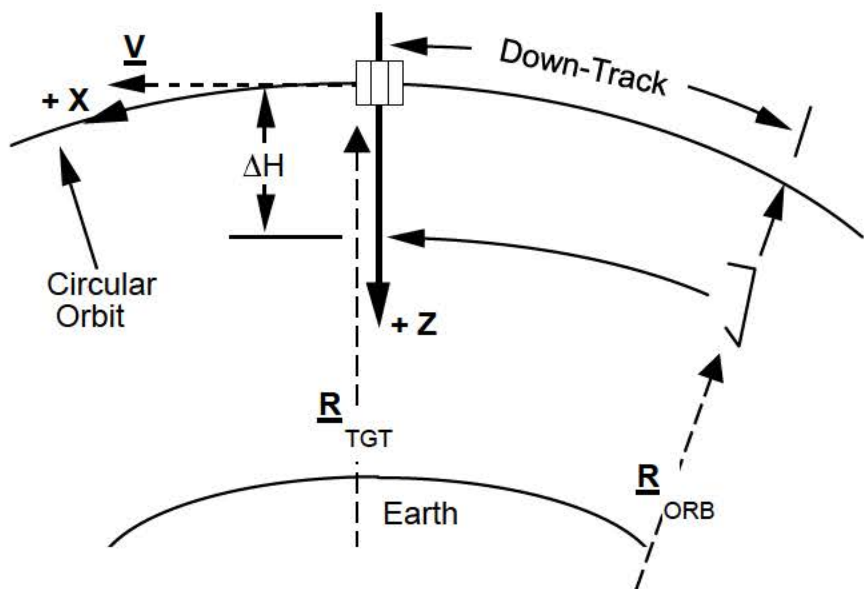


Local Vertical Curvilinear Coordinates (LVC)

The X axis is a circular arc with a radius equal to the magnitude of the TARGET position vector. For circular orbits, the X axis is along the orbital path of the TARGET.

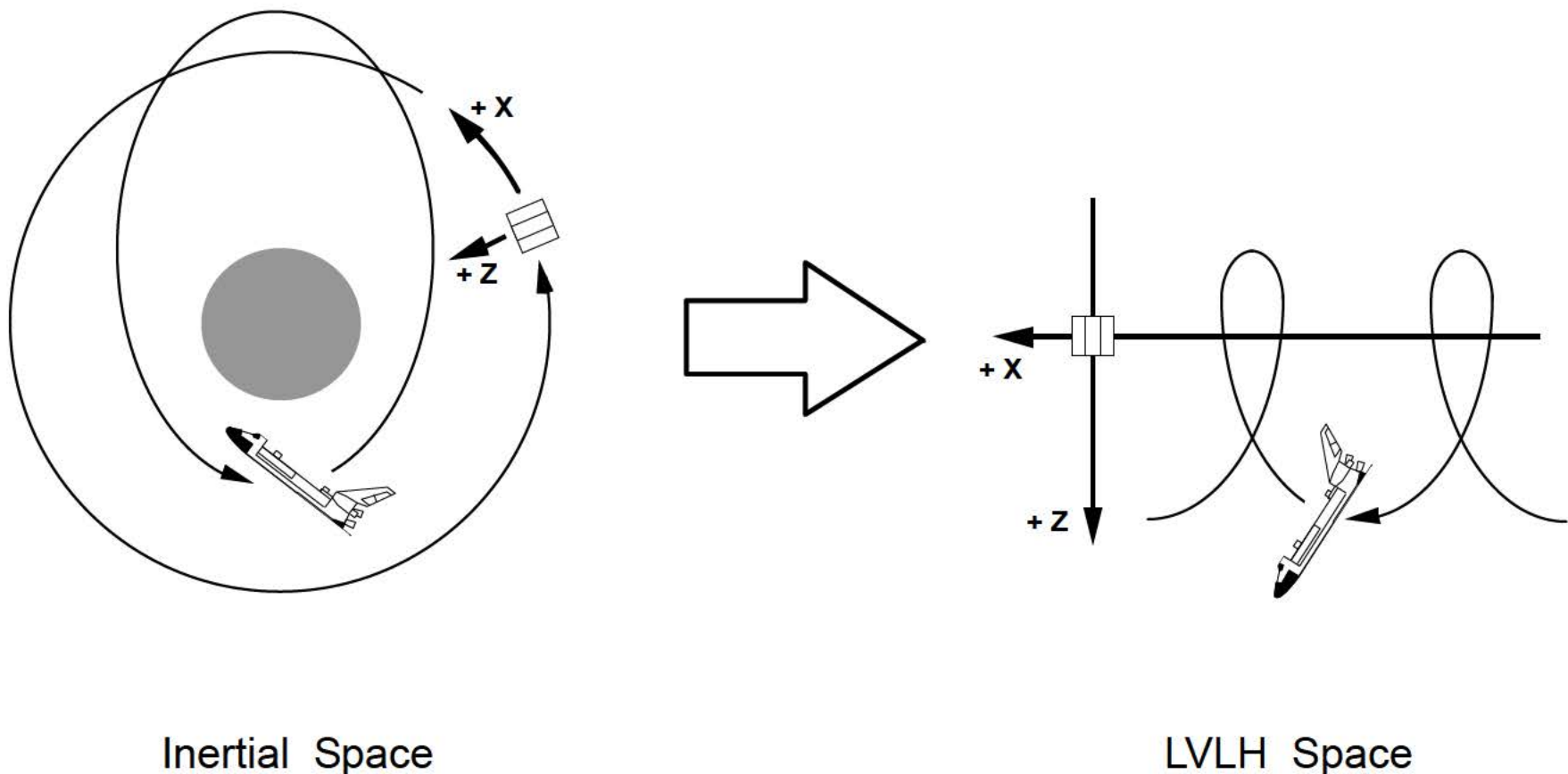
Down-track is the arc length along the X axis from the TARGET to the point where a line collinear with the ORBITER position vector would intersect the X axis.

Relative altitude is determined by subtracting the magnitudes of the TARGET and ORBITER position vectors.

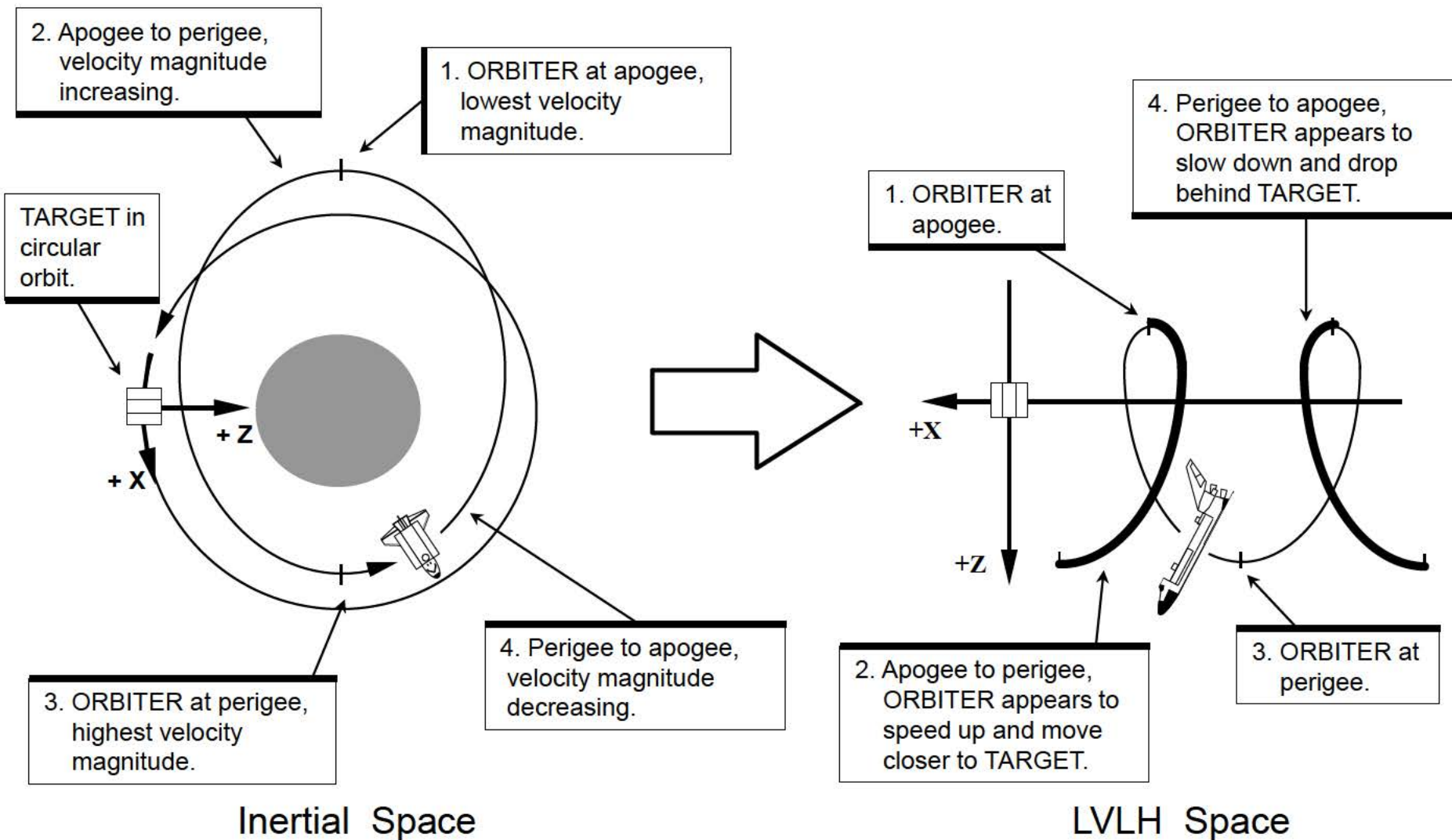


3.5 Relative Motion Projected Into the Local Vertical Plane

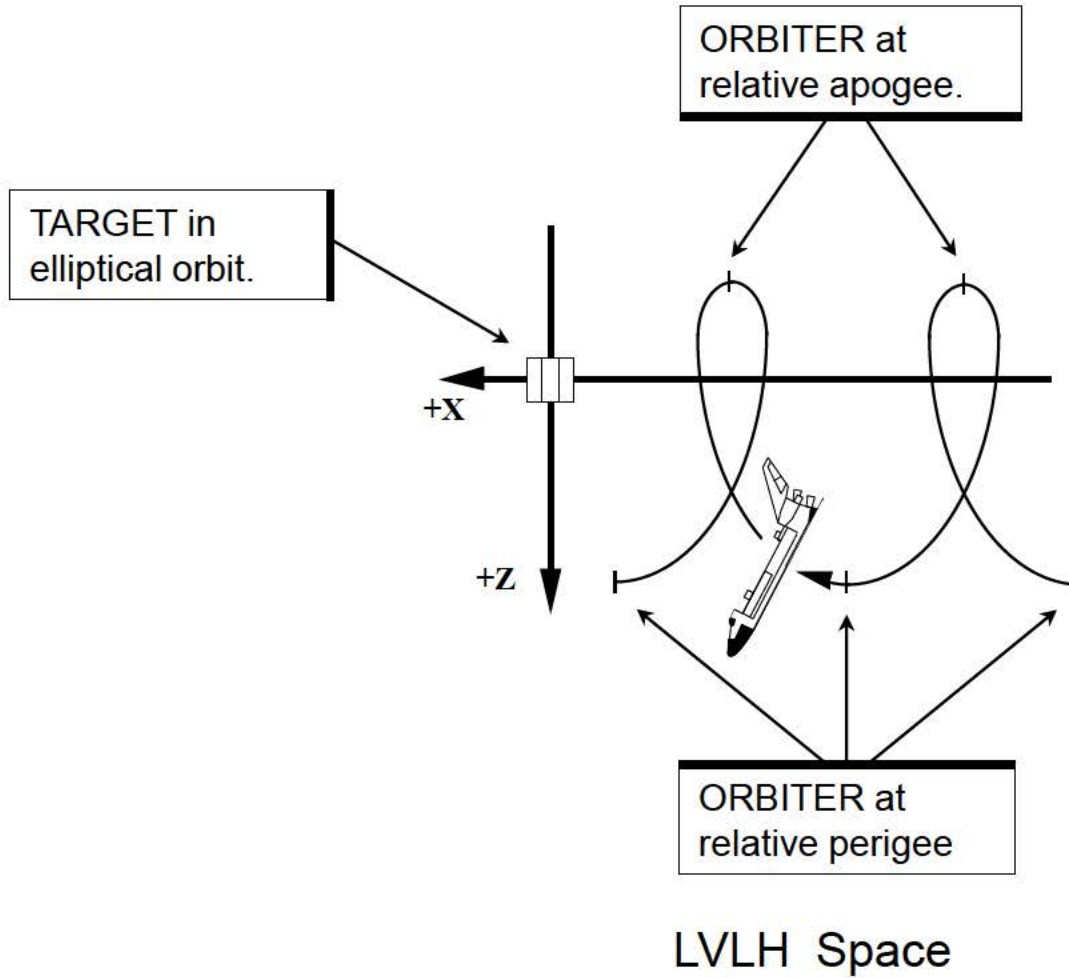
Orbiter motion in the local vertical plane is the most difficult to interpret. If the ORBITER is in an elliptical orbit that intersects the circular target orbit, the trajectory in LVLH curvilinear space would look like this:



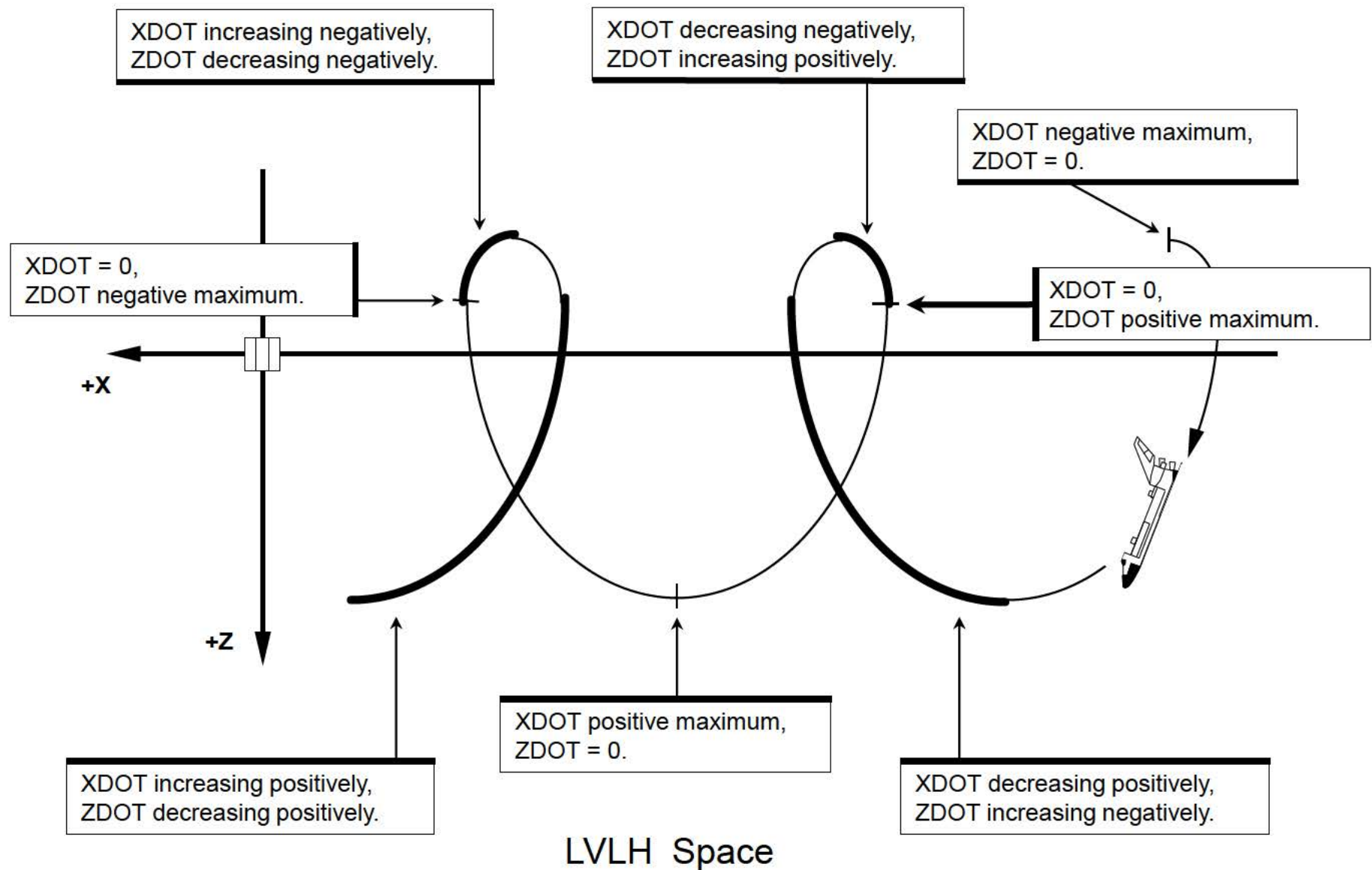
For circular orbits, the magnitude of the velocity vector is constant. The magnitude of the velocity vector varies for elliptical orbits. It has its greatest value at perigee and its lowest value at apogee. This results in the “loop de loop” (or “wifferdil”) trajectory when an elliptical orbit is viewed in LVLH space.



If the TARGET is in an elliptical orbit, the high and low points of the ORBITER's trajectory in LVLH space may not correspond to the ORBITER's apogee and perigee. For the elliptical case, these points are known as "relative apogee" and "relative perigee."

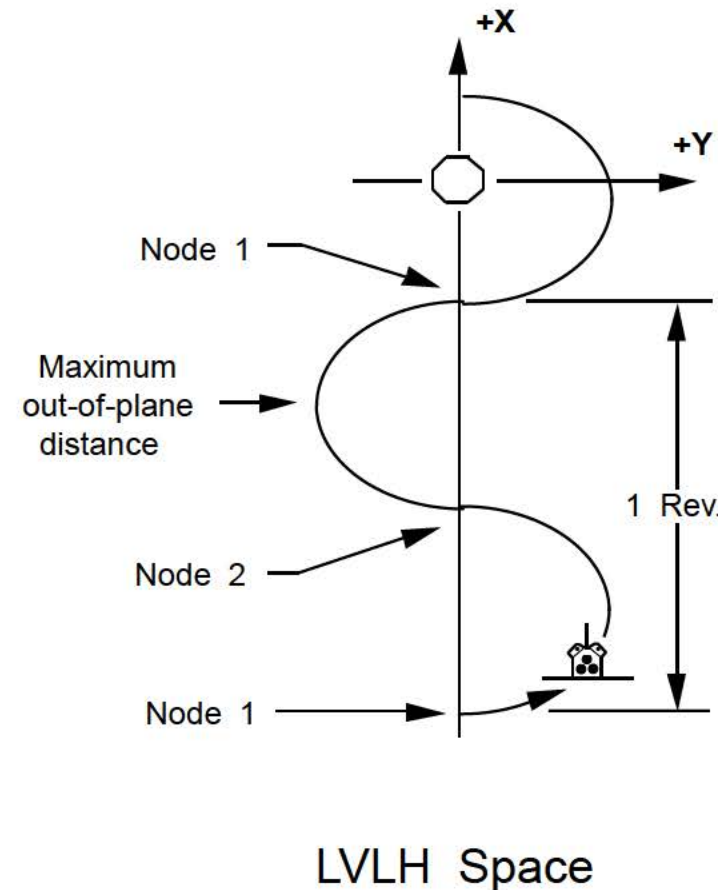
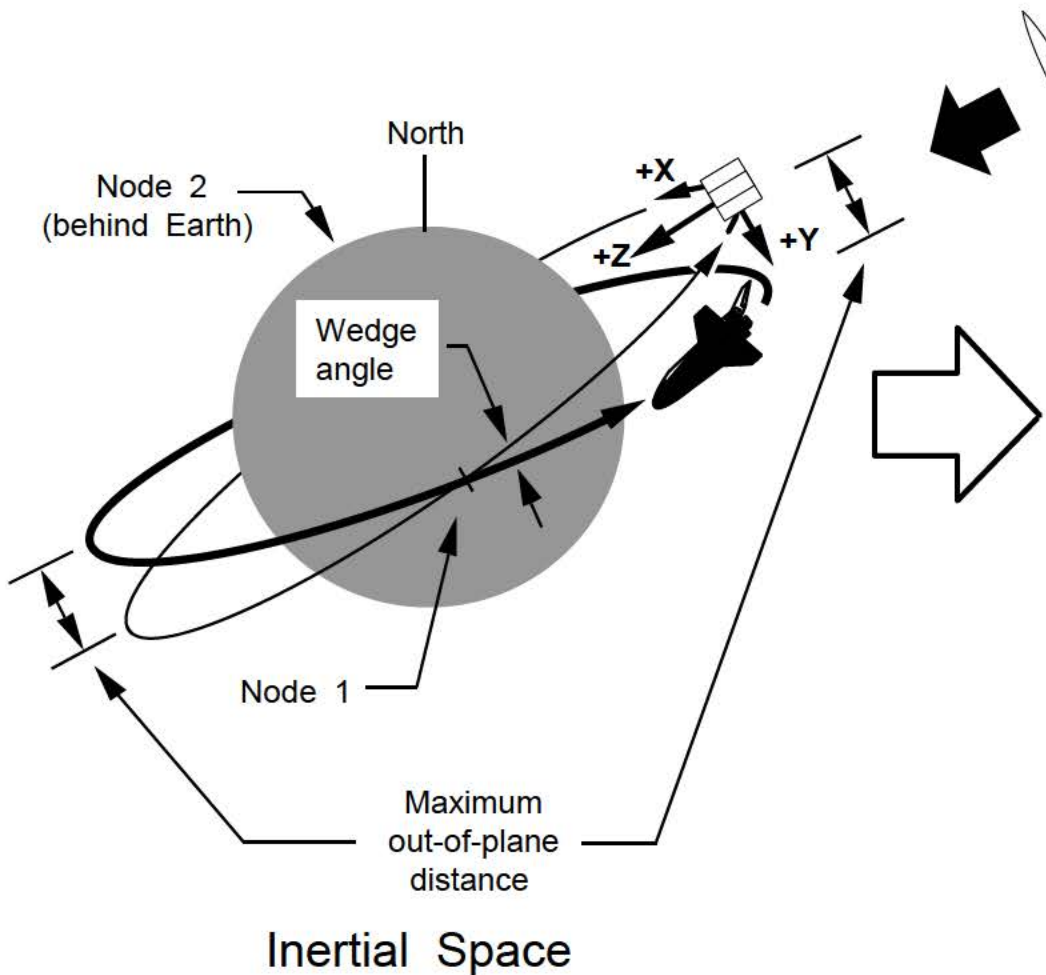


ORBITER relative velocity varies as follows :



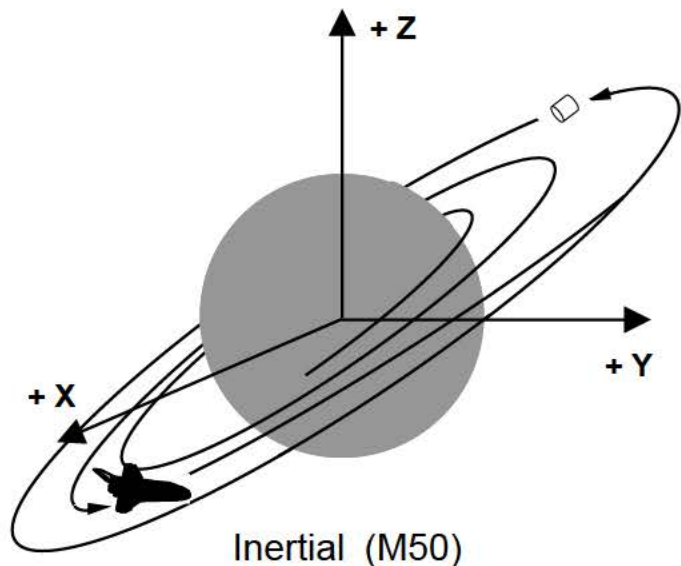
3.6 Relative Motion Projected Into the Local Horizontal Plane

When viewed in the local horizontal plane, orbiter out-of-plane motion appears to be sinusoidal due to the wedge angle between the orbiter and target orbits.

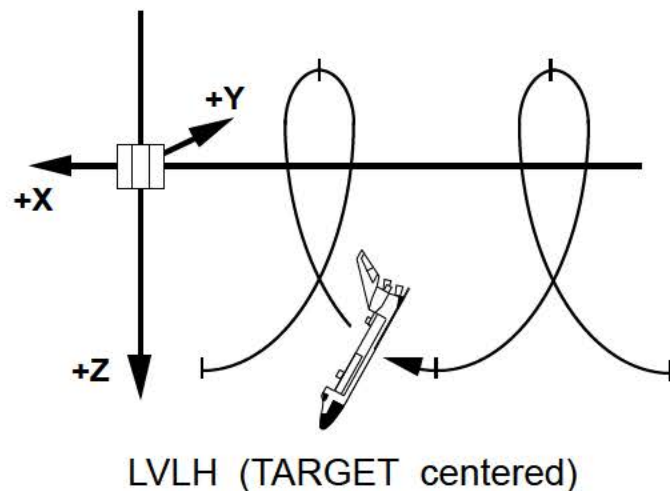


3.7 Coordinate Frame Summary

ORBITER motion during rendezvous may be viewed in the M50 (inertial) or LVLH frame. The LVLH frame is preferred since it displays ORBITER motion with respect to the TARGET.



Inertial (M50)

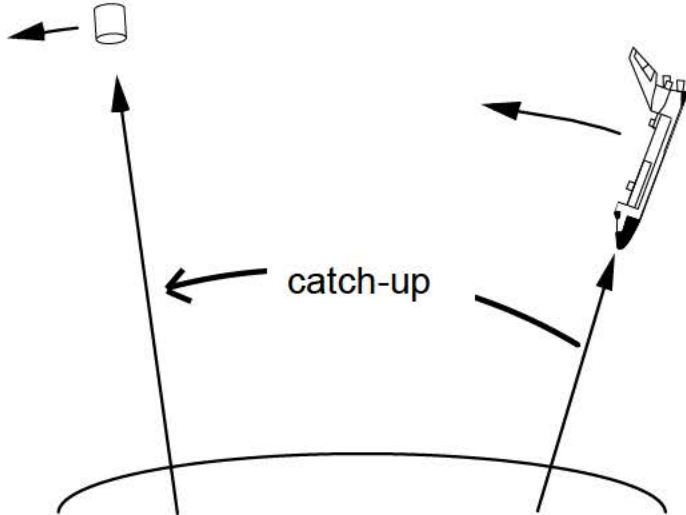


LVLH (TARGET centered)

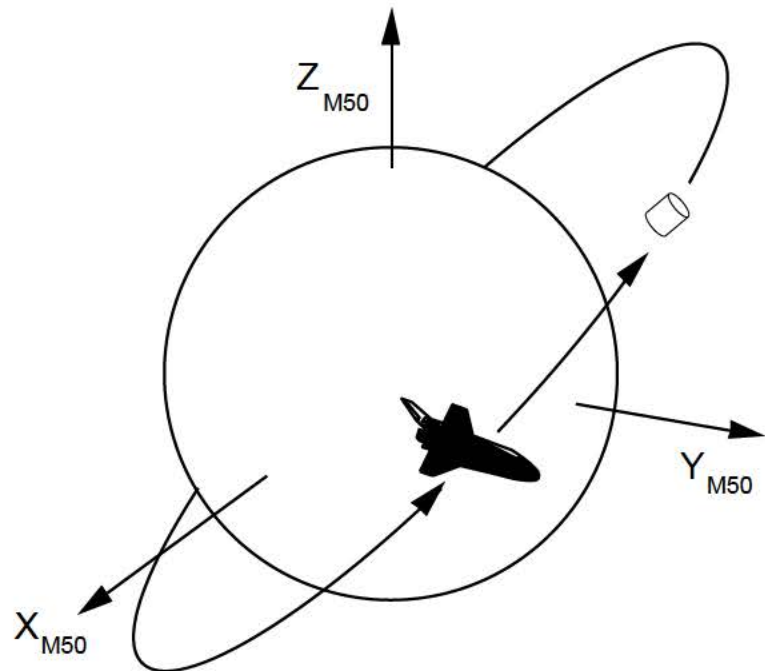
This page intentionally left blank.

4.0 Launch Windows and Constraints

To rendezvous with a TARGET, the ORBITER must be launched so that it can catch-up with the TARGET, and be in the same orbital plane as the TARGET by the day of rendezvous.



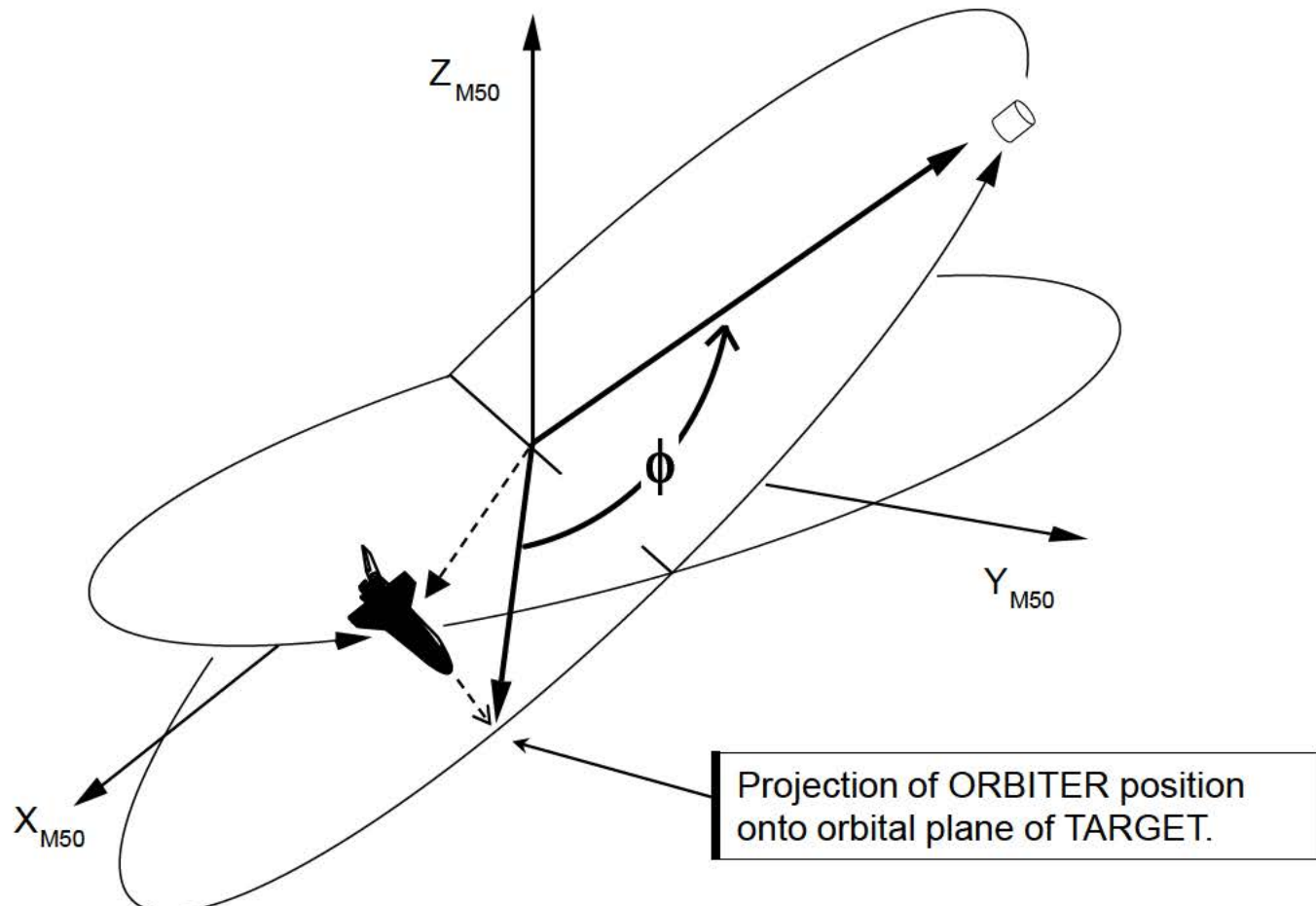
ORBITER must catch-up with TARGET on the day of rendezvous.



By the day of rendezvous, the ORBITER must be in the same orbital plane as the TARGET.

4.1 Phase Window

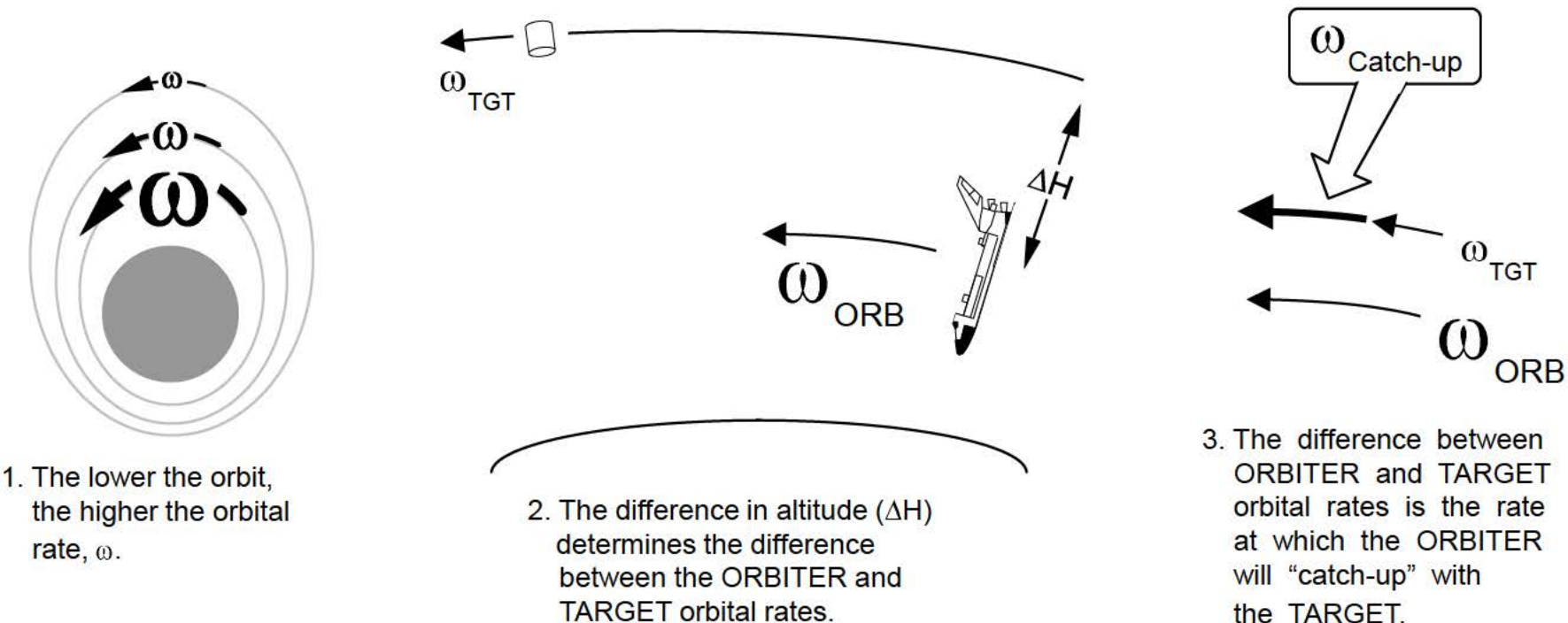
The phase angle, ϕ , is a measure of how far the TARGET is ahead (or behind) the ORBITER. Phase angle is measured in the orbital plane of the TARGET. It is the angle between the projection of the ORBITER position onto the orbital plane of the TARGET and the TARGET position vector.



Phase angle can be reduced to zero by controlling the rate at which the ORBITER approaches the TARGET.

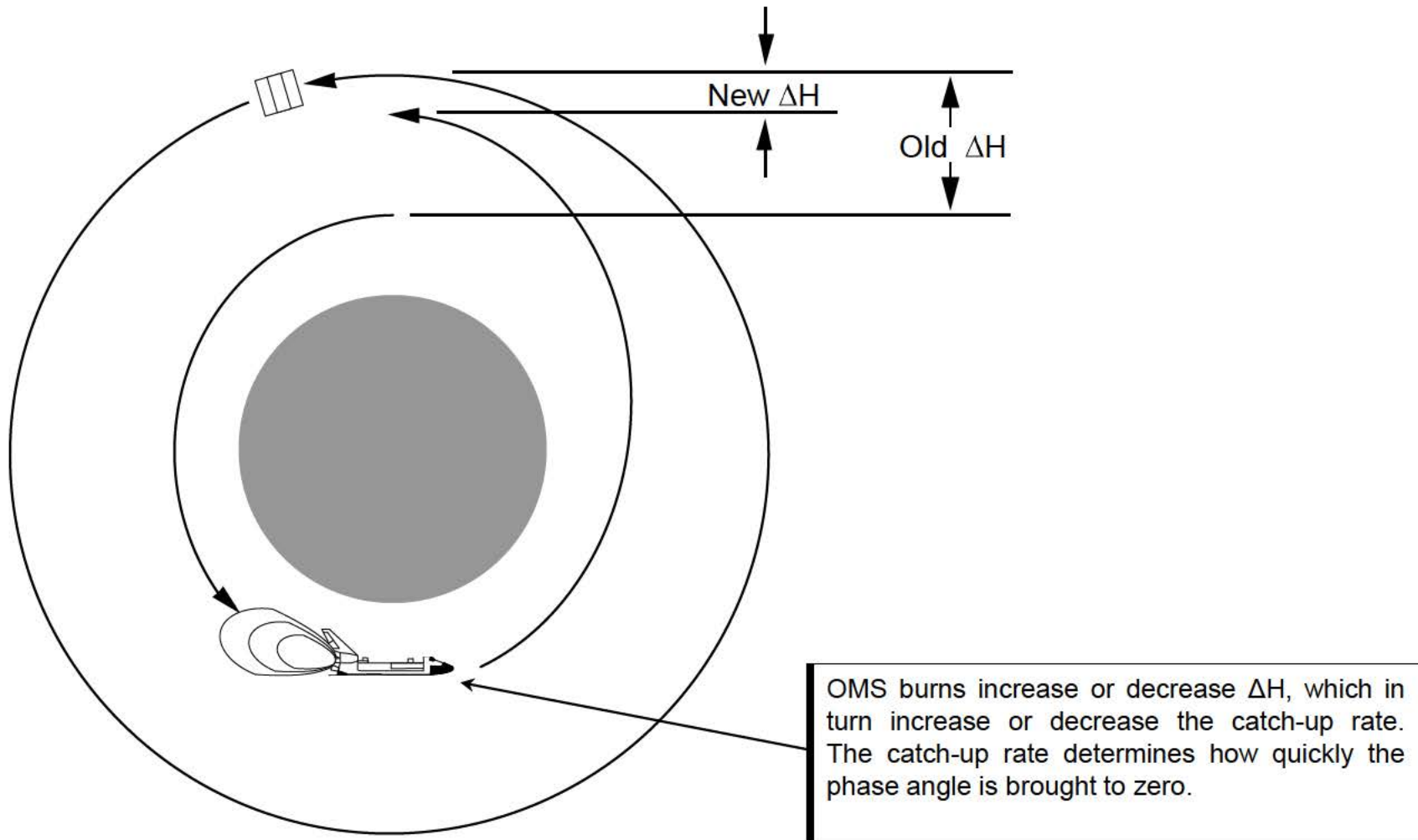
Orbital rate decreases as orbital altitude increases. If the ORBITER and TARGET are at different altitudes, they will have different orbital rates.

The difference between ORBITER and TARGET orbital rates is the rate at which the ORBITER “catches-up” with (or moves away from) the TARGET. Catch-up rate can be controlled by varying the difference in altitude (ΔH) between the ORBITER and TARGET orbits.

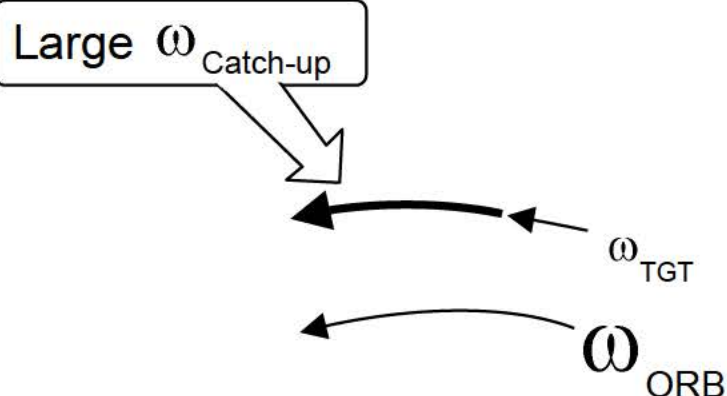
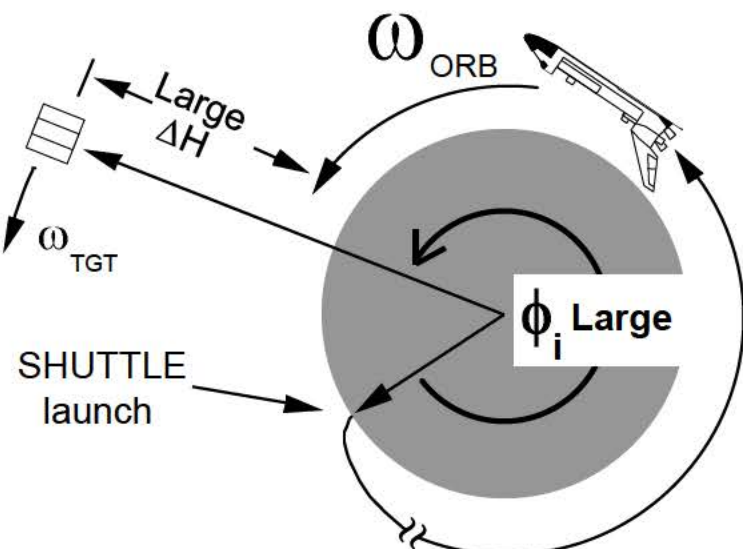


Changes in ΔH are made by performing OMS/RCS burns after orbit insertion. The amount of “phasing” that the ORBITER can accomplish is determined by the desired time of rendezvous and the altitude of the TARGET.

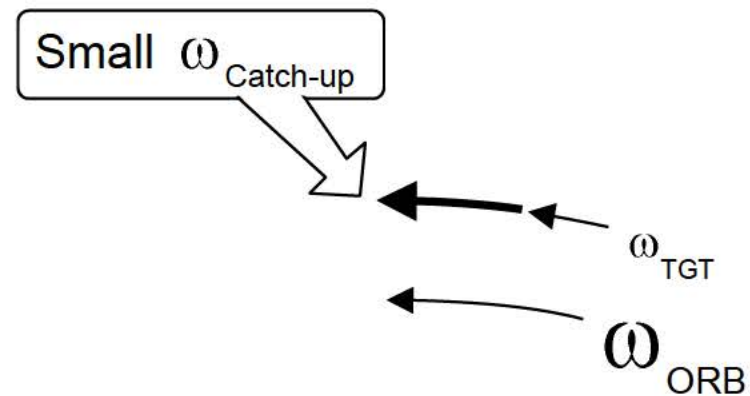
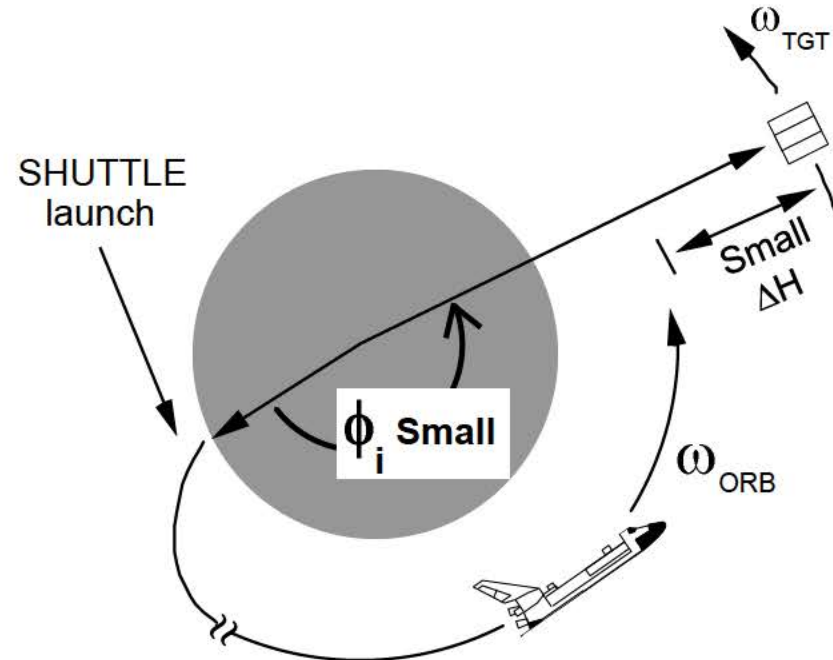
If the TARGET has the ability to change its orbit, and enough propellant is available, it can perform phasing maneuvers in conjunction with the ORBITER (see Control Box Rendezvous).



If the initial phase angle (at launch) is large, the ORBITER will have to stay in a low orbit (large ΔH) to get a high catch-up rate to reduce the phase angle.



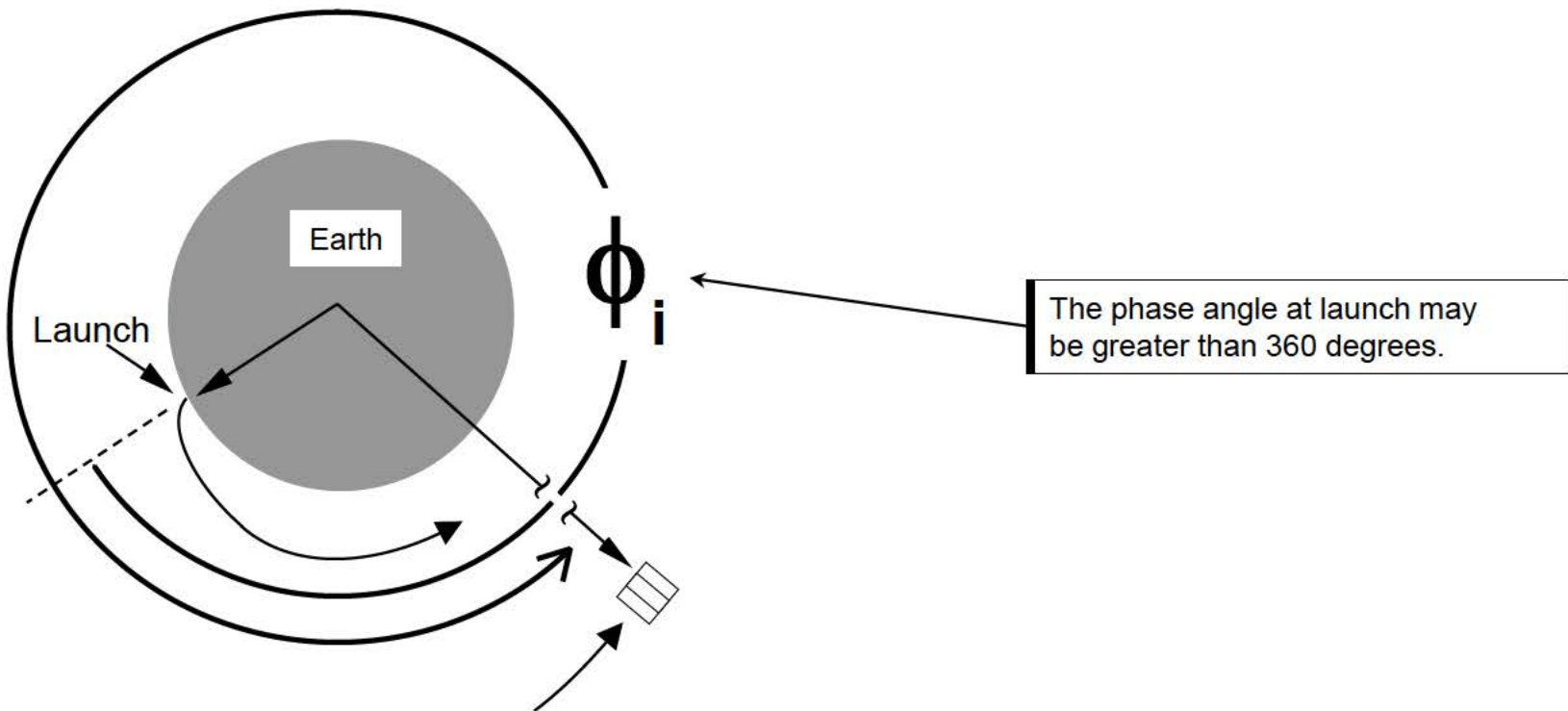
If the initial phase angle (at launch) is small, the ORBITER will fly into a high orbit (small ΔH) to get a low catch-up rate to reduce the phase angle.



The acceptable maximum and minimum phase angles at launch are determined by the phasing capability of the ORBITER (or ORBITER and TARGET if it is a control box rendezvous).

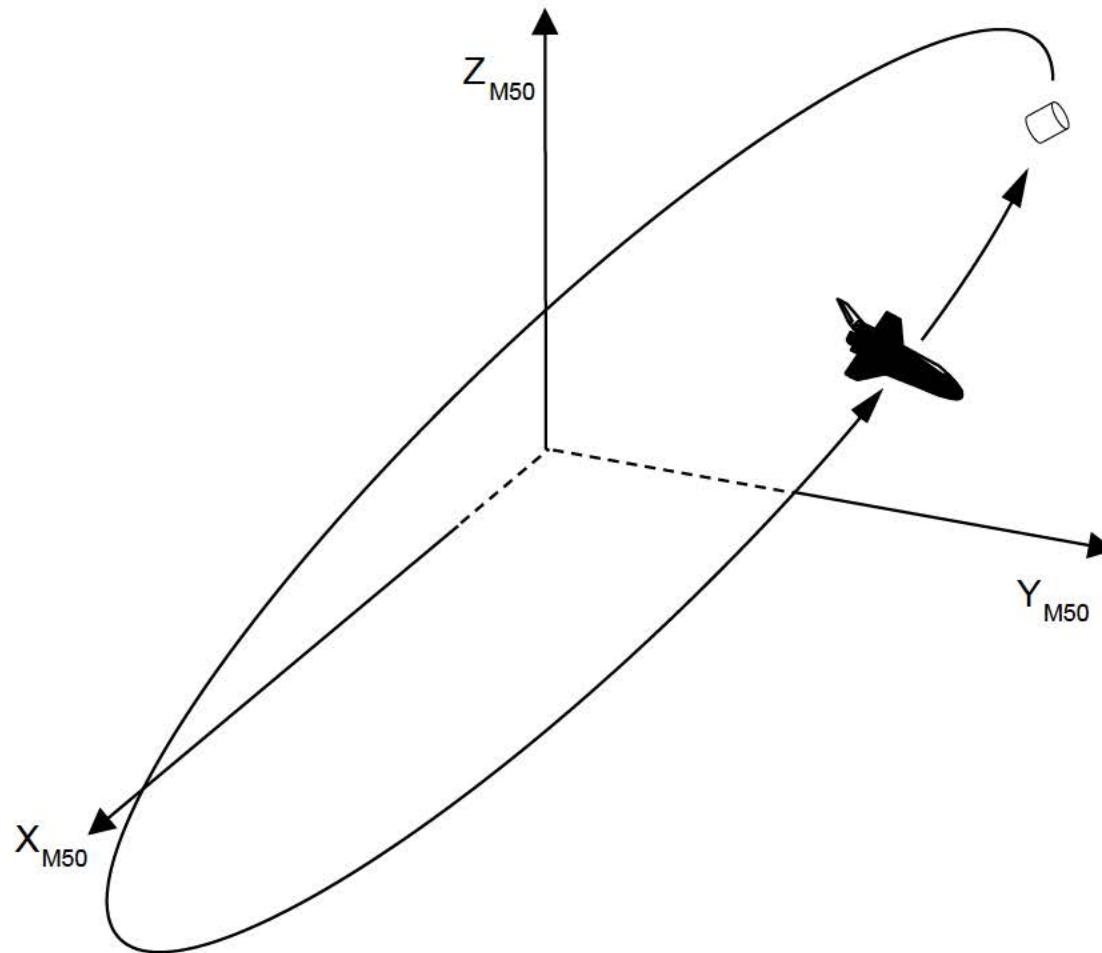
The range of time during which the SHUTTLE can launch and have a phase angle between the minimum and maximum values is called the “phase window.”

It is important to remember that the ORBITER must have a different orbital altitude than the TARGET in order to accomplish phasing.



4.2 Planar Window

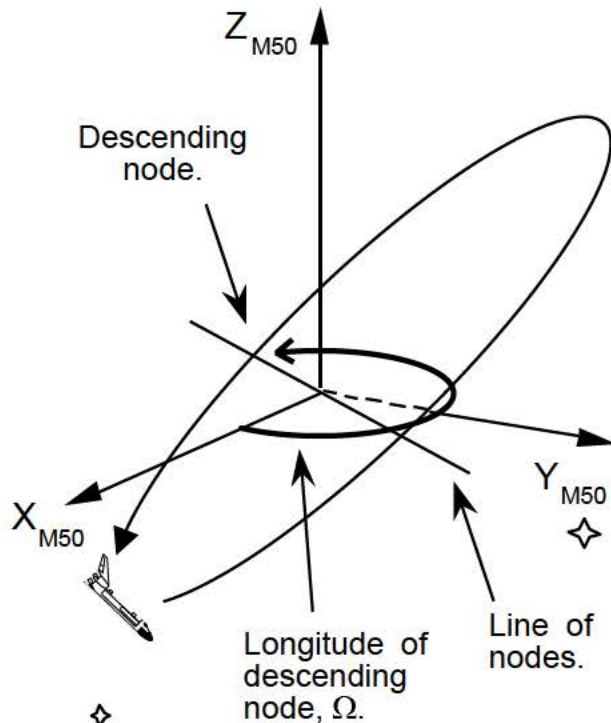
On the day of rendezvous, the ORBITER must be in the orbital plane of the TARGET. The day of rendezvous is usually several days after launch.



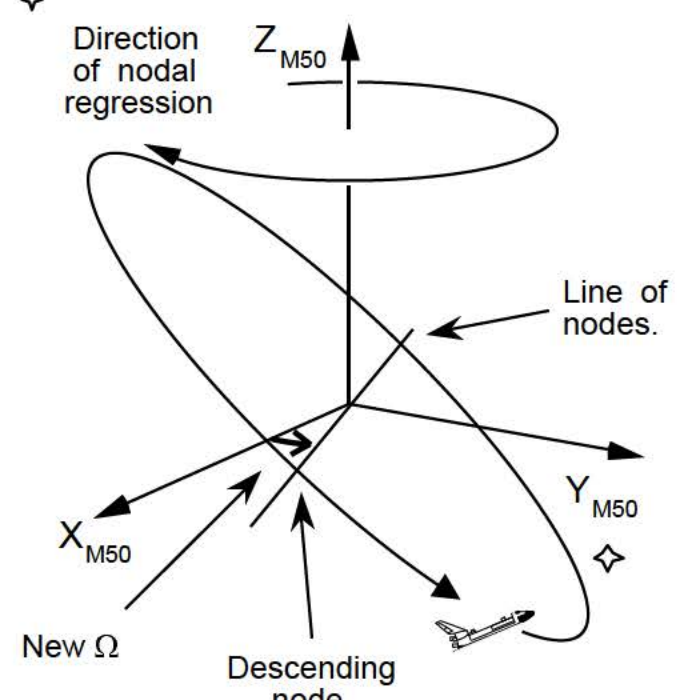
Earth is not a perfect sphere; it has a bulge around the equator. This causes orbital planes of spacecraft to “rotate” in inertial space (with respect to the stars).

A line formed by the intersection of an orbital plane and the M50 X-Y plane is called the “line of nodes.” Rotation of the orbital plane is referred to as nodal regression, since the line of nodes is rotating in inertial space.

The angle between the M50 X axis and the line of nodes (longitude of the descending node, Ω) is constantly changing. For most Shuttle orbits, this angle will change by about 7 to 8 degrees per day.

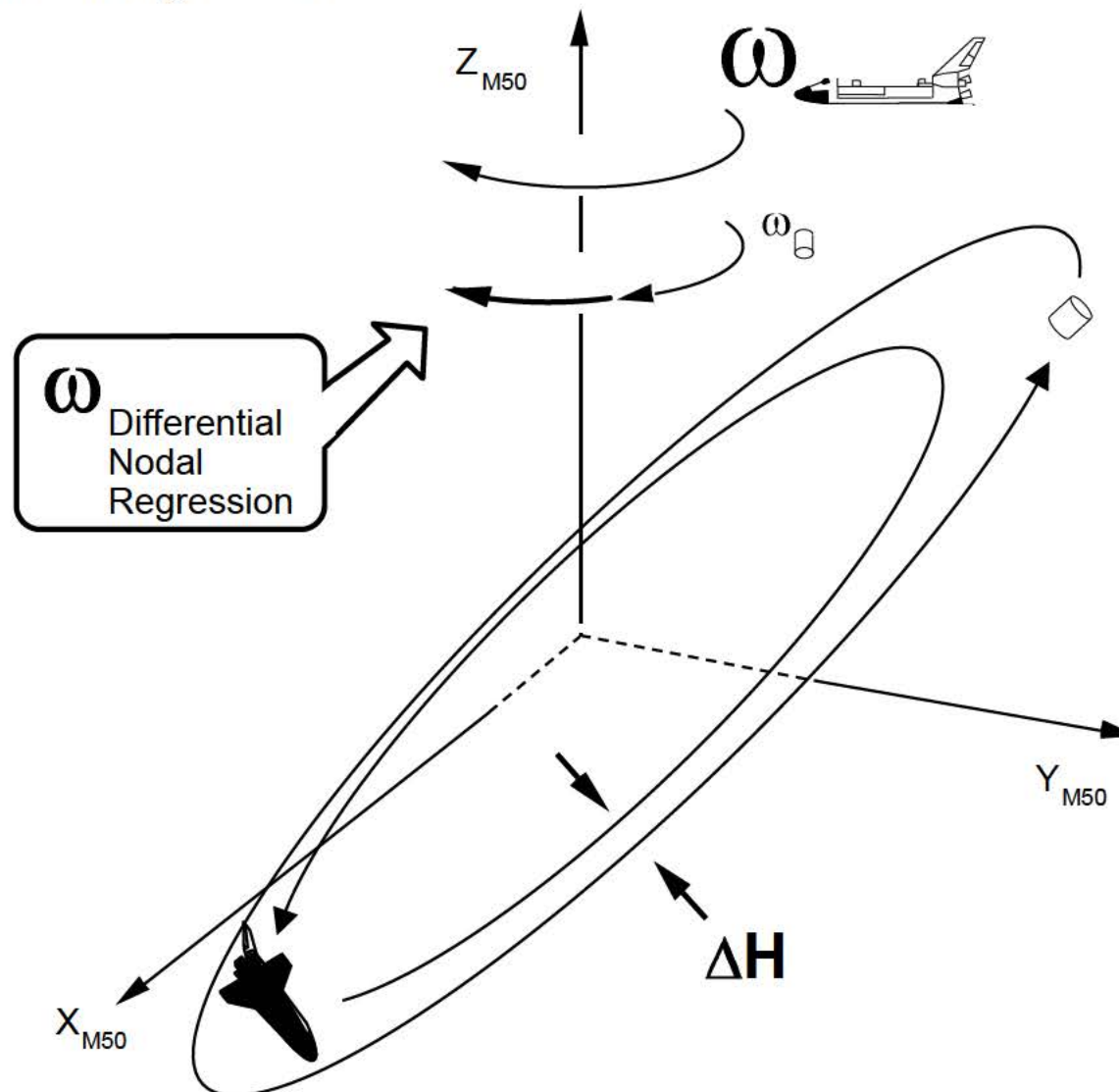


1. Initial orientation of orbital plane.

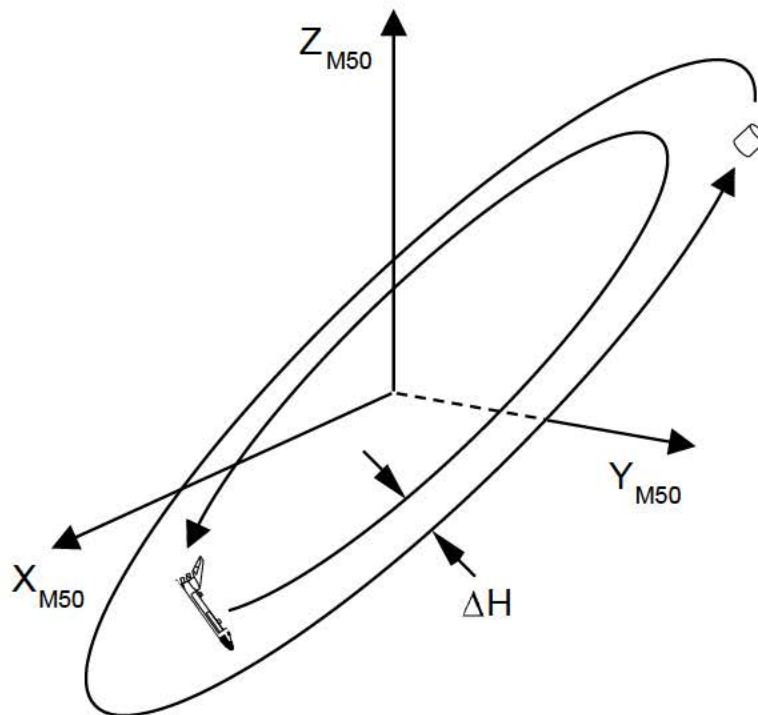


2. Later orientation of orbital plane due to nodal regression.

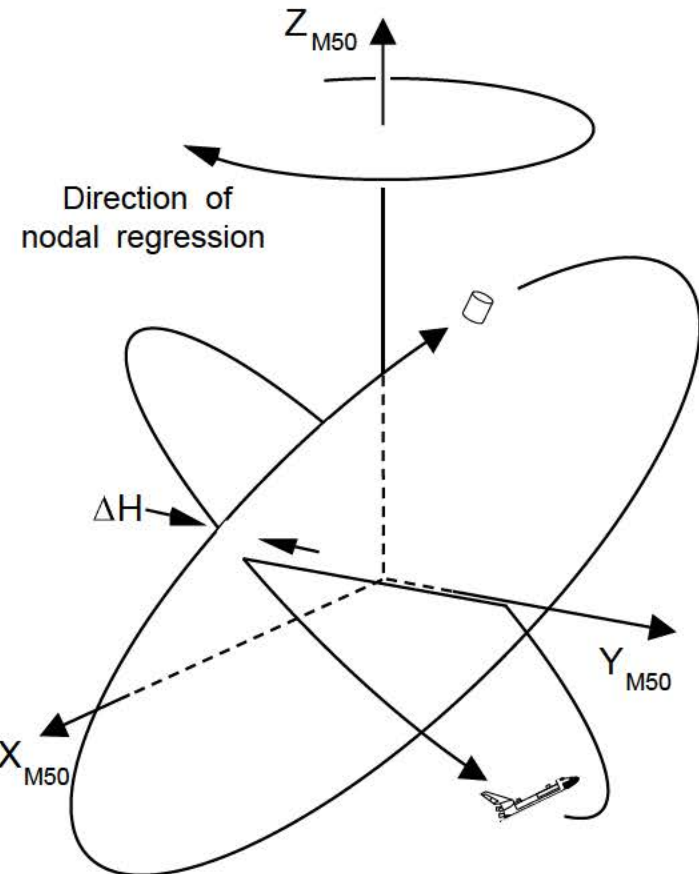
Nodal regression rate varies with altitude and inclination. The higher the orbit, the smaller the rotation rate. If the ORBITER is in a lower orbit than the TARGET, the ORBITER's orbital plane will rotate about the Z axis faster than the orbital plane of the TARGET. The difference in the nodal regression rates of the orbital planes is called the “differential nodal regression” rate.



To accomplish phasing, the ORBITER must be at a different altitude than the TARGET. If the ORBITER were launched into the orbital plane of the TARGET, it would eventually “regress” out of it due to differential nodal regression resulting from ΔH .



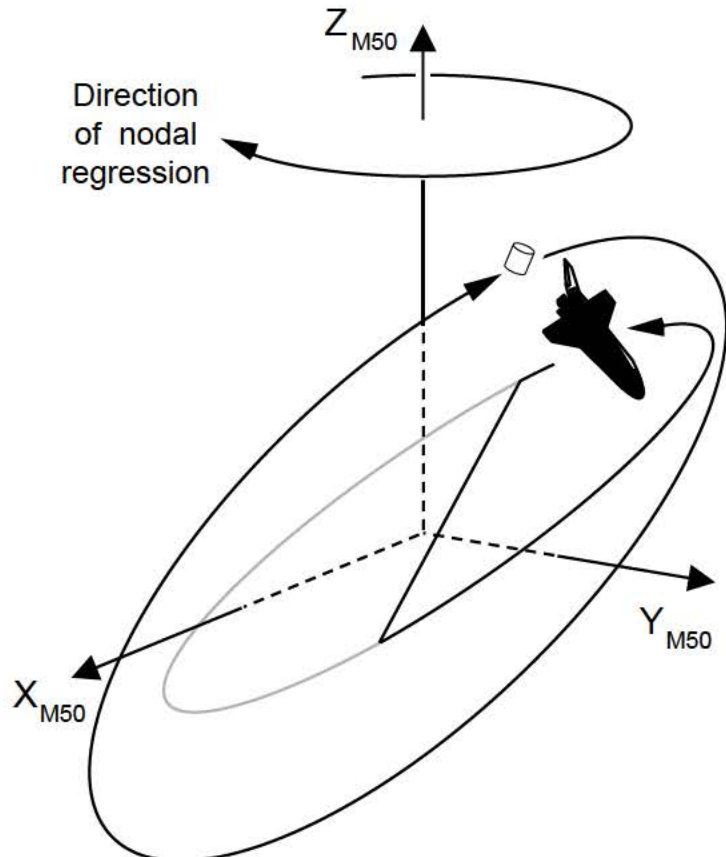
1. ORBITER and TARGET in the same orbital plane, but at different altitudes.



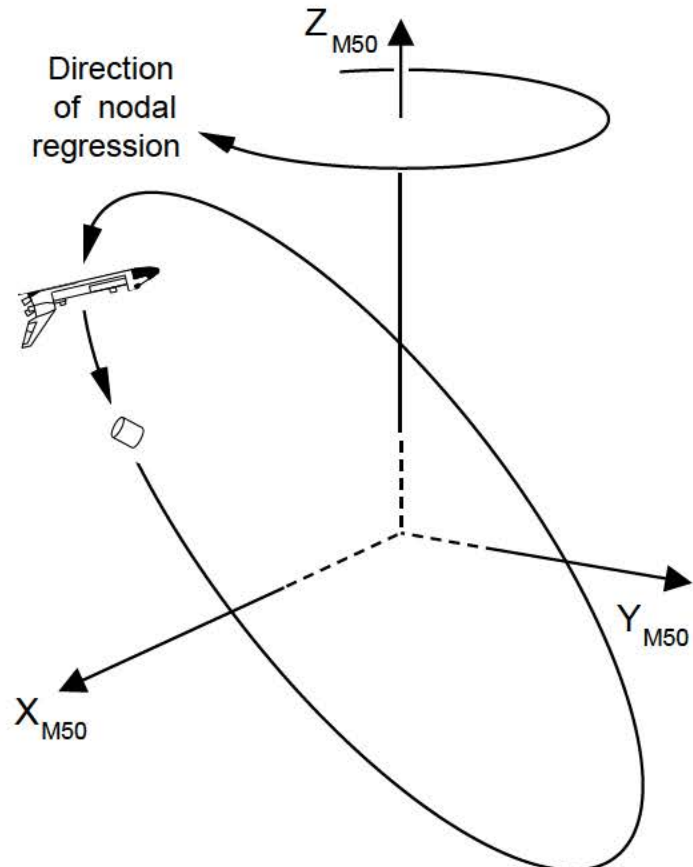
2. Differential nodal regression due to ΔH causes ORBITER to regress out of TARGET's orbital plane.

To compensate for differential nodal regression, the ORBITER is launched into a “phantom plane.” This phantom plane is designed so that it will “regress into” the orbital plane of the TARGET on the day of rendezvous.

It is important to remember that the ORBITER is not launched into the TARGET's orbital plane.



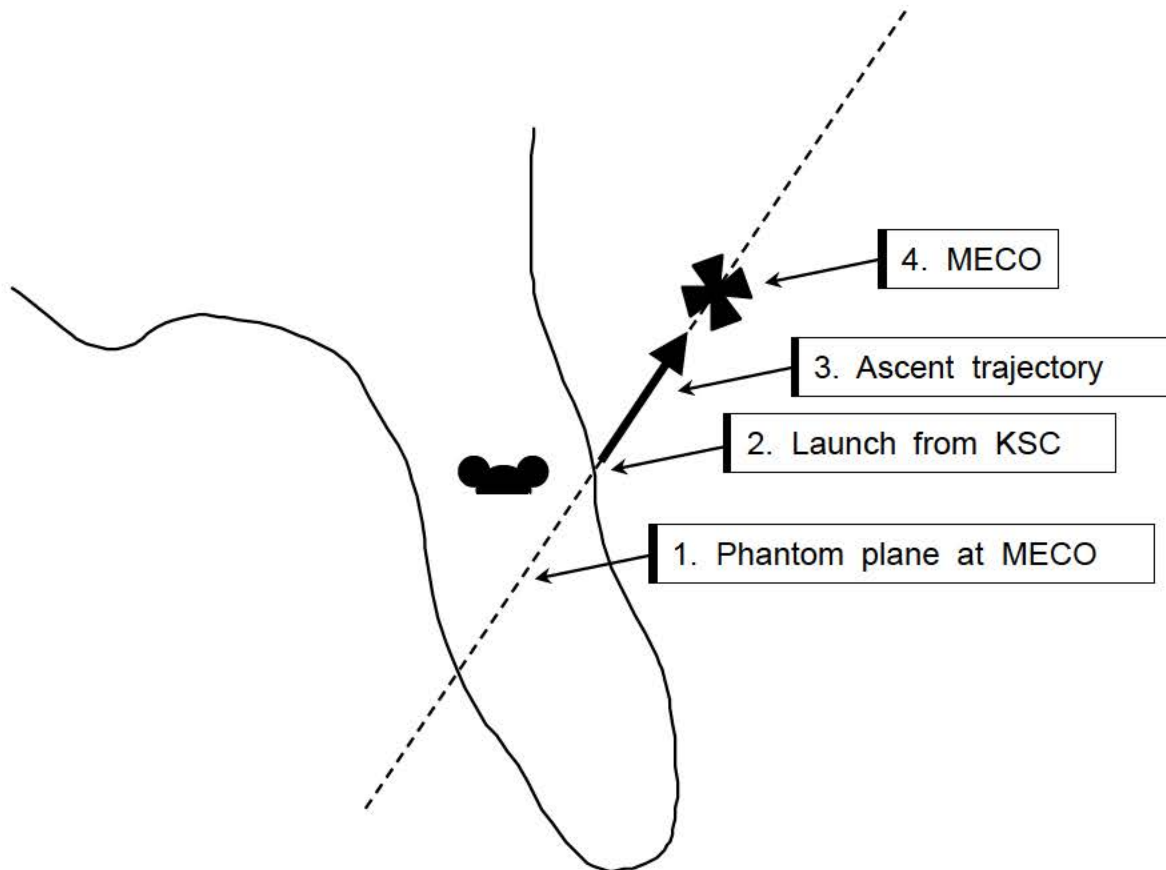
1. ORBITER is launched into phantom plane.



2. Phantom plane “regresses into”
TARGET orbital plane on day
of rendezvous.

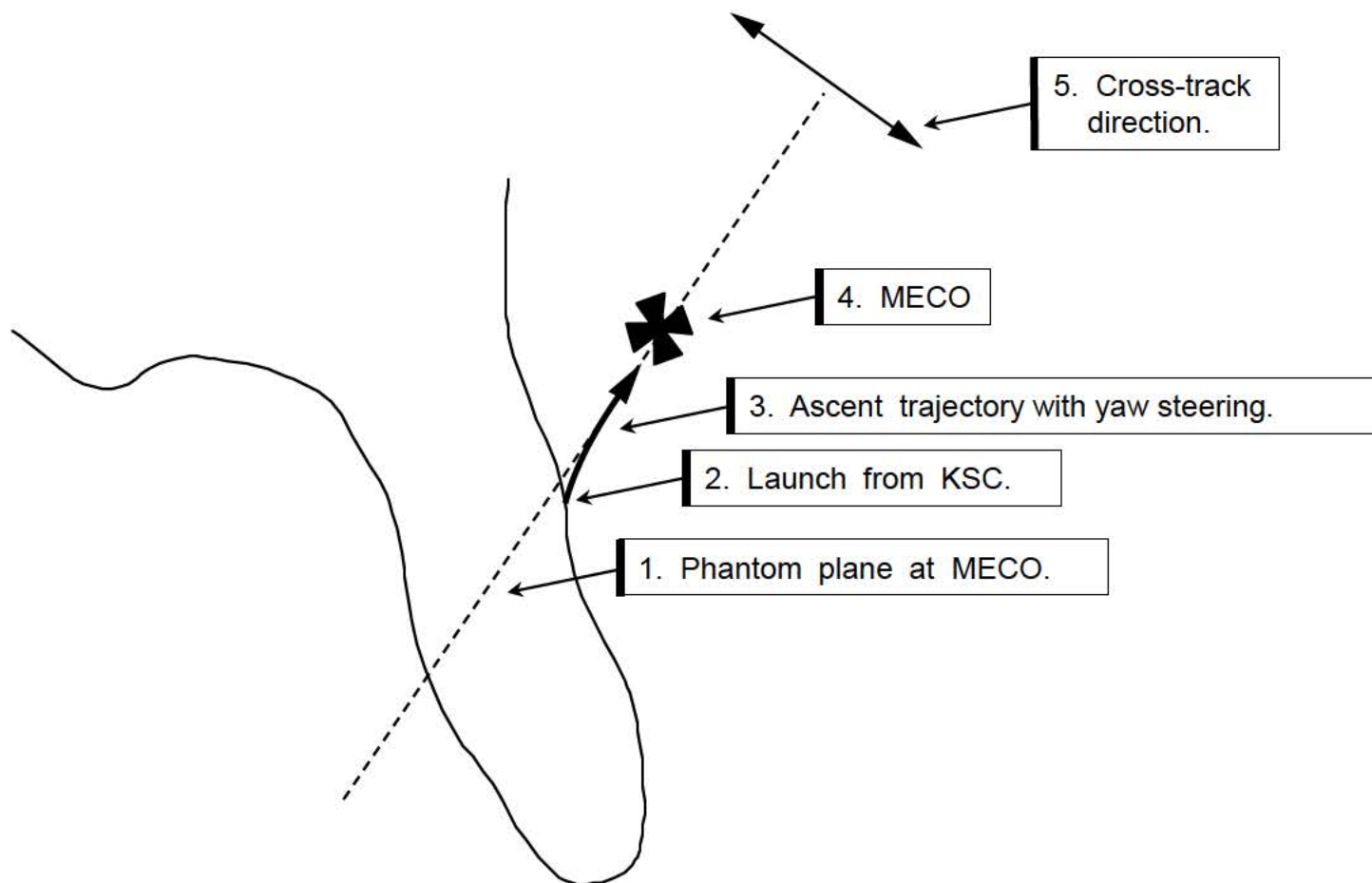
The time at which the phantom plane passes directly over the launch site is called the “in-plane time.”

If lift-off is timed so that Main Engine Cut-Off (MECO) occurs at the in-plane time, propellant used during second stage is minimized since it is used only to achieve the desired velocity and altitude at MECO.



In reality, it is impossible to guarantee that the SHUTTLE will be able to lift-off so that MECO will occur at the in-plane time. If this condition is not met, the SHUTTLE has to use some of the propellant in the External Tank to steer in the “cross-track” direction (see “5” below). This is referred to as “yaw steering.”

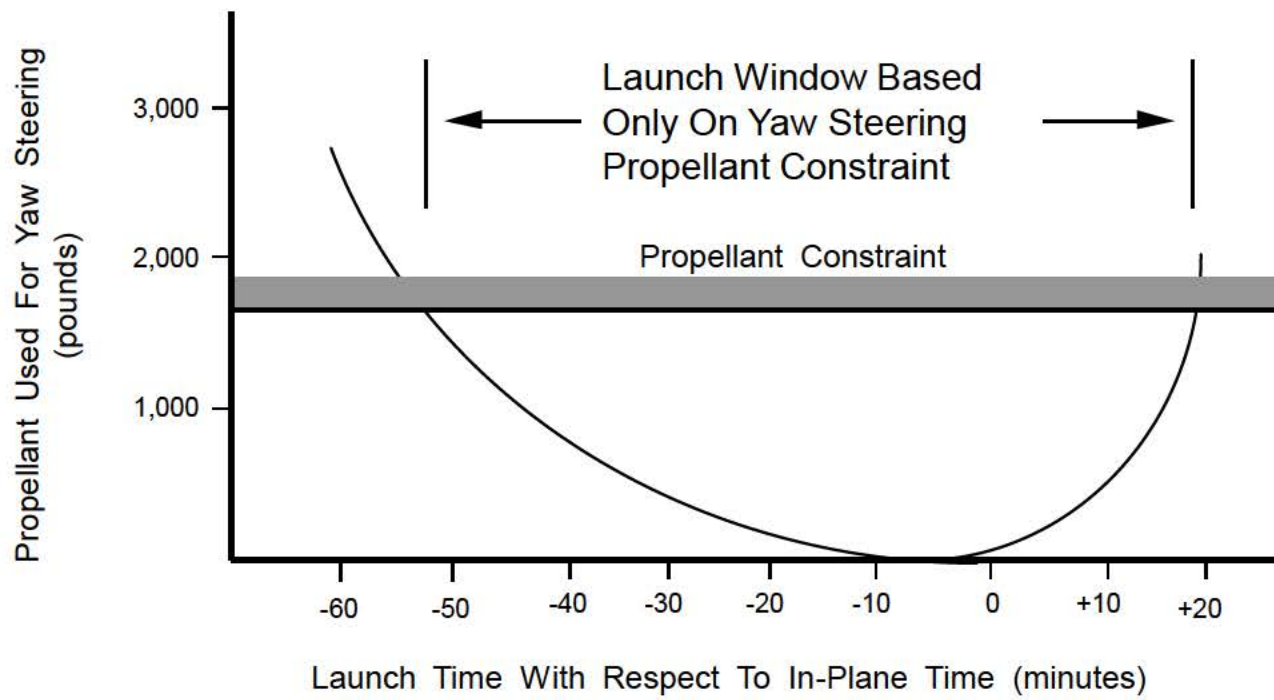
Yaw steering reduces the amount of propellant available to achieve the desired altitude and velocity at MECO.



A limited amount of SSME propellant is available for yaw steering. The actual amount used depends on how much yaw steering has to be performed. As the time between lift-off and the in-plane time increases, the amount of propellant needed for yaw steering increases.

The SHUTTLE must launch within a certain time period in order to minimize propellant consumed for yaw steering. The maximum amount of propellant that can be used for yaw steering is the “propellant constraint.”

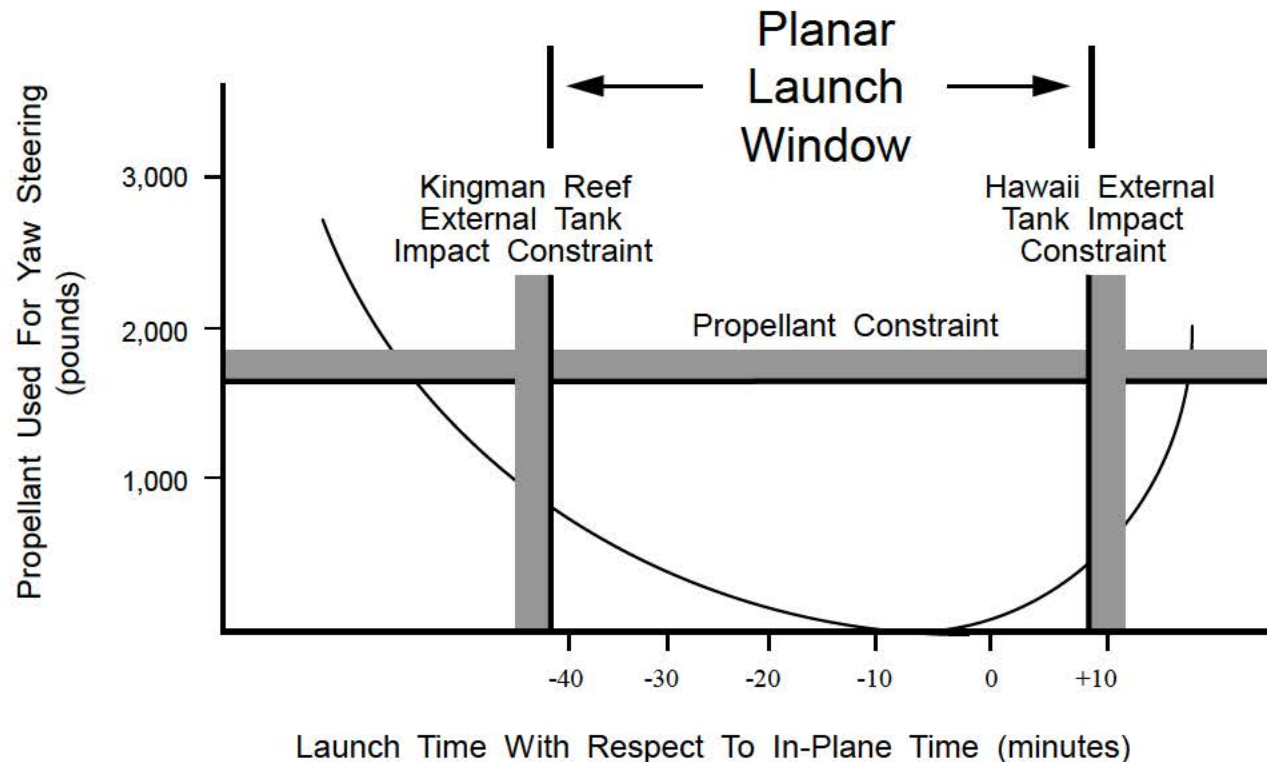
Propellant consumed by yaw steering is plotted against time with respect to the in-plane time. The propellant constraint can be superimposed on the plot to illustrate a launch window based only on propellant available for yaw steering.



The orientation of the orbital plane at MECO (longitude of descending node) depends on the time of launch. Changing the longitude of the descending node changes the area on the Earth's surface where debris resulting from External Tank break-up may impact. This area of possible impact is called a "footprint."

Mission rules exist that control how close the footprint can come to a landmass. In order to keep the ET footprint away from any landmasses, additional constraints are placed on the time of launch.

ET impact constraints and the yaw steering propellant constraint together determine the planar launch window.



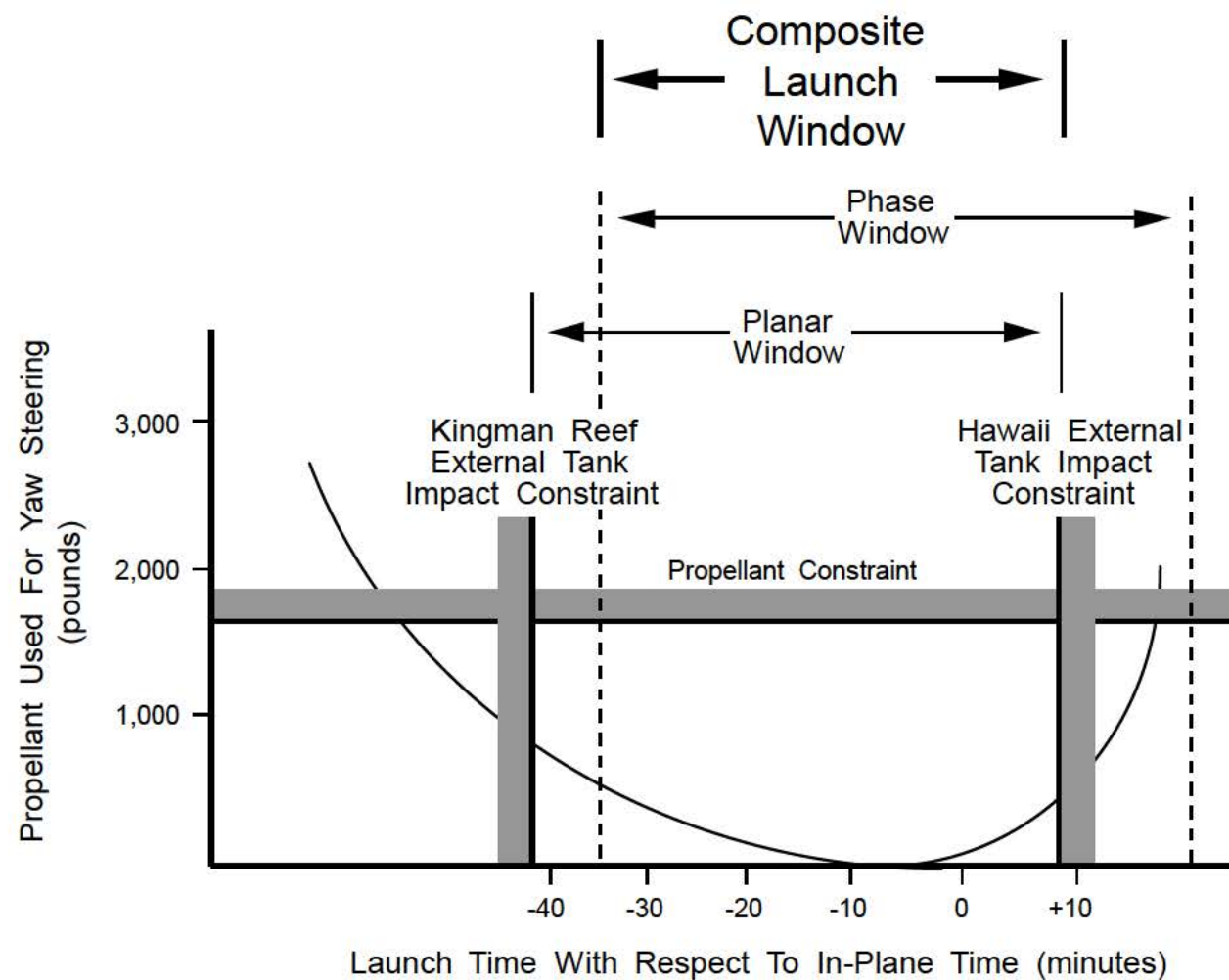
4.3 Composite Launch Window

The phase and planar windows together form the “composite” launch window.

$$\text{Composite Launch Window} = \text{Phase Window} + \text{Planar Window}$$

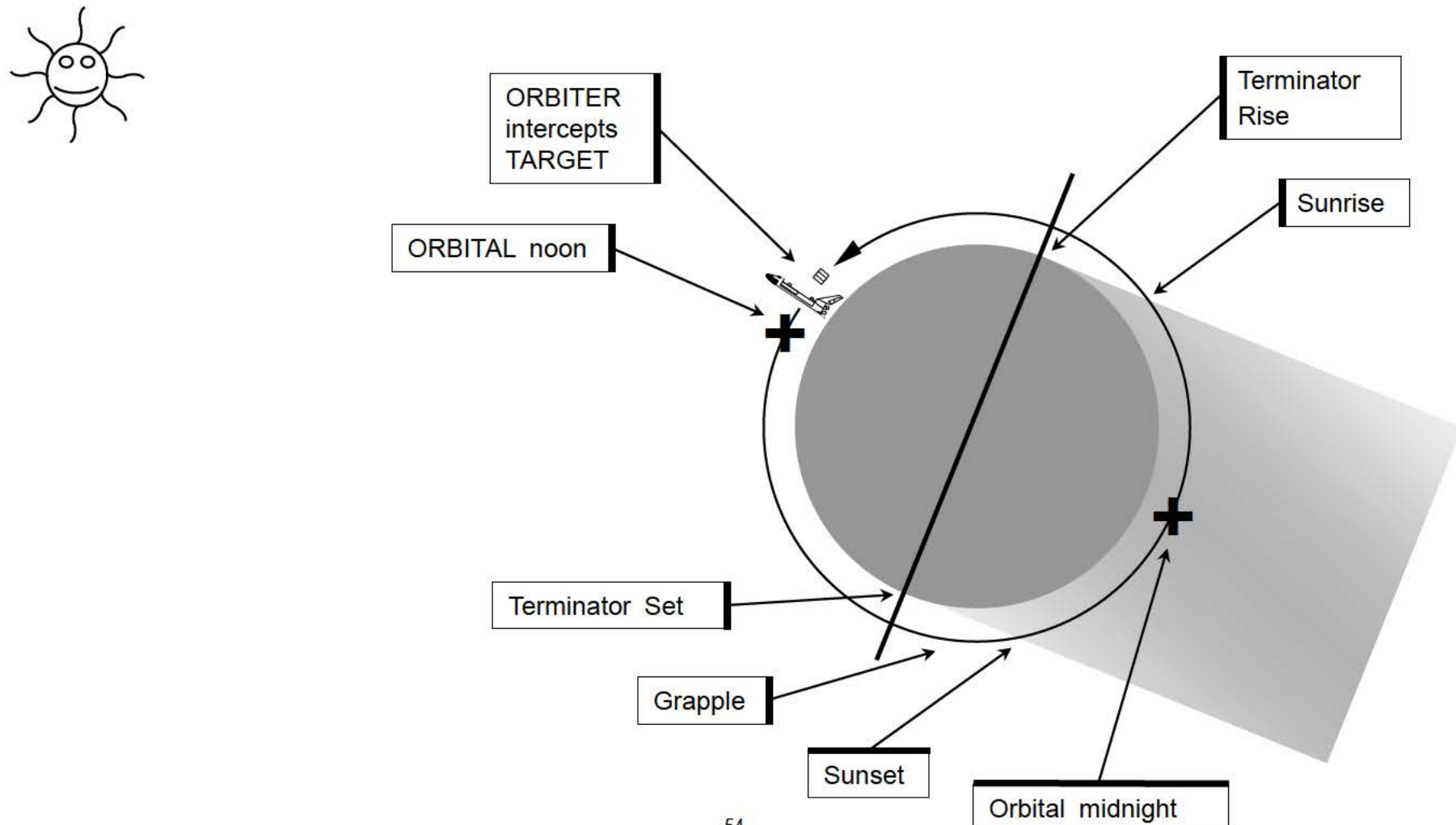
The phase window can be superimposed on the yaw steering propellant plot to illustrate the composite window.

On non-ground-up rendezvous missions, the primary constraint on the launch window is lighting at the nominal end-of-mission and abort landing sites. Landing lighting constraints are ignored for ground-up rendezvous. It would be very difficult or impossible to satisfy planar, phasing, and landing lighting constraints at the same time.

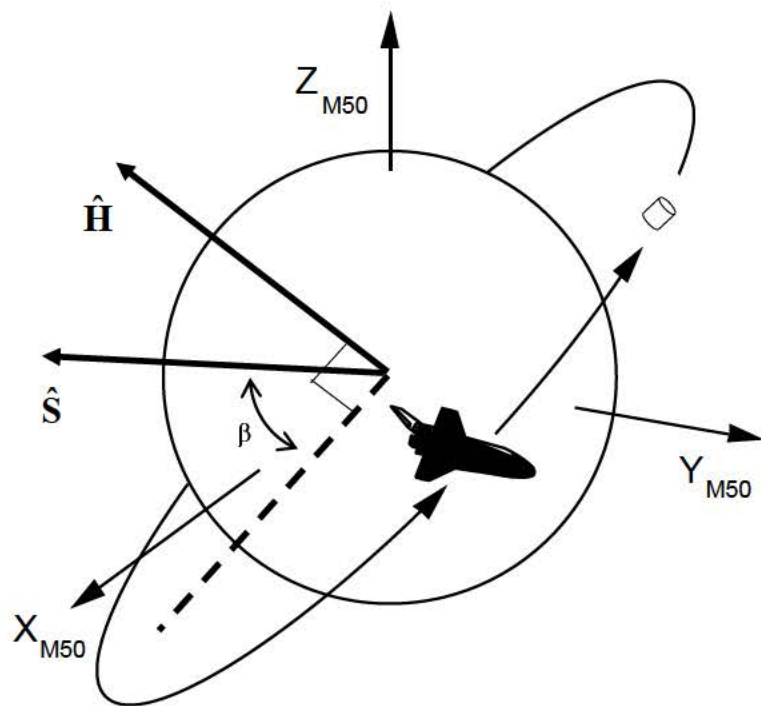
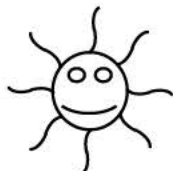


4.4 Other Constraints

Burns executed once on-orbit ensure that lighting requirements are met. The TARGET must be illuminated by sunlight during the final phase of the intercept. TARGET illumination by sunlight is also needed when the ORBITER's star tracker is used to track the TARGET.



Solar beta (β) angle is used in discussions of orbital lighting. It is the complement of the angle between the orbital plane and the solar vector. β is positive if the sun is “north” of the orbital plane, negative if it is “south” of the orbital plane. β angle is important for determining sunlight impact on crew “out the window” piloting tasks and Shuttle tile inspection requirements. The amount of sunlight for a given orbit is a function of β angle, orbital inclination and altitude. β and the amount of sunlight over an orbit will change over the course of a mission.



$$\beta = \sin^{-1} \hat{\mathbf{H}} \cdot \hat{\mathbf{S}}$$

$$\hat{\mathbf{H}} = \frac{\vec{\mathbf{R}} \times \vec{\mathbf{V}}}{|\vec{\mathbf{R}} \times \vec{\mathbf{V}}|}$$

$\hat{\mathbf{S}} \equiv$ Solar Unit Vector

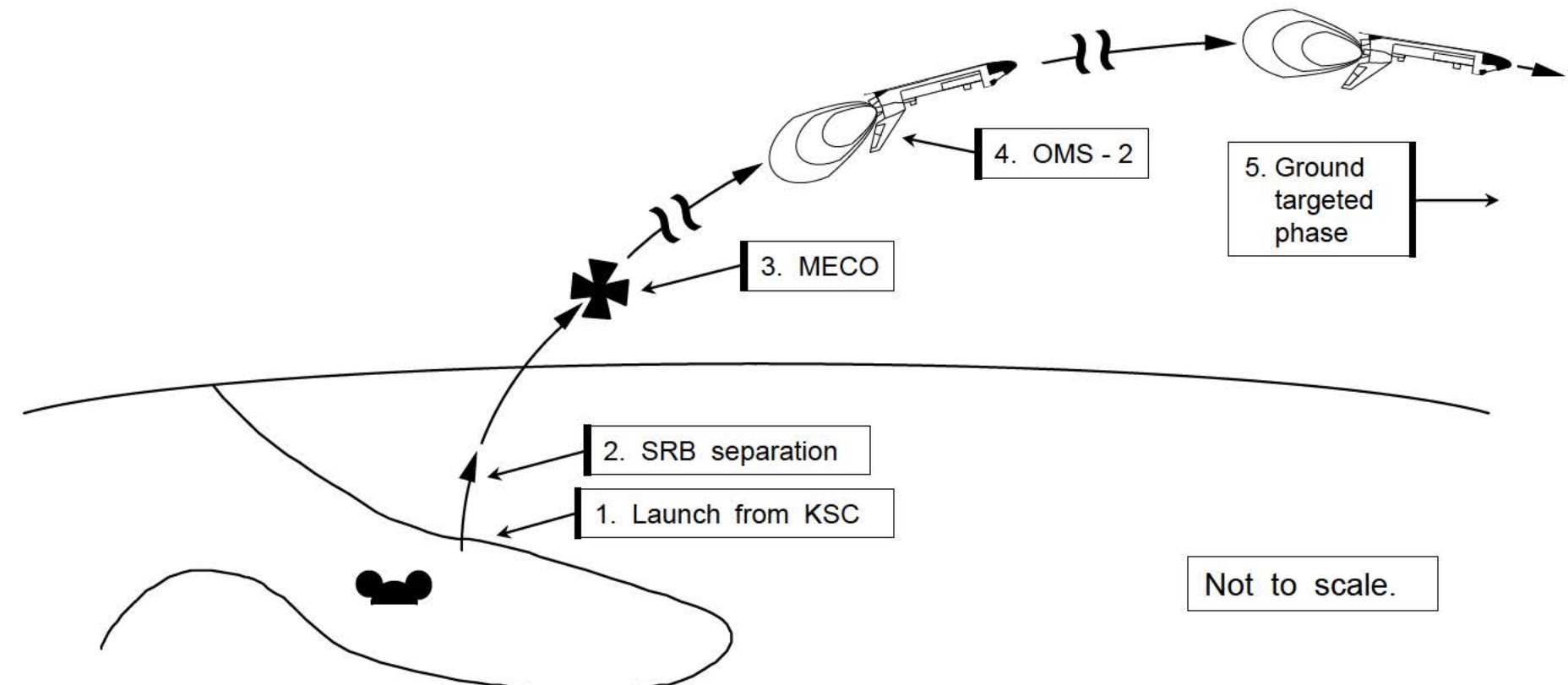
$\hat{\mathbf{H}} \equiv$ Angular Momentum
Unit Vector

Orbital lighting during the final approach to the TARGET is just one of many constraints that have to be satisfied by the burns. The burns, and the rendezvous trajectory as a whole, are designed to meet these constraints. Other constraints include:

- Propellant and non-propulsive consumables available for the mission.
- Effect of atmospheric drag on relative motion.
- Trajectory dispersions due to poor navigation or burn performance.
- Payload and experiment requirements.
- Length of the mission.
- Activities to be executed by the crew.
- Visibility of ORBITER and TARGET to ground tracking stations.
- Ability to complete mission objectives and/or safely return the ORBITER to Earth in the event of system failures on the ORBITER, TARGET or ground.

5.0 Ascent, OMS-2, and the Ground Targeted Phase

Ascent, OMS-2, and burns executed during the ground targeted phase are designed to enable the ORBITER to rendezvous with the TARGET at a designated time.



5.1 Ascent

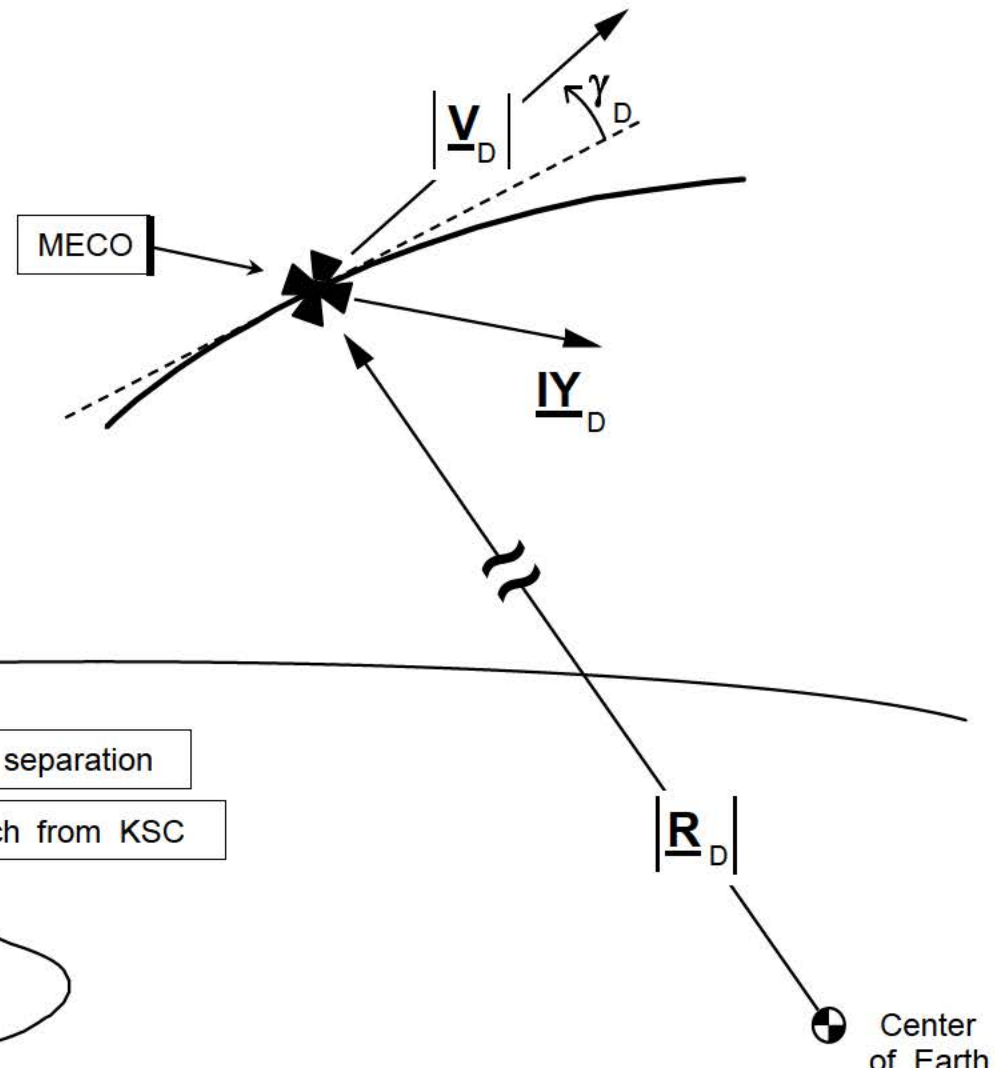
Second stage ascent guidance (PEG 1) is active from SRB separation to Main Engine Cut-Off (MECO). PEG 1 flies the SHUTTLE so that the following 4 desired (D) conditions are achieved at MECO. These "MECO targets" are ILOADED into the Flight Software. MECO targets may also be uplinked prior to launch.

$|R_D|$ Inertial position magnitude

$|V_D|$ Inertial velocity magnitude

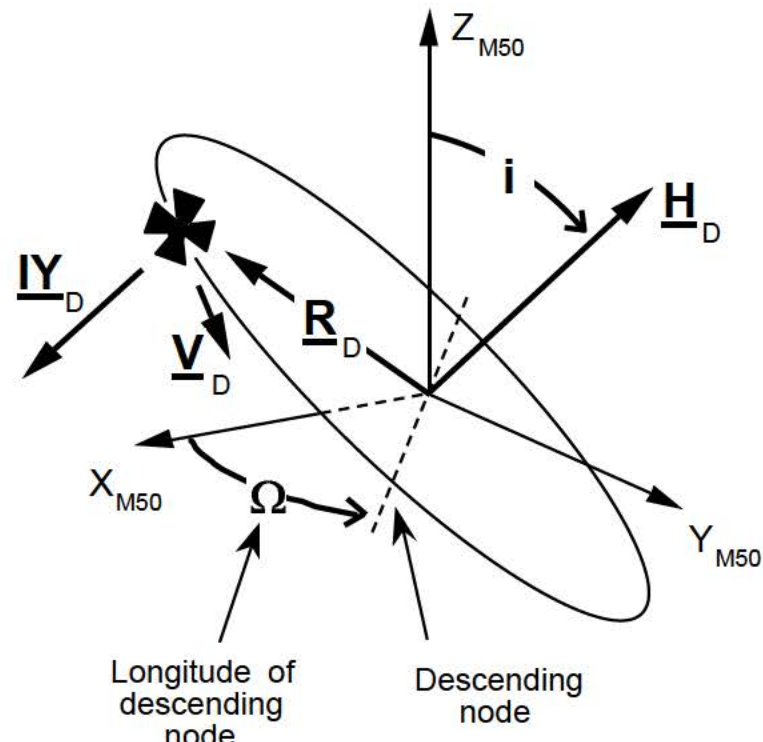
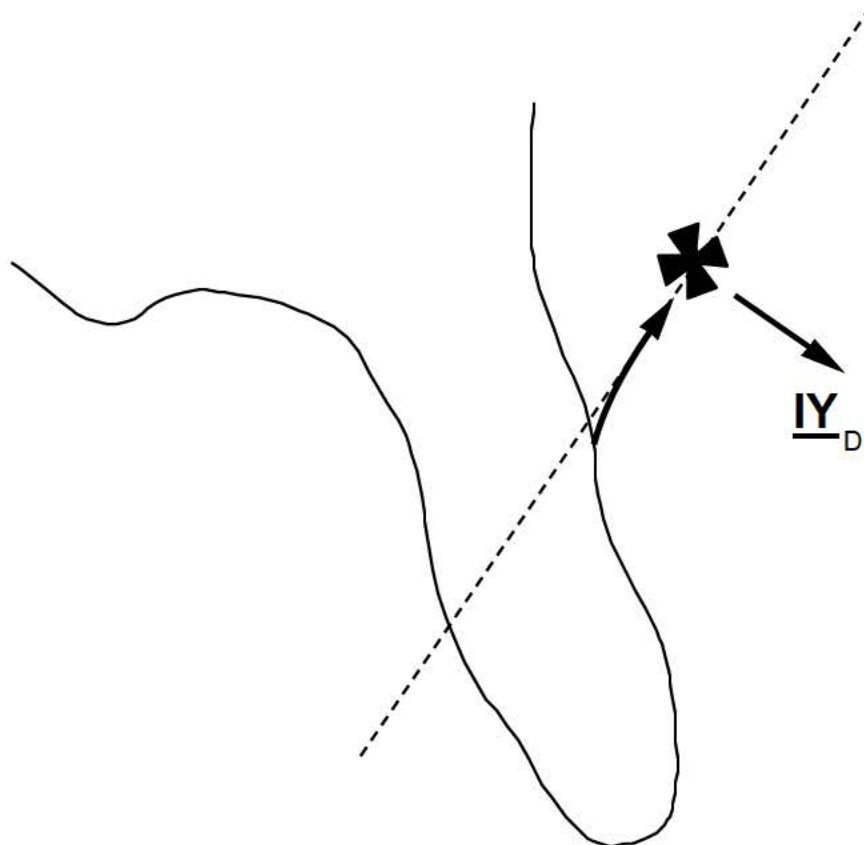
g_D Inertial flight path angle

$$IY_D = - \text{Unit} (R_D \times V_D)$$

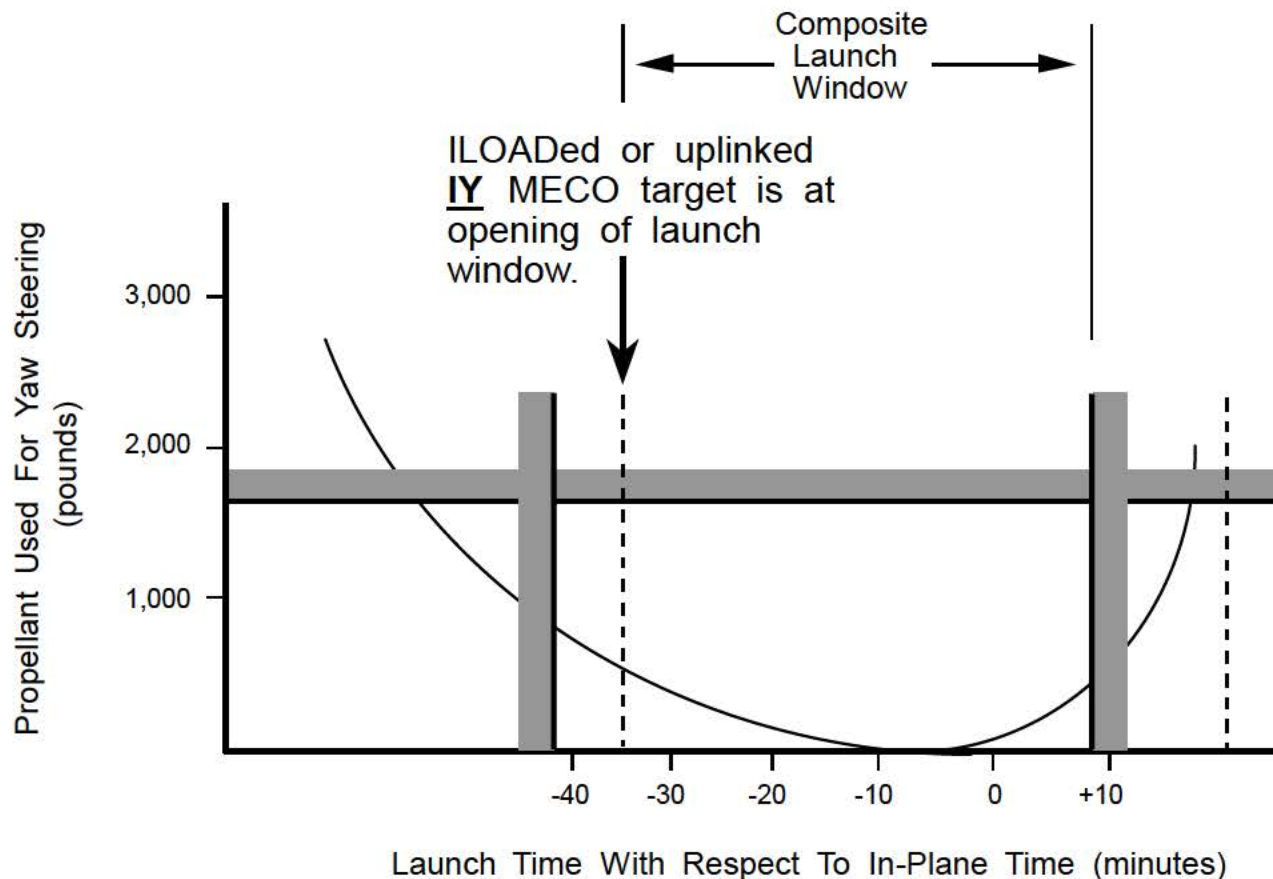


$\underline{\text{IY}}$ (the unitized negative of the angular momentum vector) defines the orbital plane that the ORBITER is to have at MECO. For a ground-up rendezvous, this is the phantom plane. **$\underline{\text{IY}}$** determines how the orbital plane is to be oriented in inertial space (inclination angle, i , and the longitude of the descending node, Ω).

$$\underline{\text{IY}}_D = - \text{Unit}(\underline{\text{R}}_D \times \underline{\text{V}}_D) = - \text{Unit}(\underline{\text{H}}_D)$$

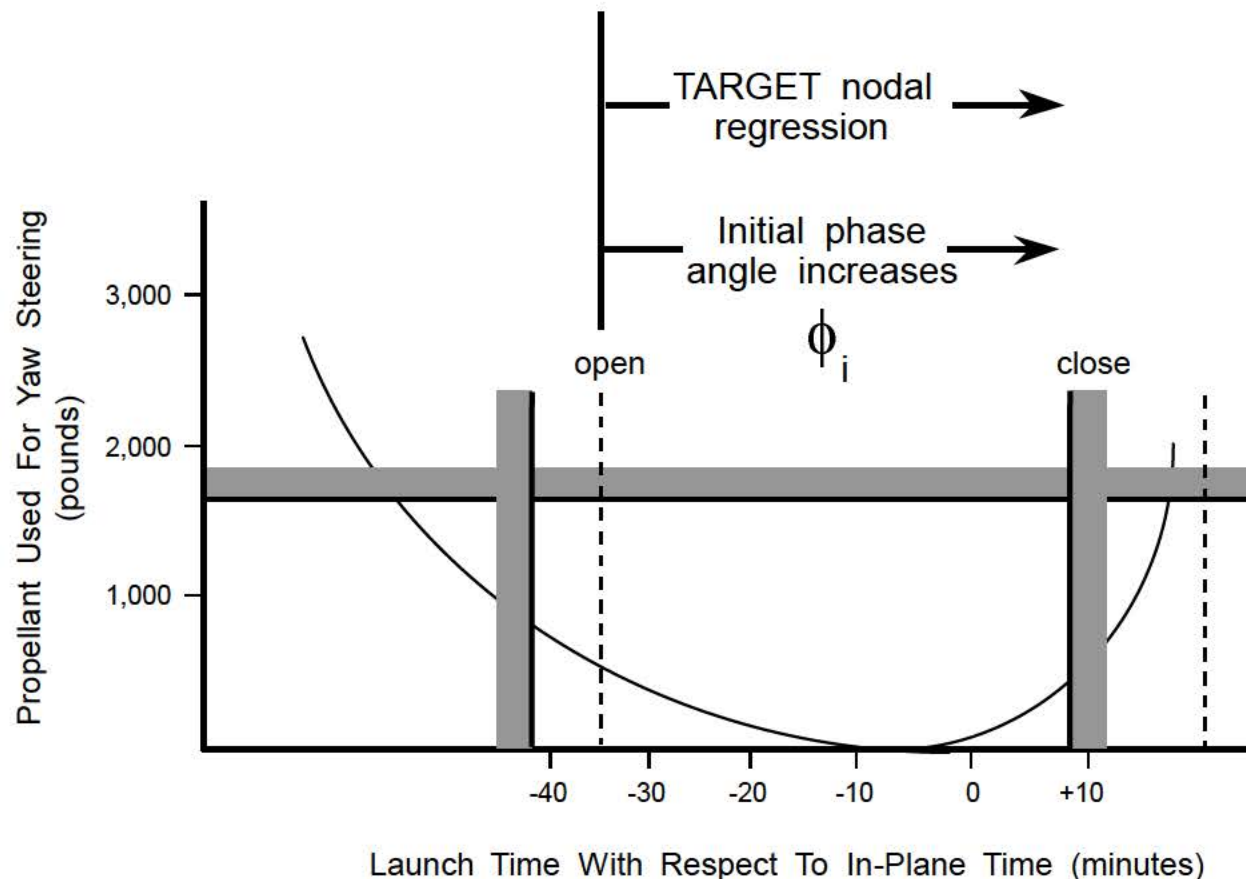


The **IY** MECO target that is ILOADED (or computed by the Flight Dynamics Officer and uplinked on launch day prior to lift - off) defines the desired phantom plane at the opening of the launch window.

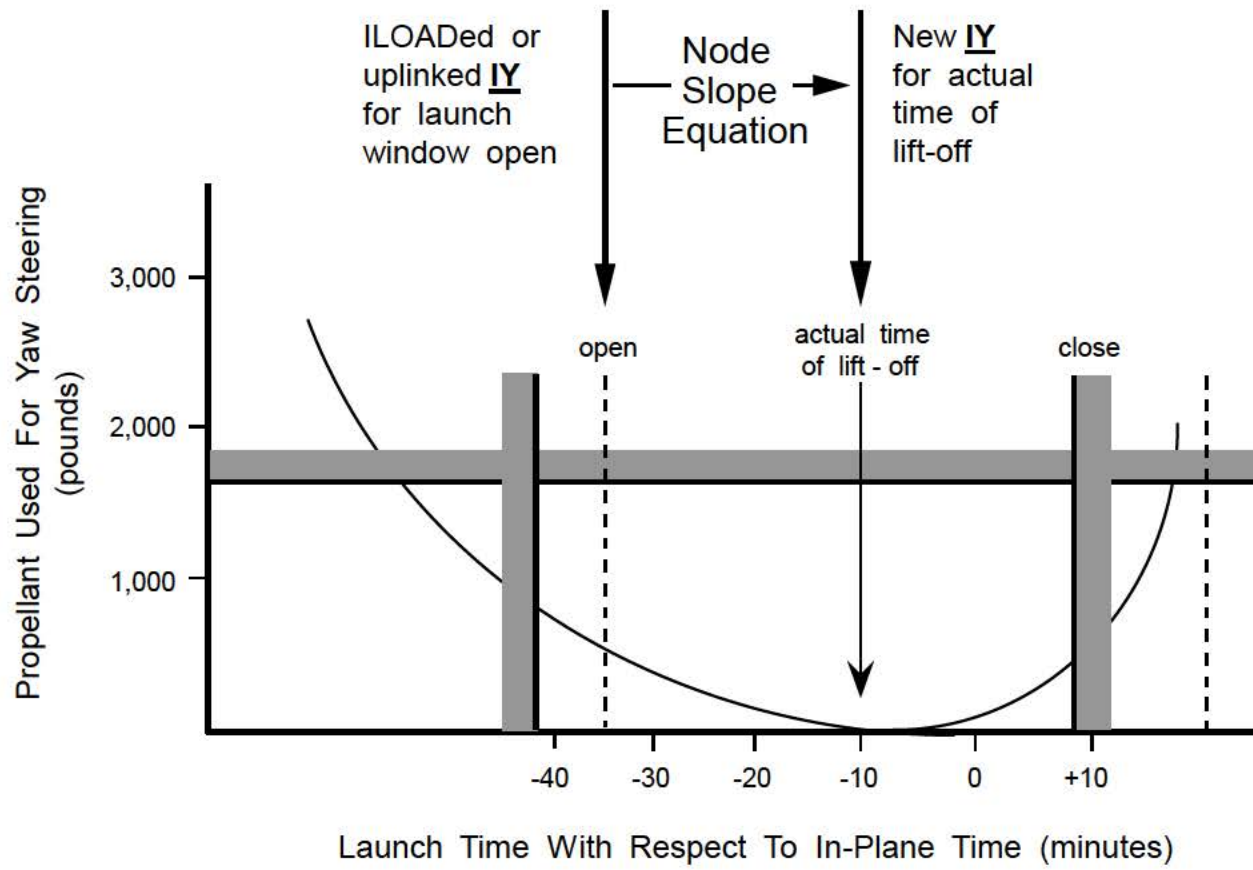


The ILOADED (or uplinked **IY**) target is computed based on the initial phase angle (φ) at the opening of the launch window. If lift-off is delayed to some later point in the launch window, the initial phase angle will be different. This will change the ΔH the ORBITER must achieve for phasing, which in turn will change the differential nodal regression rate between the orbital planes of the TARGET and ORBITER.

This change in phase angle, coupled with nodal regression of the TARGET's orbital plane during the launch window, changes the phantom plane that the ORBITER must achieve at MECO. The ILOADED (or uplinked) **IY** target is only valid for lift-off at the opening of the launch window. A new **IY** target must be computed for the actual lift-off time.

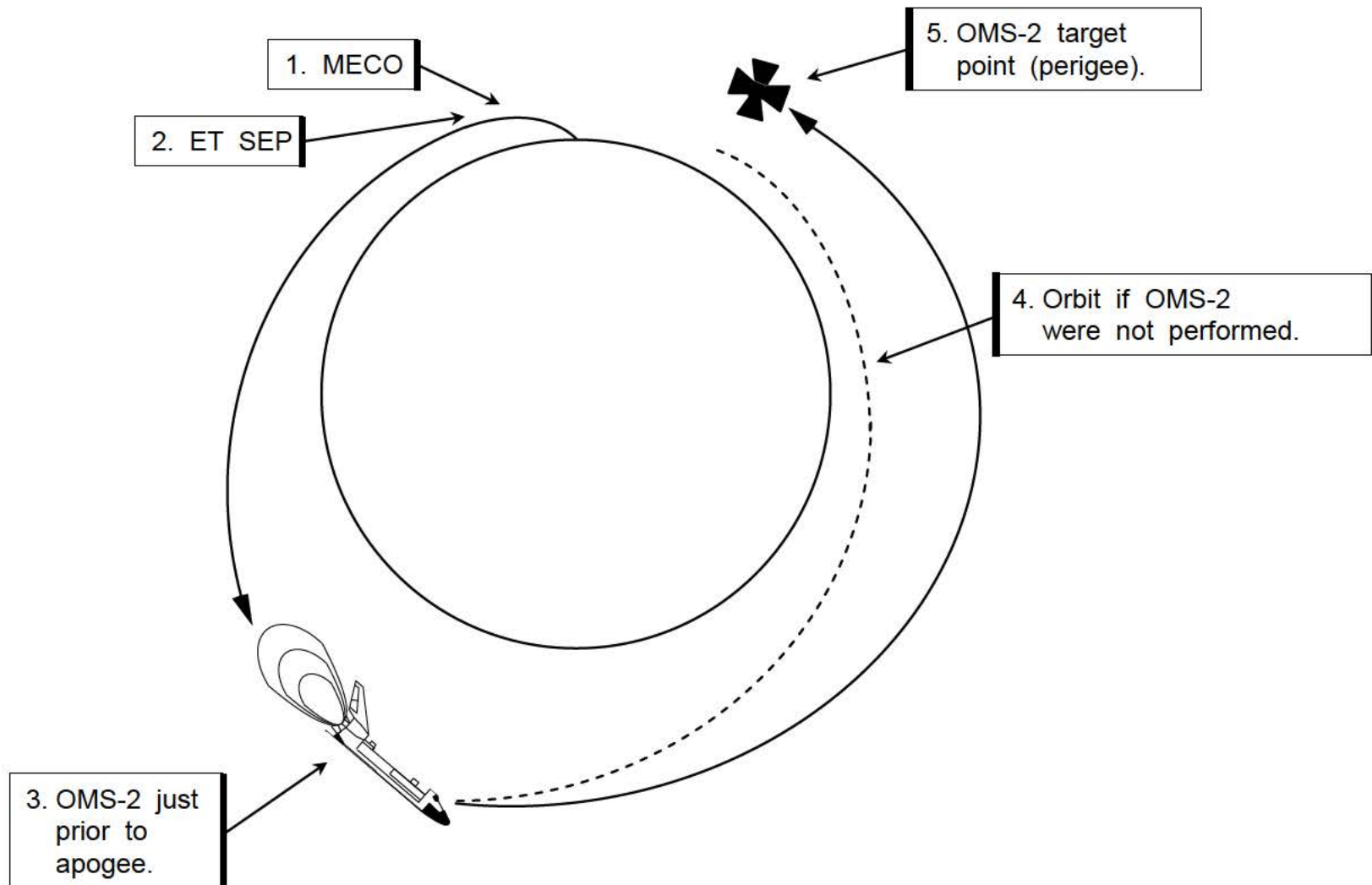


At SRB ignition, the node slope equation in ascent User Parameter Processing (UPP) computes a new IY target. This equation takes into account the change in initial phase angle and TARGET nodal regression between the opening of the launch window and the actual lift-off time.



5.2 OMS-2 Burn

After MECO, the ORBITER is in a highly elliptical orbit. Just prior to apogee, the OMS-2 maneuver is executed to raise the ORBITER's perigee. The post OMS-2 orbit could be either circular or elliptical.



Orbit insertion guidance (PEG 4) targets an OMS burn so that the ORBITER will have a certain horizontal/vertical velocity relationship ($Vv = C2 [Vh] + C1$) at a given target point. This point is defined by altitude above the surface of the Earth (**HT**) and the angle between KSC and the target point (**OT**).

OMS-2 normally targets for a perigee point. Since the vertical velocity is zero at perigee, **C1** and **C2** are set to zero.

PEG 4 Targets

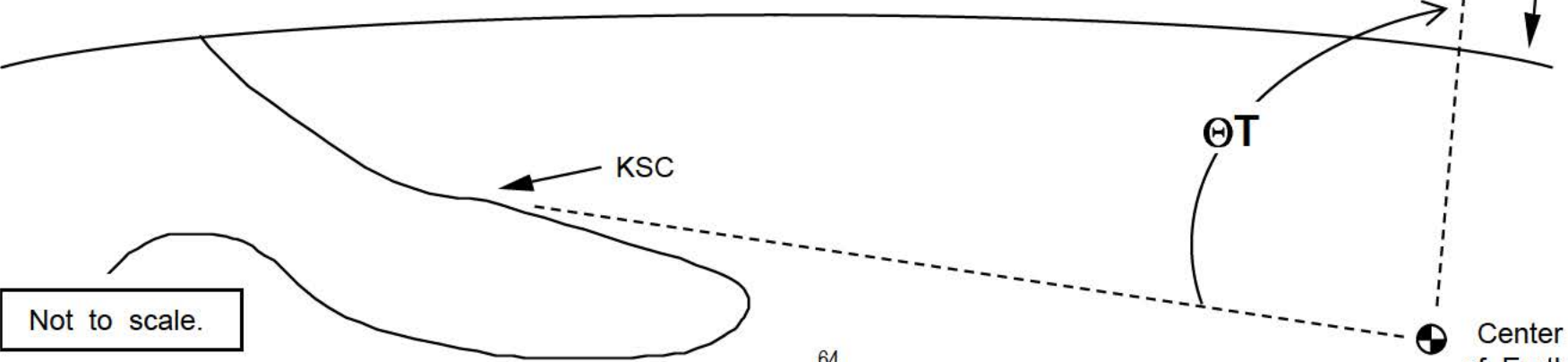
TIG Time of OMS-2 ignition.

OT Angle between KSC and target point.

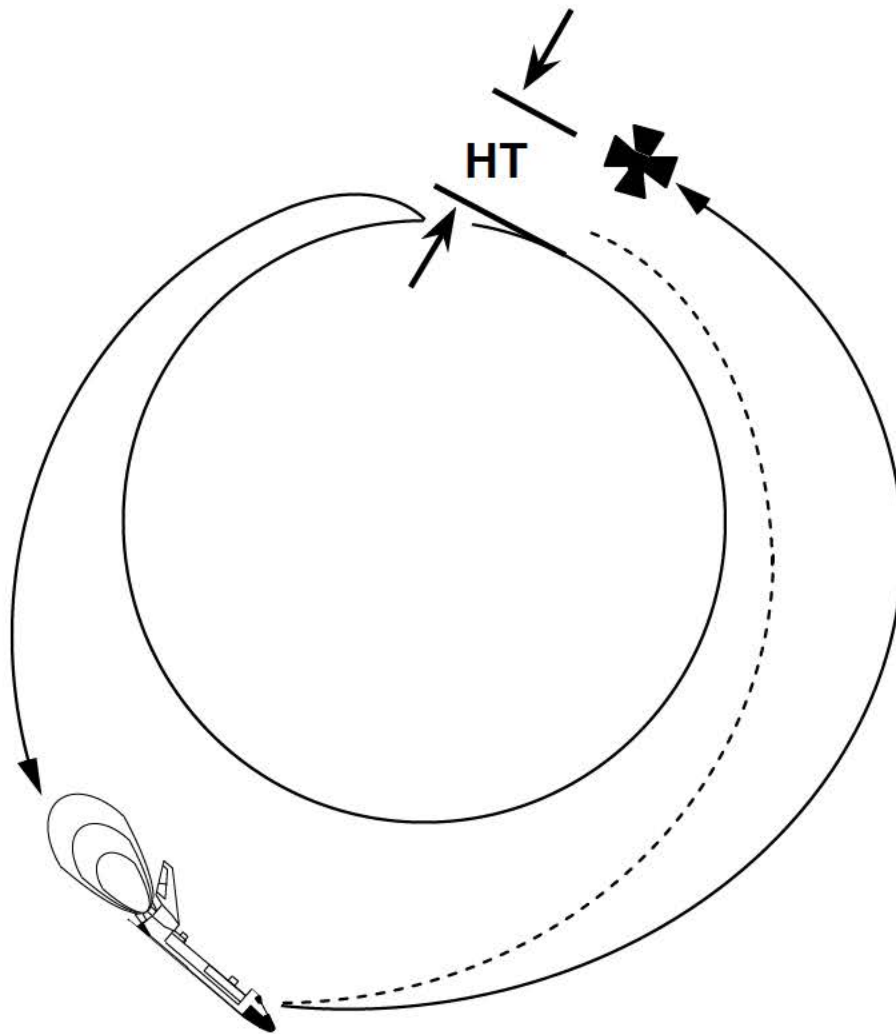
HT Altitude above Earth at target point.

C1 Coefficients for vertical / horizontal velocity relationship at target.

C2

$$Vv = C2 \times Vh + C1$$


In addition to placing the ORBITER in a safe orbit, OMS-2 can be used as a phasing maneuver. The target point altitude (**HT**) can be adjusted based on the initial phase angle at lift-off. The value of **HT** determines ΔH , which, in turn, determines the rate at which the ORBITER “catches-up” with the TARGET.

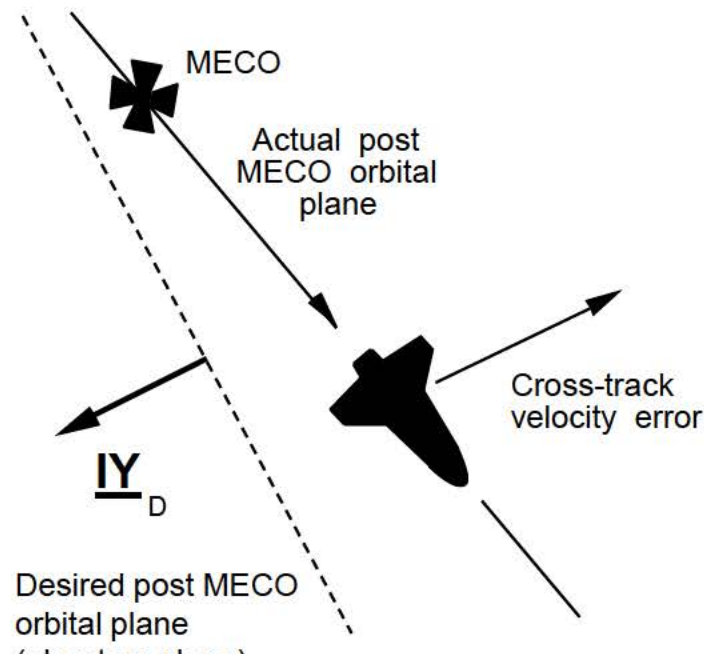


The value of **HT** to be used is computed post MECO/OMS-1 by the Flight Dynamics Officer (FDO). Flights that use this technique are called “variable perigee flights.”

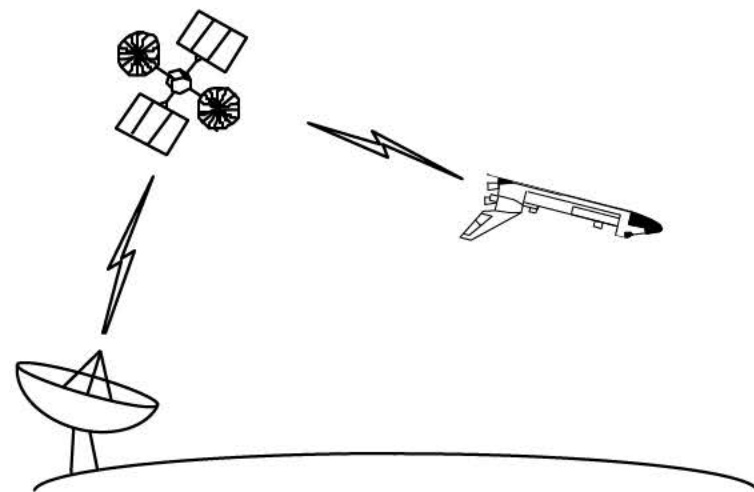
While the SHUTTLE is on the pad prior to launch, the IMUs drift off of their desired position. During ascent, this drift can result in a cross-track velocity error. This velocity error will cause the ORBITER to miss the phantom plane at MECO.

After MECO, Mission Control checks the cross-track velocity error. If it is greater than 6 feet/second, a new state vector (based on ground tracking data) is uplinked to the ORBITER. This new state vector does not contain velocity errors from pre-launch IMU drift.

The 6 feet/second rule applies only to ground-up rendezvous.



1. Due to cross-track velocity error, ORBITER misses phantom plane.

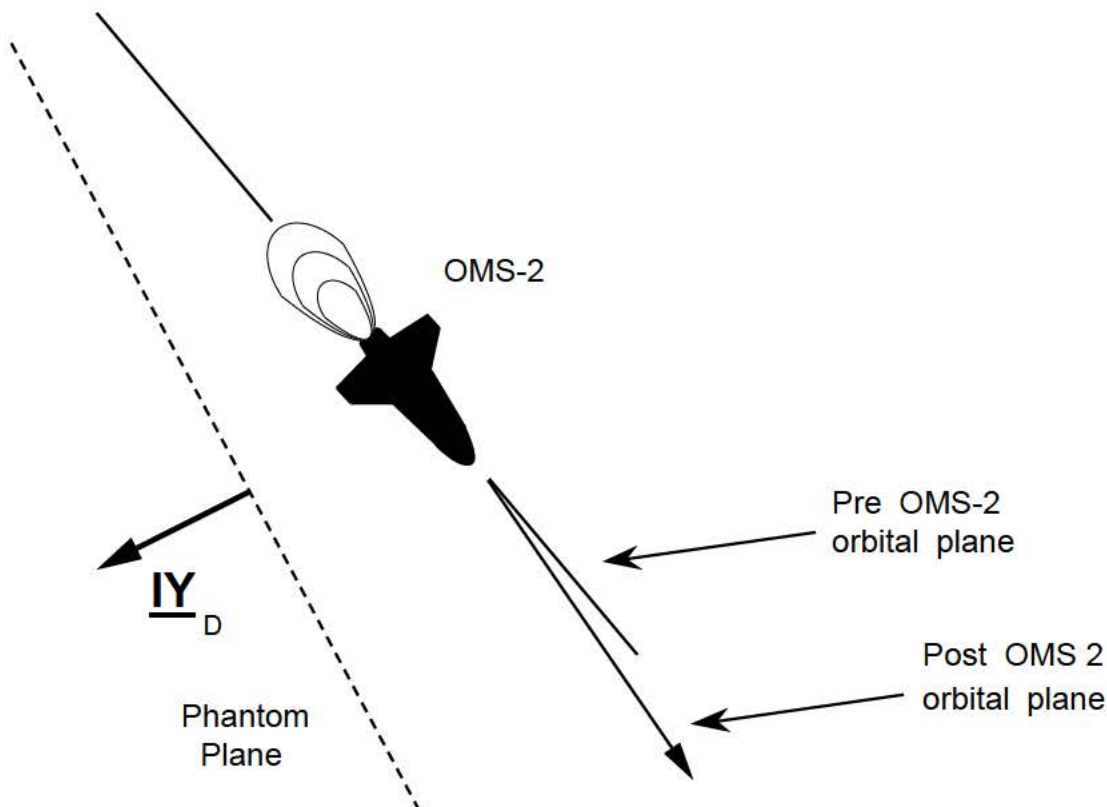


2. If post-MECO cross-track velocity error is > 6 ft./sec., a new state vector is uplinked.

OMS-2 can help reduce the planar error due to cross-track velocity error. The **IY** (phantom plane) target used by PEG 1 is also used by PEG 4.

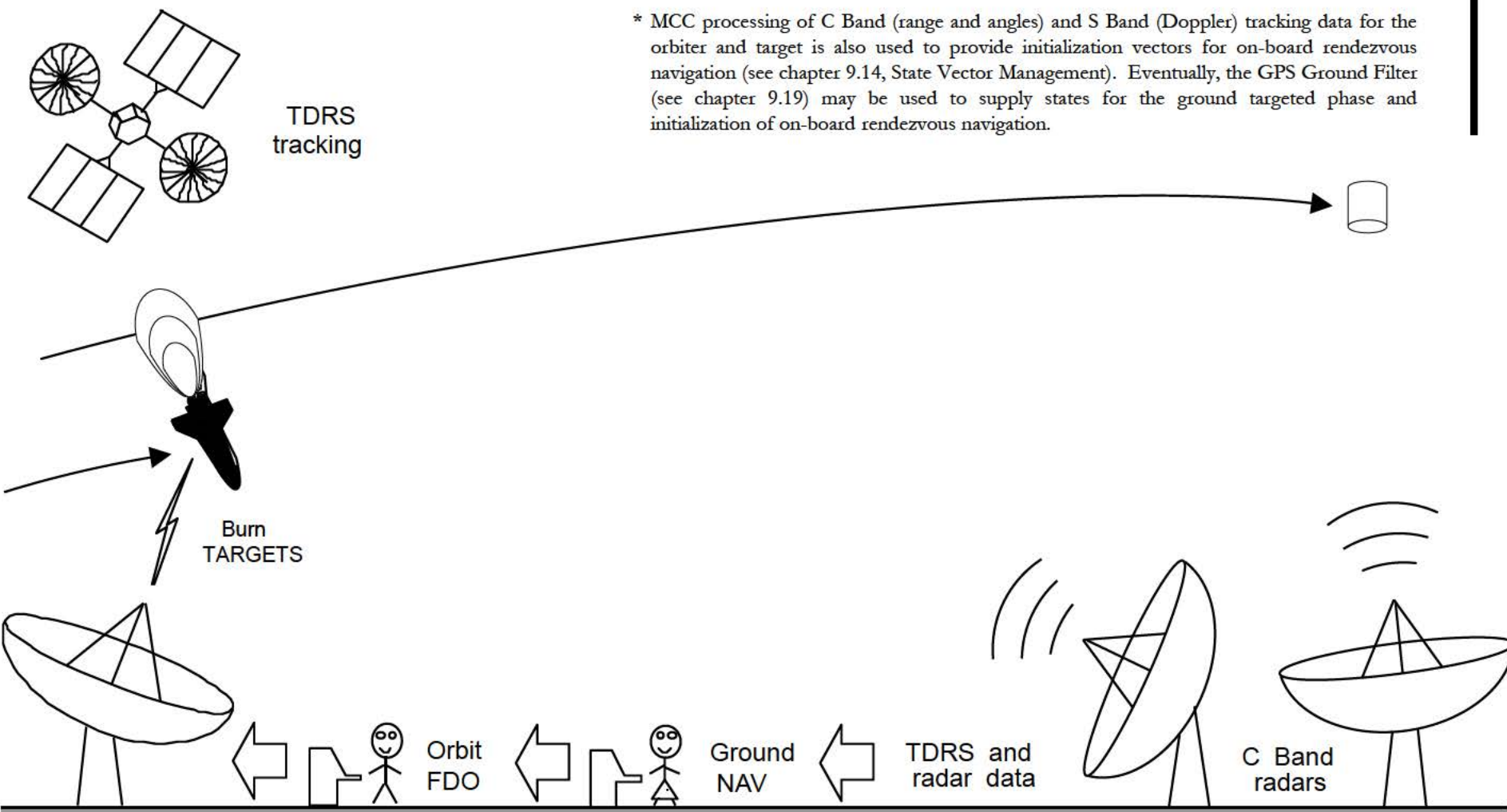
PEG 4 guidance will null the ORBITER rate that is normal to the phantom plane (or parallel to the **IY** vector).

OMS-2 will not place the ORBITER in the phantom plane, but it will reduce the size of a subsequent burn executed to correct the planar error (see NPC burn).



5.3 Ground Targeted Phase

Most of the burns executed during rendezvous are computed on the ground **using orbiter and target state vectors** based on tracking data from radar stations (**C Band**) and from the Tracking and Data Relay Satellites (TDRS, S Band).* Solutions computed by the Flight Dynamics Officer (FDO) are then uplinked or voiced up to the crew for execution. The part of the rendezvous during which ground targeted burns are performed is called the “ground targeted phase.”



Terms used for burns in both the ground and on-board targeted phases originated during development of rendezvous techniques in the early 1960s for Gemini and Apollo. Originally, the burns were assigned a numerical prefix that represented the orbit on which the maneuver was executed. It enabled personnel to tell where in the mission plan a ground targeted maneuver would be executed. The “N” in NC, NH, NPC, and NSR represents the crossing of the chaser line of apsides at which the maneuver is performed. N=1 represented the first apogee, N=1.5 the first perigee, as so on. For example, if the second NC maneuver was to be executed at the fifth apogee, the burn would be named 5C2. However, in actual practice the “N” was not usually assigned the apsidal crossing number. Over time, the numbers were dropped and the “N” remained in the burn name. The convention has been retained due to the large amount of software and documentation that refers to NC, NH, NPC, and NSR. If there is more than one burn of a type (like NC), the x (as in NCx) represents the nth burn, as in NC1, NC2, etc.

Below is a list of burn designations.

NC1 – **N**th apsides crossing, Catch-up (phasing) maneuver, 1st catch-up maneuver.

NPC – Number of common planar node, Plane Change maneuver.

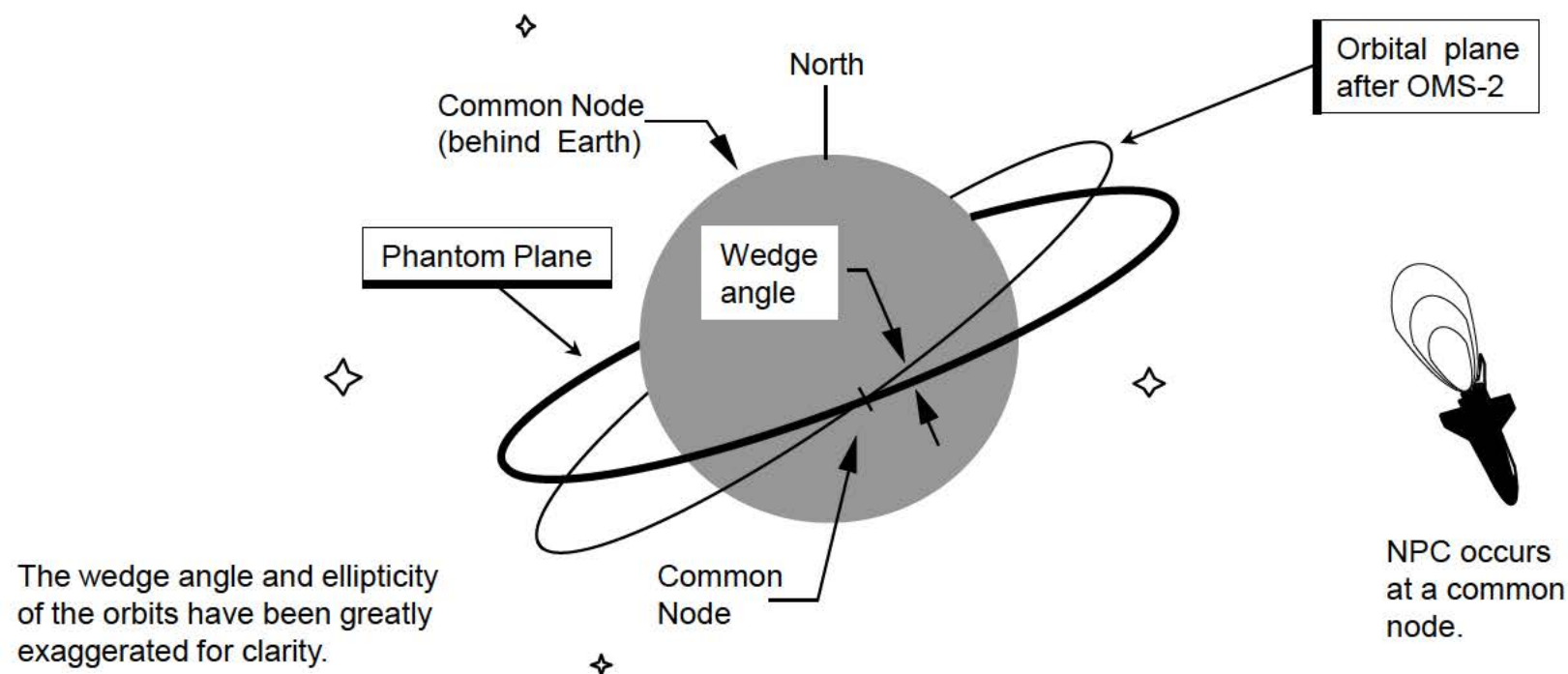
NSR – **N**th apsides crossing, Slow Rate catch-up initiation (co-elliptic orbit).

NCC – **N**th apsides crossing, Corrective Combination maneuver.

5.4 Plane Change Burn (NPC)

For a ground-up rendezvous, yaw steering is performed to place the ORBITER in the phantom plane. Dispersions during ascent may cause the actual orbital plane to be different than the desired phantom plane. The difference is measured in terms of wedge angle.

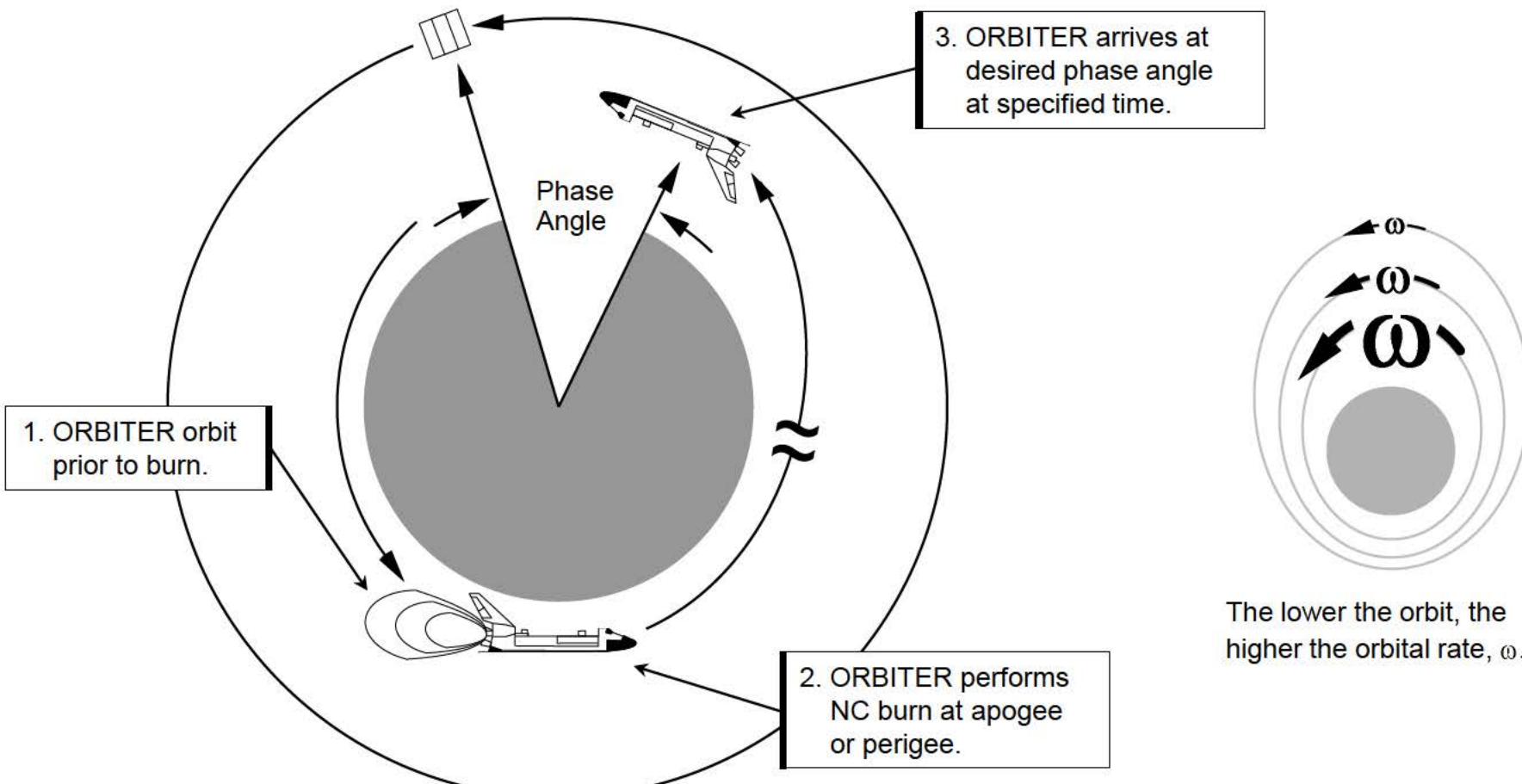
This maneuver corrects for the ascent planar dispersions by placing the ORBITER in the phantom plane. NPC is done at the point where the actual and phantom planes intersect (called the common node). Typically only one NPC maneuver is performed. **Sometimes the NPC is combined with a NH or NC burn.** This avoids having to schedule and perform a separate NPC burn and saves propellant. The root sum square for the ΔV of the combined burn is less than ΔV of the two burns done separately. This cannot be done if the common node is too far from the optimum point for the NC or NH.



5.5 Phasing Burn (NC)

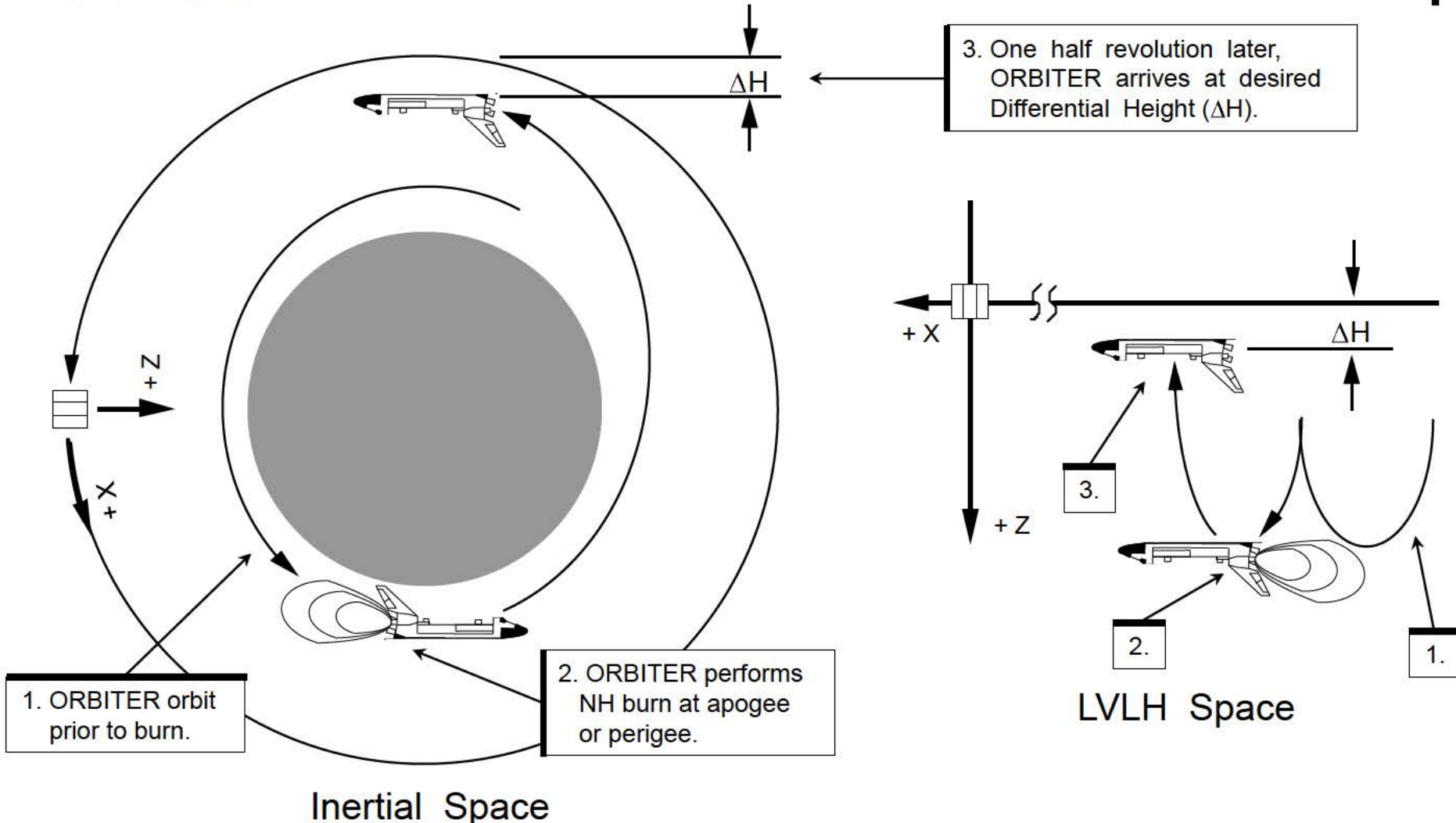
NC burns (“C” is for “closing” or “catch-up”) are used to control how quickly the ORBITER is approaching the TARGET. They may be executed either at apogee or perigee. **If a NSR burn is factored into the NC burn, it may not be performed at relative apogee or perigee.** By changing the altitude of apogee or perigee, the ORBITER can control the rate at which it orbits the Earth.

The NC burn is designed so that the orbital rate of the ORBITER will place the ORBITER at some desired down-range position (phase angle) relative to the TARGET at a designated time.



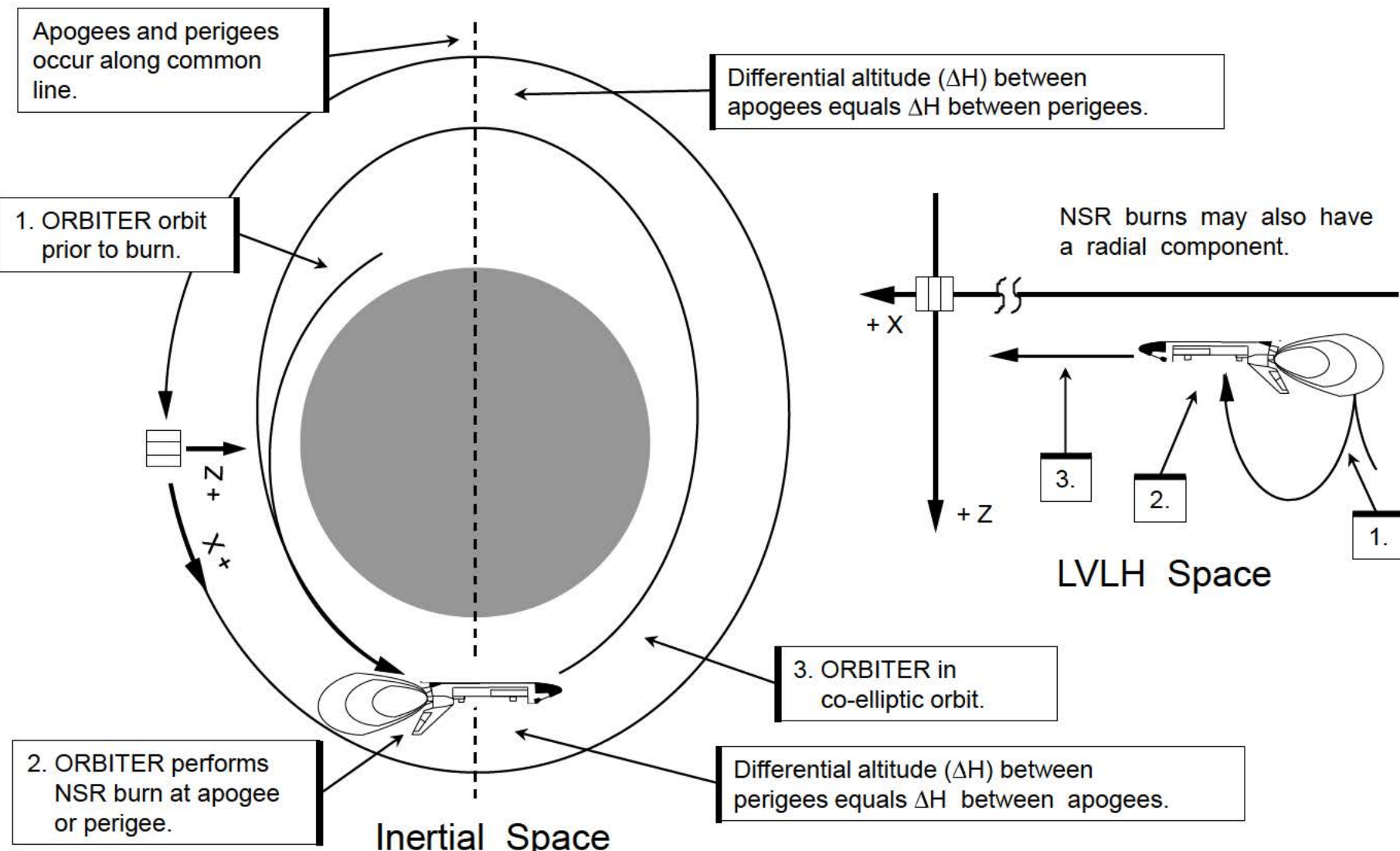
5.6 Altitude Burn (NH)

The NH burn controls the differential height (ΔH) between the ORBITER's orbit and the TARGET's orbit. It is executed at either apogee or perigee. NH is designed so that the ΔH condition is met after half a revolution (180 degrees of orbit travel). **If a NSR burn is factored into the NH burn, it may not be performed at relative apogee or perigee.**



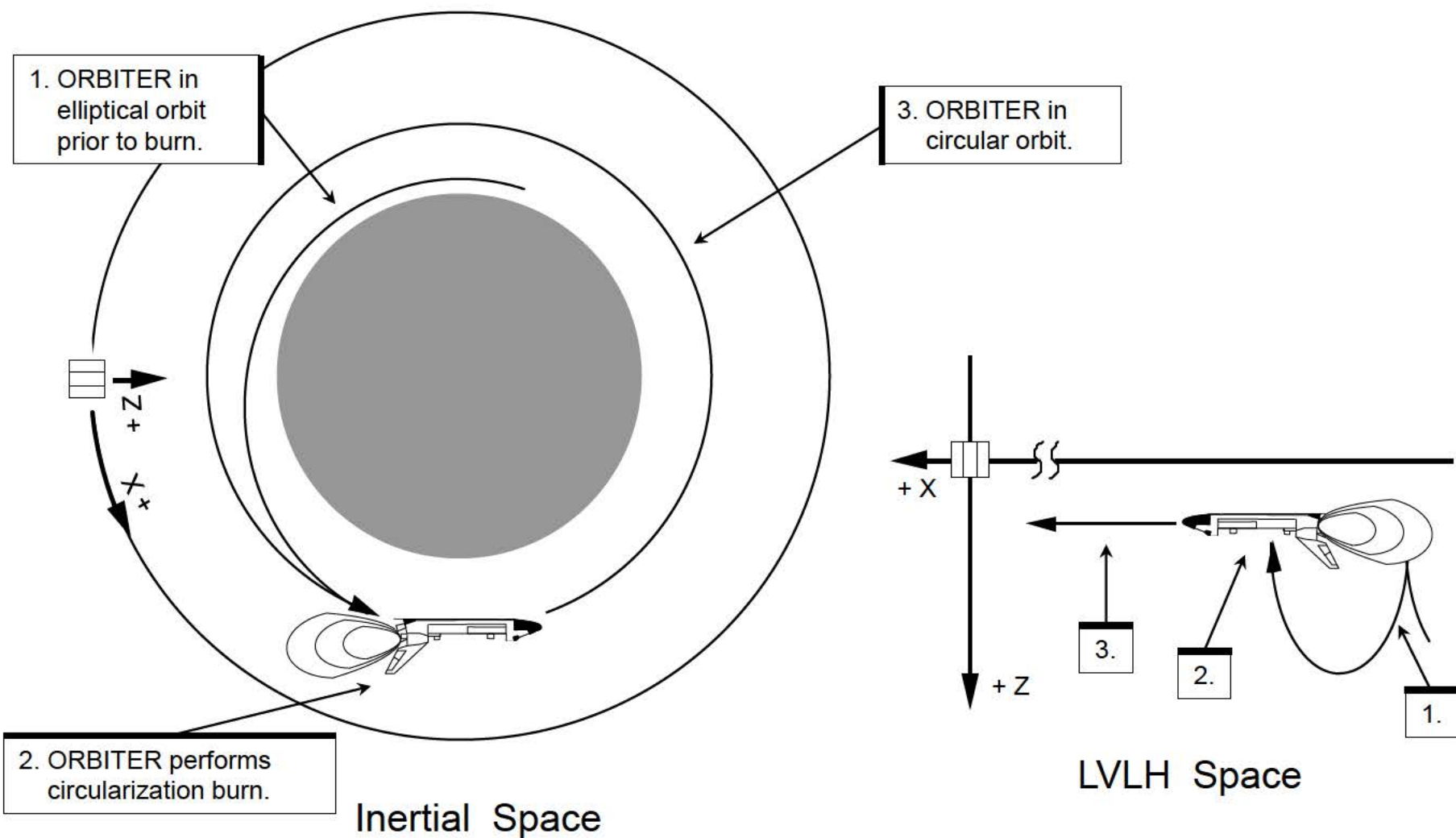
5.7 Co-Elliptic Burn (NSR)

An NSR (Slow Rate) burn places the ORBITER in a co-elliptic orbit with the TARGET. NSR burns can be used to meet lighting requirements on the day of rendezvous. However, on most rendezvous flights, the design of the profile permits lighting conditions to be met without an NSR burn.



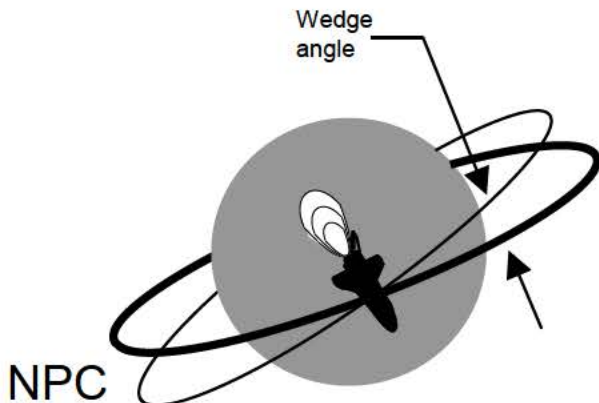
5.8 Circularization Burn (CIRC)

A fifth type of burn that may be executed is the circularization (CIRC) burn. It is performed at either apogee or perigee and changes the orbit from elliptical to circular. For a circular TARGET orbit, CIRC is equivalent to NSR.

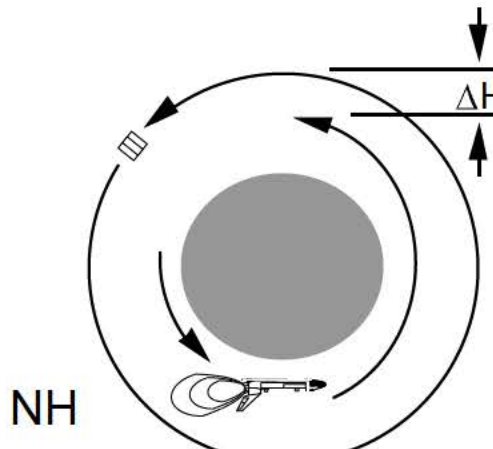


5.9 Ground Targeted Burn Summary

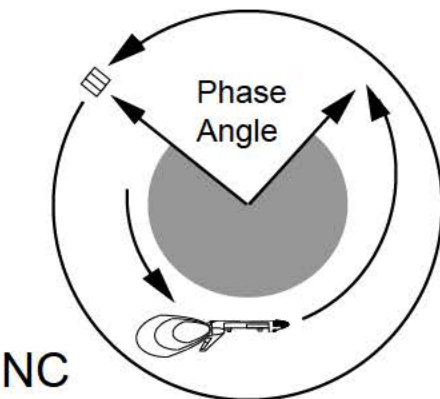
There are four main types of burns that are computed by the orbit Flight Dynamics officer based on C-band radar and TDRS tracking data. ΔV to be burned is then uplinked or voiced up to the crew. A fifth type, the circularization burn, is occasionally performed but is not shown here.



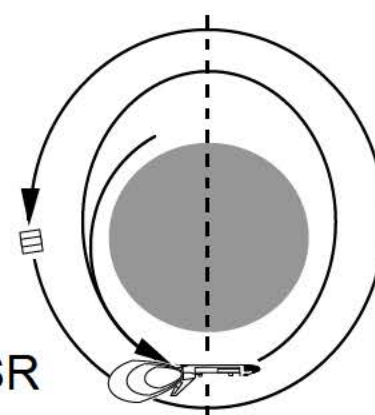
Controls wedge angle between current orbital plane and desired orbital plane.



Controls differential height between ORBITER and TARGET orbits.

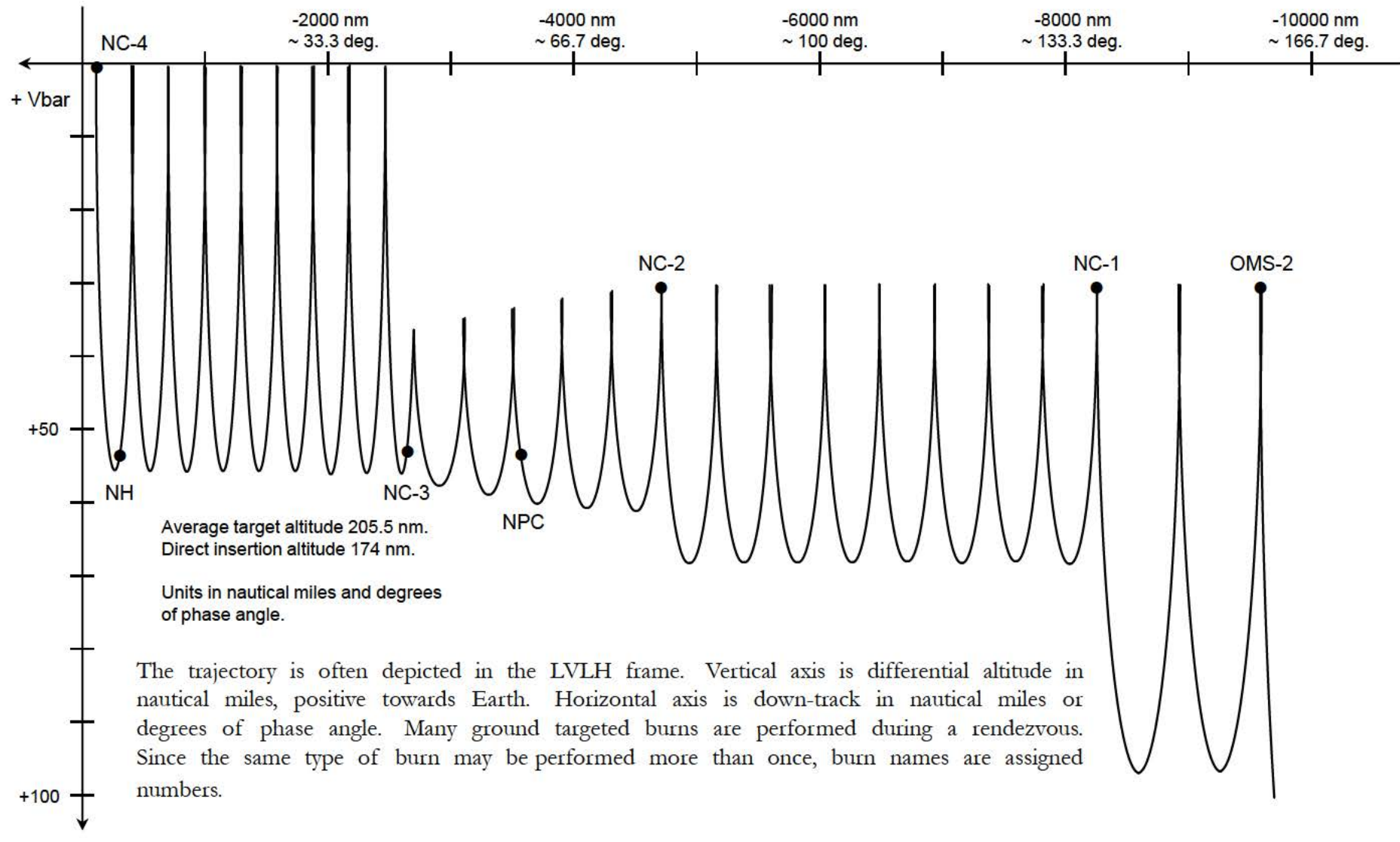


Controls down-track position of ORBITER with respect to TARGET.



Places ORBITER in orbit coelliptic with TARGET's orbit.

5.10 Ground Targeted Phase In LVLH Coordinates



The trajectory is often depicted in the LVLH frame. Vertical axis is differential altitude in nautical miles, positive towards Earth. Horizontal axis is down-track in nautical miles or degrees of phase angle. Many ground targeted burns are performed during a rendezvous. Since the same type of burn may be performed more than once, burn names are assigned numbers.

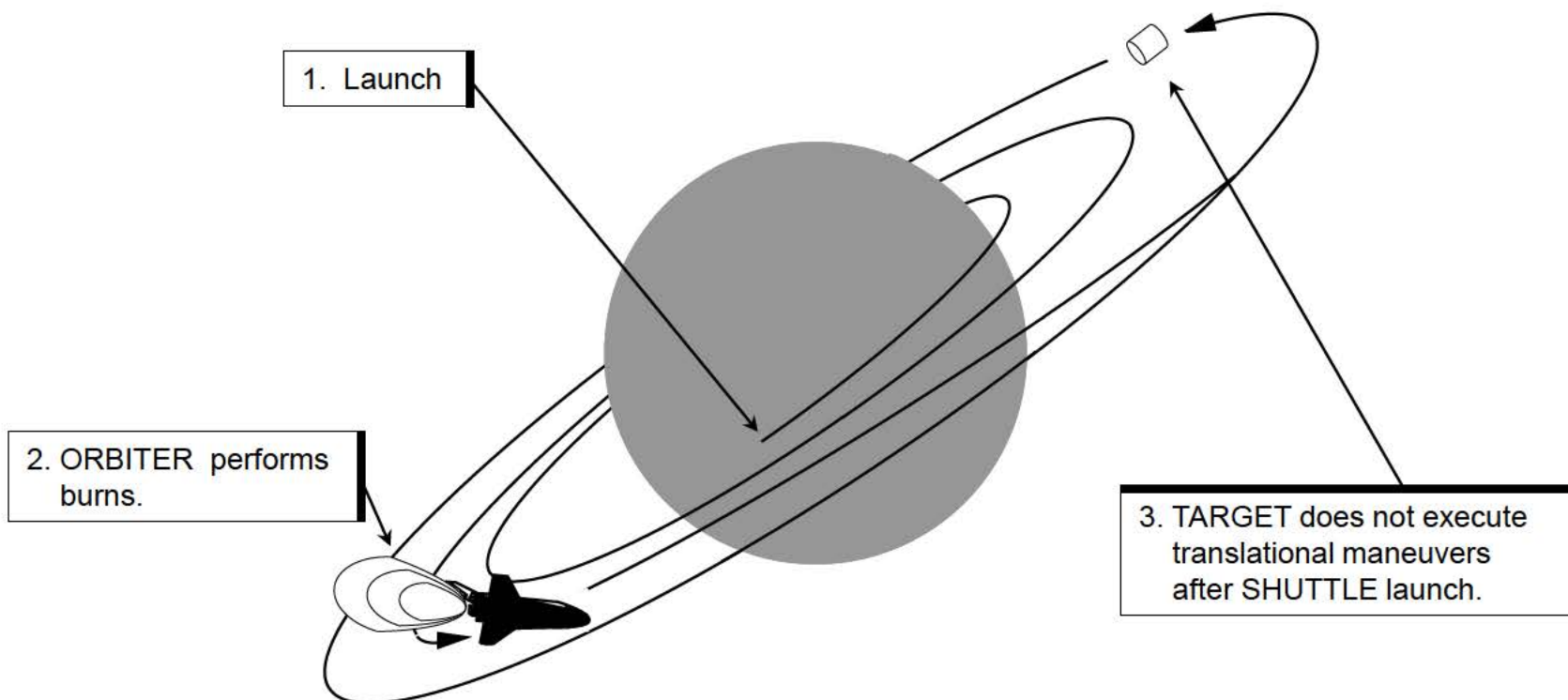
Adapted from a STS-101 OCF Cycle Rendezvous FOP Chart by Kristine Pettinger and Richard Parker.

5.11 Classical Ground-Up Rendezvous

Ground targeted burns (NPC, NC, NH and NSR) may be performed in one of four types of ground-up rendezvous profiles. The first is the “classical” ground-up rendezvous.

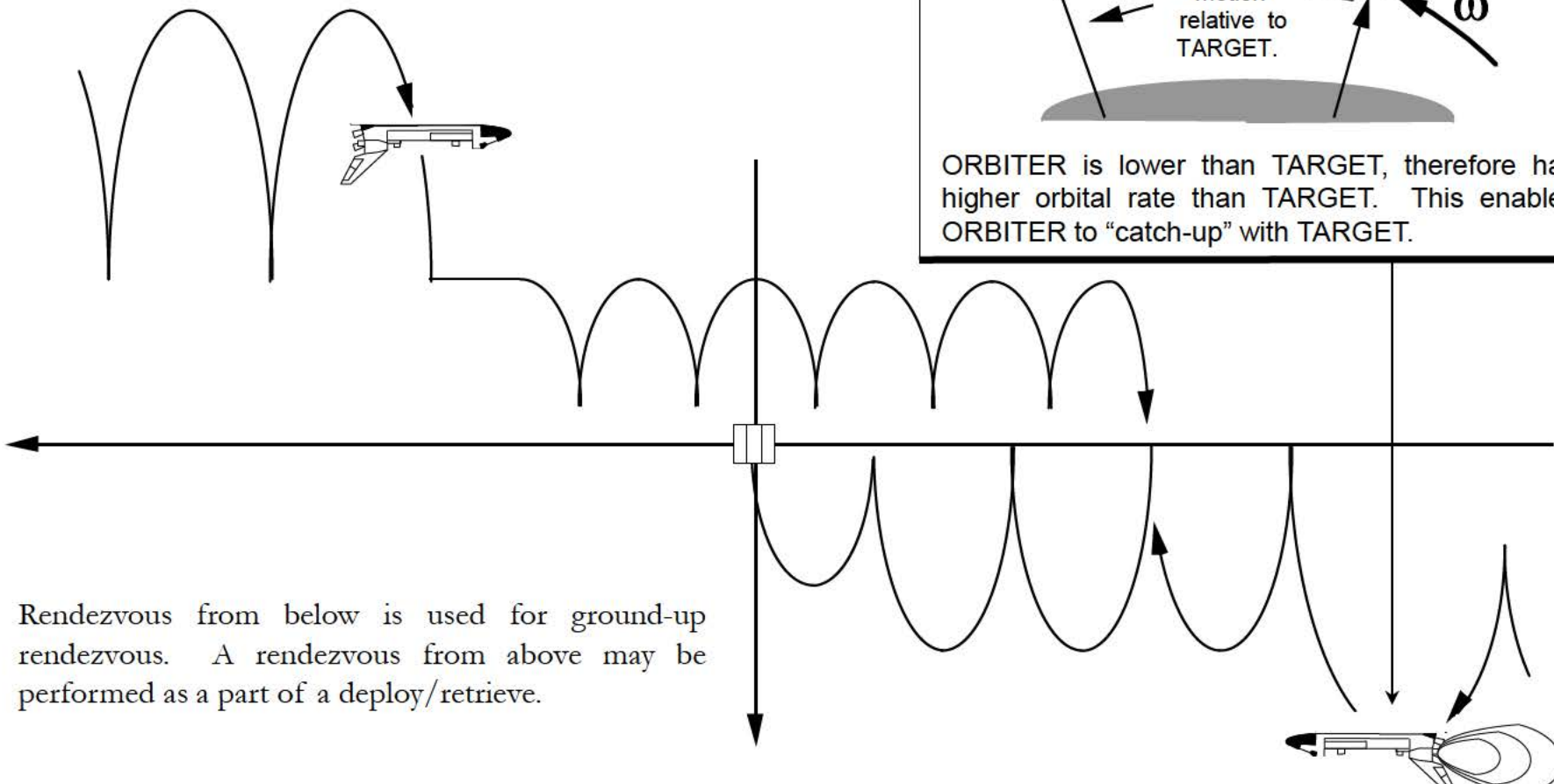
Under this profile, the TARGET is passive during the rendezvous. The ORBITER executes all of the maneuvers required for the rendezvous.

If the TARGET has a translational DV capability, it may lower its orbit prior to SHUTTLE launch to decrease ORBITER propellant expenditure.



5.12 Rendezvous From Above or Below

The ORBITER may approach the TARGET during the ground-targeted phase in one of two ways:

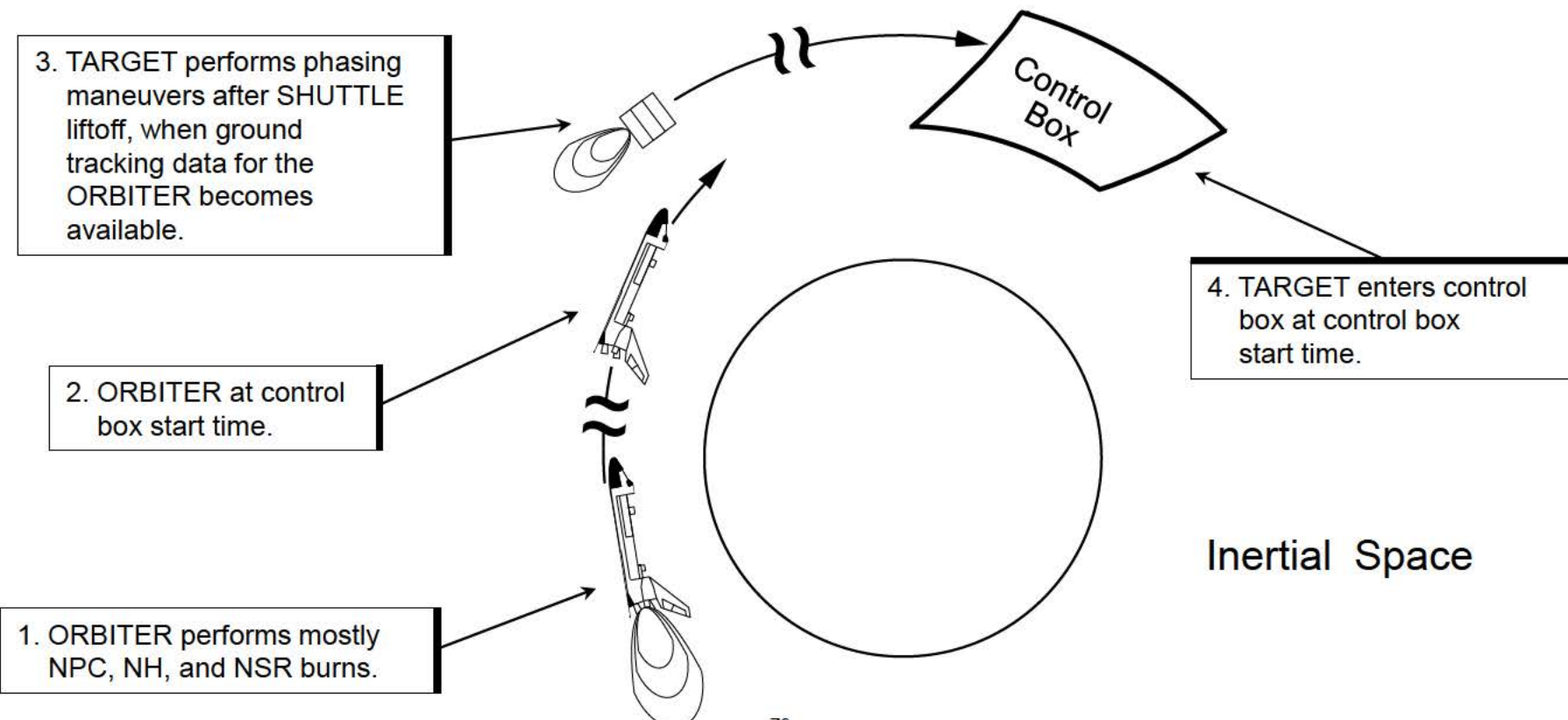


Rendezvous from below is used for ground-up rendezvous. A rendezvous from above may be performed as a part of a deploy/retrieve.

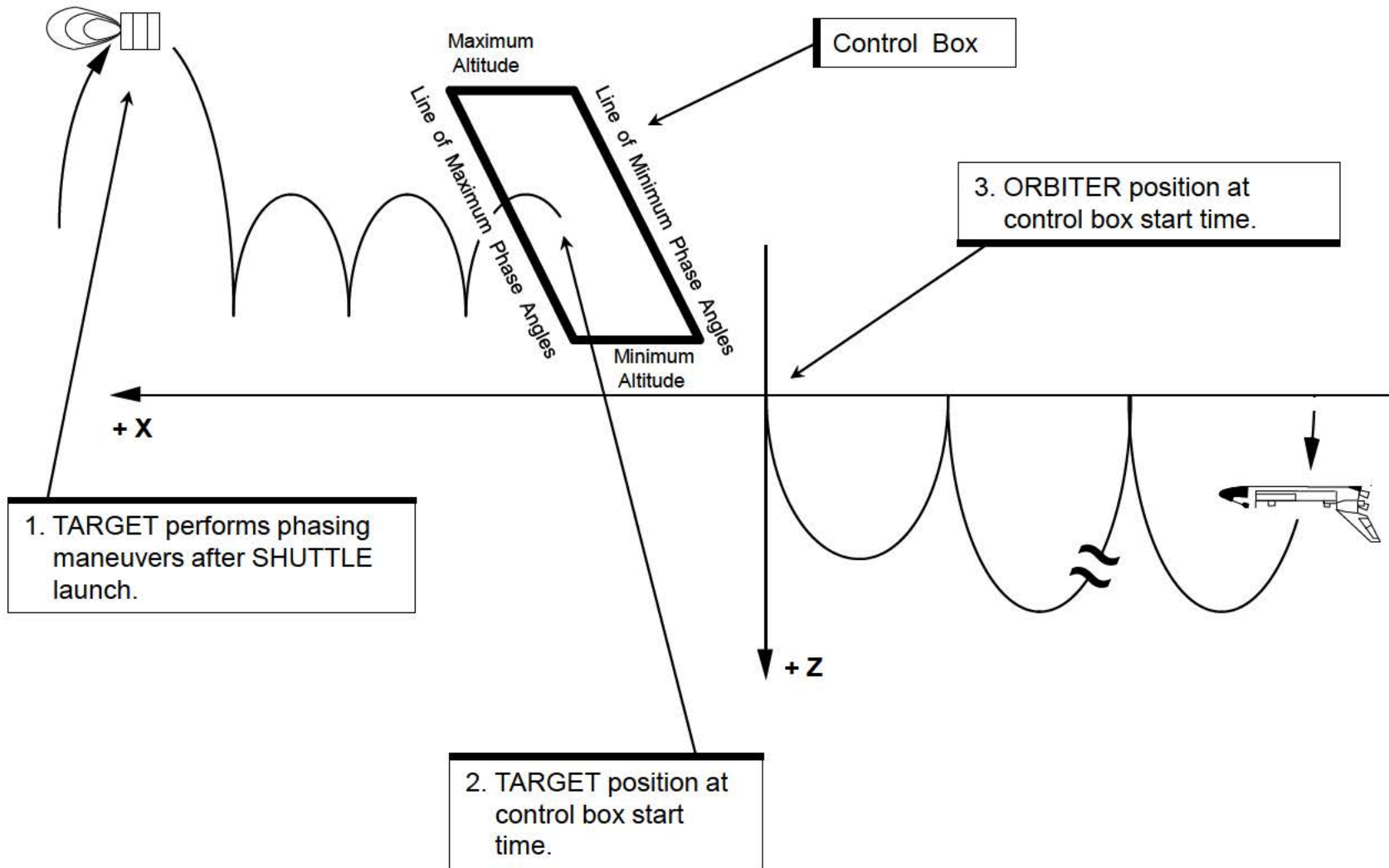
5.13 Control Box Rendezvous

If the TARGET has a translational ΔV capability (and enough propellant) it can also execute maneuvers during the rendezvous. In a “control box” rendezvous, the TARGET performs the phasing maneuvers, rather than the ORBITER. After SHUTTLE launch, the TARGET maneuvers so that it will enter the “control box” at a specified time. This reduces the ORBITER's propellant load.

After the TARGET enters the control box, it no longer executes burns. Some phasing by the ORBITER will be required after this point. The ORBITER may also execute an NPC burn to compensate for TARGET planar error introduced by TARGET phasing maneuvers.

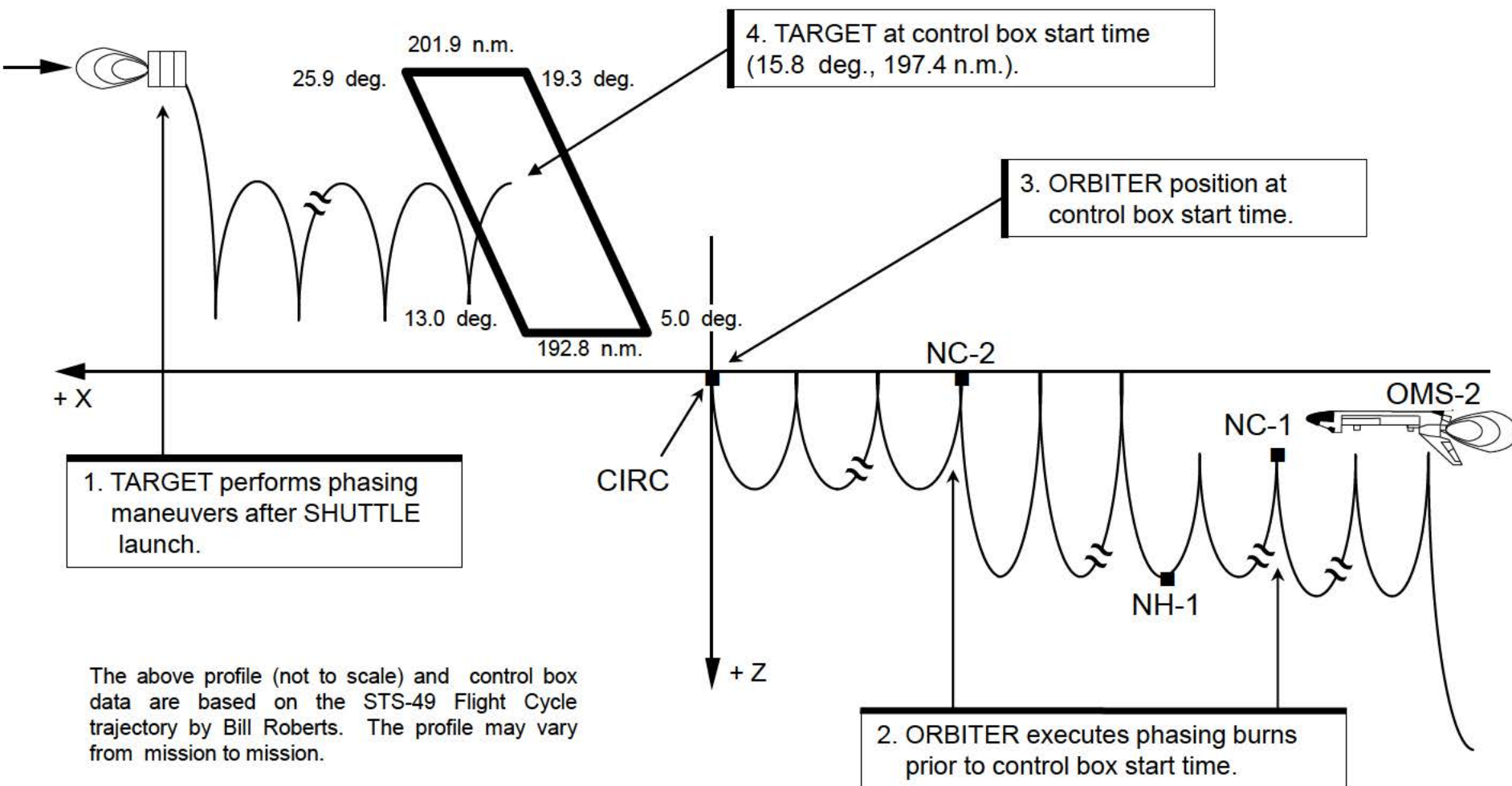


Control box rendezvous is usually viewed in LVLH. The system is centered on ORBITER position at control box start time.



5.14 Hybrid or Modified Control Box Rendezvous

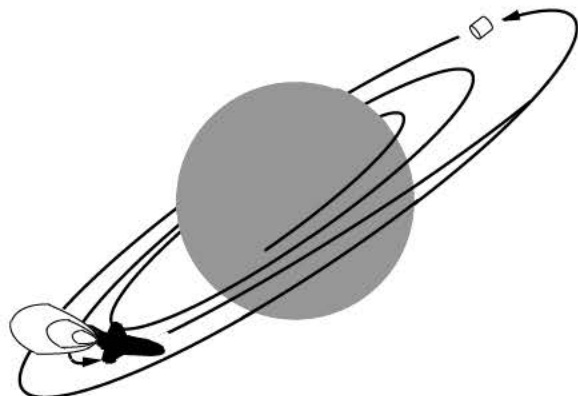
A variation of the control box rendezvous is the “hybrid” or “modified” control box rendezvous. In this scenario, the ORBITER performs some phasing maneuvers prior to control box start time.



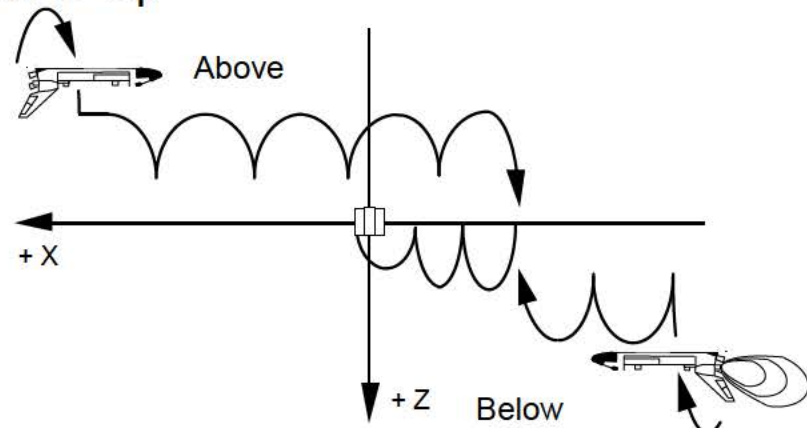
5.15 Summary of Ground-Targeted Phase Profiles

Ground targeted burns may be combined to create one of three ground-up profiles.

Classical Ground-Up

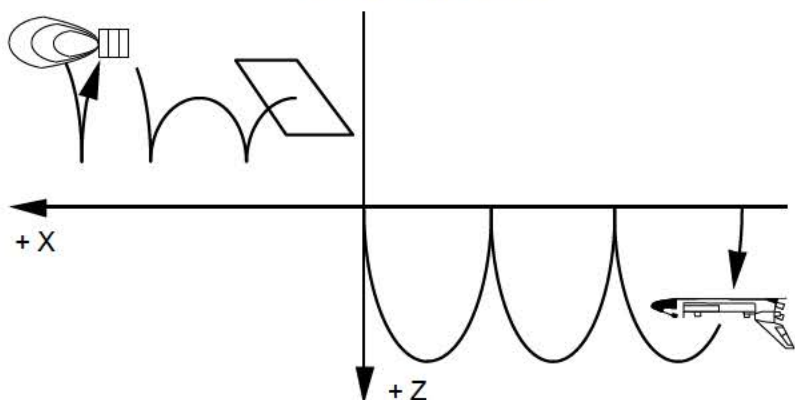


1. TARGET is passive after ORBITER launch.



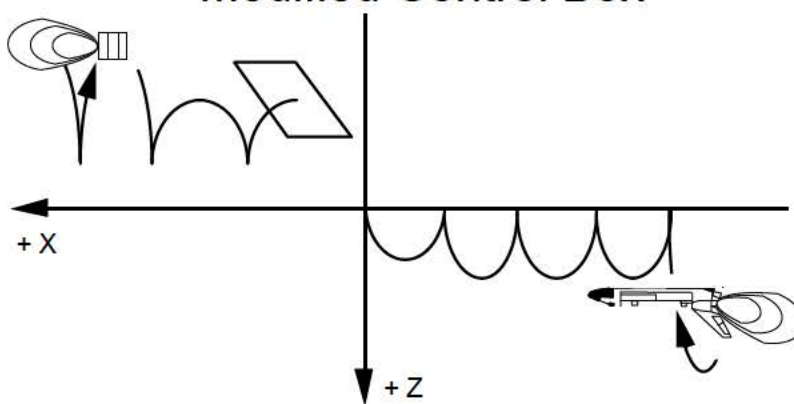
2. ORBITER approaches to TARGET.

Control Box



TARGET performs phasing maneuvers after SHUTTLE launch.

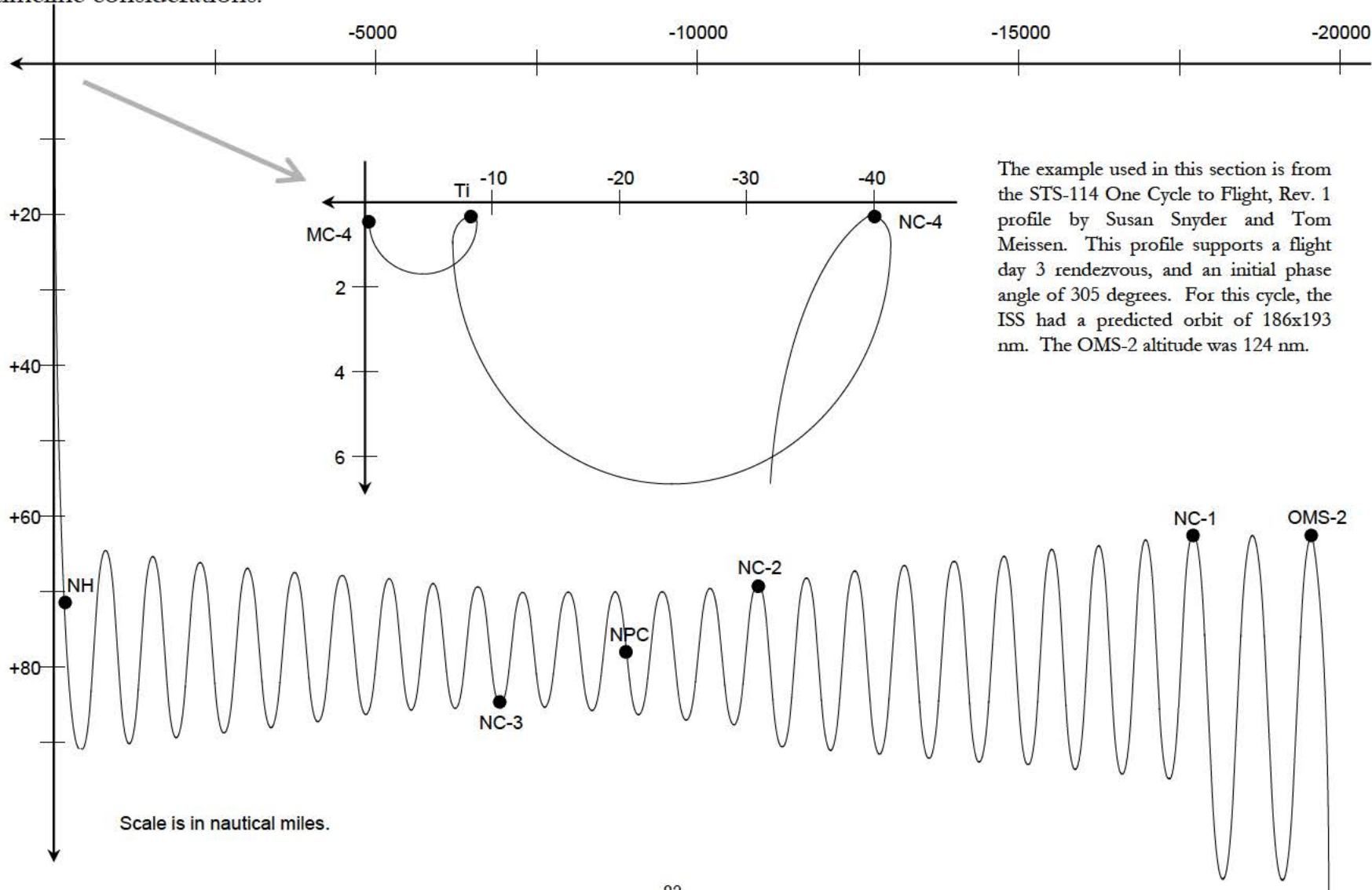
Modified Control Box



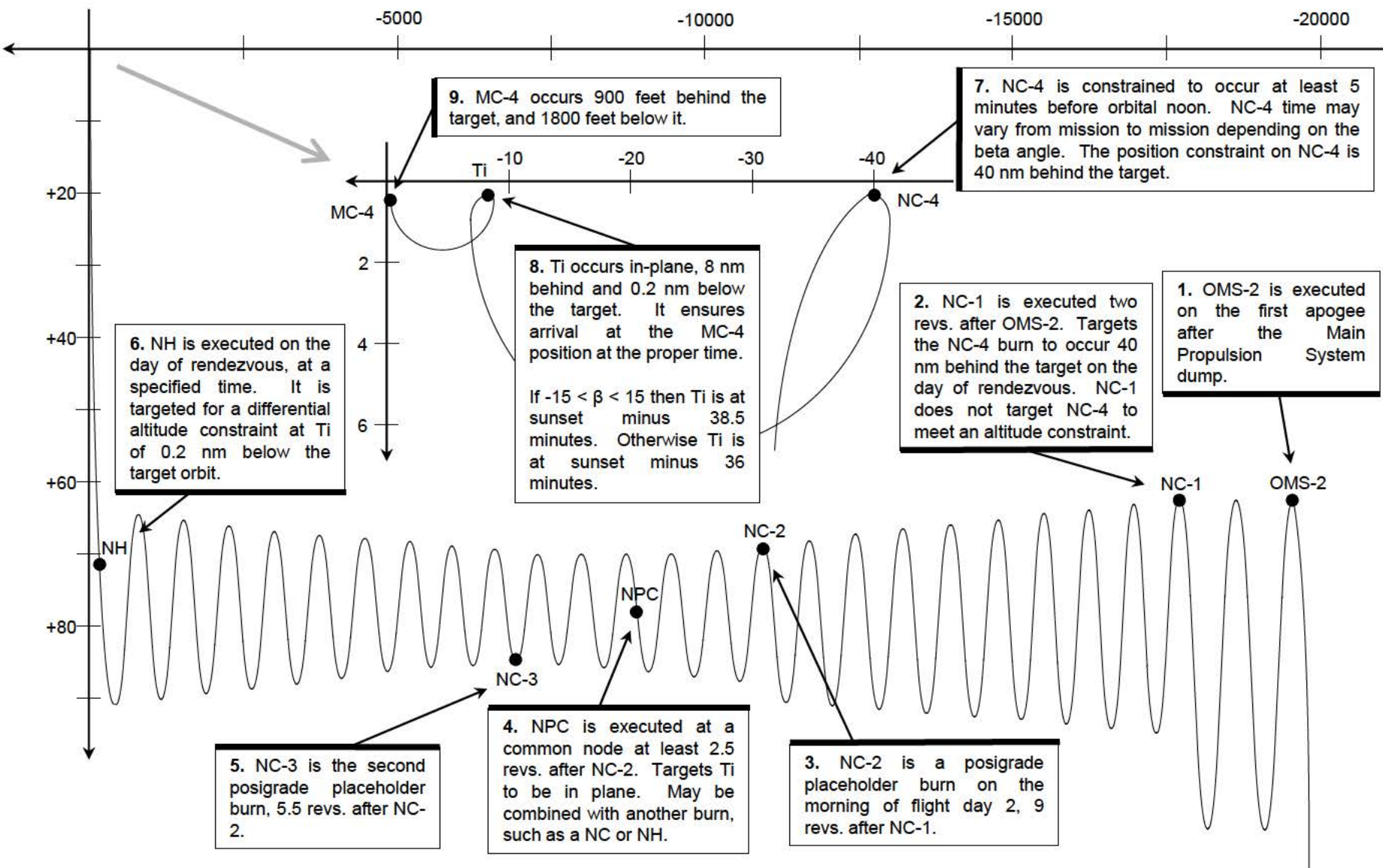
TARGET and ORBITER perform phasing maneuvers.

5.16 Designing a Ground-Up Rendezvous Profile

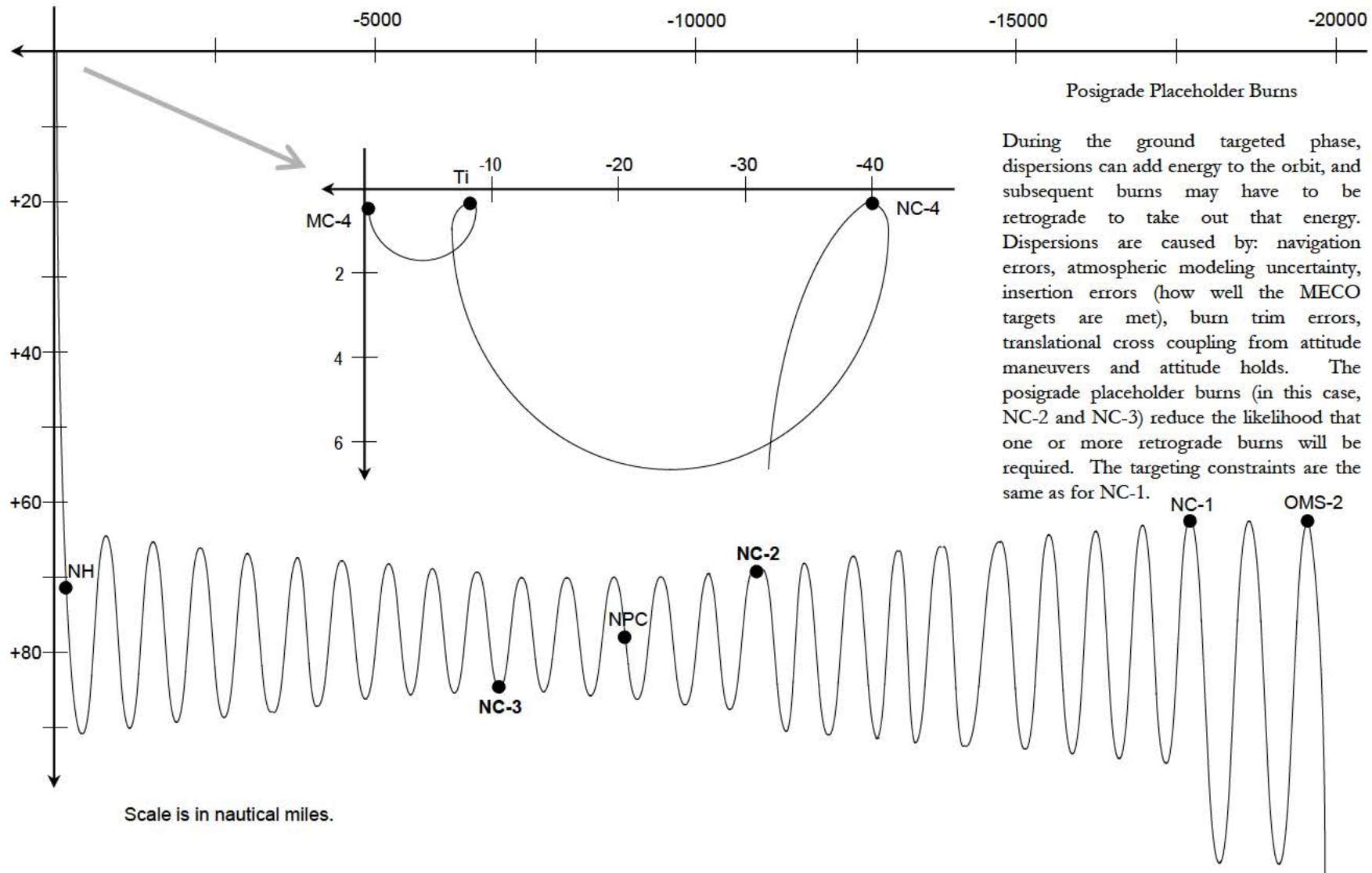
A number of phasing plans exist for the ground targeted phase. Each plan covers different initial phase angles (the phase angle from OMS-2 to the target). Plans with fewer burns on flight days 1 and 3 are preferred due to crew timeline considerations.



Each burn in the sequence is targeted so that constraints (time, relative position, lighting, direction and magnitude of a subsequent burn) will be met at a future time. The rev. counts quoted below are specific to this design for STS-114, and may be different for other missions.



A profile is iterated on until: 1) the minimum orbital altitude is not below 85 nautical miles, 2) the radial ΔV component at T_i is minimized, 3) there are no retrograde burns, 4) all downrange constraints (last NC, T_i) are satisfied, and 4) the ΔH at T_i is 0.2 nm. If the constraints cannot be met, another plan will have to be used. Nominal profiles are designed without NSR maneuvers. However, the Joint Underspeed Recovery profiles designed to enable an ISS rendezvous in the event of an ascent performance problem use NSR.

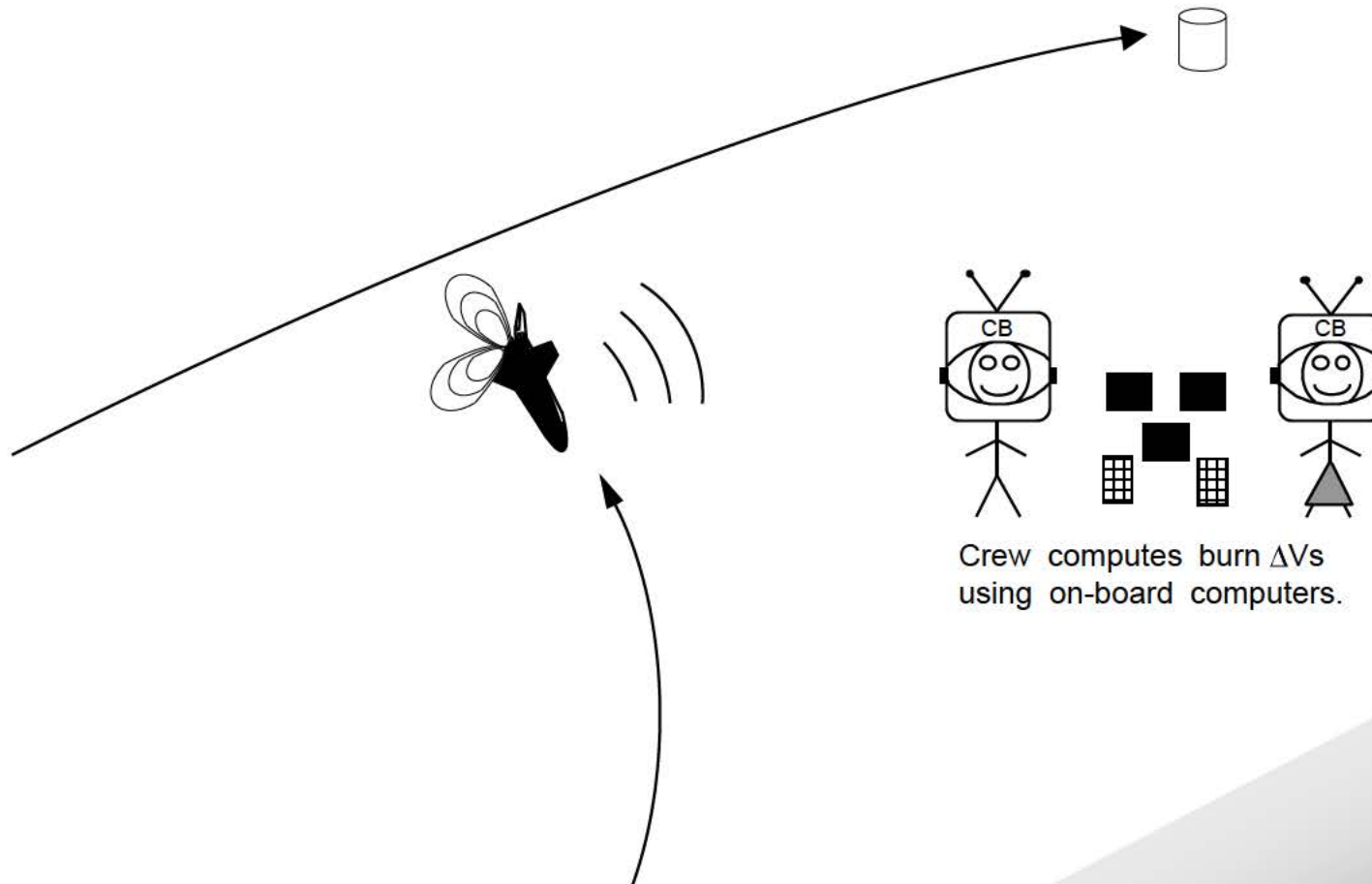


Scale is in nautical miles.

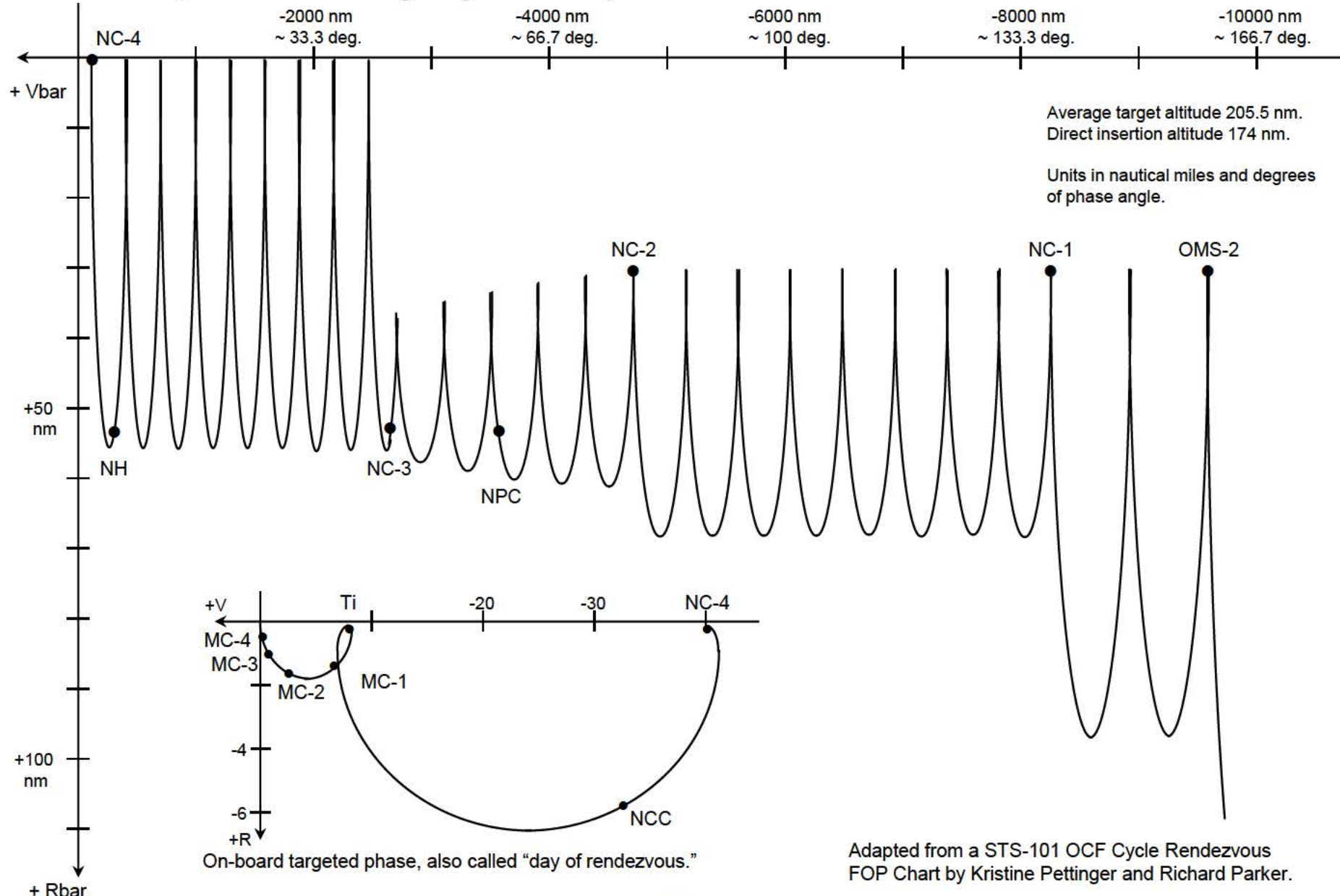
This page intentionally left blank.

6.0 Day of Rendezvous and Separations

For the ORBITER to successfully intercept the TARGET, it must have a more accurate estimate of its position and velocity relative to the TARGET than can be provided by ground and TDRS tracking. Radar and star trackers (navigation sensors) on the ORBITER are used to improve the on-board estimate of ORBITER position and velocity relative to the TARGET. The final seven burns (counting the planar null) in the rendezvous are computed on-board using the on-board ORBITER (sensor updated) and TARGET state vectors.

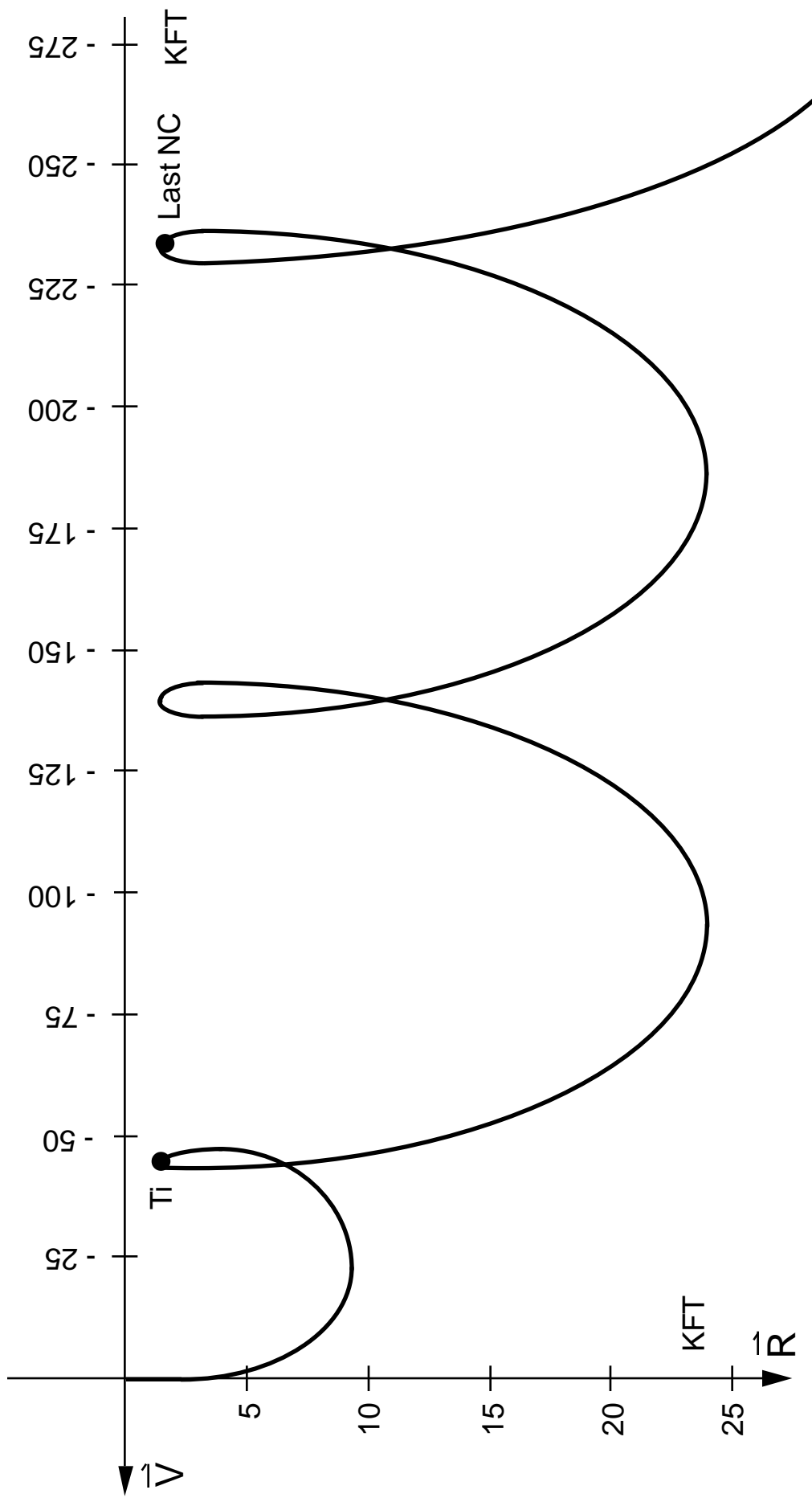


The ground targeted phase (from post OMS-2 to the final NC burn, NC-4 in this example) may last several days. The on-board targeted phase lasts anywhere from 3 to 4.5 hours.

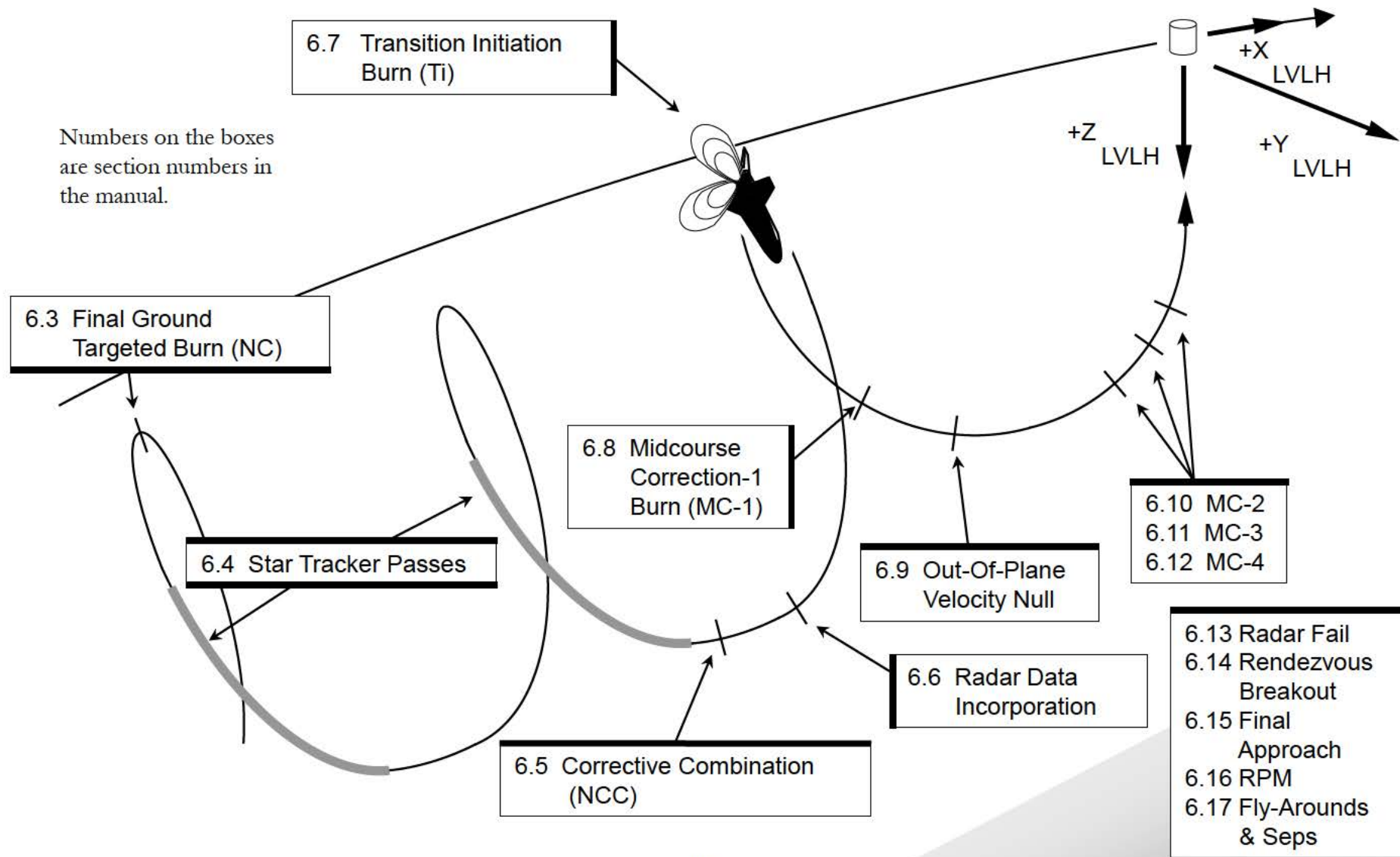


6.1 Day of Rendezvous Phase In LVLH Coordinates

Axes are usually in thousands of feet (kilofeet or KFT). The +X axis is often called the “Vbar” and the +Z axis the “Rbar.” A two rev NC to Ti profile is shown.

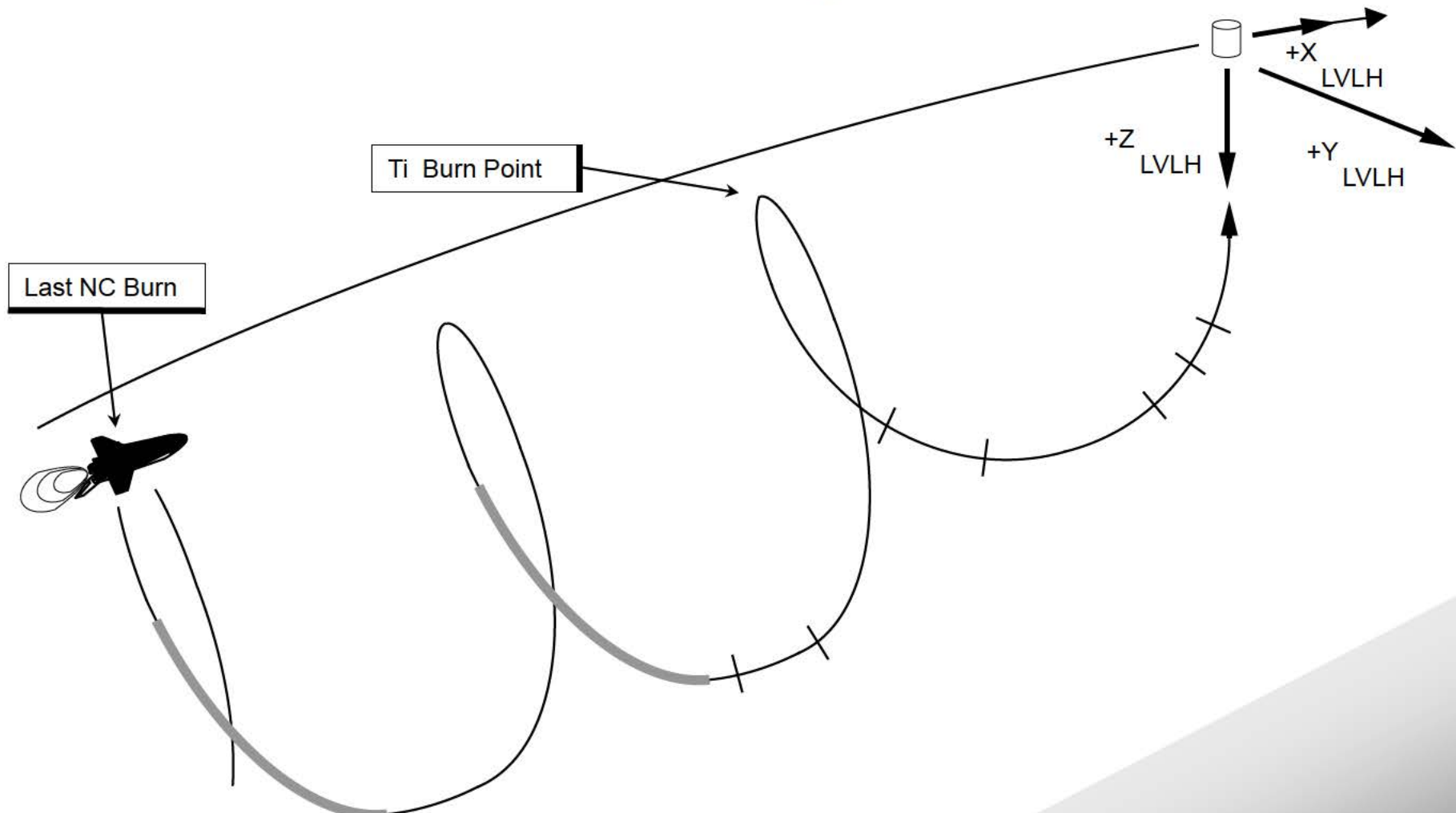


6.2 Day of Rendezvous Events Covered

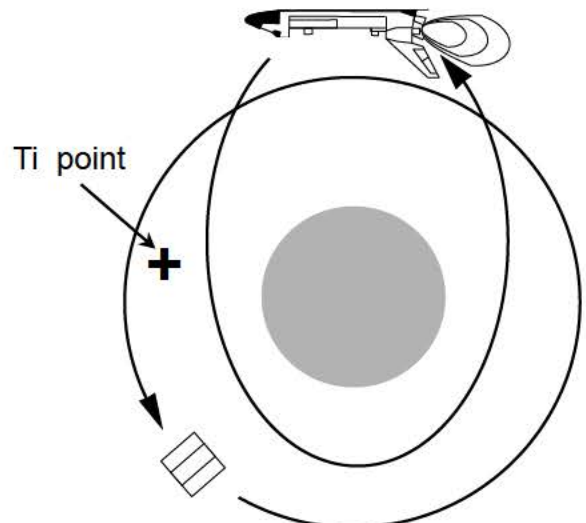


6.3 Final Ground Targeted Burn

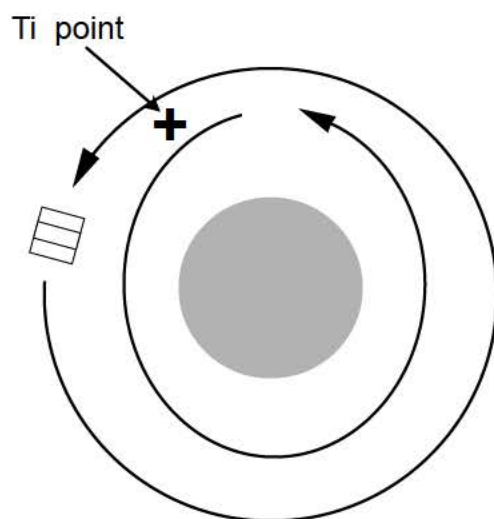
The final ground targeted burn (an NC, or phasing burn) is executed at a point normally near 40 N.M. behind the TARGET. It is designed to enable the ORBITER to arrive at the Ti point after one or two orbits.



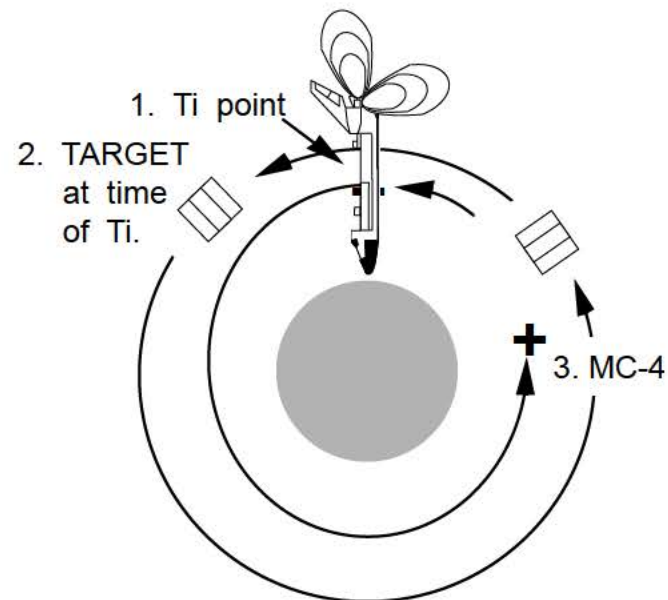
A two rev to Ti transfer is 720 degrees, a one rev transfer is 360 degrees.



A. Last NC burn executed.



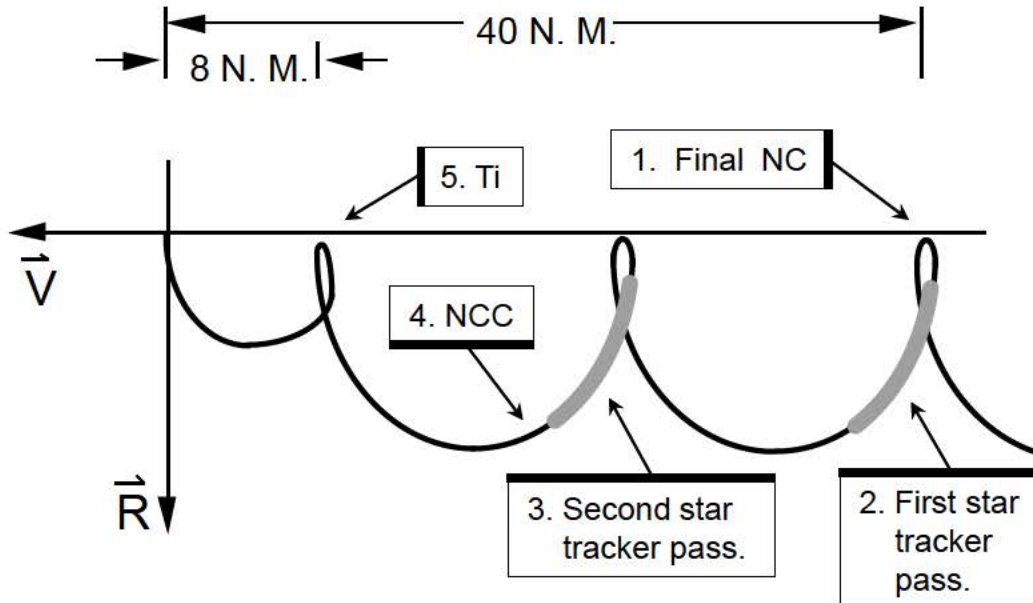
B. One revolution later.



C. Ti point reached and burn executed, intercept follows.

Note: Phase angle between ORBITER and TARGET, and the orbits have been exaggerated for clarity.

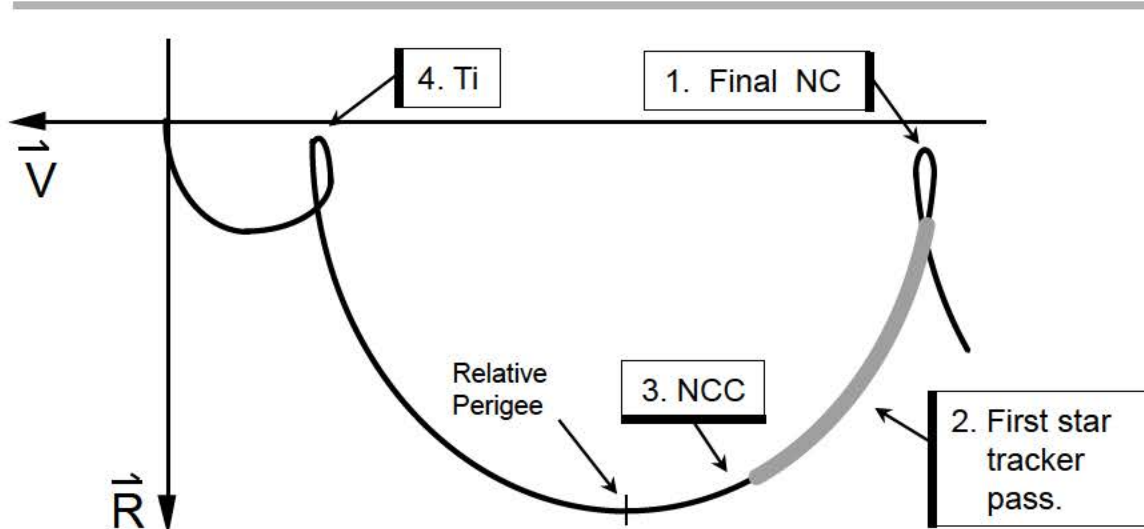
For most ground up rendezvous flights, the last NC will put the ORBITER on a 1 rev. transfer to Ti.



Two Revolutions to Ti

The final NC (at 40 nautical miles) targets the ORBITER to reach the Ti point after two ORBITER revolutions around the Earth.

Two star tracker passes are performed prior to NCC.



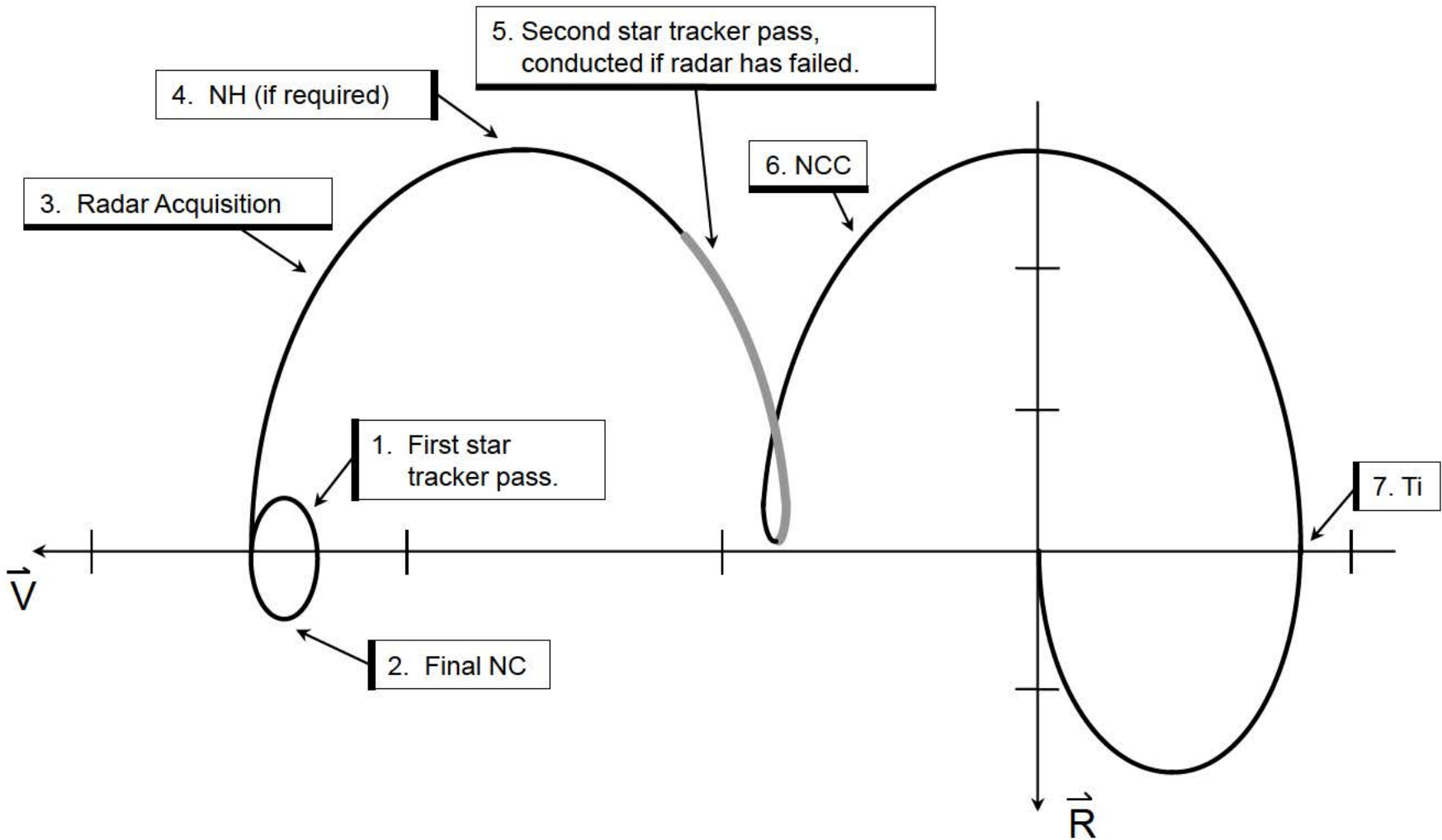
One Revolution to Ti

The final NC (at 40 nautical miles) targets the ORBITER to reach the Ti point after one ORBITER revolution around the Earth.

One tracker pass is performed prior to NCC.

ORBITER relative perigee is lower than for the 2 rev. to Ti case. This is due to the higher catch-up rate needed to do 1 rev. to Ti.

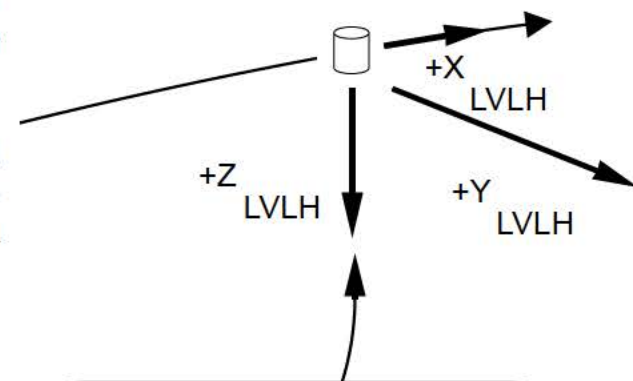
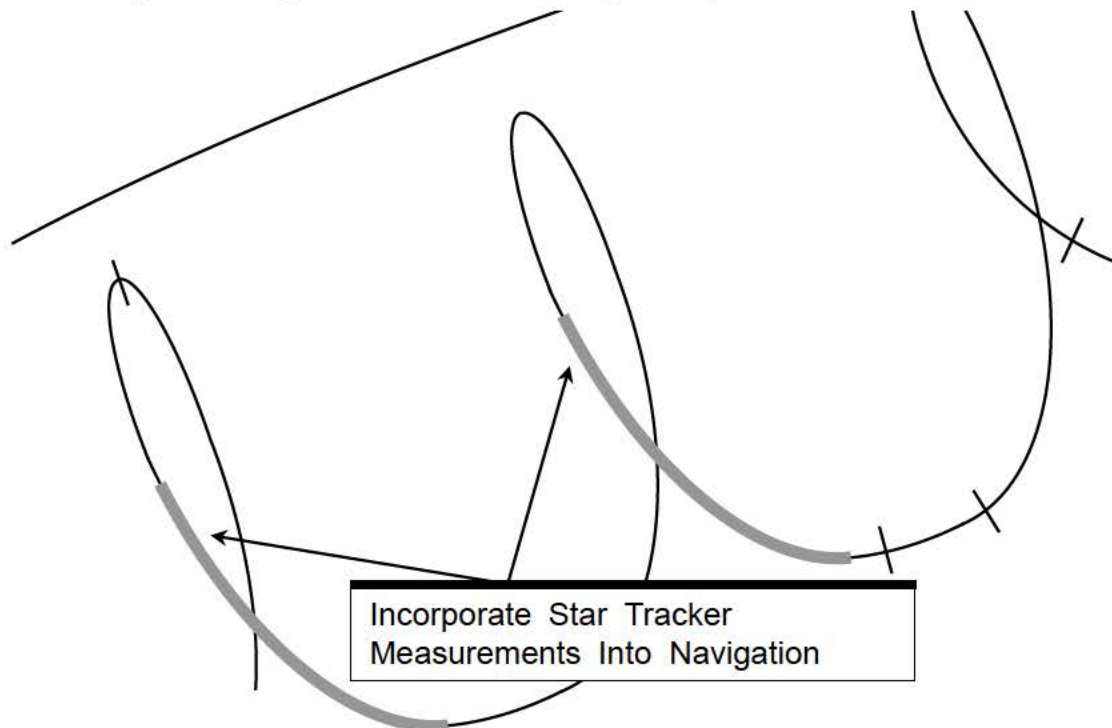
Most deploy/retrieve missions involve a two rev. to Ti transfer from in front.



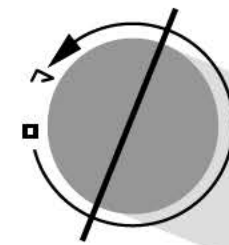
6.4 Nominal Star Tracker Passes

Two star tracker passes are performed for a two rev to Ti transfer. One is performed for the 1 rev to Ti case. Star trackers are vulnerable to bright objects, such as the Earth, Moon, and the ISS. Star tracker passes are planned to avoid known bright objects such as the Sun, Moon, and Earth limb. The bright object sensor in the star tracker will close the shutter before a known bright object enters the field of view.

Both the Image Detection Tube (IDT) and Solid State Star Trackers (SSST) have a suppression feature that will take action to protect the tracker from an object in the field of view that becomes too bright. The IDT will close the shutter. The SSST will set the star present flag to 0, or for an even brighter object will close the shutter.



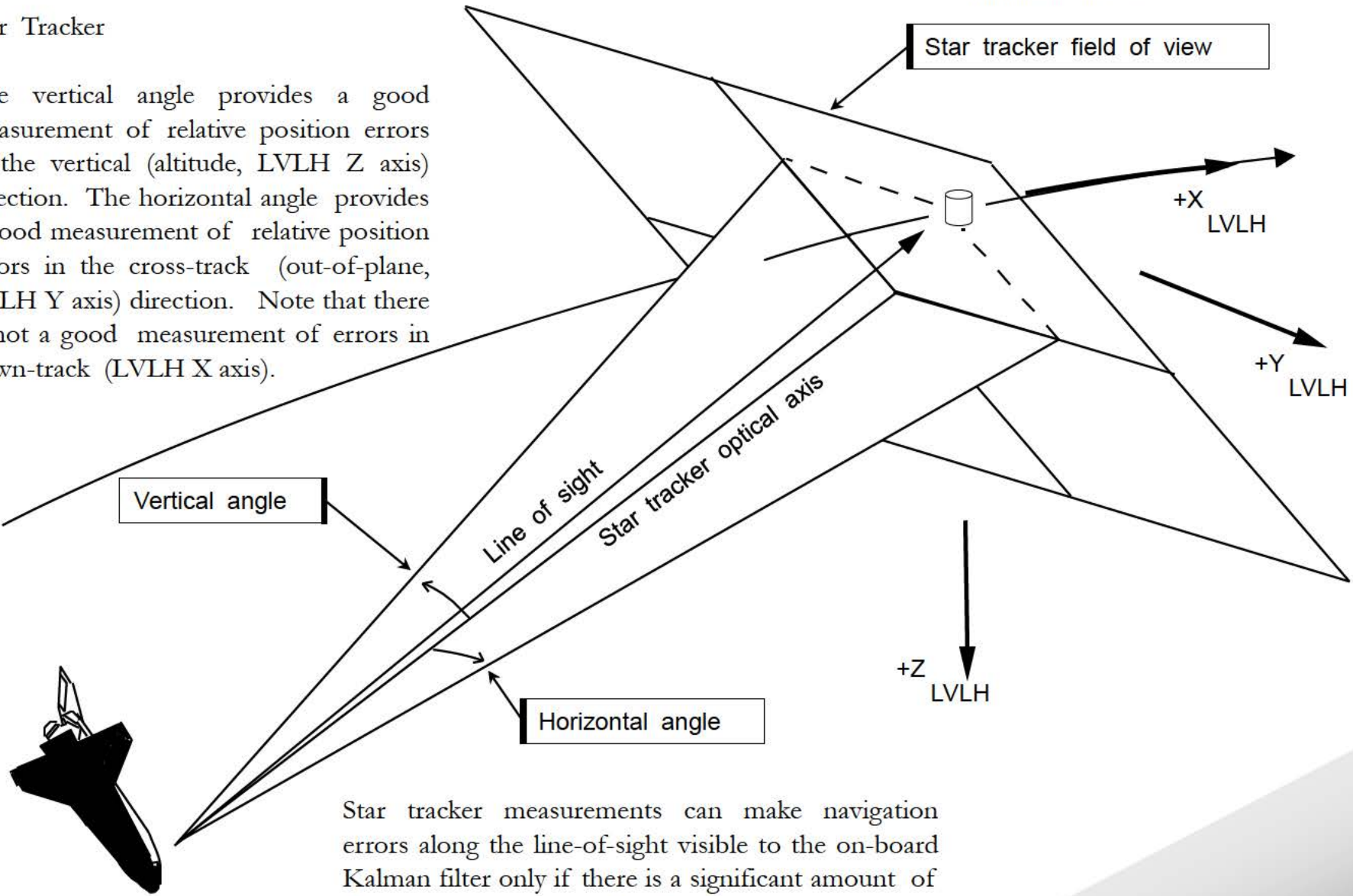
Passes are performed when the TARGET is illuminated by sunlight (orbital daylight).



Each pass starts at about orbital noon to ensure that the TARGET is front lit. The star trackers cannot reliably track a backlit TARGET.

Star Tracker

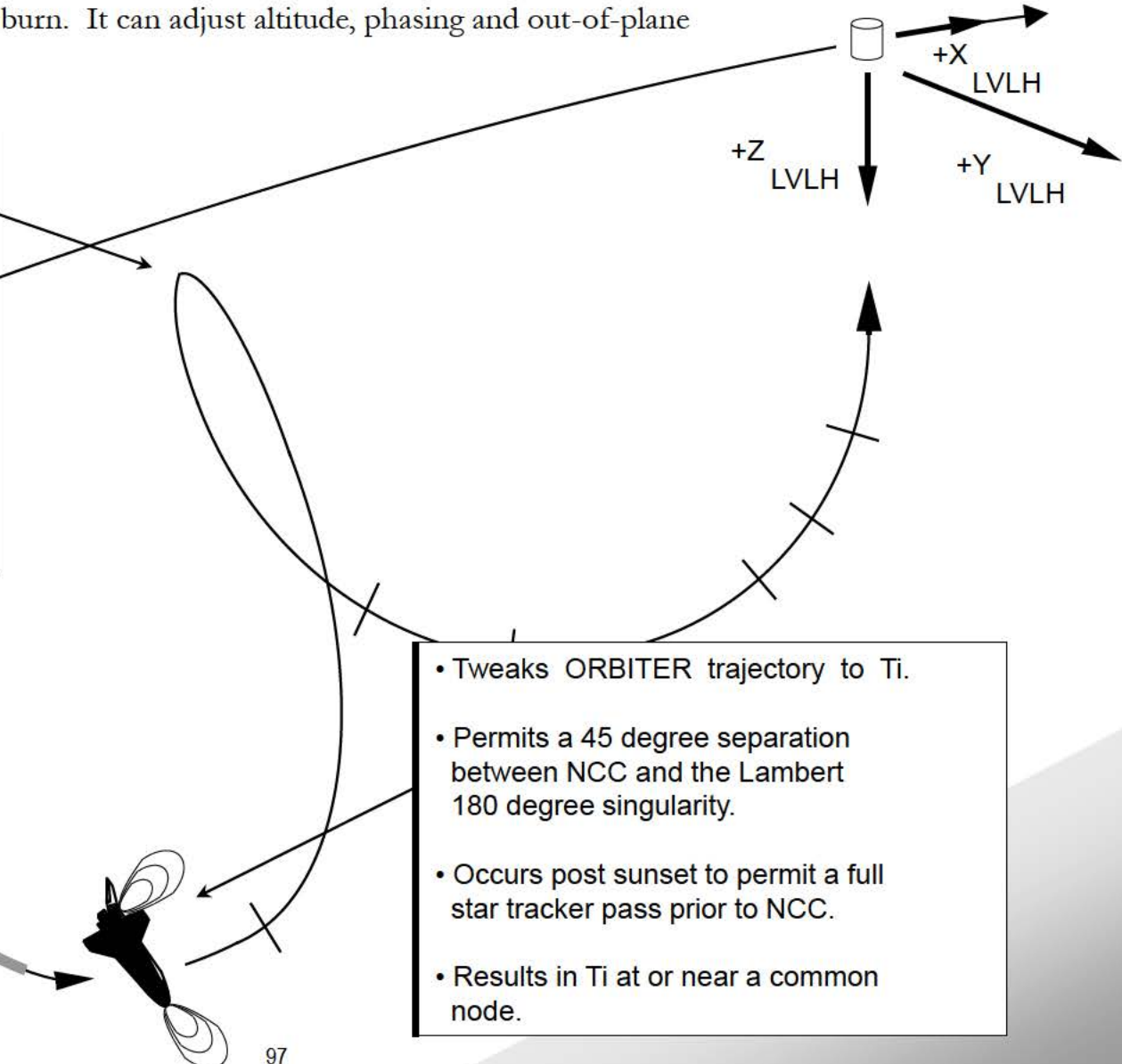
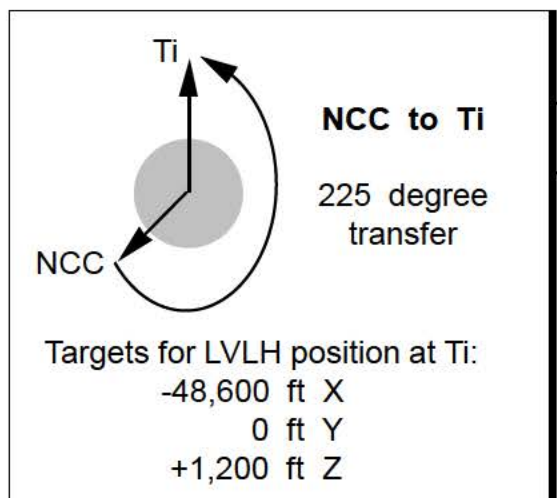
The vertical angle provides a good measurement of relative position errors in the vertical (altitude, LVLH Z axis) direction. The horizontal angle provides a good measurement of relative position errors in the cross-track (out-of-plane, LVLH Y axis) direction. Note that there is not a good measurement of errors in down-track (LVLH X axis).



Star tracker measurements can make navigation errors along the line-of-sight visible to the on-board Kalman filter only if there is a significant amount of geometry change during the star tracker pass.

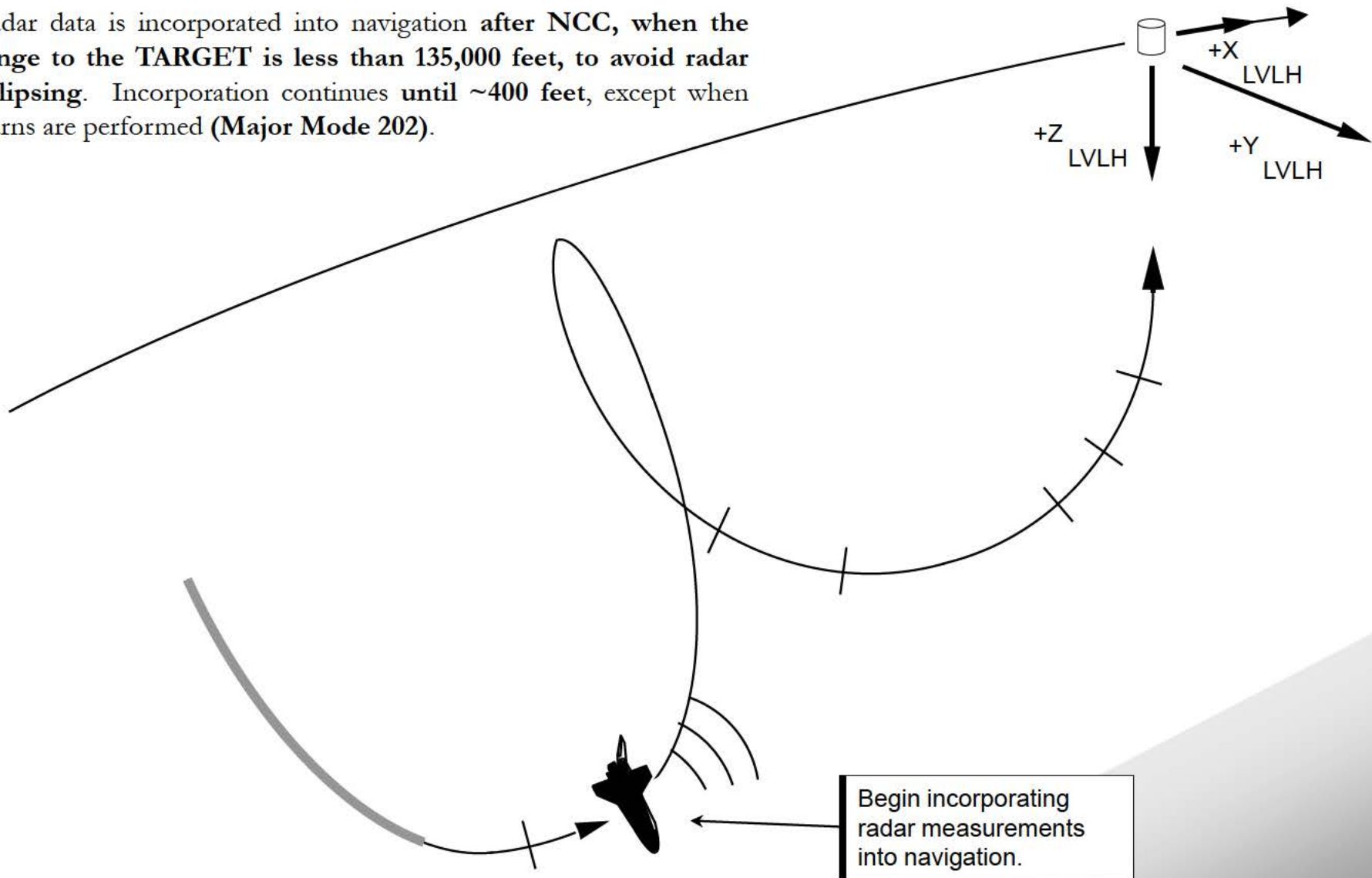
6.5 Corrective Combination Burn (NCC)

NCC is the first on-board targeted burn. It can adjust altitude, phasing and out-of-plane aspects of the trajectory.



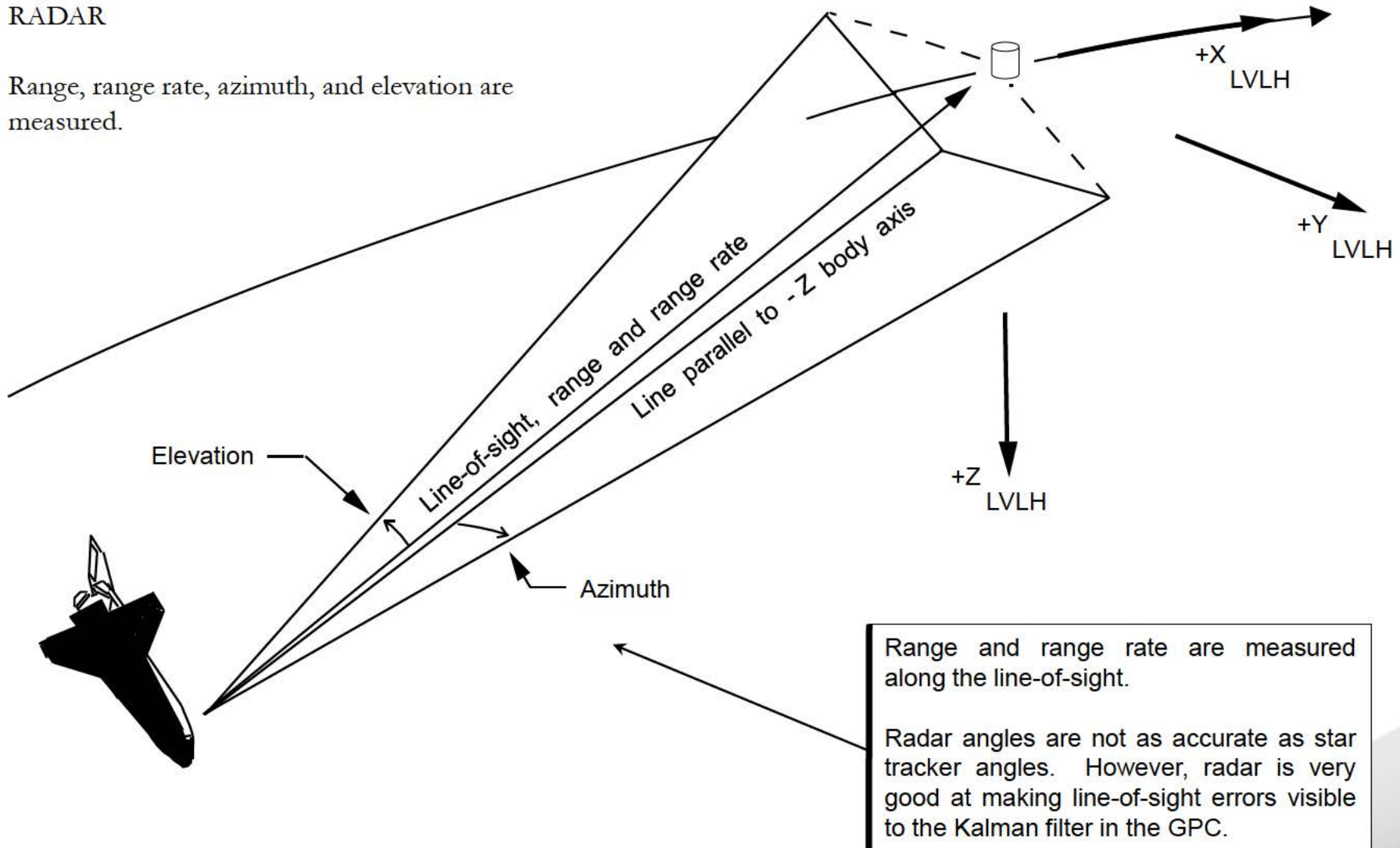
6.6 Radar Data Incorporation

Radar data is incorporated into navigation after NCC, when the range to the TARGET is less than 135,000 feet, to avoid radar eclipsing. Incorporation continues until ~400 feet, except when burns are performed (Major Mode 202).

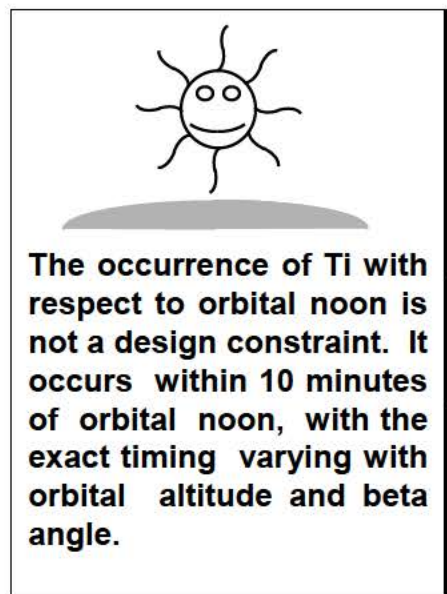


RADAR

Range, range rate, azimuth, and elevation are measured.



6.7 Transition Initiation Burn (Ti)

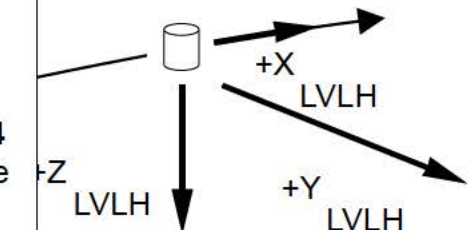
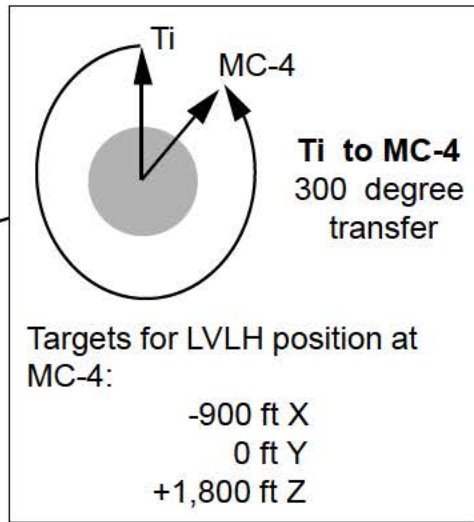


Transition Initiation Burn (Ti)

Places ORBITER on trajectory for the MC-4 (manual takeover point).

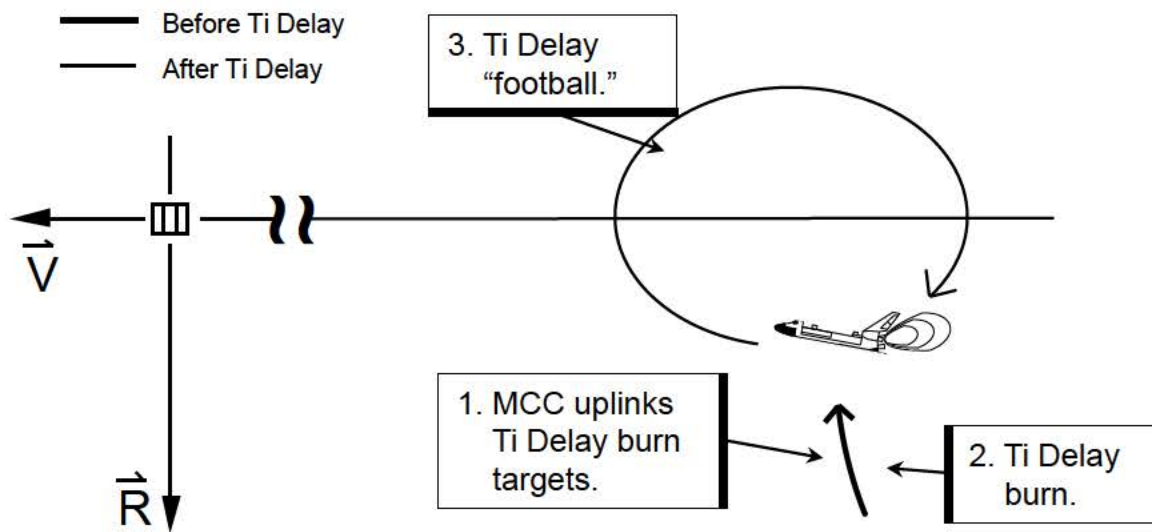
Occurs 8 nautical miles (48,600 feet) behind TARGET and 1,200 feet below X LVLH axis.

Timed to occur at sunset -38.5 minutes (β from -15° to $+15^\circ$) or -36 minutes for all other β angles, to ensure a star tracker pass after Ti in case of radar fail and to protect for RPM lighting.

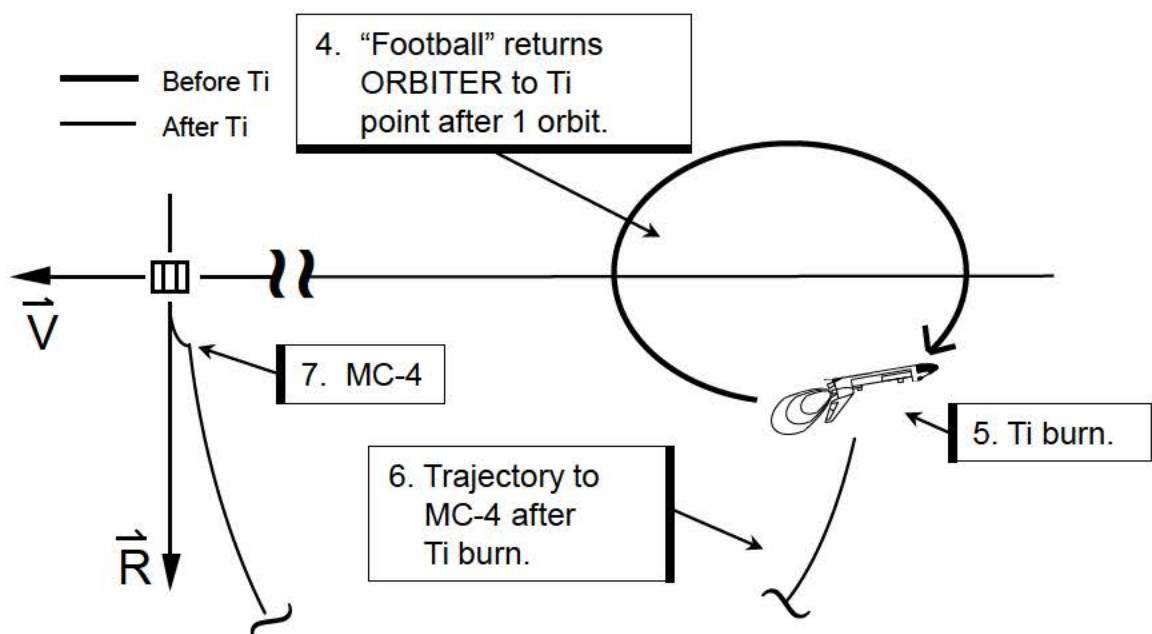


- Executing Ti below the V-Bar results in MC-4 ΔV as a mostly $+X$ RCS burn (little or no forward RCS required). It also permits the equivalent of MC-4 to be executed manually (for radar fail) with $+X$ pulses.
- Lighting constraint permits post Ti daytime star tracker pass before MC-1, and a night star tracker pass prior to MC-2.

Ti Delay Burn



The “Ti Delay” burn can be executed at Ti TIG to delay the rendezvous if a problem has developed. Ti Delay is ground targeted.



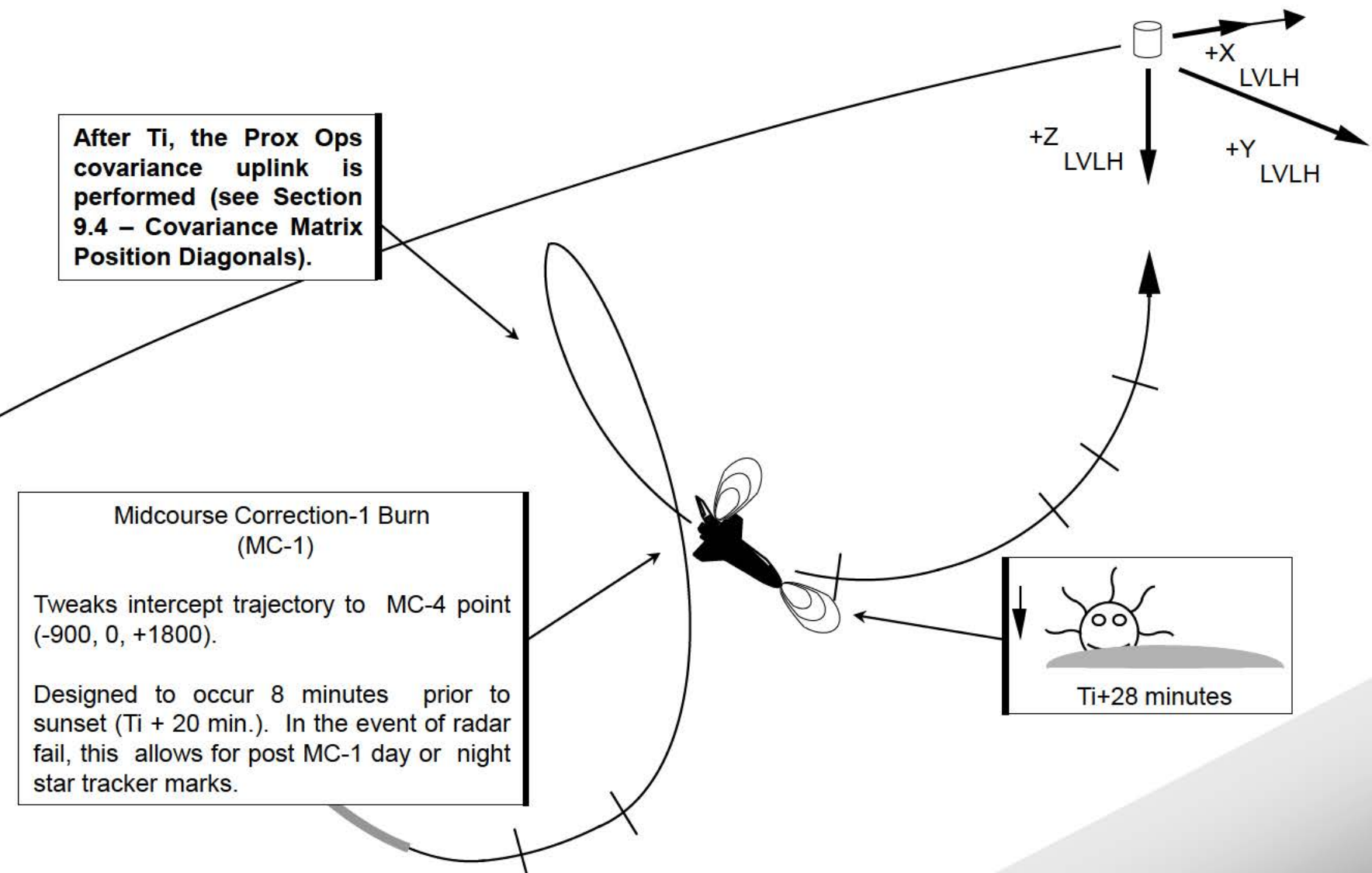
This burn places the ORBITER on a “football” shaped trajectory that will bring it back to the Ti point after 1 orbit. The Flight Dynamics Officer computes the burn so that the ORBITER will initially move away from the TARGET.

The size of the footballs on this page are exaggerated for clarity.

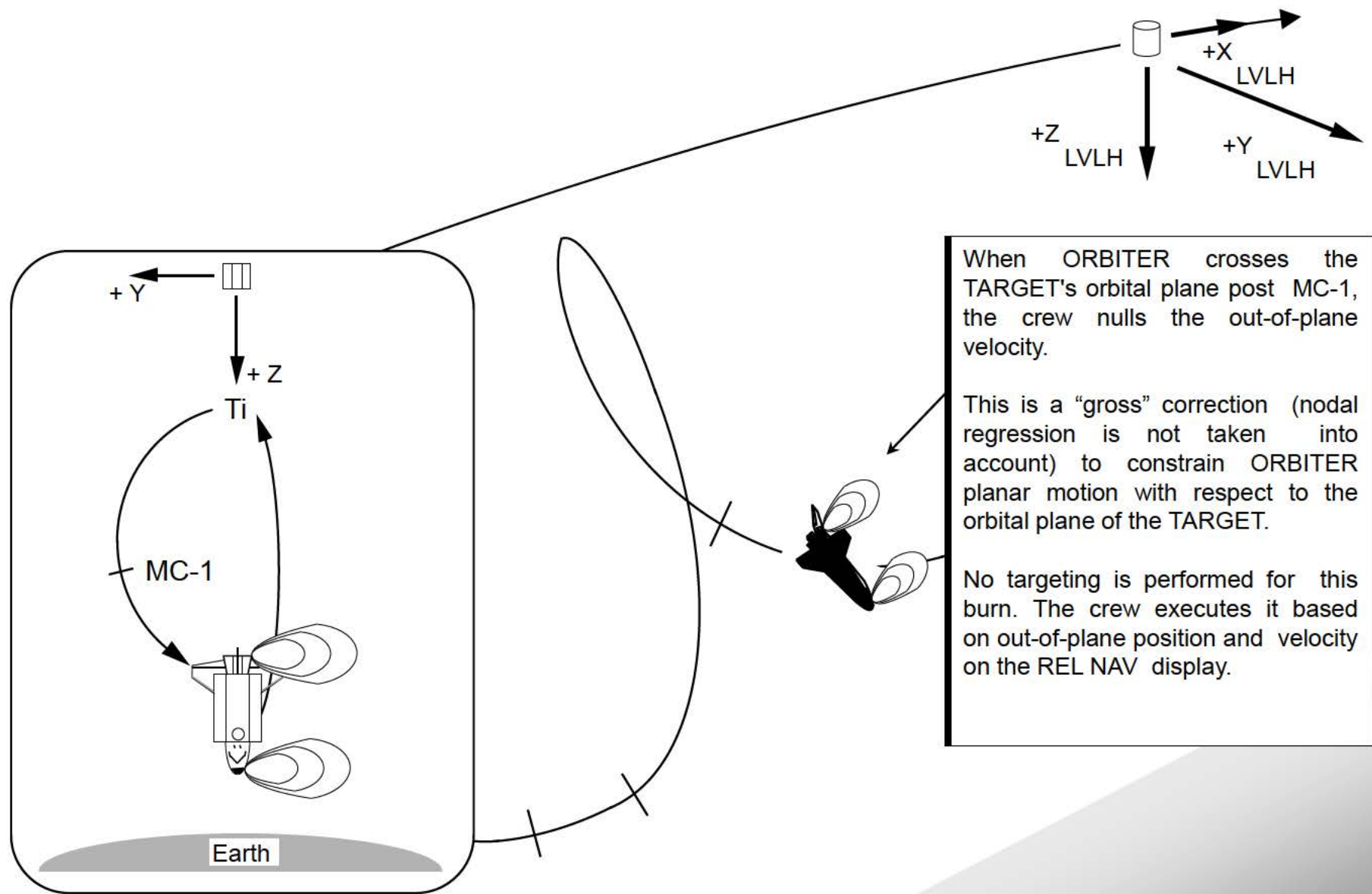
The ORBITER can stay on the football for up to three revolutions.

TIG for the new Ti burn must be computed so that proper lighting conditions will occur during the manual approach phase.

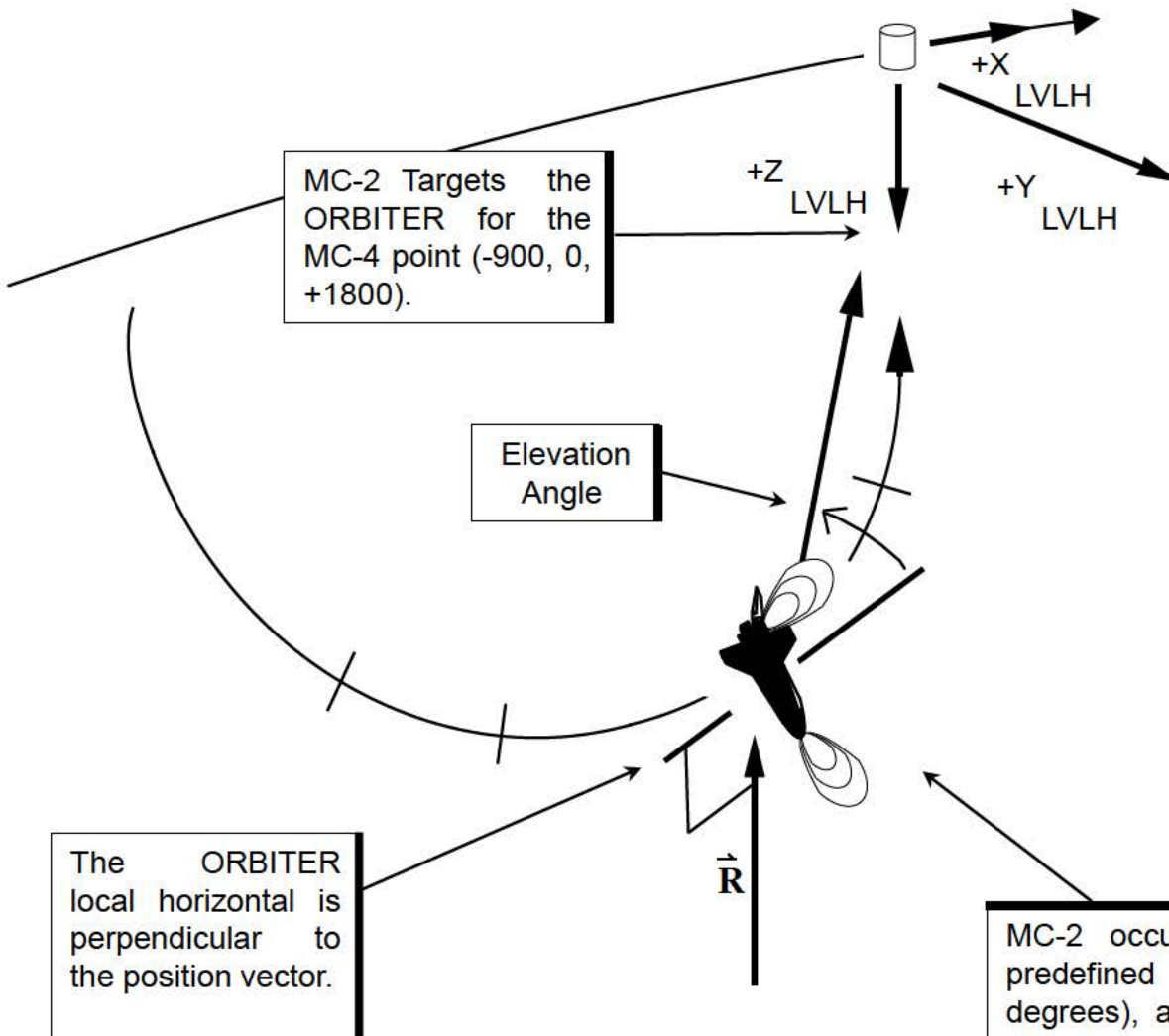
6.8 Midcourse Correction-1 Burn (MC-1)



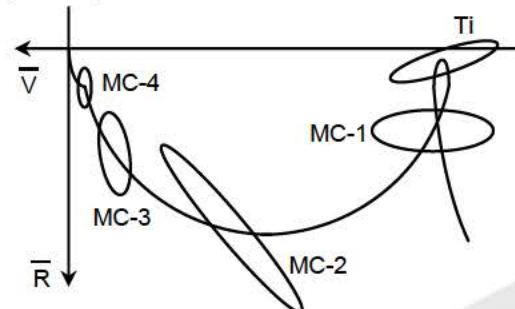
6.9 Out-of-Plane Velocity Null



6.10 Midcourse Correction-2 Burn (MC-2)

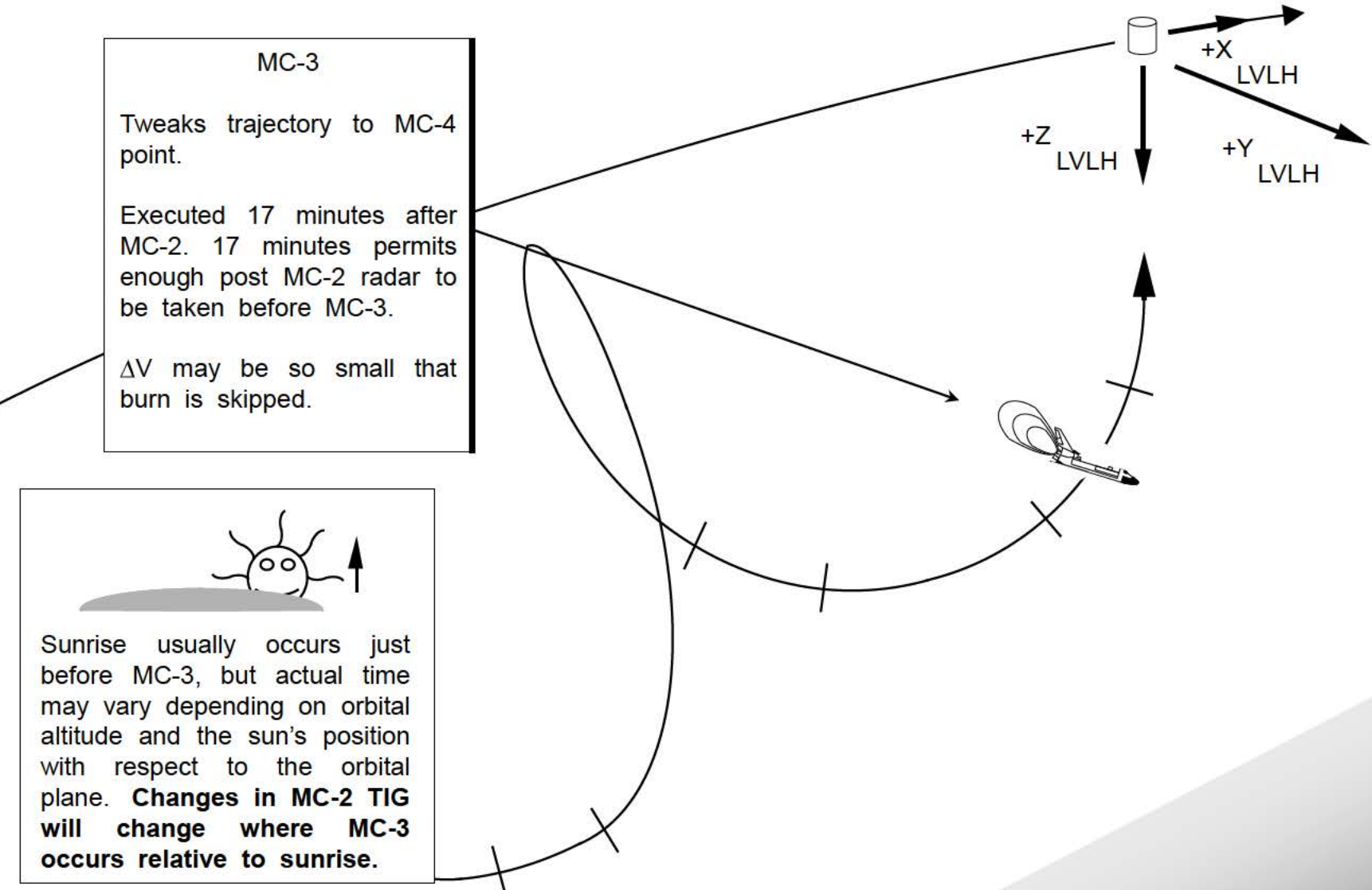


MC-2 preserves the geometry of the MC-2 to MC-4 trajectory for dispersed cases. To control downrange dispersions, the in-plane dispersion ellipse needs to be aligned with the trajectory.

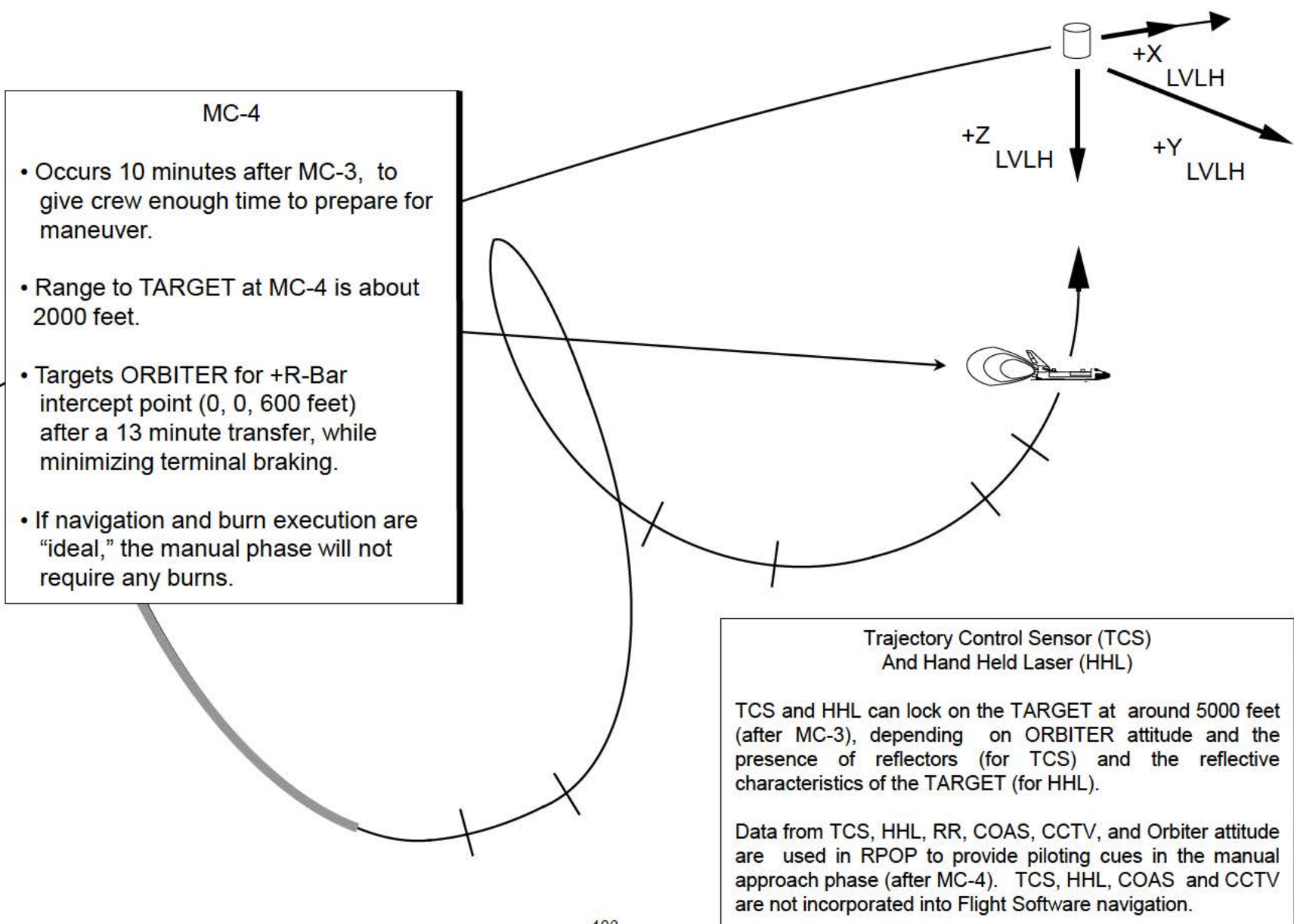


MC-2 occurs when ORBITER reaches a predefined elevation angle (around 28 degrees), around 27 minutes prior to MC-4. MC-2 TIG will vary.

6.11 Midcourse Correction-3 Burn (MC-3)

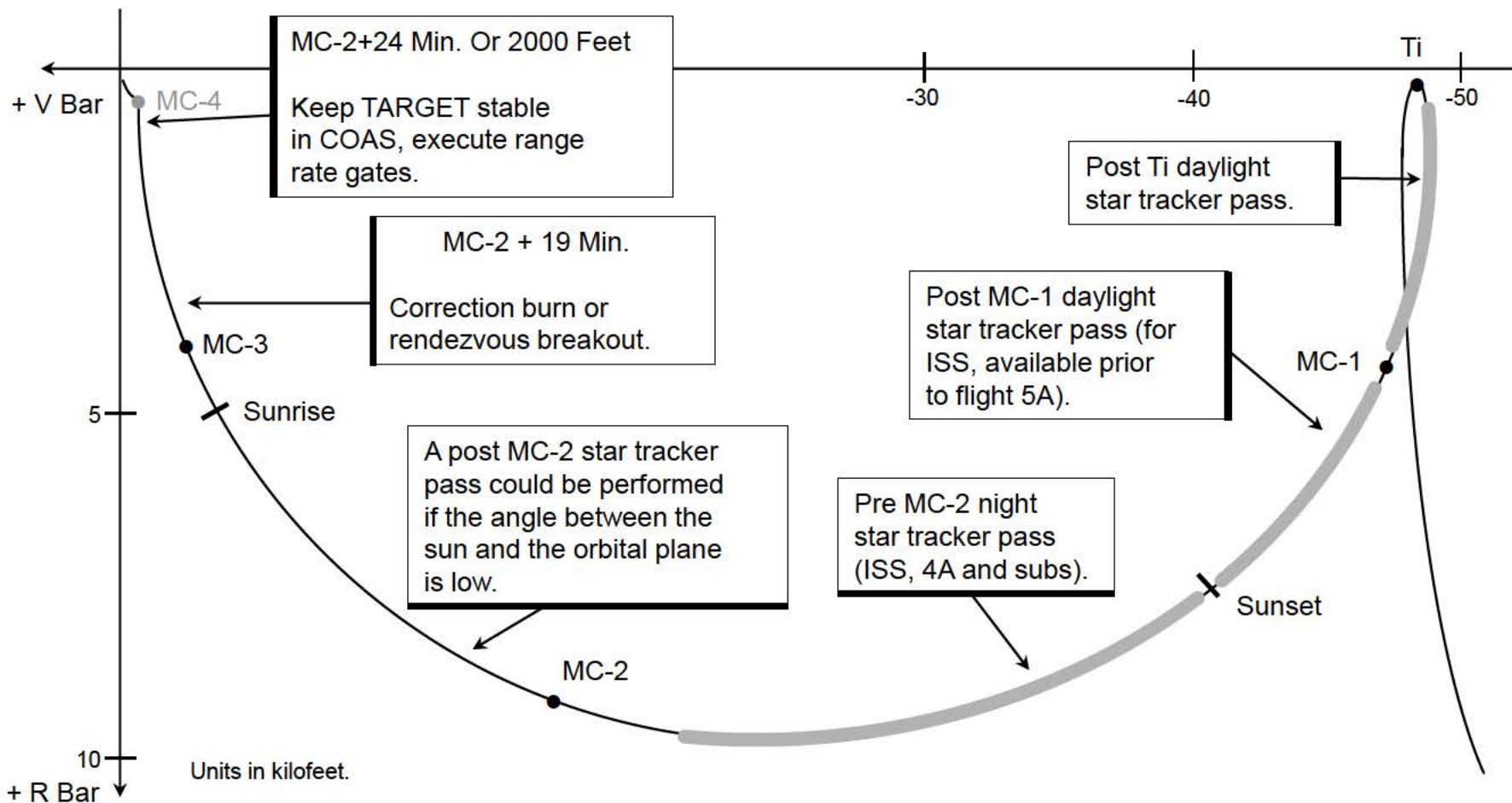


6.12 Midcourse Correction-4 Burn (MC-4)

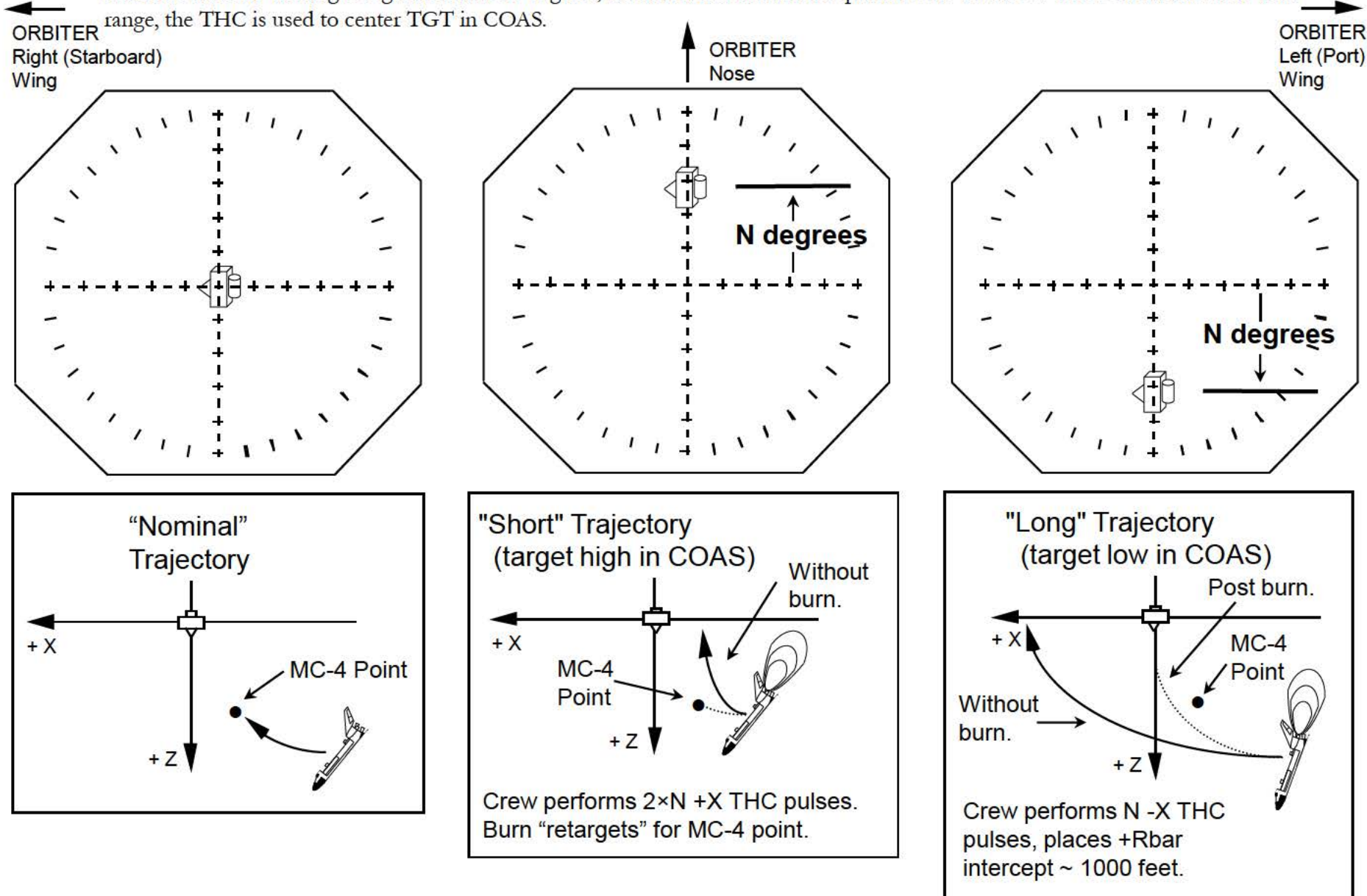


6.13 Radar Failure

In the event of a radar failure, star tracker navigation is performed after Ti (COAS navigation can also be performed, if needed). Daylight passes may be executed prior to and after MC-1. For ISS missions after flight 5A, ISS is too large and too bright for the daylight passes. A tracking light on ISS will permit night star tracker marks after sunset, post MC-1. MC-4 is not executed. Instead, a correction maneuver (or a breakout) is performed at MC-2+19 minutes (see next page). At MC-2 + 24 minutes, or range equals 2000 feet (whichever comes first), range rate gates are executed and the TARGET is kept stable in the COAS by orbiter translations.

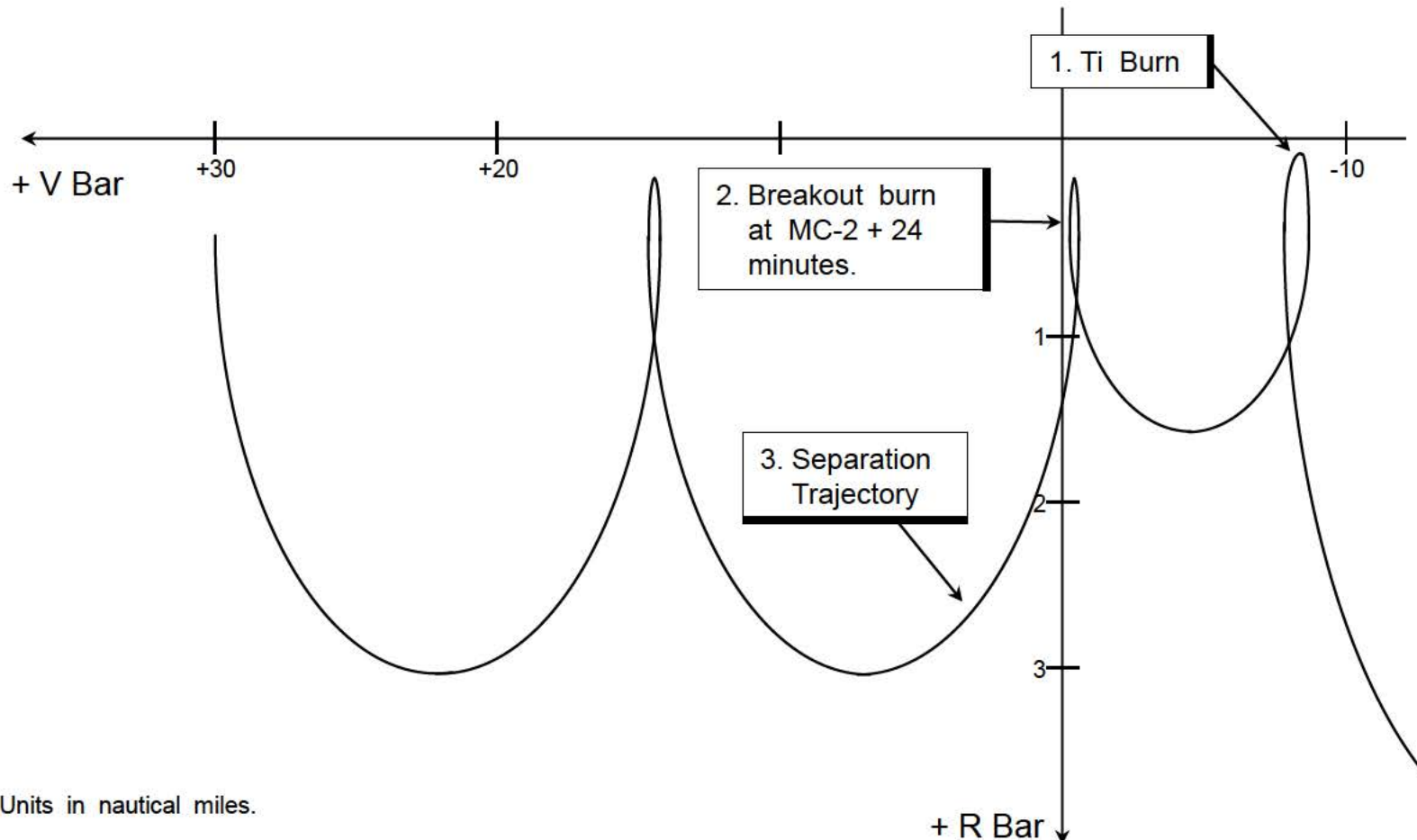


At MC-2+19 minutes, +X or -X pulses are performed depending on the vertical angle (see "N" below) in the COAS. If the absolute value of the angle is greater than 30 degrees, a rendezvous breakout is performed. At MC-2 TIG+24 min or 2000 foot range, the THC is used to center TGT in COAS.



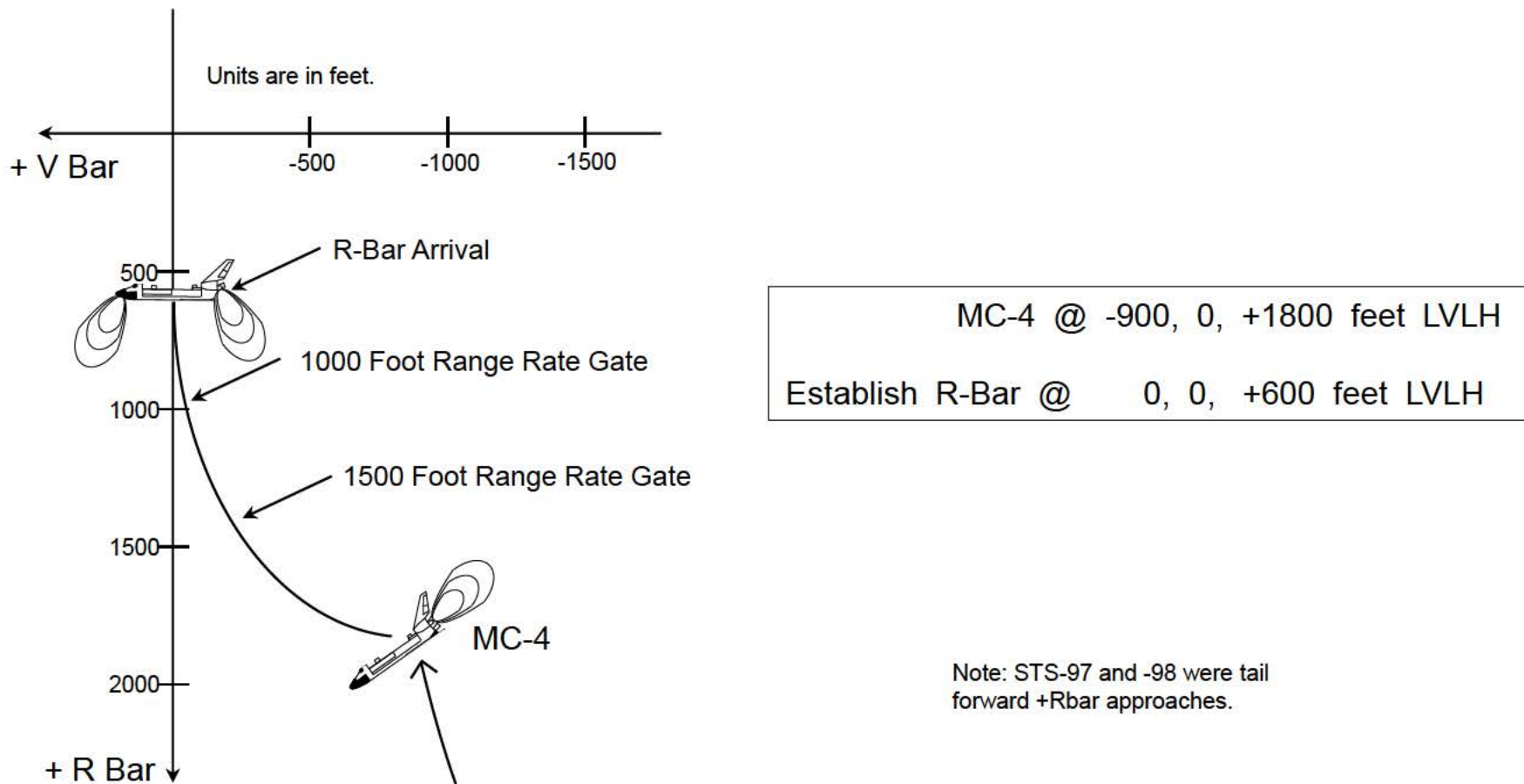
6.14 Rendezvous Breakout

If sensor data has been taken, breakout can be performed between T_i up until 500 feet on the +R-Bar. If sensor data has not been taken, breakout can be performed as late as MC-2+24 minutes. The maneuver for the Optimized Rbar Targeted (ORBT) profile involves a single, 3 foot/second retrograde burn.

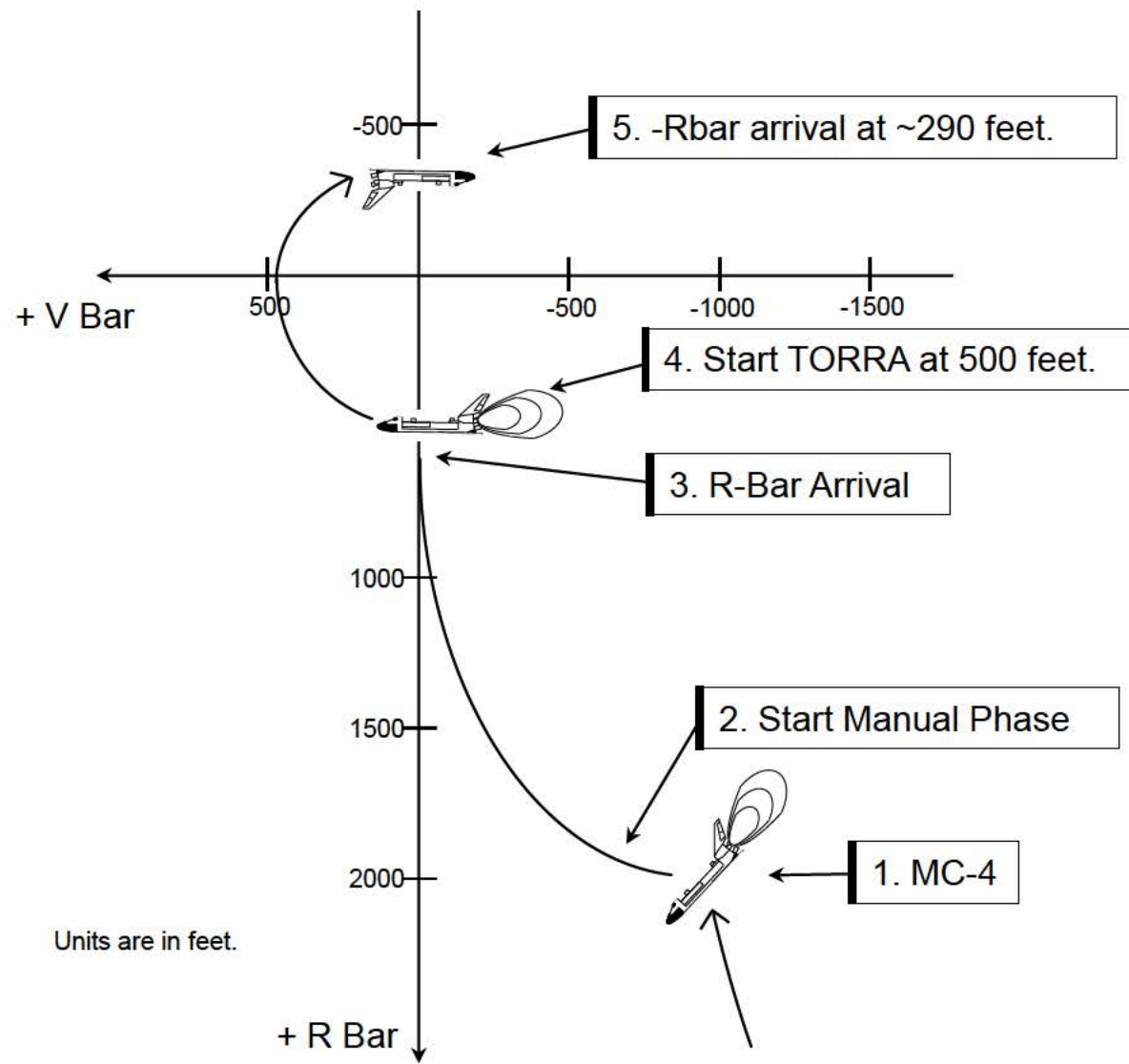


6.15 Final Approach

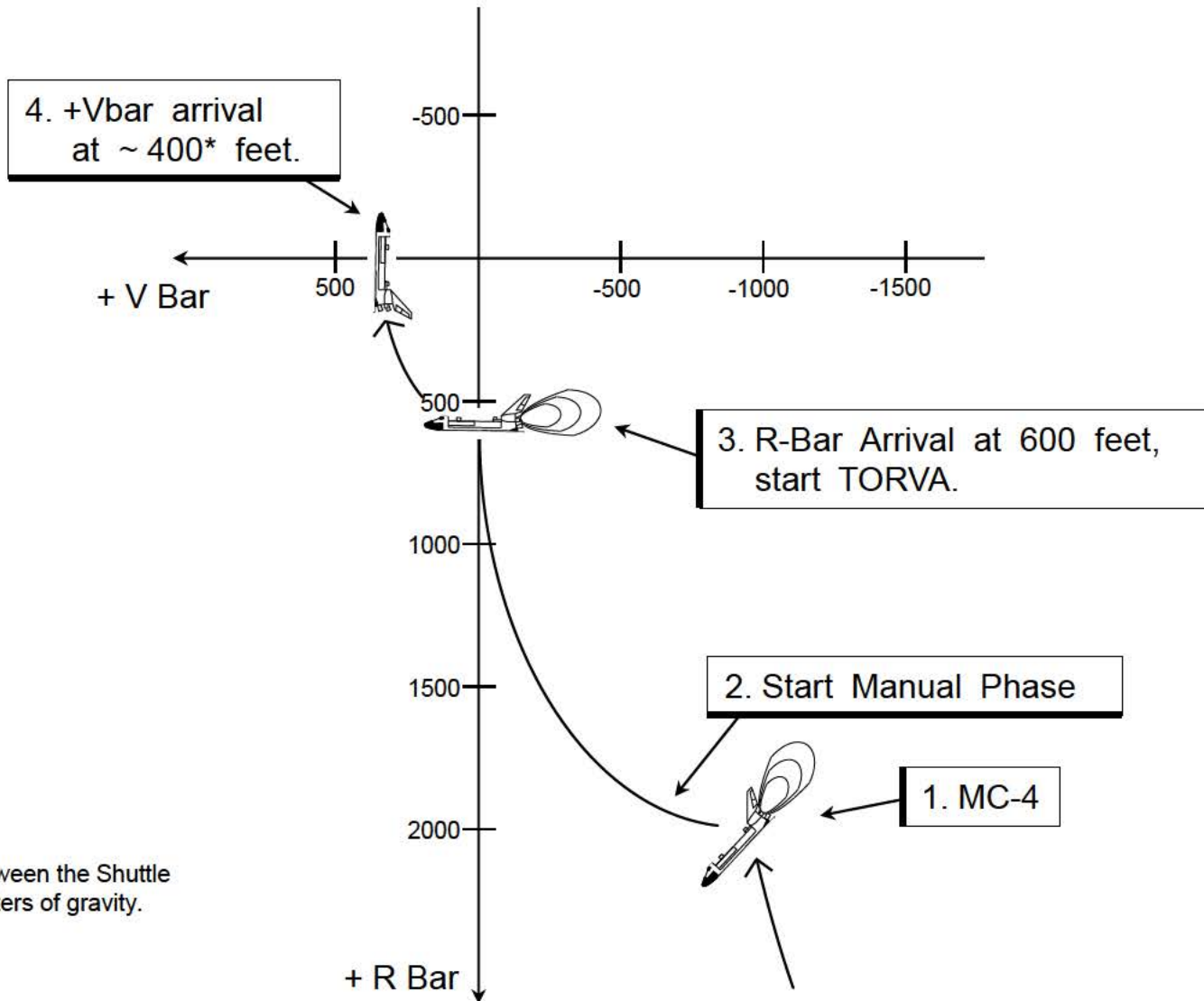
The ORBT profile design takes advantage of orbital mechanics effects to perform most of the braking inside 2000 feet, rather than using propellant to do most of it. MC-4 is the start of the manual phase (proximity operations). The commander will keep the TARGET stable in the COAS and perform range rate gates. After R-Bar arrival is established at 600 feet, procedures related to approach, fly-arounds, station keeping, grapple or docking are executed. These procedures are often mission dependent. ISS flights 4A and 5A (**STS-97 and -98**) used +Rbar approaches, as was done with Mir.



ISS flights 2A, 2A.1, 2A.2 and 3A flew to the +Rbar intercept point, then transitioned to the -Rbar using the Twice Orbital Rate +Rbar To -Rbar Approach (TORRA).



5A.1 (STS-102) and subsequent flights to ISS will fly to the +Rbar intercept point, then transition to the +Vbar using the Twice Orbital Rate Rbar To Vbar Approach (TORVA).



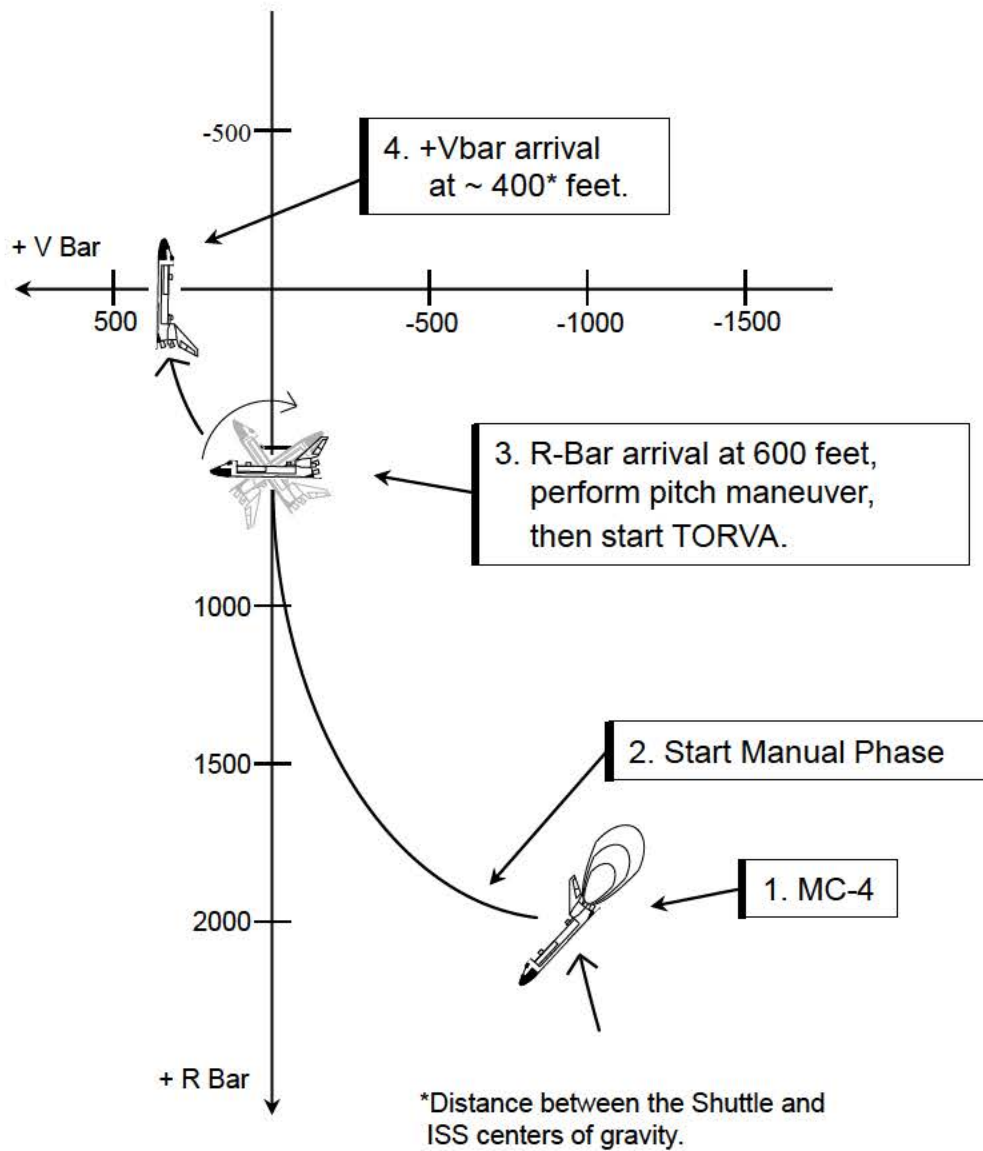
*Distance between the Shuttle and ISS centers of gravity.

6.16 Rbar Pitch Maneuver (RPM)

After the loss of *Columbia*, several methods were identified for inspecting the Orbiter's Thermal Protection System (TPS) for damage. The Rbar Pitch Maneuver, which is performed about 600 feet below the ISS, provides the ISS crew with about 1.5 minutes to photograph the underside of the orbiter.

The +Rbar is preferred over the +Vbar since the Service Module and U.S. Lab window field of views are along the nadir. The Rbar provides natural braking via orbital mechanics and provides safe relative motion during the maneuver. This is important since the crew and relative sensors (radar, TCS, HHL) cannot see the ISS during part of the rotation.

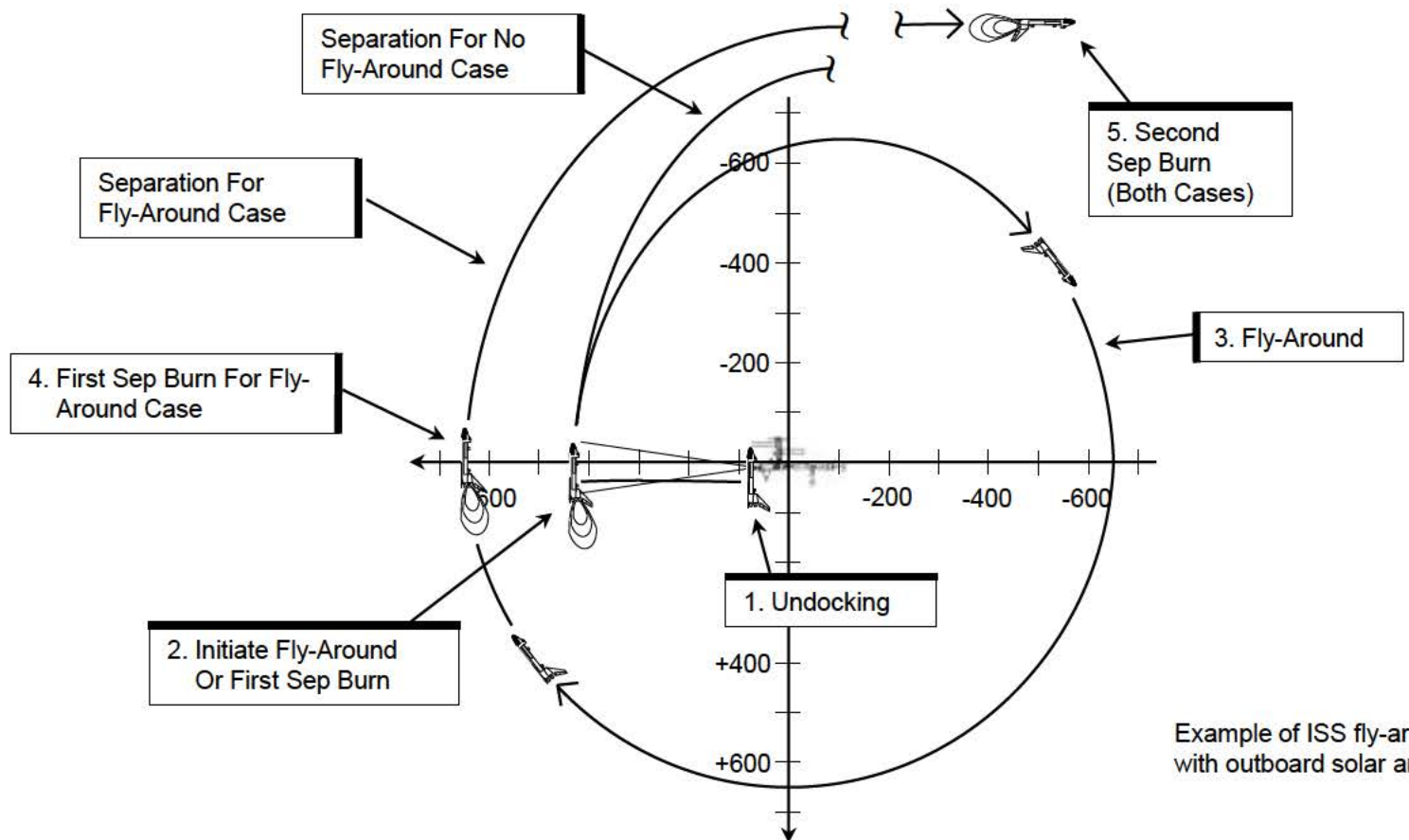
A pitch rate of 0.75 degrees/second was chosen to provide enough time for digital photography, while minimizing trajectory and attitude dispersions that could build up over the course of the maneuver. The orbiter flight control system is in FREE DRIFT for much of the RPM, to avoid plume impingement on the ISS windows, solar arrays feathered for docking, and other plume sensitive areas. A pitch maneuver was chosen over a roll maneuver since Low Z pitch firings introduce minimal coupling into the roll and yaw axes that could result in a higher than desired closing rate. The coupling that does occur offsets the orbital mechanics braking effect at 600 feet, and helps the RPM maintain a range of greater than 500 ft from ISS.



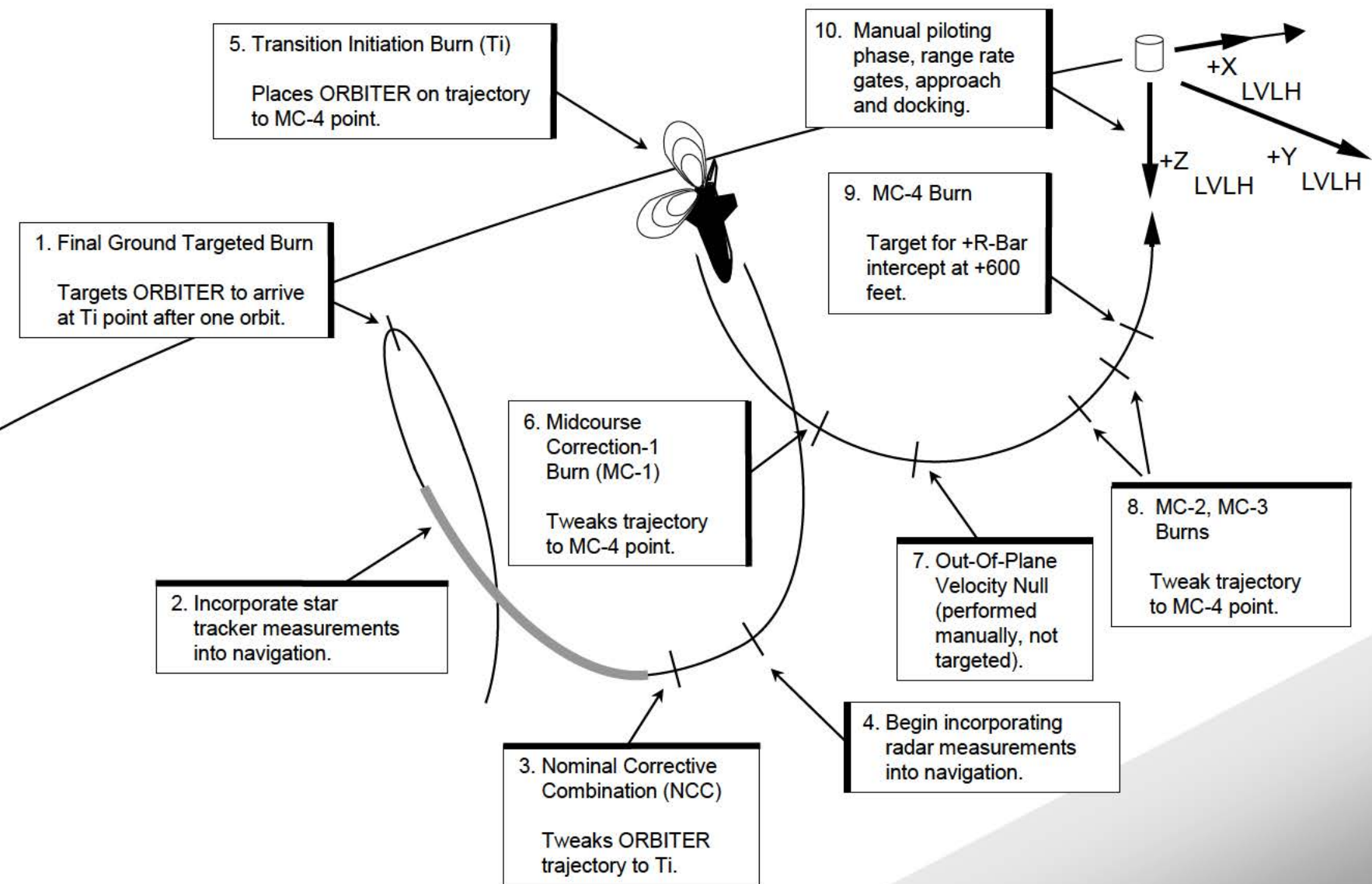
*Distance between the Shuttle and ISS centers of gravity.

6.17 Fly-Arounds and Separations

A fly-around to obtain photography of the ISS or other spacecraft may be performed before separation. Whether or not a fly-around is performed depends on propellant and crew timeline considerations. Fly-around trajectories, separation burns, and separation trajectories are dependent on target configuration and plume impingement constraints.



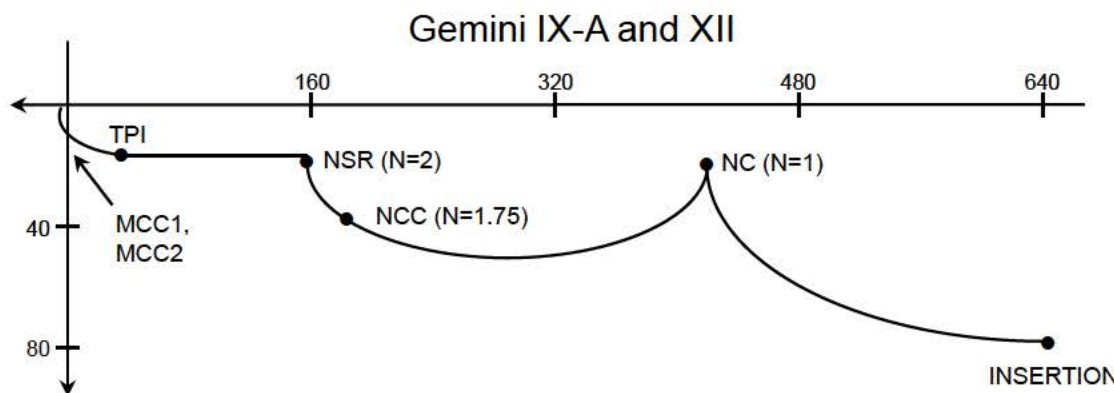
6.18 Summary of Day of Rendezvous Events



This page intentionally left blank.

7.0 Rendezvous Profile Evolution And Scenarios

This chapter covers the development of the on-board targeted phase of the rendezvous profile, from Gemini through Shuttle Optimized RBar Targeted (ORBT) rendezvous. Different rendezvous scenarios that have occurred in the shuttle program are also detailed.



7.1 Gemini

President Kennedy's goal of sending Americans to and from the moon by the end of the sixties necessitated the development of orbital rendezvous. The Gemini program was the testing ground for technologies and flight techniques needed for Apollo. In the early sixties, three rendezvous schemes were studied.

The first was the Tangential Orbit (a precursor of the Shuttle stable orbit profile). This involved launching the Gemini spacecraft into an elliptical orbit tangential to the Agena Target Vehicle (ATV) orbit. Rendezvous would occur near the apogee of the Gemini vehicles fourth orbit. However, this technique did not guarantee proper lighting conditions or relative dynamics in the terminal phase.

The second was the First Apogee (or Direct Rendezvous) profile. The Titan II booster would place the Gemini spacecraft on an intercept trajectory with the ATV. Gemini would achieve radar lock on the ATV soon after orbit insertion. However, the short amount of time for the crew to conduct on-orbit checkout of Gemini systems and rendezvous procedures made the timeline impractical. Furthermore, the trajectory was highly sensitive to ascent dispersions and lift-off delays. In the event of a dispersed trajectory, a backup rendezvous profile was needed. [In the early 1970s, this idea surfaced again. Mission 3B involved a Shuttle launch, rendezvous with and placement of a satellite in the payload bay, followed by a landing at Edwards within one revolution of launch. It too was eventually deemed impractical.]

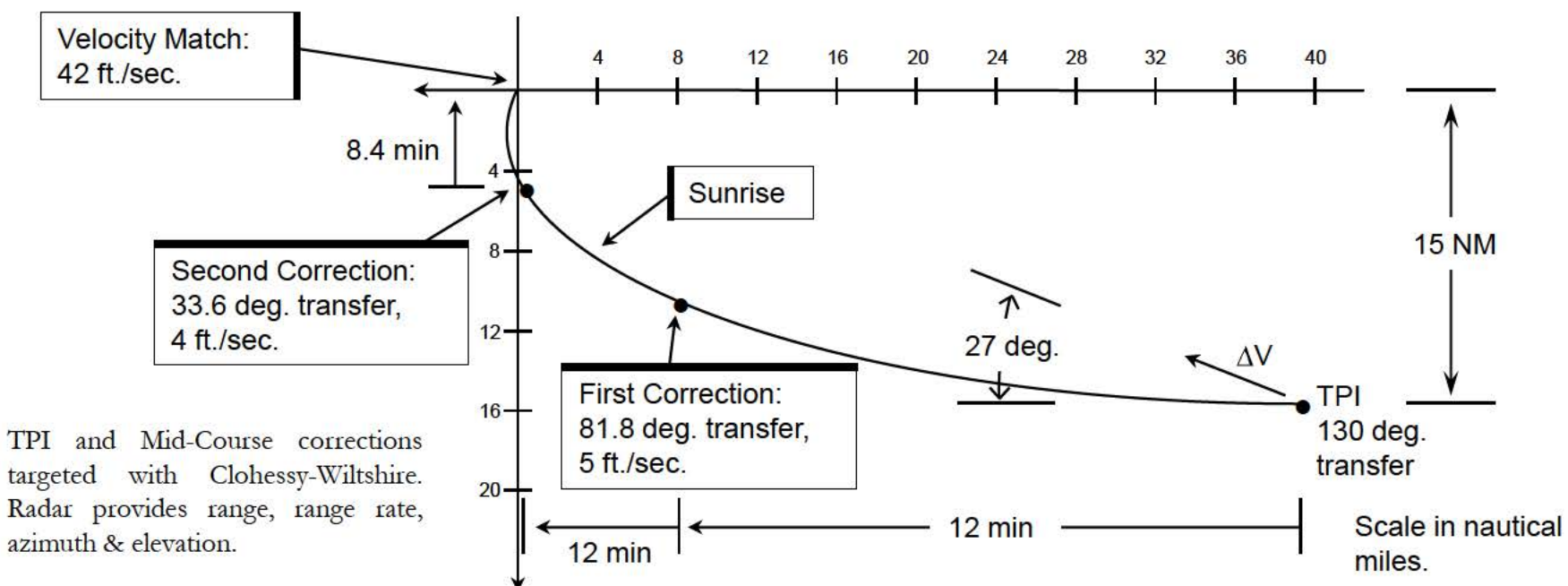
The third profile examined was the Concentric Height Profile. This used the same maneuver plan as the ground targeted phase in the Tangential Orbit profile, but had a different terminal phase. Rather than ground targeting placing the spacecraft on an intercept trajectory, it placed the Gemini in a coelliptic orbit with respect to the ATV. The length of the coelliptic phase could be controlled to ensure appropriate lighting during the terminal phase. The terminal phase would begin once certain relative geometry criteria were met. This profile was baseline for Gemini in mid 1964 (when the author was six months old).

Three different parameters had to be chosen for the terminal phase: the AH for the coelliptic orbit, the relative geometry cue upon which the terminal phase would be initiated and the angular transfer. In addition, a thrusting methodology had to be identified that would permit burn execution in the event of spacecraft system failures.

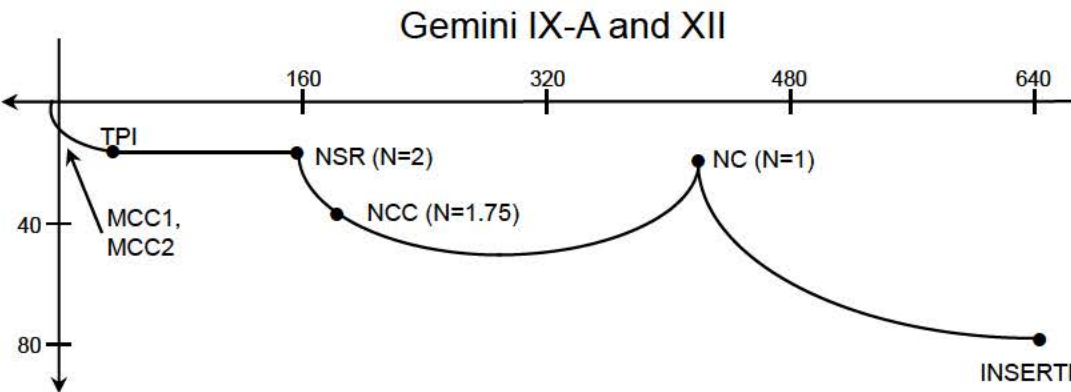
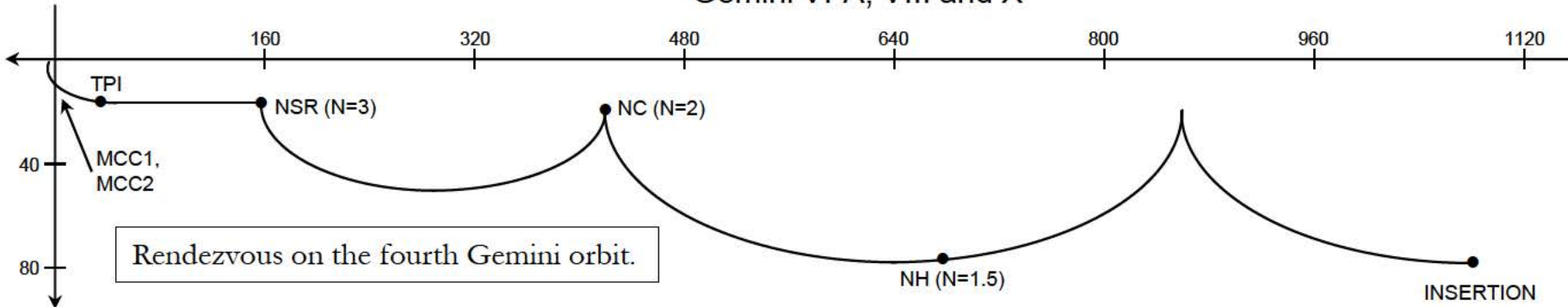
It was decided that the Terminal Phase Initiation (TPI) burn should have a ΔV that was along the line-of-sight to the ATV. The advantage of this burn over a horizontal ΔV was that it was easier to execute with backup procedures.

For the relative geometry cue, elevation angle of the ATV with respect to the Gemini local horizontal was chosen over range, relative radial velocity, time and minimum ΔV . In the presence of dispersions, range, relative radial velocity and elevation angle were equally insensitive. Elevation angle determination was the least vulnerable to equipment failures and easy to incorporate into backup procedures. Elevation angle was also a convenient attitude reference for the crew.

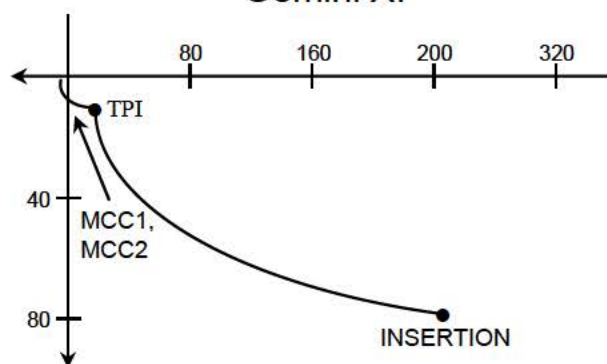
ΔH was chosen as a trade-off between visual sighting requirements, minimizing the impact of dispersions in the terminal phase, minimizing closure rate when approaching ATV and minimizing ΔV . Lower values of ΔH were favored. A transfer angle of 130 degrees was chosen. This value resulted in manual phase characteristics (inertial line-of-sight rates, range rate and lighting) that were the least sensitive to TPI TIG and ΔV dispersions.



Gemini VI-A, VIII and X

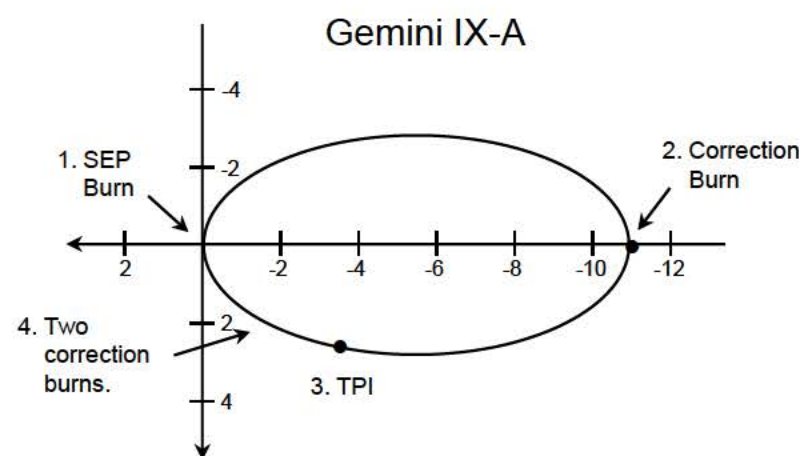
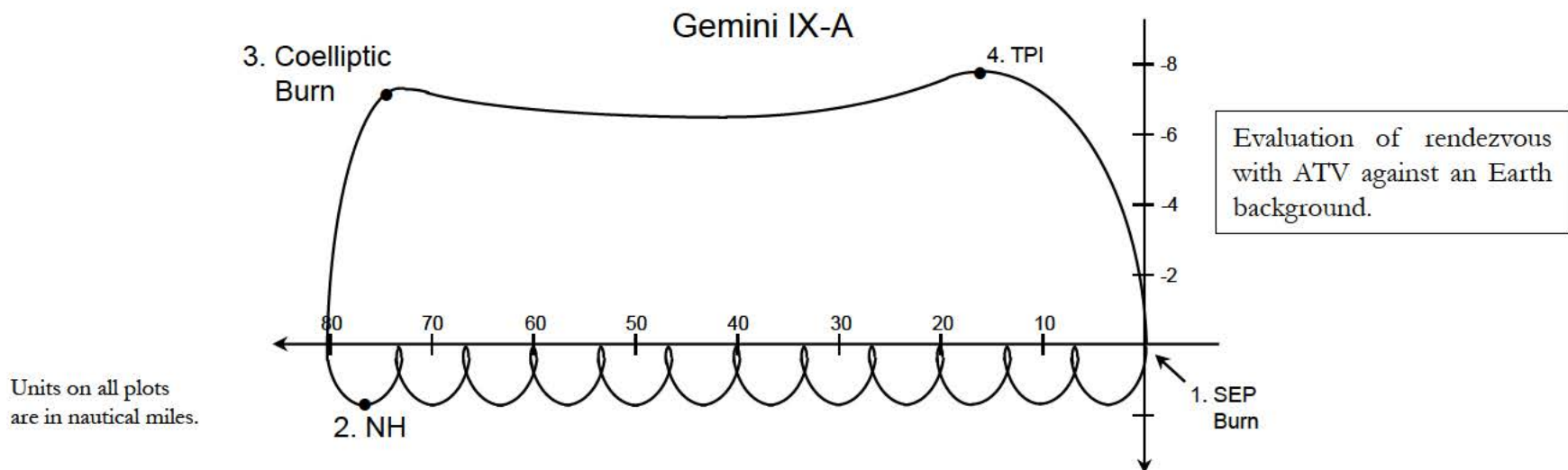


Gemini XI

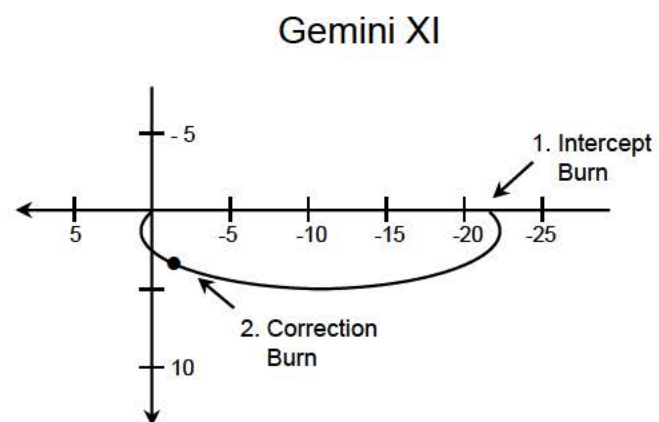


Units on all plots are in nautical miles.

Variation of the First Apogee profile. Two on-board targeted burns (one right after insertion) performed using radar data to adjust out-of-plane motion, phasing and altitude.



Evaluation of optical only rendezvous procedures to be used on Gemini X dual rendezvous. TPI was an 80 degree transfer.



Stable Orbit Profile - Intercept burn started a 292 degree transfer. Correction burn was a 34 degree transfer. Both ground targeted. Crew performed manual phase without radar.

7.2 Apollo

The rendezvous profile for the lunar missions built on the work done during Gemini. As with Gemini, it was desired to have a terminal phase whose characteristics (line-of-sight rates, closure rate, lighting) were more or less the same whether the trajectory was dispersed or not. The TPI and terminal phase design from Gemini was adapted for Apollo. The LM was the active vehicle during rendezvous. In the event of a LM systems failure, the CSM could go active.

Burns had to be small enough to permit execution with LM RCS. The LM ascent engine could not be relied upon due to lack of propellant after ascent.

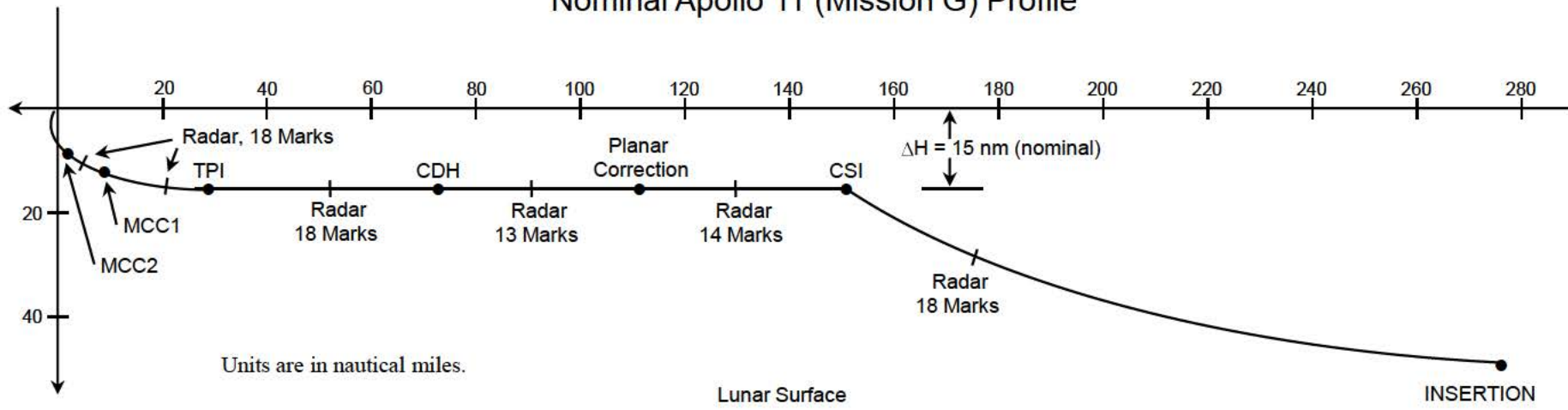
The LM had rendezvous radar (range, range rate, shaft and trunnion angles). LM rendezvous navigation using the radar was active before and after each burn. The covariance matrix was reinitialized after each burn, before more radar data was processed. LM radar had both skin track and cooperative modes. There was a transponder on the CSM to support the cooperative mode. LM burn solutions were voiced to the CSM for incorporation into the CSM navigation estimate of the LM state.

CSM used VHF ranging and a sextant for angles (with a COAS to backup the sextant), and tracked the LM throughout the rendezvous. A VHF transponder was on the LM to support VHF ranging. Sextant marks and VHF ranging marks were taken at a rate of about one per minute. Both the CSM and LM had flashing lights to aid visual tracking. The ranging limit for both the CSM and LM was about 320 nautical miles. In the event of a LM radar failure, CSM VHF ranging data could be voiced from the CSM to the LM and manually entered into the LM Auxiliary Guidance System (AGS).

State vectors from rendezvous navigation on both vehicles were available to Mission Control, and could be uplinked to either vehicle.

Apollos 9, 10, 11 and 12 used the coelliptic sequence prior to the Terminal Phase Initiation (TPI) burn. Apollo 13 was planned to use the same sequence.

Nominal Apollo 11 (Mission G) Profile



Terminal Phase Initiation (TPI)

- Elevation angle of 26.6 deg.
- ΔV along line-of-sight to CSM, provides a visual reference in the event of system failures.
- Nominal ΔV 25 ft/sec, 130 degrees transfer over 43 min.
- Magnitude of ΔV proportional to ΔH .

Plane Change (PC)

- Performed if out-of-plane $\Delta V > 5 \text{ ft/sec}$.

Coelliptic Sequence Initiation (CSI)

- Adjust catch-up rate to achieve 26.6 deg. elevation angle at mid-point of lunar darkness (TPI).
- Raise perilune to 45 nm.
- ΔH may vary from 15 nm due to ascent dispersions.
- ΔV constrained to be horizontal to avoid lowering perilune.
- Varying ΔH permits CSI to be horizontal while maintaining terminal phase timing.
- If CSM tracking indicates sizable out-of-plane dispersion, ΔV added to set up nodal crossing 90 deg after CSI (PC burn).

Insertion

- 10 nm x 45 nm orbit.
- CSM in 60 nm orbit.
- 7.5 min. powered ascent.
- Nominally 3 hours, 25 min. from insertion to station keeping on +V Bar.

Braking Gates

Range (ft)	R_Dot (ft./sec.)
6000	30
3000	20
1500	10
600	5

Constant Delta Height (CDH)

- Align lines of apsides of CSM and LM orbits.
- Establish constant ΔH .
- ΔV small for non-dispersed trajectory.

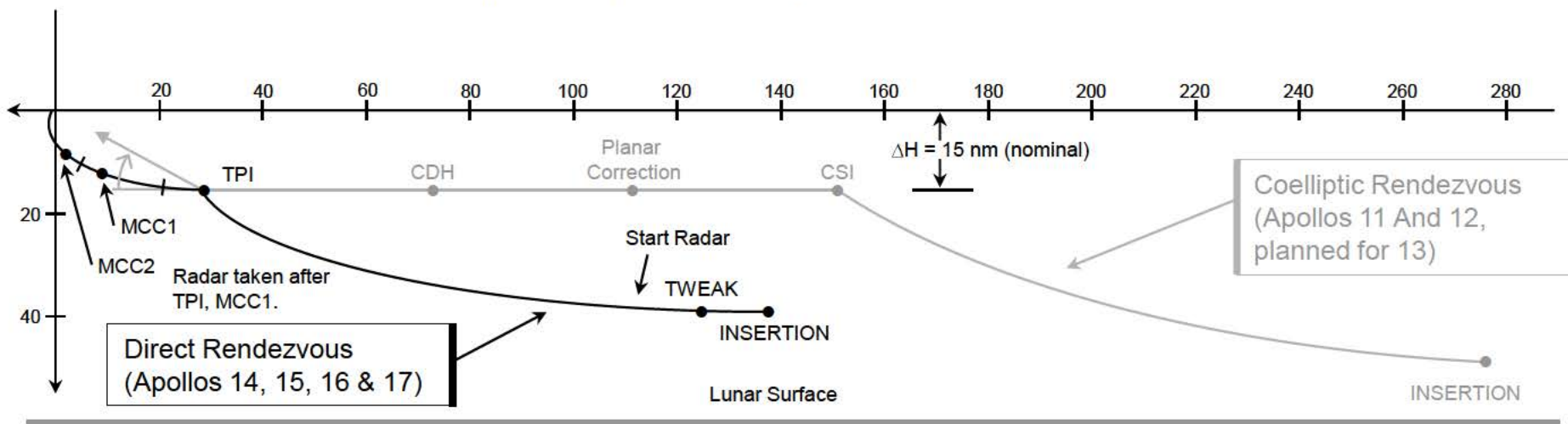
INSERTION to CSI	51 min
CSI to PC	28 min
PC to CDH	30 min
CDH to TPI	39 min
TPI to MCC1	15 min
MCC1 to MCC2	15 min
MCC2 to Station Keeping	27 min

Apollos 14, 15, 16 and 17 did not use the coelliptic sequence. Instead, the rendezvous was designed to be accomplished within the first revolution after LM orbit insertion. This saved about 2 hours compared to the coelliptic profile performed on Apollos 11 and 12 (a lunar orbit took 2 hours).

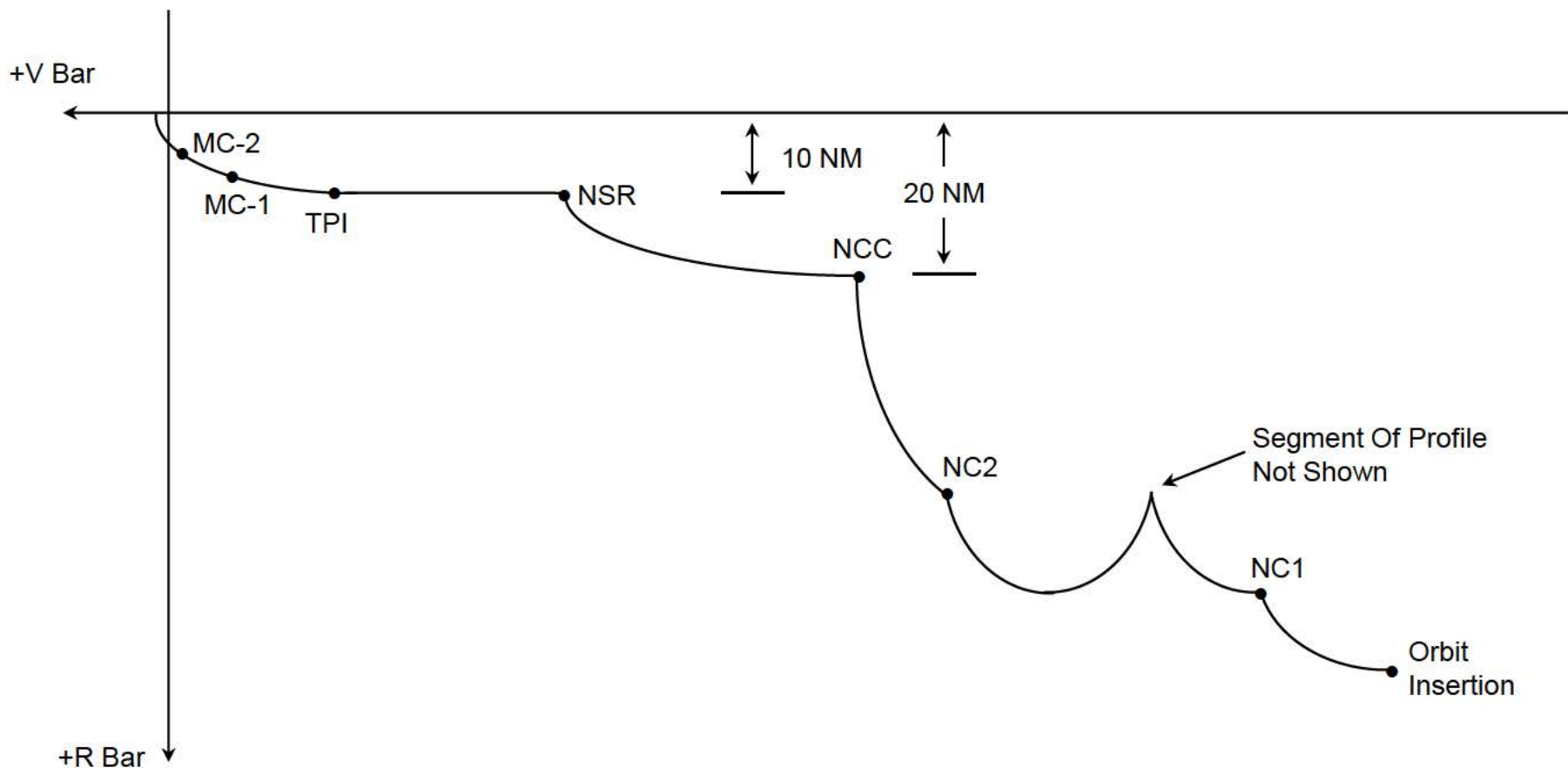
LM ascent guidance was designed to get the LM to the desired TPI geometry soon after lunar orbit insertion (38 minutes for Apollo 14, 45 minutes for Apollo 15 and 47 minutes for Apollos 16 and 17). A small correction burn was executed after insertion. If the ΔV for the tweak was greater than 60 feet/second, a “LM Bailout” procedure was executed and a CSI/CDH rendezvous would be performed. In addition, the insertion wedge angle had to be less than 0.5 degrees.

Both of the LM rendezvous profiles are illustrated below.

Apollo 14 (Mission H-3) Direct Rendezvous Profile



For Skylab and Apollo/Soyuz flights, the terminal phase was similar to the lunar flights. An NCC/NSR sequence was used prior to TPI, rather than the CSI/CDH sequence.



Shuttle rendezvous was potentially more challenging than Gemini and Apollo rendezvous. The Agena, Lunar Module, Command Service Module, Skylab and Soyuz (for Apollo Soyuz) were outfitted with Flashing lights and radar transponders. In addition, on the lunar missions, the MCC had access to rendezvous navigation data from both the IM and CSM. The Shuttle had to be able to rendezvous with passive targets (no radar transponders or lights). RCS jets placement on the Shuttle was driven by entry considerations (attitude control could couple into translational AVs). On Gemini and Apollo they were optimized for orbital flight (both Gemini and the Apollo Command Module used different RCS systems during reentry than on-orbit). Shuttle RCS jets were larger than those on Gemini and Apollo vehicles, and created plume impingement problems on targets. The Shuttle also had a limited amount of forward RCS propellant available. The Apollo CSM and LM had larger propellant reserves available for rendezvous maneuvers.

The original Shuttle rendezvous profile identified by the Mission Planning and Analysis Division (MPAD) was the Double Coelliptic (see next page). The manual phase was similar to that on Gemini/Apollo, but TPI was performed 8 minutes after sunset (to allow a star tracker pass prior to TPI and a final approach in daylight). Radar was not processed until after TPI. If the TARGET did not have a tracking light, this prevented the TPI maneuver from being executed (point at the TARGET and burn). The approach to the TARGET would be made along the +Vbar manually (see next page). The manual phase could be completed with LightScape software along with Lambert Targeting and Orthogonal Braking Logic.

By the late 1970s, plume impingement and Forward RCS budgeting resulted in serious concerns about the Double Coelliptic profile. The closing rate at the start of the manual phase could be as high as 40 feet/second. The Orthogonal Braking logic was designed to permit a +Rbar approach using only Aft RCS, but lighting and burn spacing issues prevented it from resolving the concerns with the Double Coelliptic profile.

The aid of Orbit Targeting. In the end, braking gates and Prox Ops in the Shuttle Program were performed without done on Gemini and Apollo). The Orthogonal Braking logic was placed in the Flight Software along with Lambert Targeting to permit targeting of braking gates and Proximity Operations maneuvers, rather than purely manual execution (as was to do on Gemini and Apollo). In the end, lighting gates and Prox Ops in the Shuttle Program were performed without done on Gemini and Apollo).

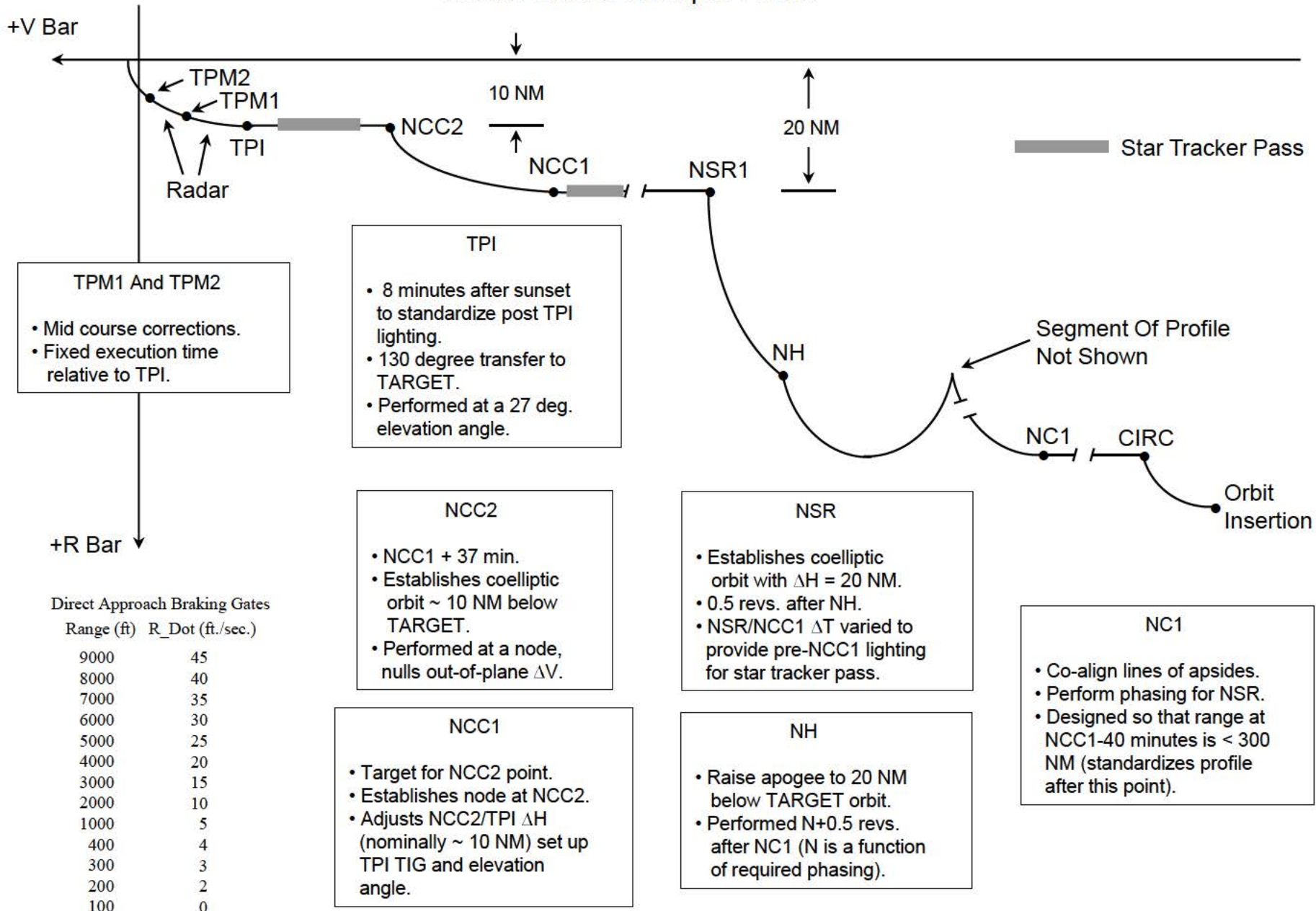
The Orthogonal Braking logic was placed in the Flight Software along with Lambert Targeting to permit targeting of braking gates and Proximity Operations maneuvers, rather than purely manual execution (as was to do on Gemini and Apollo).

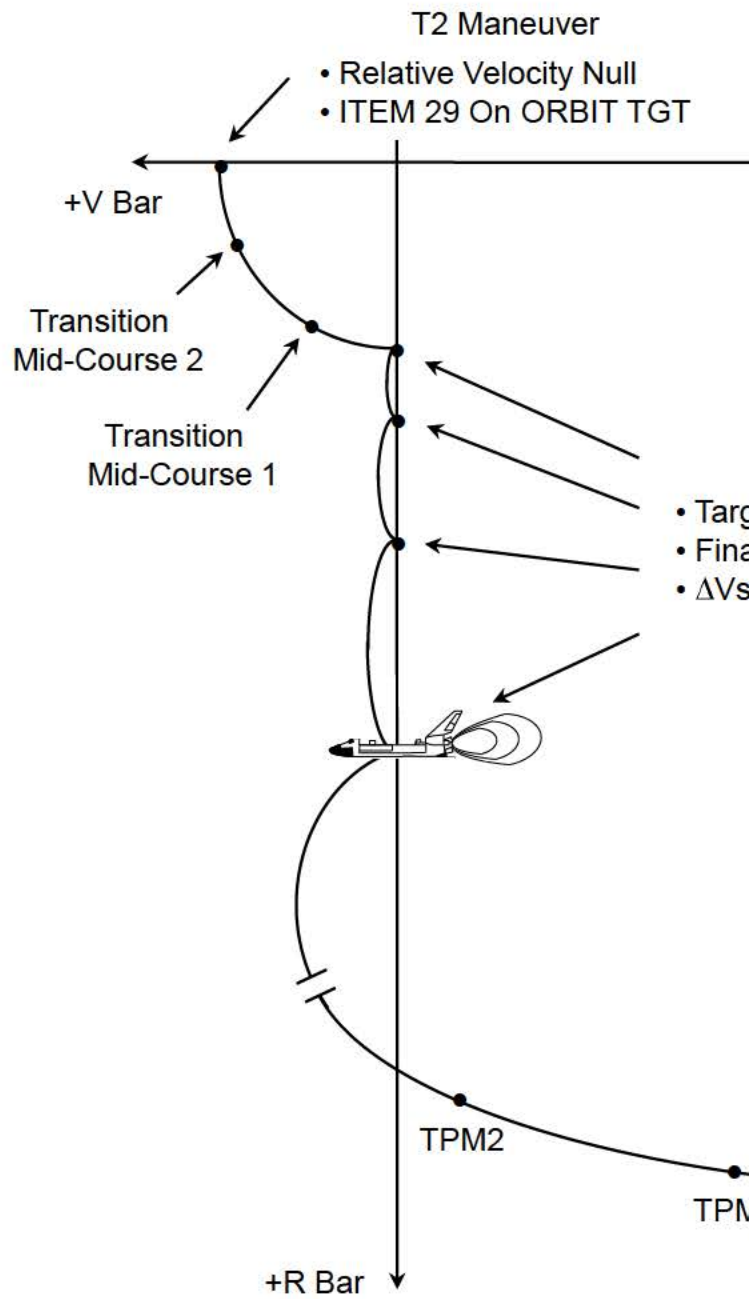
The original Shuttle rendezvous profile identified by the Mission Planning and Analysis Division (MPAD) was the Double Coelliptic (see next page). The manual phase was similar to that on Gemini/Apollo, but TPI was performed 8 minutes after sunset (to allow a star tracker pass prior to TPI and a final approach in daylight). Radar was not processed until after TPI. If the TARGET did not have a tracking light, this prevented the TPI maneuver from being executed (point at the TARGET and burn). The approach to the TARGET would be made along the +Vbar manually (see next page). The manual phase could be completed with LightScape software along with Lambert Targeting and Orthogonal Braking Logic.

The original Shuttle rendezvous profile identified by the Mission Planning and Analysis Division (MPAD) was the Double Coelliptic (see next page). The manual phase was similar to that on Gemini/Apollo, but TPI was performed 8 minutes after sunset (to allow a star tracker pass prior to TPI and a final approach in daylight). Radar was not processed until after TPI. If the TARGET did not have a tracking light, this prevented the TPI maneuver from being executed (point at the TARGET and burn). The approach to the TARGET would be made along the +Vbar manually (see next page). The manual phase could be completed with LightScape software along with Lambert Targeting and Orthogonal Braking Logic.

7.3 Shuttle Baseline Stable Orbit Rendezvous (BSOR)

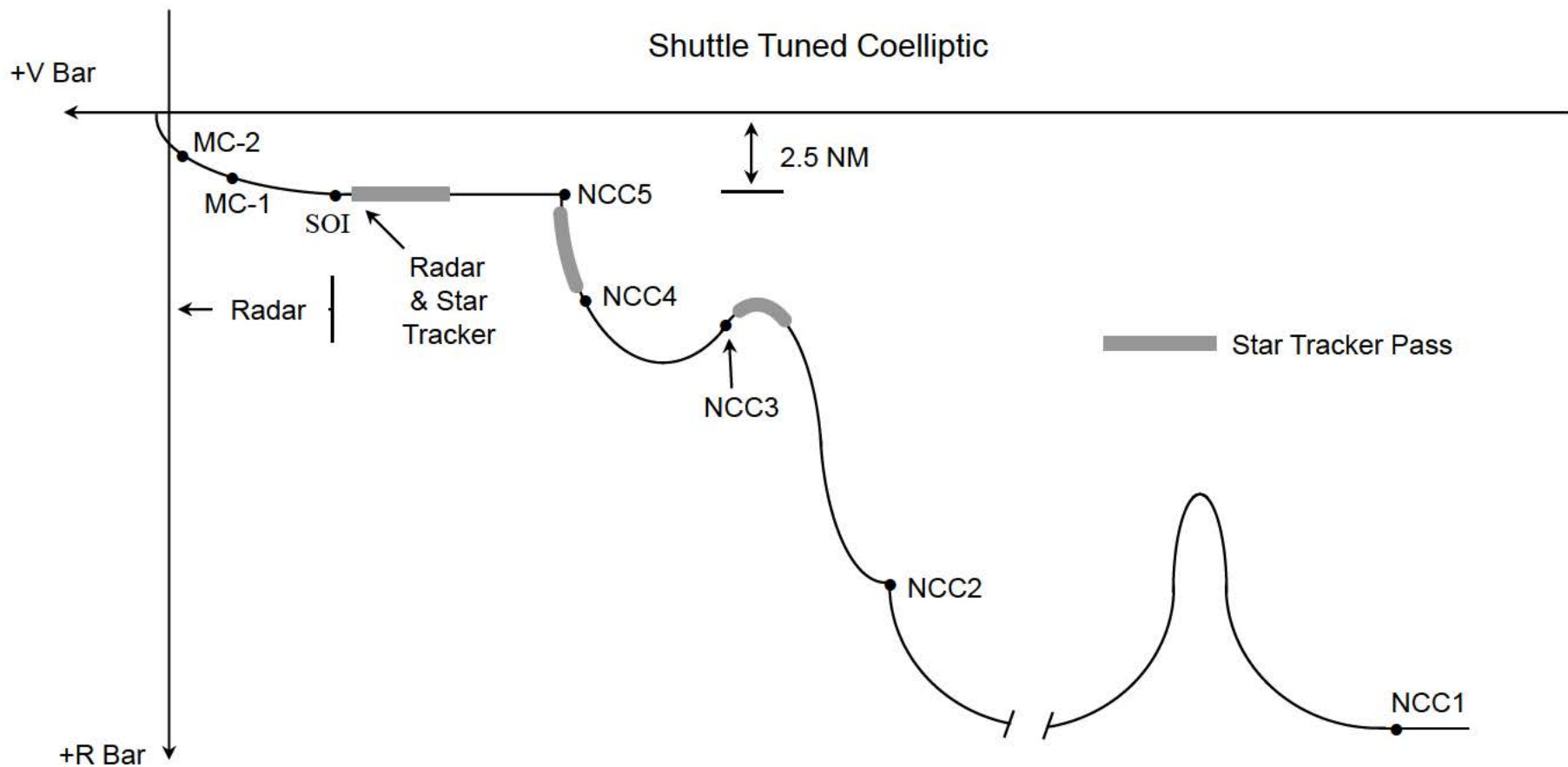
Shuttle Double Coelliptic Profile



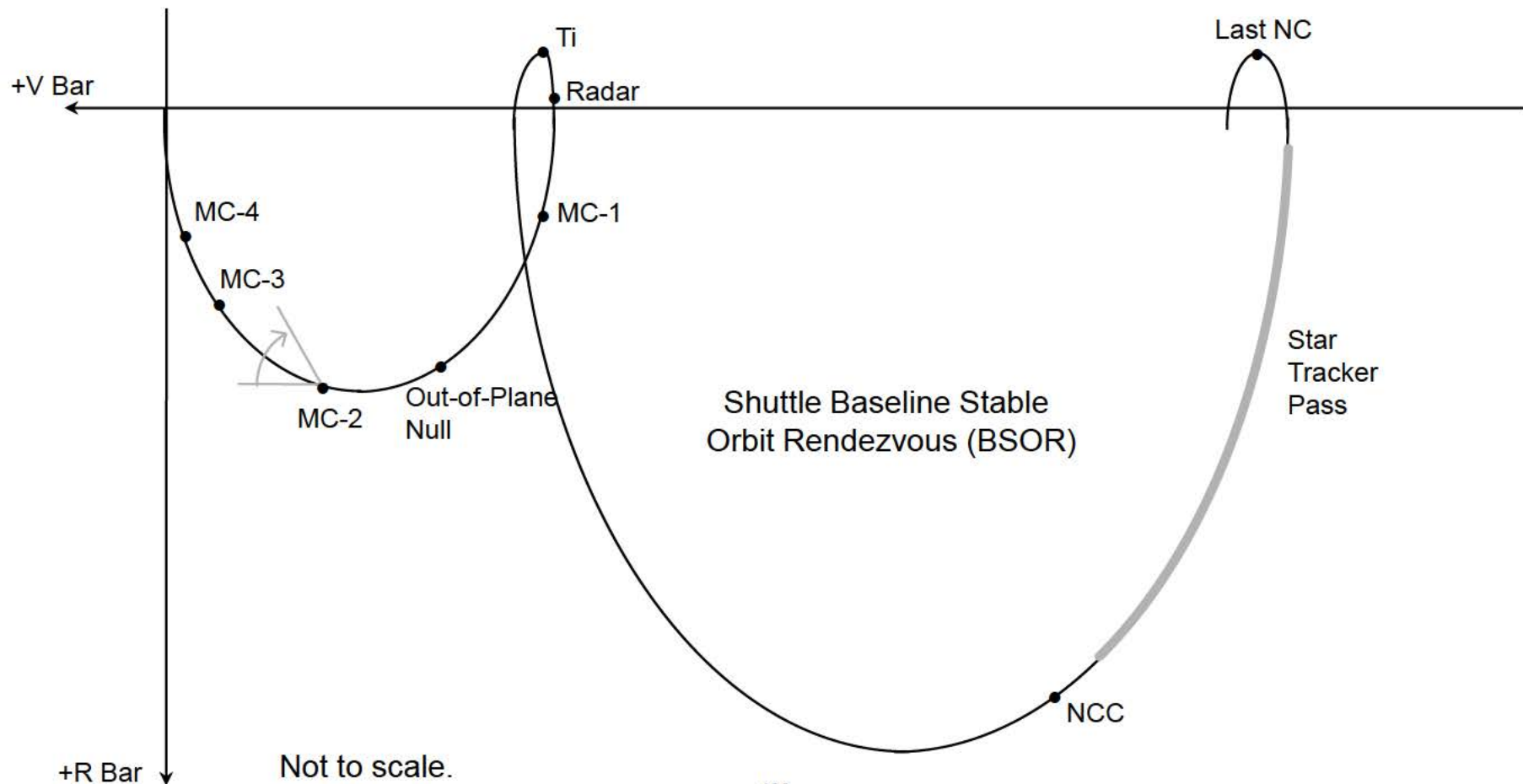


Rendezvous procedures and ORBIT TGT Flight Software development in the late 1970s permitted Manual Phase maneuvering to be computed by the Flight Software. Manual Phase could also be executed “completely manually” as was done on Gemini and Apollo.

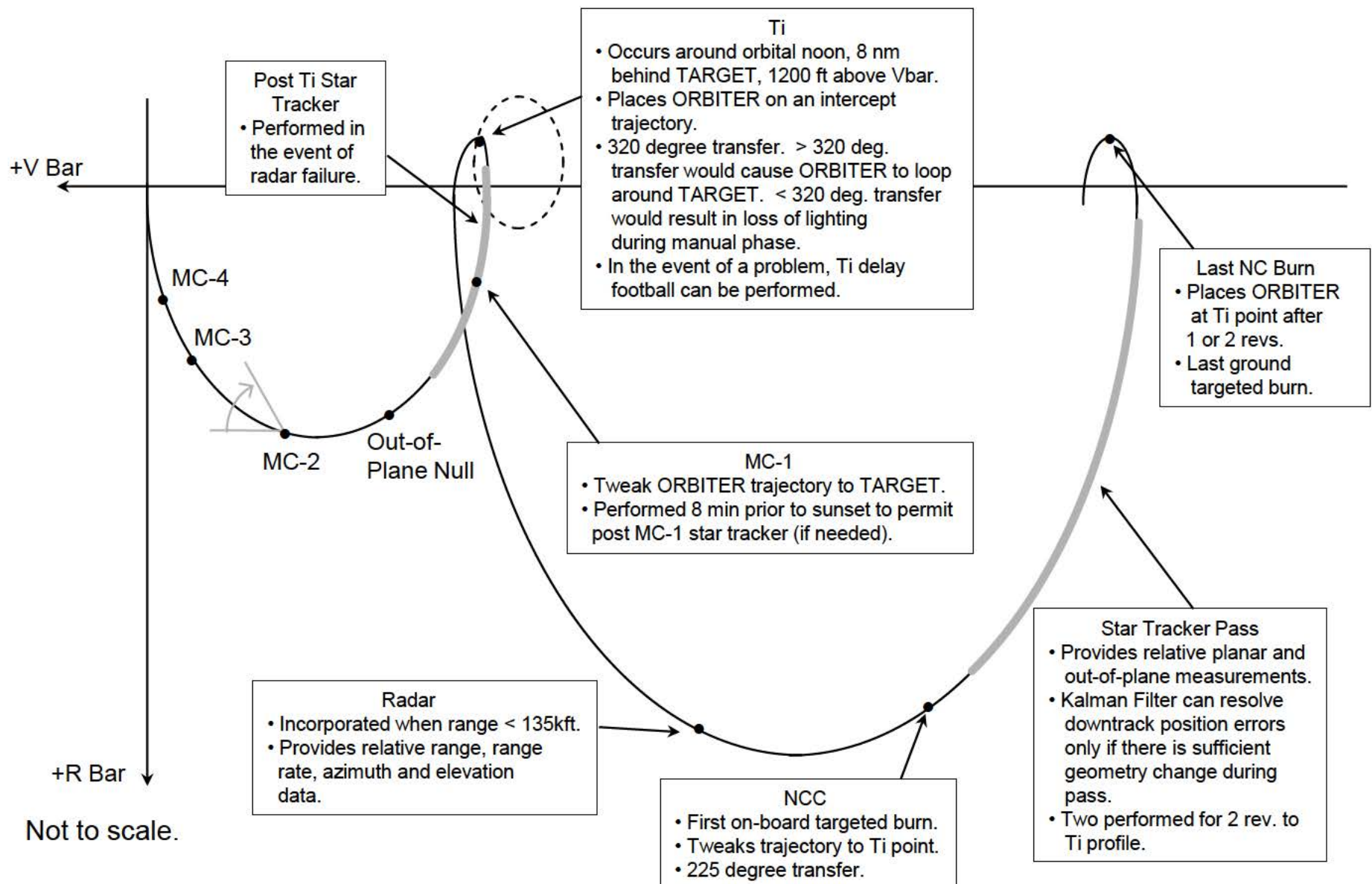
Paul Kramer of the Avionics Systems Division led a team of Engineering Directorate and Draper Labs personnel that proposed the “Tuned” Coelliptic profile. This profile retained the Gemini/Apollo terminal phase while attempting to resolve the Forward RCS and lighting concerns. The profile also involved using the on-board Lambert Targeting to target NH and NC maneuvers.



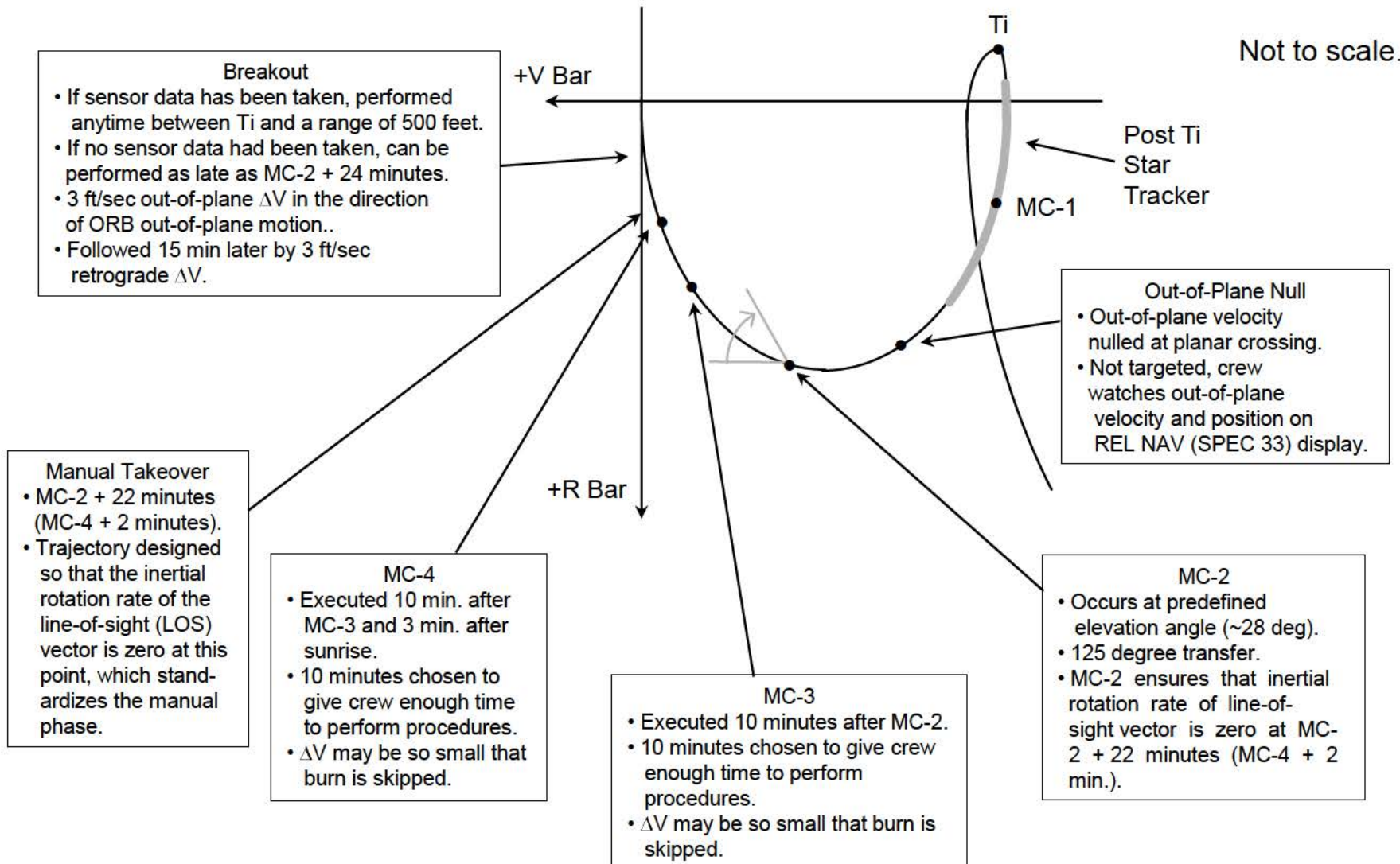
In the fall of 1981, Ed Lineberry of MPAD proposed the stable (tangential) orbit concept tried on Gemini XI. Ground targeted burns could get the orbiter to a station keeping point on the -Vbar within radar range (< 10 NM). A Transition Initiation (Ti) burn would be executed at orbital noon. The closing rate at the start of the manual phase was an order of magnitude smaller (~4 feet/second) than the Double Coelliptic profile. From the fall of 1981 to the spring of 1983 Lineberry's proposal was modified to improve performance. A star tracker pass and NCC burn prior to Ti was added to reduce nav uncertainties from the ground targeted phase and permit more accurate placement of Ti in the TARGET's orbital plane. Radar would be taken starting after Ti (the radar had a 10 nm range requirement, later radar was taken starting post NCC). MC-2 was targeted on an elevation angle (like the old TPI) to standardize the manual phase in the presence of dispersions. This avoided the terminal phase lighting and dispersion problems encountered when the Tangential Orbit profile was studied in the early 1960s. The Stable Orbit profile was baselined for Shuttle in April of 1983.



Shuttle Baseline Stable Orbit Rendezvous (BSOR) Details (Last NC Through Ti)

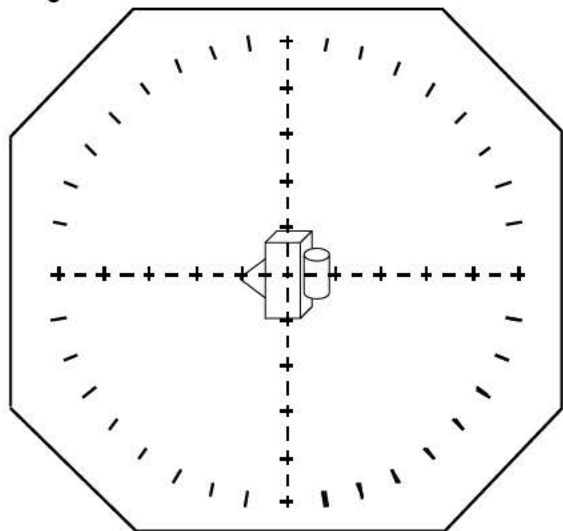


Shuttle Baseline Stable Orbit Rendezvous (BSOR) Details (Post Ti Through Intercept)

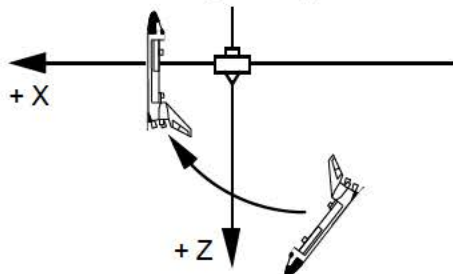


Where TARGET is in COAS at MC-2 + 22 minutes is an indication of trajectory dispersions.

←
ORBITER
Right (Starboard)
Wing

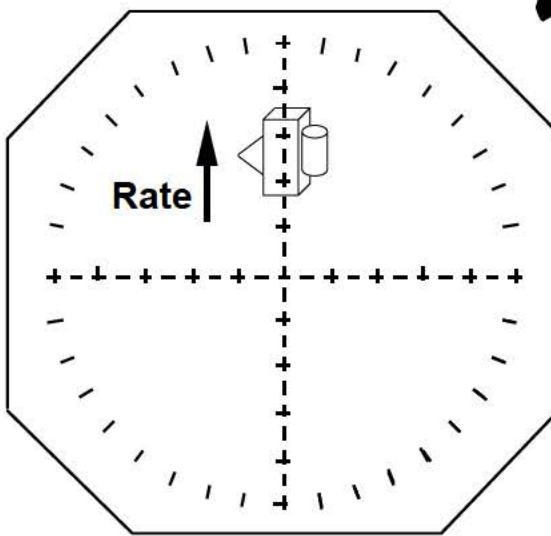


Nominal
Trajectory

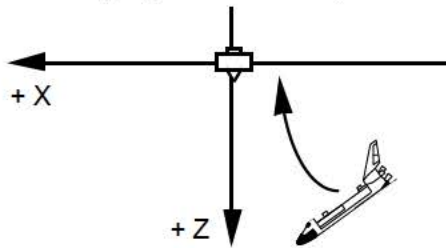


Inertial rotation
rate of line-of-sight
vector is zero.

↑
ORBITER
Nose
Line of
Sight

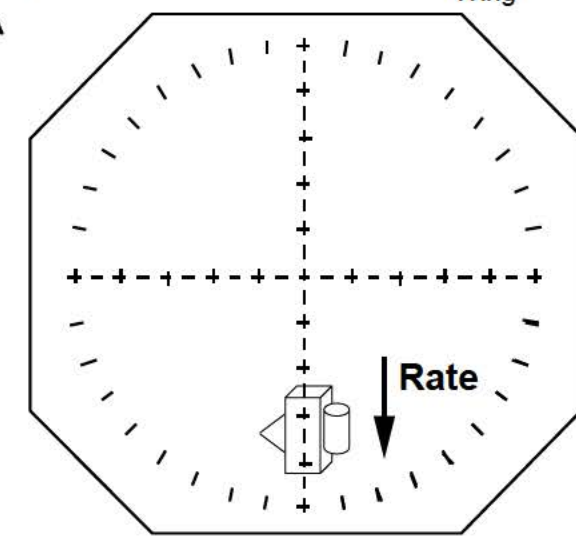


"Short" Trajectory
(high is short)

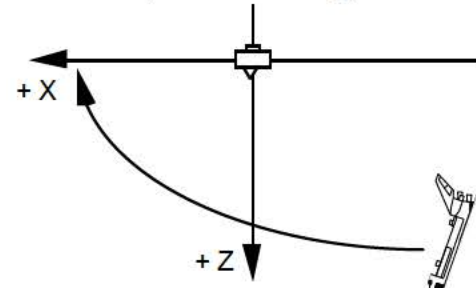


Inertial rotation rate of line-of-sight vector is non-zero. ORBITER never reaches R_BAR (+Z axis).

→
ORBITER
Left (Port)
Wing

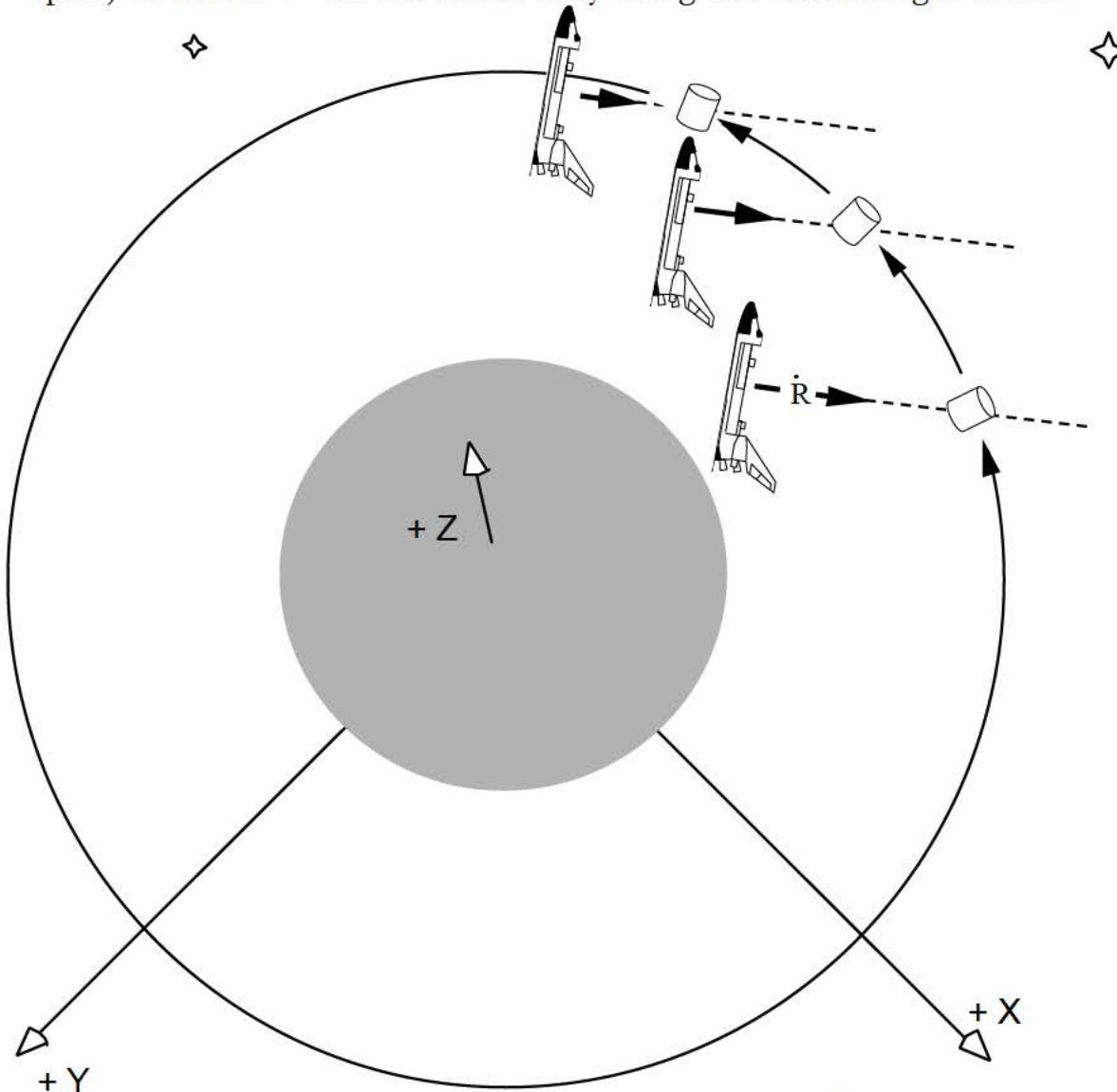


"Long" Trajectory
(low is long)



Inertial rotation rate of line-of-sight vector is non-zero.

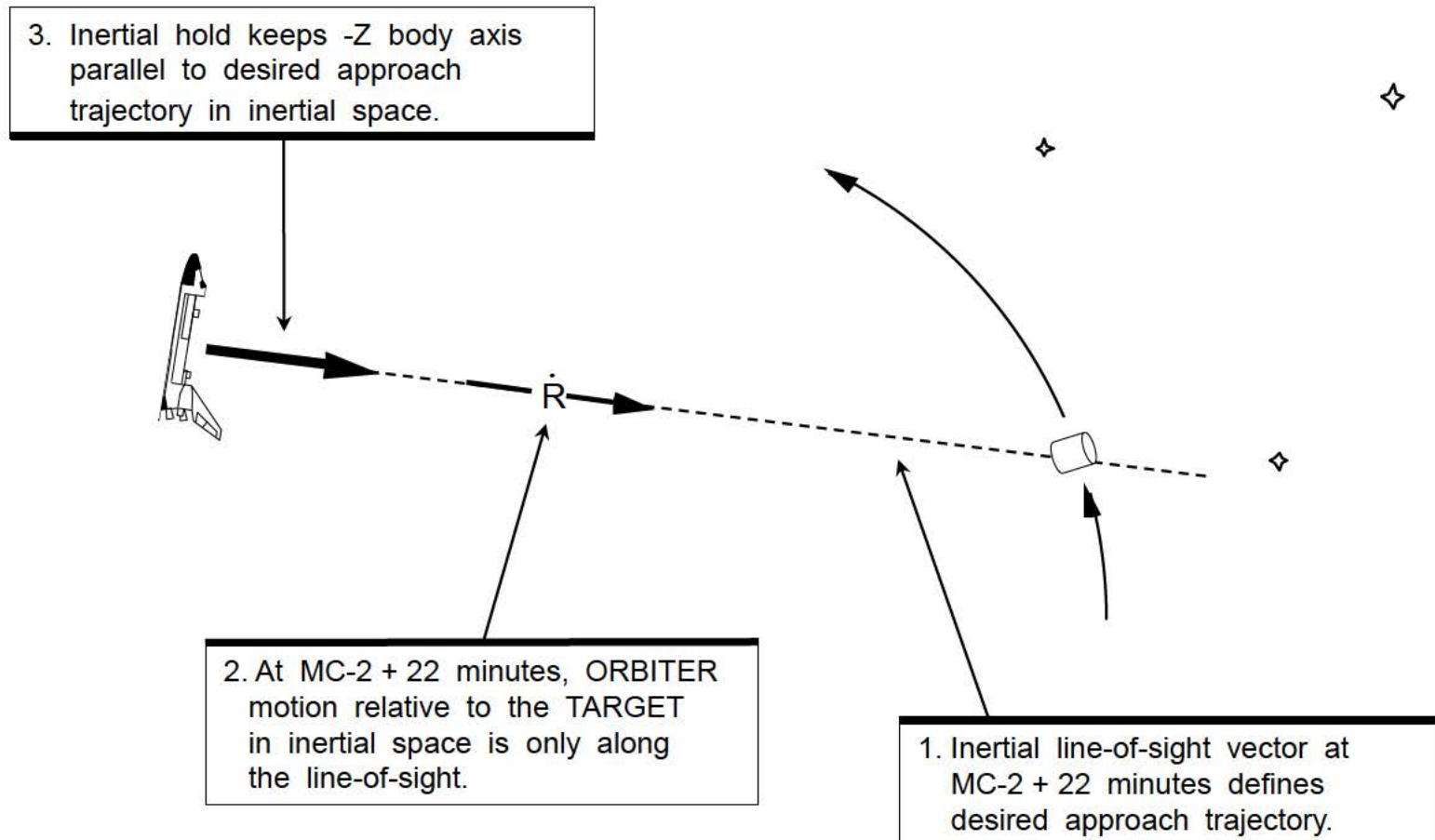
During the manual phase, the ORBITER needs to approach the TARGET along a straight line in inertial space. The rendezvous trajectory is designed so that ORBITER motion relative to the TARGET (in inertial space) at MC-2 + 22 minutes is only along the Line-of-Sight vector.



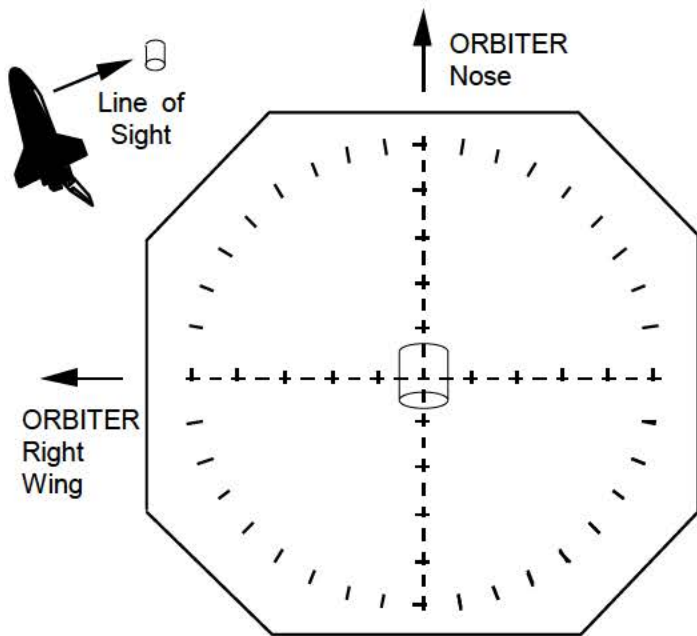
MC-2 ensures that the inertial rotation rate of line-of-sight vector is zero at MC-2 +22 minutes (MC-4 + 2 min.).

The TARGET would appear to be stationary with respect to the stars if it was orbital night at this point.

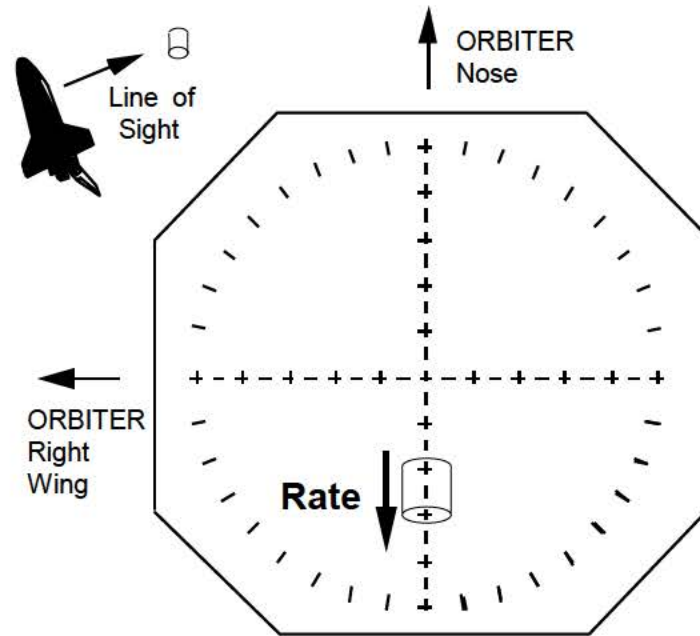
Until manual takeover, the DAP has kept the -Z body axis pointed at the TARGET. At MC-2 + 22 minutes, the crew places the ORBITER in an inertial attitude hold. During the rest of the approach to the TARGET, the -Z body axis will be parallel to the LOS vector when the inertial rotation rate of the LOS was zero.



During most of the approach to the TARGET, the boresight of the COAS can be considered to be along the -Z body axis. The COAS is used to ensure that the ORBITER stays on the correct approach path.

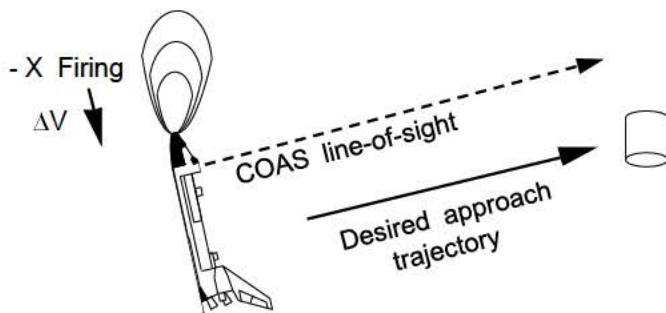
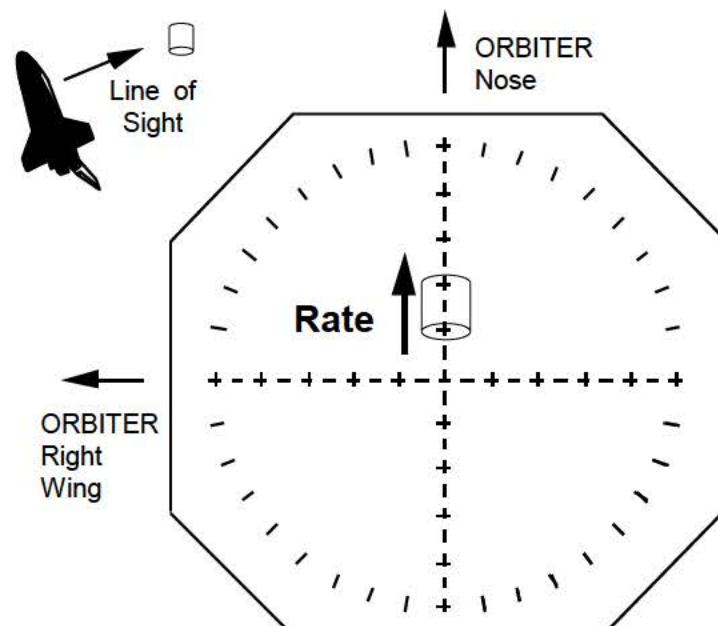
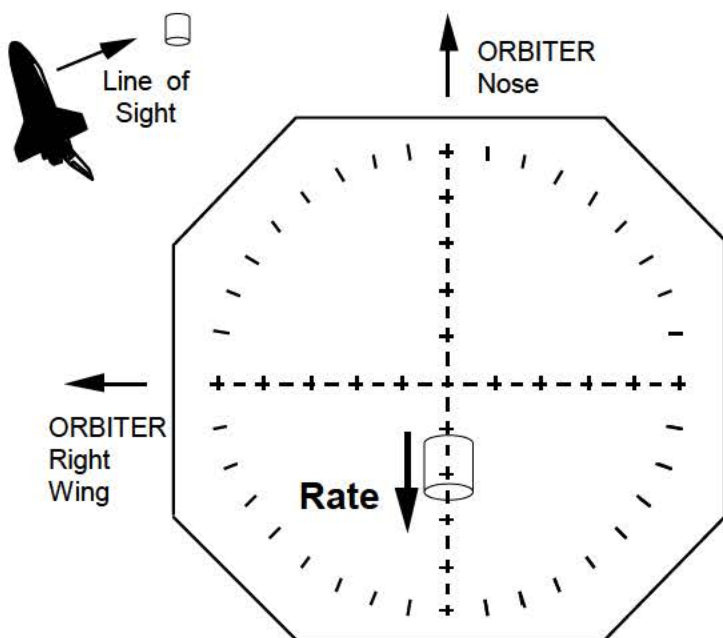


Crew keeps TARGET stable in COAS to constrain ORBITER position to the desired line-of-sight vector. TARGET does not have to be centered in COAS for proper approach to be maintained.

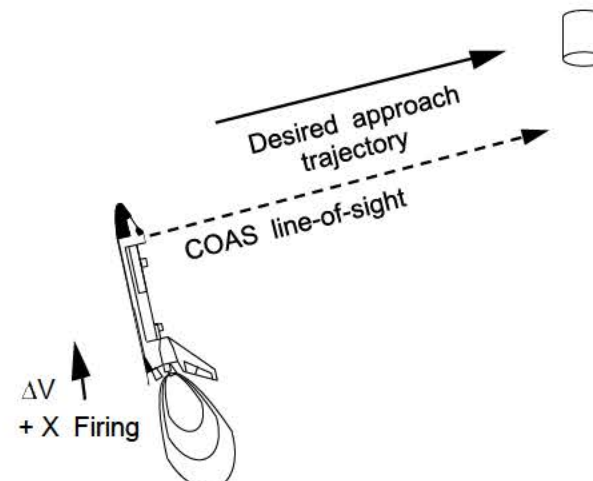


If the ORBITER begins to move off of the desired trajectory, the TARGET will appear to move in the COAS. ORBITER translation is no longer limited to the LOS vector at MC-2 + 22 minutes.

The crew uses RCS firings to keep the ORBITER on the proper trajectory.



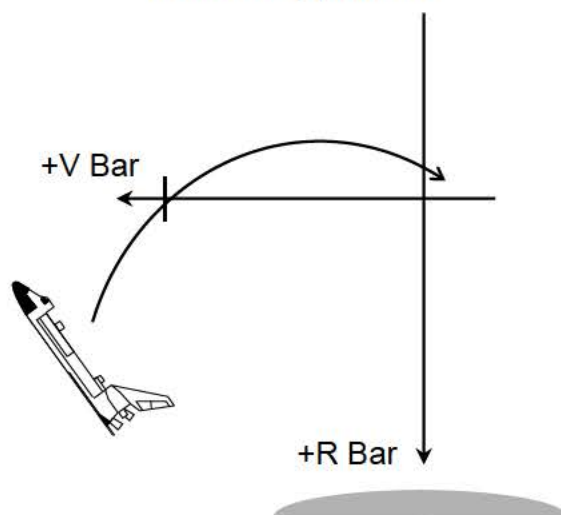
Translational -X RCS firing performed to keep TARGET stable in COAS.



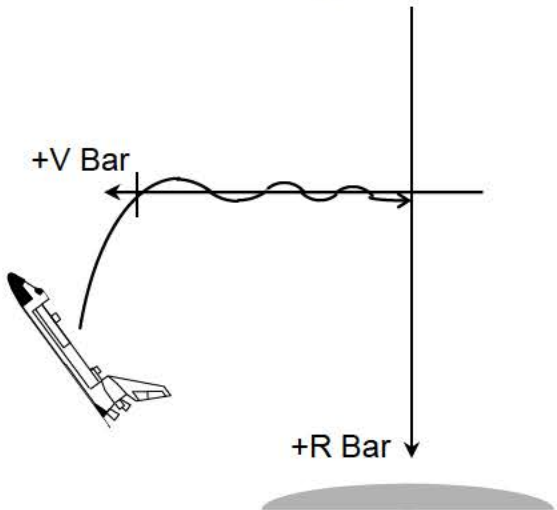
+ X RCS firing performed to keep TARGET stationary in COAS.

Historically, the most common final approach used with the Baseline Stable Orbit Rendezvous profile was the +V Bar approach. Inertial and -R Bar approaches were also performed. The manual phase was designed so that +V Bar crossing occurred at 400 feet for the +V Bar, -R Bar and Inertial approaches. The +R Bar approach was first performed as a Detailed Test Objective (DTO) on STS-66. Mir rendezvous flights 71, 74, 76, 79, 81 and 84 used a +R Bar approach with BSOR.

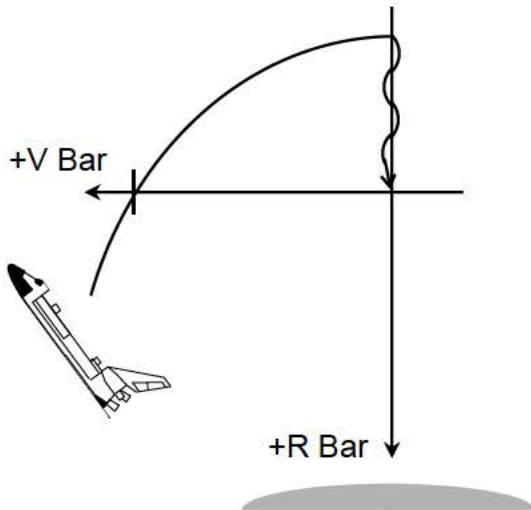
Inertial Approach



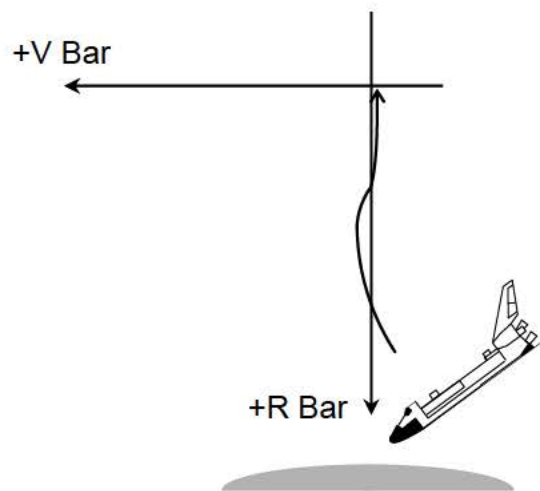
+V Bar Approach



-R Bar Approach



+R Bar Approach



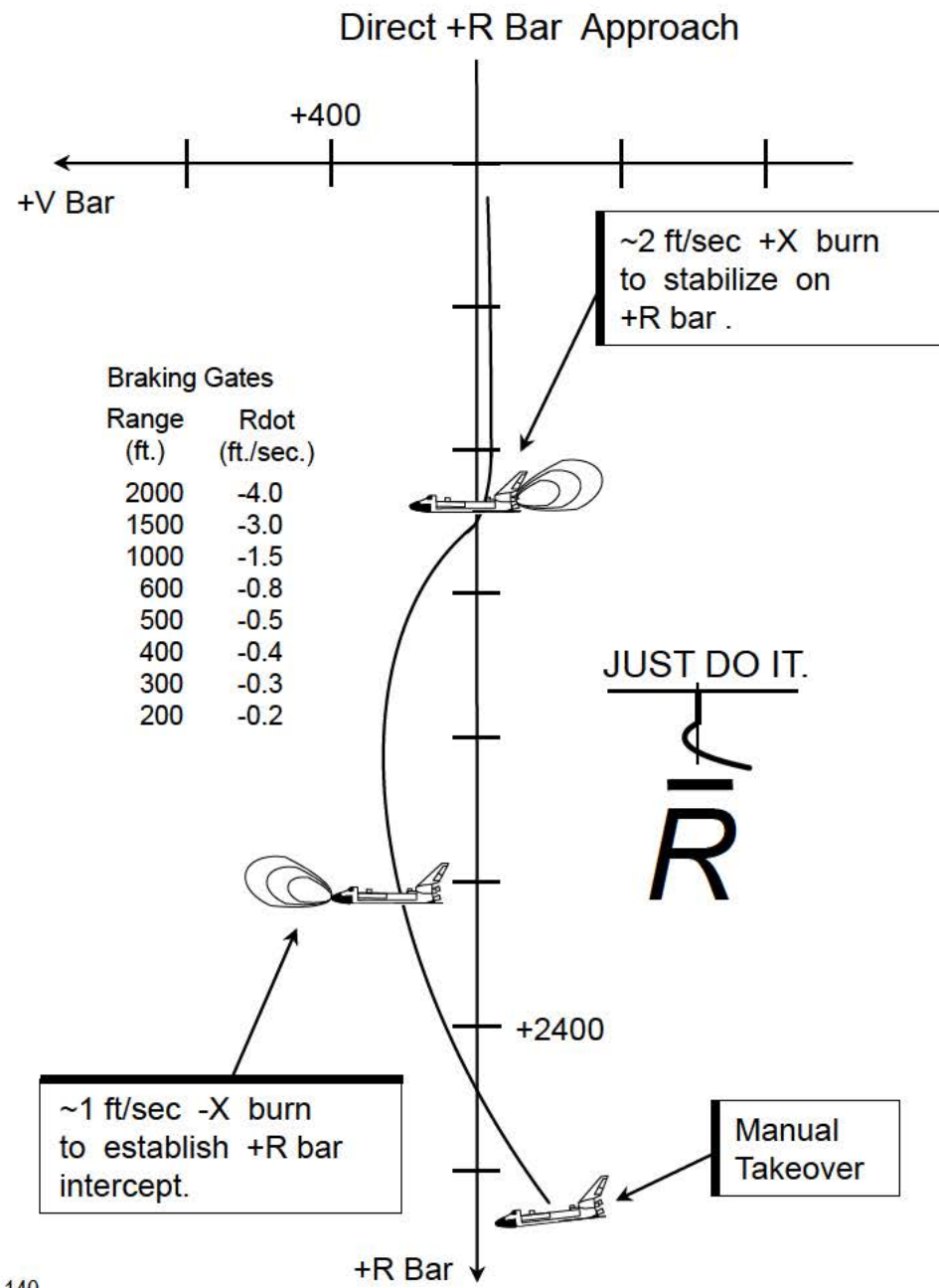
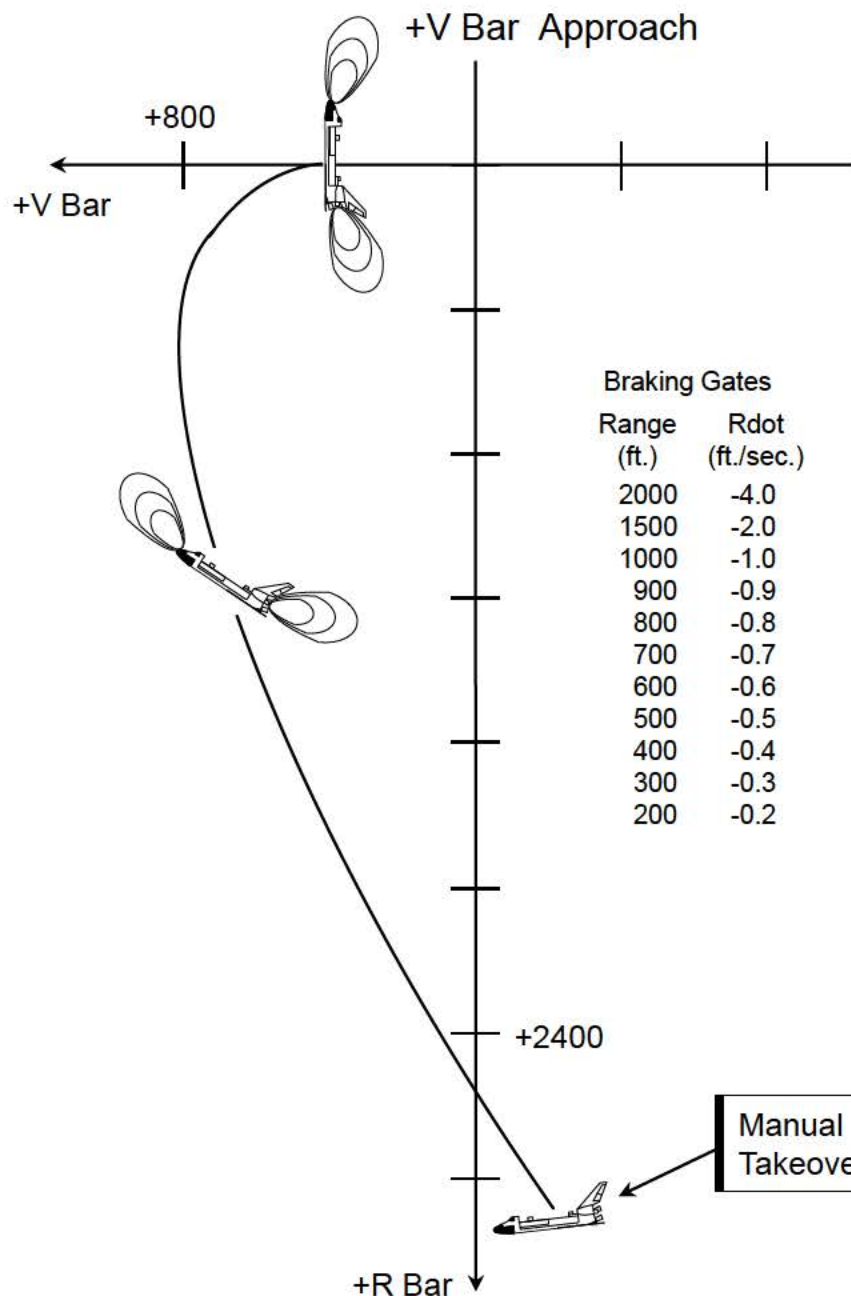
7.4 +Rbar Approach (BSOR)

The baseline stable orbit rendezvous profile was designed and adopted for mainly +Vbar approaches (a transition to the -Rbar could be performed upon arrival at the +Vbar, permitting a -Rbar approach). The difficulty with these approaches was that the amount of braking required that increased plume impingement loads on the target. For the Mir missions (as well as ISS), reducing plume impingement loads was critical. Braking in Low Z mode reduced plume impingement but dramatically increased propellant costs.

Rendezvous designers had long desired to use orbital mechanics to brake the orbiter during the manual phase, and reduce reliance on RCS thrusting. Such an approach, up the +Rbar for the proposed Skylab Rescue mission in 1978, was studied. However, a +Rbar approach required a reliable range rate sensor. Rendezvous radar did not have sufficient range rate accuracy or reliability to support a +Rbar approach. Also, it was assumed that adoption of an +Rbar approach would require changes to rendezvous targeting. For the Skylab Rescue, the +Rbar approach also had lighting problems.

In an attempt to resolve plume impingement and propellant expenditure problems with the double coelliptic profile during Proximity Operations, the Orthogonal Braking logic was developed (around 1978) and placed in Orbit Targeting. This feature was to be used to target burns while making a +Rbar approach. However, orbital noon would occur by the time the ORBITER arrived at the transition to +Vbar point, creating a bad lighting condition for the crew. Burns targeted with Orthogonal Braking were also too close to each other in terms of execution time.

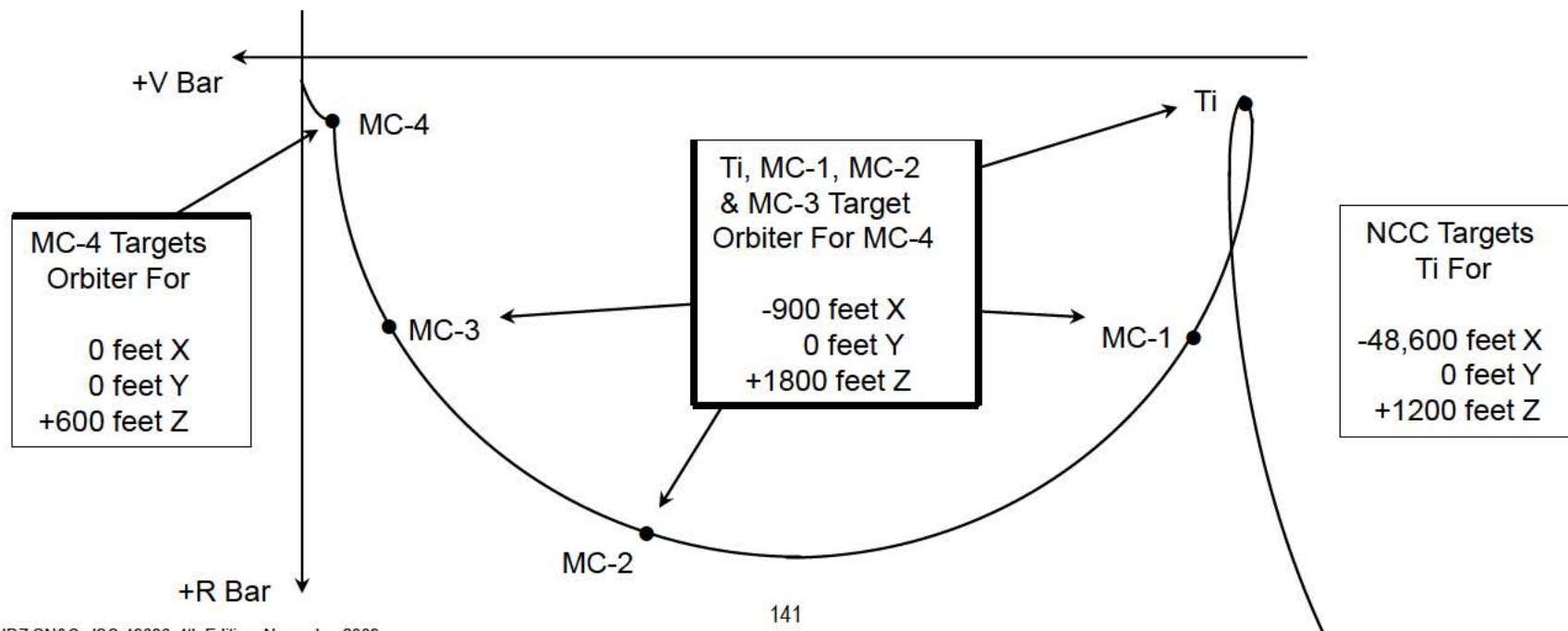
Planning for Mir and ISS rendezvous missions prompted study of the Direct +Rbar approach in 1993. Plume impingement was anticipated to be a serious concern for Mir and ISS. Use of orbital mechanics to perform braking, rather than RCS jet firings, would resolve the plume impingement issue. +Rbar would also provide a small propellant savings. Studies indicated that the new approach could be performed without changing targeting ILOADs for the BSOR profile. A +Rbar separation (backout) from Mir could also take advantage of orbital mechanics, and require less jet firings. The first flight of Hand Held Lidars (HHL) on STS-49 and the first successful flight of the Trajectory Control Sensor (TCS) on STS-64 provided the Shuttle Program with the precise range and range rate sensors needed to meet Mir and ISS docking conditions. Direct +Rbar was presented to Flight Techniques in April of 1994, and first flown on as a DTO on STS-66 to CRISTA-SPAS in November of 1994. Direct +Rbar approaches were flown with the baseline stable orbit rendezvous profile on Mir rendezvous flights 71, 74, 76, 79, 81 and 84.



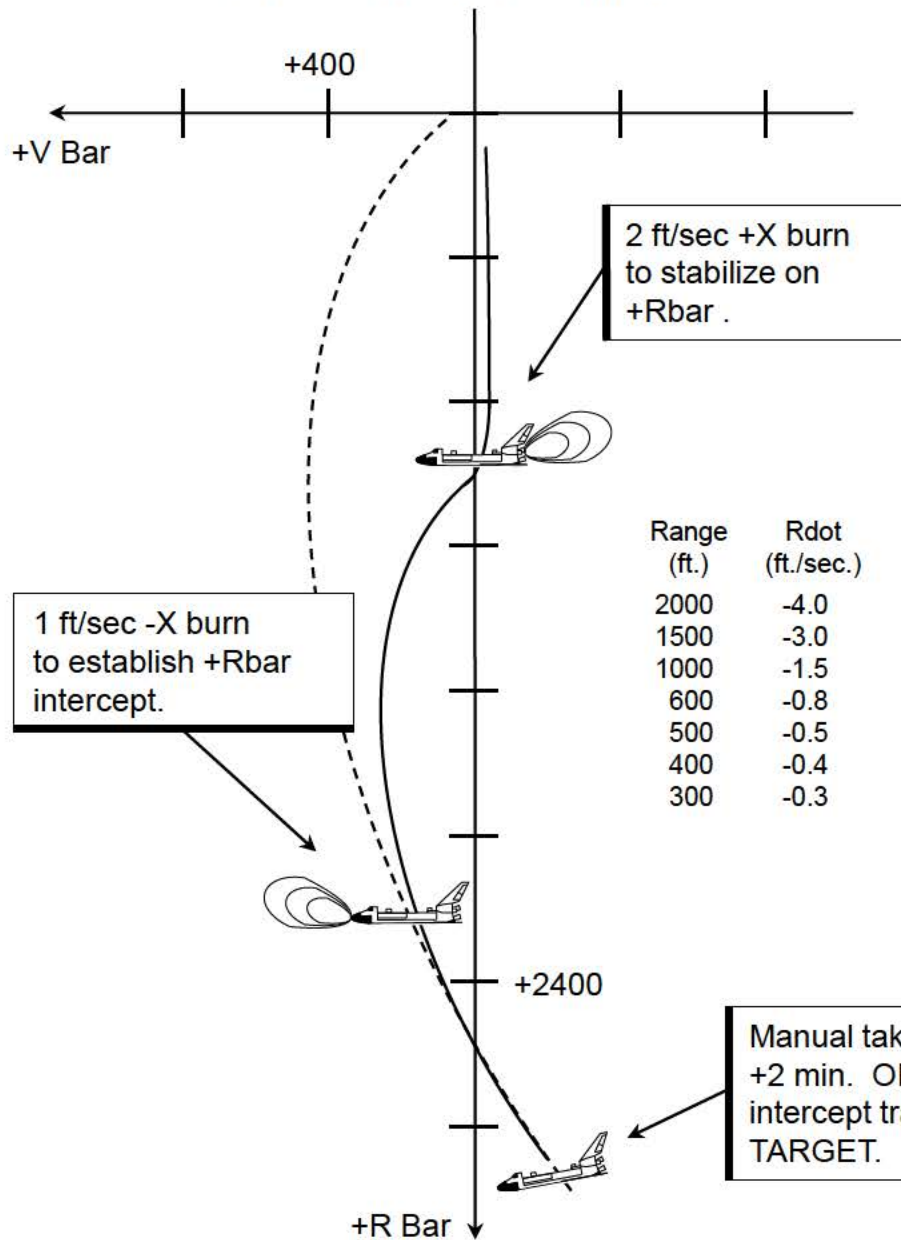
7.5 Optimized R-Bar Targeting (ORBT) Rendezvous

After adapting the Direct +Rbar approach to the Baseline Stable Orbit Rendezvous (BSOR) profile, further analysis led rendezvous designers to investigate changes to the rendezvous profile itself (before the manual phase) to further reduce propellant consumption during the manual phase. The BSOR profile was a “high energy” profile designed to support a terminal phase to the +Vbar. Since early ISS flights were designed with +Rbar approaches to minimize impingement, a new profile was designed which was optimized for the +Rbar approach.

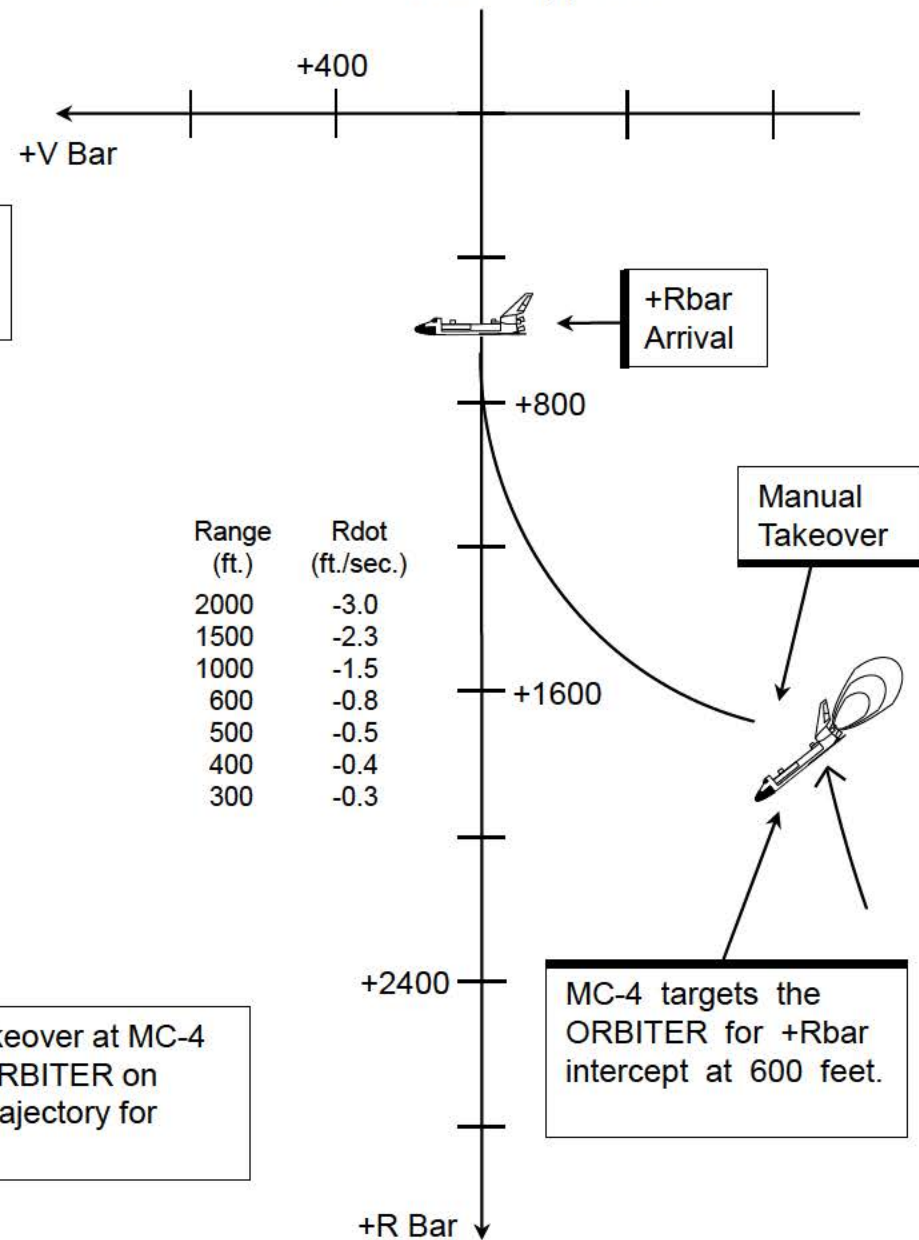
The new profile, Optimized R-Bar Targeted Rendezvous (ORBT), differs from BSOR in several ways. ORBT performs a low energy coast up the +Rbar, rather than a higher energy target intercept (BSOR). By targeting to the manual takeover point at 2000 feet (rather than intercept), manual phase trajectory dispersions are reduced and propellant consumption is cut since ORBT normally would not require +Rbar stabilization burns or braking burns. The Ti point for ORBT is below the Vbar, rather than above it (BSOR). After arriving on the +Rbar, the ORBITER can transition to the +Vbar (TORVA) or -Rbar (TORRA) if needed, using new fly-around procedures.



BSOR Direct +R Bar Approach

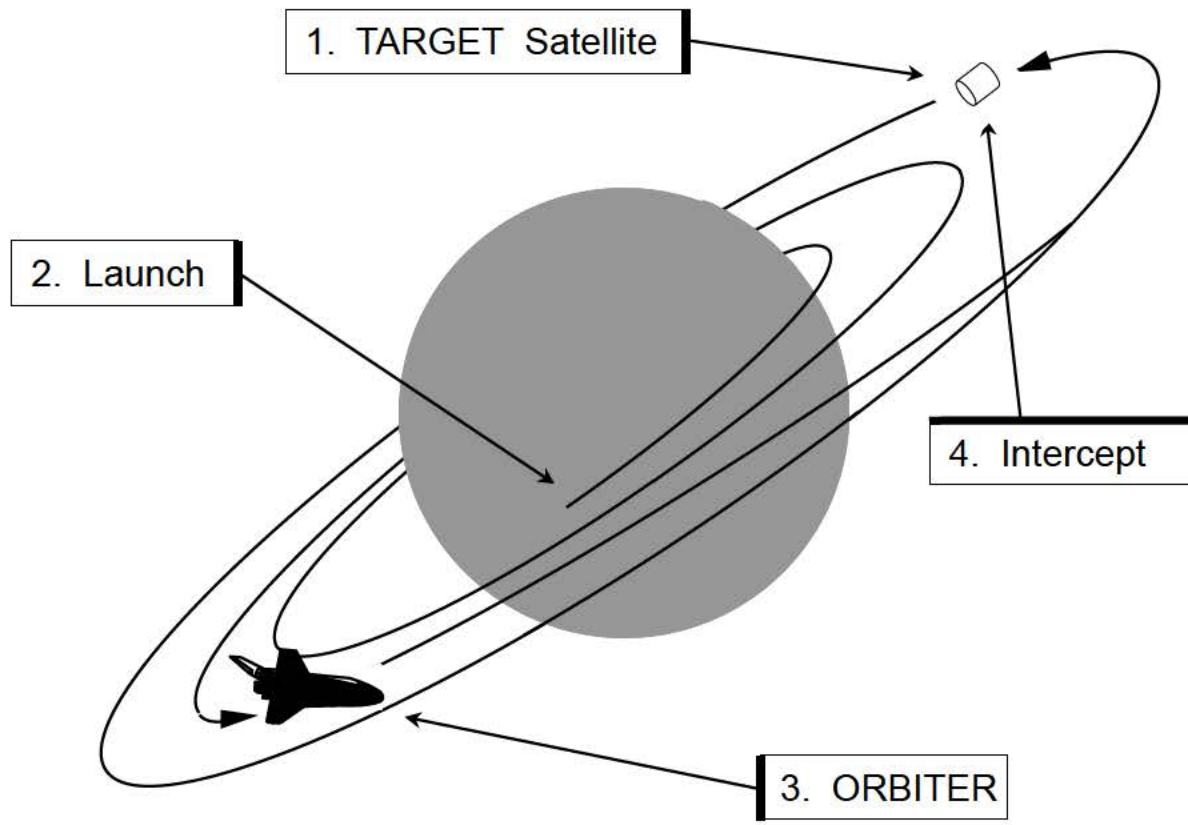


ORBT +R Bar Approach



7.6 Ground Up Rendezvous

Thus far (Chapters 4 and 5), it has been assumed that the TARGET satellite is in orbit prior to ORBITER launch (ground-up rendezvous). Although many ground-up rendezvous have been performed during the shuttle program, several rendezvous missions have been flown that were not of the ground-up type.



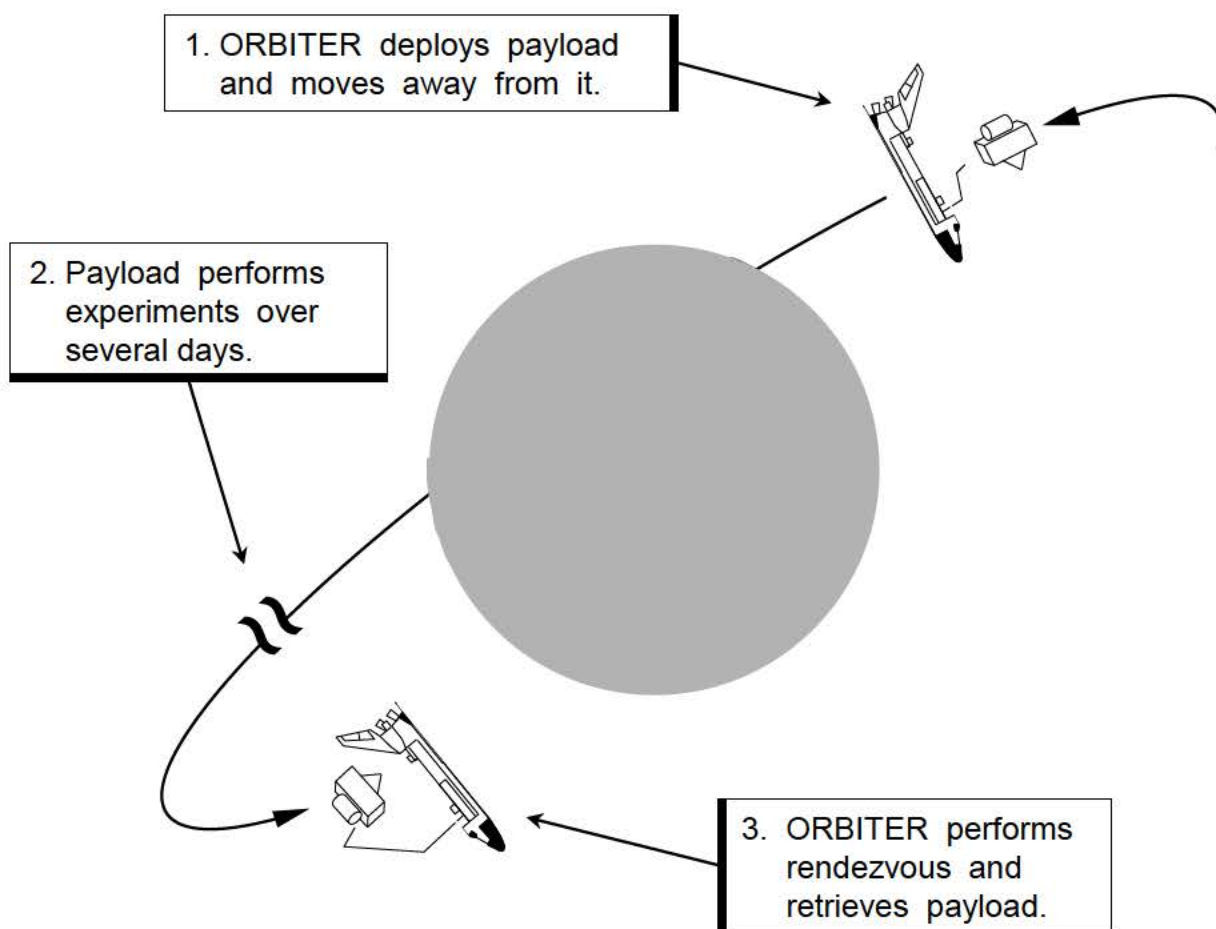
Ground-Up Rendezvous

Ground-Up Rendezvous Missions

41C	Solar Max repair
51A	Palapa B, Westar retrieval
51I	Leasat (Syncom) repair
32	LDEF retrieval
49	INTELSAT reboost
57	Eureca
61	HST
72	SFU
82	HST
103	HST
109	HST
Many	Mir
Many	ISS

7.7 Deploy/Retrieve

On other missions the ORBITER may deploy a PAYLOAD (such as a SPAS pallet). The ORBITER then “backs away” from the PAYLOAD. Several days later, the ORBITER will rendezvous with the PAYLOAD and put it back in the cargo bay.

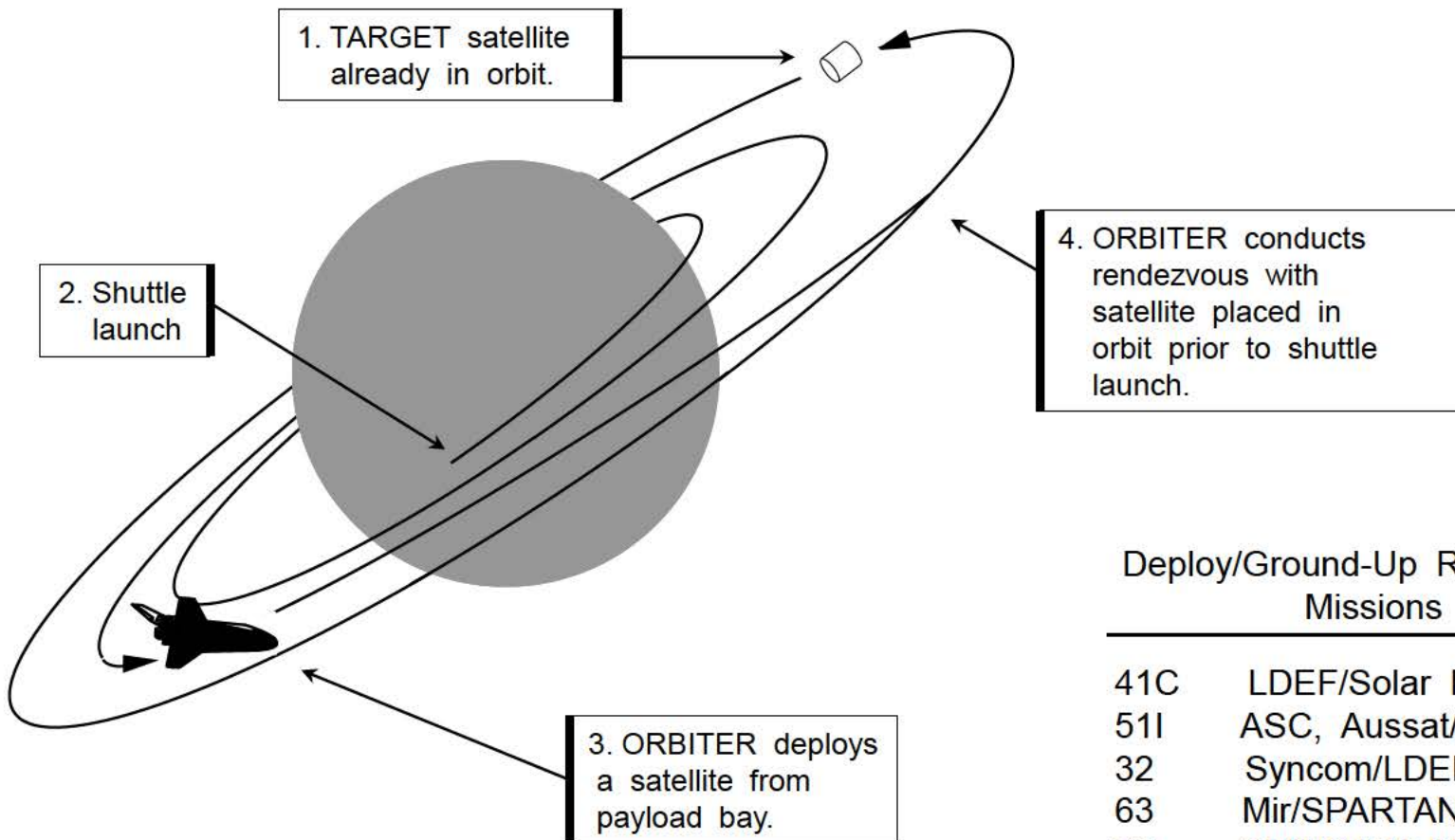


Deploy / Retrieve
Missions

	Deploy / Retrieve Missions
7	SPAS
51G	SPARTAN-101
51F	PDP
39	IBSS-SPAS II
56	SPARTAN-201-01
51	ORFEUS-SPAS 1
60	WSF-1
64	SPARTAN-201-02
66	CRISTA-SPAS 1
63	SPARTAN-204
69	SPARTAN-201-03
	WSF-2
72	OAST-Flyer
77	SPARTAN-207-IAE
	PAMS-STU
80	ORFEUS-SPAS 2
	WSF-3
85	CRISTA-SPAS 2
87	SPARTAN-201-04
95	SPARTAN-201-05

7.8 Deploy/Ground-Up Rendezvous

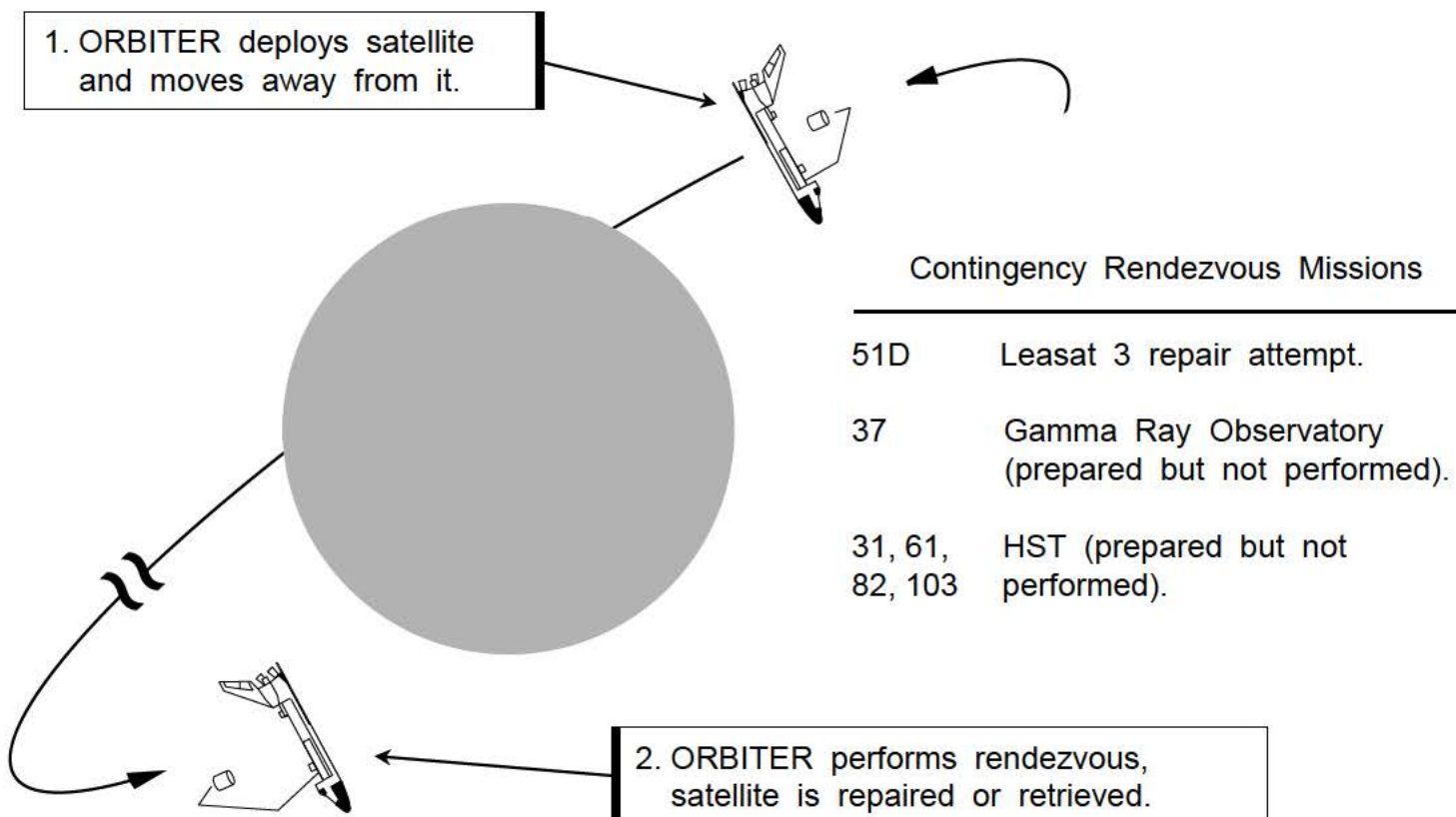
During a ground-up rendezvous mission, the ORBITER may deploy one or more satellite(s) during the ground targeted phase.



7.9 Contingency Rendezvous

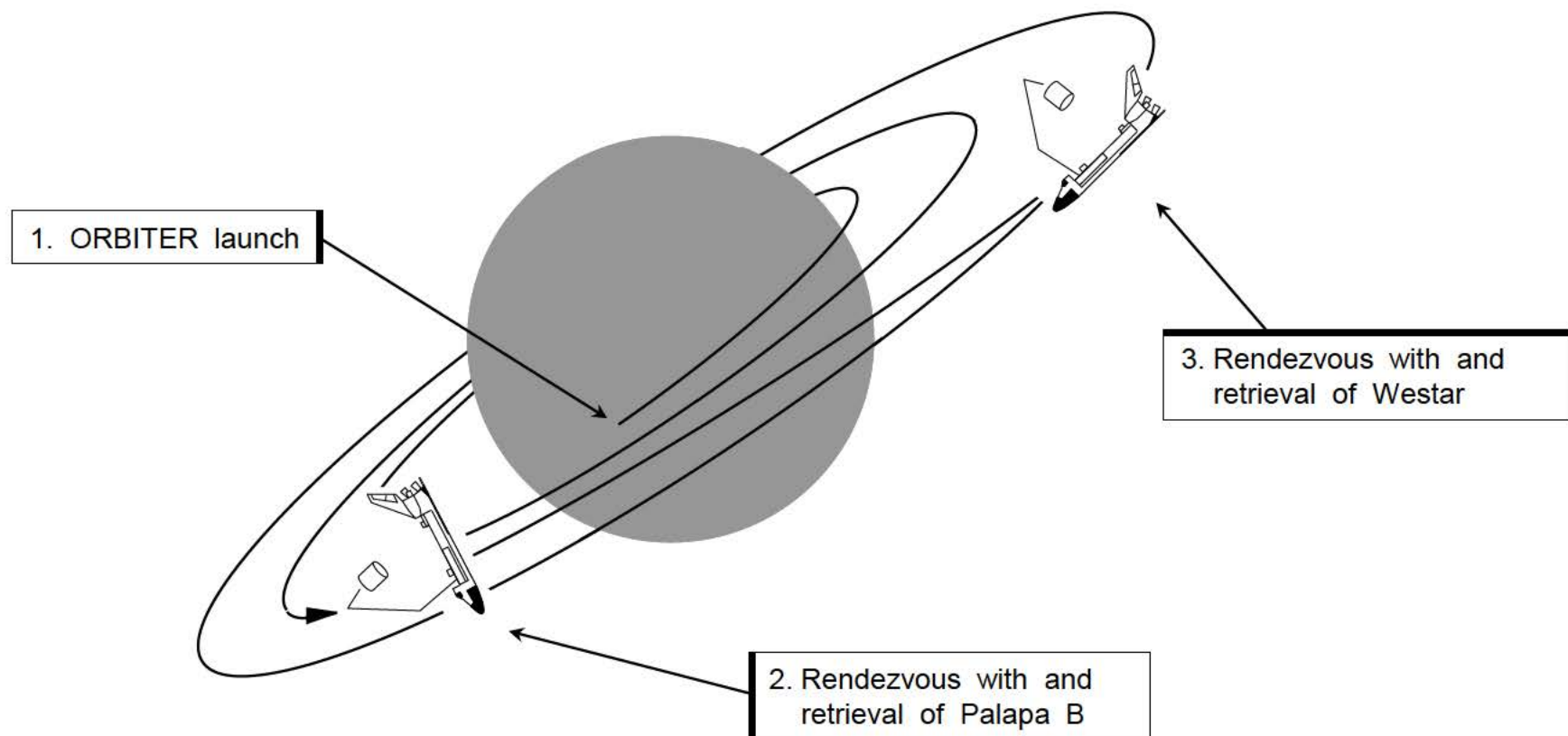
A mission may not have a rendezvous manifested, but a situation may arise which requires a rendezvous. The only example to date was 51D. 51D deployed Leasat 3, which malfunctioned. A rendezvous and an EVA were performed in an attempt to repair the Leasat. The repair effort failed, and Leasat 3 was later successfully fixed by mission 51I.

On STS-31, 61, 82, 103, and 109 contingency rendezvous were planned in the event of a malfunction of the Hubble Space Telescope (HST) after deployment.



7.10 Ground-Up Double Rendezvous

Mission 41B deployed the Palapa B and Westar satellites. Propulsion systems on both satellites failed to place them in the desired geosynchronous orbits. Both satellites were maneuvered into orbits that could be reached by the shuttle. On mission 51A, both satellites were recovered and returned to Earth.



7.11 Ground-Up Triple Rendezvous

On STS-49, Endeavor's mission was to rendezvous with and attach a new upper stage to the stranded Hughes/INTELSAT 6F communications satellite. This had been launched by a Titan in 1990, but had not been able to leave low Earth orbit for the intended geostationary orbit.

Only one rendezvous was planned and executed on May 10, 1992, but Mission Specialist Pierre Thout was unable to "catch" the INTELSAT with a special tool during a spacewalk.

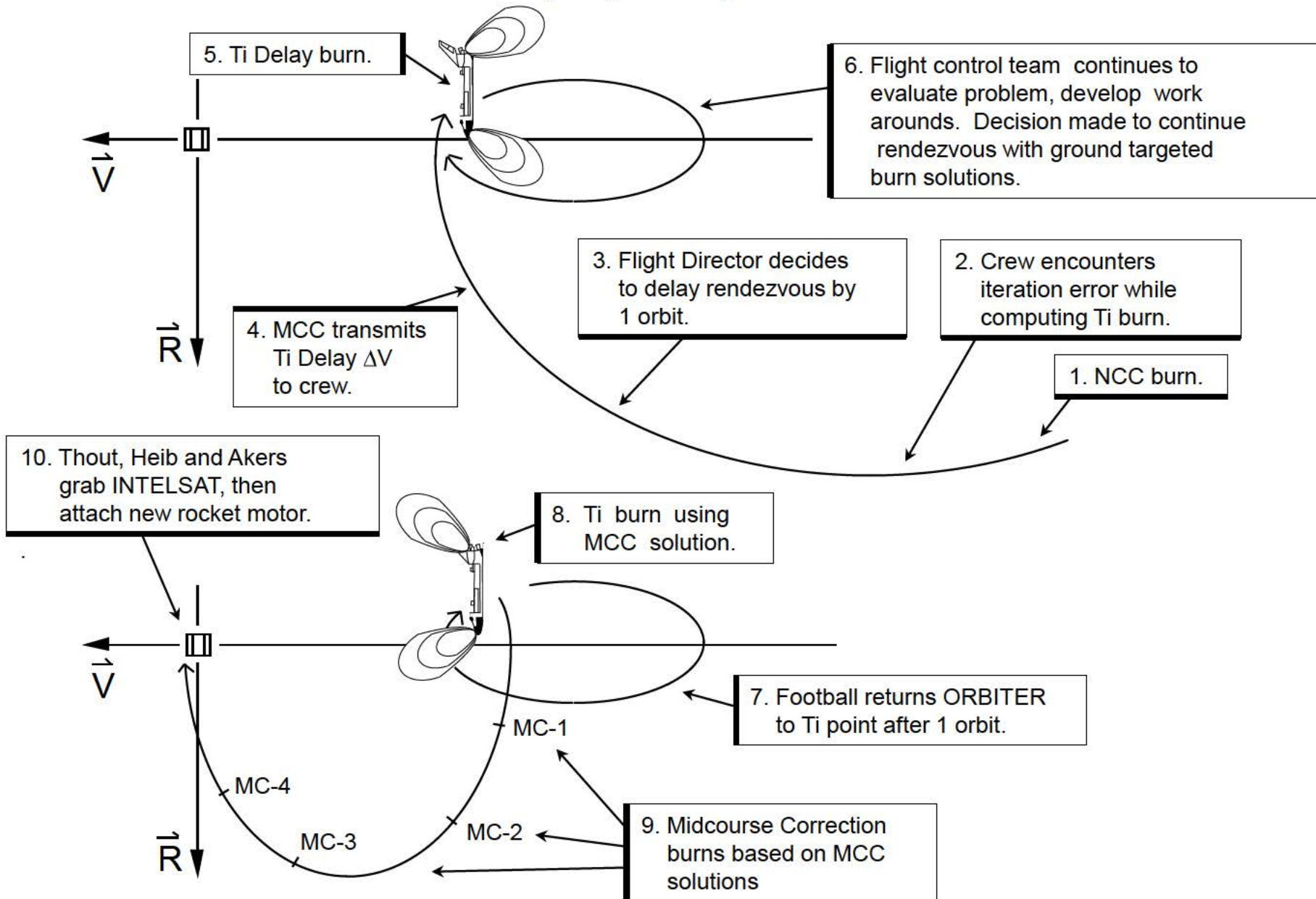
A second rendezvous was performed a day later. MC-2 had to be computed based on time since the T1_LOAD for MC-2 was zeroed during the May 10 rendezvous (BASE TIME reset to MC-2 TIG). The capture attempt using the tool failed again.

A third rendezvous was performed on May 13. During the computation for the Ti burn, a targeting iteration error occurred. A Ti delay burn was performed to give flight controllers more time to evaluate the problem and develop an alternate targeting procedure. After 1 rev the Ti burn was executed using Δ Vs computed by the Flight Dynamics Officer (FDO). The remaining burns (MC-1, -2, -3, -4) were also computed by the FDO and voiced to the crew.

This time the capture attempt succeeded through the use of three spacewalking astronauts grabbing the INTELSAT. A new rocket motor was bolted on the INTELSAT. After deployment the INTELSAT eventually reached its desired position in geostationary orbit.

The Lambert targeting problem was later traced to the use of both single- and double-precision variables. This mission marked the first time 3 rendezvous were performed on a U.S. mission, MC-2 was computed on-board based on time, a Ti delay was executed, and the final rendezvous burns were executed based on FDO computations.

Events related to STS-49 Lambert targeting anomaly :



This page intentionally left blank.

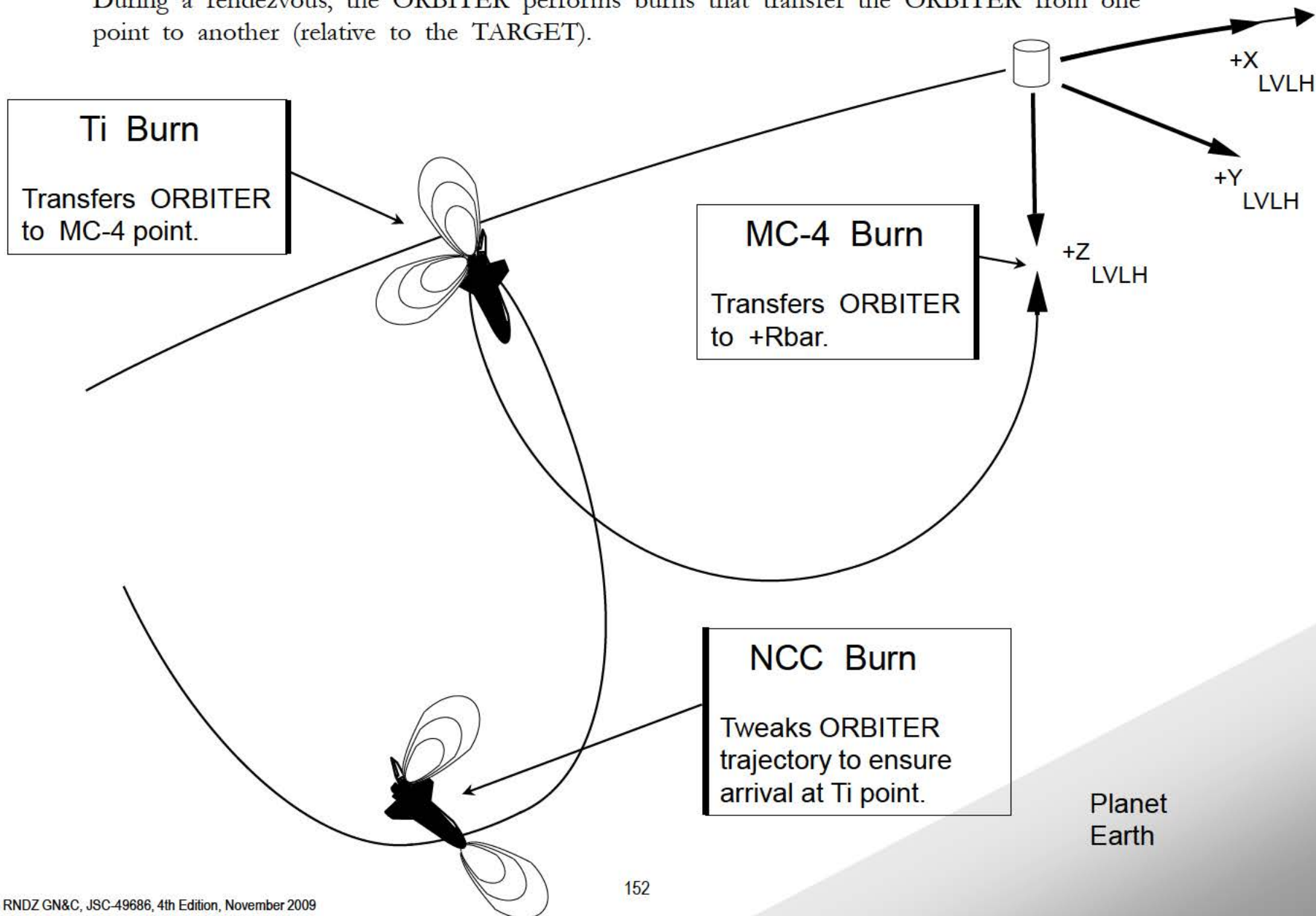
8.0 On-Board Rendezvous Targeting And Guidance

The ORBIT TGT display is used by the crew to compute on-board targeted burn solutions.

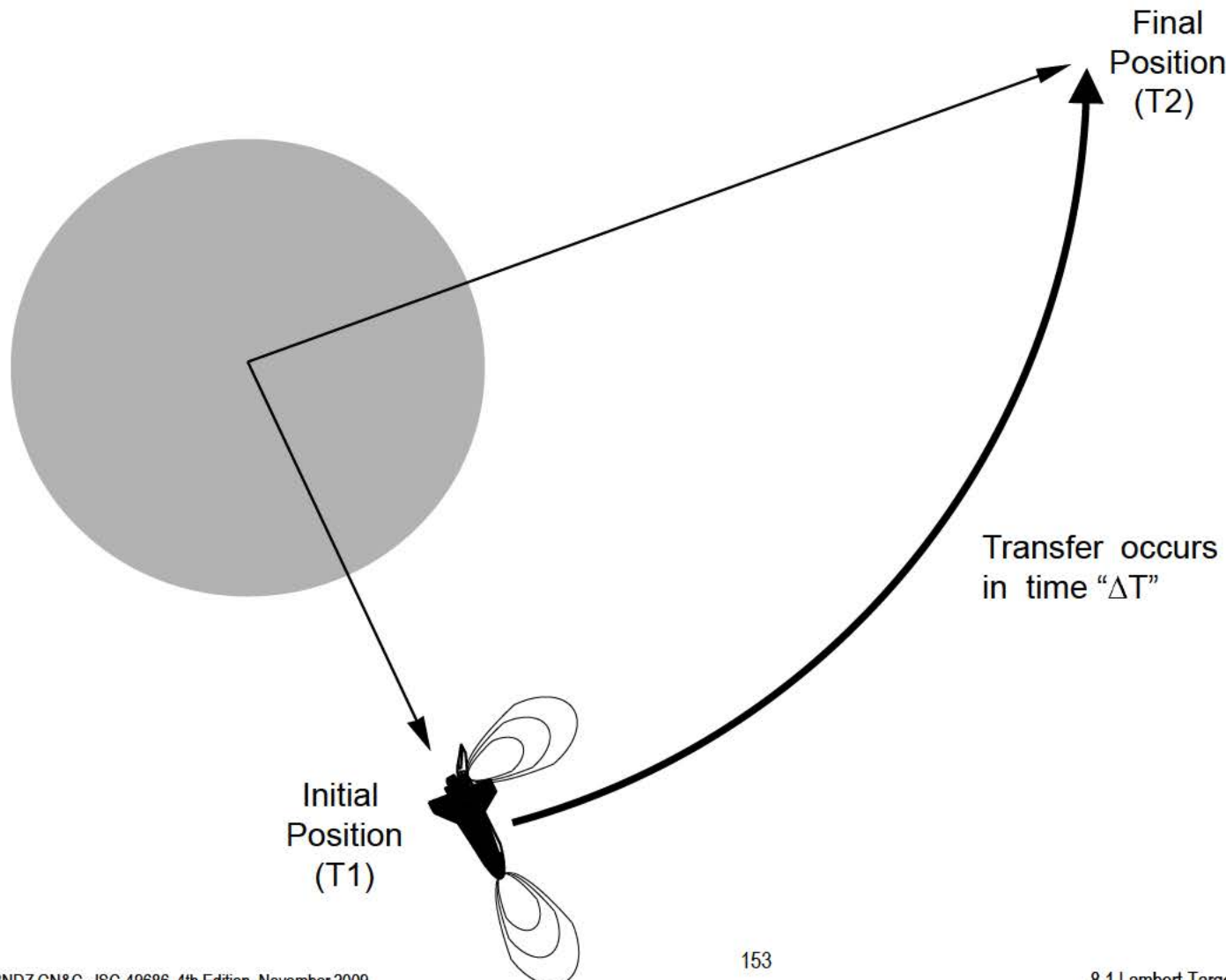
2021 / 034 /	ORBIT TGT	1 001 / 14 :21 :31 000 / 00 :03 :42	
MNVR	TIG	ΔV_x ΔV_y ΔV_z ΔV_t	
10	1 / 14 :25 :13	+ 8 .3 - 0 .4 - 0 .2 + 8 .3	
		PRED MATCH = 17	
INPUTS		CONTROLS	
1	TGT NO	10	T2 TO T1 25
2	T1 TIG	1 / 14 :25 :13	LOAD 26
6	EL	0 .00	COMPUTE T1 28
7	ΔX / DNRNG	[+] 52 .61	COMPUTE T2 29
8	ΔY	[+] 0 .15	
9	ΔZ / ΔH	[+] 0 .11	
10	$\Delta \dot{X}$	[+] 11 .53	
11	$\Delta \dot{Y}$	[+] 0 .57	
12	$\Delta \dot{Z}$	[+] 1 .14	
13	T2 TIG	1 / 15 :42 :06	ORB ITER STATE
17	ΔT	[+] 76 .9	218 / 20 :36 :14 .458
18	ΔX	[+] 0 .90	X - 6161 .856
19	ΔY	[+] 0 .00	Y +20949 .483
20	ΔZ	[+] 1 .80	Z + 3959 .738
21	BASE TIME	1 / 14 :25 :13	VX - 16 .303619
			VY - 1 .165214
			VZ - 19 .145939
ITEM 28 EXEC			

8.1 Lambert Targeting

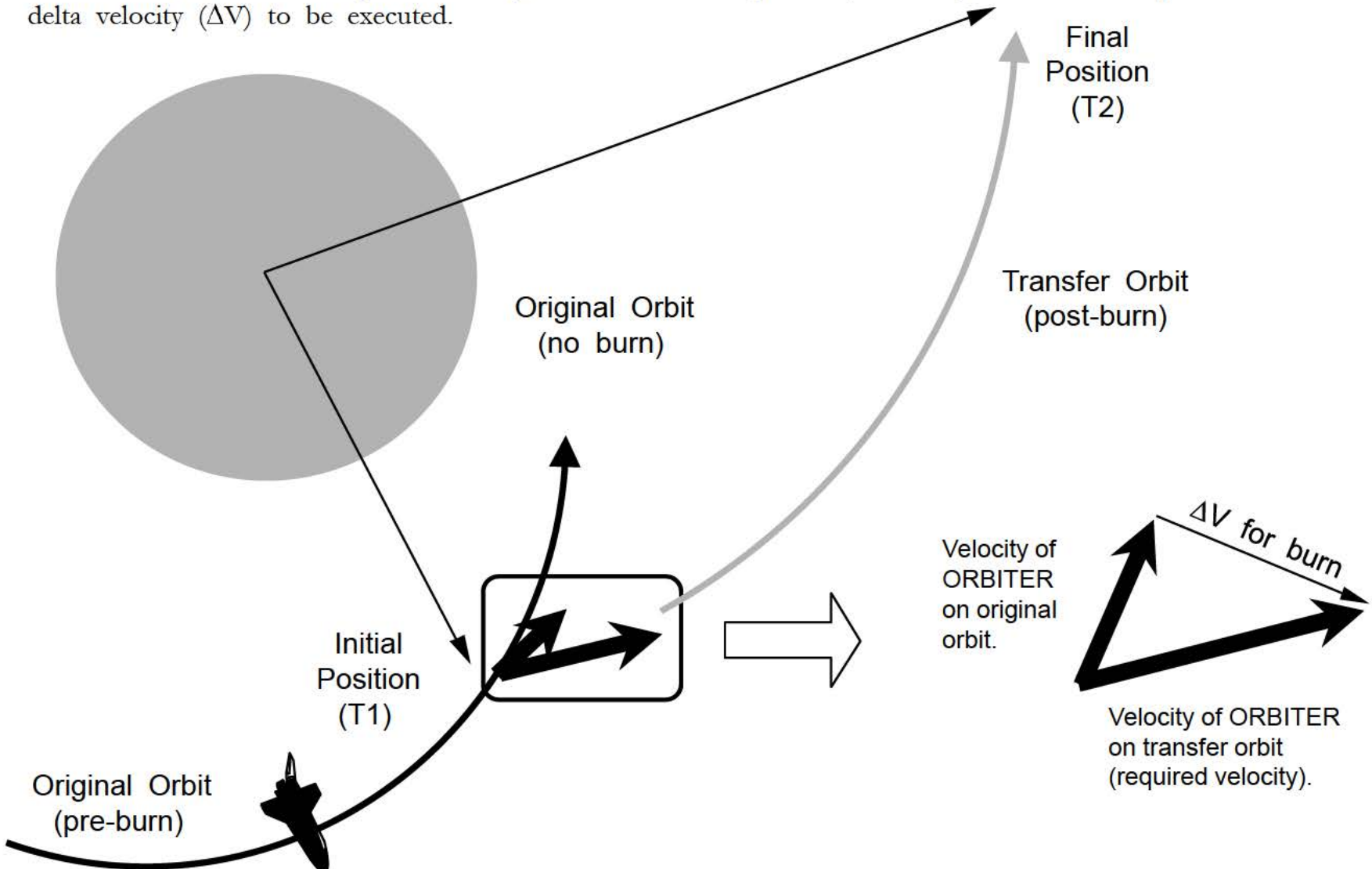
During a rendezvous, the ORBITER performs burns that transfer the ORBITER from one point to another (relative to the TARGET).



The algorithm used to compute rendezvous burns is called LAMBERT TARGETING. Given an initial position, a final position and a transfer time (ΔT), LAMBERT computes the velocity required to get from an initial position to a final position over a period of time ΔT . The initial point (where the burn is executed) is sometimes called “T1” and the final point is sometimes called “T2.”

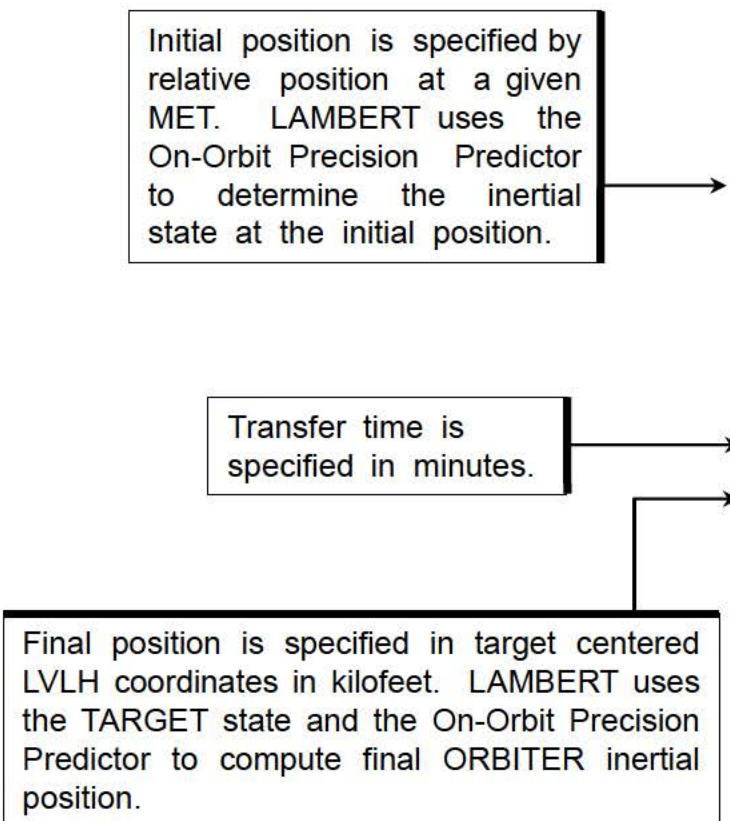


A burn must be executed at the initial position to place the ORBITER on the transfer orbit. LAMBERT computes the ORBITER's required velocity at the initial point to achieve the transfer. The difference between the required velocity and the actual (pre-burn) velocity at the initial point is the delta velocity (ΔV) to be executed.



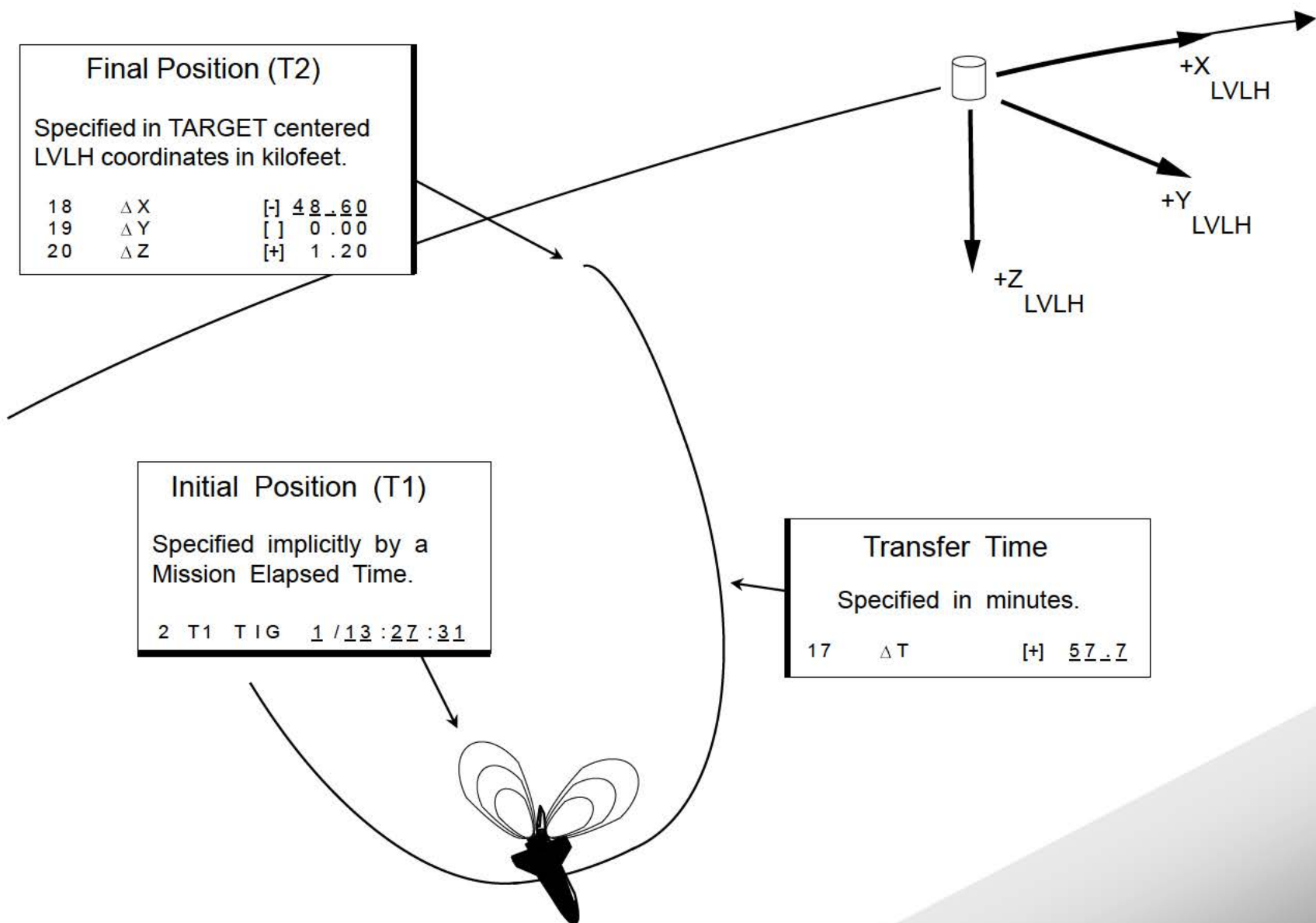
8.2 Display Inputs

The LAMBERT algorithm performs computations in inertial (M50) space. In order to make the interface between the crew and LAMBERT “user friendly,” initial position is defined implicitly in terms of relative position (target centered curvilinear LVLH coordinates) at a given mission elapsed time (MET) and the final position is likewise given in relative coordinates at the given MET + transfer time. This final position is sometimes called the “target offset.” The two positions and transfer time can be called “display inputs.” A burn computation is initiated by an “ITEM 28 EXEC.”



2021 / 034 /		ORBIT	TGT	1 001 / 13 :01 :41 000 / 00 :23 :49
MNVR	TIG	ΔV_x	ΔV_y	ΔV_z
9	1 / 13 :27 :31	+ 0.0	- 0.1	+ 0.1
		PRED	MATCH =	55.3
INPUTS				
1	TGT NO	9		CONTROLS
2	T1 TIG	1 / 13 :27 :31		T2 TO T1 25
6	EL	0 . 00		LOAD 26
7	ΔX / DNRNG	[] 0.00		COMPUTE T1 28*
8	ΔY	[] 0.00		COMPUTE T2 29
9	ΔZ / ΔH	[] 0.00		
10	$\Delta \dot{X}$	[] 0.00		
11	$\Delta \dot{Y}$	[] 0.00		
12	$\Delta \dot{Z}$	[] 0.00		
13	T2 TIG	0 / 00 :00 :00		ORBITER STATE
17	ΔT	[+] 57 . 7		218 / 19 :18 :24 . 974
18	ΔX	[-] 48 . 60		X - 15369 . 250
19	ΔY	[] 0.00		Y +11027 . 125
20	ΔZ	[+] 1 . 20		Z +11577 . 291
21	BASE TIME	1 / 14 :25 :13		VX - 3 . 447589
				VY - 20 . 218801
				VZ - 14 . 607606
ITEM 28 EXEC				

Display inputs in LVLH space:



8.3 Target Sets

ILOADs that define the transfer time and initial and final points are grouped in TARGET SETS. Each set is numbered and can be called up on the display via ITEM 1. The set for a particular burn must be called up before the burn can be computed. There are 40 TARGET SETS available. Shaded parameters on the display are members of or are derived from members of TARGET SET 9.

The diagram shows a flow from a 'Target Sets' table on the left to a detailed ILOAD display on the right. An arrow points from the 'MC-2 on time' row in the table to the corresponding row in the display.

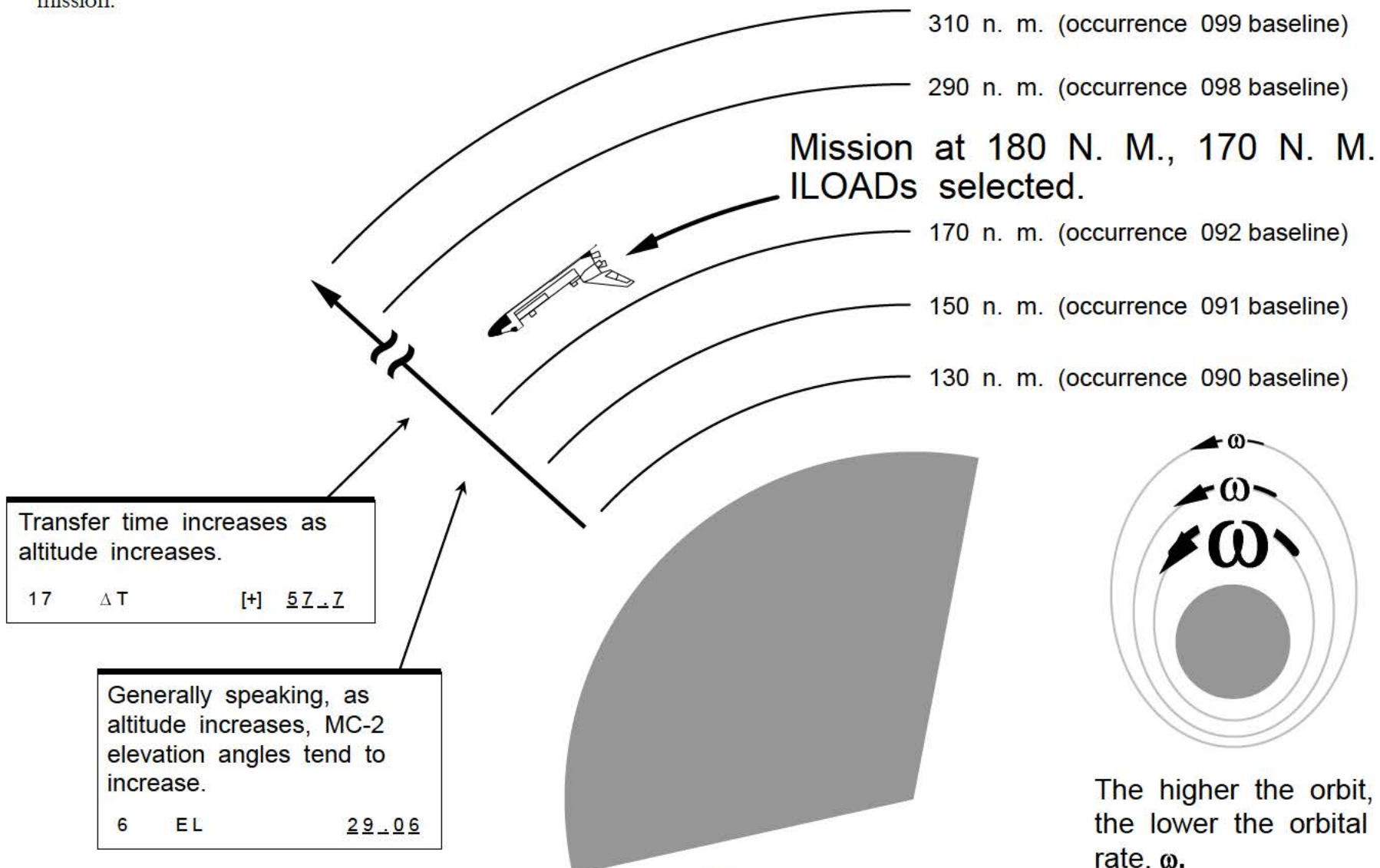
Target Sets	
NCC	9
Ti	10
MC-1	11
MC-2	12
MC-3	13
MC-4	14
MC - 2 on time	19

2021 / 034 /		ORBIT TGT	1 001 / 13 :01 :41		
MNVR	TIG	ΔV_X	ΔV_Y	ΔV_Z	ΔV_T
0 *	0 / 00 :00 :00	0 .0	0 .0	0 .0	0 .0
		PRED	MATCH =		0
INPUTS					
1	TGT NO		9	CONTROLS	
2	T1 TIG	1 / 13 :27 :31		T2 TO T1	25
6	EL	0 .00		LOAD	26
7	ΔX / DNRNG	[]	0 .00	COMPUTE T1	28
8	ΔY	[]	0 .00	COMPUTE T2	29
9	ΔZ / ΔH	[]	0 .00		
10	$\Delta \dot{X}$	[]	0 .00		
11	$\Delta \dot{Y}$	[]	0 .00		
12	$\Delta \dot{Z}$	[]	0 .00		
13	T2 TIG	0 / 00 :00 :00			
17	ΔT	[+]	57 .7	ORBITER STATE	
18	ΔX	[+]	48 .60	218 / 19 :16 :25 .934	X - 14819 .653
19	ΔY	[+]	0 .00		Y +13326 .229
20	ΔZ	[+]	1 .20		Z +19737 .695
21	BASE TIME	1 / 14 :25 :13		VX - 5 .768583	
				VY - 28 .346205	
				VZ - 16 .251806	
ITEM 1 + 9 EXEC					

In addition to transfer time, initial point and final point, each TARGET set contains an ILOAD called LAMB. If LAMB is set to ON, the LAMBERT algorithm is used to compute the burn. If set to OFF, the Clohessy-Wiltshire algorithm is used.

Currently only LAMBERT is used. There is no indication on ORBIT TGT of which method is used.

Transfer time (ΔT) and MC-2 elevation angle (EL) vary according to orbital altitude. Generic ILOADs for each TARGET SET are defined for altitudes from 130 N. M. to 310 N. M. at 20 N. M. intervals. TARGET SETS defined for a particular altitude make up an “occurrence.” The occurrence selected is the one with an altitude at or just below the orbital altitude of the mission.



8.4 Display Outputs

Once the computation is complete (when the “*” next to ITEM 28 disappears), the burn solution, ORBITER LVLH state at the initial point, and the time of arrival at the final point are given. These can be called “display outputs.”

- Maneuver number (target set number).*
- Time of Ignition (TIG).*
- Delta velocity to be executed is given in the orbiter centered LVR frame at T1 in feet/second.

Miss distance (in feet) at the end of each targeting iteration.

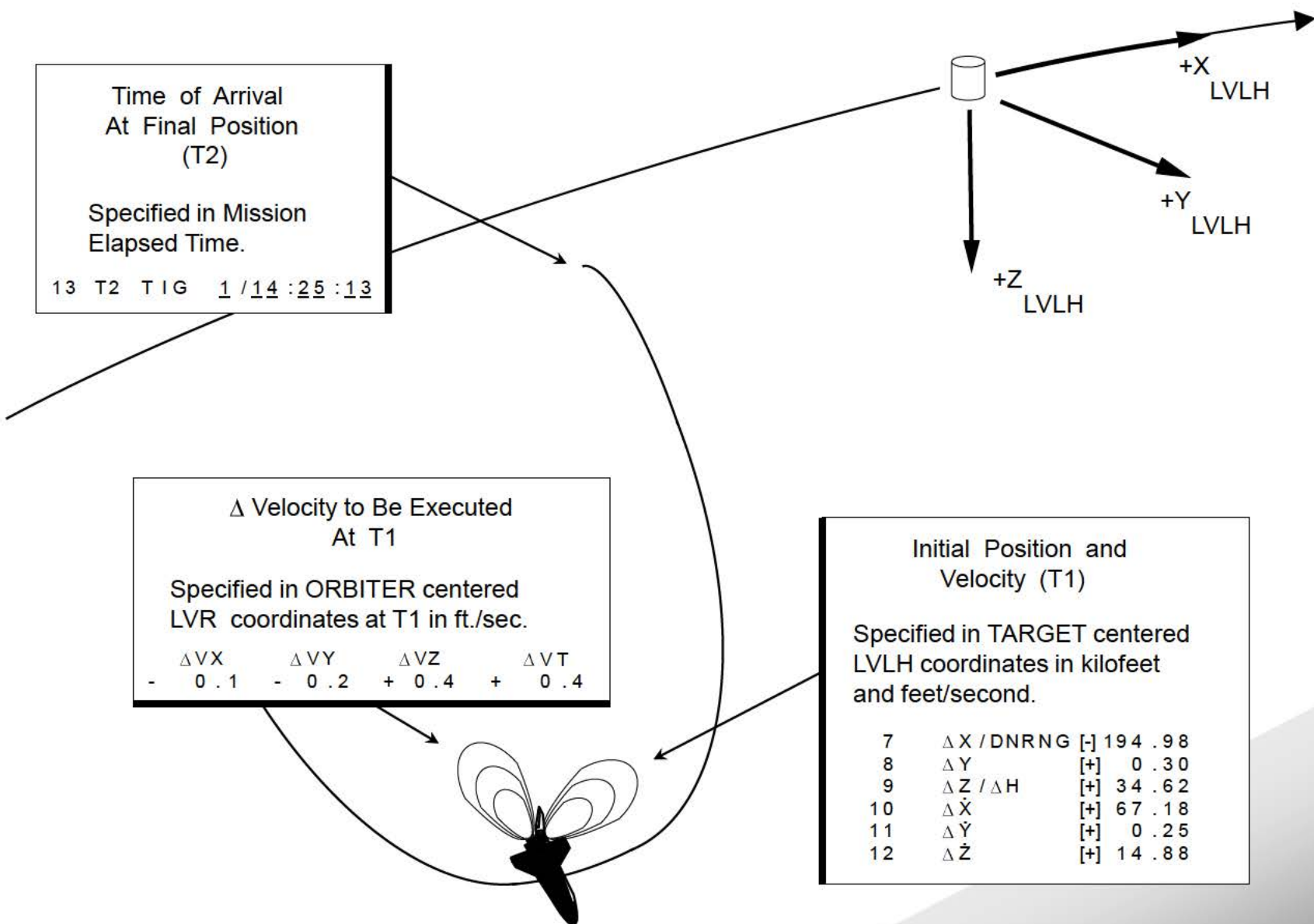
Initial (or burn) position and velocity is computed in target centered LVLH in kilofeet and ft/sec.

Time of arrival at final position is given in Mission Elapsed Time (MET).

2021 / 034 /		ORBIT	TGT	1 001 / 13 :01 :41	
MNVR	TIG	ΔV_X	ΔV_Y	ΔV_Z	ΔV_T
9	1 / 13 :27 :31	- 0 .1	- 0 .2	+ 0 .4	+ 0 .4
PRED MATCH = 2					
INPUTS					CONTROLS
1 TGT NO				9	T2 TO T1 25
2 T1 TIG		1 / 13 :27 :31			LOAD 26
6 EL		0 .00			COMPUTE T1 28
7 ΔX / DNRNG	[+]	194 .98			COMPUTE T2 29
8 ΔY	[+]	0 .30			
9 ΔZ / ΔH	[+]	34 .62			
10 $\Delta \dot{X}$	[+]	67 .18			
11 $\Delta \dot{Y}$	[+]	0 .25			
12 $\Delta \dot{Z}$	[+]	14 .88			
13 T2 TIG		1 / 14 :25 :13			
17 ΔT	[+]	57 .7			ORBITER STATE
18 ΔX	[+]	48 .60			218 / 19 :39 :47 .578
19 ΔY	[+]	0 .00			X - 4756 .307
20 ΔZ	[+]	1 .20			Y - 16423 .261
21 BASE TIME		1 / 14 :25 :13			Z - 14042 .513
					VX +16 .973446
					VY - 14 .712980
					VZ +11 .500532
ITEM 28 EXEC					

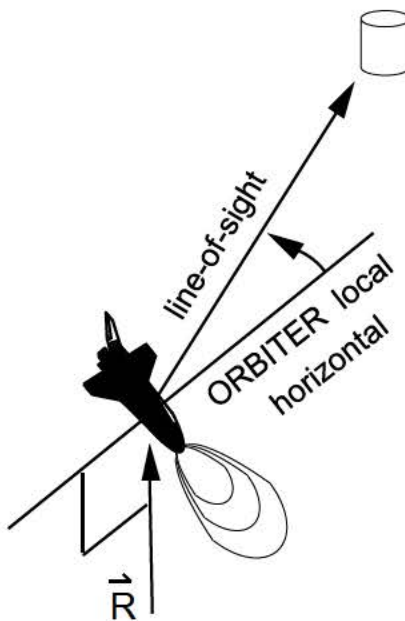
* Maneuver number and TIG at the top of the display are updated once targeting is complete. Execution of ITEM 1 does not change this data.

Display outputs in LVLH space:



8.5 Elevation Angle Option

Unlike the NCC, Ti, MC-1, MC-3 and MC-4 burns, the MC-2 burn is determined by the ORBITER's position relative to the TARGET, instead of time. The time constraint is included in the ILOADs, but is overridden by a non-zero elevation angle. This is done to ensure a sunrise just prior to MC-4 and to maintain the MC-2 to MC-4 geometry in dispersed cases. TARGET SET 12 is normally used for MC-2.

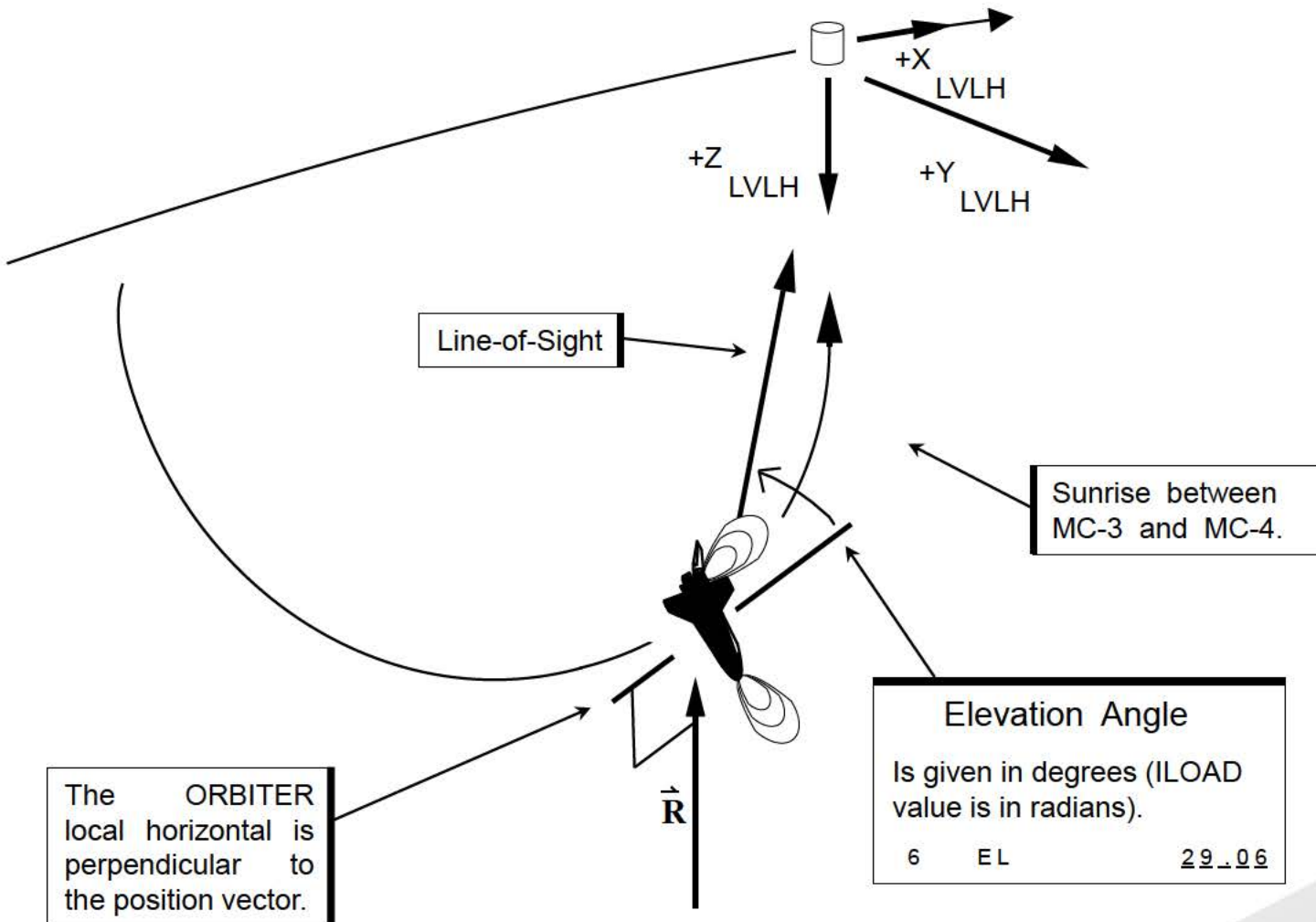


Elevation angle is the angle measured from the ORBITER's local horizontal to the line of sight vector to the TARGET. The ILOADed angle varies with altitude but is between 28.45 and 30.25 degrees.

2021 / 034 /		ORBIT	TGT	1 001 / 14 : 47 : 23	
MNVR	TIG	ΔV_X	ΔV_Y	ΔV_Z	ΔV_T
11	1 / 14 : 47 : 22	+ 0.2	+ 0.1	- 0.1	+ 0.2
PRED MATCH = 125					
INPUTS					
1	TGT NO	12			
2	T1 TIG	1 / 15 : 15 : 06			
6	EL	29.07			
7	ΔX / DNRNG	[]	0.00		
8	ΔY	[]	0.00		
9	ΔZ / ΔH	[]	0.00		
10	$\Delta \dot{X}$	[]	0.00		
11	$\Delta \dot{Y}$	[]	0.00		
12	$\Delta \dot{Z}$	[]	0.00		
13	T2 TIG	0 / 00 : 00 : 00			
17	ΔT	[+]	27.0		
18	ΔX	[+]	0.90		
19	ΔY	[+]	0.00		
20	ΔZ	[+]	1.80		
21	BASE TIME	1 / 14 : 25 : 13			
CONTROLS					
T2	TO T1	25			
LOAD		26			
COMPUTE	T1	28*			
COMPUTE	T2	29			
ORBITER STATE					
218	/ 21 : 2 : 9.658				
X	- 12897.821				
Y	- 5071.080				
Z	- 17293.485				
VX	+ 10.019524				
VY	- 23.107965				
VZ	- 0.659777				

ITEM 28 EXEC

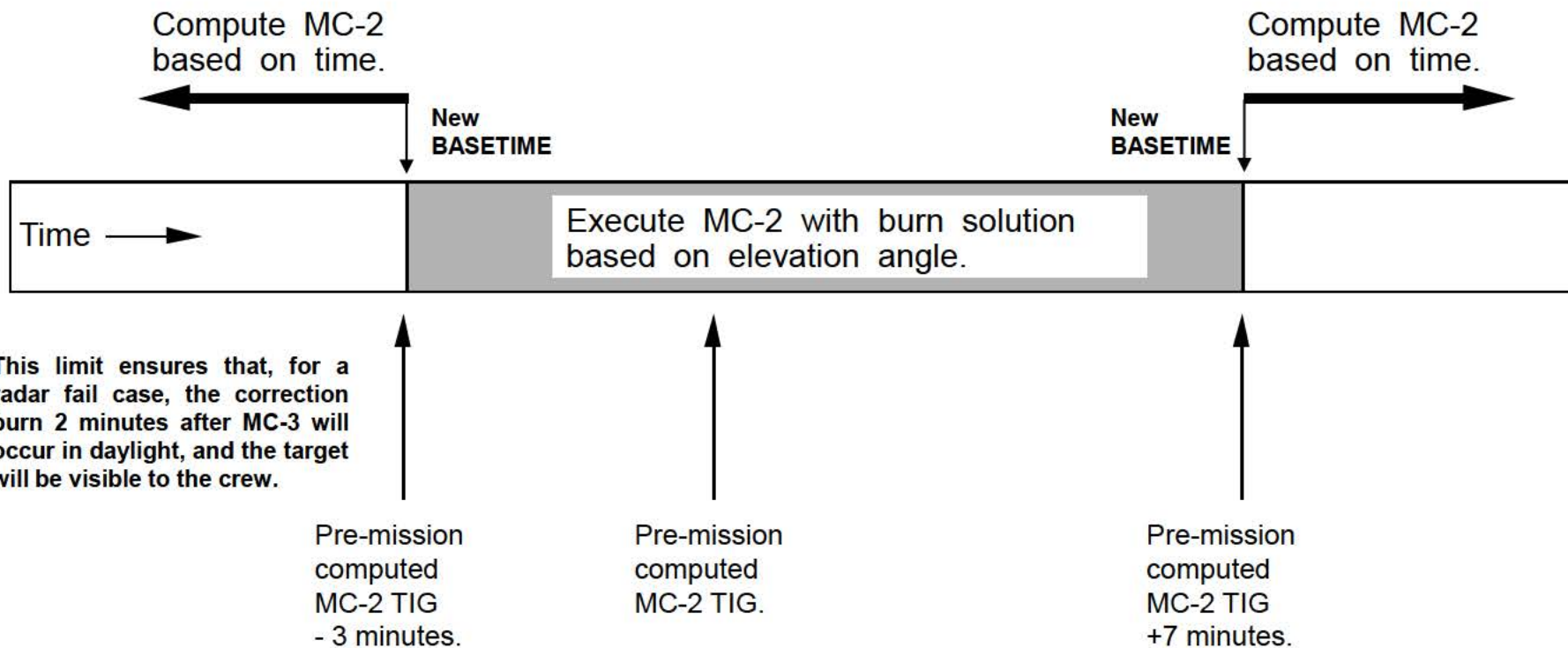
Burning MC-2 on an elevation angle standardizes the manual approach phase and keeps the in-plane dispersion ellipse aligned with the trajectory. This helps maintain control over dispersions later in the profile.



8.6 MC-2 Time of Ignition (TIG) Slip

Due to navigation errors, sensor errors, burn trim errors and 6 degree-of-freedom effects, the time at which the desired elevation angle occurs may differ from the pre-mission value. If there is too much of a difference, part of the manual approach may take place at night.

To protect the manual approach in daylight requirement, MC-2 is computed based on time if too much of a slip occurs using the elevation angle. The crew compares the computed TIG against the limits illustrated below. If the TIG falls outside the shaded area, **the crew sets the BASETIME to the planned TIG –3 minutes or +7 minutes and then computes the burn with TARGET SET 19.**

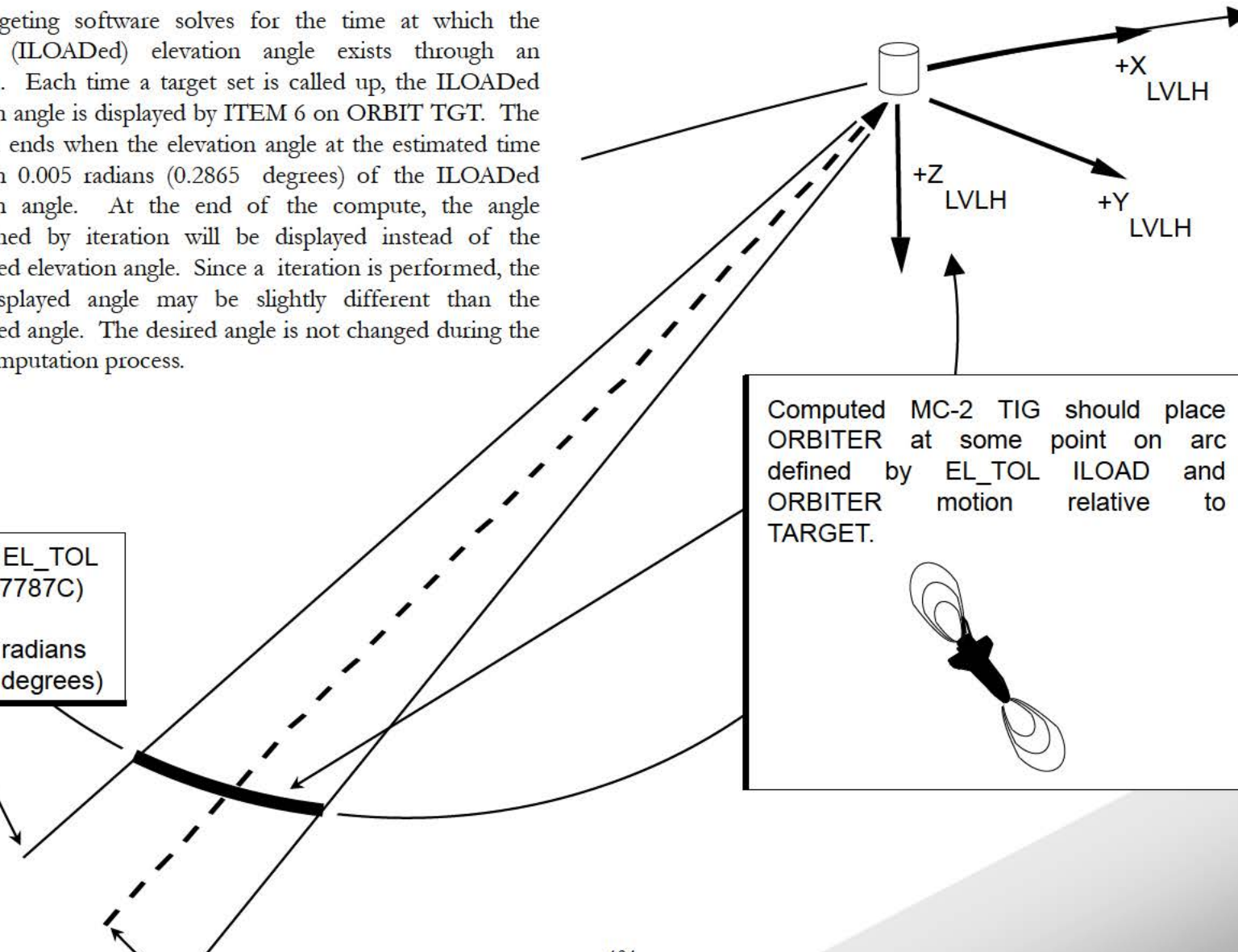


8.7 Elevation Angle Tolerance

The targeting software solves for the time at which the desired (ILOADed) elevation angle exists through an iteration. Each time a target set is called up, the ILOADed elevation angle is displayed by ITEM 6 on ORBIT TGT. The iteration ends when the elevation angle at the estimated time is within 0.005 radians (0.2865 degrees) of the ILOADed elevation angle. At the end of the compute, the angle determined by iteration will be displayed instead of the ILOADed elevation angle. Since a iteration is performed, the final displayed angle may be slightly different than the ILOADed angle. The desired angle is not changed during the burn computation process.

ILOAD EL_TOL
(V96U7787C)

0.005 radians
(0.2865 degrees)



8.8 Targeting With TIG In The Past

If the displayed TIG for the target set in question is in the past, an asterisk will appear in the upper left hand corner between the maneuver number and TIG. **The timer in the upper right hand corner of the display will be counting up.** The asterisk will remain until another compute is completed, or a new target set is called up. This example is of a post Ti burn recompute from a STS-101 SPF Level 8 rendezvous case. The original Ti ΔV, from the last targeting prior to burn execution, is displayed. Note also the PRED MATCH value. Values of PRED MATCH are displayed while targeting is converging on a solution.

2021 / 034 /	ORBIT TGT	1 001 / 14 :26 :15 000 / 00 :01 :02
MNVR	TIG	ΔVX ΔVY ΔVZ ΔVT
10 *	1 / 14 :25 :13	+ 8.3 - 0.4 - 0.2 + 8.3
		PRED MATCH = 1706
INPUTS		CONTROLS
1 TGT NO	10	T2 TO T1 25
2 T1 TIG	1 / 14 :25 :13	LOAD 26
6 EL	0 . 00	COMPUTE T1 28*
7 ΔX / DNRNG	[] 0 . 00	COMPUTE T2 29
8 ΔY	[] 0 . 00	
9 ΔZ / ΔH	[] 0 . 00	
10 ΔX	[] 0 . 00	
11 ΔY	[] 0 . 00	
12 ΔZ	[] 0 . 00	
13 T2 TIG	0 / 00 :00 :00	ORBITER STATE
17 ΔT	[+] 76 . 9	218 / 20 :40 :58 . 618
18 ΔX	[+] 0 . 90	X - 10396 . 955
19 ΔY	[] 0 . 00	Y +19542 . 842
20 ΔZ	[+] 1 . 80	Z - 1591 . 274
21 BASE TIME	1 / 14 :25 :13	VX - 13 . 248472
		VY - 8 . 650884
		VZ - 19 . 589226
ITEM 28 EXEC		

When a computation is performed with TIG in the past, TIG is reset to the current time plus 60 seconds (LOAD PROX_DTMIN_LAMB (V96U7777C) for Lambert). If the burn is based on elevation angle, the angle will be ignored.

Upon completion, the new TIG and transfer time (ΔT , ITEM 17) will be displayed. The timer in the upper right hand corner should be counting down and have a value less than 60 seconds.

2021 / 034 /	ORBIT	TGT	1 001 / 14 :26 :20 000 / 00 :00 :46
MNVR	TIG	ΔV_X ΔV_Y ΔV_Z ΔV_T	
10	1 / 14 :27 :06	- 0 .1 + 0 .1 + 0 .1 + 0 .2	PRED MATCH = 14
INPUTS	CONTROLS		
1 TGT NO	T2 TO T1	25	
2 T1 TIG	LOAD	26	
6 EL	COMPUTE T1	28	
7 ΔX / DNRNG	COMPUTE T2	29	
8 ΔY			
9 ΔZ / ΔH			
10 $\Delta \dot{X}$			
11 $\Delta \dot{Y}$			
12 $\Delta \dot{Z}$			
13 T2 TIG	ORB ITER	STATE	
17 ΔT	218 / 20 :41 :	2 .458	
18 ΔX	X - 10447 .730		
19 ΔY	Y +19509 .437		
20 ΔZ	Z - 1666 .482		
21 BASE TIME	VX - 13 .196834		
	VY - 8 .747557		
	VZ - 19 .581139		
ITEM 28 EXEC			

8.9 Base Time

During a mission, events rarely occur at the time determined during pre-mission planning. This can cause the burn times to change. BASE TIME is used to easily adjust the burn times. Instead of specifying an absolute time (such as GMT or MET) when a burn is to occur, each burn is given an execution time relative to BASE TIME. By changing BASE TIME, the crew can adjust the ignition times of the burns, or even move the rendezvous profile to a different day of the flight.

The equation used to compute the TIG is :

$$T1_TIG = \text{BASE_TIME} + T1_ILOAD$$

T1_ILOAD is an ILOAD that specifies when the burn occurs relative to BASE TIME. Each burn has a T1_ILOAD value.

For NCC, Ti, MC-1 and the first MC-2 compute the BASE TIME is the time of Ti.

When a MC-2 (elevation angle) compute is performed, BASE TIME is reset to MC-2 TIG. MC-3 and MC-4 TIGs are determined using the new BASE TIME.

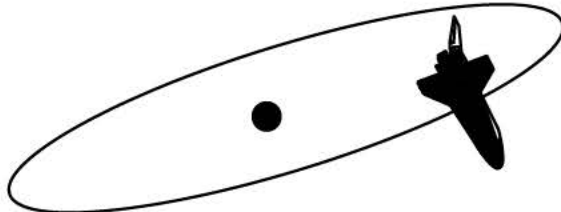
After the crew enters BASE TIME, a LOAD must be performed to overwrite the ILOADed BASE TIME. "ITEM 26 EXEC" is usually done with TARGET SET 1 called up, although any target set (other than zero) could be used.

2021 / 034 /		ORBIT	TGT	1 001 / 13 : 01 : 39	000 / 00 : 00 : 00
MNVR	TIG	ΔV_x	ΔV_y	ΔV_z	ΔV_t
0 *	0 / 00 : 00 : 00	0 . 0	0 . 0	0 . 0	0 . 0
		PRED	MATCH	=	0
INPUTS					
1	TGT NO			1	
2	T1 TIG	0 / 00 : 00 : 00			
6	EL		00 . 00		
7	ΔX / DNRNG	[]	0 . 00		
8	ΔY	[]	0 . 00		
9	ΔZ / ΔH	[]	0 . 00		
10	ΔX	[]	0 . 00		
11	ΔY	[]	0 . 00		
12	ΔZ	[]	0 . 00		
13	T2 TIG	0 / 00 : 00 : 00			
17	ΔT	[]	00 . 0		
18	ΔX	[]	0 . 00		
19	ΔY	[]	0 . 00		
20	ΔZ	[]	0 . 00		
21	BASE TIME	1 / 14 : 25 : 13			
CONTROLS					
	T2 TO T1	25			
	LOAD	26			
	COMPUTE T1	28			
	COMPUTE T2	29			
ORBITER STATE					
218	/ 19 : 16 : 25 . 934				
X	- 14819 . 863				
Y	+13326 . 029				
Z	- 9737 . 765				
VX	- 5 . 768653				
VY	- 18 . 346425				
VZ	- 16 . 251186				
ITEM 26 EXEC					

8.10 Prediction Match

The LAMBERT algorithm was derived through the use of several assumptions about the forces acting on the ORBITER.

LAMBERT World



- Point mass Earth.
- No atmospheric drag.
LAMBERT is only valid for conic orbits.

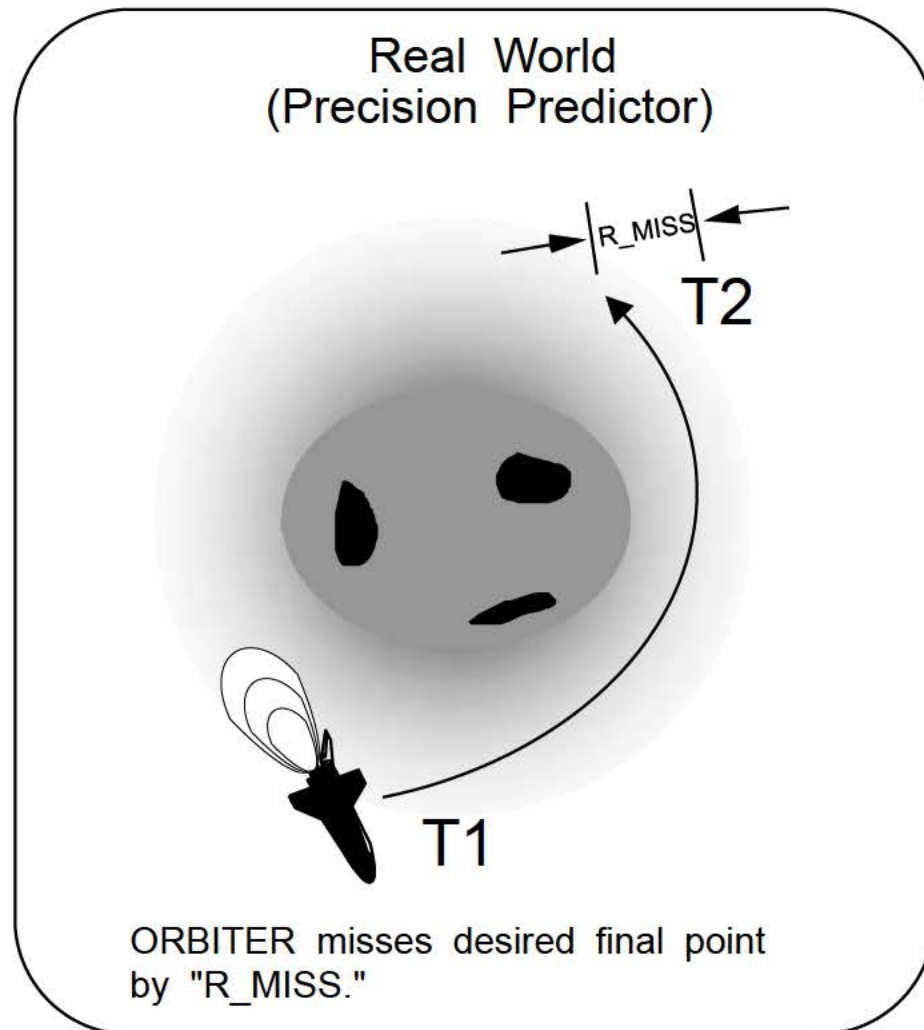
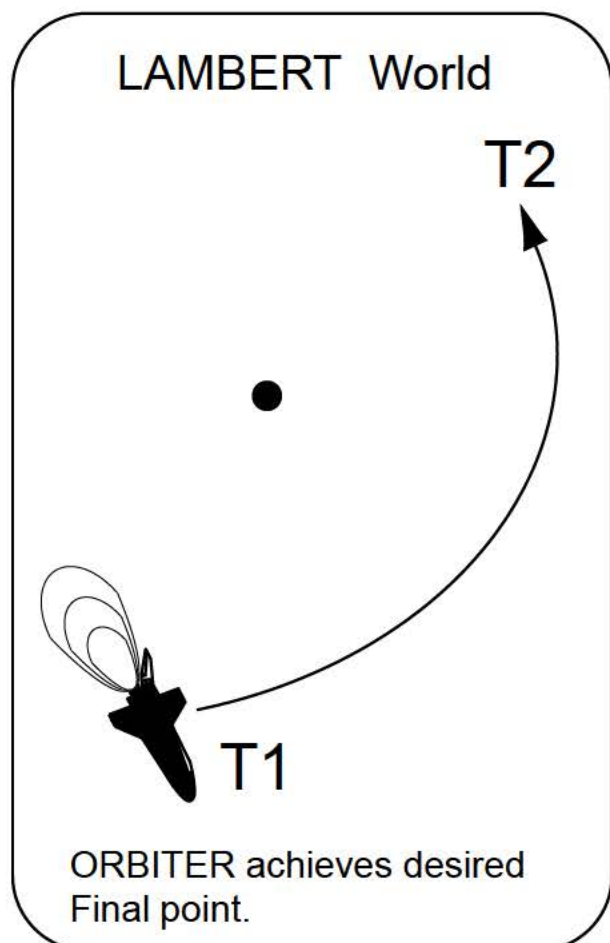
Real World



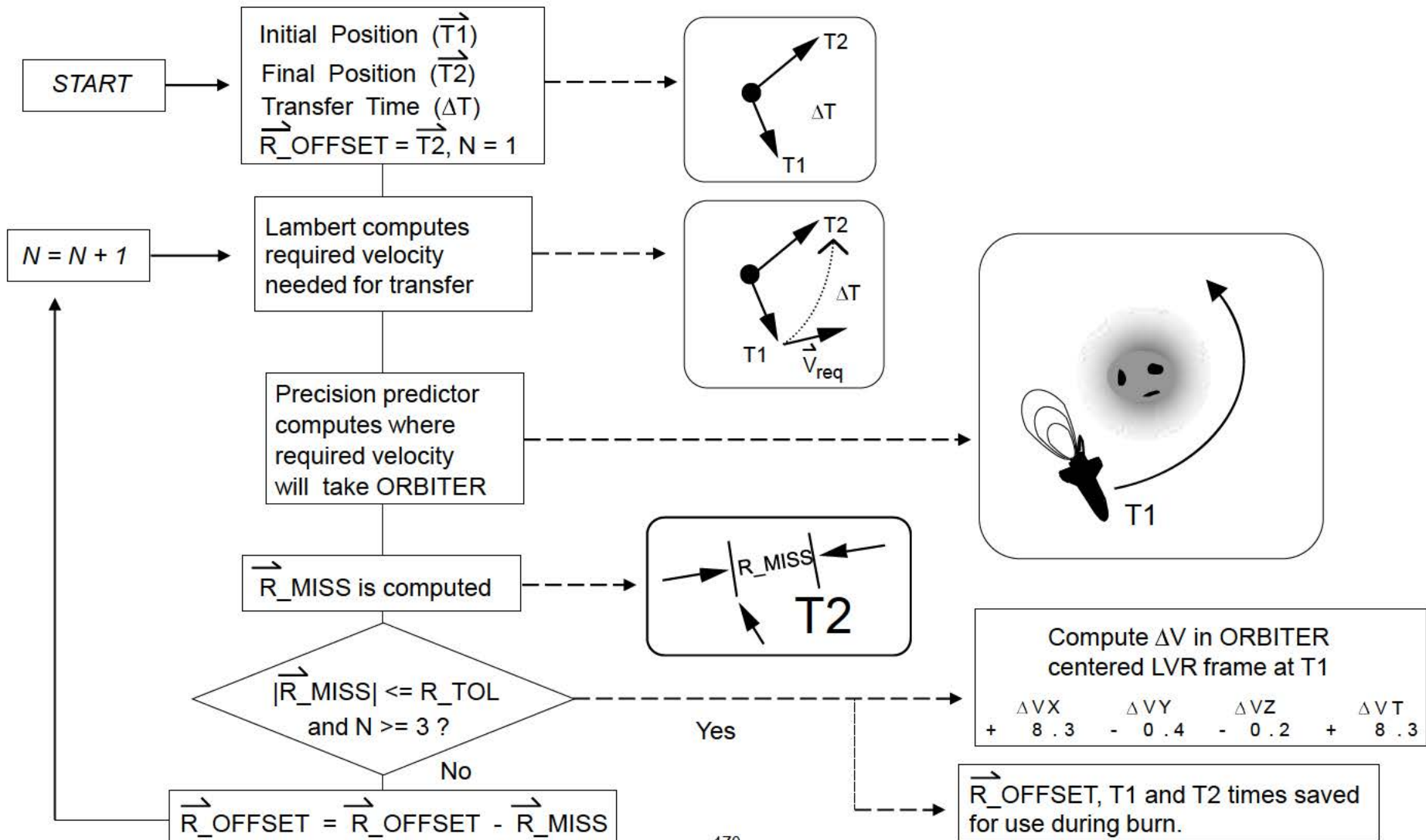
- Non-spherical Earth with uneven mass distribution.
- Atmospheric drag.

The Flight Software approximates the “real world” via the On-Orbit Precision Predictor (equations of motion) and math models for gravitational harmonics and atmospheric drag.

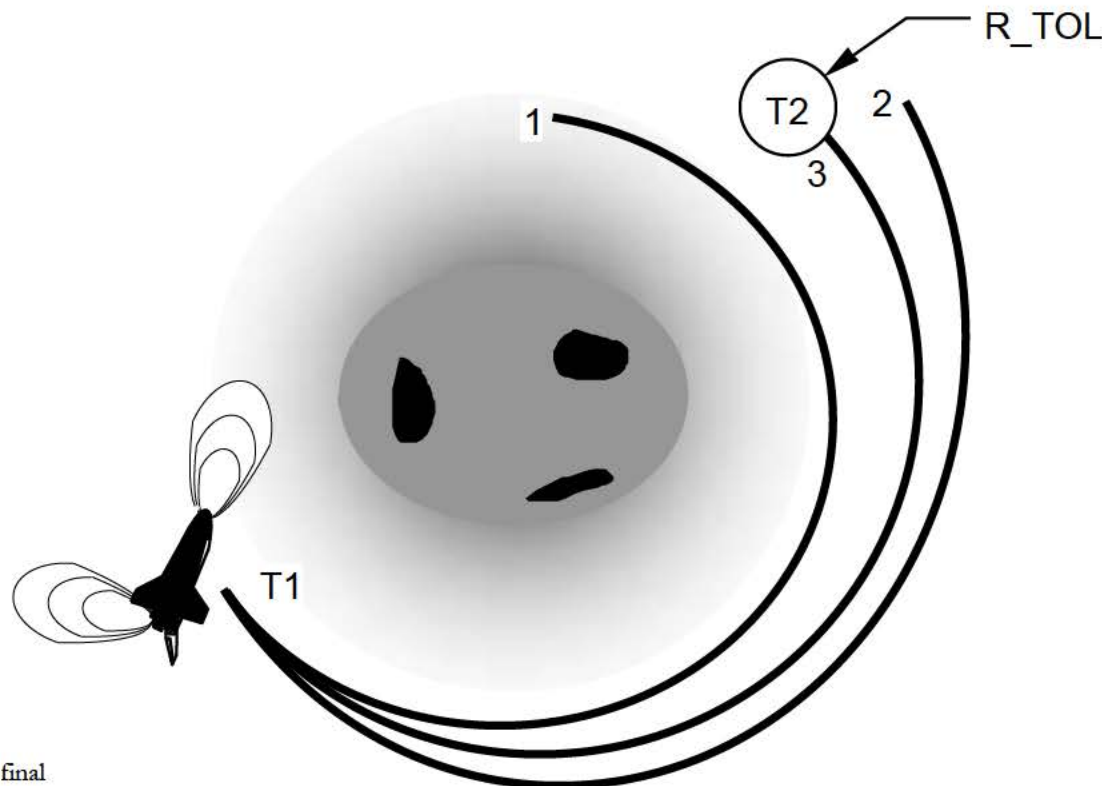
Display inputs are converted from time and LVLH position to initial and final M50 positions, respectively, by using the On-Orbit Precision Predictor. LAMBERT then uses the positions and transfer time to compute the required velocity. However, if the ORBITER has the required velocity at T1, it will not reach the desired final position. This is due to the assumptions made when deriving the LAMBERT equations.



The targeting software iteratively adjusts the targeted final position to get around this problem. Once LAMBERT has computed the required velocity, the Precision Predictor is used to determine where the ORBITER will be at the end of the transfer if the burn is executed. \vec{R}_{MISS} is computed by subtracting the desired final position (T_2) from the predicted position. If \vec{R}_{MISS} is greater than an ILOADed tolerance (R_{TOL}), the targeted final position (\vec{R}_{OFFSET}) is adjusted by the amount \vec{R}_{MISS} , and the LAMBERT procedure is repeated. This process must be performed a minimum of 3 times (ILOAD NMIN, V96U7516C).



With each iteration, the value of R_MISS should decrease until R_MISS is less than or equal to R_TOL. R_TOL may be thought of as being the radius of a sphere with the desired final position (T2) at the center of the sphere. The number of iterations needed depends upon the value of R_TOL and the ILOADed minimum (3) and maximum (10) number of iterations.



Note: The direction the predicted final position approaches the desired final position that is shown here is based on analysis of R_MISS data from Level 8 simulations. R_TOL was 10 feet. NCC and the Mid-Courses required 3 iterations, Ti required 4.

While the computation is in progress, values of R_MISS are displayed below the delta velocity. It is labeled PRED MATCH, or PREDICTION MATCH. Upon completion, the final value should be less than or equal to R_TOL.

Final value
of R_MISS
in feet.

2021 / 034 /		ORBIT TGT		1 001 / 14 :21 :31	
				000 / 00 :03 :42	
MNVR	TIG	ΔV_X	ΔV_Y	ΔV_Z	ΔV_T
10	1 / 14 :25 :13	+ 8 .3	- 0 .4	- 0 .2	+ 8 .3
PRED MATCH = 17					
INPUTS			CONTROLS		
1	TGT NO	10	T2 TO T1	25	
2	T1 TIG	1 / 14 :25 :13	LOAD	26	
6	EL	0 .00	COMPUTE T1	28	
7	ΔX / DNRNG	[+] 52 .61	COMPUTE T2	29	
8	ΔY	[+] 0 .15			
9	ΔZ / ΔH	[+] 0 .11			
10	$\Delta \dot{X}$	[+] 11 .53			
11	$\Delta \dot{Y}$	[+] 0 .57			
12	$\Delta \dot{Z}$	[+] 1 .14			
13	T2 TIG	1 / 15 :42 :06	ORBITER STATE		
17	ΔT	[+] 76 .9	218 / 20 :36 :14 .458		
18	ΔX	[+] 0 .90	X - 6161 .856		
19	ΔY	[+] 0 .00	Y +20949 .483		
20	ΔZ	[+] 1 .80	Z + 3959 .738		
21	BASE TIME	1 / 14 :25 :13	VX - 16 .303619		
ITEM 28 EXEC					
VY - 1 .165214					
VZ - 19 .145939					

8.11 Orbiter State

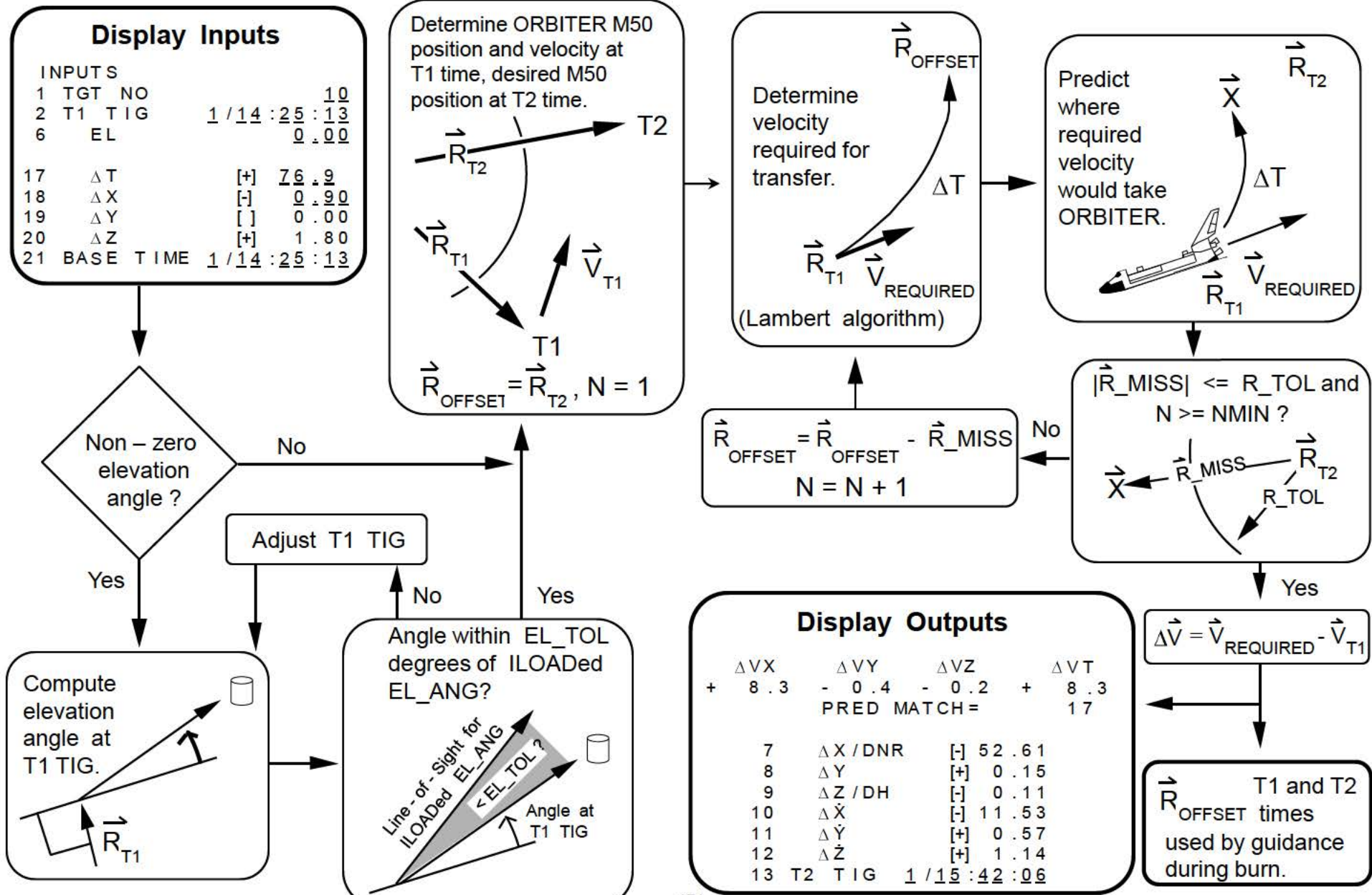
During the flight, the crew uses computers in the cockpit that are not a part of the ORBITER's avionics system. Some of these computers need an ORBITER state vector. The M50 state vector is displayed on ORBIT TGT so that the crew can key it into another computer. ORBIT TGT was chosen to display ORBITER STATE since it had more unoccupied space than other displays.

ORBITER inertial state vector is given in M50 coordinates in kilofeet and kilofeet/second.

The crew can freeze the display by pressing the "SPEC" button on the DEU keyboard. This prevents the displayed state vector from being updated while the crew is reading it.

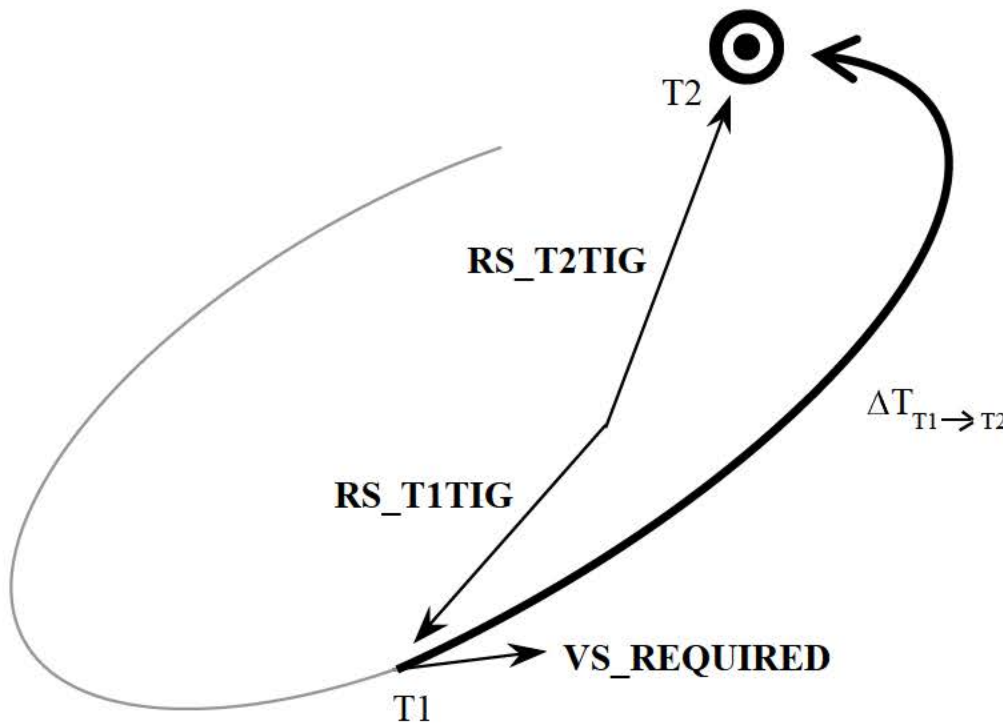
2021 / 034 /	ORBIT TGT	1 001 / 14 :21 :31 000 / 00 :03 :42
MNVR	TIG	ΔV_x ΔV_y ΔV_z ΔV_t
10	1 / 14 :25 :13	+ 8 .3 - 0 .4 - 0 .2 + 8 .3
		PRED MATCH = 17
INPUTS		CONTROLS
1 TGT NO	10	T2 TO T1 25
2 T1 TIG	1 / 14 :25 :13	LOAD 26
6 EL	0 .00	COMPUTE T1 28
7 ΔX / DNRNG	[+] 52 .61	COMPUTE T2 29
8 ΔY	[+] 0 .15	
9 ΔZ / ΔH	[+] 0 .11	
10 $\Delta \dot{X}$	[+] 11 .53	
11 $\Delta \dot{Y}$	[+] 0 .57	
12 $\Delta \dot{Z}$	[+] 1 .14	
13 T2 TIG	1 / 15 :42 :06	
17 ΔT	[+] 76 .9	
18 ΔX	[+] 0 .90	
19 ΔY	[+] 0 .00	
20 ΔZ	[+] 1 .80	
21 BASE TIME	1 / 14 :25 :13	
ITEM 28 EXEC		ORBITER STATE 218 / 20 :36 :14 .458 X - 6161 .856 Y +20949 .483 Z + 3959 .738 VX - 16 .303619 VY - 1 .165214 VZ - 19 .145939

8.12 Lambert Targeting Summary

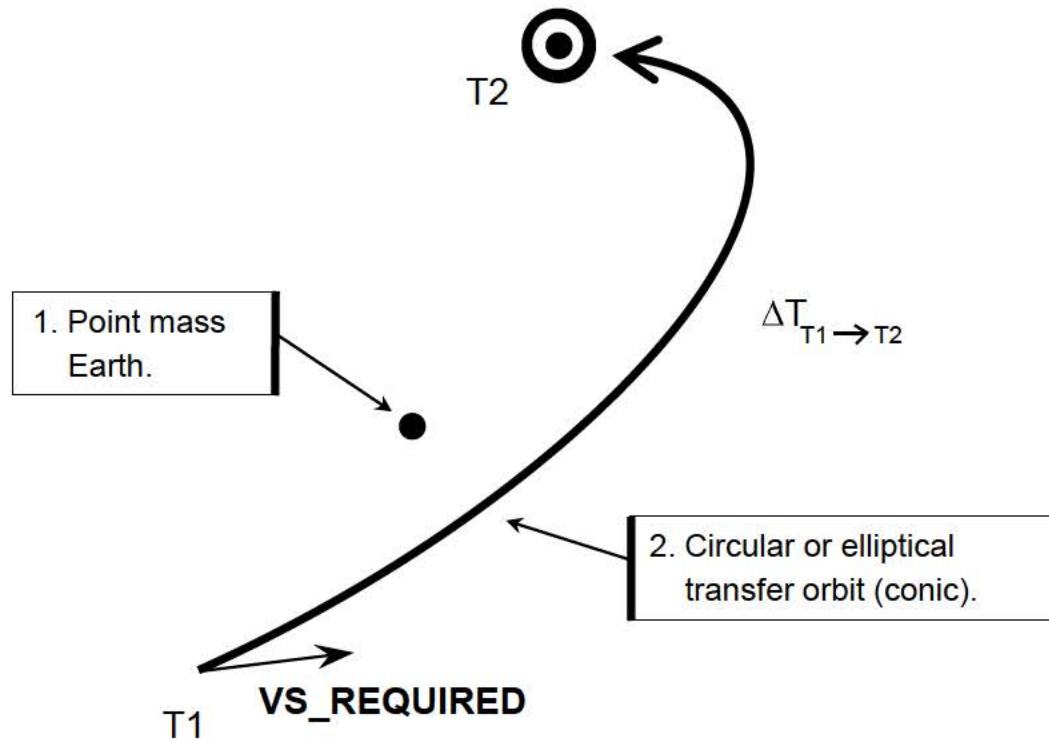


8.13 A Closer Look at the Precision Velocity Required Computation

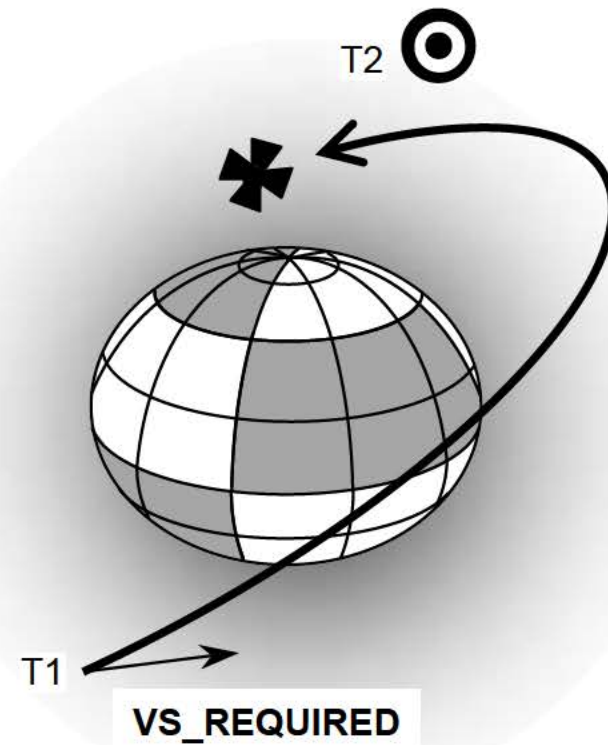
The Lambert algorithm used in the FSW computes the velocity required (**VS_REQUIRED**) to transfer from an initial point (**RS_T1TIG** or **RS_IPO**) to a final point (**RS_T2TIG**) over a given transfer time (ΔT).



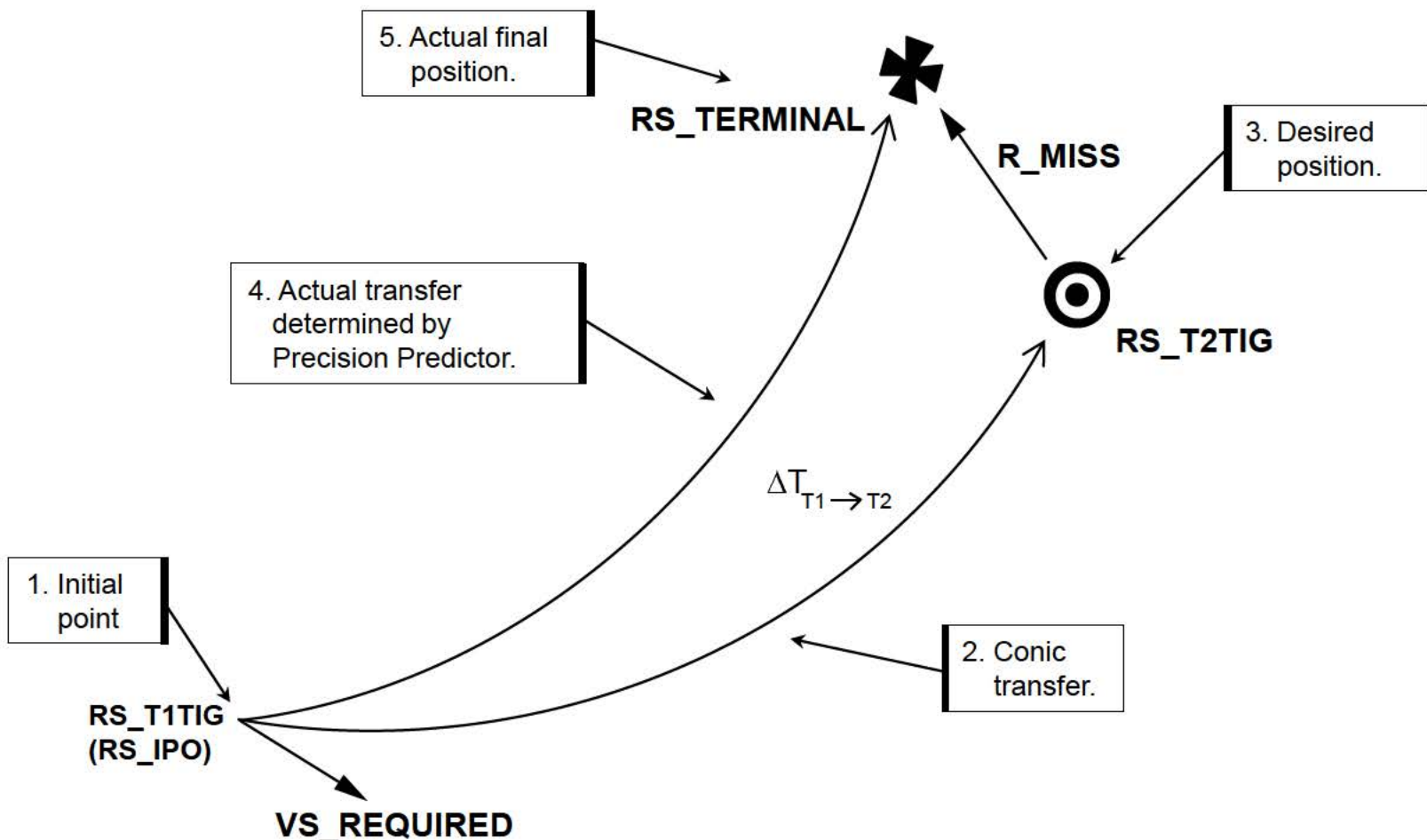
Lambert's theorem is valid for conic orbits. The Lambert algorithm in the FSW is valid for circular and elliptical orbits. Central force gravity (point mass Earth) is assumed to be the only force acting on the orbiter during the transfer.



In reality, there are more forces than just central force gravity acting on the orbiter. These include atmospheric drag and gravitational harmonics due to a non-spherical Earth of uneven mass distribution. If the orbiter possessed the **VS_REQUIRED** computed by Lambert at T1, the orbiter would miss the T2 position by several hundred thousand feet.

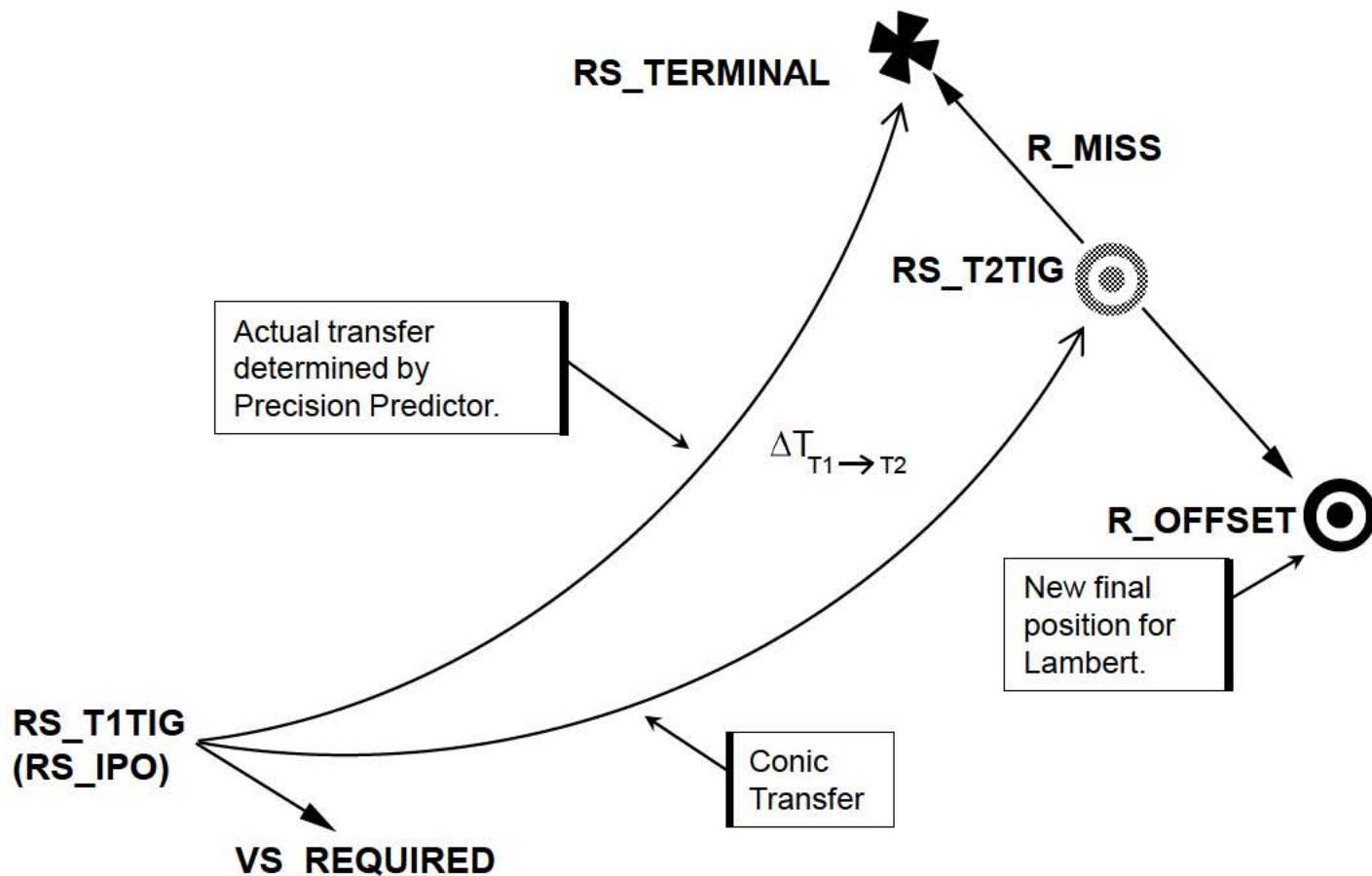


The FSW gets around the central force gravity assumption by determining where **VS_REQUIRED** would take the orbiter if the burn were to be executed. This is done by the On-Orbit Precision Predictor. The post-burn state at the initial point (**RS_IPO** and **VS_REQUIRED**) is predicted forward over the transfer time (ΔT). The Precision Predictor uses a 4x2 gravity model and atmospheric drag (constant drag coefficient) to make the predicted state at T2 as “realistic” as possible. The miss vector (**R_MISS**) can then be determined by subtracting the desired position (**RS_T2TIG**) from the actual position (**RS_TERMINAL**) at the end of the transfer.

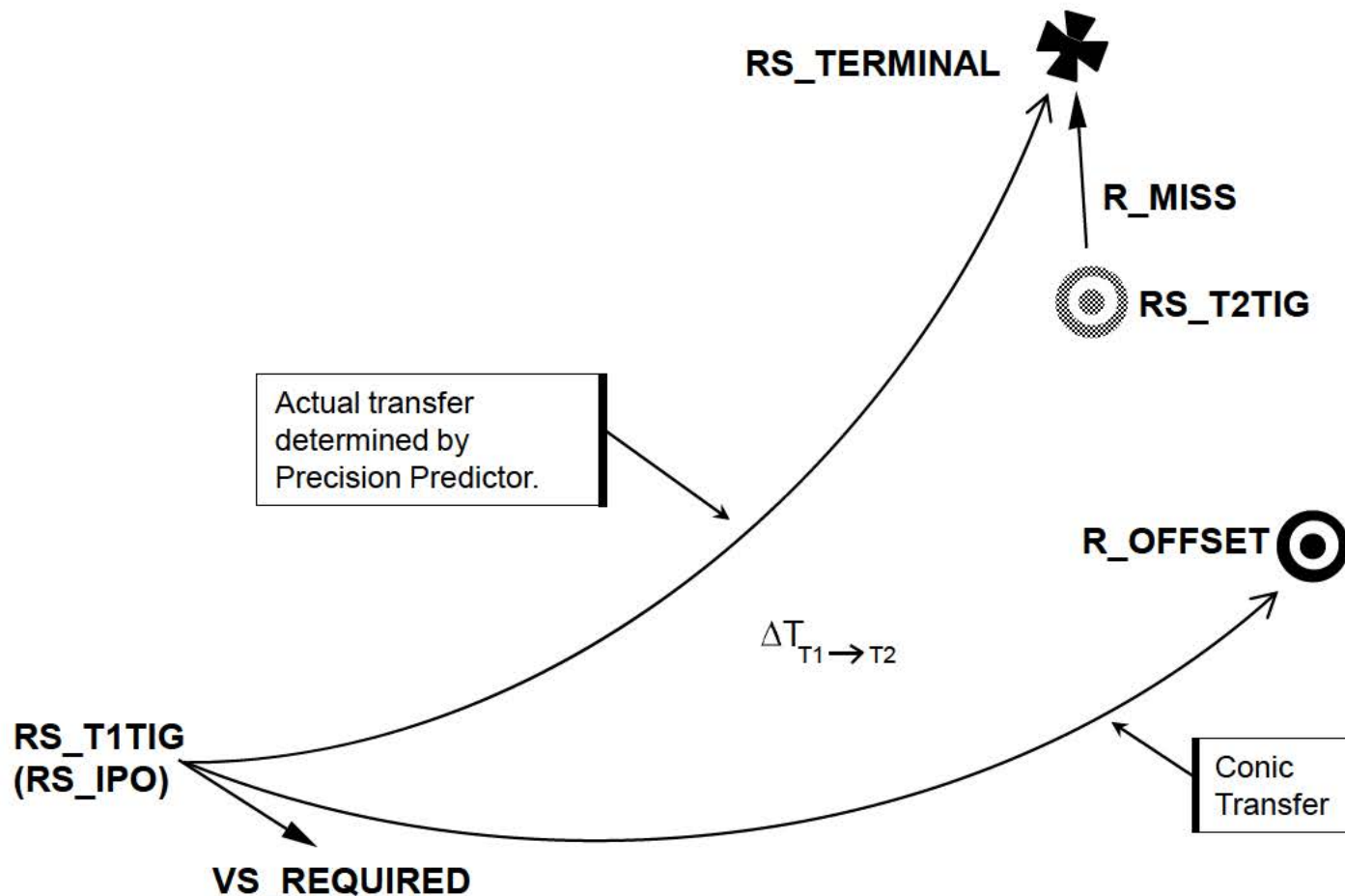


In the initial Lambert computation, the burn was targeted with **RS_T2TIG** as the desired final position. To compensate for the central force assumption, the Lambert computation is repeated with a new target point.

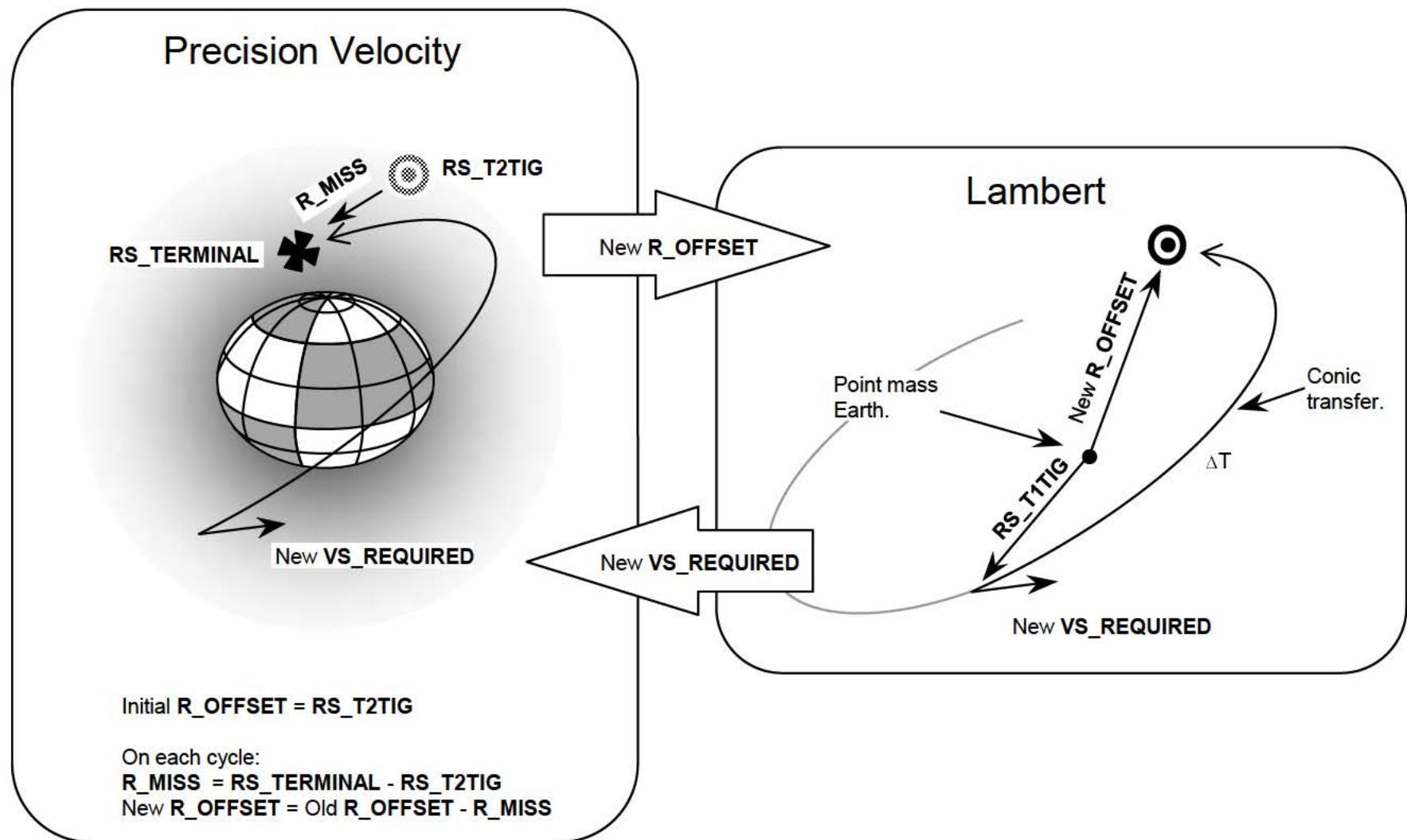
The new target point (**R_OFFSET**) is found by subtracting the miss vector (**R_MISS**) from the desired final point (**RS_T2TIG**). This means that the next Lambert computation will determine a required velocity (**VS_REQUIRED**) needed for a conic transfer from **RS_IPO** to the **R_OFFSET** position.



After the second Lambert computation, the Precision Predictor then determines where the required velocity will take the orbiter (a new **RS_TERMINAL**). A new value for **R_MISS** is then determined by subtracting **RS_T2TIG** from **RS_TERMINAL**. The value for **R_OFFSET** to be used by Lambert in the next iteration is computed by subtracting **R_MISS** from the old **R_OFFSET**. It is important to note that although the desired final position given to Lambert is changed (**R_OFFSET**), **R_MISS** is still computed with respect to the actual desired final position, **RS_T2TIG**.

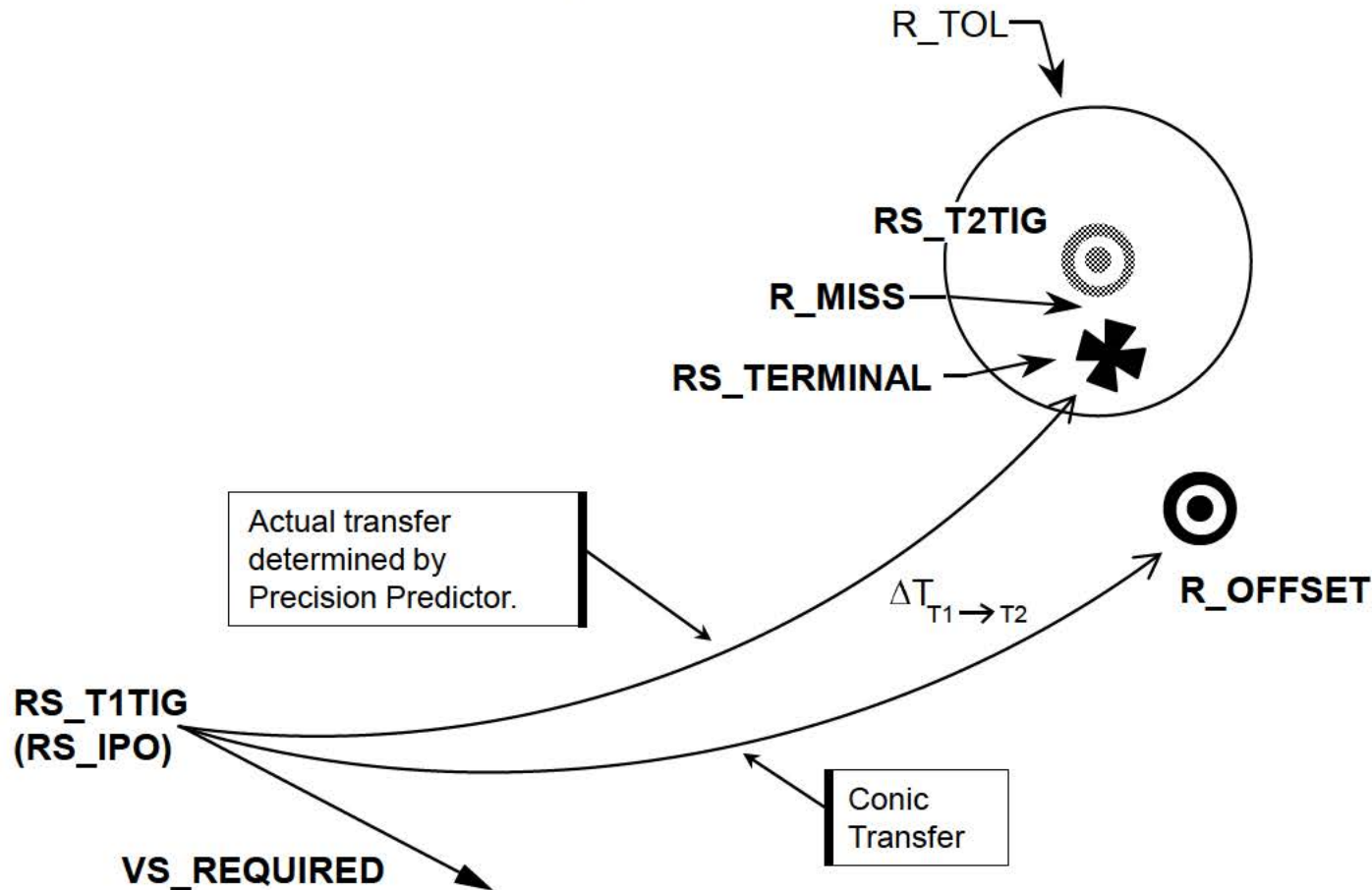


This process is performed a minimum of 3 times (ILOAD NMIN, V96U7516C), but no more than 10 times (ILOAD N_MAX_ITER, V96U7790C).

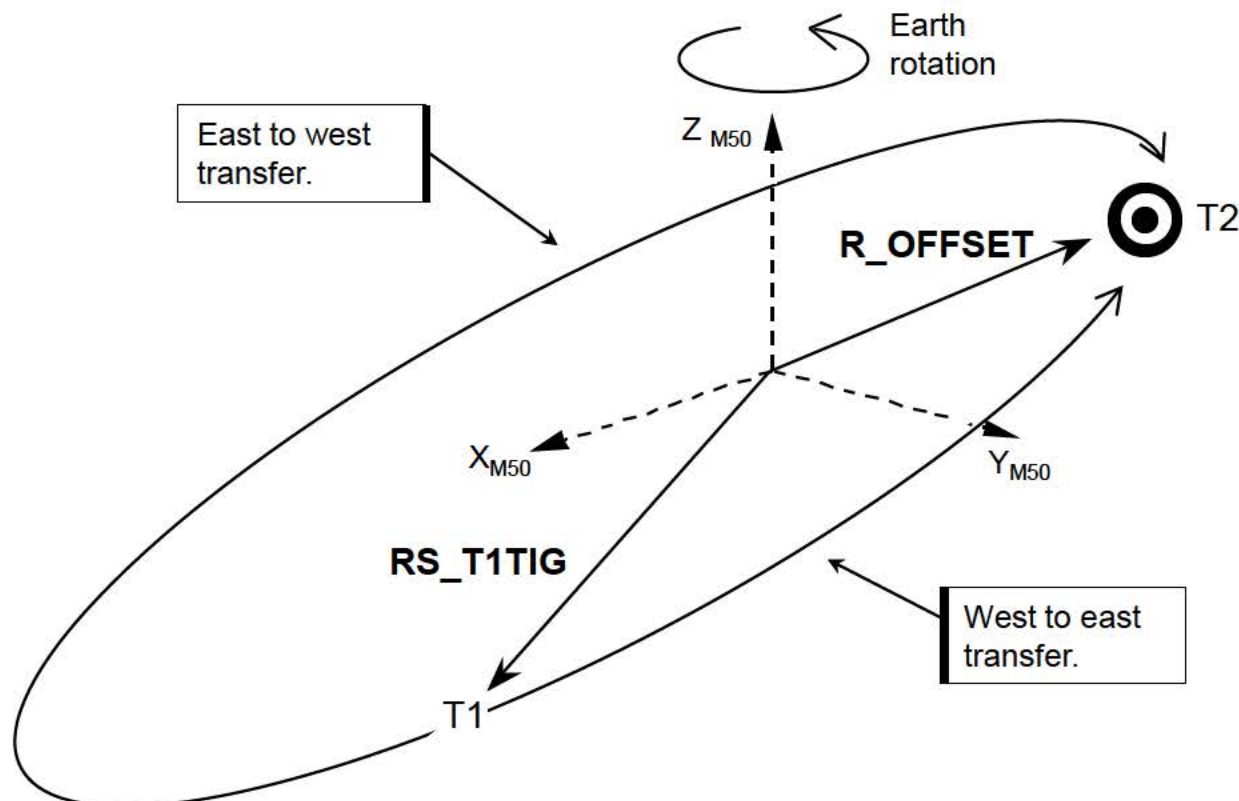


If, on any one of iterations 3 through 10, the magnitude of the **R_MISS** vector falls below an ILOADED tolerance (**R_TOL**, V967789C), an acceptable value for **VS_REQUIRED** has been found. **R_TOL** can be thought of as a sphere defining a space of acceptable final positions at the end of the transfer. **RS_T2TIG** is at the center of the sphere.

When this condition is achieved, the targeting algorithm is considered to be converged.



Lambert algorithms determine transfer trajectories between two points with a given transfer time. However, for each set of initial conditions, a “west to east” or “east to west” transfer may be computed.



VS_REQUIRED is computed by Lambert in horizontal and radial components:

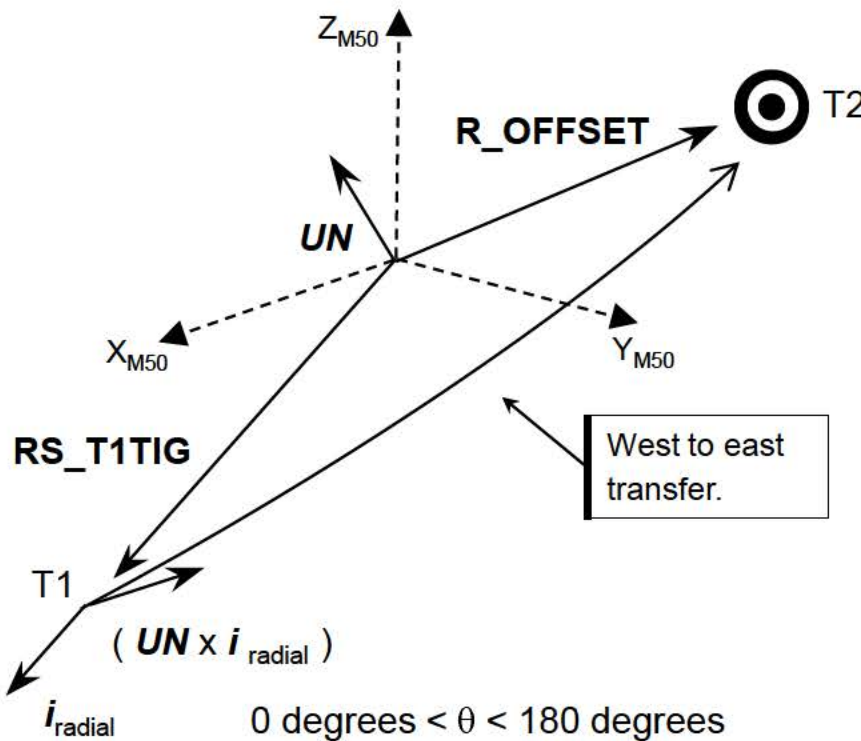
$$\mathbf{VS_REQUIRED} = V_{\text{radial}} \mathbf{i}_{\text{radial}} + V_{\text{horizontal}} (\mathbf{UN} \times \mathbf{i}_{\text{radial}})$$

The unit vectors are determined as follows:

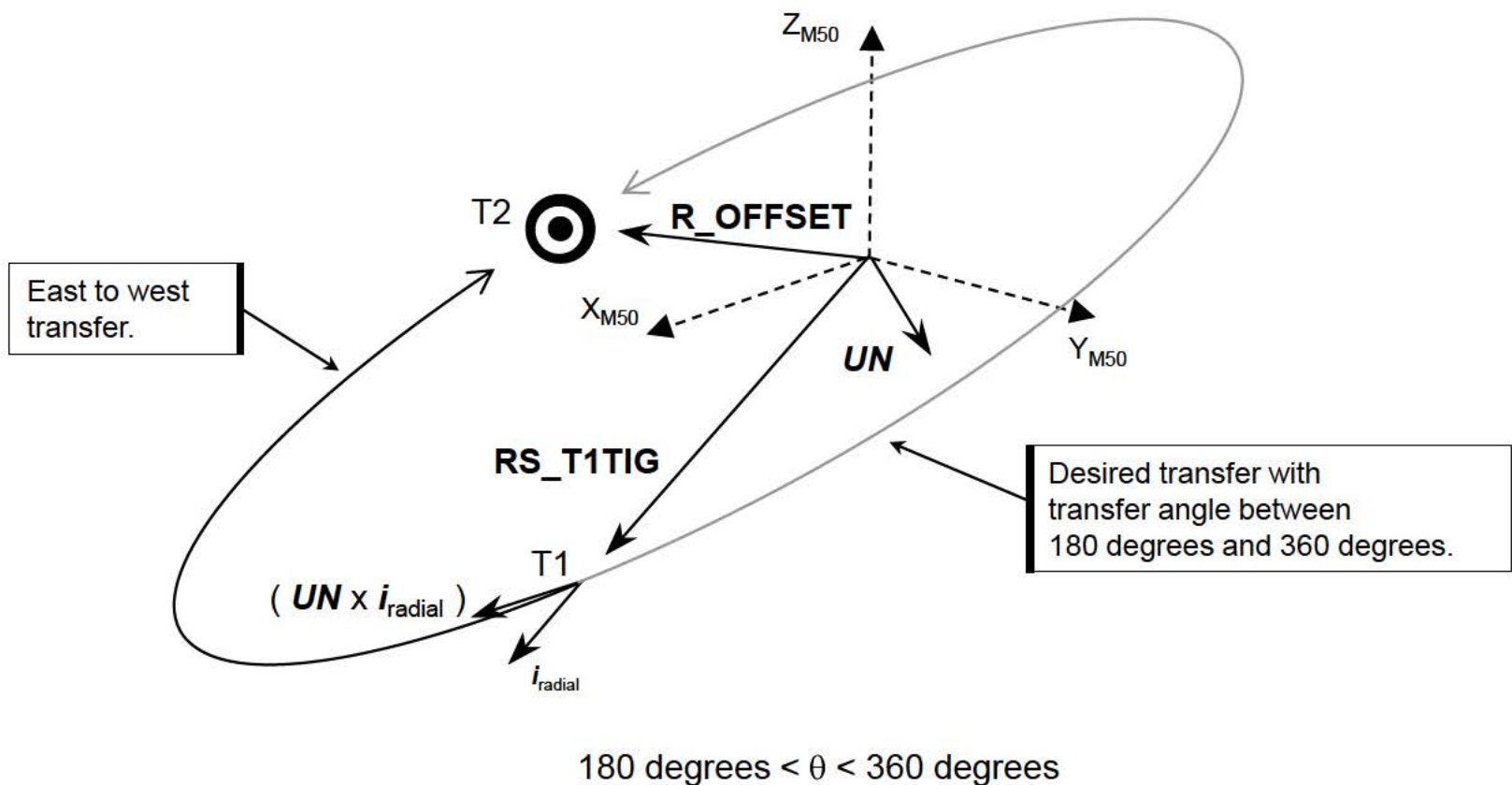
$$\mathbf{UN} = \text{unit}(\mathbf{RS_T1TIG} \times \mathbf{R_OFFSET})$$

$$\mathbf{i}_{\text{radial}} = \text{unit}(\mathbf{RS_T1TIG})$$

If the transfer angle (θ) is between 0 degrees and 180 degrees, the Z M50 component of \mathbf{UN} is positive, which results in a horizontal **VS_REQUIRED** component in a “west to east” direction.



Transfer angles between 180 degrees and 360 degrees result in a ***UN*** with a negative Z M50 component. This results in a horizontal **VS_REQUIRED** component for a “east to west” transfer. Since shuttle orbits are “west to east,” this is not desirable.



The Precision Velocity Task protects against this by changing the sign of UN . A unit vector in the direction of the pre-burn angular momentum vector is computed:

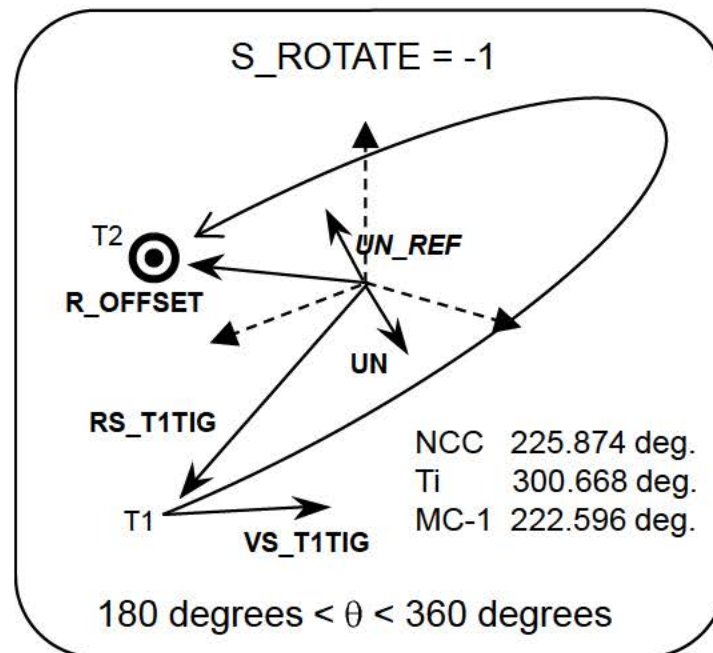
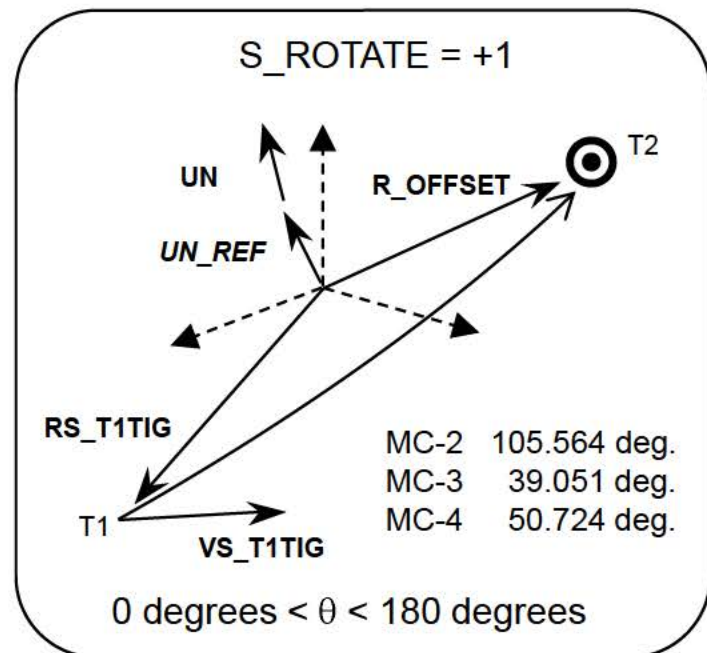
$$\text{UN_REF} = \text{unit}(\text{RS_T1TIG} \times \text{VS_T1TIG})$$

UN is then computed:

$$\text{UN} = \text{RS_T1TIG} \times \text{R_OFFSET}$$

Next, the sign of the dot product of UN and UN_REF is taken:

$$\text{S_ROTATE} = \text{SIGN}(\text{UN} \cdot \text{UN_REF})$$

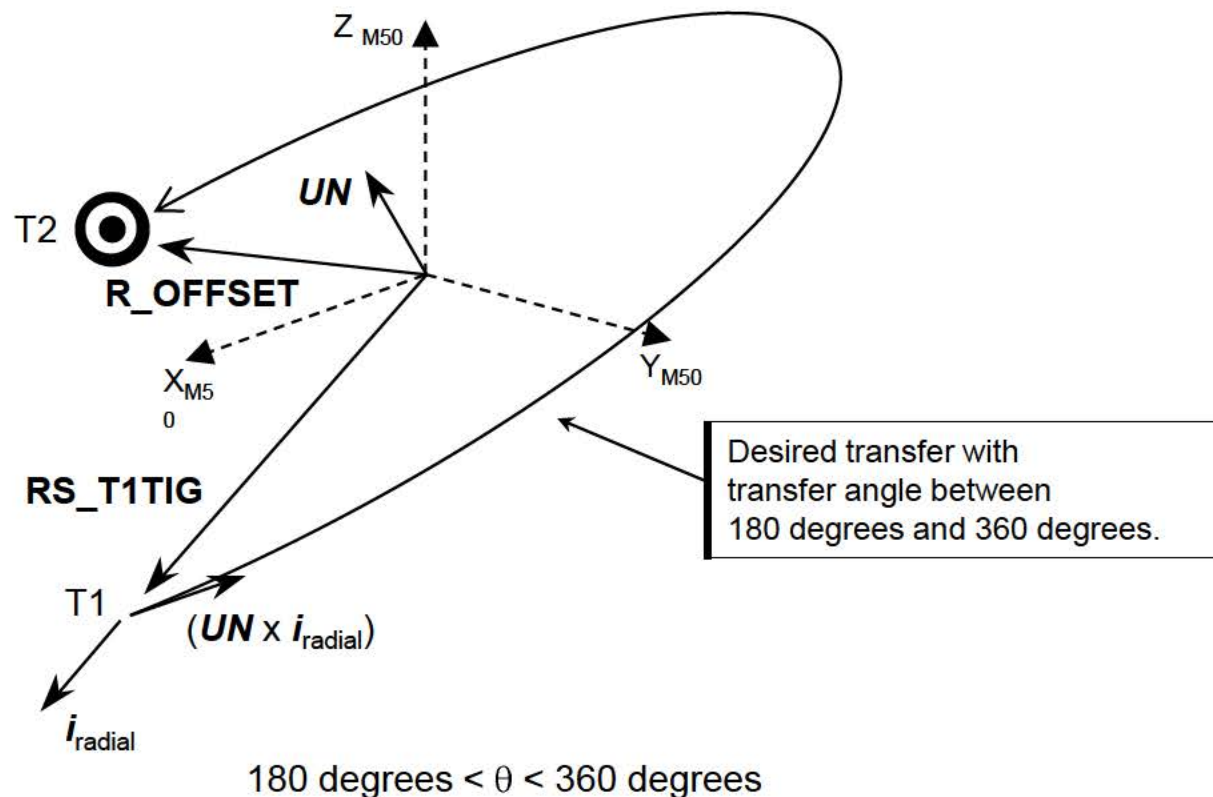


Transfer angles were taken from an ORBT simulation.

UN is then converted to a unit vector:

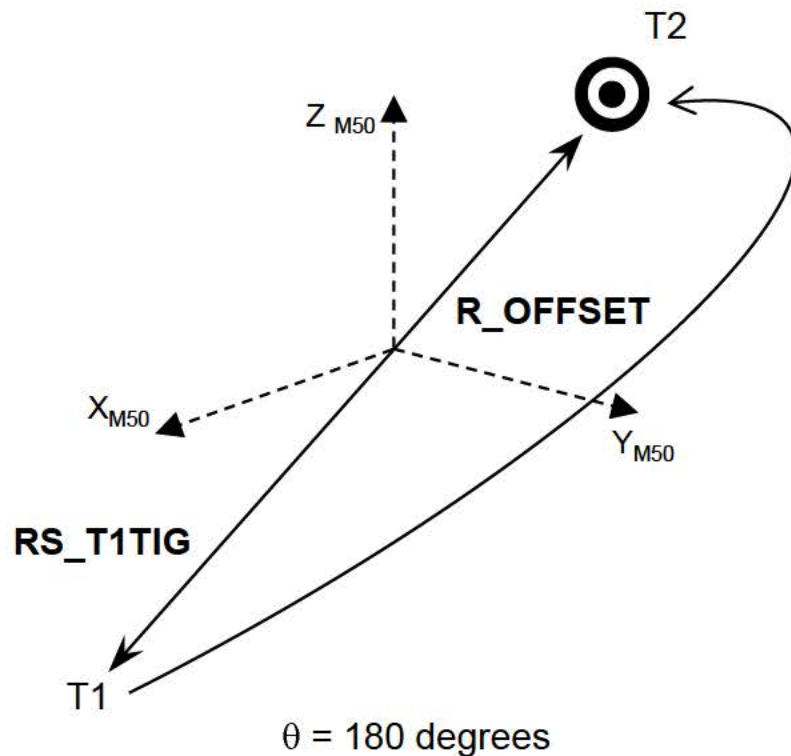
$$\mathbf{UN} = \mathbf{UN} / (\text{S_ROTATE} | \mathbf{UN} |)$$

This results in a **VS_REQUIRED** horizontal component that is in the desired direction. The **S_ROTATE** value computed during Lambert targeting is also used by cyclic Lambert guidance during burns.



When **RS_T1TIG** and **R_OFFSET** are collinear, the transfer plane is no longer defined:

$$| \mathbf{RS_T1TIG} \times \mathbf{R_OFFSET} | = |\mathbf{RS_T1TIG}| |\mathbf{R_OFFSET}| \sin(180) = 0$$



To test for the 180 degrees singularity condition, the Precision Velocity task computes the transfer angle (θ) from **RS_T1TIG** to **R_OFFSET**. Since burn execution takes a finite amount of time to complete, the transfer angle at both TIG and at burn completion is computed.

How post burn θ is computed:

$$\text{Post burn } \theta = \text{Pre-burn } \theta - \omega (\text{VG_MAG/ACC})$$

ω = orbital rate of orbiter at T1, computed from **RS_T1TIG** and **VS_T1TIG**.

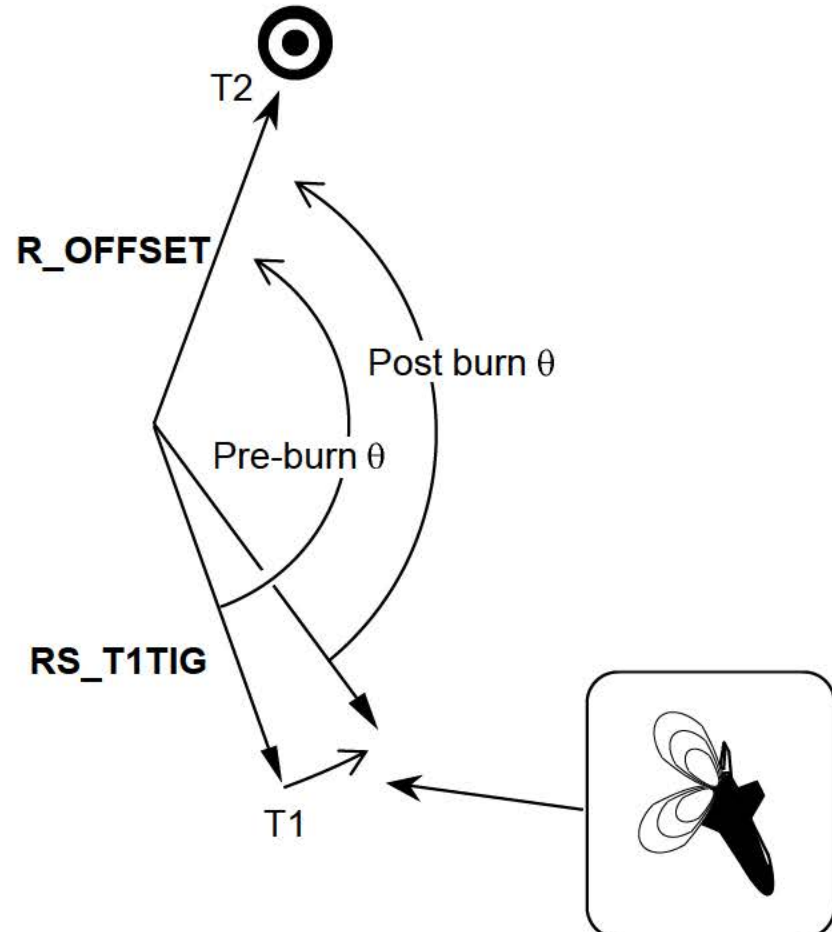
VG_MAG = VGO magnitude based on **VS_REQUIRED** from previous call to Lambert and **VS_T1TIG**.

ACC = THRUST/M

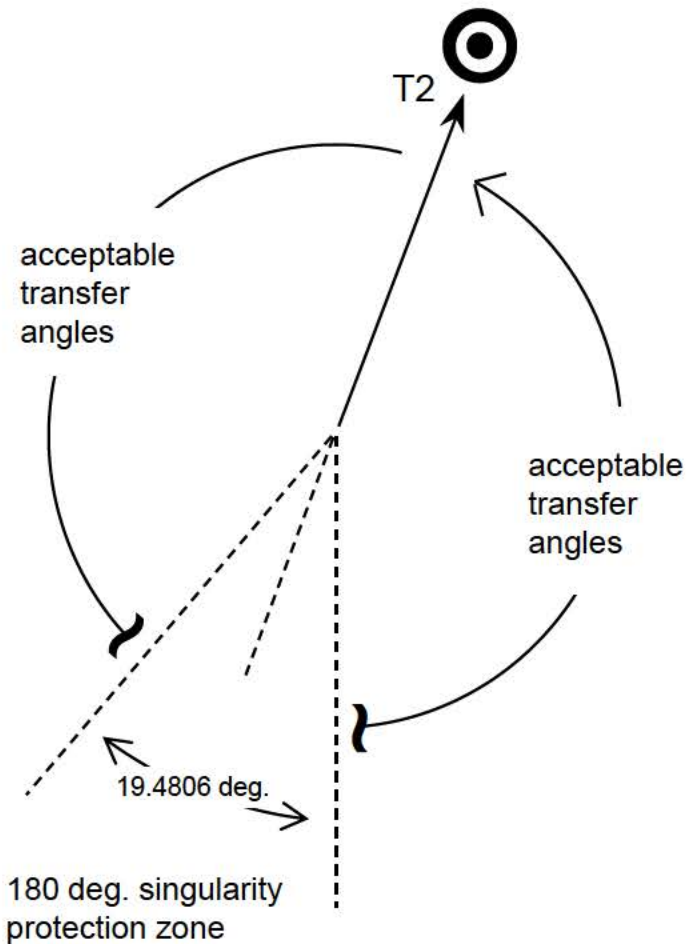
THRUST = 6000 (1 OMS engine), ILOAD V96U7524C

M = Orbiter mass (MNVR EXEC)

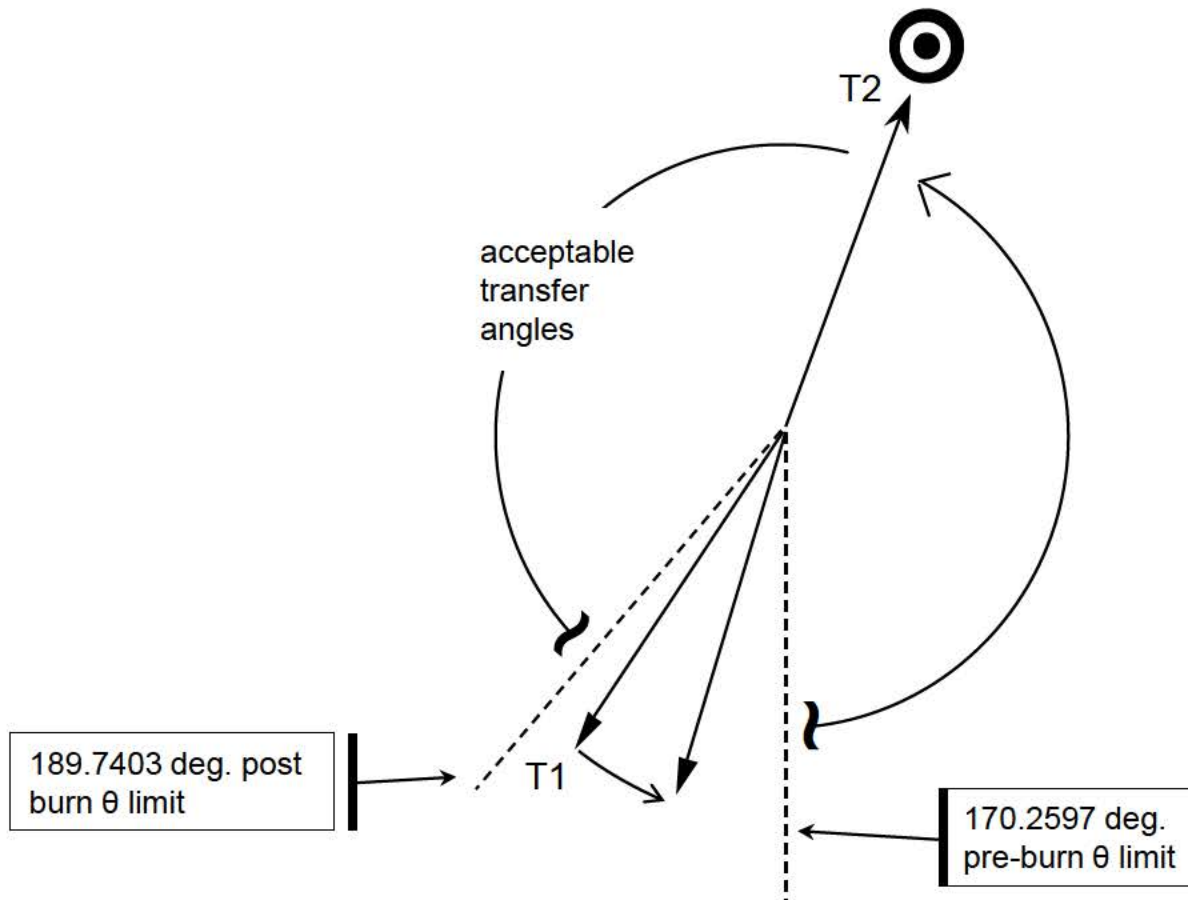
VG_MAG/ACC represents the time it would take to execute the burn, assuming a single OMS engine is used. When multiplied by the orbiter's orbital rate (ω), the angular change in orbiter position during the burn is obtained.



A singularity protection zone is defined by ILOAD CONE (V96U7791C), which has a value of 0.17 radians, or 9.7403 degrees.



If part or all of the burn arc falls within the singularity protection zone, **UN** must be defined in a manner not involving **RS_T1TIG x R_OFFSET**. **S_ROTATE** is set to 0 for use later by Lambert cyclic guidance.

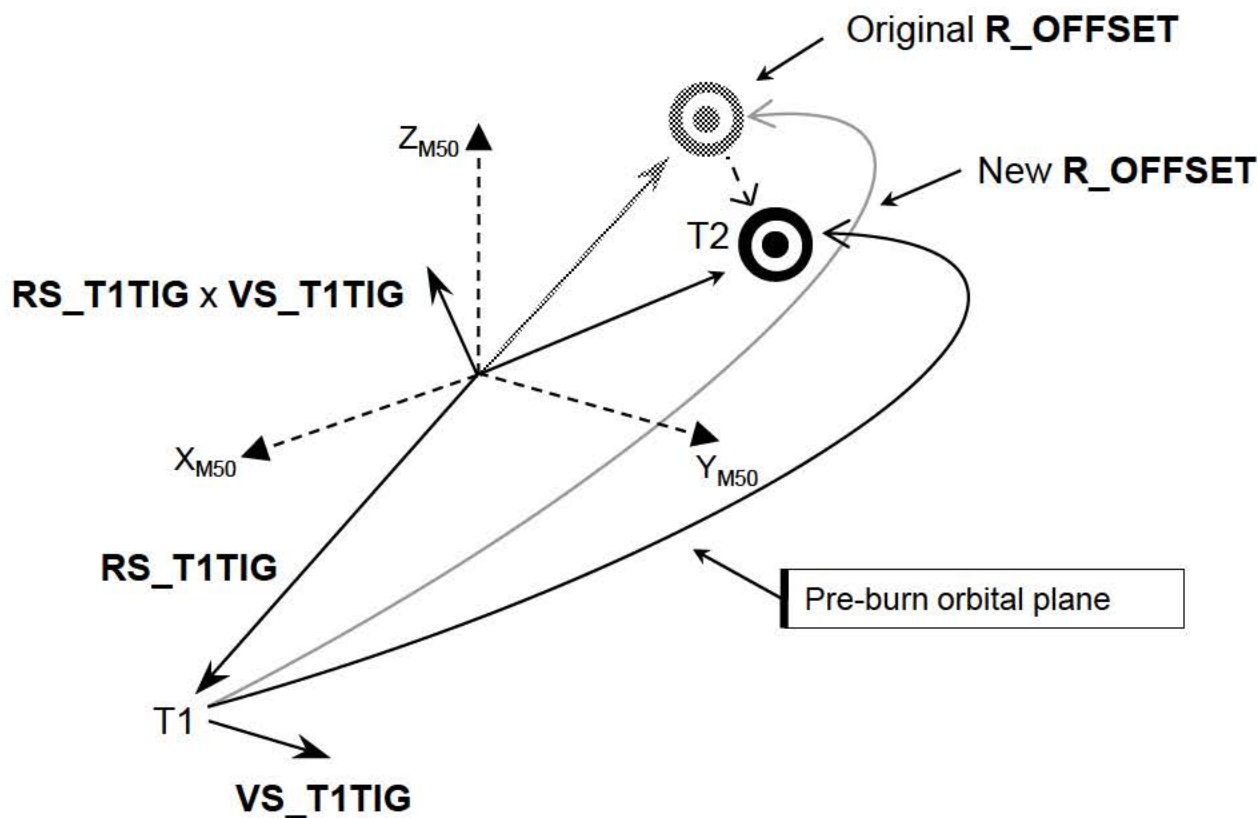


Pre-burn $\theta < 189.7403$ degrees
and
Post burn $\theta > 170.2597$ degrees

In this case, \mathbf{UN} is defined as the cross product of the pre-burn position ($\mathbf{RS_T1TIG}$) and velocity ($\mathbf{VS_T1TIG}$) vectors. $\mathbf{R_OFFSET}$ projected into the Shuttle pre-burn orbital plane.

$$\mathbf{R_OFFSET} = \mathbf{R_OFFSET} - [\mathbf{R_OFFSET} \bullet \text{UNIT}(\mathbf{RS_T1TIG} \times \mathbf{VS_T1TIG})] (\mathbf{RS_T1TIG} \times \mathbf{R_OFFSET})$$

scalar (dot product) vector

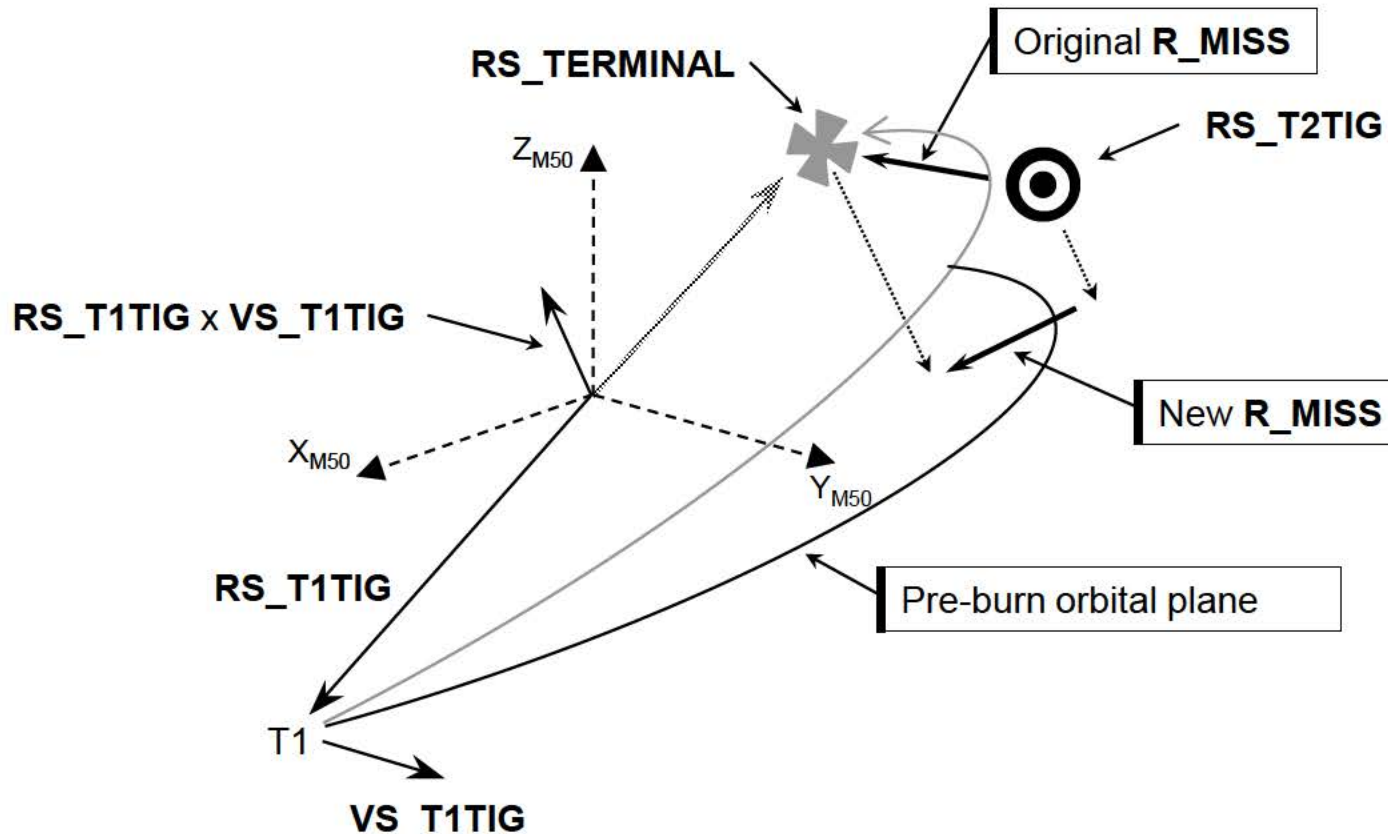


θ within 180 degree singularity protection region.

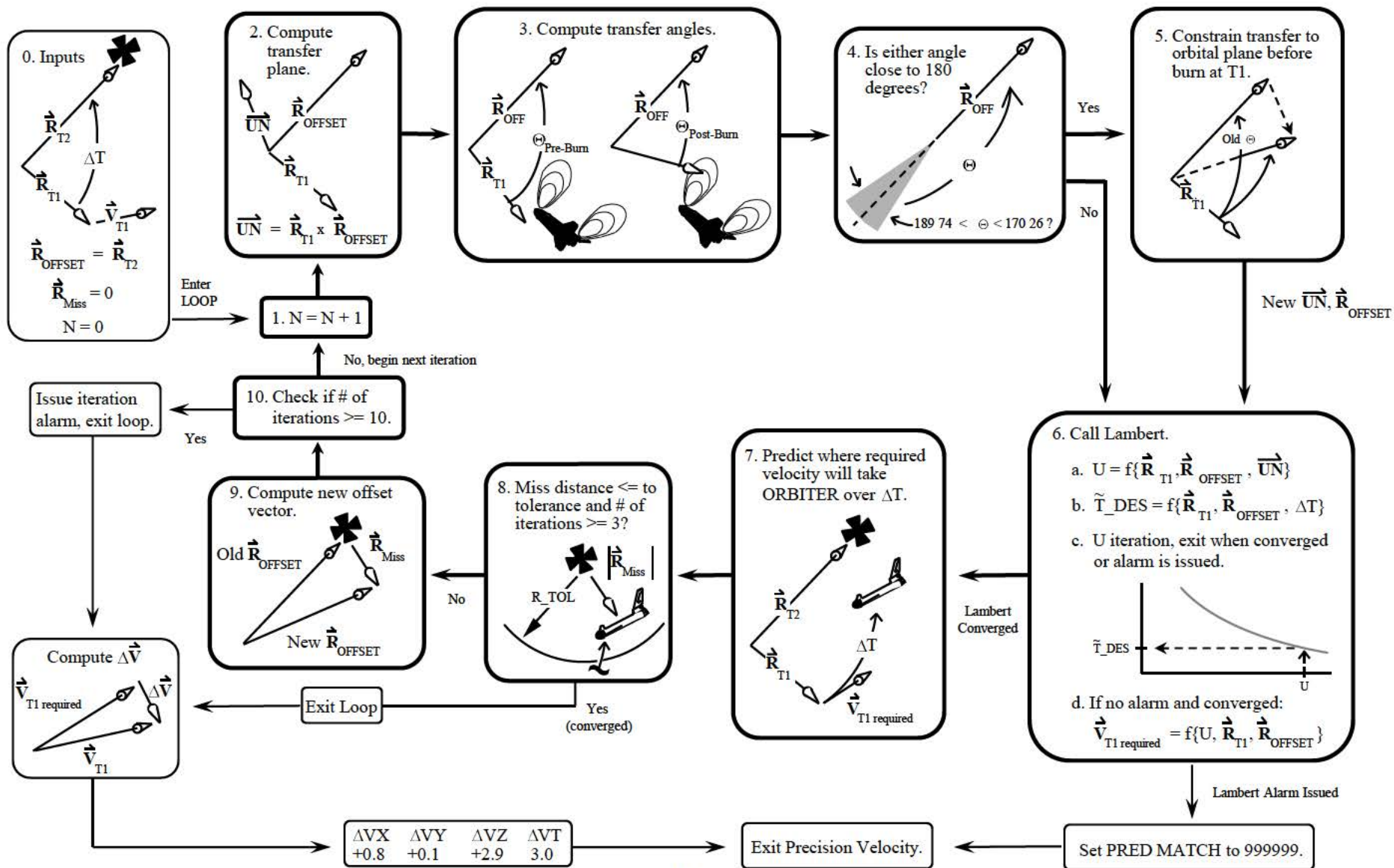
After **VS_REQUIRED** is computed and predicted forward in time to determine the miss vector (**R_MISS**), **R_MISS** is projected into the pre-burn orbital plane. **R_OFFSET** is then adjusted by the new **R_MISS**. This adjustment to **R_MISS** is performed only if part or all of the burn arc falls within the 180 degree singularity region.

$$\mathbf{R_MISS} = \mathbf{R_MISS} - [\mathbf{R_MISS} \bullet \text{UNIT}(\mathbf{RS_T1TIG} \times \mathbf{VS_T1TIG})] (\mathbf{RS_T1TIG} \times \mathbf{VS_T1TIG})$$

scalar (dot product) vector

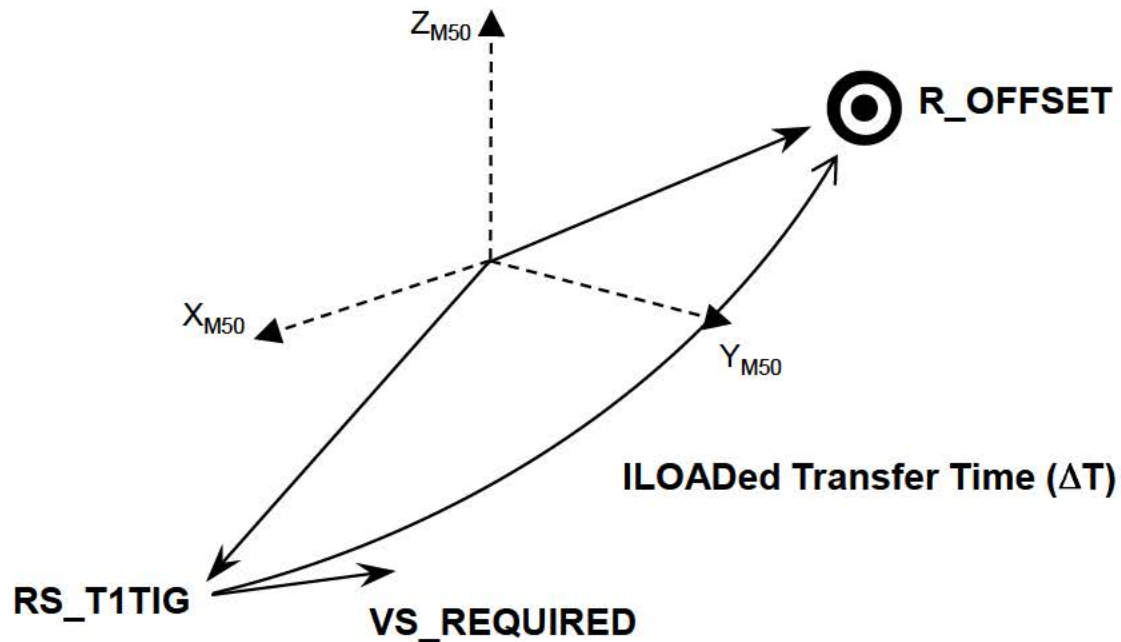


Simplified Precision Velocity Required Algorithm Chart

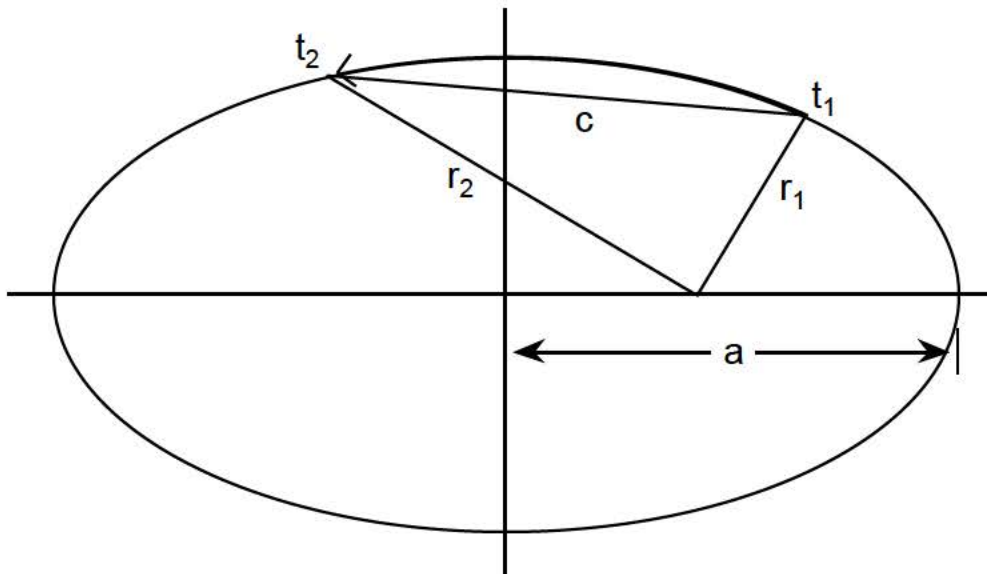


8.14 A Closer Look at the Lambert Algorithm

The Lambert algorithm uses a transfer time equation to compute the required velocity to transfer from the initial to the final positions in ΔT .



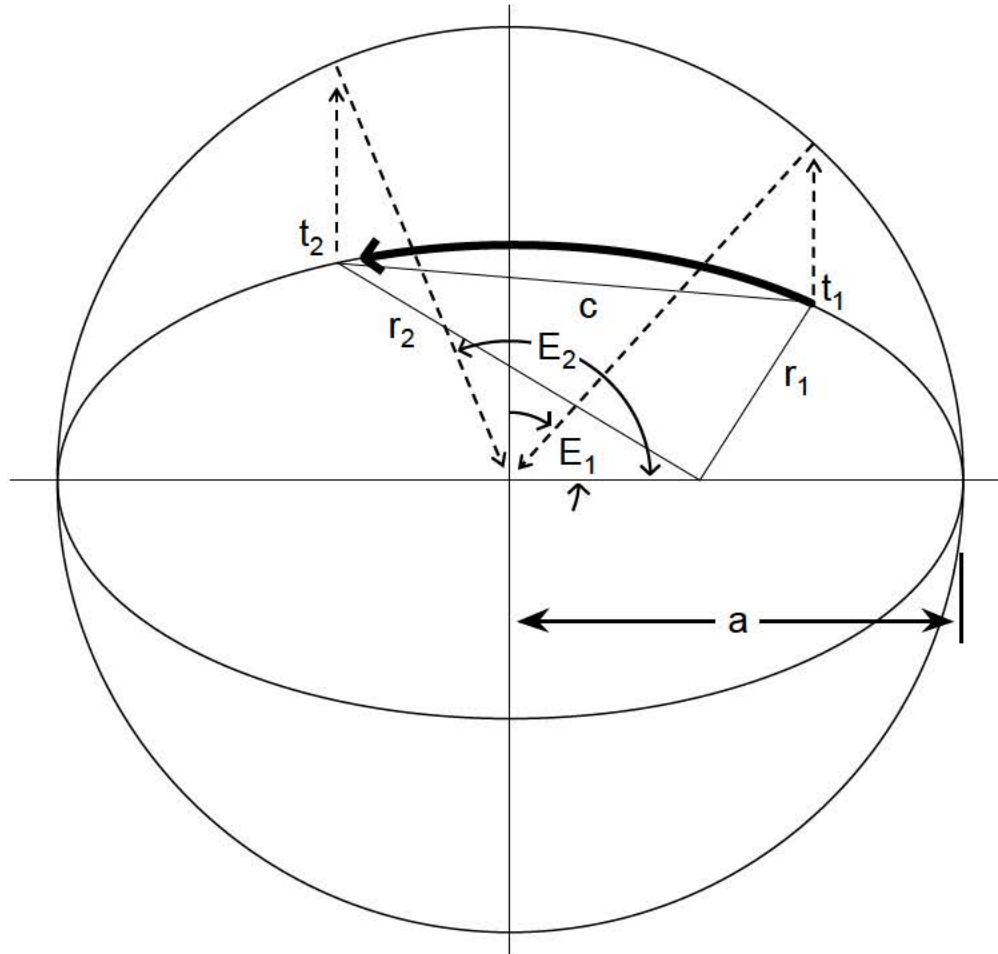
In 1761, Johann Heinrich Lambert (1728 - 1777) published a treatise on the orbital properties of comets. This work, contained a theorem (Lambert's Theorem) that related the transfer time ($t_2 - t_1$) between two points on an ellipse (or any conic section) to the sum of the distances ($r_1 + r_2$) from the occupied focus (center of attraction), the semi-major axis of the ellipse (a), and the linear distance between the two points (c).



$$t_2 - t_1 = f(a, r_1 + r_2, c)$$

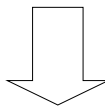
The foundation for deriving the Lambert transfer time equation is Kepler's equation. Kepler's equation relates the transfer time ($t_2 - t_1$) between two points on a conic section to eccentricity (e) and semi-major axis (a) of the conic, and the change in eccentric anomaly ($E_2 - E_1$).

$$t_2 - t_1 = \sqrt{\frac{a^3}{\mu}} [E_2 - E_1 - e(\sin E_2 - \sin E_1)]$$

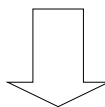


Kepler's equation can be transformed so that it is a function of the three Lambert parameters (a , $r_1 + r_2$, and c). Like Kepler's equation, it is transcendental (requiring an iterative solution). The time-of-flight equation used in the Flight Software is used to compute a normalized transfer time (\tilde{t}) using a transfer geometry parameter (λ) and a semi-major axis parameter (u).

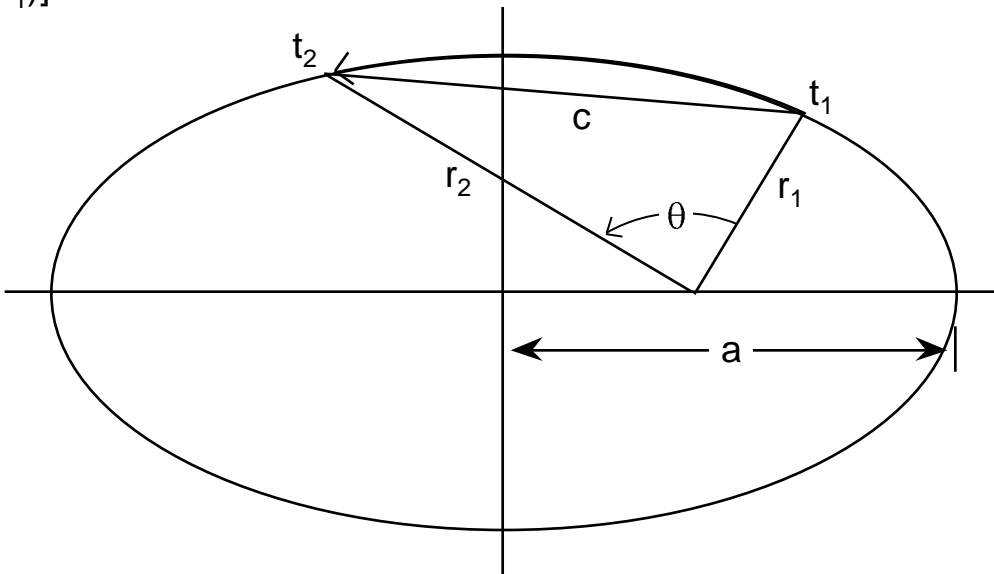
$$t_2 - t_1 = \sqrt{\frac{a^3}{\mu}} [E_2 - E_1 - e(\sin E_2 - \sin E_1)]$$



$$t_2 - t_1 = f(a, r_1 + r_2, c)$$



$$\tilde{t} = f(\lambda, u) = \sqrt{\frac{2\mu}{s^3}} (t_2 - t_1)$$



$$\lambda = \frac{\sqrt{r_2 r_1}}{s} \cos \frac{\theta}{2} = \pm \sqrt{\frac{s - c}{s}}$$

$$u = \sqrt{1 - \frac{1}{2a}} \quad s = \frac{1}{2}(r_1 + r_2 + c)$$

The particular transfer time equation and associated Lambert variables used by the Shuttle Flight Software was first published by Lancaster, Blanchard, and Devaney (LBD)* in 1966. Battin* independently formulated the same set of variables, and published his results in 1968. Lancaster and Blanchard* published a NASA Technical note in 1969, giving more details than their earlier paper. Battin's book* also contains a treatment of these parameters. The most exhaustive study of the Lambert variables and transfer time equation used by the Shuttle was published by Gooding* in 1988.

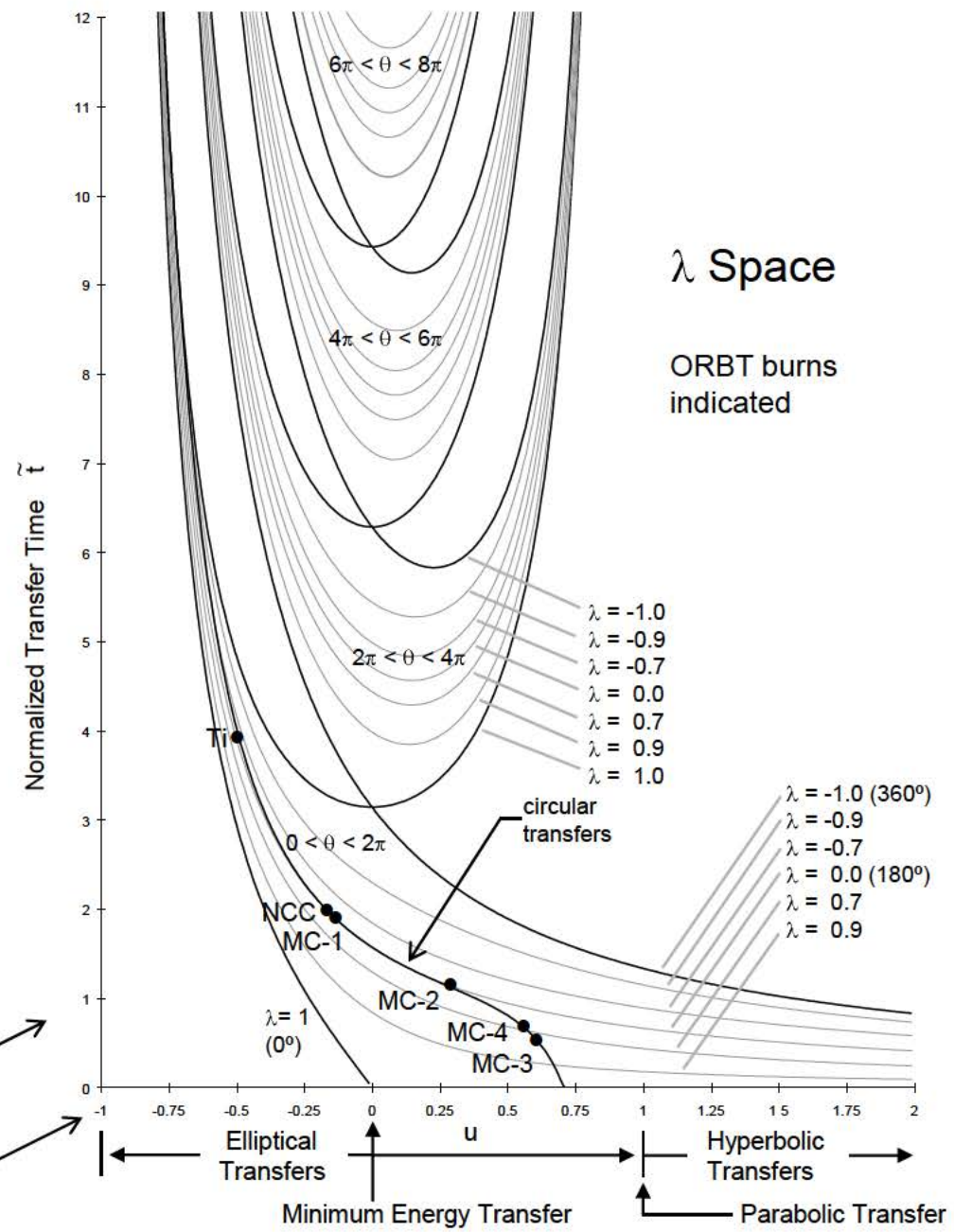
The elliptic version of the Lambert algorithm for the Shuttle was derived by Stan Shepperd of the Charles Stark Draper Laboratory in the late 1970s. Shepperd's work was documented in an informal, but readable memo by Don Pearson* in 1980. In 1979, Bobby Uzzell* of the NASA/JSC Mission Planning and Analysis Division also documented the Shuttle Lambert algorithm.

The transfer time equation detailed in LBD, Battin, and Gooding can be used for transfers less than or greater than 360 degrees, and for elliptic, circular, parabolic, and hyperbolic transfers. A plot of the normalized transfer time as a function of u ("λ space") is given at the right. The Shuttle transfer time equation is only good for circular and elliptical transfers less than 360 degrees.

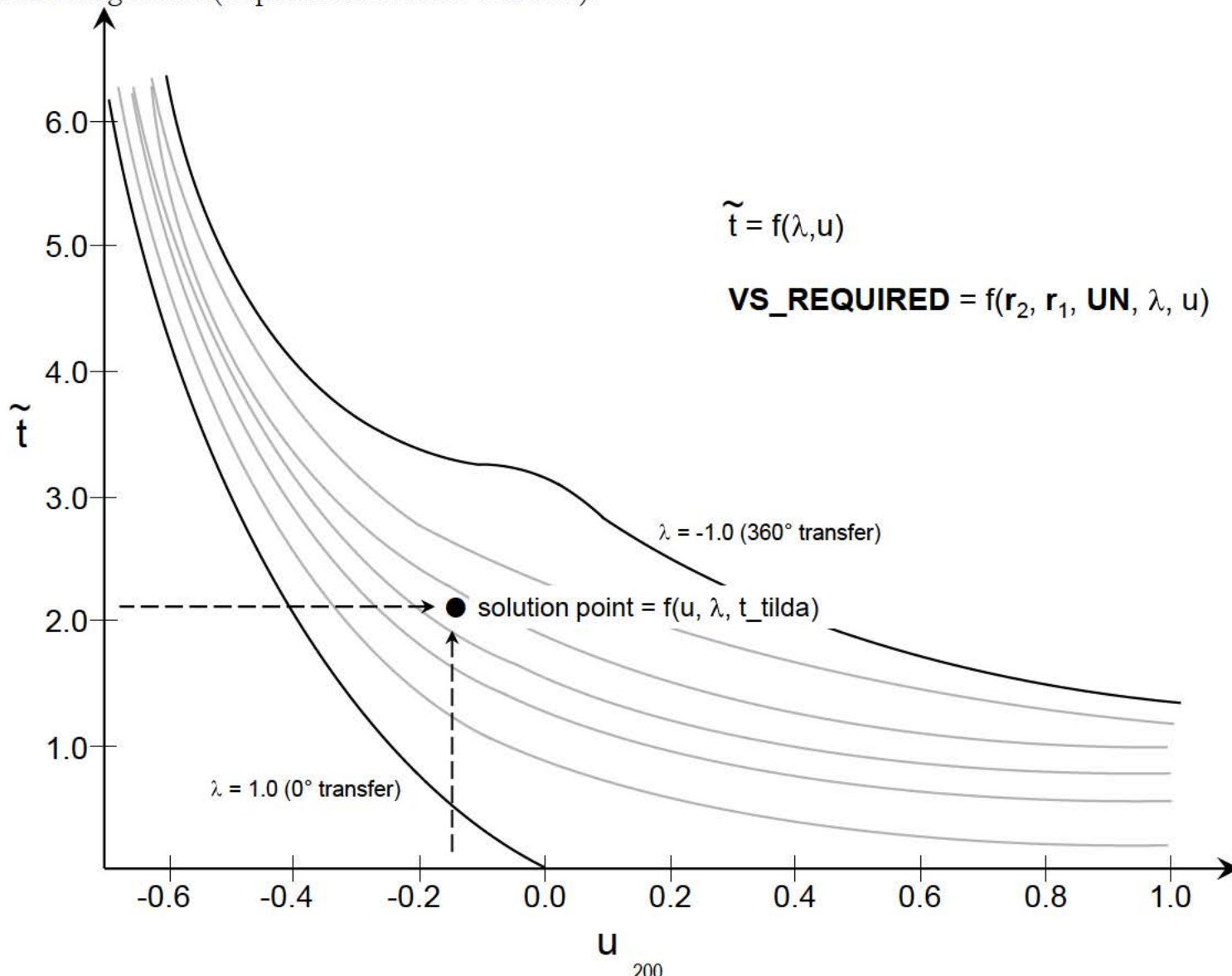
* See the bibliography for complete citations.

$$\text{Normalized Transfer Time } \tilde{t} = \sqrt{\frac{2\mu}{s^3}} (t_1 - t_0)$$

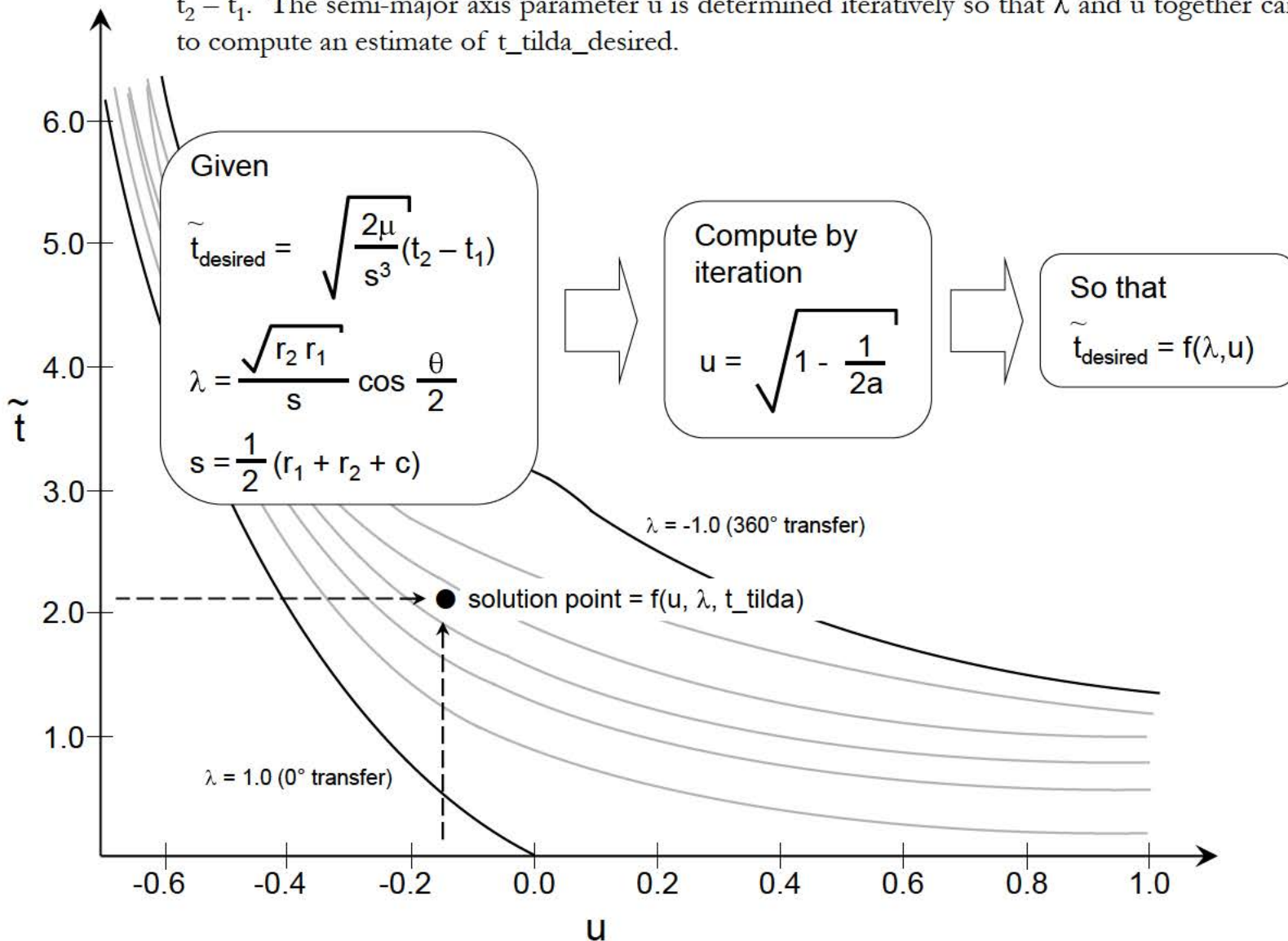
$$\text{Semi-major Axis Parameter } u = +/- \sqrt{1 - \frac{s}{2a}}$$



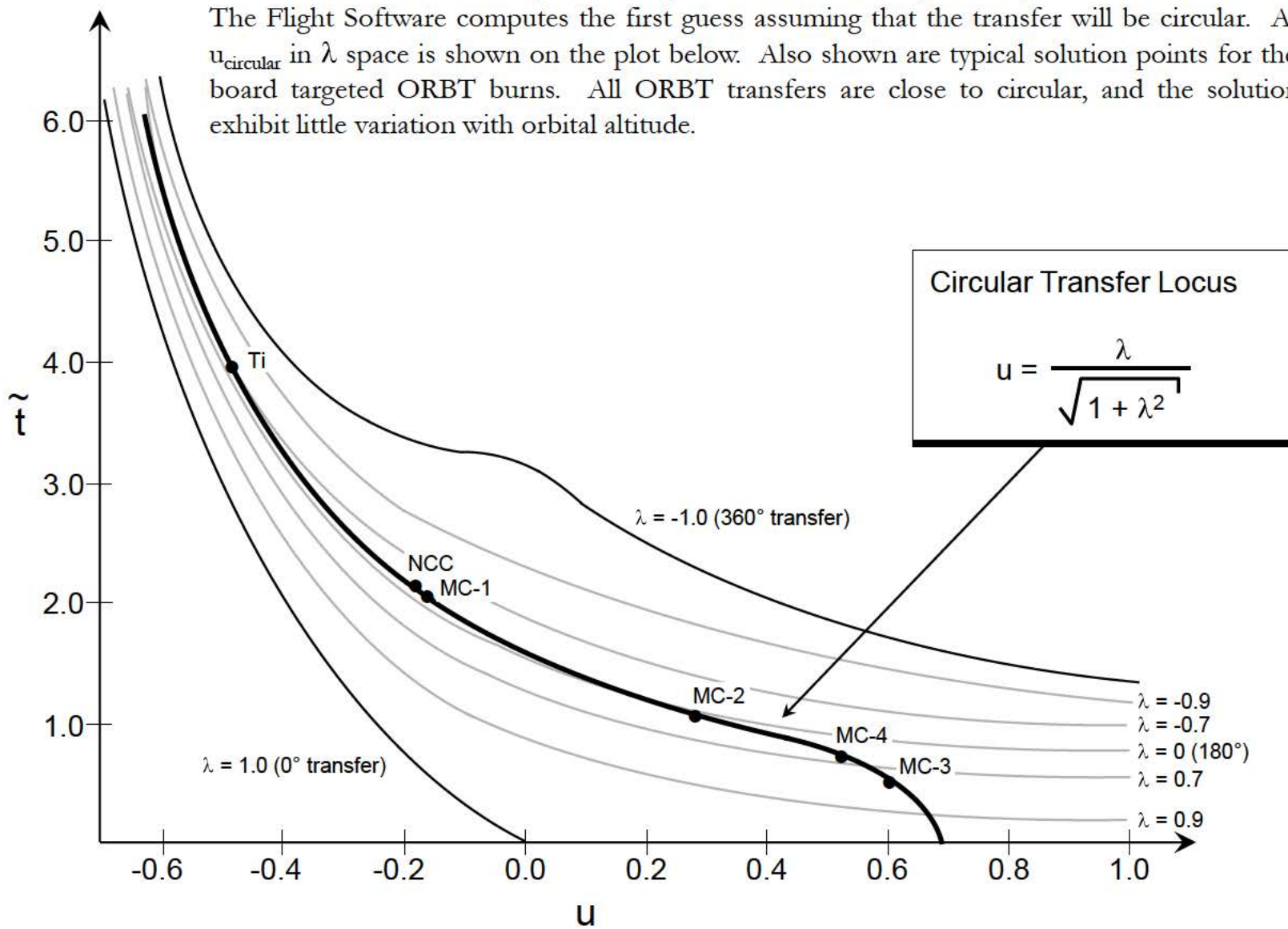
If the t_{tilde} , λ , and u values for a particular set of input parameters are known, the required velocity to achieve the transfer may be computed. This section of the λ space is that covered by the Shuttle Lambert algorithm (elliptical and circular transfers).



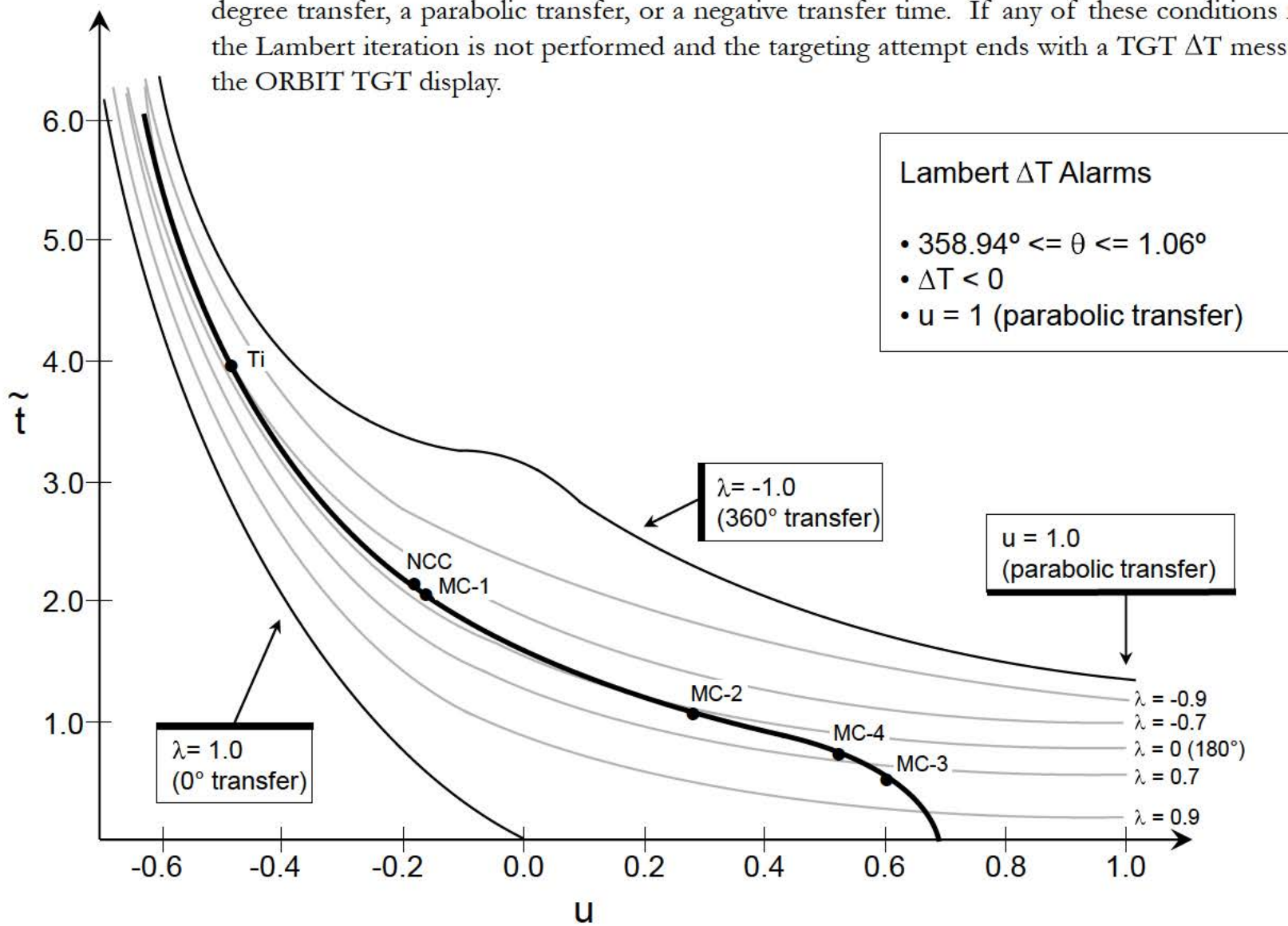
Of the four terms in Lambert's theorem, $(t_2 - t_1, a, r_2 + r_1, c)$, the only unknown is a , the semi-major axis of the transfer orbit. The Flight Software $t_{\text{tilda_desired}}$ and λ are determined from r_1 , r_2 , c , and $t_2 - t_1$. The semi-major axis parameter u is determined iteratively so that λ and u together can be used to compute an estimate of $t_{\text{tilda_desired}}$.



Before the iteration can begin, a first guess of the semi-major axis parameter u must be obtained. The Flight Software computes the first guess assuming that the transfer will be circular. A plot of u_{circular} in λ space is shown on the plot below. Also shown are typical solution points for the six on-board targeted ORBT burns. All ORBT transfers are close to circular, and the solution points exhibit little variation with orbital altitude.

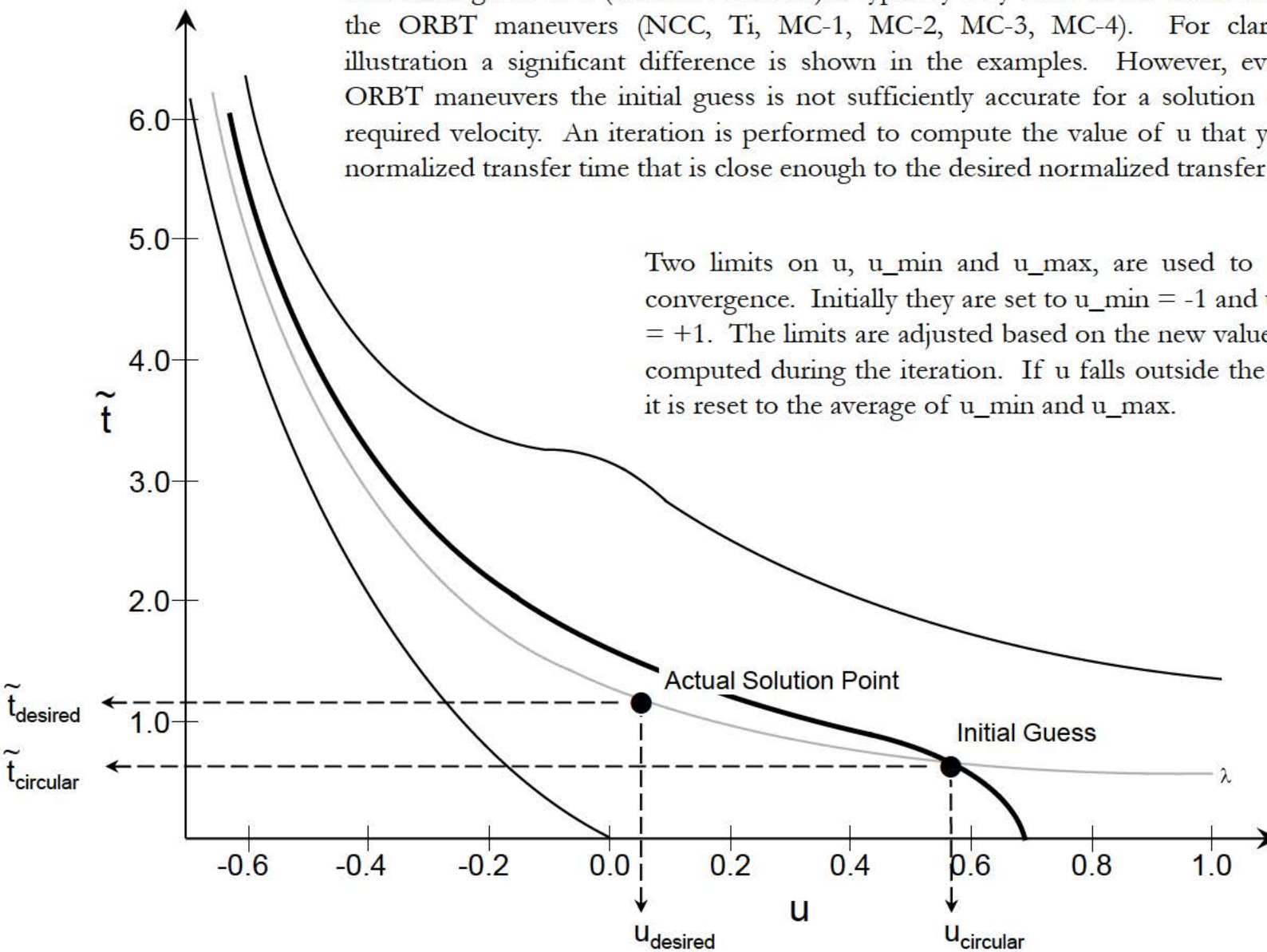


A check is made to ensure that the input trajectory parameters do not represent close to a 360 or 0 degree transfer, a parabolic transfer, or a negative transfer time. If any of these conditions is met, the Lambert iteration is not performed and the targeting attempt ends with a TGT ΔT message on the ORBIT TGT display.



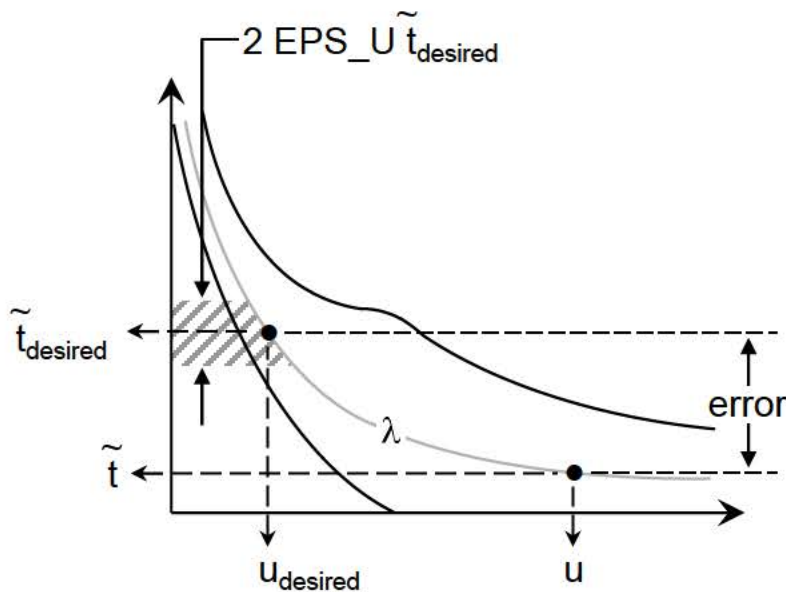
The initial guess of u (a circular transfer) is typically very close to the actual value for the ORBT maneuvers (NCC, Ti, MC-1, MC-2, MC-3, MC-4). For clarity of illustration a significant difference is shown in the examples. However, even for ORBT maneuvers the initial guess is not sufficiently accurate for a solution of the required velocity. An iteration is performed to compute the value of u that yields a normalized transfer time that is close enough to the desired normalized transfer time.

Two limits on u , u_{\min} and u_{\max} , are used to ensure convergence. Initially they are set to $u_{\min} = -1$ and $u_{\max} = +1$. The limits are adjusted based on the new values of u computed during the iteration. If u falls outside the limits, it is reset to the average of u_{\min} and u_{\max} .

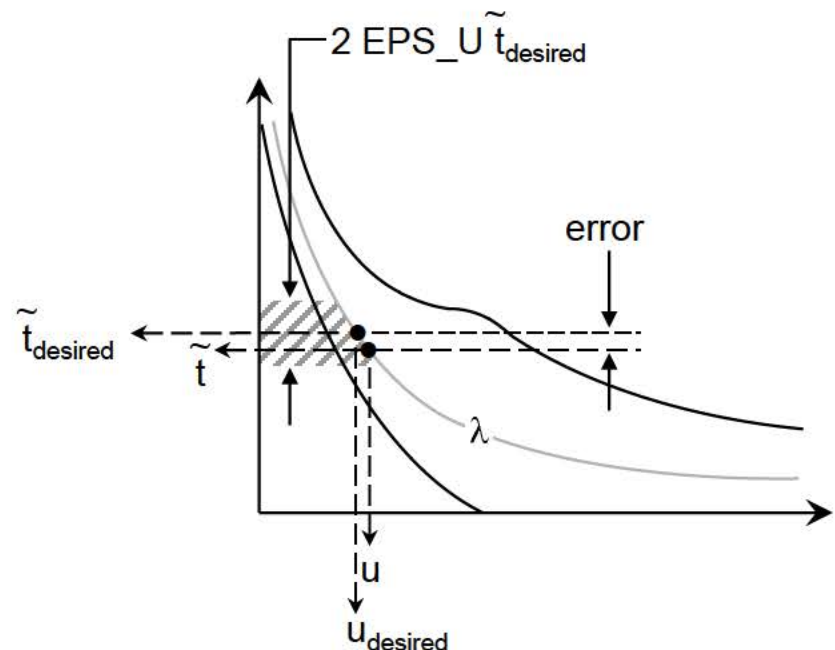


For each value of u determined during the iteration, a corresponding value of the normalized transfer time (\tilde{t}) is computed. Once \tilde{t} is within a specified tolerance of $\tilde{t}_{desired}$, the iteration is declared converged and a required velocity vector can be computed.

Check: $| \text{error} | < \text{EPS_U } \tilde{t}_{desired}$

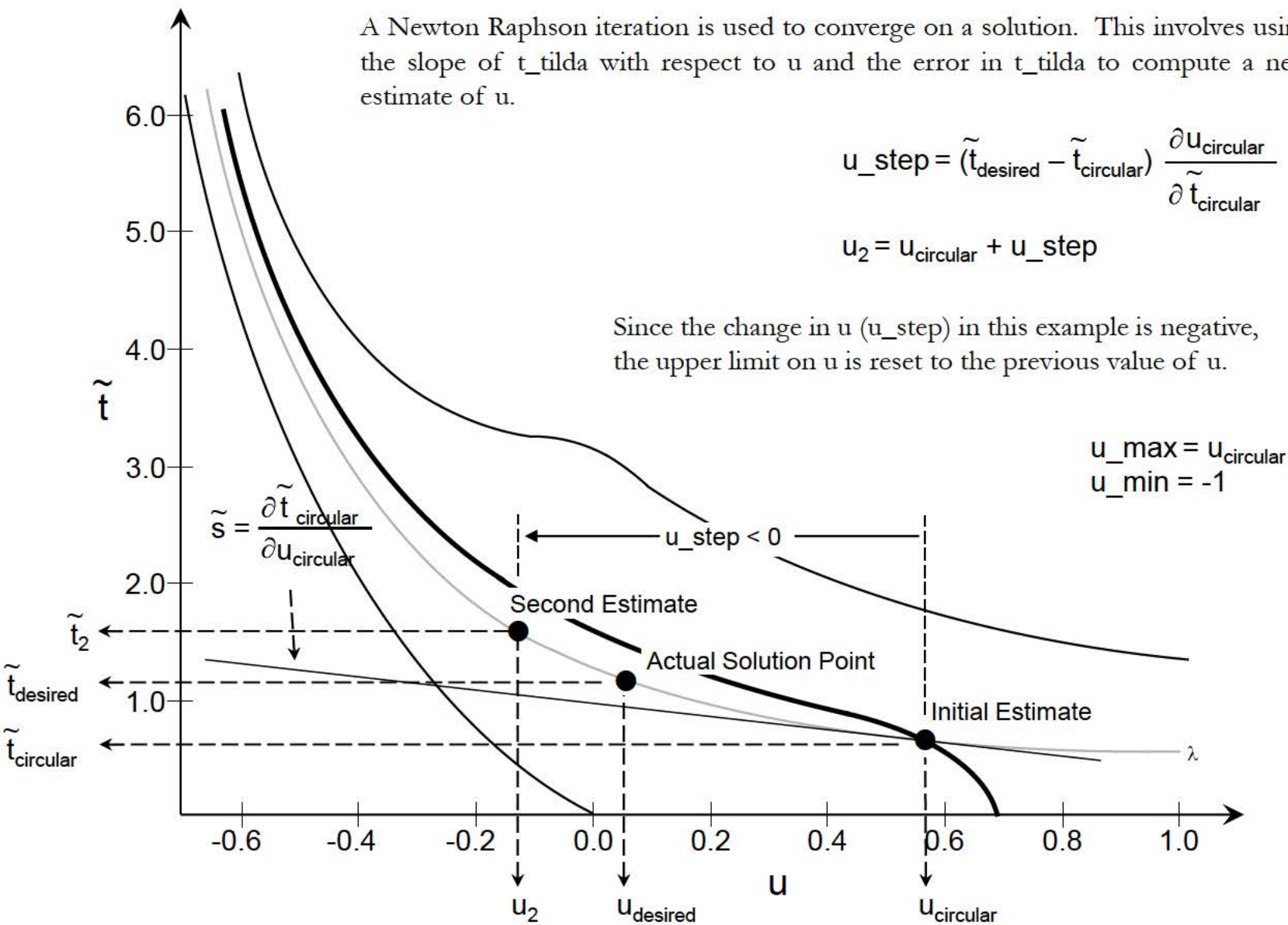


Not Converged, $|\text{error}| > \text{EPS_U } \tilde{t}_{desired}$



Converged, $|\text{error}| < \text{EPS_U } \tilde{t}_{desired}$

A Newton Raphson iteration is used to converge on a solution. This involves using the slope of \tilde{t} with respect to u and the error in \tilde{t} to compute a new estimate of u .



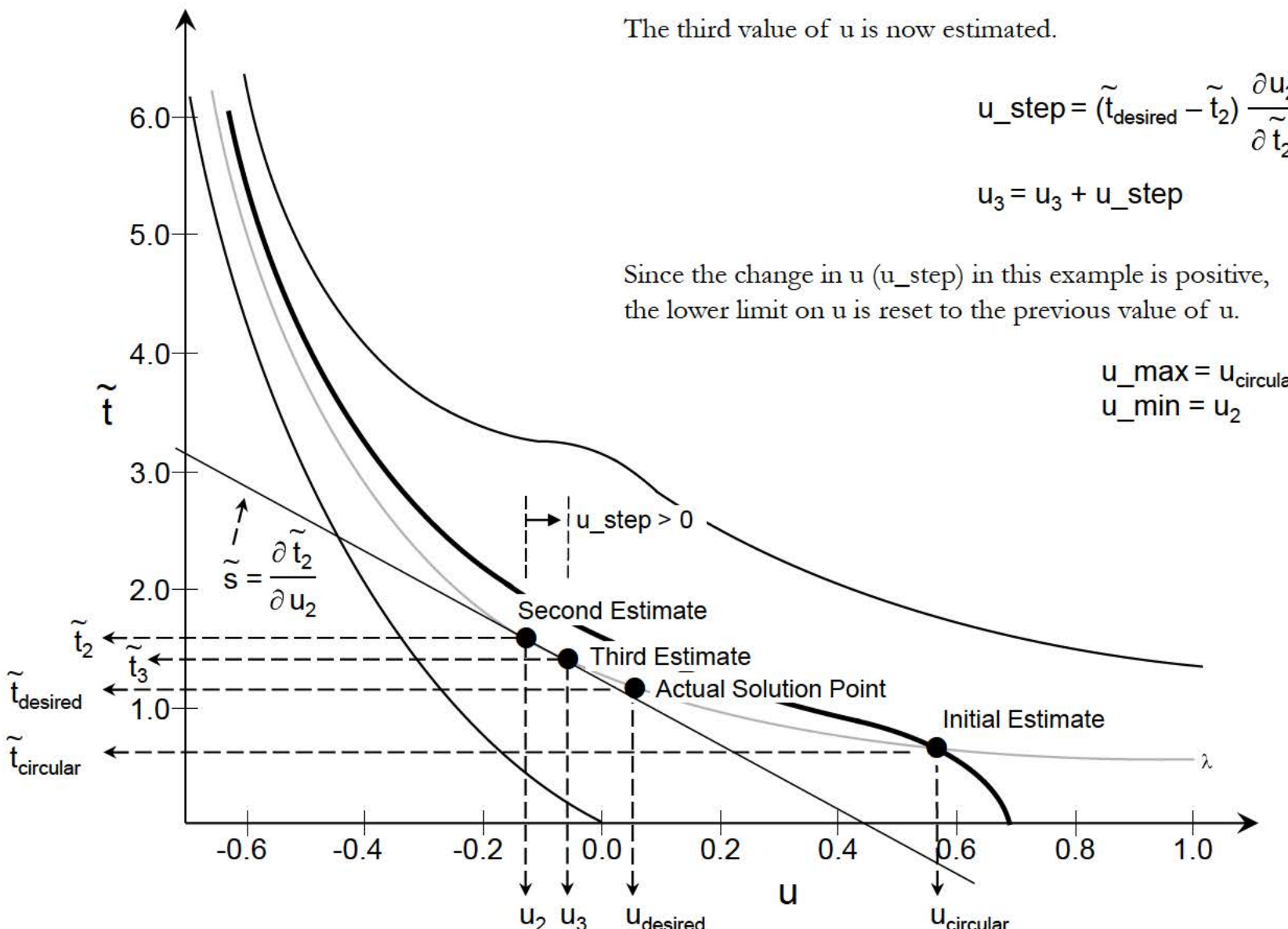
The third value of u is now estimated.

$$u_{\text{step}} = (\tilde{t}_{\text{desired}} - \tilde{t}_2) \frac{\partial u_2}{\partial \tilde{t}_2}$$

$$u_3 = u_2 + u_{\text{step}}$$

Since the change in u (u_{step}) in this example is positive, the lower limit on u is reset to the previous value of u .

$$\begin{aligned} u_{\text{max}} &= u_{\text{circular}} \\ u_{\text{min}} &= u_2 \end{aligned}$$



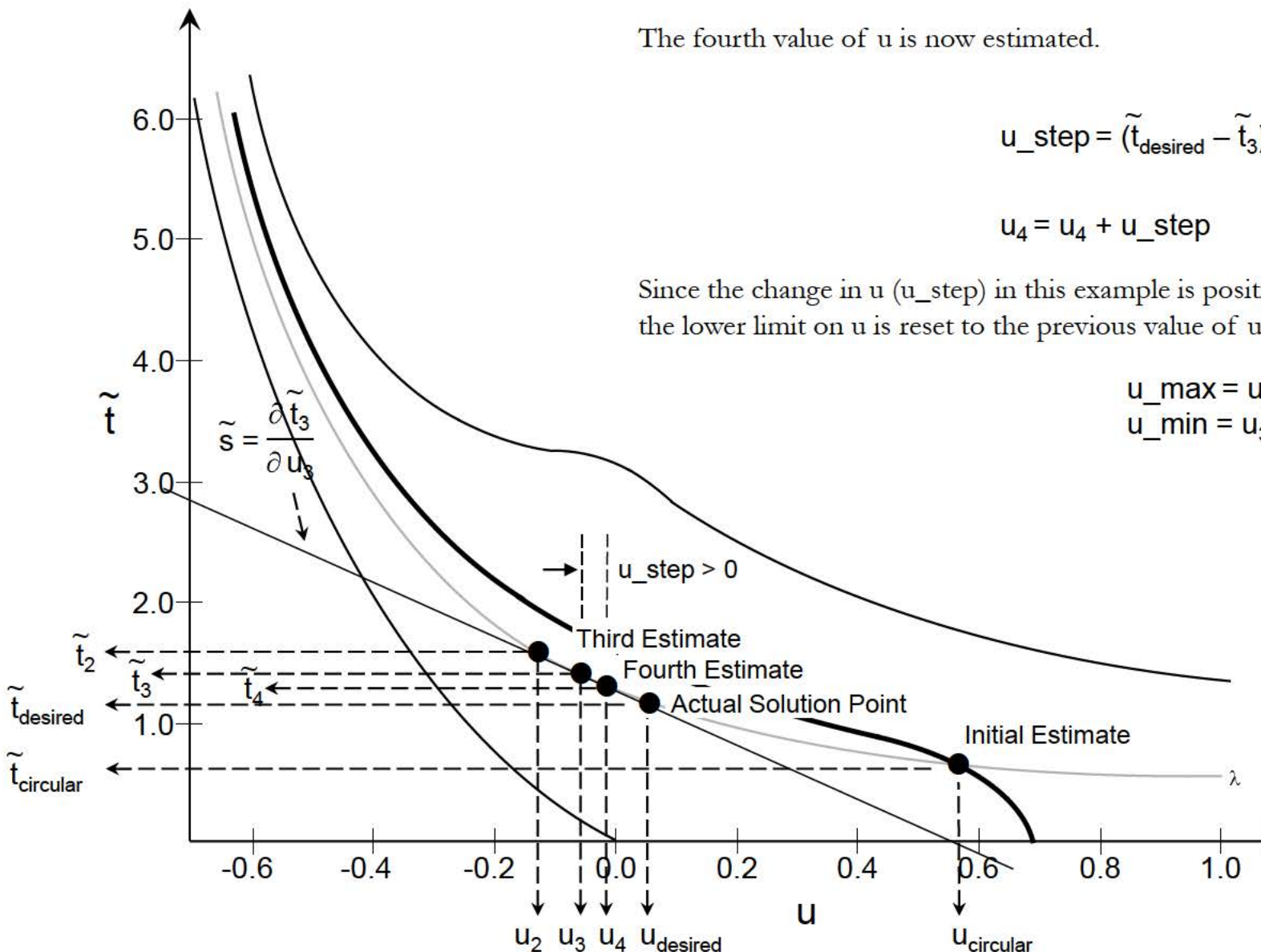
The fourth value of u is now estimated.

$$u_{\text{step}} = (\tilde{t}_{\text{desired}} - \tilde{t}_3) \frac{\partial u_3}{\partial \tilde{t}_3}$$

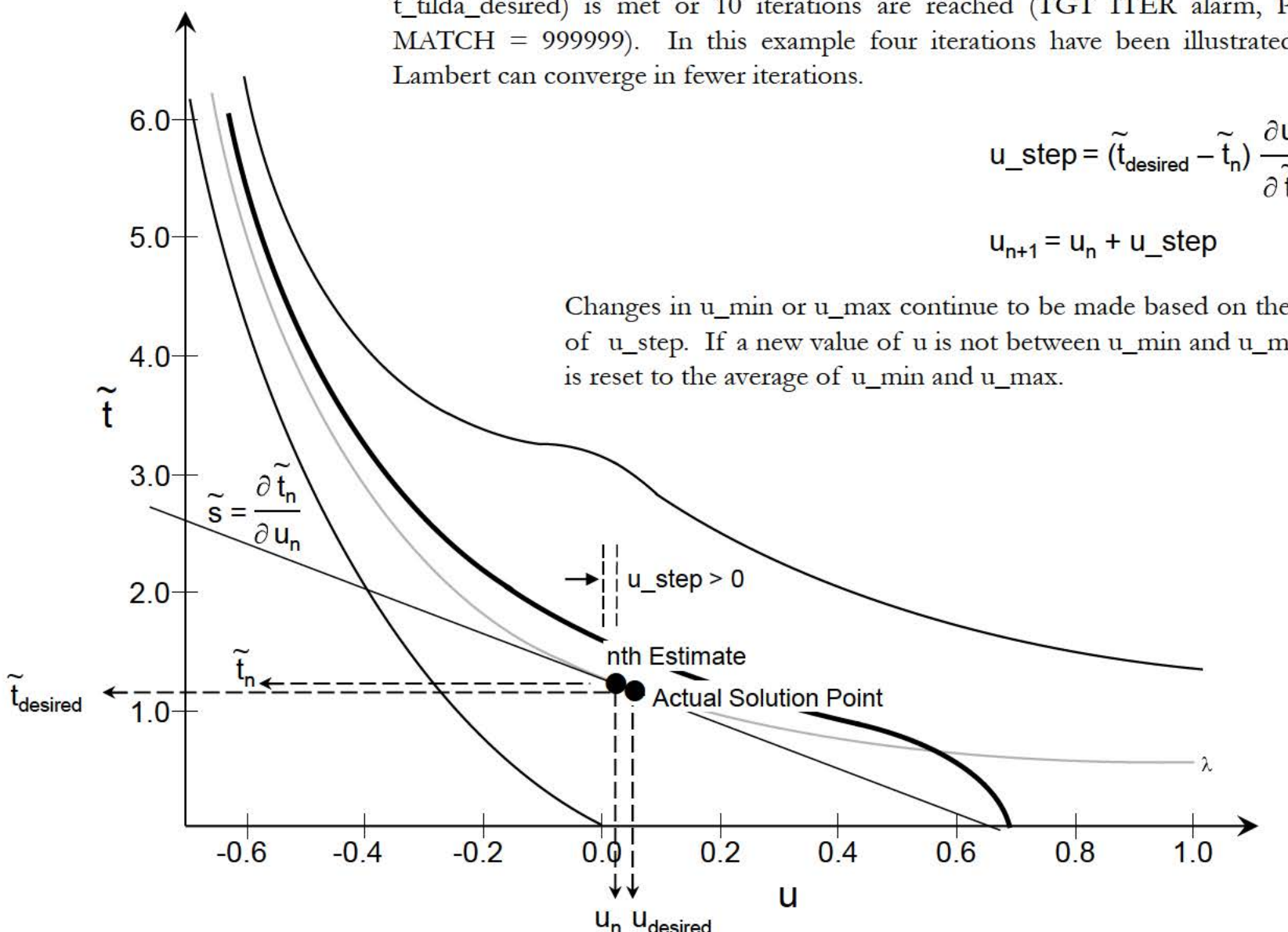
$$u_4 = u_3 + u_{\text{step}}$$

Since the change in u (u_{step}) in this example is positive, the lower limit on u is reset to the previous value of u .

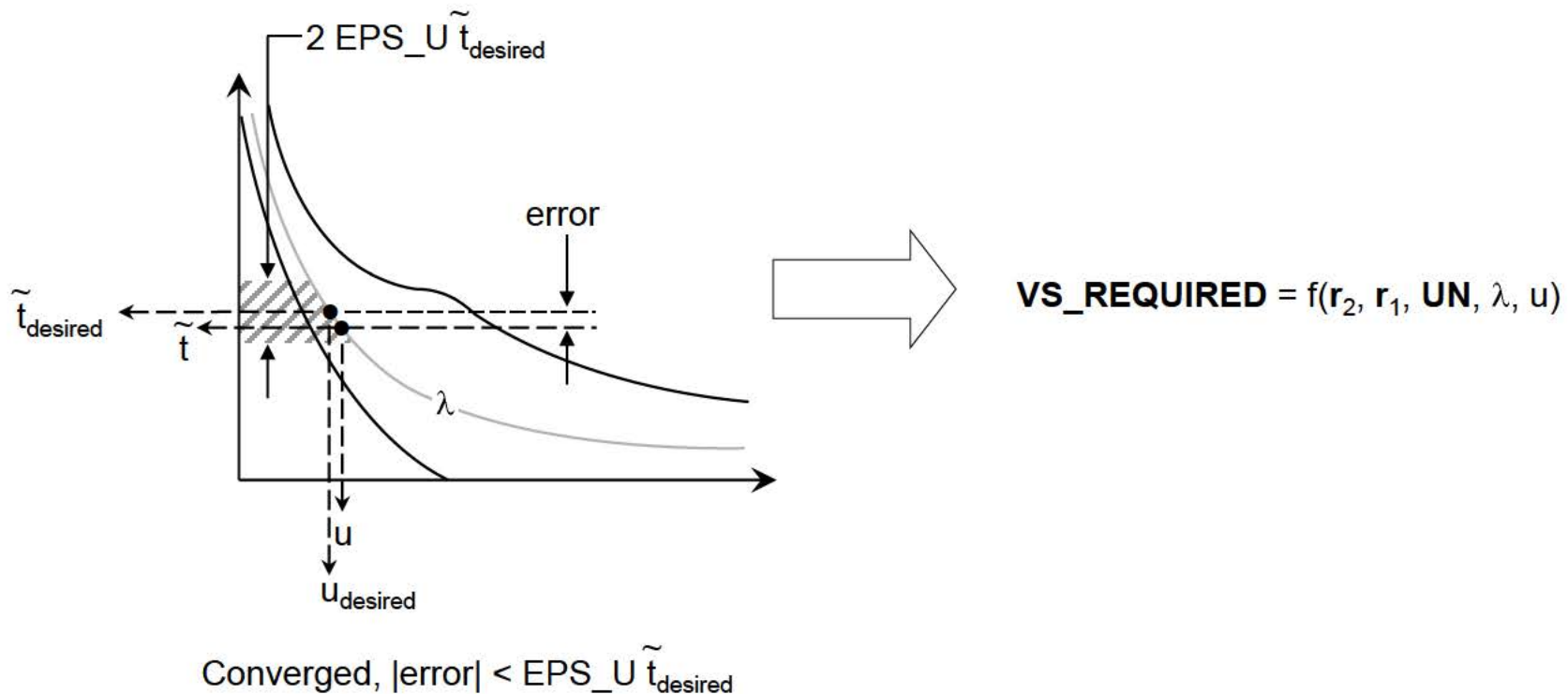
$$\begin{aligned} u_{\text{max}} &= u_{\text{circular}} \\ u_{\text{min}} &= u_3 \end{aligned}$$



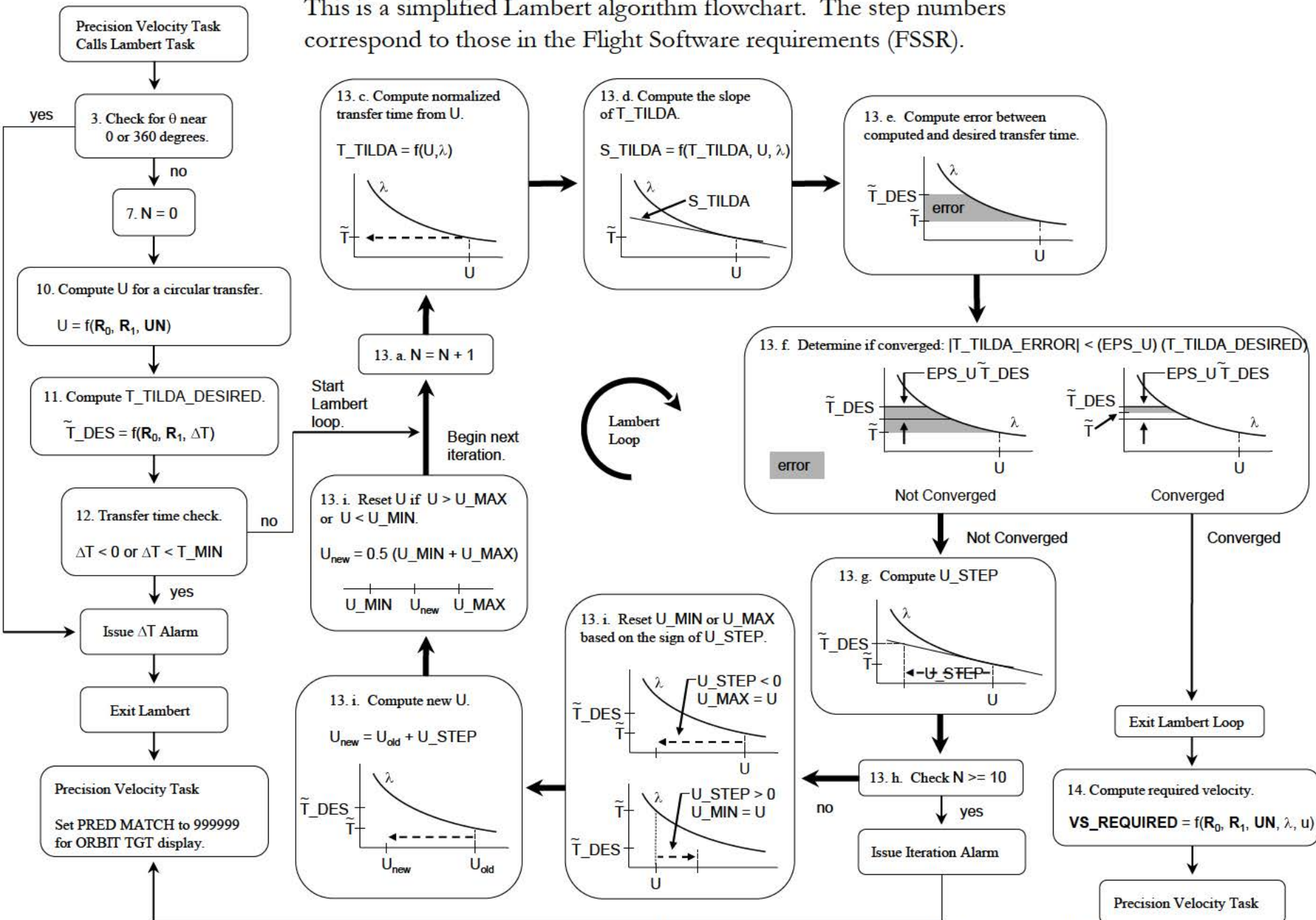
The iteration continues until the convergence criteria ($|\text{error}| < \text{eps}_u$ or $t_{\tilde{\text{t}}\text{da}_{\text{desired}}} = 999999$) is met or 10 iterations are reached (TGT ITER alarm, PRED MATCH = 999999). In this example four iterations have been illustrated, but Lambert can converge in fewer iterations.



If the iteration converges, a required velocity vector can then be computed. This velocity vector is then flown out by the Precision Velocity Required task.

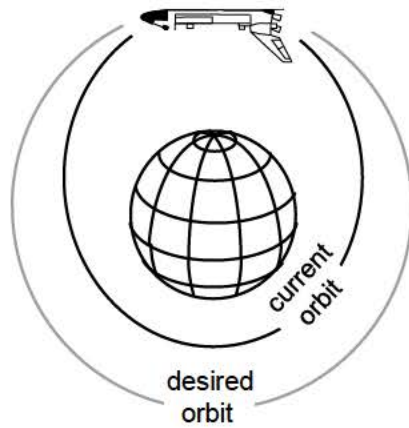


This is a simplified Lambert algorithm flowchart. The step numbers correspond to those in the Flight Software requirements (FSSR).



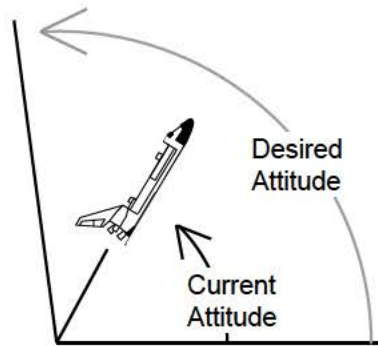
8.15 Guided and Unguided Burns

To accomplish mission objectives, a spacecraft must control both its translational and rotational dynamics. Guidance determines how vehicle thrust vector should be pointed so that the mission can be successfully executed. The term “guidance” isn’t normally associated with the control of rotational dynamics, but there is a “guidance” aspect to flight control (determining desired rate or attitude) and a “navigation” type of function (computing current attitude and rate).



Translational

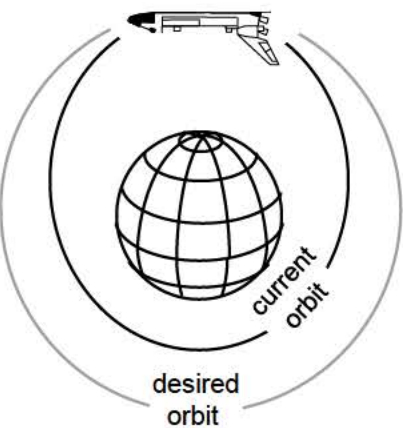
- position
- velocity



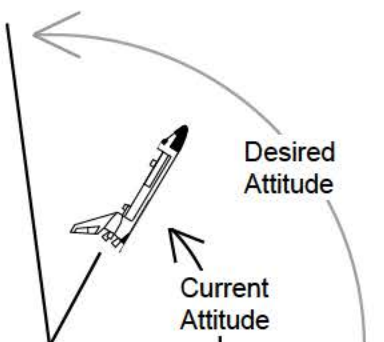
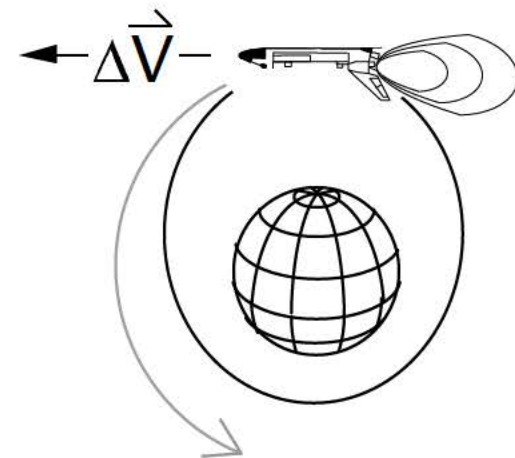
Rotational

- attitude
- rate

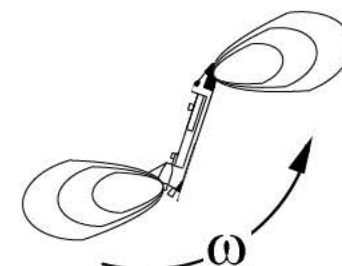
Guidance algorithms exist for both translation (such as Lambert or Powered Explicit Guidance) and rotation (such as Universal Pointing).



Translational guidance computes commands to change translational state.

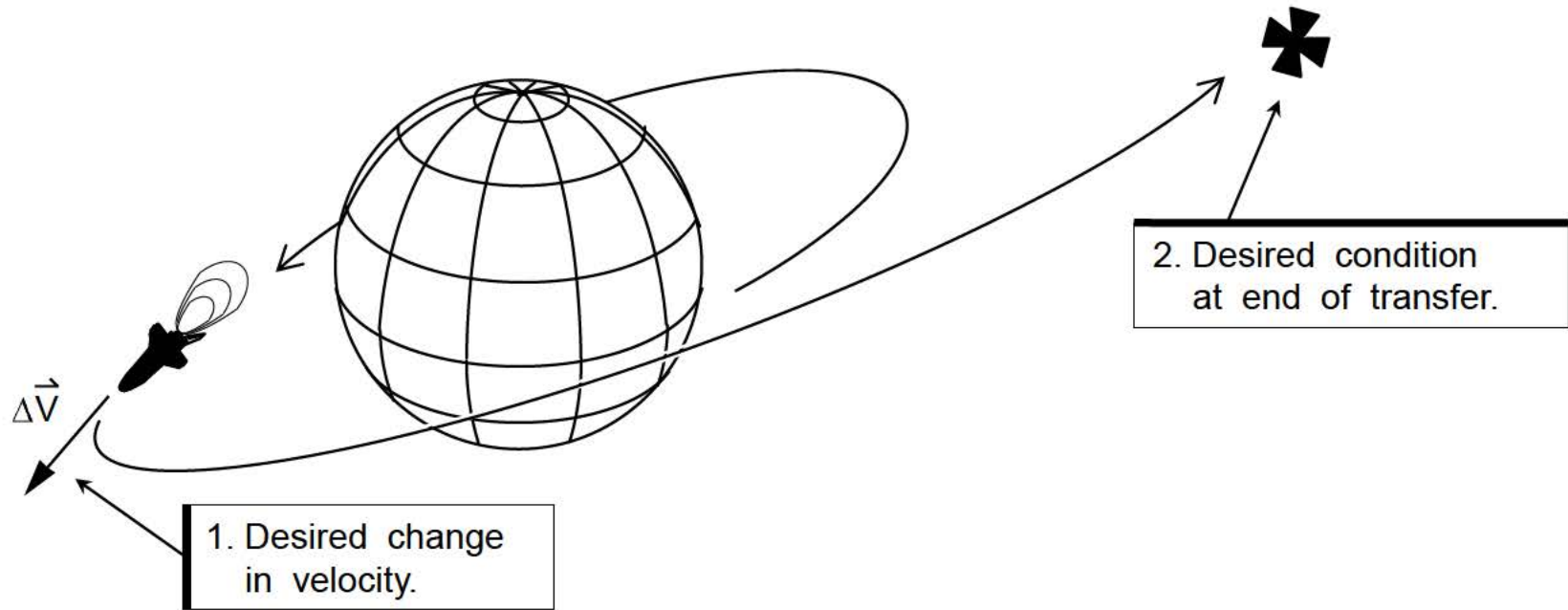


Rotational guidance computes commands to change rotational state (commands to flight control).



For a spacecraft to accomplish its mission it must be able to change its translational dynamics to meet some desired condition (or conditions) at a future time. Desired position and/or velocity to be achieved are called "targets" or "trajectory constraints."

The job of translational targeting and guidance is to determine the velocity change (ΔV) needed so that the targets are met. The point at which the targets are to be achieved may be at engine cut-off or some time after the end of the burn. It is important to remember that targets (or constraints) can also include the acceleration level during powered flight and time of engine cut-off (propellant available).

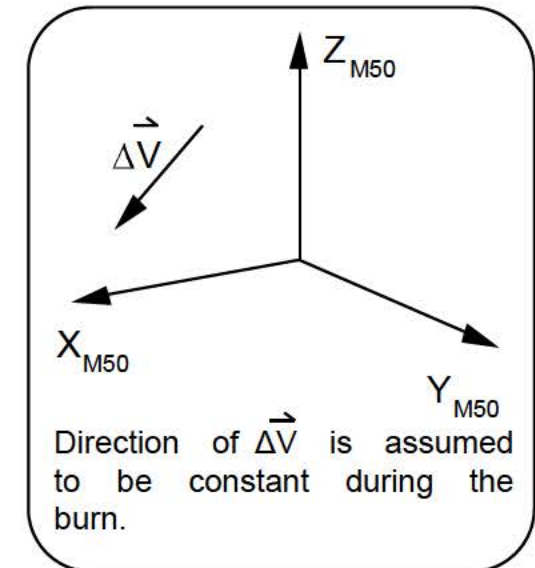
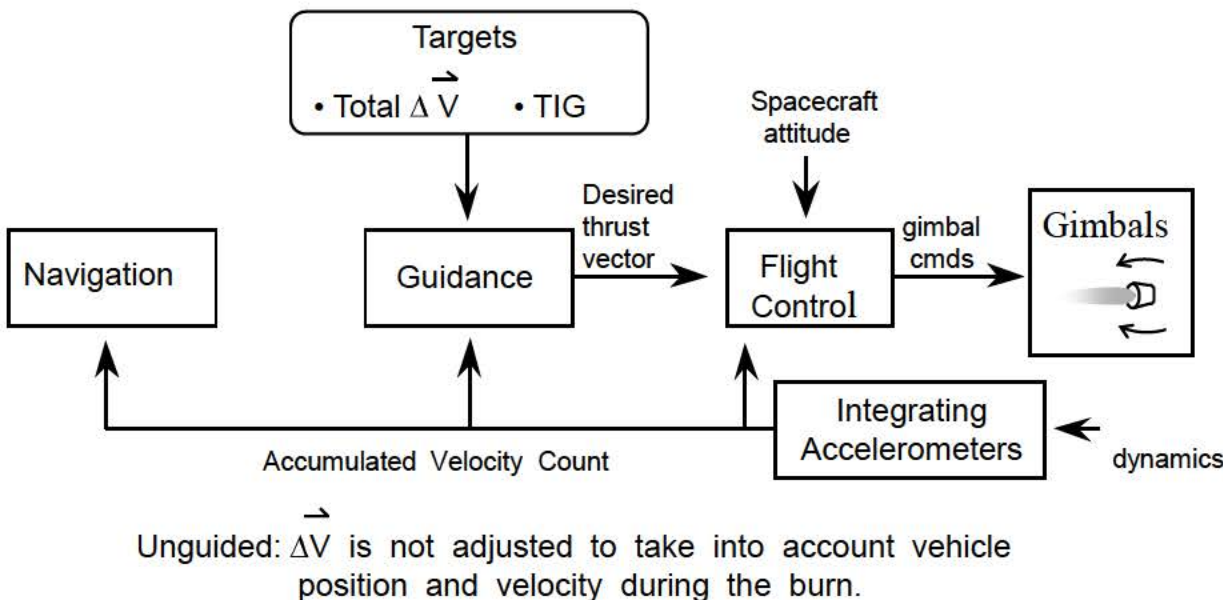


A closed loop unguided burn uses the simplest form of guidance. For on-orbit, exoatmospheric applications, the ΔV vector needed to achieve the burn targets and the Time-of-Ignition (TIG) are computed prior to the burn. During the burn, the ΔV vector is not recomputed based on current position and velocity. Hence the “unguided” nature of this guidance scheme.

Once the burn begins, guidance decrements the ΔV vector based on the sensed velocity obtained from accelerometers on an inertial platform. Hence the “closed loop” nature of this scheme. Guidance values for the ΔV vector are used to compute a desired thrust vector, T.

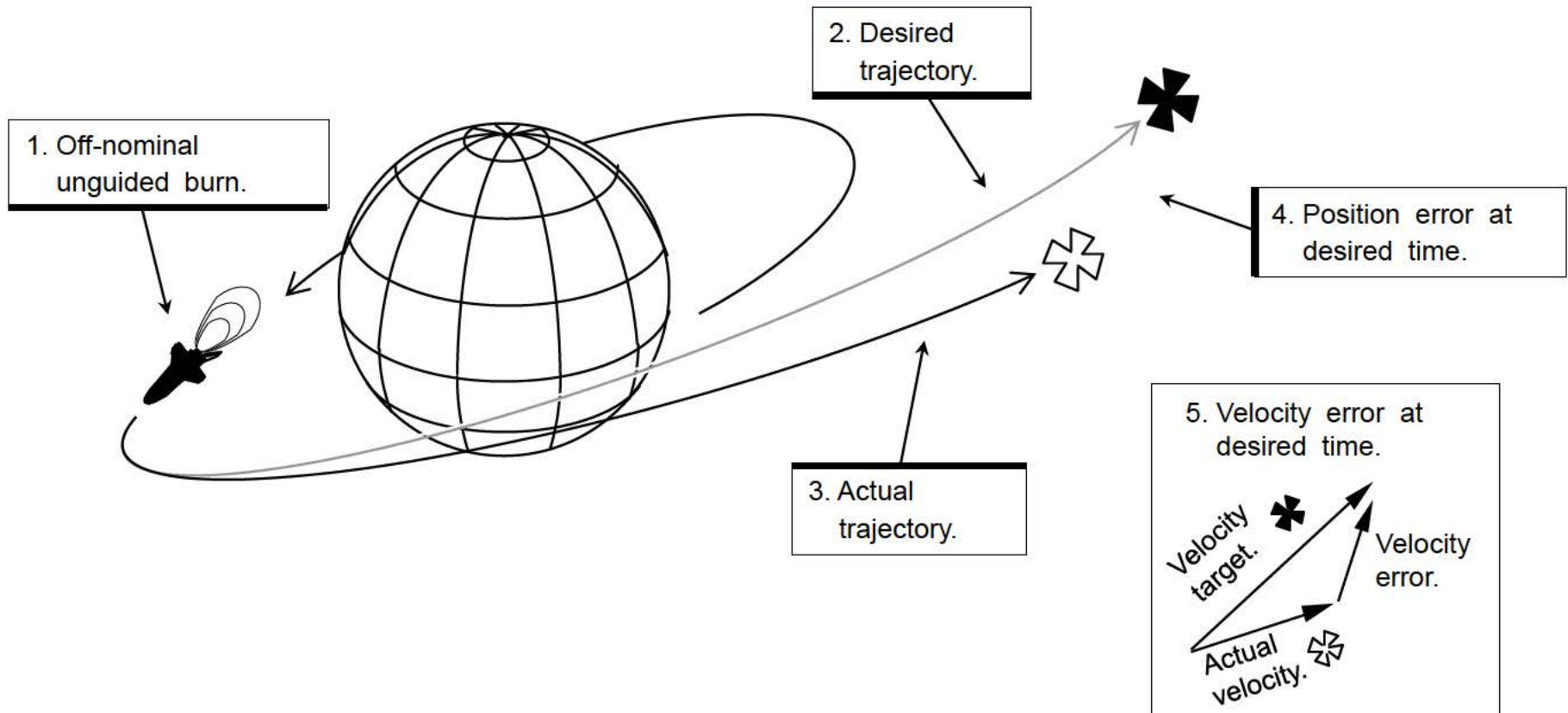
Flight control uses the desired thrust vector, sensed velocity and spacecraft attitude to ensure that the vehicle is burning in the proper direction.

Sensed velocity changes during the burn are used by navigation to determine current position and velocity.



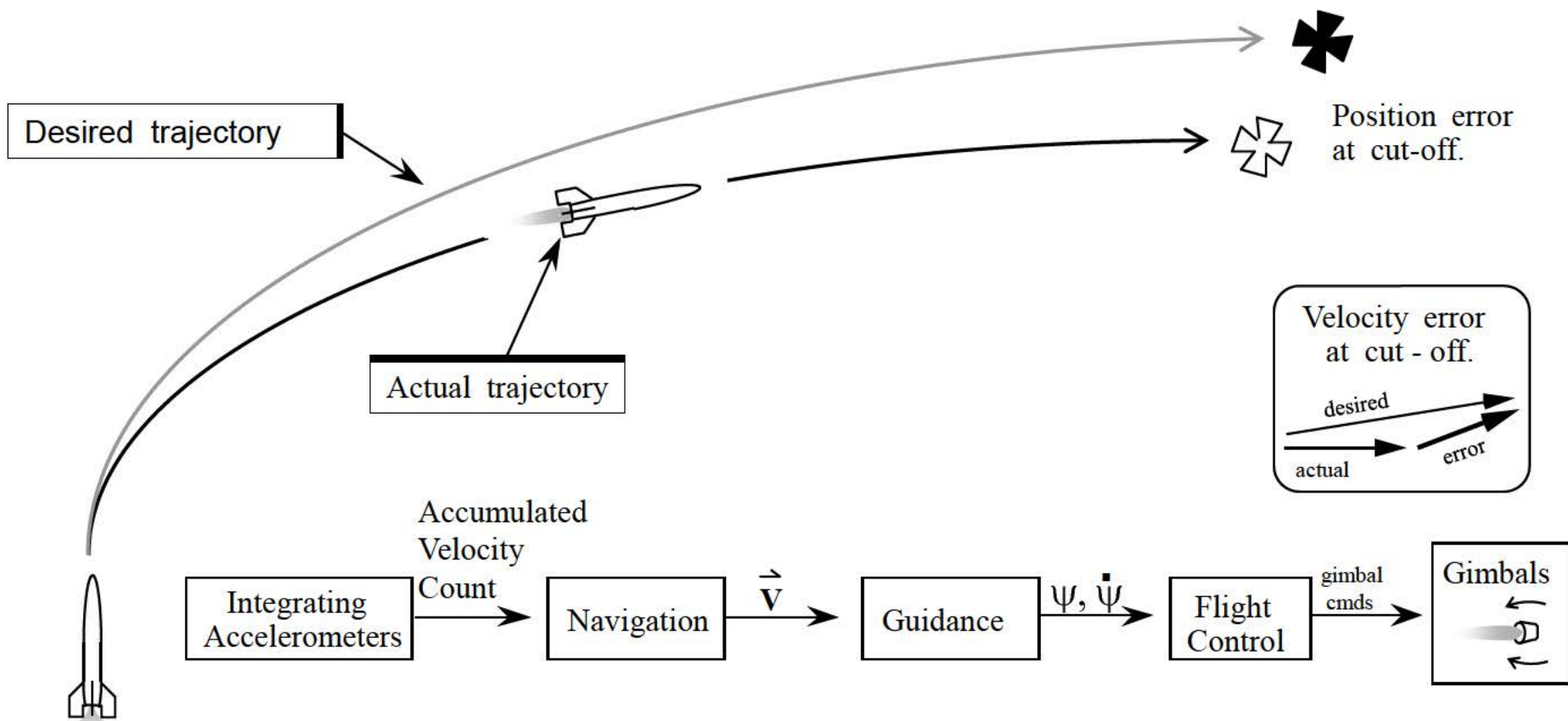
If ignition does not occur exactly at TIG, or if propulsion system performance is off-nominal, or if a propulsion system failure occurs requiring a downmode to another propulsion system, the spacecraft may not meet its trajectory targets. An unguided burn is not capable of compensating for off-nominal burn execution.

Closed loop unguided burns are used for trajectory adjustments that do not require a high degree of accuracy, such as orbit shaping burns.



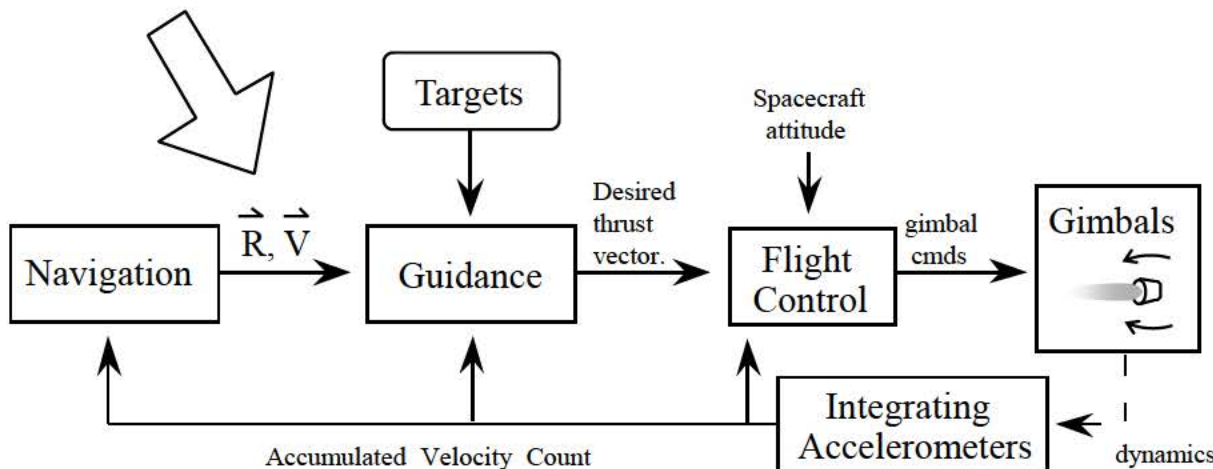
Pre-computed guidance commands used for atmospheric flight of sounding rockets and satellite launchers. It is not possible to obtain optimal, closed form equations for guidance parameters for powered flight within the atmosphere. Guidance may contain a table of desired thrust vector pitch angles (ψ) or thrust vector pitch rates ($\dot{\psi}$). The value of ψ or $\dot{\psi}$ used at a particular point could depend on elapsed time from lift off or rocket velocity (table look-up). ψ or $\dot{\psi}$ could also be computed real time from a set of equations.

These values would be computed assuming certain atmospheric conditions (temperature, winds, atmospheric pressure) and nominal engine performance. However, if atmospheric conditions and/or engine performance on the day of launch deviate from the expected, the rocket will not meet its targets at engine cut-off.

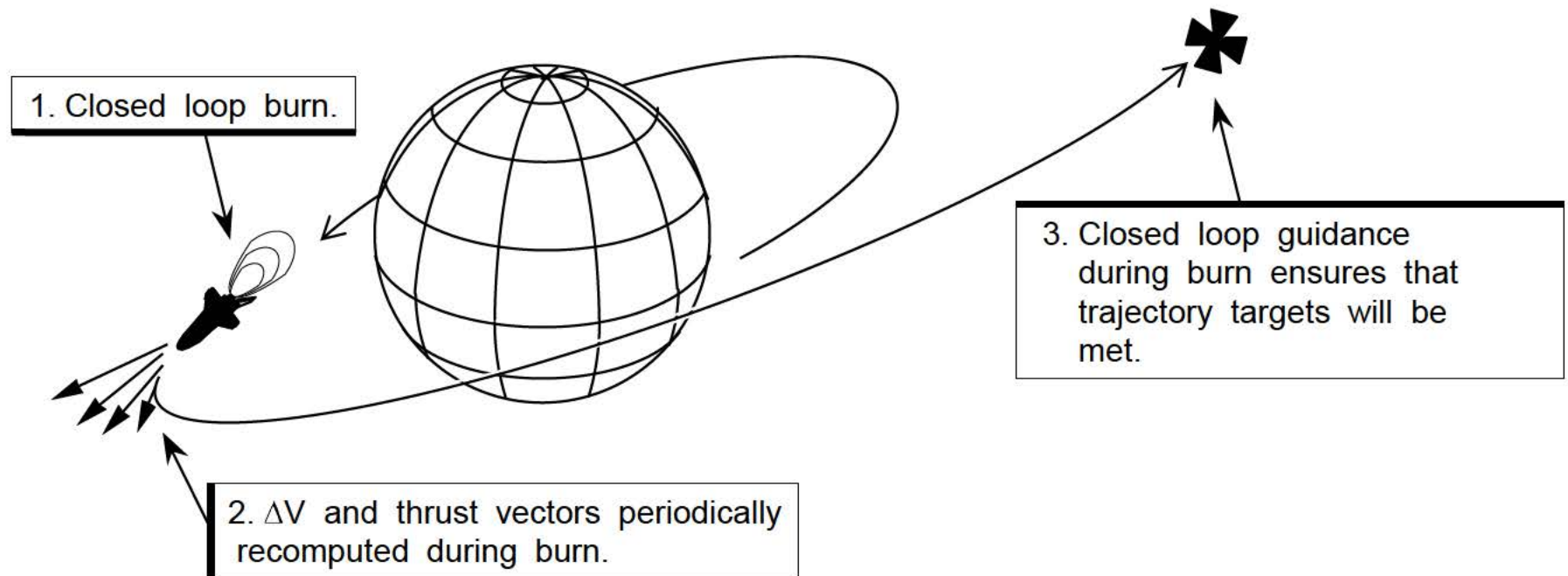


A closed loop guided burn enables a spacecraft to meet its trajectory targets in spite of off nominal engine performance or missed time of ignition. As with a closed loop unguided burn, a closed loop guided burn decrements the ΔV vector based on sensed velocity.

However, throughout the burn guidance will also periodically re-compute the total velocity vector required to meet the trajectory targets based on current spacecraft position and velocity obtained from navigation. The ΔV vector is then tweaked based on the recomputed total velocity required. A desired thrust vector is then computed for use by Flight Control.

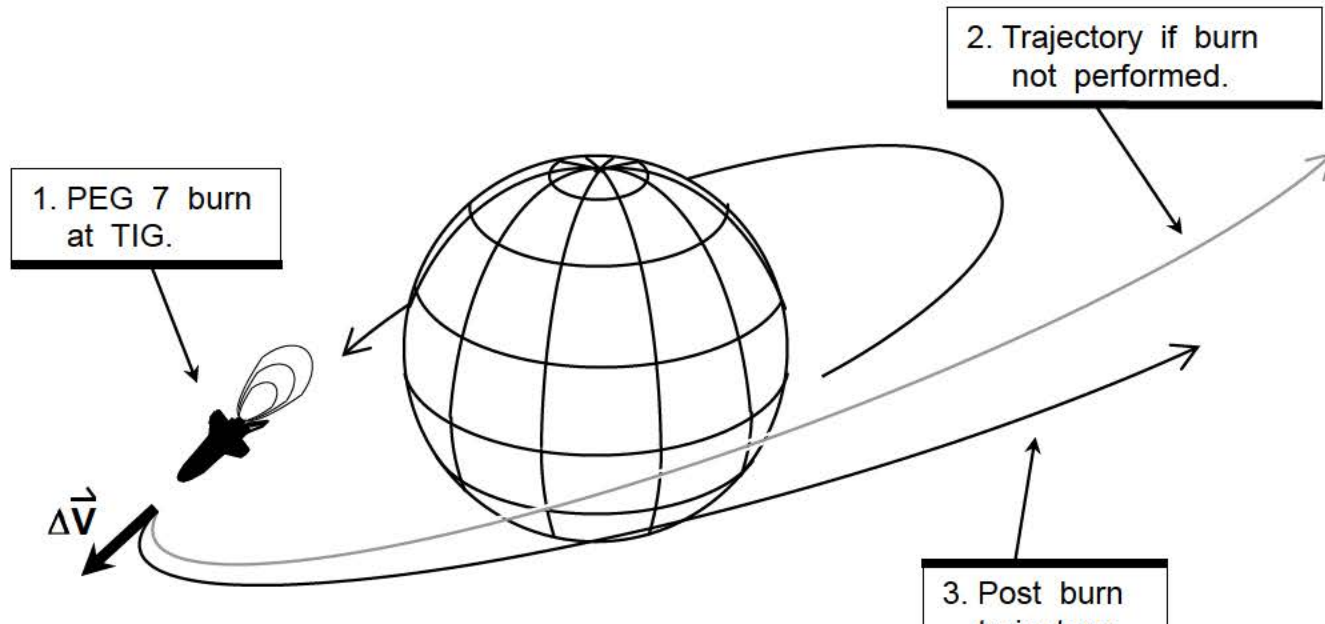


Closed loop guided burns are used for burns requiring a high degree of accuracy, such as rendezvous.



8.16 PEG 7 (External ΔV)

PEG 7 (Powered Explicit Guidance mode 7, also called External ΔV) is an closed loop unguided burn algorithm used during burns in OPS 2 (there is also a PEG 7 option in OPS 3). The ΔV to be executed is provided to PEG 7 in Local Vertical Rectilinear (LVR) coordinates centered on the orbiter state at ignition. A Lambert targeted burn may be executed via PEG 7, but this is not normally done.



PEG 7 Targets

TIG Time of ignition.

$\vec{\Delta V}$ Velocity change vector in ORBITER centered LVR coordinates at TIG.

ΔV and TIG may be obtained from the Flight Dynamics Officer (FDO) in Mission Control. Burn parameters (propulsion system, TV roll, weight, burn attitude, TIG and PEG 7 ΔV s) may be uplinked or voiced to the crew.

This is a MNVR EXEC display at TIG. Note that “EXT ΔV ” is displayed. If the ΔV targets were larger, the current and targeted apogee and perigee would differ. The “targeted” apogee and perigee are computed by applying the ΔV targets to the predicted TIG state to determine a predicted burn out state, then computing the resulting apogee and perigee.

2021 / /		ORBIT MNVR EXEC			1 010 / 18 :52 :43	
OMS BOTH 1*					000 / 00 :00 :00	
L 2		BURN ATT			ΔV TOT 111 .8	
R 3		24 R 186			TGO 1 :07	
RCS SEL 4		25 P 185				
5 TV ROLL 180		26 Y 322				
TRIM LOAD		MNVR 27 AUTO			VGO X + 107 .80	
6 P [-]0 .1		TTG			Y + 0 .29	
7 LY [+].5 .7		REI			Z + 29 .68	
8 RY [+].5 .7		TTA 38 :13				
9 WT 235359		GMBL			HA HP	
10 TIG		L R			TGT 199 +177	
10 / 18 :52 :43 .3		P - 0 .3 - 0 .3			CUR 194 +184	
TGT PEG 4		Y - 5 .8 +5 .8				
14 C1		PRI 28* 29*			35 ABORT TGT	
15 C2 [] -		SEC 30 31				
16 HT -		OFF 32 33			FWD RCS	
17 @ T -		GMBL CK 34			ARM 36	
18 PRPLT []		EXT ΔV			DUMP 37	
TGT PEG 7					OFF 38 *	
19 ΔV X [] 0_0					SURF DRIVE	
20 ΔV Y [+].100_0					ON 39	
21 ΔV Z [-].50_0					OFF 40 *	
LOAD 22 / TIMER 23						
EXEC						

This is the MNVR EXEC display after completion of the EXT ΔV burn. Note that the PEG 7 ΔVs remain constant, while the body axis ΔVs, ΔV magnitude and TGO have decreased. Current apogee and perigee match the targeted values after burn completion.

2021 / /	ORBIT	MNVR EXEC	1 010 / 18 :53 :53
OMS BOTH 1*			000 / 00 :01 :10
L 2	BURN ATT		ΔVTOT 1 .8
R 3	24 R 190		TGO :01
RCS SEL 4	25 P 194		VGO X + 0 .20
5 TV ROLL 180	26 Y 323		Y - 0 .00
TRIM LOAD	MNVR 27 AUTO		Z + 0 .02
6 P [-]0 .1	TTG		HA HP
7 LY [+]5 .7	REI		TGT 199 +177
8 RY [+]-5 .7	TTA 27 :45		CUR 198 +177
9 WT 232813	GMBL		
10 TIG	L R		
10 / 18 :52 :43 -3	P +1 .0 +0 .8		
TGT PEG 4	Y -5 .5 +5 .8		
14 C1	PRI 28 *	29 *	35 ABORT TGT
15 C2 [] -	SEC 30	31	FWD RCS
16 HT -	OFF 32	33	ARM 36
17 θ T -	GMBL CK	34	DUMP 37
18 PRPLT []	EXT ΔV		OFF 38 *
TGT PEG 7			SURF DRIVE
19 ΔVX [] 0 .0			ON 39
20 ΔVY [+]-100 .0			OFF 40 *
21 ΔVZ [-] 50 .0			
LOAD 22 / TIMER 23			
EXEC			

8.17 Lambert Cyclic Guidance

The Shuttle performs Lambert targeted burns once the on-board targeted (or relative navigation) phase of the rendezvous begins on the day of rendezvous. These burns are the Corrective Combination (NCC), Transition Initiation (Ti), and four Mid-course Correction (MC) burns. During Apollo the Terminal Phase Initiation (TPI) and Terminal Phase Mid-Course (TPM) burns were also Lambert targeted and Lambert guided. The phase of rendezvous where Lambert guidance was used during Apollo and Shuttle set up the vehicle for the initiation of final approach and/or proximity operations.

The phase of rendezvous where Lambert guidance was used during Apollo and Shuttle is more sensitive to trajectory dispersions than ground targeted phase where External ΔV guidance is used. Trim residuals are important for minimizing trajectory dispersions. For either a manually piloted or automated vehicle, control of dispersions is important at the proximity operations start point to ensure safe relative motion and conserve propellant. Lambert guidance ensures accurate trim residuals as the ΔV changes based on changing transfer geometry after time of ignition. Guided burns provide more accurate trim residuals at the end of the burn than External ΔV .

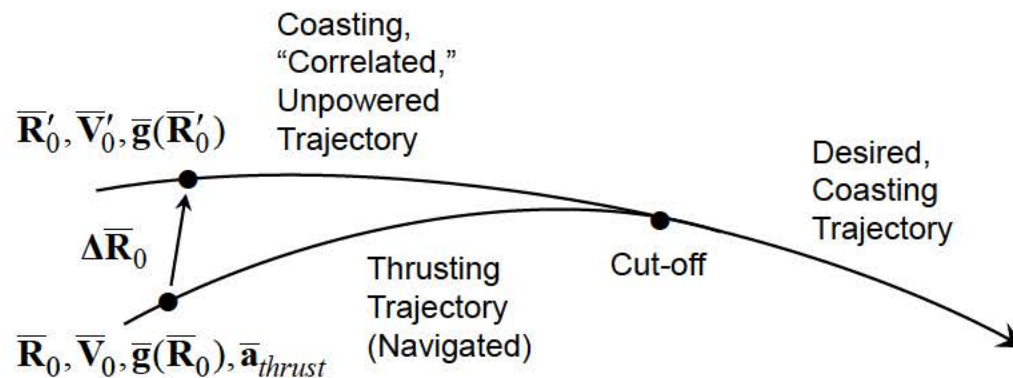
The implementation of Lambert Cyclic Guidance for the Space Shuttle was based on Apollo, with a modification developed by Tim Brand that is discussed on pages 29 and 30 of Battin's *An Introduction to the Mathematics and Methods of Astrodynamics*. The motivation behind Brand's development was to improve Lambert guidance performance over that seen on Apollo. This included lower attitude rates during the burn and a more accurate $\Delta \underline{V}$ estimate to improve cut-off performance.

Apollo Lambert guidance computed $\Delta \underline{V}$ using the following equation:

$$\Delta \bar{\mathbf{V}} = \bar{\mathbf{V}}(\bar{\mathbf{R}})_{\text{required}} - \bar{\mathbf{V}}$$

Pre-burn Lambert targeting computed the desired inertial aimpoint position vector and the semi-major axis of the transfer orbit. Values of required velocity (\bar{V}_r) during the burn were computed using a Lambert equation assuming that the semi-major axis of the transfer orbit remained constant during the burn. This assumption eliminated the need for iterative solutions of the Lambert time-of-flight equation during the burn. Between computations of \bar{V}_r using the Lambert time-of-flight equation the \mathbf{b} vector was used to extrapolate VGO along with IMU sensed velocity updates.

Brand's improved approach to Lambert guidance involved defining a coasting, non-thrusting "correlated" trajectory that coincided with the thrusting trajectory at cut-off. Primed quantities in the below illustration and in equations refer to the coasting trajectory. The required velocity is computed using the coasting trajectory, rather than the thrusting trajectory. In addition, the performance margin of the Shuttle AP-101B (later AP-101S) computer permitted an iterative solution of the Lambert time of flight equation every 3.84 seconds. Unlike Apollo, the semi-major axis of the transfer orbit was not assumed to be constant over the burn arc. A \mathbf{b} vector was not needed to extrapolate VGO between Lambert guidance passes.



This algorithm is known as Lambert Cyclic Guidance since it is used on the Space Shuttle. However, Correlated Velocity Guidance is not restricted to using a required velocity vector from Lambert targeting. The required velocity vector could come from some other type of targeting algorithm.

$\Delta \bar{\mathbf{V}}$ is defined as the difference between the velocities of the coasting (correlated) and thrusting trajectories.

$$\Delta \bar{\mathbf{V}}_0 = \bar{\mathbf{V}}'_0 - \bar{\mathbf{V}}_0$$

The position and velocity vectors at cut-off can be computed based on the thrusting trajectory parameters:

$$\bar{\mathbf{V}}_{cut-off} = \bar{\mathbf{V}}_0 + \int_{t_0}^{t_{cut-off}} \bar{\mathbf{a}}_{thrust} + \bar{\mathbf{g}}(\bar{\mathbf{R}}) dt$$

$$\bar{\mathbf{R}}_{cut-off} = \bar{\mathbf{R}}_0 + \int_{t_0}^{t_{cut-off}} \bar{\mathbf{V}} dt$$

The position and velocity vectors at cut-off can also be computed based on the coasting trajectory parameters:

$$\bar{\mathbf{V}}_{cut-off} = \bar{\mathbf{V}}'_0 + \int_{t_0}^{t_{cut-off}} \bar{\mathbf{g}}(\bar{\mathbf{R}}') dt$$

$$\bar{\mathbf{R}}_{cut-off} = \bar{\mathbf{R}}'_0 + \int_{t_0}^{t_{cut-off}} \bar{\mathbf{V}}' dt$$

The ΔV can be computed as follows:

$$\Delta \bar{\mathbf{V}}_0 = \bar{\mathbf{V}}'_0 - \bar{\mathbf{V}}_0 = \frac{\int_{t_0}^{t_{cut-off}} \bar{\mathbf{g}}(\bar{\mathbf{R}}') dt}{\int_{t_0}^{t_{cut-off}} \bar{\mathbf{a}}_{thrust} + \bar{\mathbf{g}}(\bar{\mathbf{R}}) dt}$$

$$\Delta \bar{\mathbf{V}}_0 = \bar{\mathbf{V}}'_0 - \bar{\mathbf{V}}_0 = \frac{\int_{t_0}^{t_{cut-off}} \bar{\mathbf{g}}(\bar{\mathbf{R}}') - \bar{\mathbf{g}}(\bar{\mathbf{R}}) - \bar{\mathbf{a}}_{thrust} dt}{\int_{t_0}^{t_{cut-off}} \bar{\mathbf{a}}_{thrust} dt}$$

The integration is simplified by assuming 1) the direction of the thrust acceleration vector is constant, 2) the magnitude of the thrust acceleration vector is constant, and 3) the difference in gravitational acceleration between the coasting and thrusting trajectories, $\Delta \mathbf{g}$, is small enough to be neglected:

$$\Delta \bar{\mathbf{g}} = \bar{\mathbf{g}}(\bar{\mathbf{R}}') - \bar{\mathbf{g}}(\bar{\mathbf{R}}) \approx \bar{\mathbf{0}}$$

This simplifies the $\Delta \mathbf{V}$ integration to:

$$\Delta \bar{\mathbf{V}}_0 = \bar{\mathbf{V}}'_0 - \bar{\mathbf{V}}_0 = \frac{\int_{t_0}^{t_{cut-off}} -\bar{\mathbf{a}}_{thrust} dt}{\int_{t_0}^{t_{cut-off}} -\bar{\mathbf{a}}_{thrust} dt} = -\bar{\mathbf{a}}_{thrust} (t_{cut-off} - t_0)$$

The position vector difference between the coasting and thrusting trajectories is computed as:

$$\Delta \bar{\mathbf{R}}_0 = \bar{\mathbf{R}}'_0 - \bar{\mathbf{R}}_0 = \frac{\int_{t_0}^{t_{cut-off}} \bar{\mathbf{V}}'_0 - \bar{\mathbf{V}}_0 dt}{\int_{t_0}^{t_{cut-off}} \Delta \bar{\mathbf{V}}_0 dt} = \frac{\int_{t_0}^{t_{cut-off}} -\bar{\mathbf{a}}_{thrust} (t_{cut-off} - t)^2 dt}{\int_{t_0}^{t_{cut-off}} -\bar{\mathbf{a}}_{thrust} (t_{cut-off} - t)^2 dt} = -\frac{1}{2} \bar{\mathbf{a}}_{thrust} (t_{cut-off} - t_0)^2$$

The equations for $\Delta \underline{\mathbf{V}}$ and $\Delta \underline{\mathbf{R}}$ can be used to compute $\Delta \underline{\mathbf{R}}$ in a manner that does not involve time-to-go.

$$t_{cut-off} - t_0 = \frac{|\Delta \bar{\mathbf{V}}_0|}{|\bar{\mathbf{a}}_{thrust}|}$$

$$|\Delta \bar{\mathbf{R}}_0| = -\frac{1}{2} |\bar{\mathbf{a}}_{thrust}| (t_{cut-off} - t_0)^2 = -\frac{1}{2} |\bar{\mathbf{a}}_{thrust}| \left[\frac{|\Delta \bar{\mathbf{V}}_0|}{|\bar{\mathbf{a}}_{thrust}|} \right]^2$$

$$|\Delta \bar{\mathbf{R}}_0| = -\frac{1}{2} \frac{|\bar{\mathbf{a}}_{thrust}|}{|\bar{\mathbf{a}}_{thrust}|} \frac{|\Delta \bar{\mathbf{V}}_0|^2}{|\bar{\mathbf{a}}_{thrust}|} = -\frac{1}{2} \frac{|\Delta \bar{\mathbf{V}}_0|^2}{|\bar{\mathbf{a}}_{thrust}|}$$

The magnitude of the position change is assumed to be along the unit vector of the $\Delta \underline{\mathbf{V}}$.

$$\Delta \bar{\mathbf{R}}_0 = |\Delta \bar{\mathbf{R}}_0| \frac{\Delta \bar{\mathbf{V}}_0}{|\Delta \bar{\mathbf{V}}_0|} = -\frac{1}{2} \frac{|\Delta \bar{\mathbf{V}}_0|^2}{|\bar{\mathbf{a}}_{thrust}|} \frac{\Delta \bar{\mathbf{V}}_0}{|\Delta \bar{\mathbf{V}}_0|} = -\frac{1}{2} \frac{|\Delta \bar{\mathbf{V}}_0|}{|\bar{\mathbf{a}}_{thrust}|} \Delta \bar{\mathbf{V}}_0$$

$\Delta\mathbf{R}$ is then used to compute the coasting trajectory position vector that is used to compute required velocity.

$$\Delta\bar{\mathbf{R}}_0 = \bar{\mathbf{R}}'_0 - \bar{\mathbf{R}}_0$$

$$\bar{\mathbf{R}}'_0 = \bar{\mathbf{R}}_0 + \Delta\bar{\mathbf{R}}_0 = \bar{\mathbf{R}}_0 - \frac{1}{2} \frac{|\Delta\bar{\mathbf{V}}_0|}{|\bar{\mathbf{a}}_{thrust}|} \Delta\bar{\mathbf{V}}_0$$

The value of $\bar{\mathbf{R}}_0$ prime is provided to a targeting algorithm by guidance for the computation of a required velocity vector. $\Delta\bar{\mathbf{V}}$ is then computed as:

$$\Delta\bar{\mathbf{V}}_0 = \bar{\mathbf{V}}(\bar{\mathbf{R}}'_0)_{required} - \bar{\mathbf{V}}_0$$

The equation for $\Delta\bar{\mathbf{R}}$ can be used to justify neglecting the gravitational difference between the coasting and thrusting trajectories.

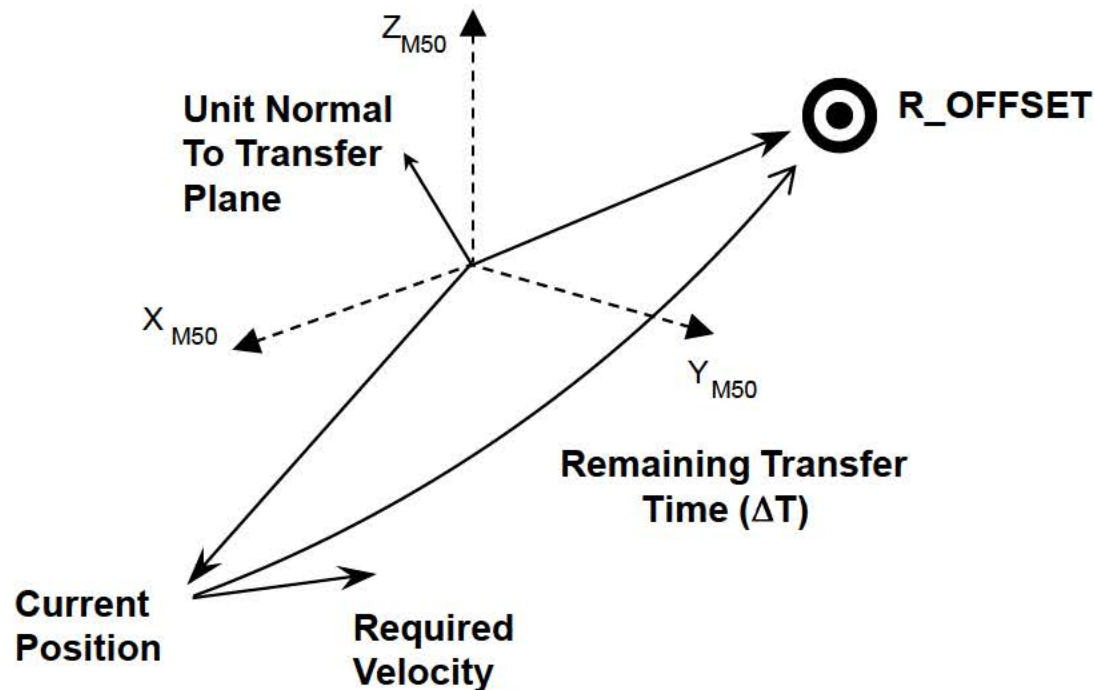
$$\Delta\bar{\mathbf{g}} = \bar{\mathbf{g}}(\bar{\mathbf{R}}) - \bar{\mathbf{g}}(\bar{\mathbf{R}}') = \frac{\partial \bar{\mathbf{g}}}{\partial \bar{\mathbf{R}}} \Delta\bar{\mathbf{R}} = - \frac{\partial \bar{\mathbf{g}}}{\partial \bar{\mathbf{R}}} \left[\frac{1}{2} \frac{|\Delta\bar{\mathbf{V}}|}{|\bar{\mathbf{a}}_{thrust}|} \Delta\bar{\mathbf{V}} \right]$$

$\Delta\bar{\mathbf{g}}$ is a function of the square of $\Delta\bar{\mathbf{V}}$ and decreases during the maneuver. Using the coasting trajectory position vector as an input to the Lambert algorithm resulted in a nearly constant attitude during the burn and more accurate $\Delta\bar{\mathbf{V}}$ values.

If targeting completes without an alarm generated by the Lambert task, a flag will be set indicating that Lambert Cyclic Guidance is to be used for the burn. Five parameters are passed by targeting to Lambert Cyclic Guidance: the R_OFFSET vector, the time of ignition, time of arrival, guidance flag and the S_ROTATE flag. The value of S_ROTATE (-1, 0 or +1) is used to ensure that the plane of the transfer (cross product of the initial and final positions) is defined correctly.

During the burn, Lambert Cyclic Guidance recomputes the required velocity to make the transfer, taking into account the decrease in transfer time and change in the ORBITER position and velocity. R_OFFSET is not recomputed. The result of the Lambert computation is used to “tweak” (not replace) the Δ Vs on the MNVR EXEC display.

Onboard targeted burns (NCC, Ti, MC-1 through MC-4) are all normally executed using Lambert Cyclic Guidance.



Lambert Cyclic Guidance executes once when the LOAD (ITEM 22) is performed, and every 3.84 seconds from TIG-15 seconds through MM 201 PRO.

This is a MNVR EXEC display at TIG for a Lambert guided burn. Note the difference in the current and targeted perigee.

The guidance mode will change to EXT ΔV if a PEG 7 target uplink is performed or if any of ITEMS 1 through 13 or 19 through 21 are entered by the crew. Also, if any of ITEMS 7 through 12 on the ORBIT TGT display were non-zero when the ITEM 28 was performed, guidance will be set to EXT ΔV .

2021 / /	ORBIT	MNVR EXEC	1 001 / 17 :27 :30 000 / 00 :00 :00
OMS BOTH 1			
L 2 *	BURN ATT		ΔV TOT 9 . 1
R 3	24 R 120		TGO 0 :11
RCS SEL 4	25 P 232		
5 TV ROLL 0	26 Y 017		VGO X + 8 . 48
TRIM LOAD	MNVR 27 AUTO		Y + 2 . 01
6 P [-]0 . 1	TTG		Z + 2 . 49
7 LY [+5 . 2	REI		
8 RY [-]5 . 2	TTP 39 :23		HA HP
9 WT 244124	GMBL		TGT 195 +182
10 TIG	L R		CUR 195 +178
1 / 17 :27 :30 . 0	P - 0 . 3 - 0 . 3		
TGT PEG 4	Y + 5 . 1 - 5 . 1		
14 C1	PRI 28 * 29 *	35 ABORT TGT	
15 C2 [] -	SEC 30 31		
16 HT -	OFF 32 33	FWD RCS	
17 0 T -	GMBL CK 34	ARM 36	
18 PRPLT []	LAMBERT	DUMP 37	
TGT PEG 7		OFF 38 *	
19 ΔV X [+] 9 - 0		SURF DRIVE	
20 ΔV Y [-] 0 - 3		ON 39	
21 ΔV Z [-] 0 - 0		OFF 40 *	
LOAD 22 / TIMER 23			
EXEC			

This is the MNVR EXEC display after completion of the Lambert guided burn. Note that the PEG 7 Δ Vs decreased, along with the body axis Δ Vs, Δ V magnitude and TGO. Current and targeted apogee and perigee match.

Before OI-32 (STS-120, Oct.-Nov. 2007), Lambert guided burns had to be completed within 90 seconds of TIG or be retargeted. Beyond 90 seconds, the error in the Δ Vs exceeded the trim limits (0.2 feet/second in each axis).

2021 / /	ORBIT	MNVR EXEC	1 001 / 17 :28 :10
OMS BOTH 1			000 / 00 :00 :40
L 2*	BURN ATT		Δ VTOT 0 .1
R 3	24 R 125		TGO 0 :01
RCS SEL 4	25 P 223		
5 TV ROLL 0	26 Y 004	MNVR 27 AUTO	VGO X - 0 .12
TRIM LOAD		TTG	Y + 0 .07
6 P [-]0 .1		REI	Z + 0 .05
7 LY [+5 .2		TTP 36 :20	
8 RY [-]5 .2		GMBL	HA HP
9 WT 243863		L R	TGT 195 +182
10 TIG		P +0 .9 +0 .9	CUR 195 +182
1 / 17 :27 :30 .0		Y +4 .1 -6 .1	
TGT PEG 4	PRI 28 * 29 *	35 ABORT TGT	
14 C1	SEC 30 31		
15 C2 [] -	OFF 32 33	FWD RCS	
16 HT -	GMBL CK 34	ARM 36	
17 θ T -	LAMBERT	DUMP 37	
18 PRPLT []		OFF 38 *	
TGT PEG 7		SURF DRIVE	
19 ΔVX [] 0_-1		ON 39	
20 ΔVY [+] 0_-1		OFF 40 *	
21 ΔVZ [+] 0_-1			
LOAD 22 / TIMER 23			
EXEC			

On OI-32 (first flight STS-120, Oct.-Nov. 2007), an improvement was made to Lambert Cyclic Guidance that removed the 90 second maneuver execution time limit. No changes were made to the display. However, the improvement eliminated the “jump” seen in the Δ Vs between TIG-15 seconds (Lambert Cyclic Guidance initiation) and TIG.

2021 / /	ORBIT	MNVR EXEC	1 001 / 17 :27 :30 000 / 00 :00 :00
OMS BOTH 1			
L 2 *	BURN ATT		Δ VTOT 9 .1
R 3	24 R 120		TGO 0 :11
RCS SEL 4	25 P 232		
5 TV ROLL 0	26 Y 017	MNVR 27 AUTO	VGO X + 8 .48
TRIM LOAD		TTG	Y + 2 .01
6 P [-]0 .1		REI	Z + 2 .49
7 LY [+5 .2		TTP 39 :23	
8 RY [-]5 .2		GMBL	HA HP
9 WT 244124		L R	TGT 195 +182
10 TIG		P - 0 .3 - 0 .3	CUR 195 +178
1 / 17 :27 :30 .0		Y + 5 .1 - 5 .1	
TGT PEG 4			
14 C1	PRI 28 *	29 *	35 ABORT TGT
15 C2 [] -	SEC 30	31	FWD RCS
16 HT -	OFF 32	33	ARM 36
17 0 T -	GMBL CK	34	DUMP 37
18 PRPLT []	LAMBERT		OFF 38 *
TGT PEG 7			SURF DRIVE
19 Δ VX [+] 9 .0			ON 39
20 Δ VY [-] 0 .3			OFF 40 *
21 Δ VZ [-] 0 .0			
LOAD 22 / TIMER 23			
EXEC			

No jumps in Δ Vs before TIG

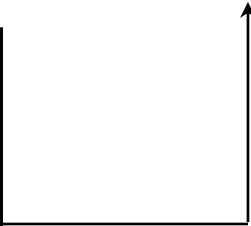
8.18 Targeting And Guidance Alarms

Under certain conditions, alarms or illegal entry messages will be annunciated during targeting with the ORBIT TGT display. These messages are designed to alert the crew and MCC personnel to a problem which would prevent successful computation of a maneuver.

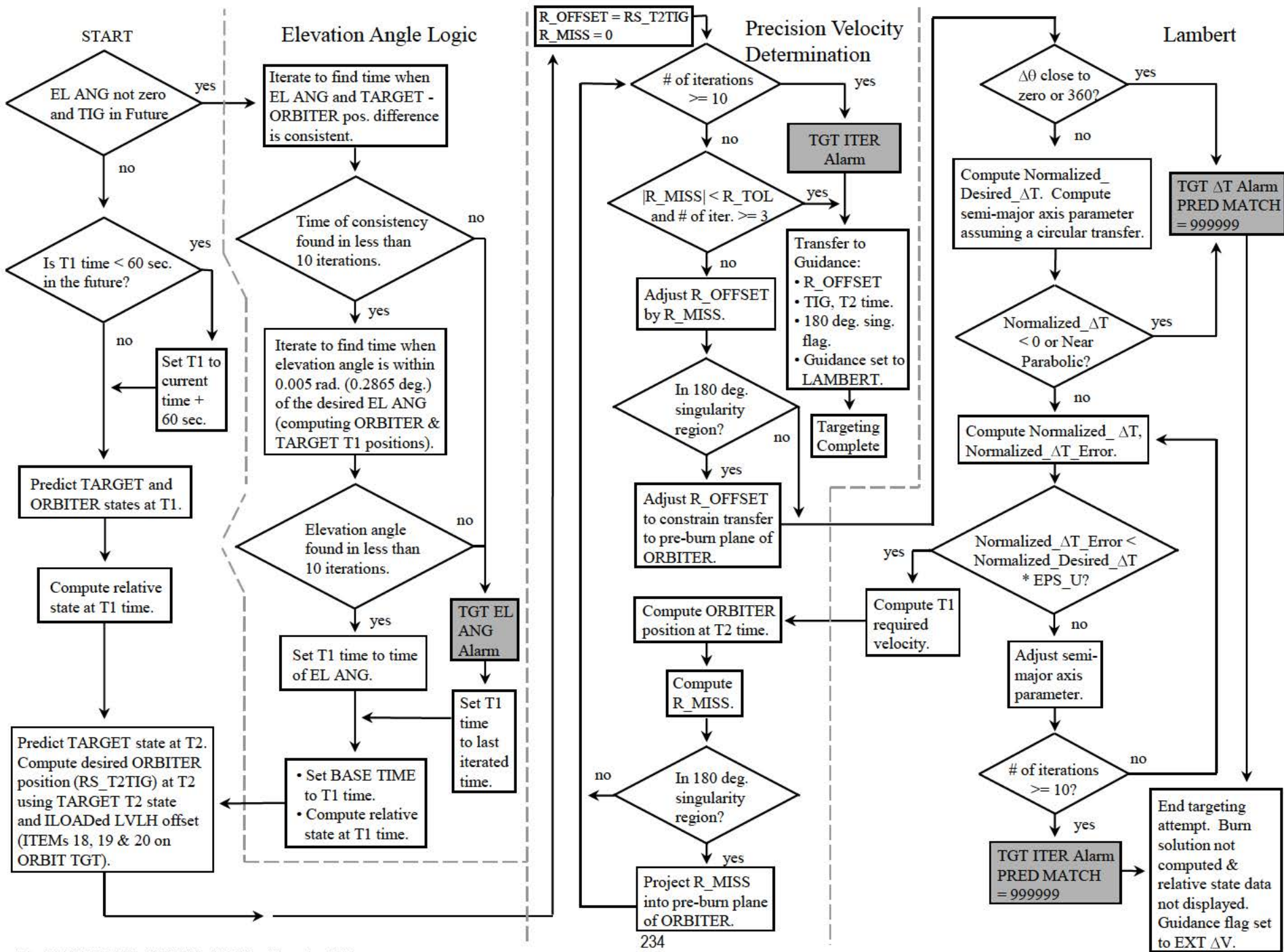
For Lambert targeted burns, alarms may also be annunciated during the LOAD (ITEM 22) on the MNVR EXEC display (not shown on this page) and during cyclic guidance (TIG - 15 seconds through MM201 PRO).

2021 / 034 /		ORB IT	TGT	1 005 / 21 :01 :23
MNVR	TIG	ΔV_X	ΔV_Y	000 / 00 :16 :32
10	5 / 21 :17 :55	- 1 .6	- 0 .8	ΔV_Z
		PRED	MATCH =	ΔVT
				999 999
INPUTS		CONTROLS		
1	TGT NO	5 / 21 :17	:55	1.0
2	T1 TIG	0	:00	25
6	EL	0	:00	LOAD
7	ΔX / DNRNG	[]	0 :00	COMPUTE T1
8	ΔY	[]	0 :00	COMPUTE T2
9	ΔZ / ΔH	[]	0 :00	28
10	ΔX	[]	0 :00	
11	ΔY	[]	0 :00	
12	ΔZ	[]	0 :00	
13	T2 TIG	0 / 00 :00	:00	29
17	ΔT	[+]	81 :4	ORBITER STATE
18	ΔX	[]	0 :00	134 / 20 :41 :16 :720
19	ΔY	[]	0 :00	X + 20708 :850
20	ΔZ	[]	0 :00	Y - 5777 :582
21	BASE TIME	5 / 21 :17	:55	Z - 5214 :796
				VX + 8 :590280
				VY + 21 :319779
				VZ + 10 :402009
TGT ITER		1	21 :01 :22	
ITEM 28 EXEC				

Alarms and illegal entries appear on the line above the ITEM entries on all on board displays.



The next page contains an illustration of the Lambert targeting process, with the places where alarms are generated indicated. The pages following the flow diagram contain tables concerning the alarms, and examples of alarms that have occurred.



Alarms During Lambert Targeting (Orbit Targeting Display)

Alarm	Targeting	FSSR Task/ FSW Module	Cause	Related FSSR/FSW Parameters
TGT EL ANG	Lambert	Elevation Angle Iteration Task (ELITER)	Time could not be found in less than 10 iterations when target position is on the same side (above/below) of orbiter local horizontal as desired target position specified by ILOADed elevation angle.	ALARM_B, DELTA_H EL_ANG (from ILOAD array) EL_DH_TOL (ILOAD V96U7788C) IC_MAX (ILOAD V96U7517C)
		GWX_ORB_TGT_ELITER*	Displayed elevation angle should be equal to pre-compute value. Elevation angle and displayed relative altitude at T1 (ITEM 9 on ORBIT TGT) will not be consistent (ΔZ negative).	CGZB_ORB_TGT_EL_ANG_ALARM CGZB_ORB_TGT_SFFAIL, DELTA_H CGZV_ORB_TGT_EL_ANG (ILD array) CGZV_EL_DH_TOL (ILD V96U7788C) CGZV_ICMAX (ILOAD V96U7517C)
TGT ΔT PRED MATCH = 999999	Lambert	Elevation Angle Iteration Task (ELITER)	Time could not be found in less than 10 iterations when the elevation angle was within EL_TOL of the ILOADed angle.	ALARM_B, EL_ERR EL_TOL (ILOAD V96U7787C) IC_MAX (ILOAD V96U7517C)
		GWX_ORB_TGT_ELITER*	Difference between pre-compute and post compute displayed elevation angles will be greater than or equal to EL_TOL (0.286478898 degrees). Elevation angle and displayed relative altitude at T1 (ITEM 9 on ORBIT TGT) will be consistent (ΔZ positive).	CGZB_ORB_TGT_EL_ANG_ALARM CGZB_ORB_TGT_SFFAIL CGZV_X_DEP CGZV_EL_TOL (ILOAD V96U7787C) CGZV_ICMAX (ILOAD V96U7517C)
	Lambert	Lambert	Transfer angle is close to 0 or 360 degrees.	ALARM_D, ALARM_KILL, EP_TRANSFER (ILOAD V96U7514C) GWY_DELTA_T_ALARM_REQ CGZB_TARGETING_TGT_DT_ALARM CGZB_ALARM_KILL CGZV_EP_TRANSFER (ILOAD)
		GWY_ORB_TGT_LAMBERT	Pre-iteration normalized transfer time (T_TILDA_DESIRED) is negative or \leq parabolic transfer time (T_MIN).	ALARM_D, ALARM_KILL DU (ILOAD V96U7513C) GWY_DELTA_T_ALARM_REQ CGZB_TARGETING_TGT_DT_ALARM CGZB_ALARM_KILL CGZV_DU (ILOAD)

* SFFAIL is set to "ON" in the Newton Raphson Iteration Task (ITERV, GWQ_ORB_TGT_ITERV). ELITER then sets the elevation angle alarm to "ON."

Alarm	Targeting	FSSR Task/ FSW Module	Cause	Related FSSR/FSW Parameters
TGT ITER PRED MATCH = 999999	Lambert	Lambert GWY_ORB_TGT_LAMBERT	This did not occur in under 10 iterations: 1. $ T_{TILDA_ERROR} < T_{TILDA_DESIRED} (\text{EPS_U})$ *	ALARM_A ALARM_KILL EPS_U (ILOAD V96U7515C) N_MAX_ITER (ILOAD V96U7790C) GWY_LAMBERT_ALARM_REQ CGZB_ALARM_KILL CGZV_EPS_U (ILOAD) CGZV_N_MAX (ILOAD)
TGT ITER	Lambert	Precision Velocity Required Task (PREVR) GWW_ORB_TGT_PREVR	Difference between predicted position at T2 time (RS_TERMINAL) and desired position (RS_T2TIG) could not be reduced to or below R_TOL in under 10 iterations.	ALARM_A N_MAX_ITER (ILOAD V96U7790C) R_TOL (ILOAD V96U7789C) CGZB_TARGETING_LAMBERT_ALARM CGZV_N_MAX (ILOAD V96U7790C) CGZV_R_TOL (ILOAD V96U7789C)
TGT ΔT	Lambert	PROX_EXEC GKQ_ORB_TGT_ITEM_PROC	Lambert targeting was requested (ITEM 28) but the transfer time (ITEM 17) and T2 TIG (ITEMs 13-16 are zero).	ALARM_D COMP_PROX_DT T2_TIG CGZB_TARGETING_TGT_DT_ALARM CGZV_COMP_PROX_DT CGZV_ORB_TGT_TIME.TOTAL_SECS\$(2;)

* The U_STEP exit was deleted by CR 90974A (Orbit Targeting Lambert Iteration Loop Exit Logic Correction) on OI-26A.

This example of a TGT ITER alarm is from a SPF recreation of an alarm that occurred during third INTELSAT rendezvous on STS-49 (OI-21) due to the Lambert parameter mixed precision problem (fixed with CR 90701A, Orbit Targeting Iteration Loop Correction on OI-22). The software problem within the Lambert task prevented convergence on a solution in under 10 iterations. Note that PRED MATCH is set to “999999,” and the T1 relative state and the T2 (arrival) time is not displayed. This occurs if the alarm is generated within the Lambert module of the Flight Software. The Δ Vs are left over from a previous computation. A TGT ITER or TGT Δ T alarm issued from the Lambert task during pre-burn targeting (PRED MATCH set to “999999”) will result in EXT Δ V being displayed on the MNVR EXEC display in MM 202.

2021 / 034 /	ORBIT	TGT	1 005 / 21 :01 :23 000 / 00 :16 :32
MNVR	TIG	Δ VX Δ VY Δ VZ Δ VT	
10	5 / 21 :17 :55	- 1.6 - 0.8 - 3.4 + 3.8	PRED MATCH = 999999
INPUTS			CONTROLS
1 TGT NO		10	T2 TO T1 25
2 T1 TIG	5 / 21 :17 :55		LOAD 26
6 EL		0 .00	COMPUTE T1 28
7 Δ X / DNRNG	[]	0 .00	COMPUTE T2 29
8 Δ Y	[]	0 .00	
9 Δ Z / Δ H	[]	0 .00	
10 Δ X	[]	0 .00	
11 Δ Y	[]	0 .00	
12 Δ Z	[]	0 .00	
13 T2 TIG	0 / 00 :00 :00		ORB ITER STATE
17 Δ T	[+]	81 .4	134 / 20 :41 :16 .720
18 Δ X	[]	0 .00	X + 20708 .850
19 Δ Y	[]	0 .00	Y - 5777 .582
20 Δ Z	[]	0 .00	Z - 5214 .796
21 BASE TIME	5 / 21 :17 :55		VX + 8 .590280
TGT ITER		1	VY + 21 .319779
ITEM 28 EXEC			VZ + 10 .402009
			21 :01 :22

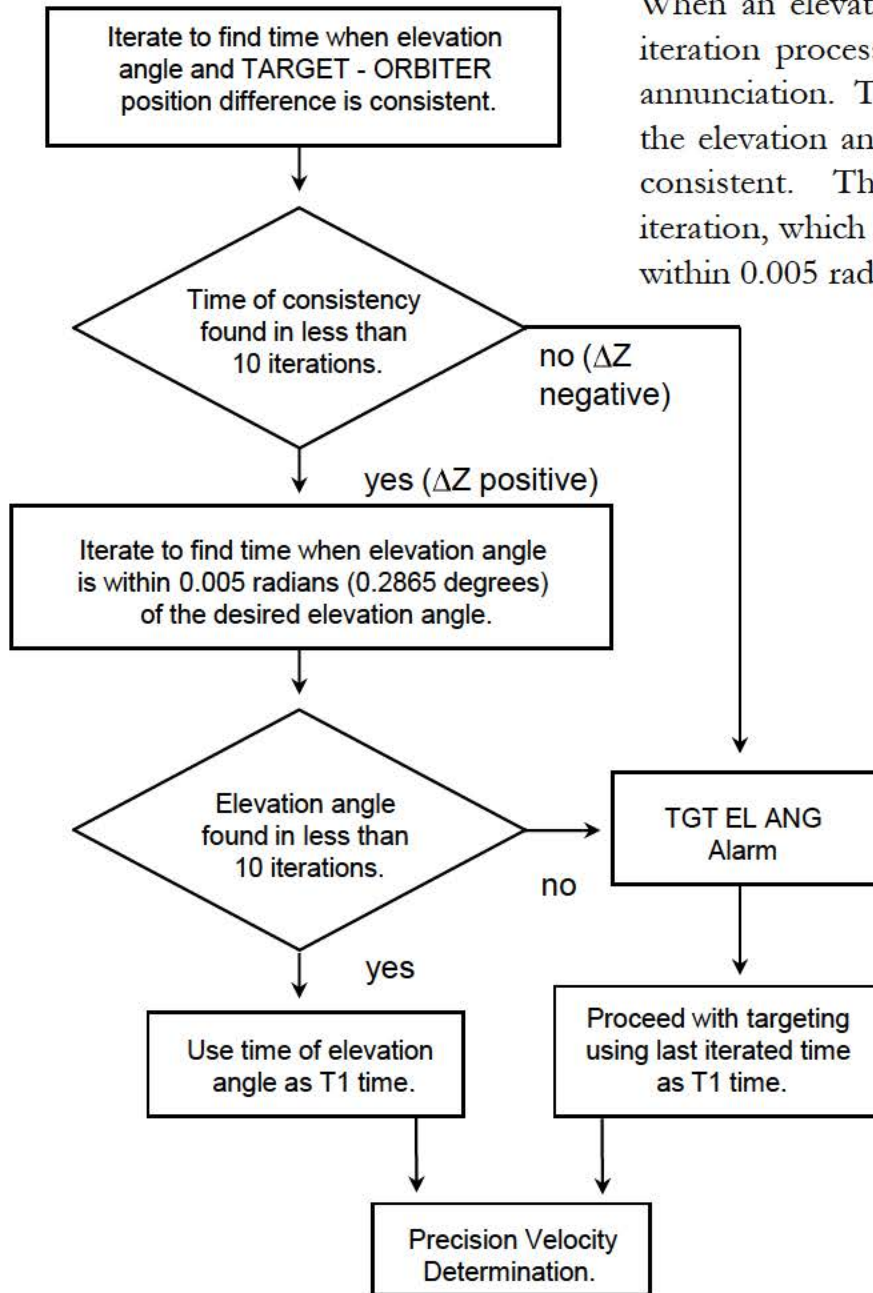
This example of a “TGT ITER” alarm is from a SPF recreation of an alarm that occurred during a STS-51 integrated sim, due to the Lambert parameter inconsistency (T_TILDA_ERROR and U_STEP exits, DR 106677 on OI-22, fixed with CR 90974A, Orbit Targeting Lambert Iteration Loop Exit Logic Correction on OI-26A). The software problem prevented the Precision Velocity Required task from converging on a ΔV that resulted in a miss distance of less than or equal to R_TOL within 10 iterations. Note that PRED MATCH, the T1 relative state and the T2 time are displayed. PRED MATCH is 326 feet, larger than the R_TOL value of 250 feet. The DV solution is from the targeting attempt that failed to meet the convergence criteria.

2021 / 034 /	ORBIT	TGT	1 005 / 05 :50 :55 000 / 00 :29 :07
MNVR	TIG	ΔV_X ΔV_Y ΔV_Z ΔV_T	
10	5 / 06 :20 :02	- 0.5 - 0.5 - 2.8 + 2.9	PRED MATCH = 326
INPUTS			
1	TGT NO	10	CONTROLS
2	T1 TIG	5 / 06 :20 :02	T2 TO T1 25
6	EL	0 .00	LOAD 26
7	ΔX / DNRNG	[+] 53 .20	COMPUTE T1 28
8	ΔY	[+] 0 .03	COMPUTE T2 29
9	ΔZ / ΔH	[+] 2 .33	
10	$\Delta \dot{X}$	[+] 7 .84	
11	$\Delta \dot{Y}$	[+] 0 .46	
12	$\Delta \dot{Z}$	[+] 2 .04	
13	T2 TIG	5 / 07 :40 :13	ORBITER STATE
17	ΔT	[+] 80 .2	187 / 4 :14 :49 .148
18	ΔX	[] 0 .00	X +18846 .669
19	ΔY	[] 0 .00	Y - 5584 .581
20	ΔZ	[] 0 .00	Z - 9639 .251
21	BASE TIME	5 / 06 :20 :02	VX + 9 .297170
TGT ITER		1	VY + 23 .106035
ITEM 28 EXEC			VZ + 4 .709670
			05 :50 :52

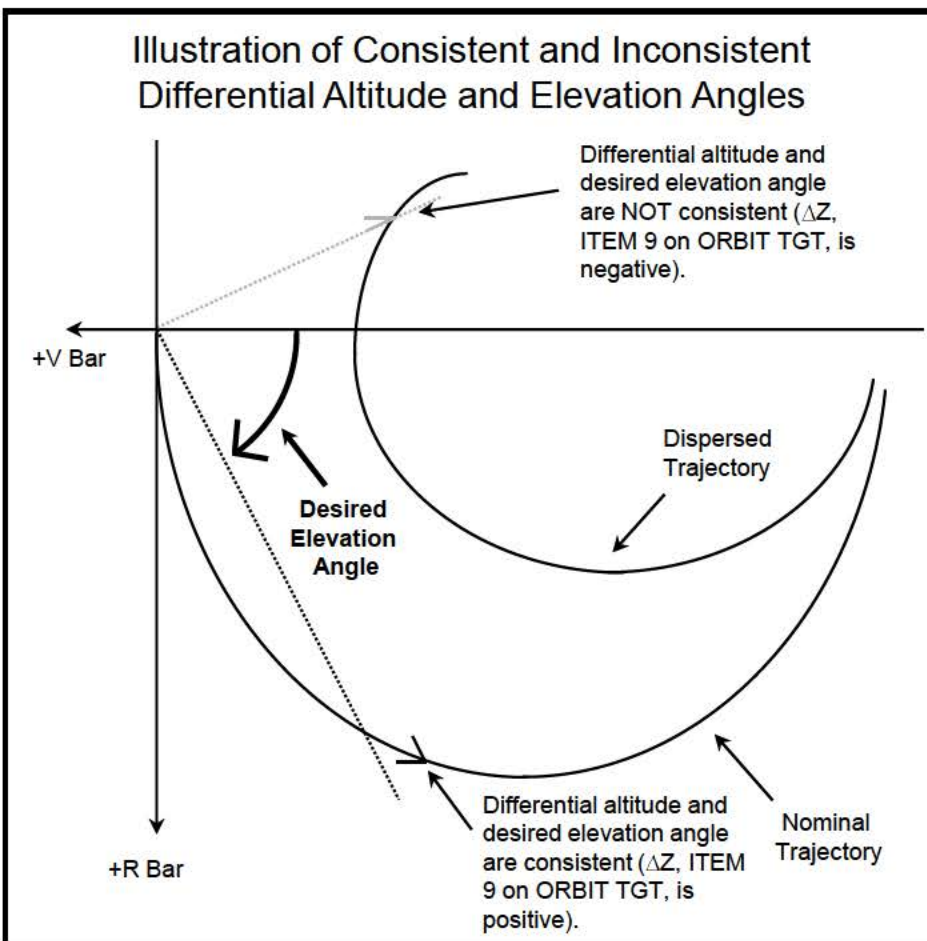
If the crew were to enter MM 202 after the TGT ITER alarm from the Precision Velocity Required task (PRED MATCH not equal to 999999), the display would appear as below. Note that the guidance mode is LAMBERT and that the burn solution appears in the PEG 7 slots.

This display is from the same SPF run as the ORBIT TGT display on the previous page.

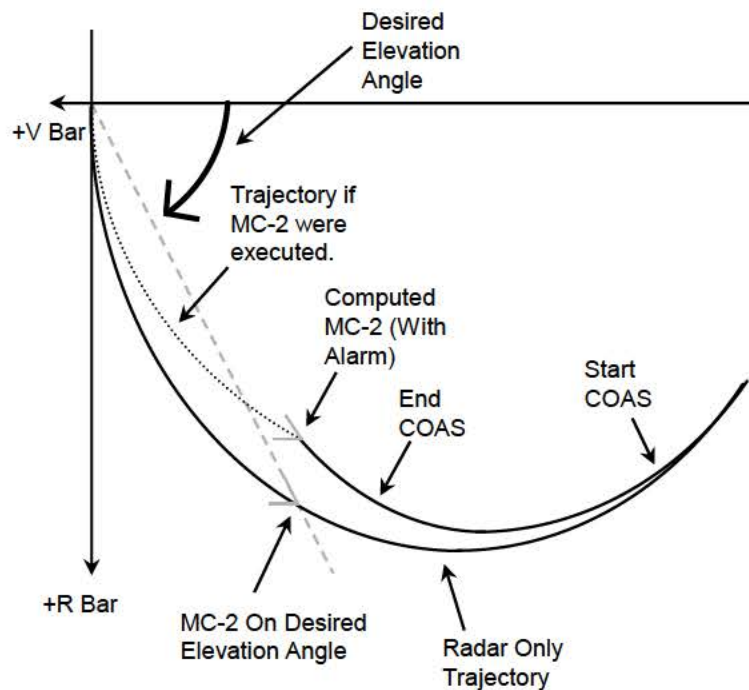
2021 / /	ORBIT MNVR EXEC	1 001 / 17 : 22 : 31 000 / 00 : 04 : 59
OMS BOTH 1	BURN ATT	ΔV TOT
L 2	24 R	TGO
R 3	25 P	VGO X
RCS SEL 4 *	26 Y	Y
5 TV ROLL 0	MNVR 27 AUTO	Z
TRIM LOAD	TTG	
6 P [-] 0 . 3	REI	
7 LY [-] 5 . 7	TTA 1 : 59	HA HP
8 RY [+] 5 . 7	GMBL	
9 WT 244124	L R	
10 TIG 1 / 17 : 27 : 30 _ 0	P - 0 . 3 - 0 . 3	TGT CUR 195 + 178
TGT PEG 4	Y - 6 . 5 + 6 . 5	
14 C1	PRI 28 * 29 *	35 ABORT TGT
15 C2 [] -	SEC 30 31	FWD RCS
16 HT -	OFF 32 33	ARM 36
17 θ T -	GMBL CK 34	DUMP 37
18 PRPLT []	LAMBERT	OFF 38 *
TGT PEG 7		SURF DRIVE
19 Δ VX [+] 8 . 9		ON 39
20 Δ VY [-] 0 . 4		OFF 40 *
21 Δ VZ [-] 0 . 1		
LOAD 22 / TIMER 23		
OPS 202 PRO		



When an elevation angle constraint is placed on the T1 position, there are two iteration processes, both of which can fail and trigger a TGT EL ANG alarm annunciation. The objective of the first iteration process is to find a time at which the elevation angle and the altitude difference between the orbiter and target are consistent. The time of consistency (if found) is used to start the second iteration, which involves finding the time of the burn when the elevation angle is within 0.005 radians (0.2865 degrees) of the desired (ILOADED) elevation angle.



Below is an example of an elevation angle alarm resulting from the failure to find the desired elevation angle in less than 10 iterations to within 0.005 radians (0.2865 degrees). This is from a STS-31 SPF simulation. A trajectory dispersion resulted from VERN firings during a pre MC-2 COAS pass. COAS procedures and DAP configuration in the simulation were not “optimal” for a COAS pass. The original ILOADED elevation angle was 29.49 degrees. The last elevation angle computed, along with the associated time (T1 TIG and BASE TIME), is displayed. Note the large radial ΔV . Original TIG was 2/23:56:27. The TIG slip was 5:59 into the future. Note that ΔZ is positive (the elevation angle and relative altitude are consistent).



2021 / 034 /		ORBIT	TGT	1 002 / 23 : 59 : 11			
MNVR	TIG		000 / 00 : 03 : 15	ΔV_x	ΔV_y	ΔV_z	ΔV_t
12	3 / 00 : 02 : 26			- 2 . 6	- 0 . 3	+ 7 . 3	+ 7 . 8
		PRED	MATCH =				1
INPUTS							CONTROLS
1	TGT NO						T2 TO T1 25
2	T1 TIG	3 / 00 : 02 : 26					LOAD 26
6	EL		27 . 28				COMPUTE T1 28
7	ΔX / DNRNG			[-]	21 . 87		COMPUTE T2 29
8	ΔY			[-]	0 . 17		
9	ΔZ / ΔH			[+]	10 . 99		
10	$\Delta \dot{X}$			[+]	24 . 10		
11	$\Delta \dot{Y}$			[+]	0 . 13		
12	ΔZ			[-]	8 . 54		
13	T2 TIG	3 / 00 : 35 : 08					
17	ΔT			[+]	32 . 7		
18	ΔX			[]	0 . 00		
19	ΔY			[]	0 . 00		
20	ΔZ			[]	0 . 00		
21	BASE TIME	3 / 00 : 02 : 26					
ORB ITER STATE							
348	/ 13 : 55 :	3 . 086	X -	6325 . 265			
			Y +	21916 . 260			
			Z +	1416 . 696			
			VX -	20 . 771492			
			VY -	6 . 755435			
			VZ +	11 . 832053			
				23 : 59 : 04			
TGT EL ANG							1
ITEM 28 EXEC							

Alarms During Maneuver Execute Processing and Burn Execution

Alarm	Targeting	FSSR Task/ FSW Module	Cause	Related FSSR/FSW Parameters
TGT ΔT	Lambert	Lambert	Transfer angle is close to 0 or 360 degrees.	ALARM_D, ALARM_KILL, EP_TRANSFER (ILOAD V96U7514C) GWY_DELTA_T_ALARM_REQ CGZB_TARGETING_TGT_DT_ALARM CGZB_ALARM_KILL CGZV_EP_TRANSFER (ILOAD)
		GWY_ORB_TGT_LAMBERT	Pre-iteration normalized transfer time (T_TILDA_DESIRED) is negative or <= parabolic transfer time (T_MIN).	ALARM_D, ALARM_KILL DU (ILOAD V96U7513C) GWY_DELTA_T_ALARM_REQ CGZB_TARGETING_TGT_DT_ALARM CGZB_ALARM_KILL CGZV_DU (ILOAD)
TGT ITER	Lambert	Lambert	This did not occur in under 10 iterations: 1. T_TILDA_ERROR < T_TILDA_DESIRED (EPS_U) *	ALARM_A ALARM_KILL EPS_U (ILOAD V96U7515C) N_MAX_ITER (ILOAD V96U7790C) GWY_LAMBERT_ALARM_REQ CGZB_ALARM_KILL CGZV_EPS_U (ILOAD) CGZV_N_MAX (ILOAD)

* The U_STEP exit was deleted by CR 90974A (Orbit Targeting Lambert Iteration Loop Exit Logic Correction) on OI-26A.

At LOAD (ITEM 22) and during Lambert Cyclic Guidance (TIG - 15 seconds through MM 201 PRO), a TGT ΔT or TGT ITER alarm could be annunciated by the Lambert task. During Cyclic Guidance, a Lambert solution (using targeting parameters computed during the previous targeting via ORBIT TGT) is computed every 3.84 seconds to determine a “tweak” to the displayed LVLH and body axis ΔVs on MNVR EXEC. If a TGT ΔT or TGT ITER alarm occurs, a ΔV “tweak” is not computed. Guidance mode will remain LAMBERT, and the displayed ΔVs will continue to be decremented based on the IMU sensed accumulated velocity counts.

2021 / /	ORBIT	MNVR EXEC	1 001 / 14 :25 :13
OMS BOTH 1			000 / 00 :00 :00
L 2 *	BURN ATT		
R 3	24 R 076		ΔVTOT 8 .2
RCS SEL 4	25 P 144		TGO 0 :10
5 TV ROLL 0	26 Y 354		VGO X + 7 .68
TRIM LOAD	MNVR 27 AUTO		Y + 1 .37
6 P [-]0 .1	REI		Z + 2 .61
7 LY [+5 .2	TTP 44 :28		
8 RY [+5 .2	GMBL	HA HP	
9 WT 243836	L R	TGT 209 +200	
10 TIG	P - 0 .3 - 0 .3	CUR 209 +196	
1 / 14 :25 :13 .0	Y + 5 .1 - 5 .1		
TGT PEG 4			
14 C1	PRI 28 * 29 *	35 ABORT TGT	
15 C2 [] -	SEC 30 31		
16 HT -	OFF 32 33	FWD RCS	
17 θ T -	GMBL CK 34	ARM 36	
18 PRPLT []	LAMBERT	DUMP 37	
TGT PEG 7		OFF 38 *	
19 ΔVX [+] 8_-3		SURF DRIVE	
20 ΔVY [-] 0_-4		ON 39	
21 ΔVZ [-] 0_-2		OFF 40 *	
LOAD 22 / TIMER 23			
TGT ITER	1	14 :25 :09	
EXEC			

Alarms During Clohessy-Wiltshire and Orthogonal Braking Targeting (Orbit Targeting Display)

Note: CW and Orthogonal Braking are not normally executed.
Alarms are included "for the record."

Alarm	Targeting	FSSR Task/ FSW Module	Cause	Related FSSR/FSW Parameters
TGT ΔT PRED MATCH = 999999	Orthogonal Braking: Lambert or Clohessy- Wiltshire	OMEGA_DT _COMP GWH_ORB_T GT_OMEGA_ DT_COMP*	Transfer time for orthogonal braking could not be found in under 10 iterations.	ALARM_D, ALARM_KILL IC_MAX (ILOAD V96U7517C) CGZB_ORB_TGT_SFFAIL CGZB_TARGETING_TGT_DT_ALARM CGZB_ALARM_KILL CGZV_ICMAX (ILOAD)
	Clohessy- Wiltshire**	OFFSET_TGT GWM_ORB TGT_OFFSET _TGT	1/K < EP_TRANSFER: protects from the roots of the equation $8 - 8\cos(\omega t) - 3\omega t \sin(\omega t)$. Roots at $2\pi n$ ($n = 0, 1, 2, 3, \dots$) and 506.42, 880.31, 1246.02, 1609.15, ... degrees. Roots approach $(2n+1)\pi$ as n approaches infinity.	ALARM_D, ALARM_KILL EP_TRANSFER (ILOAD V96U7514C) CGZB_TARGETING_TGT_DT_ALARM CGZB_ALARM_KILL CGZV_EP_TRANSFER (ILOAD)
TGT ITER	Clohessy- Wiltshire	PROX_TGT _SUP GWG_ORB_ TGT_SUP NON_LAMB	Difference between desired and predicted relative positions at T2 time has increased 2 iterations in a row.	ALARM_C, ERR, D_MISS1, D_MISS2 CALARM, CGZB_CW_SING_ALARM GWG_ERR, GWG_D_MISS1 GWG_D_MISS2
			1. A ΔV could not be found in under 10 iterations for which the miss distance is less than a computed tolerance. or 2. The change in ΔV for any 3 successive iterations out of the maximum of 10 was not less than 0.05 feet/second.	ALARM_C, ERR, I_LOW N_MAX_ITER (ILD V96U7790C) R_MAX R_TOL_CW (ILD V99U7446C) CALARM, CGZB_CW_SING_ALARM GWG_ERR, GWG_I_LOW, CGZV_N_MAX, GWG_R_MAX CGZV_R_TOL_CW

* SFFAIL is set to "ON" in the Newton Raphson Iteration Task (ITERV, GWQ_ORB_TGT_ITERV). OMEGA_DT_COMP then sets the transfer time alarm to "ON".

** During Lambert or CW targeted orthogonal braking, OFFSET_TGT (CW equations) will be called by OMEGA_DT_COMP. There are no targeting alarms for relative velocity null (T2) targeting.

8.19 Illegal Entries On The Orbit Targeting Display

This section illustrates the conditions under which ILLEGAL ENTRY messages will be annunciated on the ORBIT TGT display.



2021 / 034 /	ORBIT TGT	1 001 / 13 :01 :39 000 / 00 :00 :00	
MNVR	TIG	ΔV_x ΔV_y ΔV_z ΔV_t	
0 *	0 / 00 :00 :00	0 . 0 0 . 0 0 . 0 0 . 0	
		PRED MATCH = 0	
INPUTS		CONTROLS	
1	TGT NO	9	T2 TO T1 25
2	T1 TIG	1 / 13 :27 :31	LOAD 26
6	EL	00 . 00	COMPUTE T1 28
7	ΔX / DNRNG	[] 0 . 00	COMPUTE T2 29
8	ΔY	[] 0 . 00	
9	ΔZ / ΔH	[] 0 . 00	
10	$\Delta \dot{X}$	[] 0 . 00	
11	$\Delta \dot{Y}$	[] 0 . 00	
12	$\Delta \dot{Z}$	[] 0 . 00	
13	T2 TIG	0 / 00 :00 :00	ORBITER STATE
17	ΔT	[+] 57 . 7	218 / 19 :16 :25 . 934
18	ΔX	[+] 48 . 60	X - 14819 . 863
19	ΔY	[] 0 . 00	Y +13326 . 029
20	ΔZ	[+] 1 . 20	Z - 9737 . 765
21	BASE TIME	1 / 14 :25 :13	VX - 5 . 768653
			VY - 18 . 346425
			VZ - 16 . 251186
ILLEGAL ENTRY ITEM 28 EXEC			

Prior to the initiation of targeting computations, rendezvous navigation must be enabled (ITEM 1). Below is a REL NAV display prior to the initiation of rendezvous navigation.

2021/033/	REL NAV	1 001/13:01:07
RNDZ NAV ENA 1	SV UPDATE	000/00:00:00
KU ANT ENA 2	POS	AVG G ON 5*
MEAS ENA 3	VEL	
NAV		GPS
SV SEL 4	RR ATRK	STAT P 1σ DES
RNG	RNG 0.000↓	1 NI 31
		2 * 75 32
		3 NI 33
		SV TRANSFER
		FLTR MINUS PROP
		POS
		VEL
		FLTR TO PROP 8
NODE	0 P 0.0↓	PROP TO FLTR 9
	0 R 0.0↓	ORB TO TGT 10
		TGT TO ORB 11
FILTER		EDIT OVRD
S TRK 12*	RR 13 COAS 14	AUT INH FOR
STAT	X	17 18* 19
FLTR UPDATE 15	ORB Y	20 21* 22
COVAR REINIT 16		23 24* 25
RES ID	RATIO ACPT REJ	
RNG		42 43* 44
R		
V/ EL / Y		
H/ AZ / X		
GPS P + 0.19	0.4	
V + 0.27	0.3	

Once rendezvous navigation has been enabled, an asterisk will appear beside ITEM 1. Relative position and velocity data (all non-zero), along with the selected state vector (ITEM 4), will also be present. Prior to sensor (radar, star tracker or COAS) mark incorporation, zeros will appear under SV UPDATE, RESID, RATIO, MARK ACPT, REJ and FLTR MINUS PROP.

Rendezvous navigation can only be initialized once a target state vector uplink is performed.

2021/033/	REL NAV	1 001/13:01:09
RNDZ NAV ENA 1*	SV UPDATE	000/00:00:00
KU ANT ENA 2	POS 0.00	AVG G ON 5*
MEAS ENA 3	VEL 0.00	GPS
NAV		STAT P 1σ DES
SV SEL 4 PROP	RR ATRK	1 NI 31
RNG 246.287	RNG 0.000↓	2* 75 32
R + 1.31	R 0.00↓	3 NI 33
θ 239.14	EL 0.0↓	SV TRANSFER
Y - 0.16	AZ 0.0↓	FLTR MINUS PROP
Y + 0.4	ωP 0.0↓	POS 0.00
NODE 13:07:29	ωR 0.0↓	VEL 0.00
FILTER		FLTR TO PROP 8
S TRK 12* RR 13 COAS 14		PROP TO FLTR 9
STAT X		ORB TO TGT 10
FLTR UPDATE 15 ORB Y		TGT TO ORB 11
COVAR REINIT 16		EDIT OVRD
RES ID RATIO ACPT REJ		AUT INH FOR
RNG 0.00 0.0 0 0		17 18* 19
R 0.00 0.0 0 0		20 21* 22
V/ EL / Y 0.00 0.0 0 0		23 24* 25
H/ AZ/ X 0.00 0.0 0 0		42 43* 44
GPS P + 0.19 0.4		
V + 0.27 0.3		
ITEM 1 EXEC		

If an ITEM 28 or 29 is executed prior to rendezvous navigation initialization, an ILLEGAL ENTRY will result. No targeting computations will be performed.

2021 / 034 /	ORBIT TGT	1 001 / 13 : 01 : 39 000 / 00 : 00 : 00
MNVR	TIG	ΔV_x ΔV_y ΔV_z ΔV_t
0 *	0 / 00 : 00 : 00	0.0 0.0 0.0 0.0
		PRED MATCH = 0
INPUTS		CONTROLS
1 TGT NO		T2 TO T1 25
2 T1 TIG	1 / 13 : 27 : 31	LOAD 26
6 EL	00 . 00	COMPUTE T1 28
7 ΔX / DNRNG	[] 0.00	COMPUTE T2 29
8 ΔY	[] 0.00	
9 ΔZ / ΔH	[] 0.00	
10 $\Delta \dot{X}$	[] 0.00	
11 $\Delta \dot{Y}$	[] 0.00	
12 $\Delta \dot{Z}$	[] 0.00	
13 T2 TIG	0 / 00 : 00 : 00	ORB ITER STATE
17 ΔT	[+] 57 . 7	218 / 19 : 16 : 25 . 934
18 ΔX	[+] 48 . 60	X - 14819 . 863
19 ΔY	[] 0.00	Y +13326 . 029
20 ΔZ	[+] 1 . 20	Z - 9737 . 765
21 BASE TIME	1 / 14 : 25 : 13	VX - 5 . 768653
		VY - 18 . 346425
		VZ - 16 . 251186
→ ILLEGAL ENTRY ITEM 28 EXEC		

If any ORBIT TGT item entries are made while targeting (ITEM 28 or 29) is in progress, an illegal entry message will result. There will be no impact on targeting.

An “ITEM 1+9 EXEC” is shown as an example.

2021 / 034 /	ORBIT TGT	1 001 / 13 :01 :39 000 / 00 :00 :00
MNVR	TIG	ΔV_x ΔV_y ΔV_z ΔV_t
0 *	0 / 00 :00 :00	0 . 0 0 . 0 0 . 0 0 . 0
PRED MATCH = 0		
INPUTS		CONTROLS
1 TGT NO	9	T2 TO T1 25
2 T1 TIG	1 / 13 :27 :31	LOAD 26
6 EL	00 . 00	COMPUTE T1 28*
7 ΔX / DNRNG	[] 0 . 00	COMPUTE T2 29
8 ΔY	[] 0 . 00	
9 ΔZ / ΔH	[] 0 . 00	
10 $\Delta \dot{X}$	[] 0 . 00	
11 $\Delta \dot{Y}$	[] 0 . 00	
12 $\Delta \dot{Z}$	[] 0 . 00	
13 T2 TIG	0 / 00 :00 :00	ORB ITER STATE
17 ΔT	[+] 57 . 7	218 / 19 :16 :25 . 934
18 ΔX	[-] 48 . 60	X - 14819 . 863
19 ΔY	[] 0 . 00	Y + 13326 . 029
20 ΔZ	[+] 1 . 20	Z - 9737 . 765
21 BASE TIME	1 / 14 :25 :13	VX - 5 . 768653 VY - 18 . 346425 VZ - 16 . 251186
ILLEGAL ENTRY ITEM 1+9 EXEC		

If an attempt is made to enter data for any of ITEMS 2 through 20 while target set 0 is up, an illegal entry message will result.

An update to T1 TIG is shown as an example.

2021 / 034 /	ORBIT TGT	1 001 / 13 :01 :39 000 / 00 :00 :00
MNVR	TIG	ΔV_X ΔV_Y ΔV_Z ΔV_T
0 *	0 / 00 :00 :00	0 .0 0 .0 0 .0 0 .0
		PRED MATCH = 0
INPUTS		
1 TGT NO	0	CONTROLS
2 T1 TIG	0 / 00 :00 :00	T2 TO T1 25
6 EL	00 .00	LOAD 26
7 ΔX / DNRNG	[] 0 .00	COMPUTE T1 28
8 ΔY	[] 0 .00	COMPUTE T2 29
9 ΔZ / ΔH	[] 0 .00	
10 ΔX	[] 0 .00	
11 ΔY	[] 0 .00	
12 ΔZ	[] 0 .00	
13 T2 TIG	0 / 00 :00 :00	ORBITER STATE
17 ΔT	[] 00 .0	218 / 19 :16 :25 .934
18 ΔX	[] 0 .00	X - 14819 .863
19 ΔY	[] 0 .00	Y +13326 .029
20 ΔZ	[] 0 .00	Z - 9737 .765
21 BASE TIME	0 / 00 :00 :00	VX - 5 .768653
		VY - 18 .346425
		VZ - 16 .251186
ILLEGAL ENTRY		
ITEM 2+4 EXEC		

Targeting (ITEM 28 or 29) cannot be requested for target set 0.

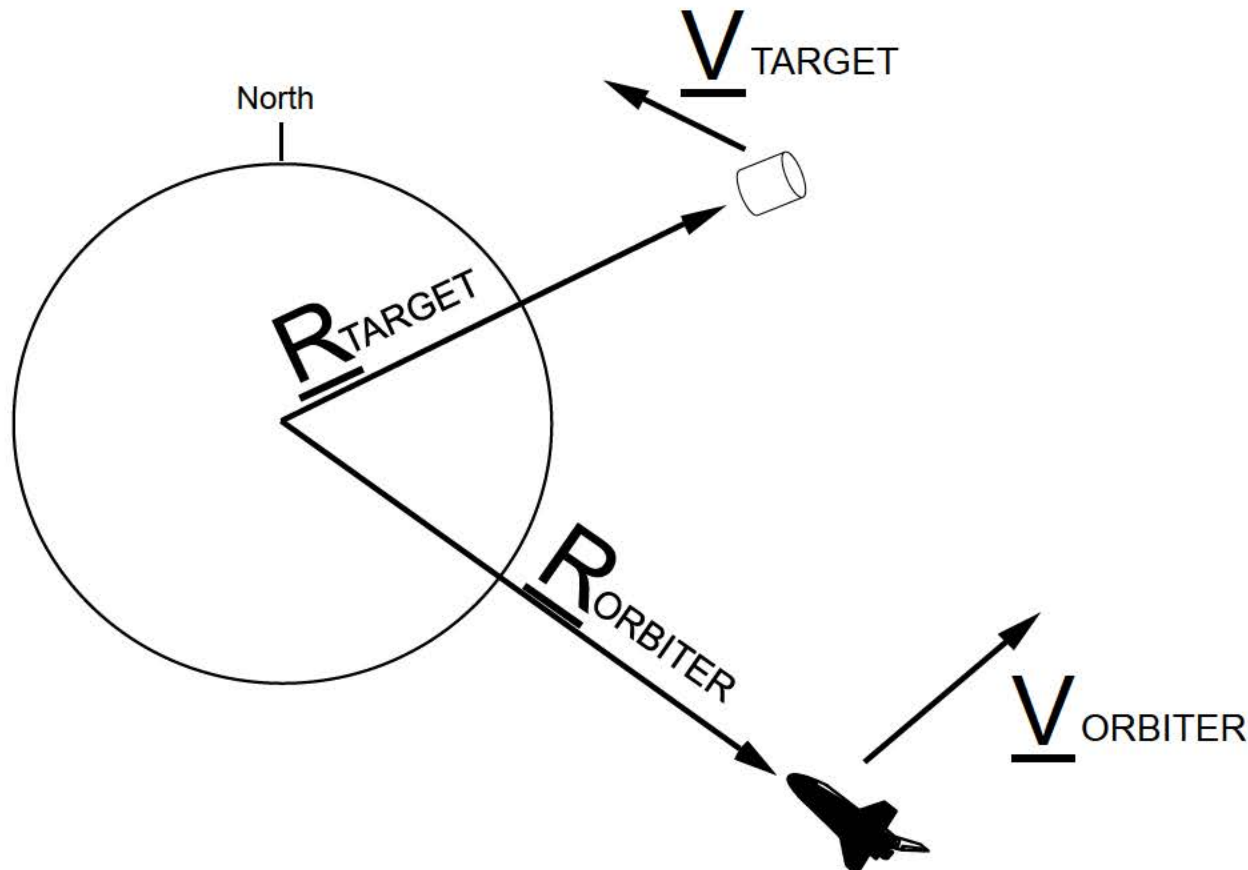
2021 / 034 /		ORBIT	TGT	1 001 / 13 :01 :39 000 / 00 :00 :00
MNVR	TIG	ΔV_x	ΔV_y	ΔV_z
0 *	0 / 00 :00 :00	0 . 0	0 . 0	0 . 0
		PRED	MATCH =	0
INPUTS				CONTROLS
1	TGT NO	0		
2	T1 TIG	0 / 00 :00 :00		T2 TO T1 25
6	EL	00 . 00		LOAD 26
7	ΔX / DNRNG	[] 0 . 00		COMPUTE T1 28
8	ΔY	[] 0 . 00		COMPUTE T2 29
9	ΔZ / ΔH	[] 0 . 00		
10	ΔX	[] 0 . 00		
11	ΔY	[] 0 . 00		
12	ΔZ	[] 0 . 00		
13	T2 TIG	0 / 00 :00 :00		ORBITER STATE
17	ΔT	[] 00 . 0		218 / 19 :16 :25 . 934
18	ΔX	[] 0 . 00		X - 14819 . 863
19	ΔY	[] 0 . 00		Y +13326 . 029
20	ΔZ	[] 0 . 00		Z - 9737 . 765
21	BASE TIME	0 / 00 :00 :00		VX - 5 . 768653
				VY - 18 . 346425
				VZ - 16 . 251186
ILLEGAL ENTRY				
ITEM 28 EXEC				

A LOAD (ITEM 26) cannot be performed if a BASE TIME (ITEMS 21 through 24) has not been entered.

2021 / 034 /	ORBIT TGT	1 001 / 13 :01 :39 000 / 00 :00 :00
MNVR	TIG	ΔV_x ΔV_y ΔV_z ΔV_t
0 *	0 / 00 :00 :00	0 . 0 0 . 0 0 . 0 0 . 0
		PRED MATCH = 0
INPUTS		
1 TGT NO	0	
2 T1 TIG	0 / 00 :00 :00	
6 EL	00 . 00	
7 ΔX / DNRNG	[]	0 . 00
8 ΔY	[]	0 . 00
9 ΔZ / ΔH	[]	0 . 00
10 $\Delta \dot{X}$	[]	0 . 00
11 $\Delta \dot{Y}$	[]	0 . 00
12 $\Delta \dot{Z}$	[]	0 . 00
13 T2 TIG	0 / 00 :00 :00	
17 ΔT	[]	00 . 0
18 ΔX	[]	0 . 00
19 ΔY	[]	0 . 00
20 ΔZ	[]	0 . 00
21 BASE TIME	0 / 00 :00 :00	
ILLEGAL ENTRY ITEM 26 EXEC		
CONTROLS		
T2 TO T1 25		
LOAD 26		
COMPUTE T1 28		
COMPUTE T2 29		
ORBITER STATE		
218 / 19 :16 :25 . 934		
X - 14819 . 863		
Y +13326 . 029		
Z - 9737 . 765		
VX - 5 . 768653		
VY - 18 . 346425		
VZ - 16 . 251186		

9.0 Rendezvous Navigation

To facilitate on-board targeting of burns and pointing of navigation sensors at the TARGET, the on-board computers must maintain an estimate of ORBITER and TARGET position and velocity. These estimates are known as state vectors and are maintained by the navigation Flight Software.

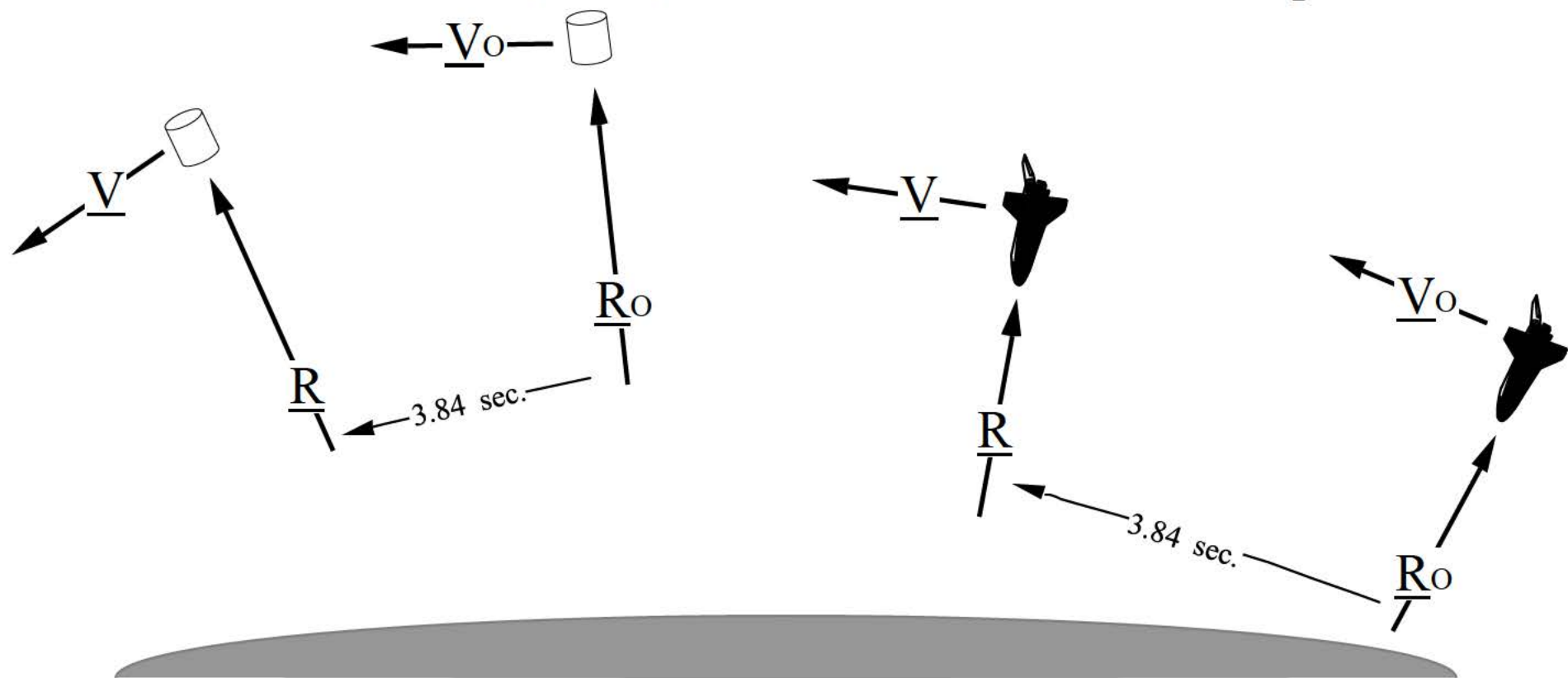


9.1 State Vector Propagation

An algorithm known as “SUPER_G” maintains the ORBITER and TARGET state vectors. Every 3.84 seconds, the previous state vectors are propagated to the current time.

$$*\underline{\dot{R}} = \underline{R}_o + \underline{\dot{R}}_o \Delta T + \frac{\underline{\ddot{R}}_o \Delta T^2}{2} + \frac{\underline{\ddot{\dot{R}}}_o \Delta T^3}{3}$$

$$*\underline{\dot{V}} = \underline{V}_o + \underline{\dot{V}}_o \Delta T + \frac{\underline{\ddot{V}}_o \Delta T^2}{2}$$

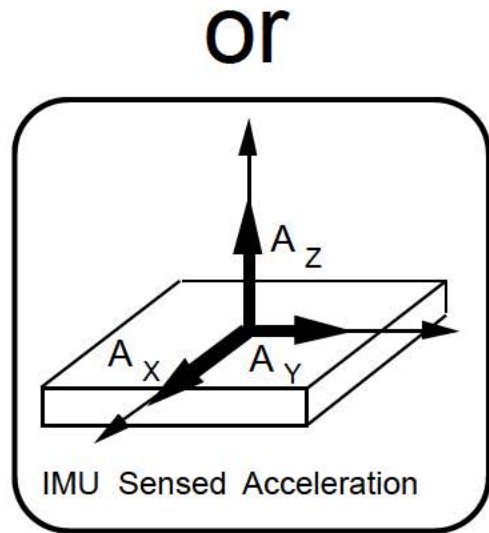
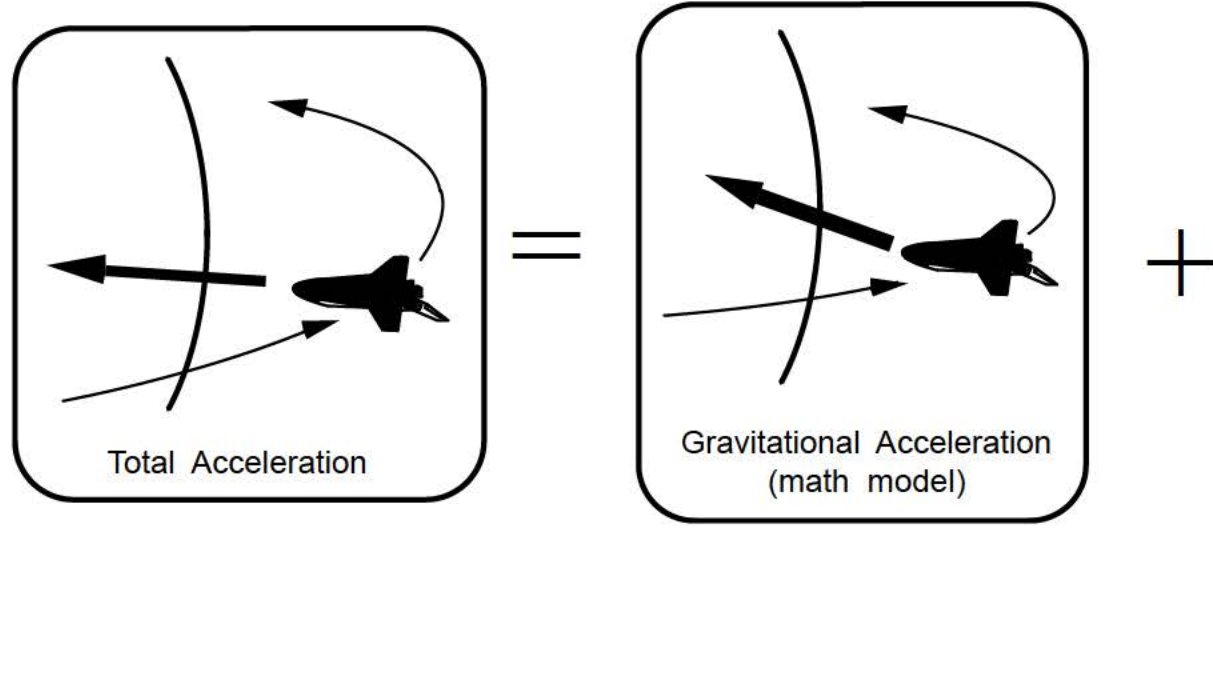
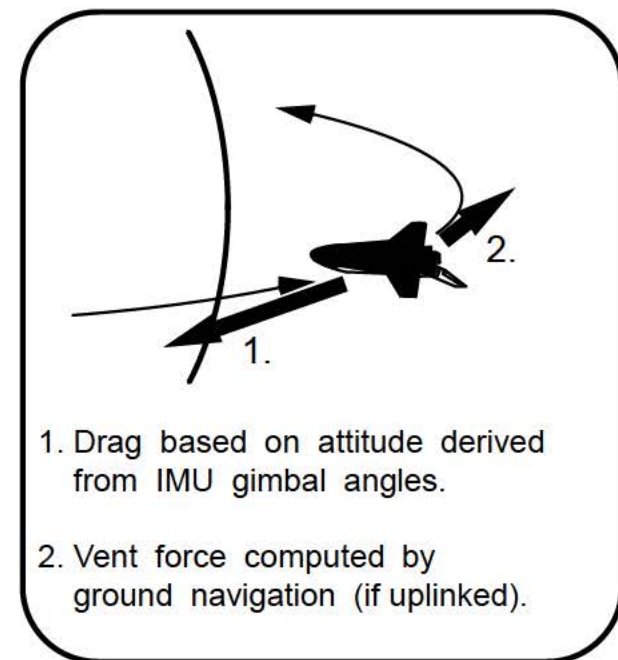


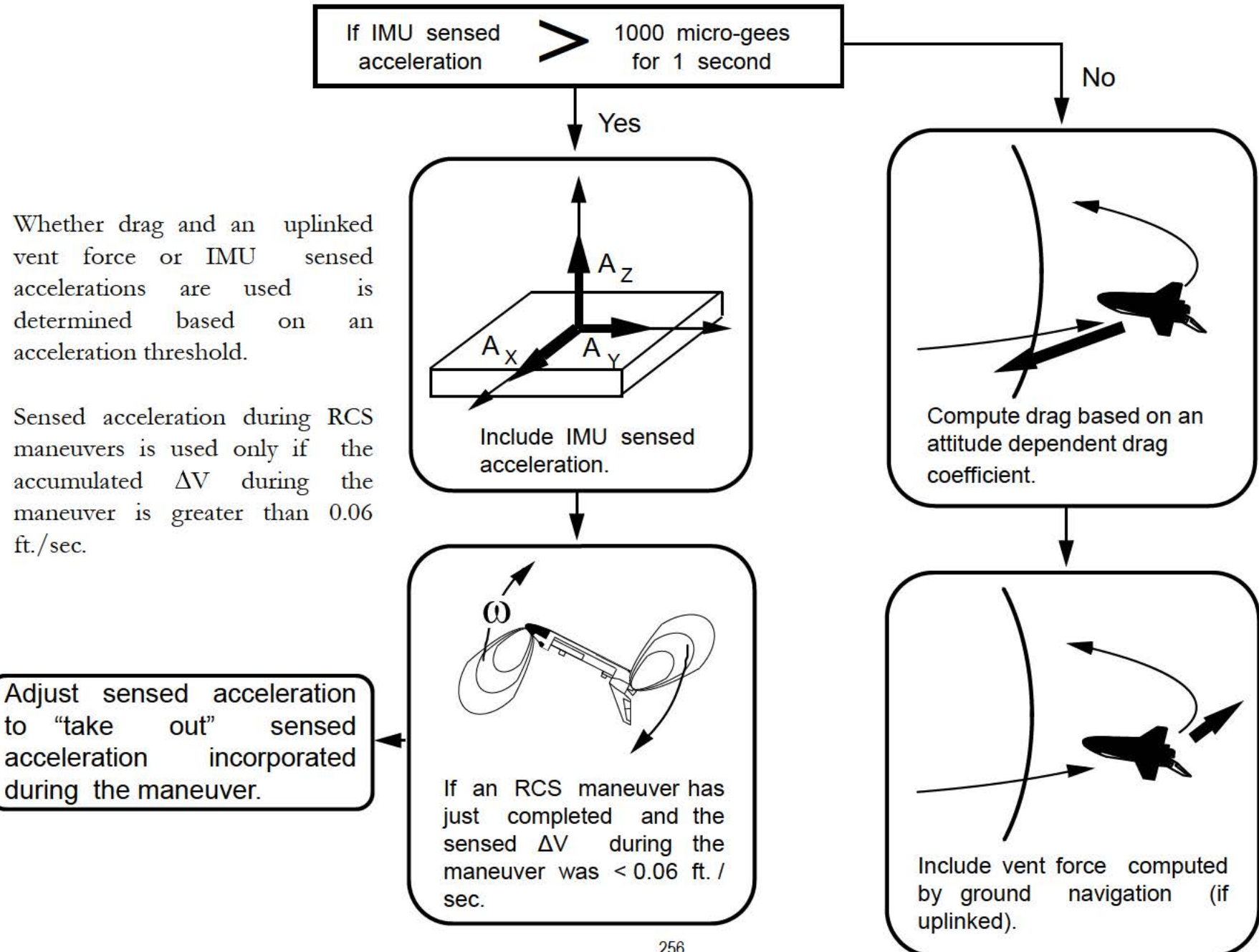
* Note: These are the starting equations for the derivation of the SUPER_G algorithm. The highest order terms (often called the "jerk terms") do not appear explicitly in the Flight Software. They are approximated in the derivation by determining the change in acceleration over the last navigation cycle (3.84 seconds).

Accelerations used in propagation of the ORBITER state vector include gravitational acceleration, atmospheric drag, a ground navigation computed vent force, and sensed acceleration from the IMUs.

If IMU sensed acceleration is used, the drag and vent forces are not used.

A vent force is computed by ground navigation based on radar and TDRS tracking of the ORBITER. The force is used to compensate for unmodeled accelerations and RCS translational acceleration not detected by the IMUs.





2011 / 021 /	IMU ALIGN			1 006 / 22 :39 :35
IMU				000 / 00 :00 :00
	1	2	3	
STAT	OK	OK	OK	ALIGN ENA
TEMP	21	22	23	IMU 1 10* REF STAR 13*
STBY				2 11* IMU 14
OPER	4*	5*	6*	3 12* TYPE 15 TORQUE
DES	7	8	9	
				EXEC 16*
ACC				TERM 17
	1	2	3 X	
X	+0 .00	+0 .03	-0 .01	IMU BITE MASK
Y	+0 .02	+0 .00	+0 .02	1 0000 24
Z	-0 .00	-0 .00	-0 .01	2 0000 25
				3 0000 26
ANG				
	1	2	3	
X	16 .47	16 .65	16 .72	NAV ΔV THRESH
Y	284 .33	284 .31	284 .31	18 3840
Z	186 .56	186 .29	186 .32	
ΔX	+ 0 .04	- 0 .04	+ 0 .03	MM READ 19X
ΔY	+ 0 .03	- 0 .04	+ 0 .04	
ΔZ	+ 0 .04	- 0 .04	+ 0 .03	
ITEM 16 EXEC				

Note: OI-32 Display Format

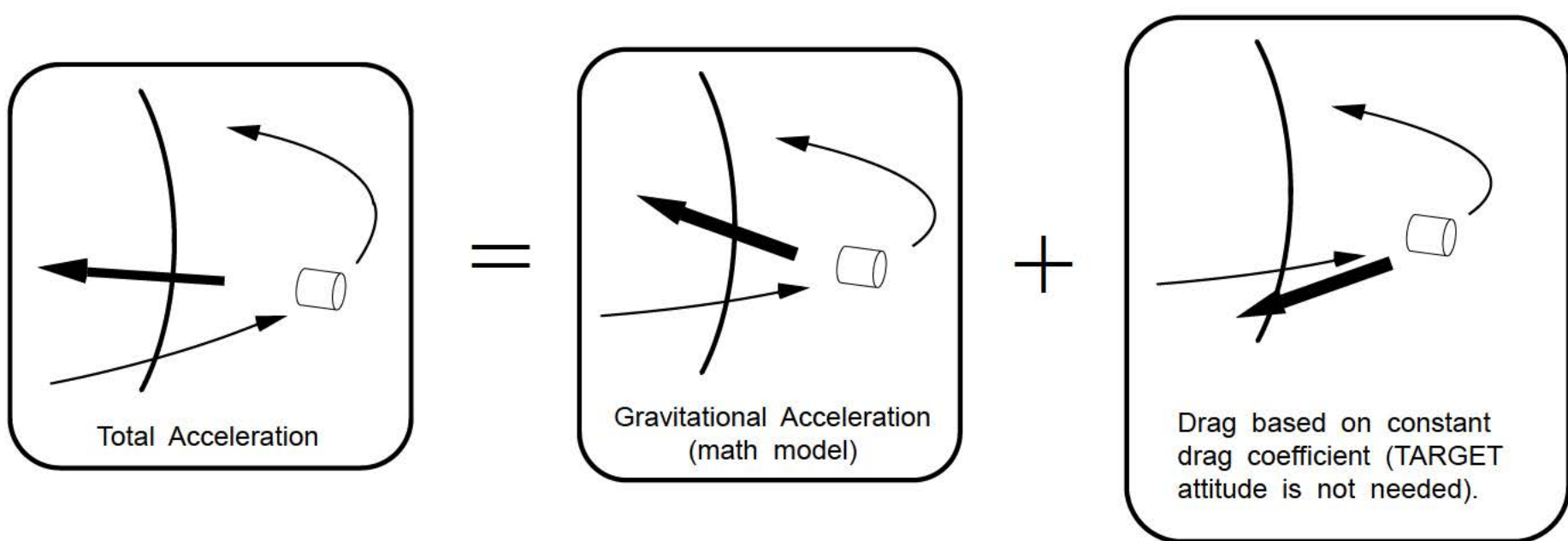
$$\frac{1000 \text{ micro-gees}}{\text{second}} \times 3.84 \text{ seconds} = 3840 \text{ micro-gees}$$

Since the state vector propagation software (SUPER_G) runs every 3.84 seconds, it does not check the IMU sensed acceleration every second.

Rather than comparing the sensed acceleration against the 1000 micro-gees/second threshold, it uses a threshold that takes into account the execution rate of SUPER_G.

The adjusted acceleration threshold is displayed on the IMU ALIGN display (SPEC 21). It can be changed by the crew via this display.

TARGET acceleration is computed based on math models. No external sensor data is used.



The drag vector (\mathbf{D}) is computed using drag coefficient (C_D), atmospheric density (ρ), area (A), Earth relative velocity vector (\mathbf{V}_{REL}), and the vehicle mass (M).

$$\mathbf{D} = -\frac{1}{2} \frac{C_D K_{FACTOR} \rho A |\mathbf{V}_{REL}|}{M} \mathbf{V}_{REL}$$

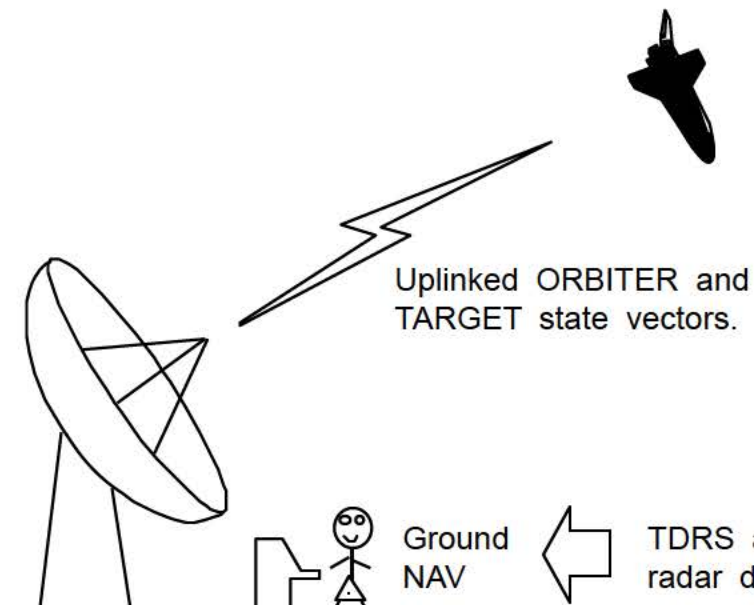
An additional parameter, the K_{FACTOR} , is included to permit adjustment of the drag computation due to uncertainties in mass, area, drag coefficient, or atmospheric density. The K_{FACTOR} is ILOADed at 1.0, but alternate values for either the ORBITER or TARGET can be determined on the ground and uplinked by Mission Control.

Drag computation for TARGET state vector propagation and precision prediction will use the K_{FACTOR} . However, ORBITER K_{FACTOR} is only used during state vector propagation.

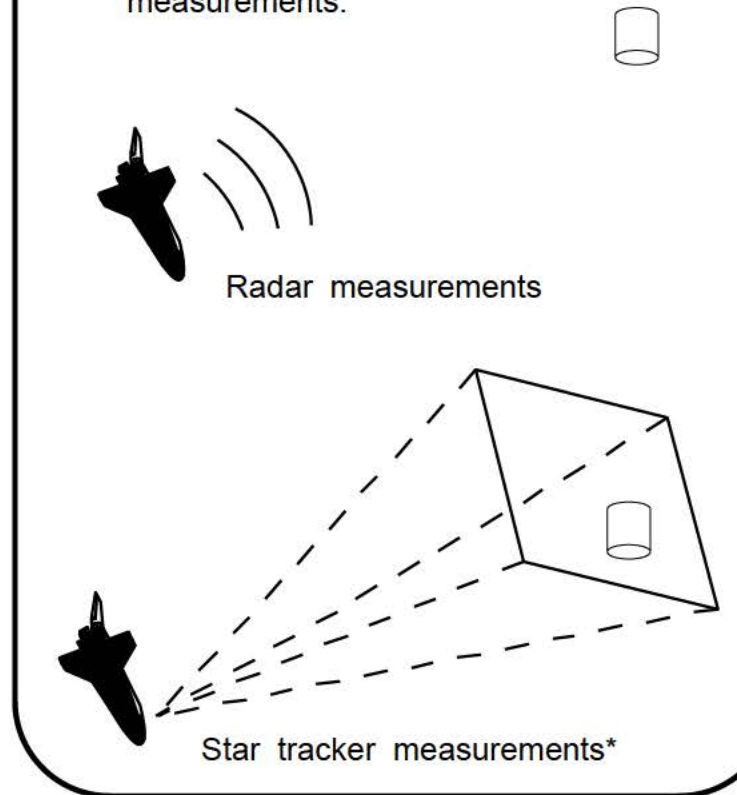
9.2 State Updates and Sensor Measurement Residuals

In order for the crew to compute on-board targeted burns, a more accurate estimate of ORBITER position and velocity relative to the TARGET is needed than can be provided by ground tracking. A more accurate estimate of relative position and velocity is obtained through the use of navigation sensors on the ORBITER.

1. Ground navigation supplies on-board navigation with an ORBITER and a TARGET state vector.



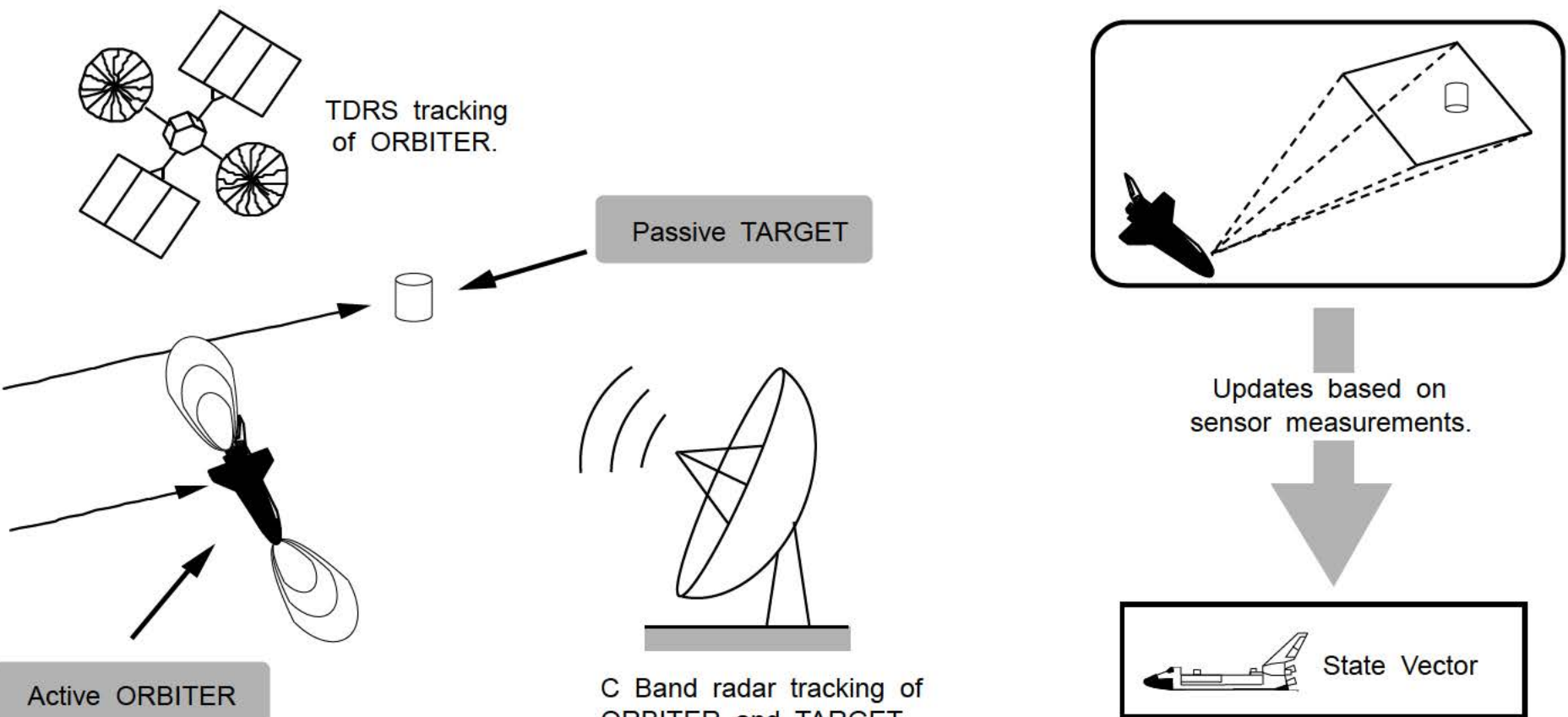
2. Estimate of relative position and velocity is improved via sensor measurements.



* A third sensor, the Crew Optical Alignment Sight (COAS), is available but is not normally used.

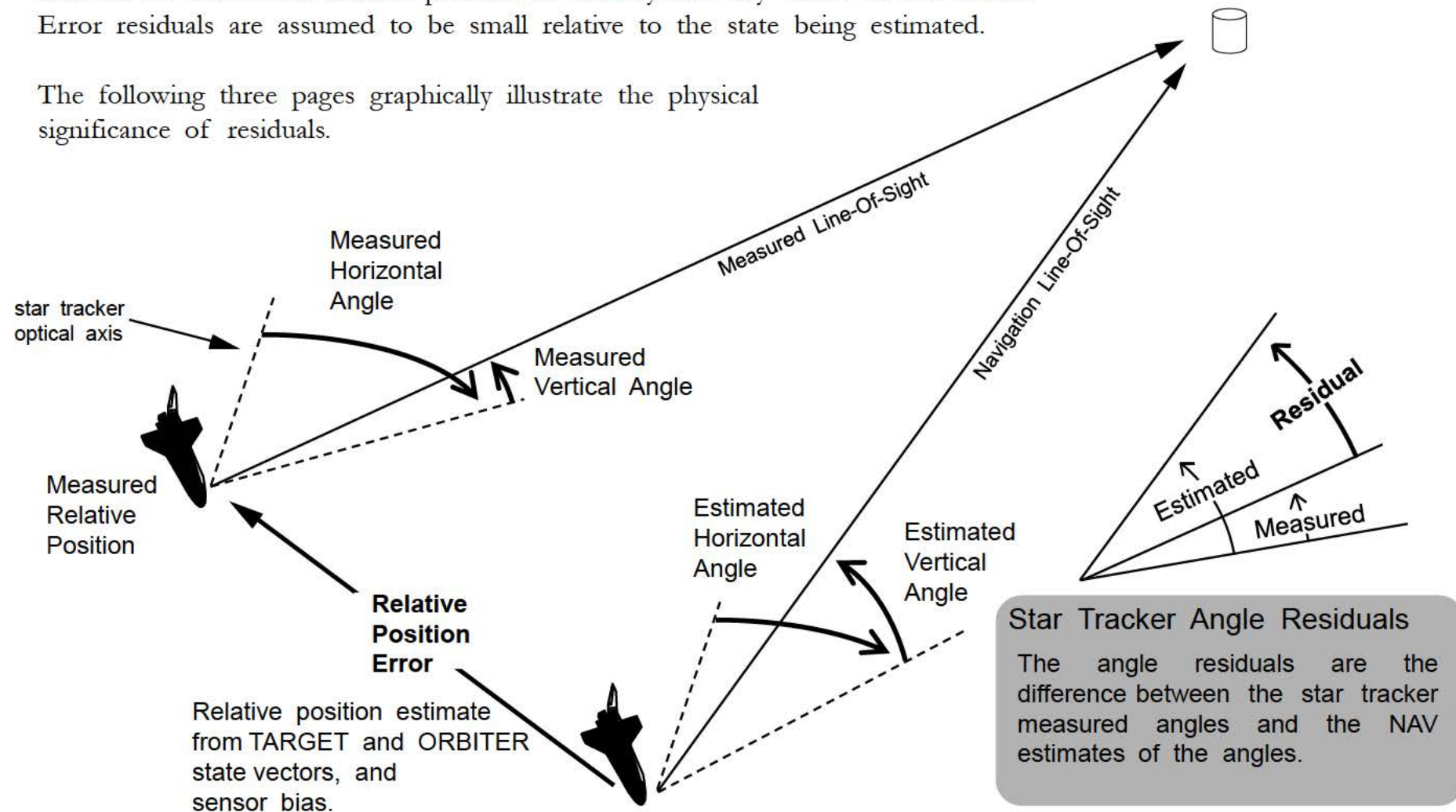
During rendezvous, the ORBITER and the TARGET are tracked by ground radars and the Tracking and Data Relay Satellite (TDRS). The ORBITER executes maneuvers which change its orbit. The TARGET typically does not do any maneuvering which may change its orbit during the on-board targeted phase. For this reason, the ground tracking estimate of TARGET position and velocity is considered to be more accurate than the ORBITER estimate of position and velocity.

Since the ORBITER state is assumed to be less accurate than the TARGET state, sensor measurements are applied to the ORBITER state vector based on the measured relative state with respect to the TARGET.



A residual is the difference between a sensor measurement and the navigation estimate of what the measurement should be. The NAV estimate is computed from the ORBITER and TARGET state vectors and sensor bias. A residual results from the error in the NAV estimate of ORBITER relative position or velocity and any errors in the sensor. Error residuals are assumed to be small relative to the state being estimated.

The following three pages graphically illustrate the physical significance of residuals.



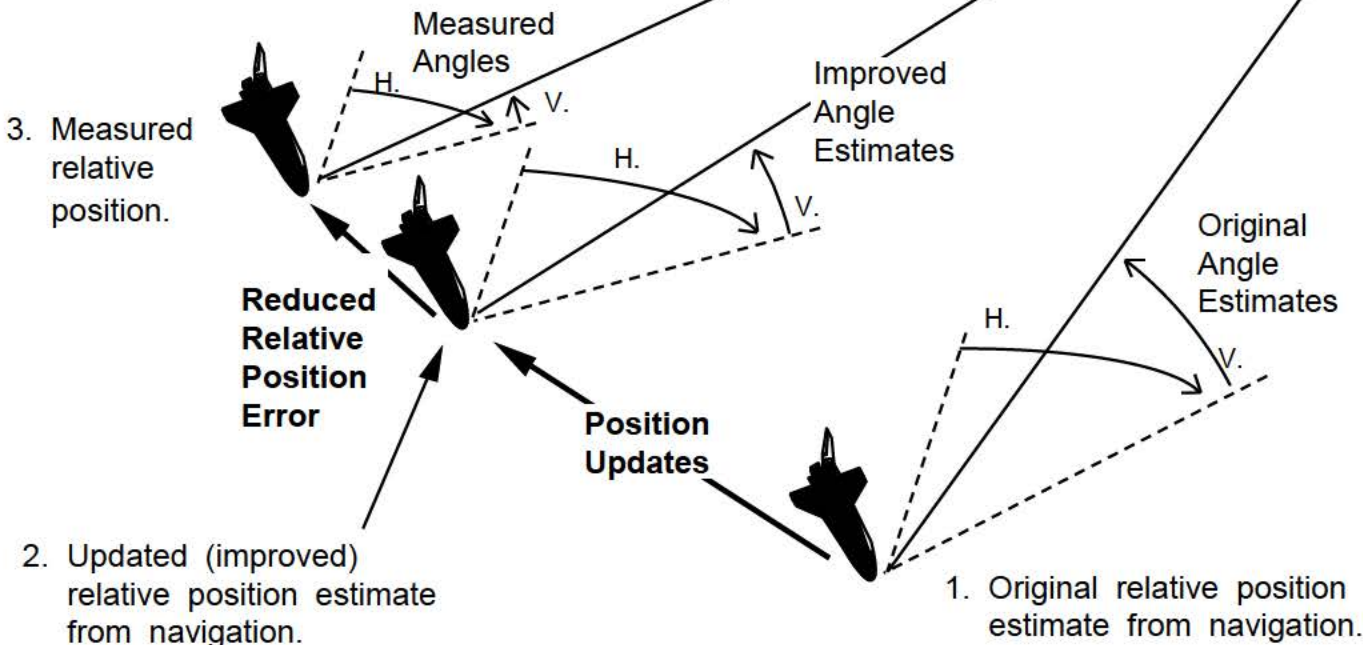
Star Tracker Angle Residuals During Pass

While star tracker measurements are incorporated, the NAV estimate of ORBITER relative position (with respect to the TARGET) will gradually approach the measured position. The updates work to reduce the relative position error. As a result, the navigation estimates of vertical (V) and horizontal (H) angles will begin to converge on the measured values.

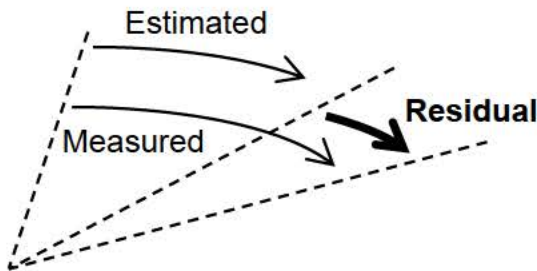


Star Tracker	Angular Meas.	Angular Meas. W/R to Orbit Plane
-Z	H V	In-plane Out-of-plane
-Y	H V	Out-of-plane In-plane

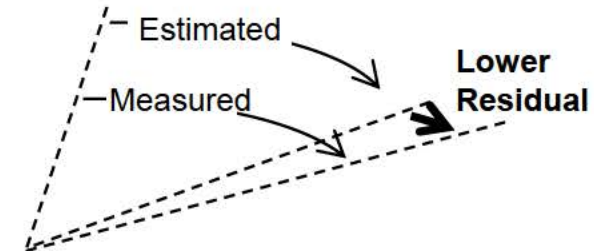
This table assumes nominal -Z or -Y star tracking attitude. -Z is illustrated on this page. The -Z star tracker boresight is offset from the Orbiter -Z body axis by 3°.



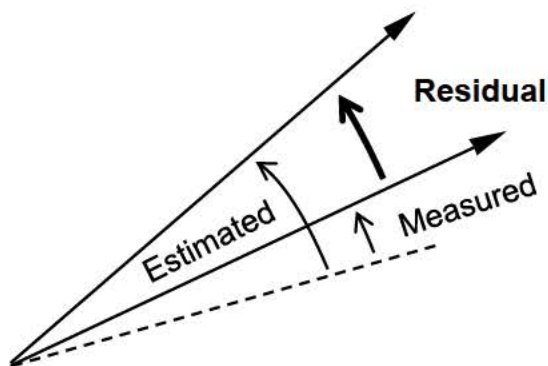
As the navigation estimates of vertical and horizontal angles converge to the measured values, the residual for each angle will decrease.



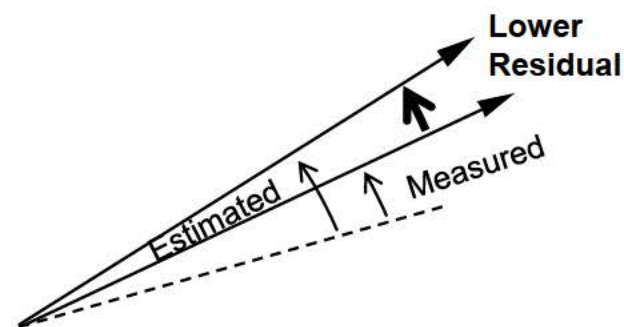
1. Horizontal residuals prior to incorporation of sensor measurements.



2. Horizontal residuals after incorporation of sensor measurements.



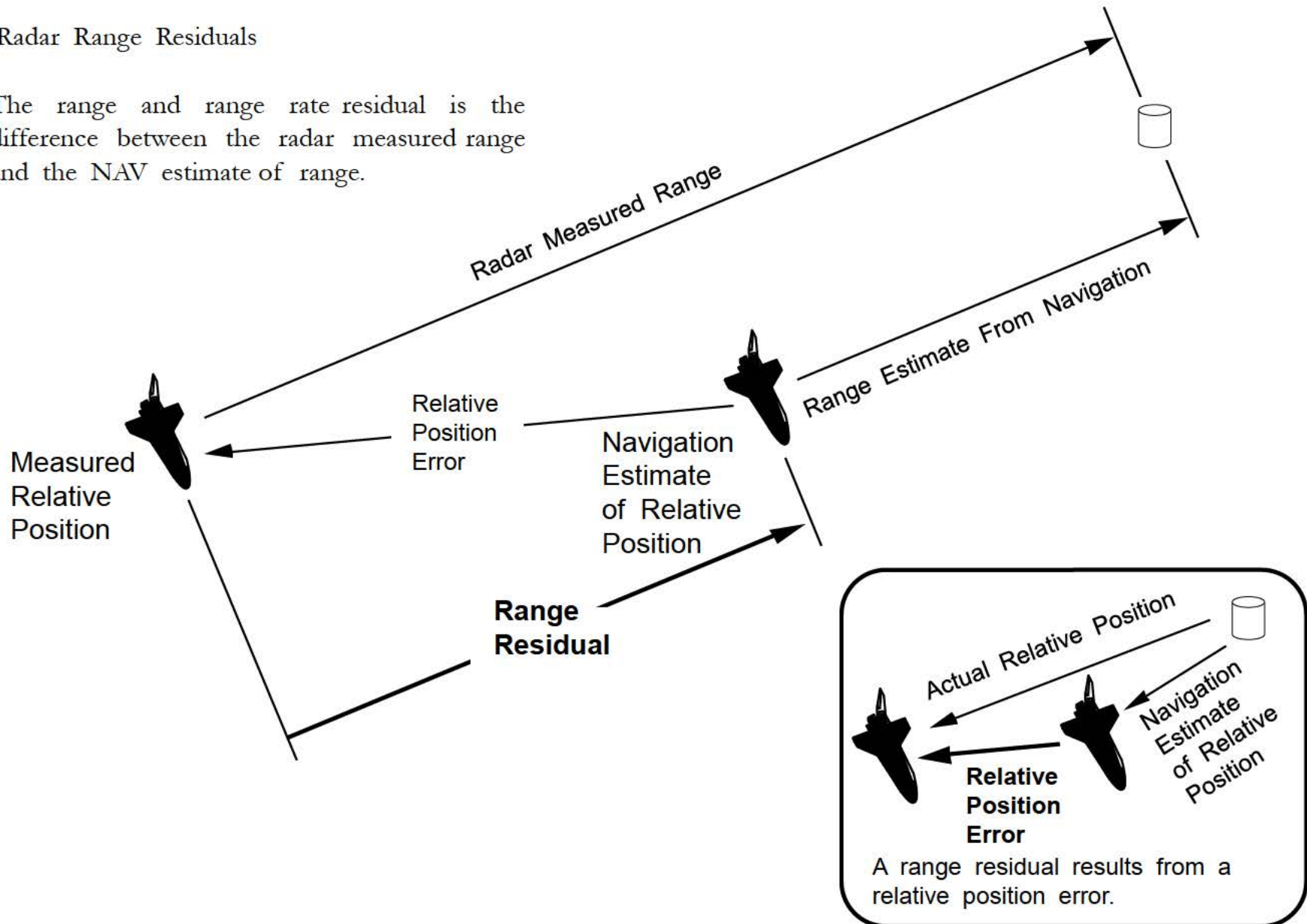
1. Vertical residuals prior to incorporation of sensor measurements.



2. Vertical residuals after incorporation of sensor measurements.

Radar Range Residuals

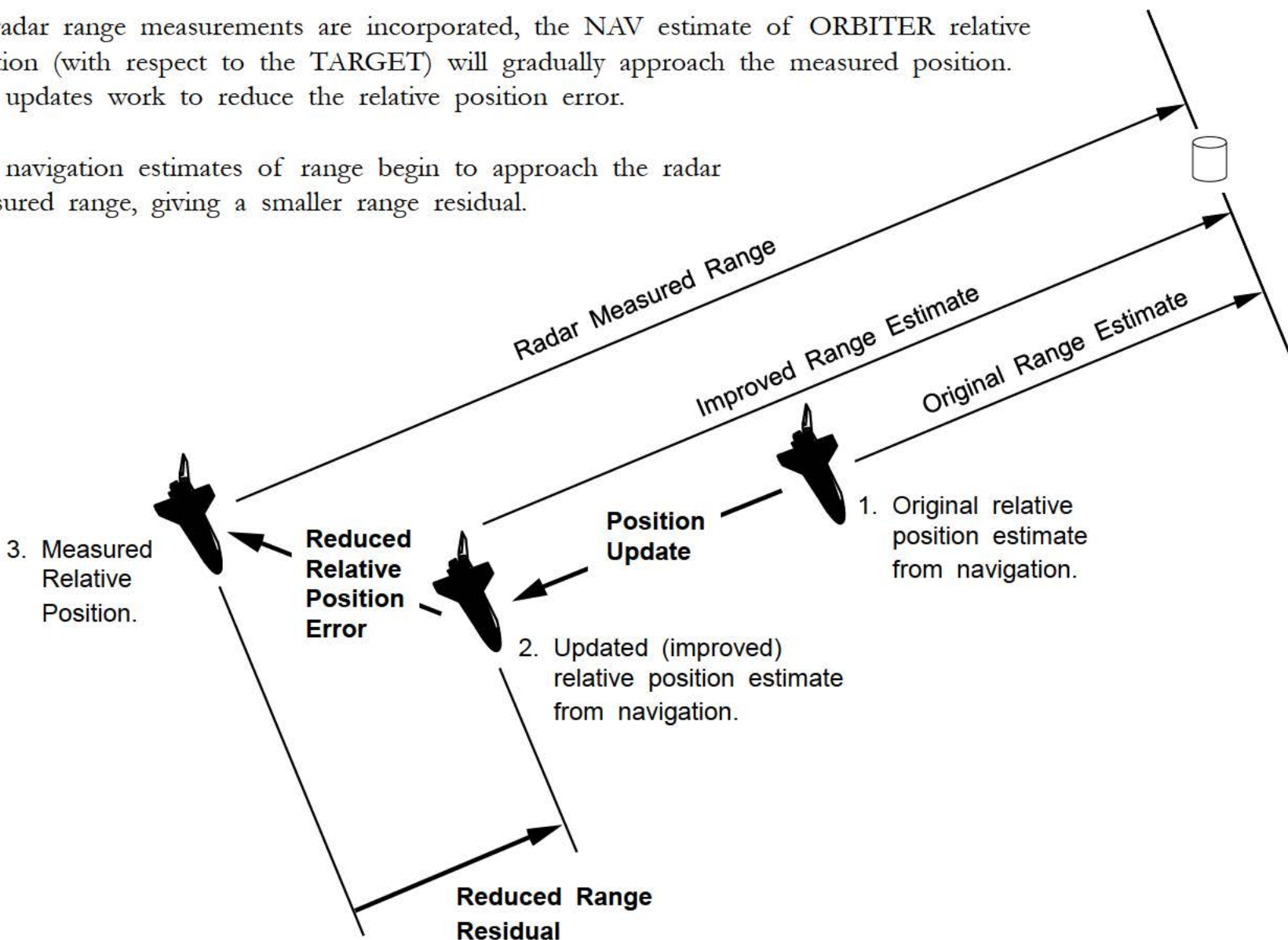
The range and range rate residual is the difference between the radar measured range and the NAV estimate of range.



Radar Range Residuals During Pass

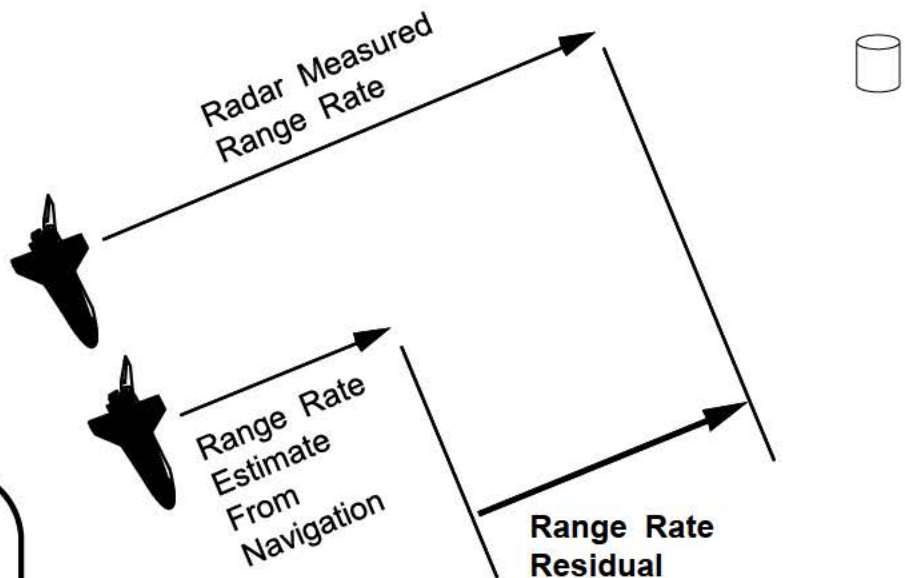
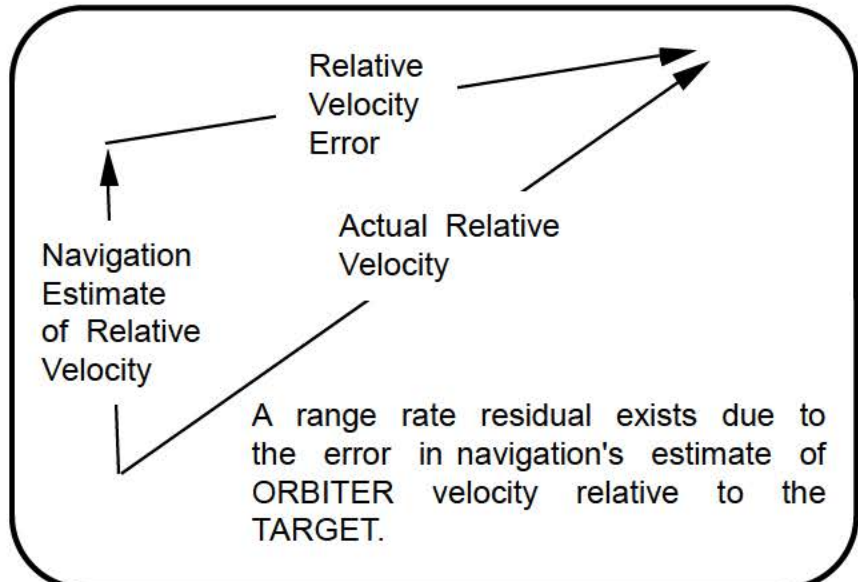
As radar range measurements are incorporated, the NAV estimate of ORBITER relative position (with respect to the TARGET) will gradually approach the measured position. The updates work to reduce the relative position error.

The navigation estimates of range begin to approach the radar measured range, giving a smaller range residual.

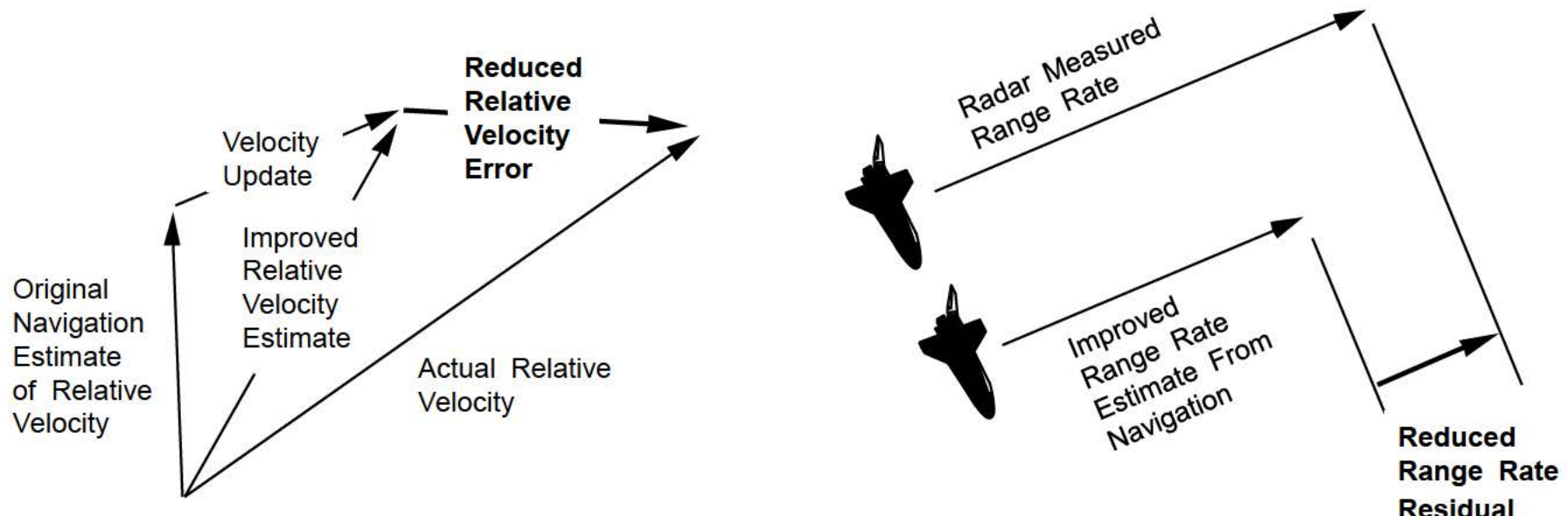


Radar Range Rate Residual

The range rate residual is the difference between the radar measured range rate and the NAV estimate of range rate.

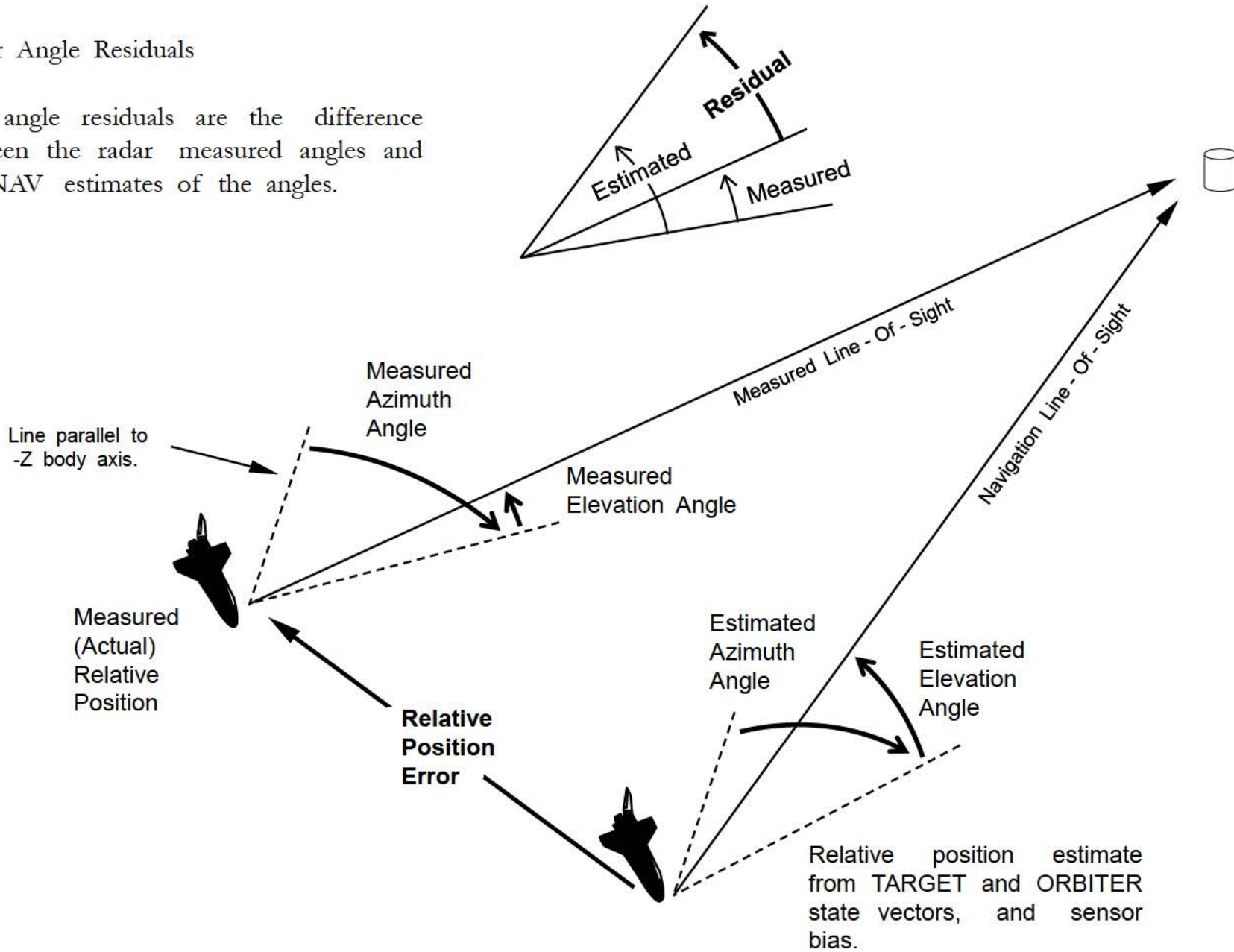


Velocity update improves navigation's estimate of relative velocity with respect to the TARGET. This reduces the relative velocity error and the range rate residual.



Radar Angle Residuals

The angle residuals are the difference between the radar measured angles and the NAV estimates of the angles.



Radar Angle Residuals During Pass

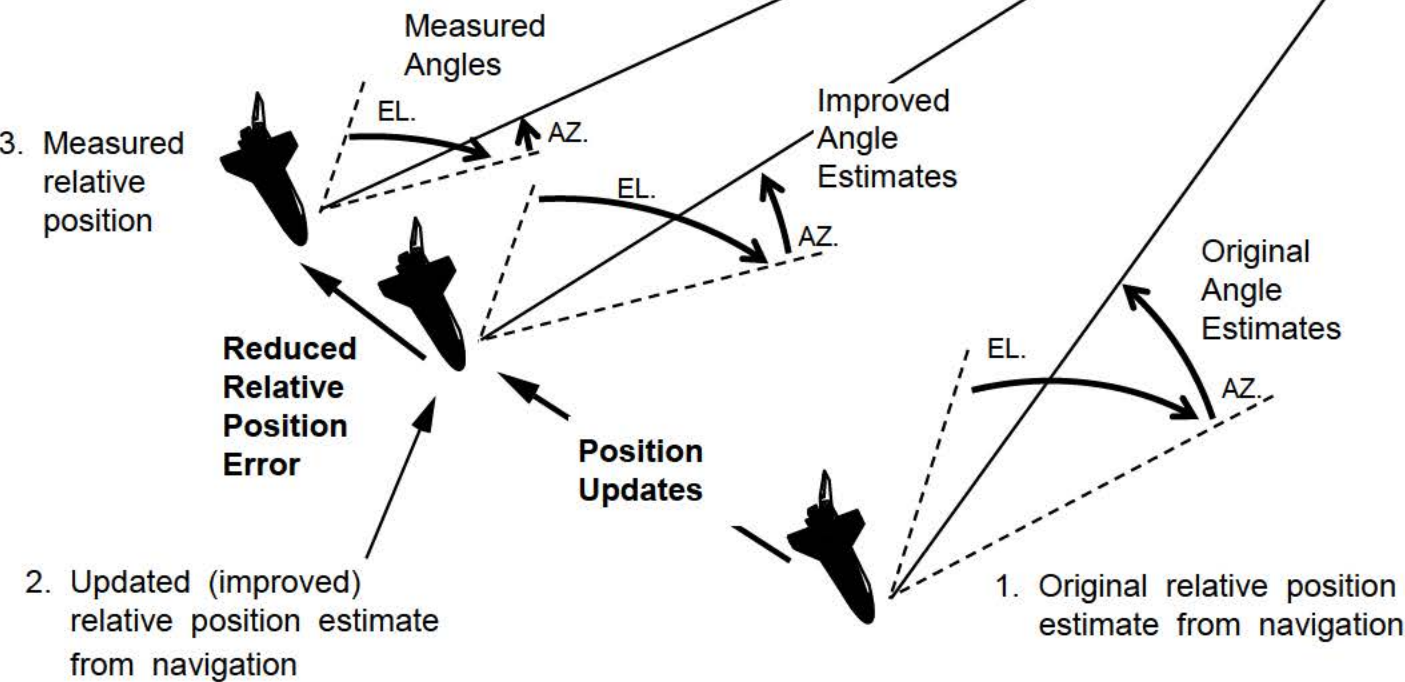
While radar measurements are incorporated, the NAV estimate of ORBITER relative position (with respect to the TARGET) will gradually approach the measured position.

The updates work to reduce the relative position error.

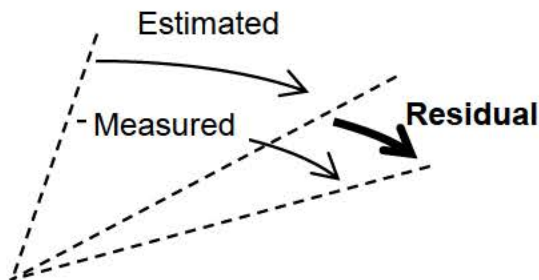
As a result, the navigation estimates of elevation and azimuth will begin to converge on the measured values.



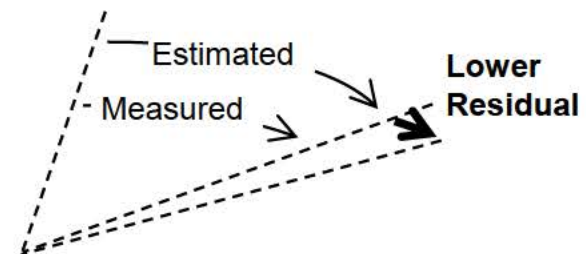
AZ. - Azimuth Angle
EL. - Elevation Angle



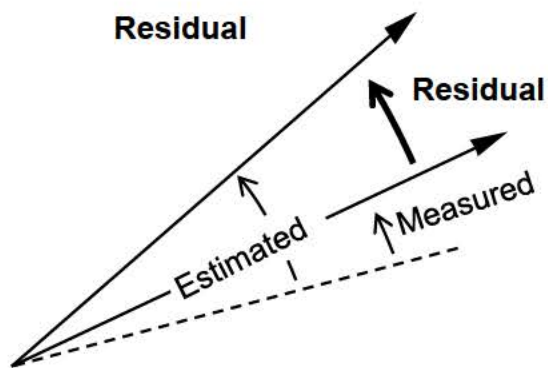
As the navigation estimates of elevation and azimuth converge to the measured values, the residual for each angle will decrease.



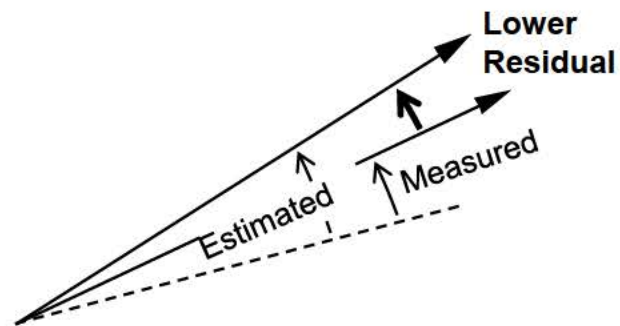
1. Azimuth residuals prior to incorporation of sensor measurements.



2. Azimuth residuals after incorporation of sensor measurements.

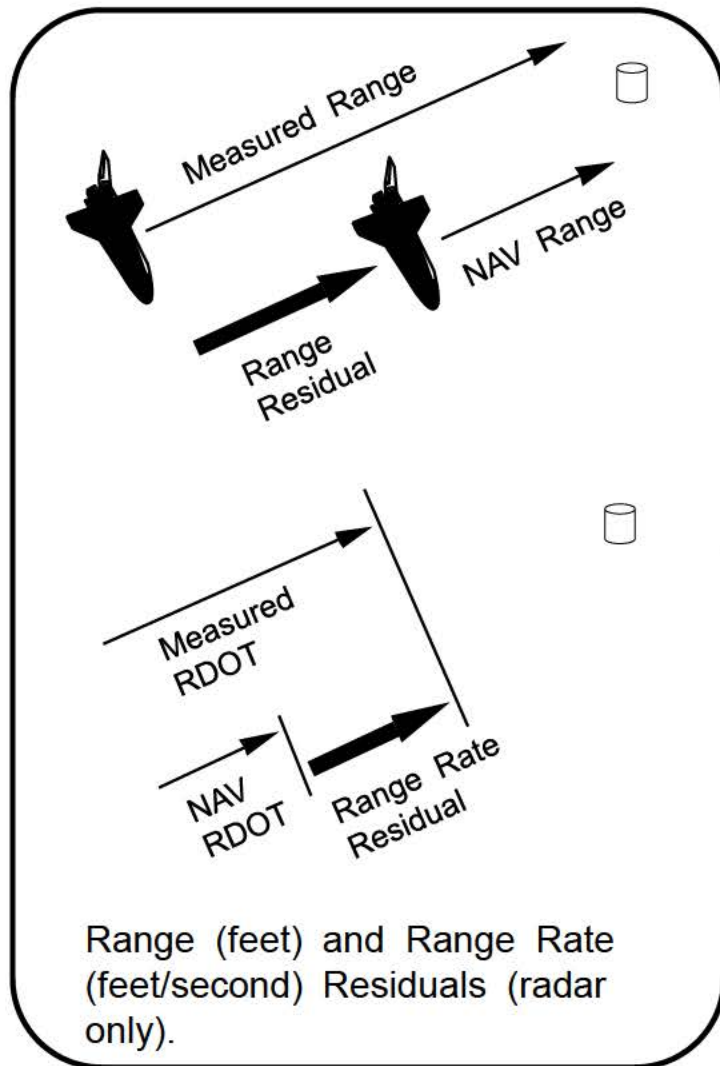


1. Elevation residuals prior to incorporation of sensor measurements.



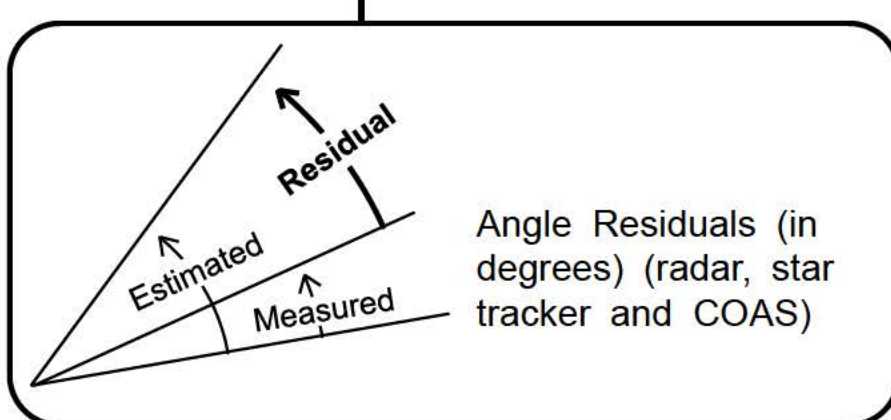
2. Elevation residuals after incorporation of sensor measurements.

Residuals are given in the lower left hand corner of the REL NAV display.



Range (feet) and Range Rate (feet/second) Residuals (radar only).

2021 / 033 /	REL NAV	1 005 / 02 : 07 : 37
RNDZ NAV ENA 1*	SV UPDATE	000 / 00 : 00 : 00
KU ANT ENA 2*	POS 0.02	Avg G ON 5*
MEAS ENA 3	VEL 0.03	
NAV		
SV SEL 4 FLTR	RR GPC	
RNG 25.721	RNG 25.610	
R - 21.19	R - 20.80	
θ 25.76	EL - 0.4	
Y + 0.08	AZ - 0.8	
Y + 0.1	ₚ P + 0.8	
NODE 2:54:00	ₚ R + 0.1	
FILTER		
S TRK 12 RR 13*	COAS 14	
STAT	X - 3.4	
FLTR UPDATE 15	ORB Y + 4.4	
COVAR REINIT 16		
RESID RATIO ACPT REJ		
RNG + 0.09 0.2 807 0		
R + 0.02 0.0 807 0		
V/EL/Y + 0.02 0.0 807 0		
H/AZ/X + 0.01 0.0 807 0		
GPS P + 0.19 0.4		
V + 0.26 0.3		
EDIT OVRD		
17* 18 19		
20* 21 22		
23* 24 25		
42 43* 44		



9.3 Kalman Filtering Overview

Every 3.84 seconds, the ORBITER state vector is propagated to the current time via the SUPER_G integrator. Every 7.68 seconds, updates in position and velocity are added to the position and velocity components of the ORBITER state. The basic equations are given below:

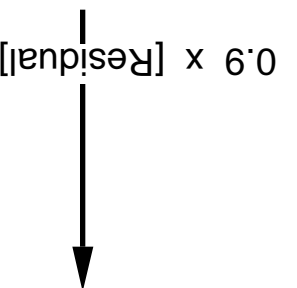
$$\begin{aligned} X_{\text{NEW}} &= \boxed{X_{\text{OLD}}, \dot{X}_{\text{OLD}} \substack{\text{Integrated} \\ \text{By SUPER_G}}} & 3.84 \text{ seconds} & & 7.68 \text{ seconds} \\ &+ \text{Position Update} \\ \\ \dot{X}_{\text{NEW}} &= \boxed{\dot{X}_{\text{OLD}}, \ddot{X}_{\text{OLD}} \substack{\text{Integrated} \\ \text{By SUPER_G}}} & 3.84 \text{ seconds} & & 7.68 \text{ seconds} \\ &+ \text{Velocity Update} \end{aligned}$$

Position and velocity updates are computed based on the sensor measurement residual. The residual can be thought of as the “error” in the ORBITER’s estimate of its relative position and velocity with respect to the TARGET. The residual also contains error from the sensors. By reducing the “error” in the ORBITER state, the ORBITER’s estimate of its position and velocity can be improved.

The Kalman filter maintains an estimate of how accurate the ORBITER state vector and navigation sensors are. These estimates are maintained in the covariance matrix. The filter determines the magnitude and direction of the position and velocity updates. Adjusting the ORBITER state in this manner makes it vulnerable to corruption by bad sensor data. To prevent this, residual edit criteria are used.

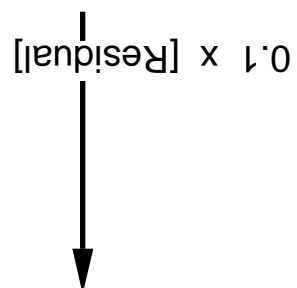
High Kalman gain, large update :

$$\text{Update} = 0.9 \times [\text{Residual}]$$



Low Kalman gain, small update :

$$\text{Update} = 0.1 \times [\text{Residual}]$$



the gain is high, more of the residual is added to the ORBITER state.

Covariance matrix estimates of state vector uncertainty and sensor errors work together to determine the Kalman gain. A low gain means that only a small part of the residual is added to the ORBITER state. If

$$\text{Update} = \text{Kalman Gain} \times [\text{Residual}]$$

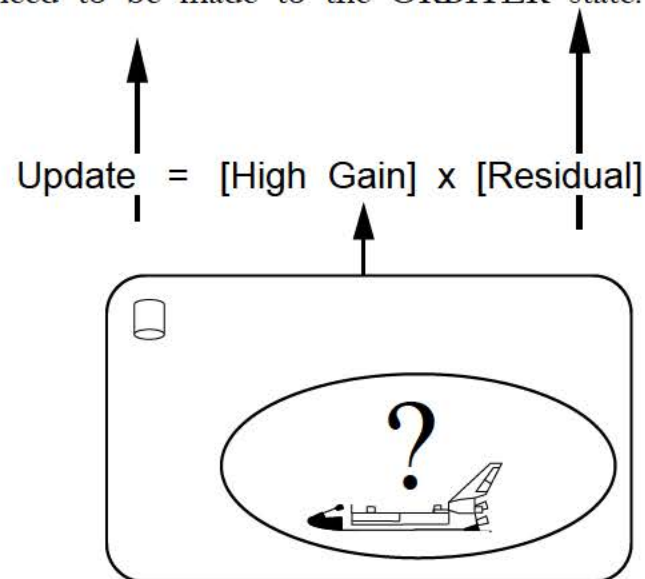
The equation for updates is :

vector and sensor accuracy.

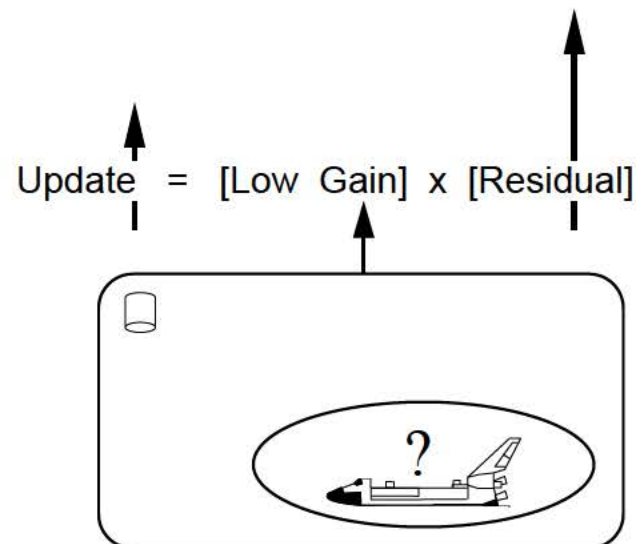
Kalman gain is computed from the covariance matrix. It is an indicator of how "believable" the residual is and to what extent sensor data is used to correct the state. This gain is multiplied by the residual to obtain the update. Kalman gain controls by how much the state is updated based on the filter's estimate of state vector and sensor accuracy.

If the covariance matrix indicates a large amount of uncertainty in the ORBITER state, the gain will tend to be high. Most of the residual will be added to the ORBITER state. If the covariance indicates a low uncertainty, the gain will tend to be low. If the ORBITER state is accurate (and therefore the relative state is accurate), little change will need to be made to the ORBITER state.

Large uncertainty, high Kalman gain,
large update :

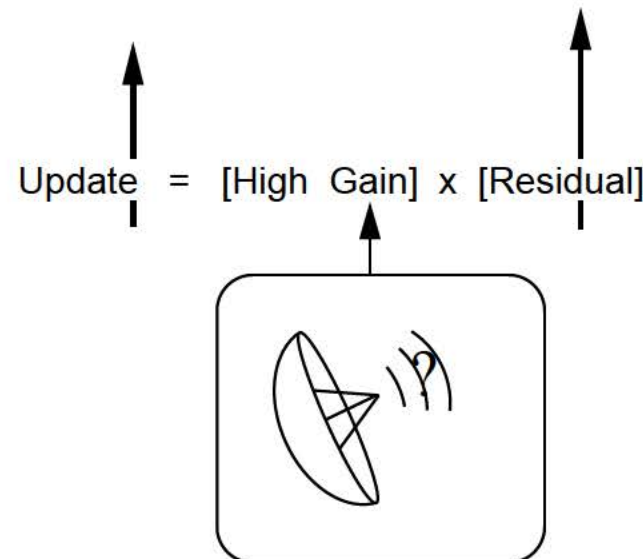


Small uncertainty, low Kalman gain,
small update :

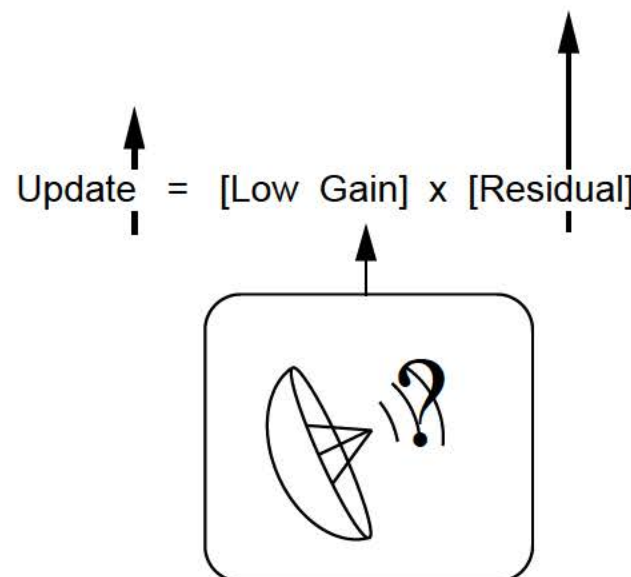


If the covariance believes the sensors to be accurate, the gain will tend to be high, otherwise it will tend to be low.

Accurate sensor, high Kalman gain,
large update :



Inaccurate sensor, low Kalman gain,
small update :



To summarize :

- Large uncertainty in position and velocity drives gain up (larger update).
- Low uncertainty in position and velocity drives gain down (smaller update).
- Inaccurate sensors drive gain down (smaller update).
- Accurate sensors drive gain up (larger update).

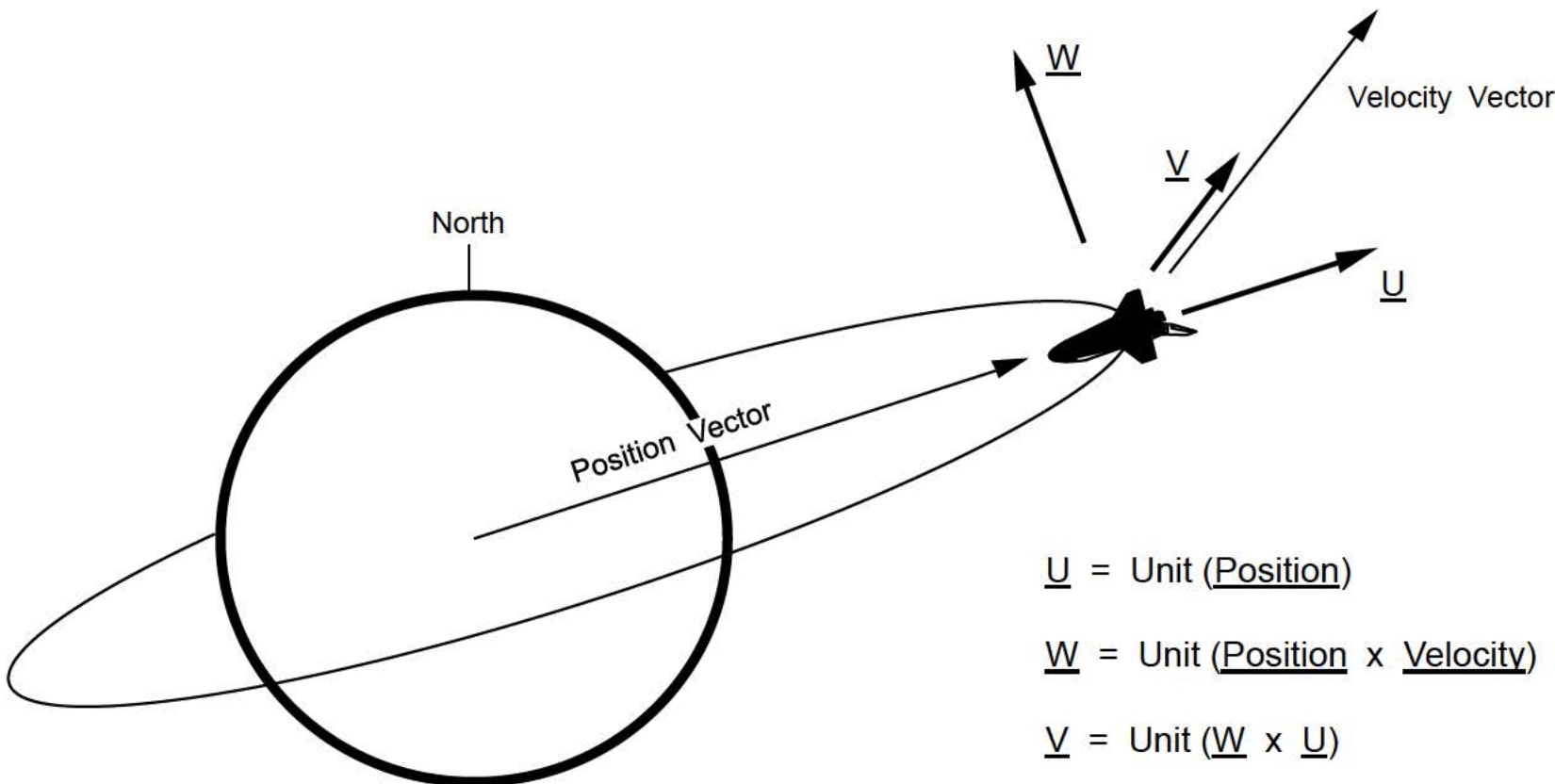
As marks are taken, the uncertainty of the filter estimate of the state will decrease, resulting in lower Kalman gain. Updates will also cause the navigation estimates of sensor measurements to converge with the actual measurements, hence lower residuals. Both of these factors will result in lower updates.

The Kalman filter estimates 13 states. Three components of an inertial position vector, three components of an inertial velocity vector, a range measurement bias, a range rate measurement bias, two angle measurement biases, and three components of an inertial un-modeled acceleration vector.

9.4 Covariance Matrix Position Diagonals

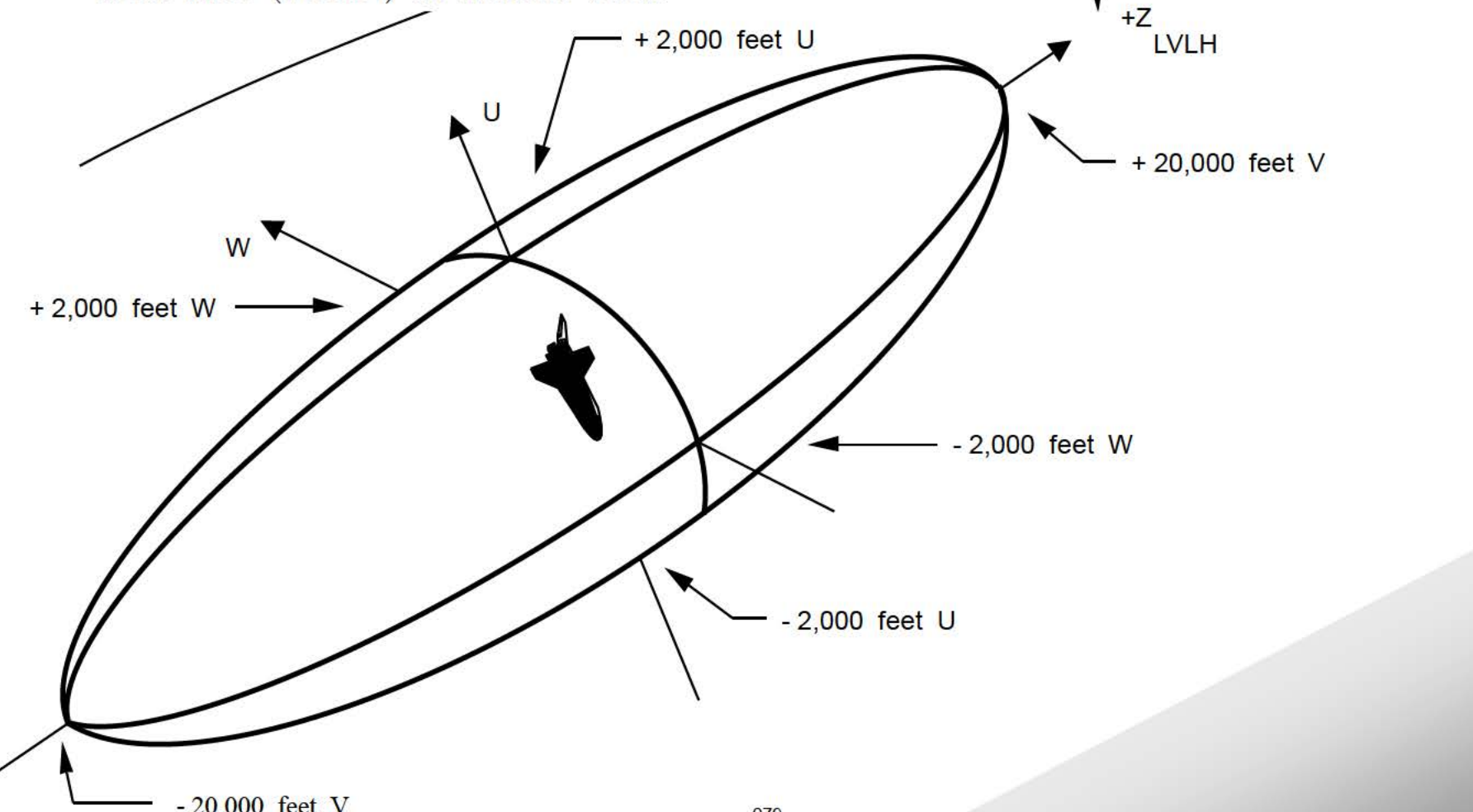
The first three diagonal terms of the covariance matrix contain the square (variance) of the uncertainty (or error) in each component of position in M50 coordinates. These three terms will normally decrease during a sensor pass as incorporated measurements improve navigation's estimate of ORBITER position and velocity (state vector). Conversely, the covariance will tend to grow during periods when sensor data is not being incorporated into navigation.

Although the covariance is in M50 coordinates, the initial values (ILOADs) are in UVW coordinates. The ILOADs are rotated into M50 when rendezvous navigation is initialized. The UVW frame is defined below:



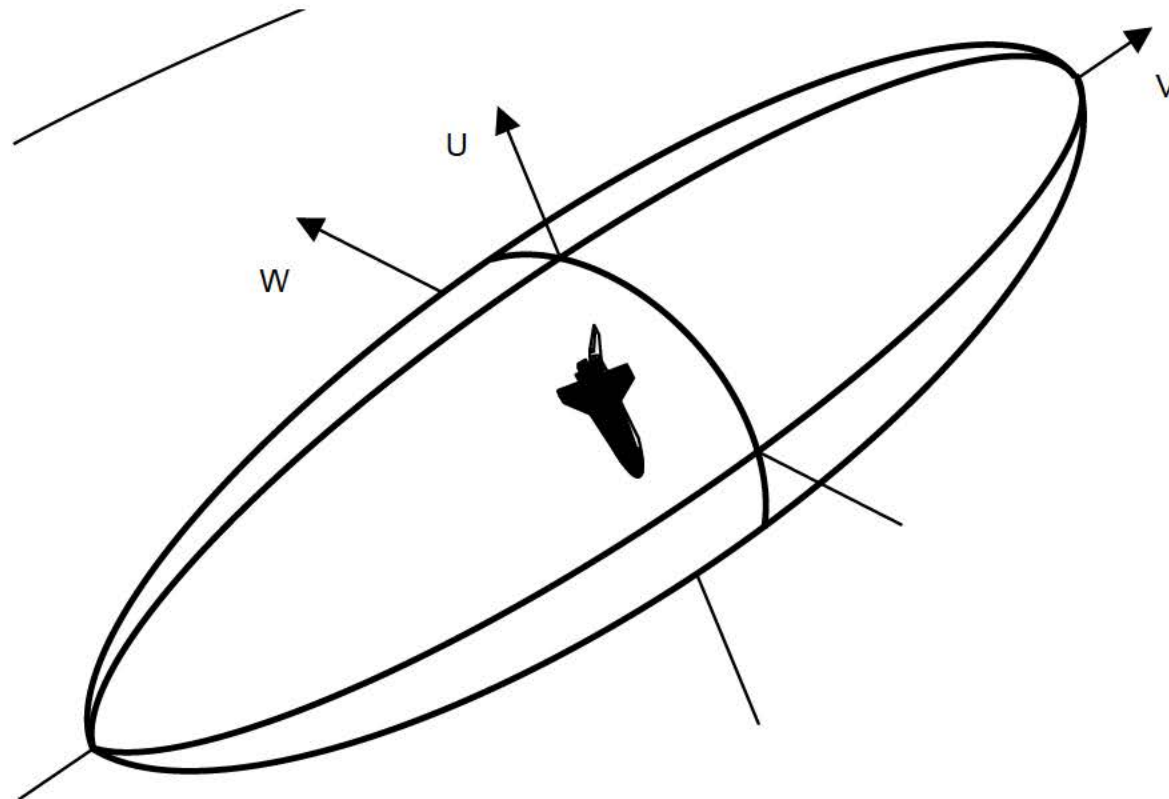
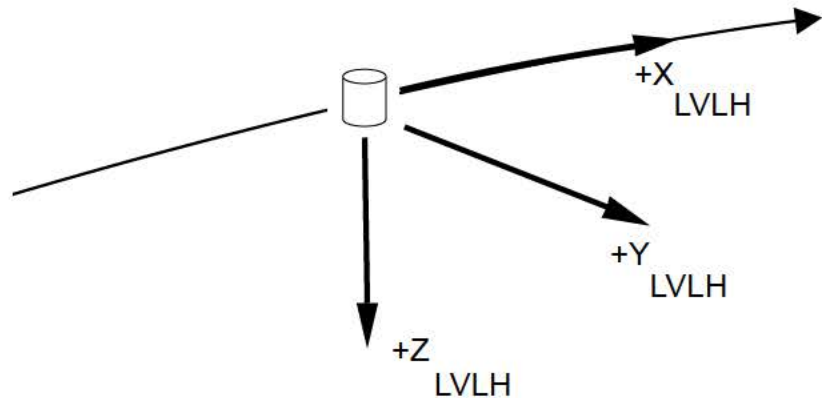
Position Diagonals - Rendezvous NAV Initialization

The three position uncertainties may be thought of as defining an error ellipsoid in UVW (and also M50) space. The ORBITER symbol represents the ORBITER relative position defined by NAV. The actual ORBITER position relative to the TARGET has a 99.9 % probability of being within a 3 sigma ellipsoid. Initial values (ILOADs) are indicated below.



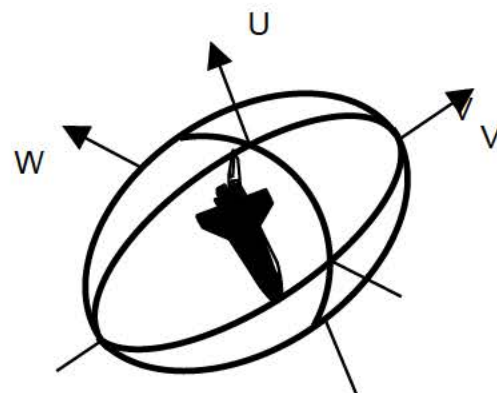
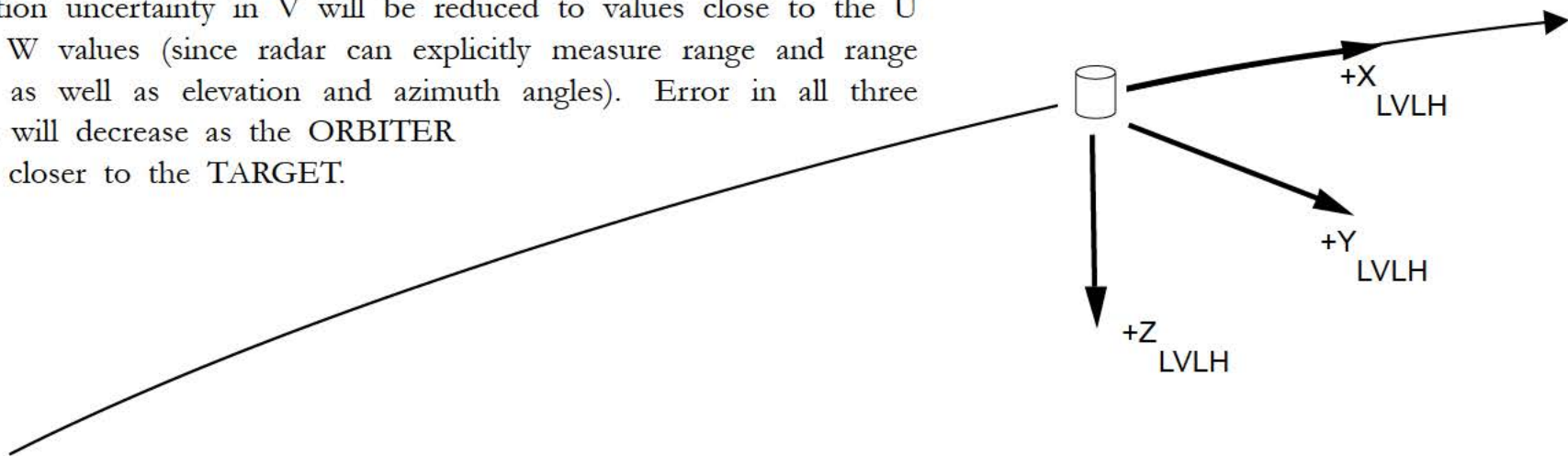
Position Diagonals - Post Star Tracker Pass

Position uncertainty will be reduced primarily in the U and W directions (since star tracker explicitly measures relative errors in altitude and cross-track), with W having a greater decrease than U. V will decrease somewhat at the end of the pass due to the geometry change in the ORBITER's trajectory relative to the TARGET.



Position Diagonals - Radar Measurement Incorporation

Position uncertainty in V will be reduced to values close to the U and W values (since radar can explicitly measure range and range rate as well as elevation and azimuth angles). Error in all three axes will decrease as the ORBITER gets closer to the TARGET.

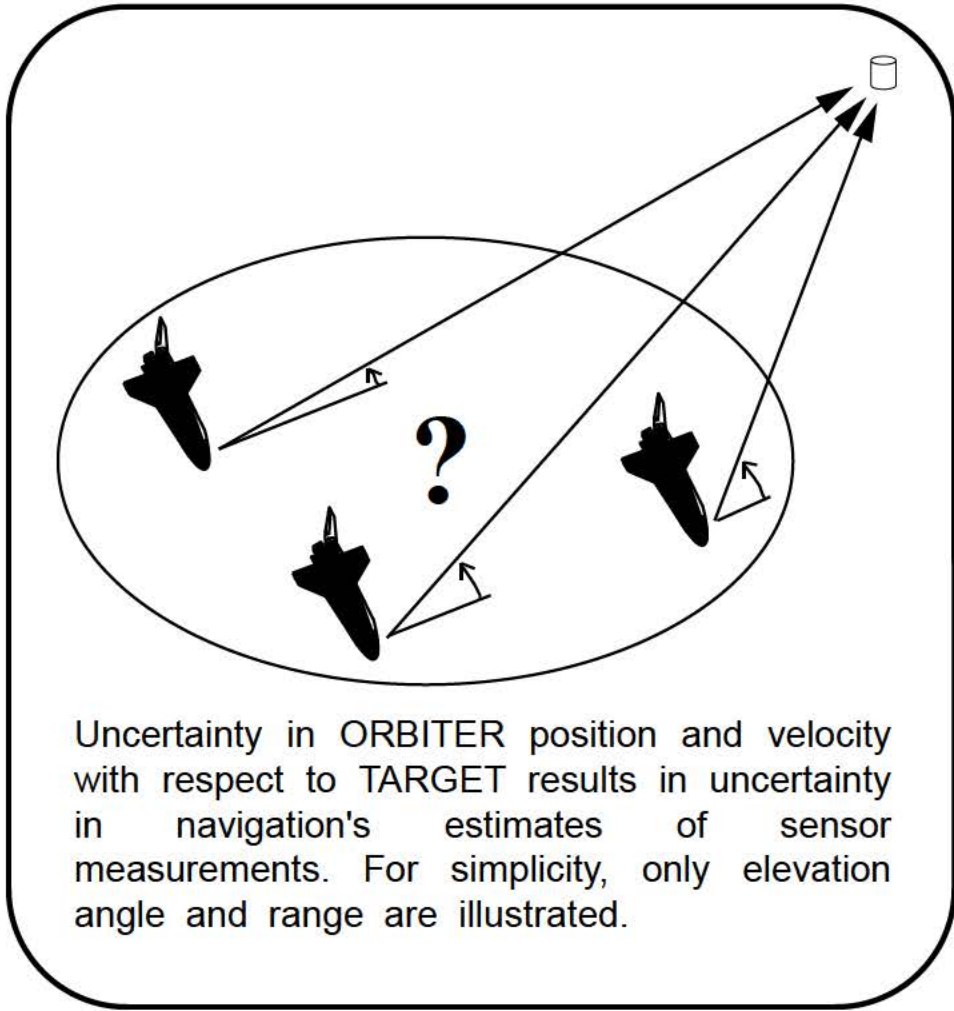


Below is a summary of the covariance matrices for rendezvous. The rendezvous covariance is ILOADED in the Flight Software. The Prox Ops covariance is uplinked after the T_i burn, and is used if a rendezvous navigation reinitialization is required after T_i . It is also uplinked to support a payload deployment. The COAS covariance is uplinked only if COAS marks are to be taken. Correlation coefficients (bottom three columns) control how much of position or velocity update is made along one axis due to a measurement update in position or velocity along another axis. If an OPS mode recall is performed after a Prox Ops or COAS covariance uplink, the current filter covariance will be reset to the uplinked covariance. If an OPS transition is performed, the covariance values will default to the ILOADED values, and the Prox Ops or COAS covariance will have to be uplinked again.

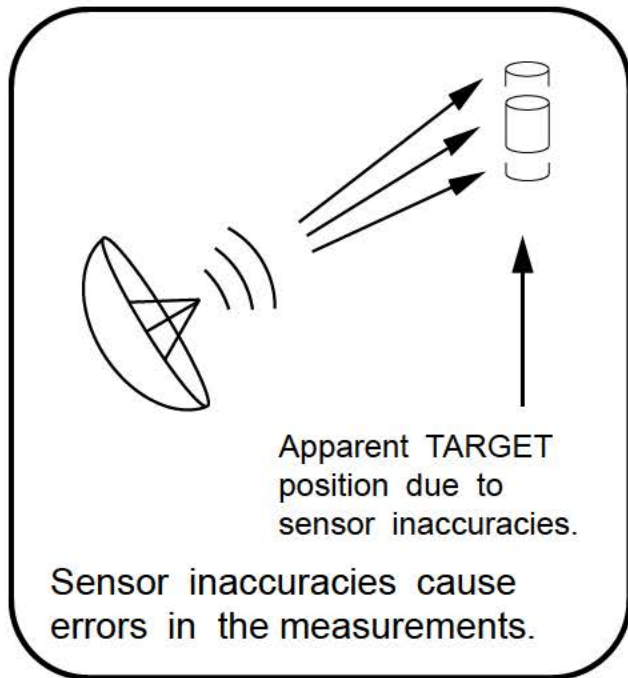
<u>Rendezvous</u>	<u>Prox Ops</u>	<u>COAS</u>
$U = 2,000$ feet	$U = 1,000$ feet	$U = 500$ feet
$V = 20,000$ feet	$V = 1,000$ feet	$V = 5,000$ feet
$W = 2,000$ feet	$W = 1,000$ feet	$W = 1,000$ feet
$\dot{U} = 21$ feet/second	$\dot{U} = 1$ feet/second	$\dot{U} = 5$ feet/second
$\dot{V} = 2$ feet/second	$\dot{V} = 1$ feet/second	$\dot{V} = 1$ feet/second
$\dot{W} = 6$ feet/second	$\dot{W} = 1$ feet/second	$\dot{W} = 1$ feet/second
$UV = 0.0$	$UV = 0.0$	$UV = 0.0$
$U\dot{U} = 0.0$	$U\dot{U} = 0.0$	$U\dot{U} = 0.0$
$U\dot{V} = -0.9$	$U\dot{V} = -0.9$	$U\dot{V} = -0.9$
$U\dot{W} = -0.9$	$U\dot{W} = -0.9$	$U\dot{W} = -0.9$
$V\dot{V} = 0.0$	$V\dot{V} = 0.0$	$V\dot{V} = 0.0$
$W\dot{W} = 0.0$	$W\dot{W} = 0.0$	$W\dot{W} = 0.0$
$\dot{U}\dot{V} = 0.0$	$\dot{U}\dot{V} = 0.0$	$\dot{U}\dot{V} = 0.0$

9.5 Ratios and Residual Edit Criteria

Both the navigation estimate of the measurement and the sensor measurement itself cannot be measured with 100% accuracy.



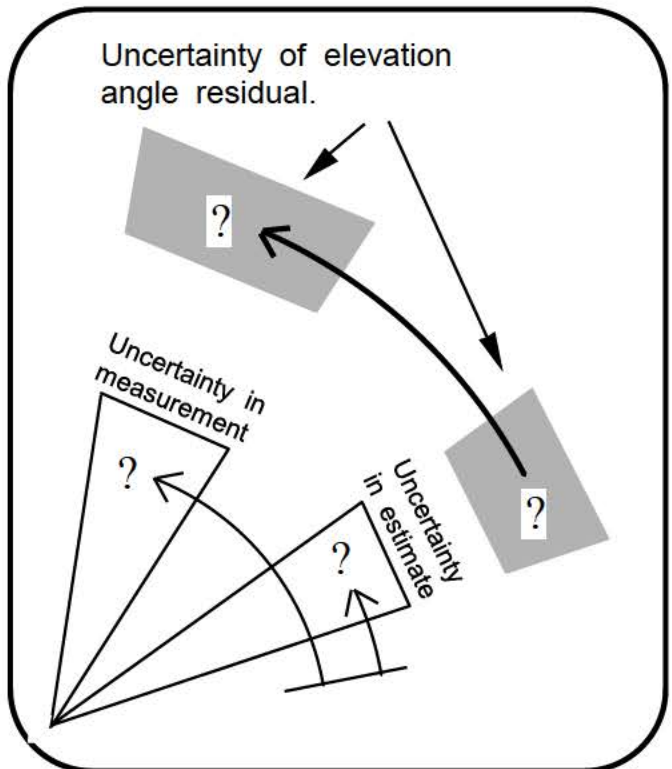
Uncertainty in ORBITER position and velocity with respect to TARGET results in uncertainty in navigation's estimates of sensor measurements. For simplicity, only elevation angle and range are illustrated.



Apparent TARGET position due to sensor inaccuracies.

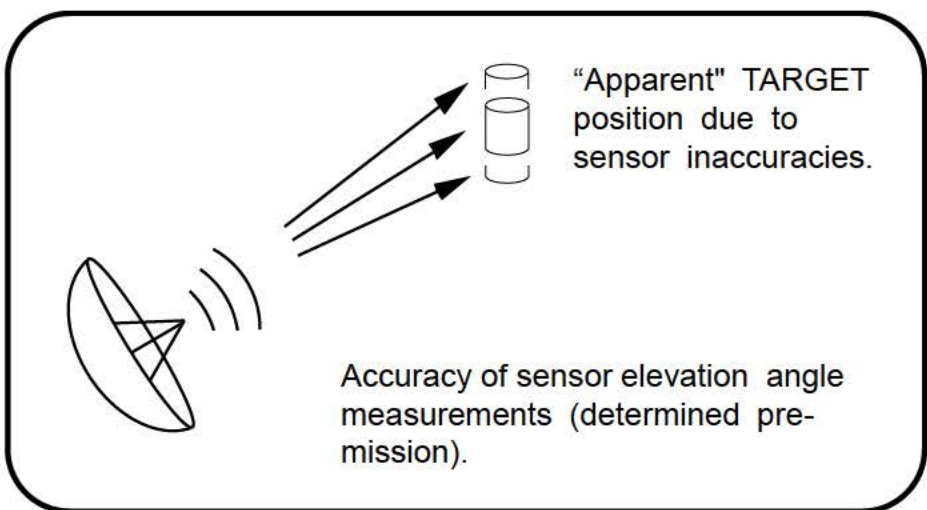
Sensor inaccuracies cause errors in the measurements.

The accuracy of the residual is dependent upon the uncertainty in navigation's estimate of the measurement and the accuracy of the sensor:



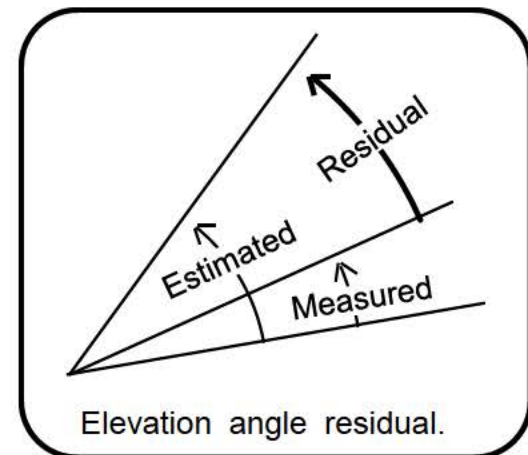
=

+



Before an update can be applied to the state vector, the residual (range, range rate, or angle) must pass a “reasonableness test.” The residual is divided by 6 times the uncertainty in the residual. If the resulting value (called a “Ratio”) is less than or equal to 1.0, the state vector is updated with that particular measurement.

This comparison of the residual with the estimated accuracy of the residual is called the “residual edit test.”

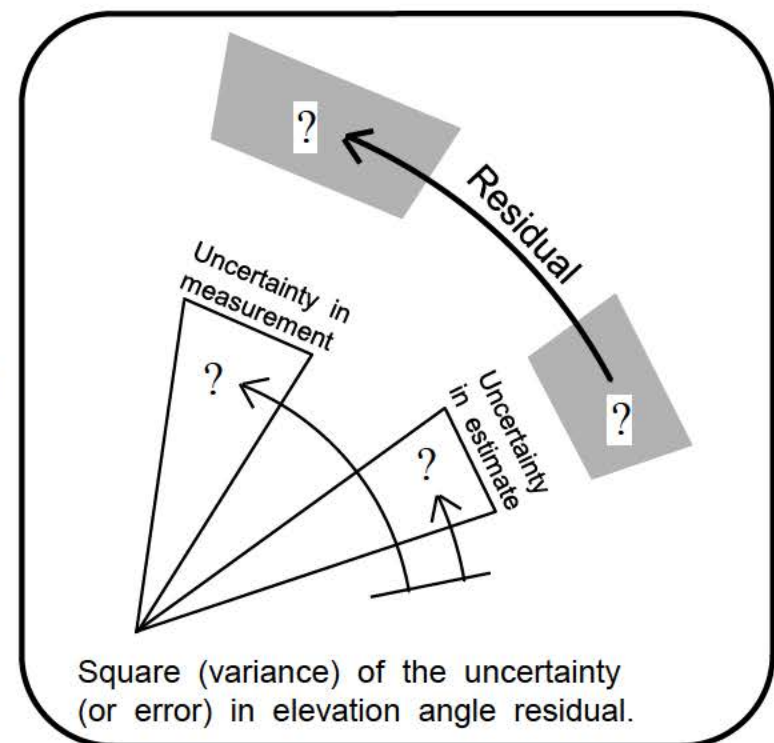


Ratio =

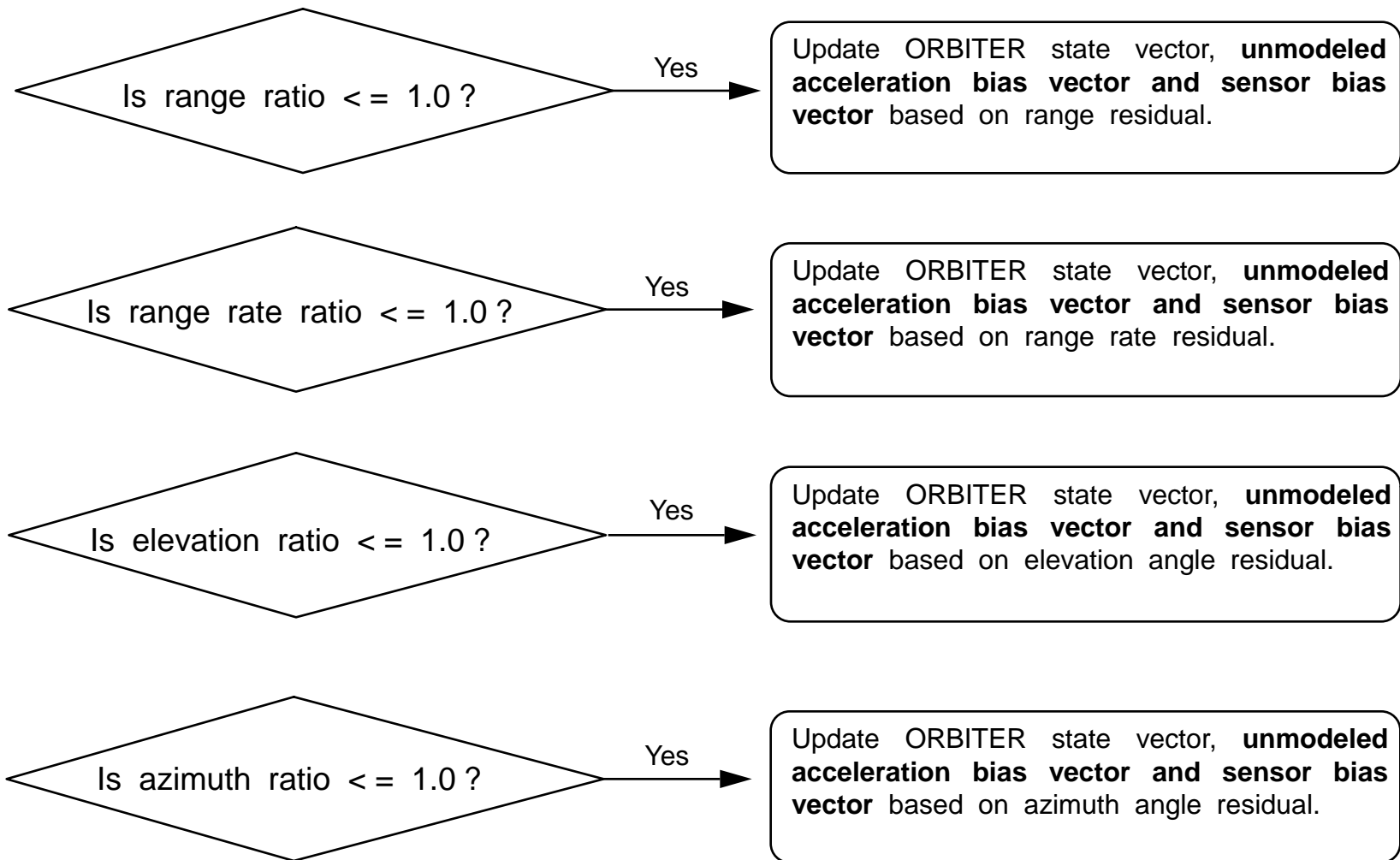
Ratios are computed independently for each measurement. Only elevation angle is shown here for clarity.

The uncertainty of the residual (computed by the Kalman filter) is considered to be “1 sigma.” It is multiplied by the number “36” (ILLOAD K_RESID_EDIT) so that residuals up to “6 sigma” will pass the test.

36



A residual edit test is performed for each measurement. If the ratio passes the test, an update is made based on that specific measurement. The two angle tests also apply to star tracker measurements (vertical and horizontal) and the COAS.



2021/033 / REL NAV				1 005/02:07:37		
RNDZ NAV ENA 1*				000/00:00:00		
KU ANT ENA 2*				AVG G ON 5*		
MEAS ENA 3				GPS		
NAV				STAT	P	1 σ DES
SV SEL 4	FLTR	RR	GPC	1		75 31
RNG 25.721		RNG 25.610		2*		75 32
R - 21.19		R - 20.80		3		75 33
θ 25.76	EL	- 0.4				
Y + 0.08	AZ	- 0.8				
Y + 0.1	Ω P	+ 0.8				
NODE 2:54:00	Ω R	+ 0.1				
FILTER						
S TRK 12	RR 13*	COAS 14				
STAT		X - 3.4				
FLTR UPDATE 15	ORB	Y + 4.4				
COVAR REINIT 16						
RESID		RATIO	ACPT	REJ	EDIT OVRD	
RNG + 0.09		0.2	807	0	AUT	INH FOR
R + 0.02		0.0	807	0	17*	18 19
V/EL/Y + 0.02		0.0	807	0	20*	21 22
H/AZ/X + 0.01		0.0	807	0	23*	24 25
GPS P + 0.19		0.4			42	43* 44
V + 0.26		0.3				

When a residual passes the residual edit test, a state update is made and the "mark acceptance" is incremented by "1".

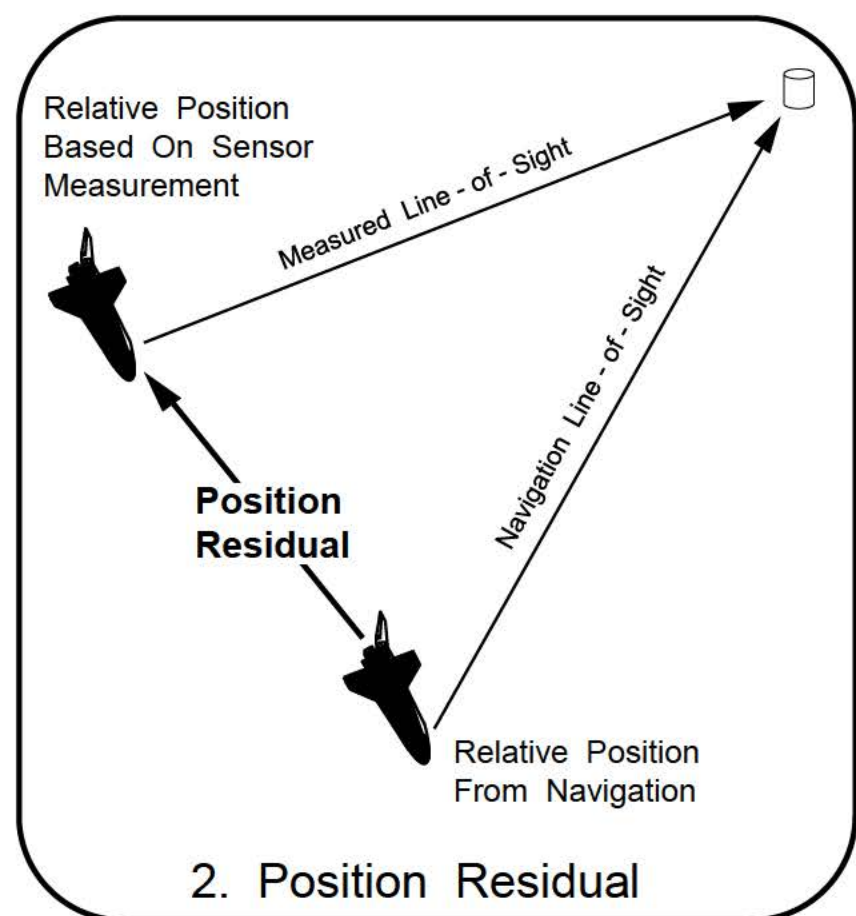
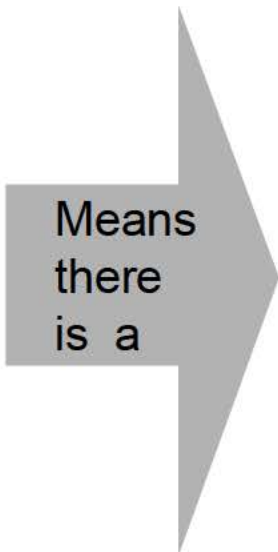
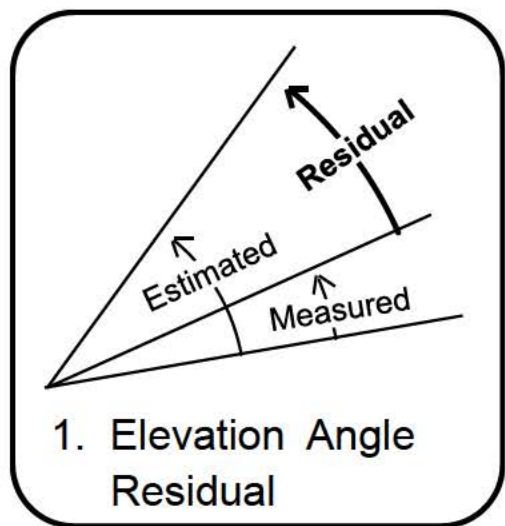
The ratio for each type of measurement is displayed.

If a residual fails the residual edit test, an update to the state vector is not performed. The "rejection" counter is incremented by "1".

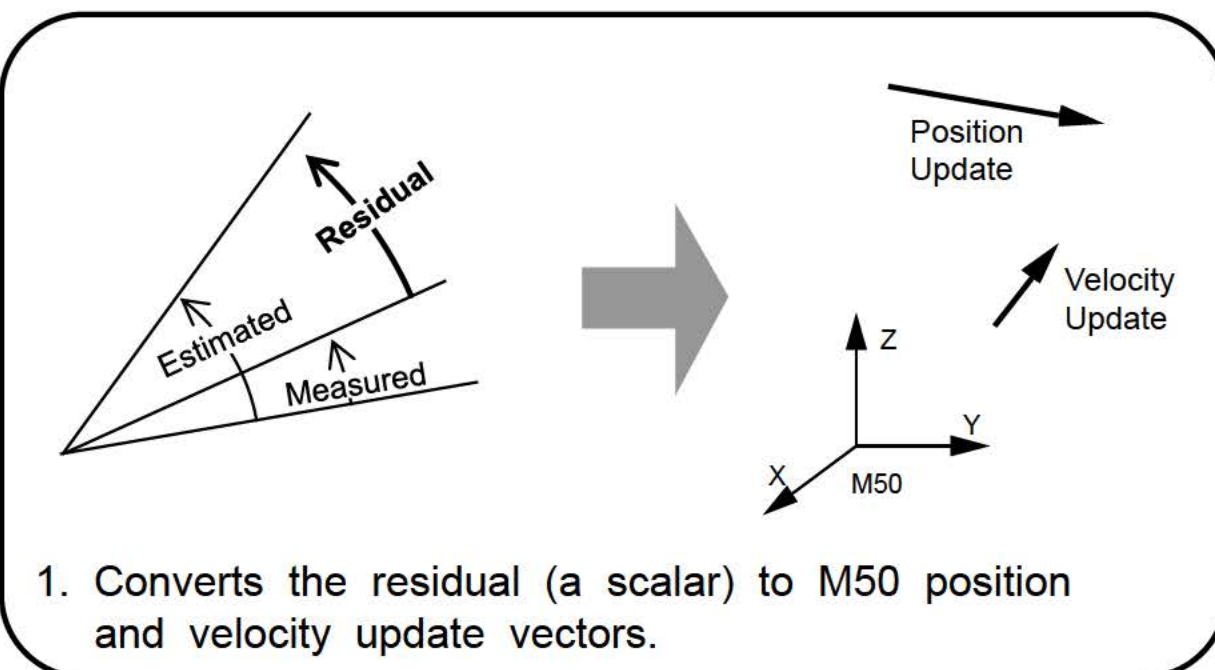
9.6 More On Kalman Gain

A measurement residual represents the amount of error in navigation's estimate of ORBITER position and/or velocity relative to the TARGET. If the navigation estimate of a measurement is in error, then navigation's estimate of ORBITER inertial position and/or velocity (state vector) has error in it.

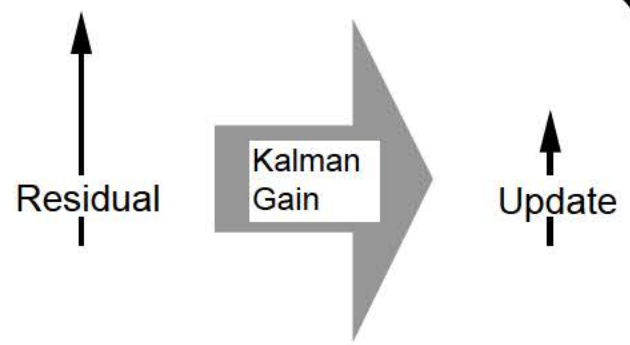
This “error” in the state vector can be called a “state vector” residual. For clarity, only an elevation angle and position residual are shown.



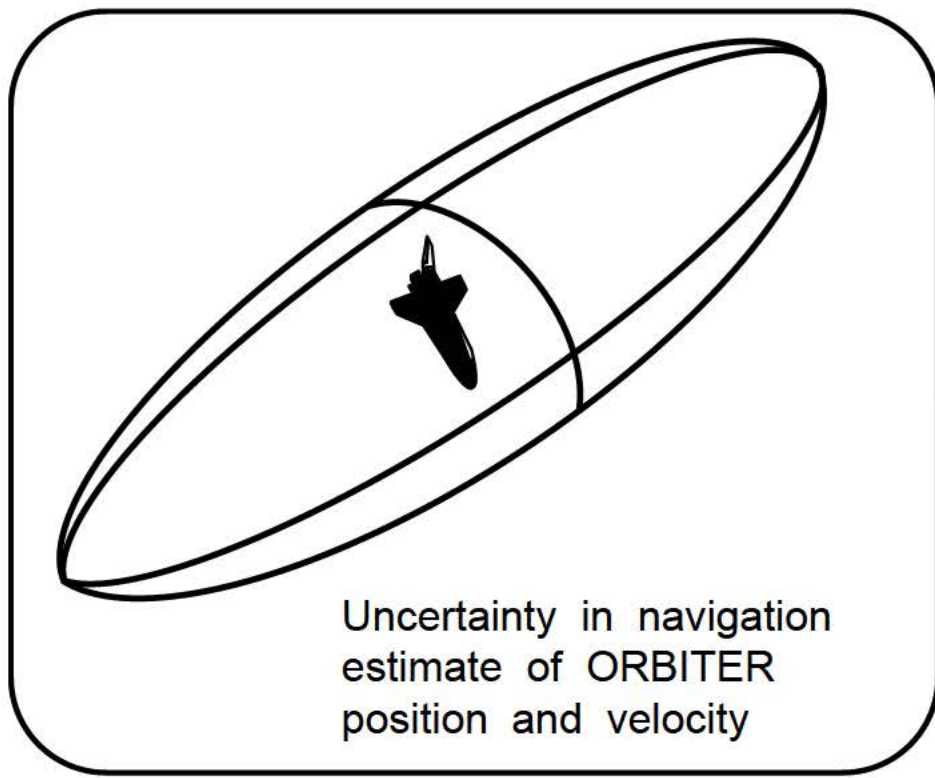
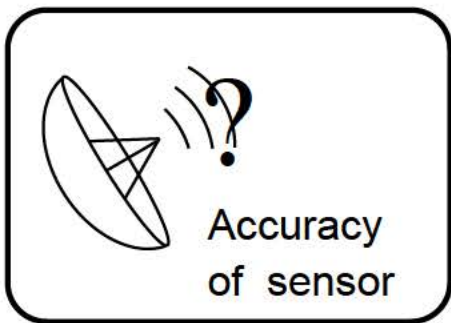
The Kalman gain vector performs the following:



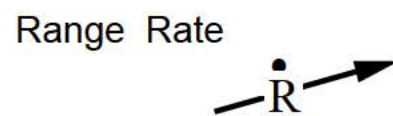
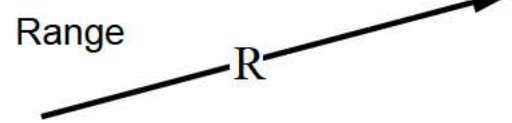
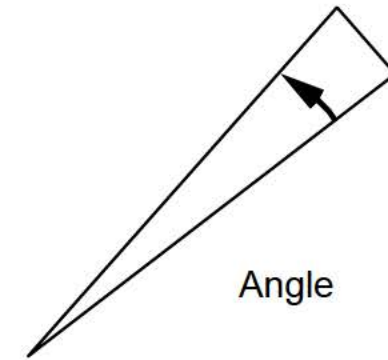
2. Determines how much of the residual (or error) is to be used to correct the ORBITER state.



Kalman gain is computed based on the following:



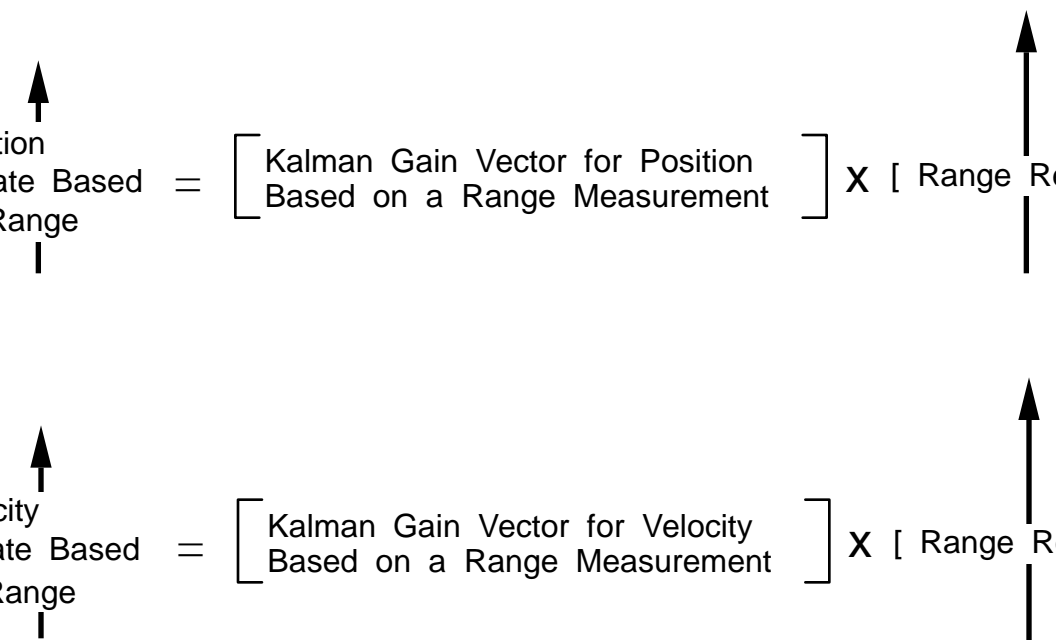
Type of measurement:



If the range residual passes the residual edit criteria test, position and velocity updates are computed and applied to the ORBITER state vector.

An important feature of the covariance matrix is that it enables velocity data to be determined from a position measurement, and position data to be determined from a velocity measurement.

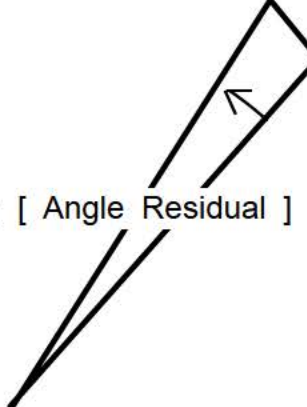
Note that two Kalman gains are computed, one for a position update and one for a velocity update.

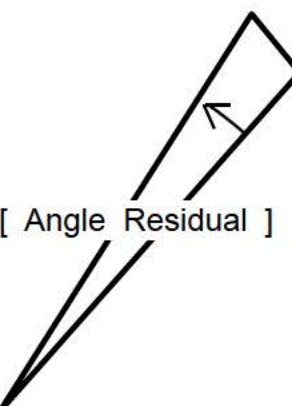
$$\begin{aligned} \text{Position Update Based on Range} &= \left[\begin{array}{c} \text{Kalman Gain Vector for Position} \\ \text{Based on a Range Measurement} \end{array} \right] \times [\text{Range Residual}] \\ \\ \text{Velocity Update Based on Range} &= \left[\begin{array}{c} \text{Kalman Gain Vector for Velocity} \\ \text{Based on a Range Measurement} \end{array} \right] \times [\text{Range Residual}] \end{aligned}$$


If the range rate residual passes the residual edit criteria test, position and velocity updates are computed and applied to the ORBITER state vector.

$$\begin{array}{l}
 \text{Position Update} \\
 \text{Based on Range} \\
 \text{Rate} \\
 | \\
 \text{Based on Range Rate Measurement} \\
 \left[\begin{array}{c} \text{Kalman Gain Vector for Position} \\ \text{Based on a Range Rate} \\ \text{Measurement} \end{array} \right] \times [\text{Range Rate Residual}] \\
 | \\
 \text{Velocity Update} \\
 \text{Based on Range} \\
 \text{Rate} \\
 | \\
 \text{Based on Range Rate Measurement} \\
 \left[\begin{array}{c} \text{Kalman Gain Vector for Velocity} \\ \text{Based on a Range Rate} \\ \text{Measurement} \end{array} \right] \times [\text{Range Rate Residual}]
 \end{array}$$

If the angle residual passes the residual edit criteria test, position and velocity updates are computed and applied to the ORBITER state vector.

$$\begin{array}{l} \text{Position} \\ \text{Update Based} \\ \text{on Angle} \end{array} = \left[\begin{array}{l} \text{Kalman Gain Vector for Position} \\ \text{Based on an Angle Measurement} \end{array} \right] \times [\text{Angle Residual}]$$


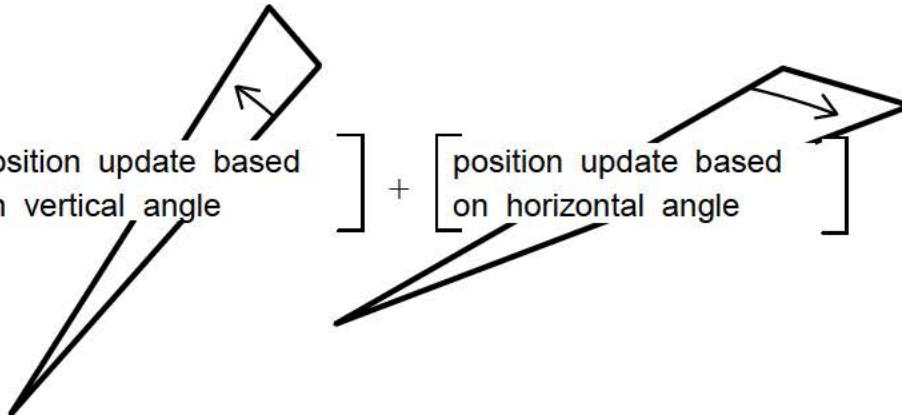
$$\begin{array}{l} \text{Velocity} \\ \text{Update Based} \\ \text{on Angle} \end{array} = \left[\begin{array}{l} \text{Kalman Gain Vector for Velocity} \\ \text{Based on an Angle Measurement} \end{array} \right] \times [\text{Angle Residual}]$$


Every 7.68 seconds, position and velocity updates are made to the ORBITER state vector. The magnitude of the position (in kilofeet) and velocity (in feet/second) update vectors are given on the Relative Navigation (REL NAV) display. These magnitudes (R_MEAS and V_MEAS in the Navigation FSSR) are the sum of the updates for each measurement type.

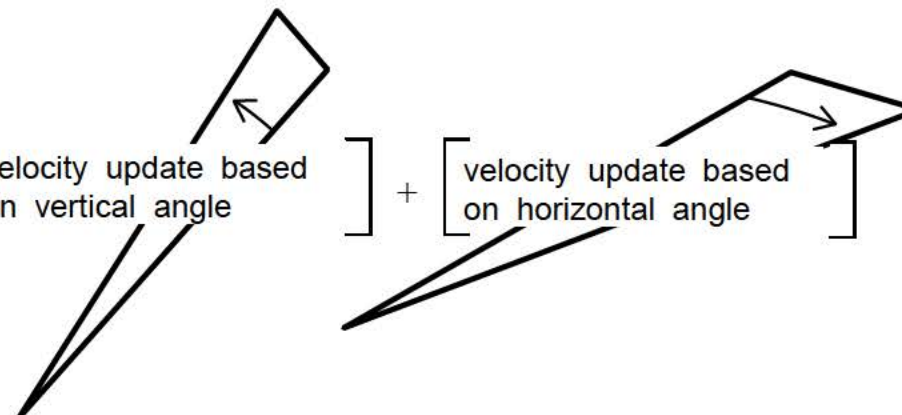
REL NAV				GPS			
RNDZ NAV ENA 1*				1 005 / 02 : 07 : 37			
KU ANT ENA 2*				000 / 00 : 00 : 00			
MEAS ENA 3				AVG G ON 5*			
NAV				STAT P 1 σ DES			
SV SEL 4	FLTR	RR	GPC	1		75	31
RNG 25.721		RNG	25.610	2*		75	32
\dot{R} - 21.19		\dot{R}	- 20.80	3		75	33
θ 25.76		EL	- 0.4	SV TRANSFER			
\dot{Y} + 0.08		AZ	- 0.8	FLTR MINUS PROP			
\ddot{Y} + 0.1		ω_P	+ 0.8	POS 4.99			
NODE 2:54:00		ω_R	+ 0.1	VEL 5.72			
FILTER							
S TRK 12	RR 13*	COAS 14		FLTR TO PROP 8			
STAT		X - 3.4		PROP TO FLTR 9			
FLTR UPDATE 15	ORB	Y + 4.4		ORB TO TGT 10			
COVAR REINIT 16				TGT TO ORB 11			
EDIT OVRD							
RNG + 0.09	RESID 0.2	ACPT 807	REJ 0	AUT 17*	INH 18	FOR 19	
\dot{R} + 0.02		807	0	20*	21	22	
V/EL / Y + 0.02		807	0	23*	24	25	
H/AZ / X + 0.01		807	0				
GPS P + 0.19	0.4			42	43 *	44	
V + 0.26	0.3						

For star tracker :

$$R_{MEAS} = \begin{bmatrix} \text{position update based} \\ \text{on vertical angle} \end{bmatrix} + \begin{bmatrix} \text{position update based} \\ \text{on horizontal angle} \end{bmatrix}$$

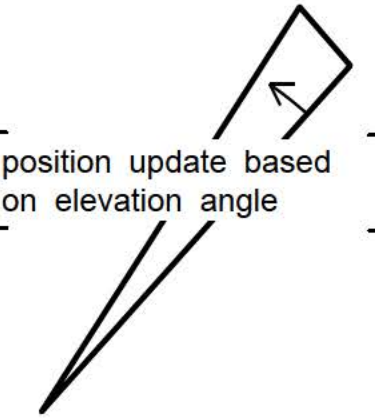
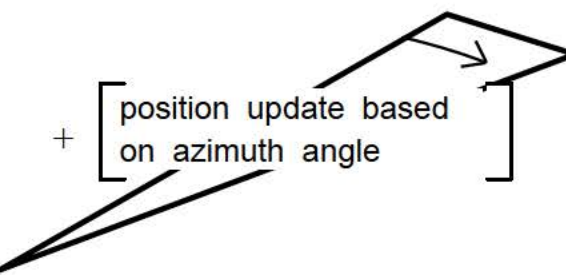


$$V_{MEAS} = \begin{bmatrix} \text{velocity update based} \\ \text{on vertical angle} \end{bmatrix} + \begin{bmatrix} \text{velocity update based} \\ \text{on horizontal angle} \end{bmatrix}$$

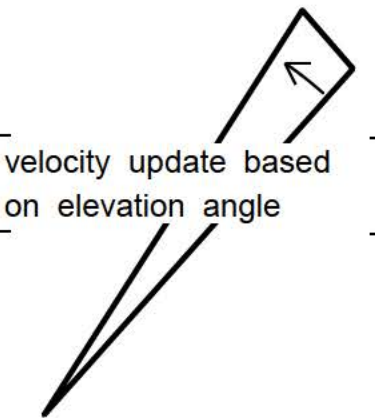
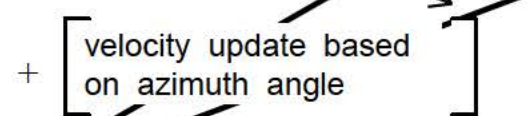


For radar :

$$R_{MEAS} = \left[\begin{array}{l} \text{position update based} \\ \text{on range} \end{array} \right] + \left[\begin{array}{l} \text{position update based} \\ \text{on range rate} \end{array} \right] + \left[\begin{array}{l} \text{position update based} \\ \text{on elevation angle} \end{array} \right]$$

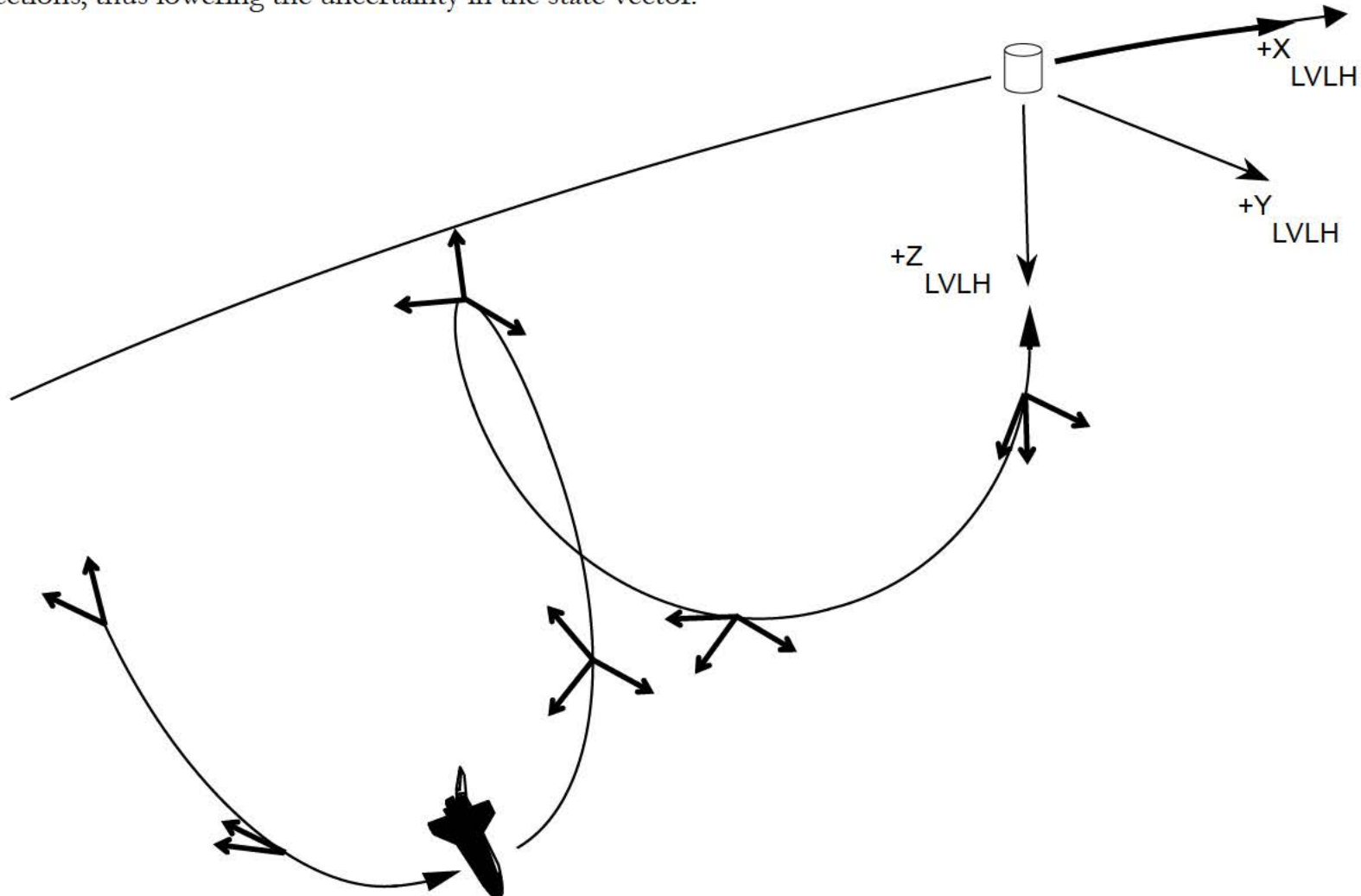


$$V_{MEAS} = \left[\begin{array}{l} \text{velocity update based} \\ \text{on range} \end{array} \right] + \left[\begin{array}{l} \text{velocity update based} \\ \text{on range rate} \end{array} \right] + \left[\begin{array}{l} \text{velocity update based} \\ \text{on elevation angle} \end{array} \right]$$



9.7 Measurement Partial

The measurement partial (**b**) is the derivative of the sensor measurement with respect to the vehicle state vector. It is found in both the Kalman gain and covariance update equations in the Kalman filter. Varying the direction of the measurement partial (via relative motion) allows the Kalman filter to update the orbiter inertial state in various directions, thus lowering the uncertainty in the state vector.



The measurement partial (sometimes also called the sensitivity or geometry) vector (**b**) relates state error ($\delta\mathbf{x}$) and the measurement residual (δq).

$$\delta q = \frac{\partial q}{\partial \bar{\mathbf{x}}} \bullet \delta_{\bar{\mathbf{x}}} = \begin{bmatrix} \frac{\partial q}{\partial \bar{\mathbf{r}}} & \frac{\partial q}{\partial \dot{\bar{\mathbf{r}}}} \end{bmatrix} \begin{bmatrix} \delta \bar{\mathbf{r}} \\ \delta \dot{\bar{\mathbf{r}}} \end{bmatrix} = \bar{\mathbf{b}} \begin{bmatrix} \delta \bar{\mathbf{r}} \\ \delta \dot{\bar{\mathbf{r}}} \end{bmatrix}$$

$$\bar{\mathbf{b}} = \begin{bmatrix} \frac{\partial q}{\partial \bar{\mathbf{r}}} & \frac{\partial q}{\partial \dot{\bar{\mathbf{r}}}} \end{bmatrix}$$

The measurement partial has an important role in the Kalman filter equations.

Kalman Gain

$$\bar{\omega} = \frac{E \bar{b}}{1.2 \bar{b} \cdot E \bar{b} + \alpha^2}$$

|

State Vector Update

$$\bar{x}_{i+1} = \bar{x}_i + \bar{\omega} \delta q$$

Covariance Update

$$E_{i+1} = E_i - \bar{\omega} (E_i \bar{b})^T$$

Parameters in the Kalman filter equations:

$\bar{\omega}$ - Kalman gain vector

E - relative covariance matrix in inertial frame

\bar{b} - measurement partial (or geometry vector) in inertial frame

$E \bar{b}$ - relative state uncertainty in the direction of the measurement (vector)

1.2 - ILOADed underweighting factor for rendezvous

$\bar{b} \cdot E \bar{b}$ - uncertainty in the measurement residual (scalar)

α^2 - ILOADed sensor variance

\bar{x} - state vector

δq - measurement residual

$\bar{\omega} \delta q$ - state vector update

$\bar{\omega} (E \bar{b})^T$ - outer product of gain vector and uncertainty in relative state
in the direction of the measurement

The range measurement partial is along the line of sight.

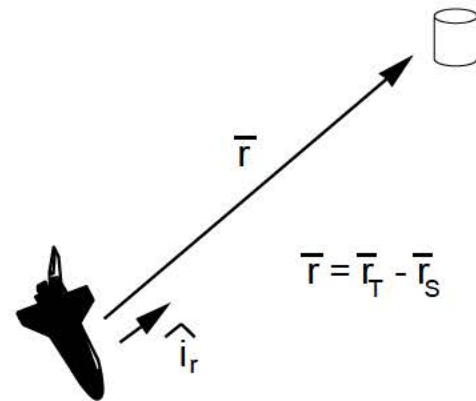
$$r^2 = \bar{r} \cdot \bar{r} = (\bar{r}_T - \bar{r}_S) \cdot (\bar{r}_T - \bar{r}_S)$$

$$2 r \delta r = -2 (\bar{r}_T - \bar{r}_S) \cdot \delta \bar{r}_S$$

$$\delta r = -\hat{i}_r \cdot \delta \bar{r}_S$$

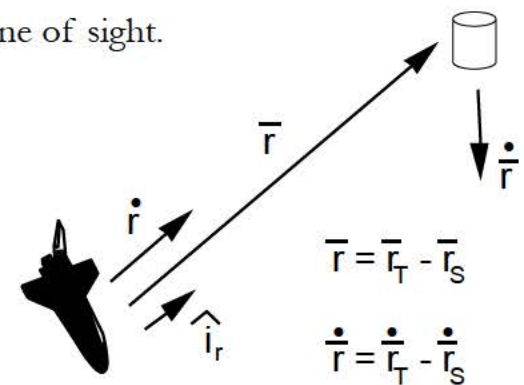
$$\therefore \bar{b} = \mp \hat{i}_r$$

"-" if orbiter state is updated
"+" if target state is updated



The range rate measurement partial has components along and normal to the line of sight.

$$\dot{r} = \hat{i}_r \cdot \dot{\bar{r}} = \frac{\bar{r} \cdot \dot{\bar{r}}}{|\bar{r}|} = \frac{(\bar{r}_T - \bar{r}_S) \cdot (\dot{\bar{r}}_T - \dot{\bar{r}}_S)}{[(\bar{r}_T - \bar{r}_S) \cdot (\bar{r}_T - \bar{r}_S)]^{1/2}}$$



$$\delta \dot{r} = - \frac{(\bar{r}_T - \bar{r}_S) \cdot \delta \dot{r}_S + (\dot{\bar{r}}_T - \dot{\bar{r}}_S) \cdot \delta \bar{r}_S}{[(\bar{r}_T - \bar{r}_S) \cdot (\bar{r}_T - \bar{r}_S)]^{1/2}} + \frac{(\bar{r}_T - \bar{r}_S) \cdot (\dot{\bar{r}}_T - \dot{\bar{r}}_S) (\bar{r}_T - \bar{r}_S) \cdot \delta \bar{r}_S}{[(\bar{r}_T - \bar{r}_S) \cdot (\bar{r}_T - \bar{r}_S)]^{3/2}}$$

$$\hat{i}_r = \frac{\bar{r}}{|\bar{r}|}$$

$$\dot{r} = \hat{i}_r \cdot \dot{\bar{r}}$$

$$\delta \dot{r} = \begin{bmatrix} \frac{-1}{|\bar{r}|} [\hat{i}_r \times (\dot{\bar{r}} \times \hat{i}_r)] \\ -\hat{i}_r \end{bmatrix}^T \begin{bmatrix} \delta \bar{r}_S \\ \dot{\bar{r}}_S \end{bmatrix}$$

$$\therefore \bar{b} = \begin{bmatrix} \frac{1}{|\bar{r}|} [\hat{i}_r \times (\dot{\bar{r}} \times \hat{i}_r)] \\ \bar{i}_r \end{bmatrix}$$

"-" if orbiter state is updated
"+" if target state is updated

Star tracker vertical angle (v) measurement partial is in the plane of the measurement along the line of sight.

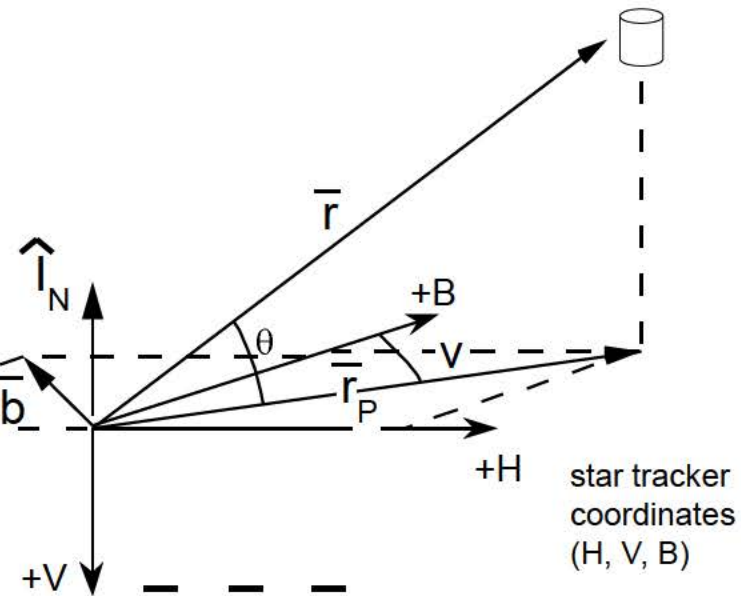
$$M_{M50 \text{ to ST}} (\bar{r}_T - \bar{r}_S) = |\bar{r}_T - \bar{r}_S| \begin{bmatrix} \cos(\theta) \sin(v) \\ -\sin(\theta) \\ \cos(\theta) \cos(v) \end{bmatrix}$$

$$-\delta \bar{r}_S = |\bar{r}| M_{M50 \text{ to ST}}^T \begin{bmatrix} \cos(\theta) \cos(v) \\ 0 \\ -\cos(\theta) \sin(v) \end{bmatrix} \delta v$$

$$\delta v = \frac{-1}{|\bar{r}_P|} \text{unit}(\bar{r}_P \times \hat{\mathbf{i}}_N) \cdot \delta \bar{r}_S$$

$$\therefore \bar{b} = \mp \frac{1}{|\bar{r}_P|} \text{unit}(\bar{r}_P \times \hat{\mathbf{i}}_N)$$

"-" if orbiter state is updated
"+" if target state is updated



$$\bar{r} = \bar{r}_T - \bar{r}_S$$

$$\hat{\mathbf{i}}_N = M_{M50 \text{ to ST}}^T \begin{bmatrix} 0 \\ -1 \\ 0 \end{bmatrix}$$

$$\bar{r}_P = \bar{r} - (\bar{r} \cdot \hat{\mathbf{i}}_N) \hat{\mathbf{i}}_N$$

Star tracker horizontal angle (h) measurement partial is in the plane of the measurement along the line of sight.

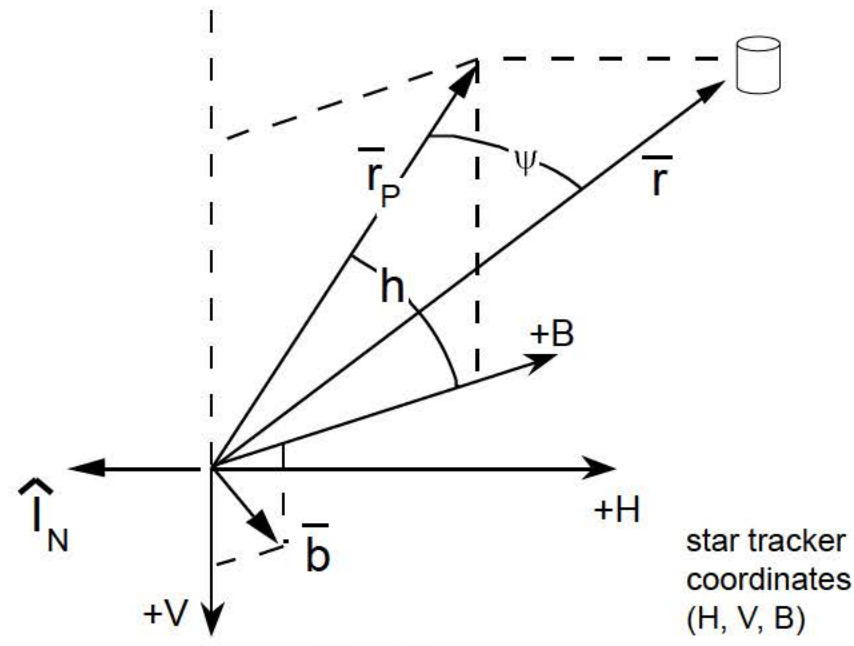
$$M_{M50 \text{ to ST}}(\bar{r}_T - \bar{r}_S) = |\bar{r}_T - \bar{r}_S| \begin{bmatrix} \sin(\psi) \\ -\cos(\psi) \sin(h) \\ \cos(\psi) \cos(h) \end{bmatrix}$$

$$-\delta \bar{r}_S = |\bar{r}| M_{M50 \text{ to ST}}^T \begin{bmatrix} 0 \\ -\cos(\psi) \cos(h) \\ -\cos(\psi) \sin(h) \end{bmatrix} \delta h$$

$$\delta h = \frac{-1}{|\bar{r}_P|} \text{unit}(\bar{r}_P \times \hat{\mathbf{l}}_N) \cdot \delta \bar{r}_S$$

$$\therefore \bar{b} = \mp \frac{1}{|\bar{r}_P|} \text{unit}(\bar{r}_P \times \hat{\mathbf{l}}_N)$$

"-" if orbiter state is updated
"+" if target state is updated



$$\bar{r} = \bar{r}_T - \bar{r}_S$$

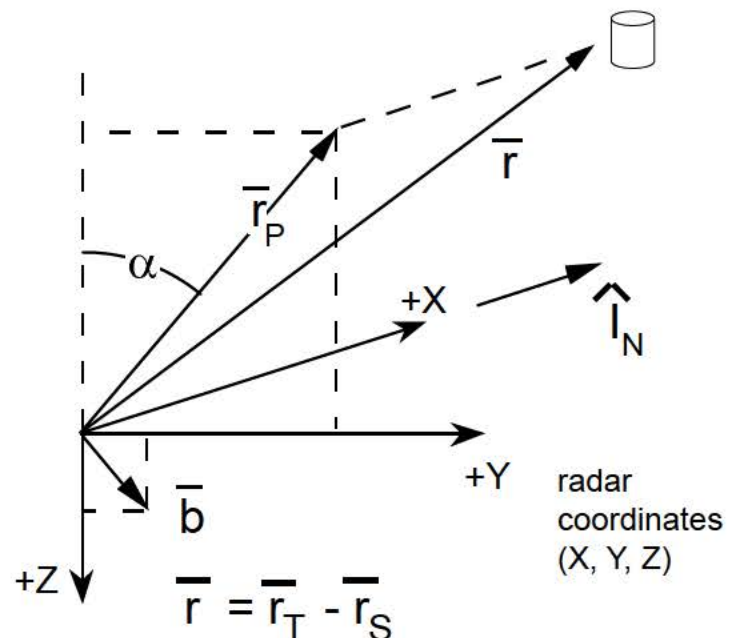
$$\hat{\mathbf{l}}_N = M_{M50 \text{ to ST}}^T \begin{bmatrix} -1 \\ 0 \\ 0 \end{bmatrix}$$

$$\bar{r}_P = \bar{r} - (\bar{r} \cdot \hat{\mathbf{l}}_N) \hat{\mathbf{l}}_N$$

Radar shaft angle (α) measurement partial.

$$\bar{b} = \mp \frac{1}{|\bar{r}_P|} \text{unit}(\bar{r}_P \times \hat{l}_N)$$

"-" if orbiter state is updated
"+" if target state is updated



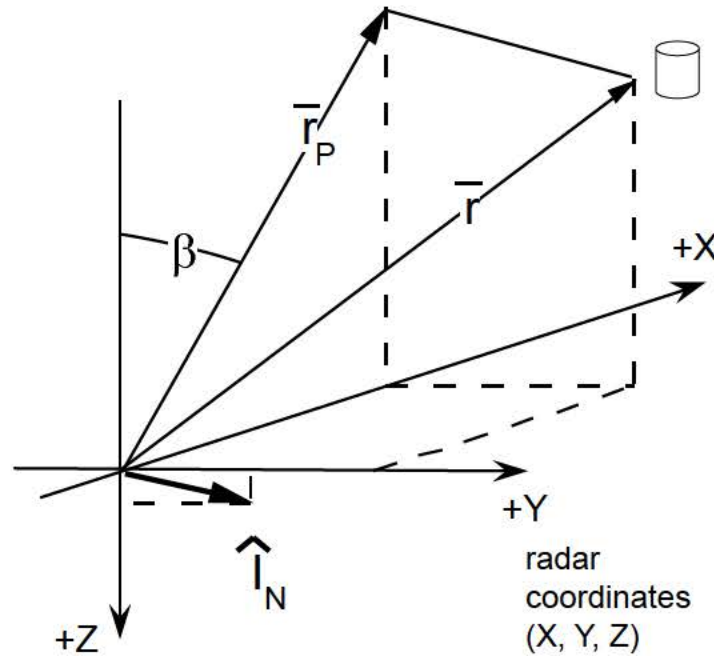
$$\hat{l}_N = M_{\text{radar to M50}} \begin{bmatrix} 1 \\ 0 \\ 0 \end{bmatrix}$$

$$\bar{r}_P = \bar{r} - (\bar{r} \cdot \hat{l}_N) \hat{l}_N$$

Radar trunnion angle (β) measurement partial.

$$\bar{b} = \mp \frac{1}{|\bar{r}_P|} \text{ unit}(\bar{r}_P \times \hat{\mathbf{i}}_N)$$

"-" if orbiter state is updated
"+" if target state is updated



$$\bar{r} = \bar{r}_T - \bar{r}_S \quad \hat{\mathbf{i}}_{+X} = \begin{bmatrix} 1 \\ 0 \\ 0 \end{bmatrix}$$

$$\hat{\mathbf{i}}_N = -\text{Unit} \left[\hat{\mathbf{i}}_r \times \begin{bmatrix} M_{\text{radar}} & \hat{\mathbf{i}}_{+X} \\ \text{to M50} & \end{bmatrix} \right]$$

$$\bar{r}_P = \bar{r} - (\bar{r} \cdot \hat{\mathbf{i}}_N) \hat{\mathbf{i}}_N$$

Summary Of Measurement Partial:

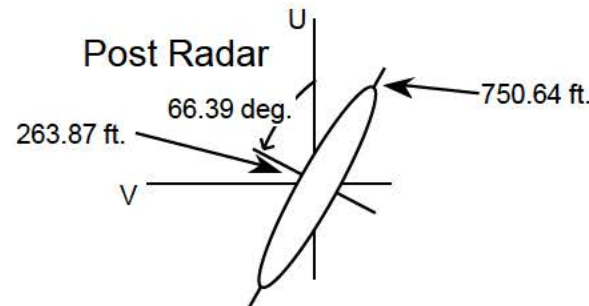
Range - Measurement partial is along the line of sight.

Range Rate - Velocity component of measurement partial is along the line of sight, position component is normal to the line of sight.

Angles - Measurement partial is perpendicular to the line of sight and in the plane of the measurement.

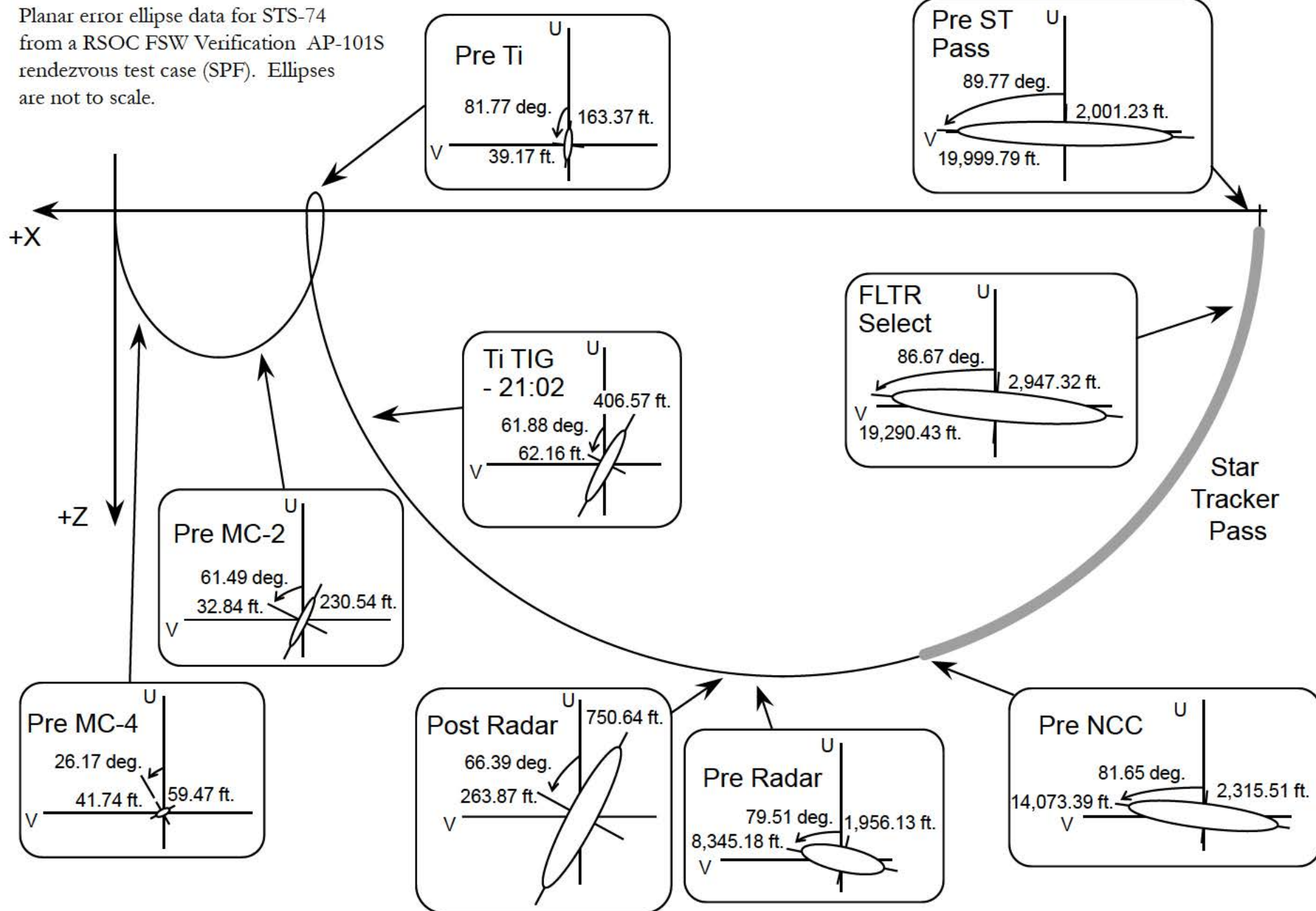
Sign of Measurement Partial – “-” for filter updates of orbiter state, “+” for updates of target state.

A covariance matrix may be represented as an equal probability ellipsoid. The covariance matrix is initialized using ILOADs in UVW for convenience, then it is rotated into the M50 frame for measurement processing during rendezvous. All covariance computations during measurement incorporation are performed in inertial (M50) space. The principal axes of the error ellipsoid are not necessarily aligned with the UVW axes, rather they are a function of the measurement partials (i.e. relative geometry).



Orientation of principal axes
with respect to U, V frame.

Planar error ellipse data for STS-74 from a RSOC FSW Verification AP-101S rendezvous test case (SPF). Ellipses are not to scale.

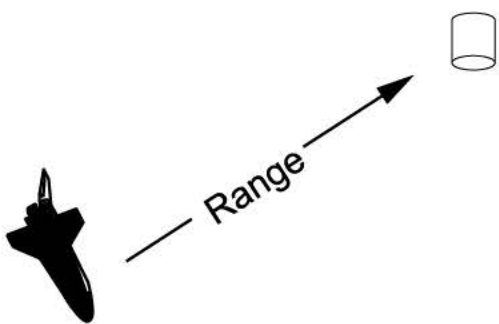


9.8 On - Board Navigation Derived Relative State Data

The Relative Navigation (REL NAV, SPEC 33) display contains ORBITER relative position and velocity parameters computed from ORBITER and TARGET state vectors. LVLH data is not given, but range, range rate, elevation angle, out-of-plane position, and out-of-plane velocity are given.

2021/033 /			REL NAV			1 005/02:07:37		
RNDZ	NAV	ENA 1*	SV UPDATE			000/00:00:00		
KU ANT	ENA 2*		POS	0.02		AVG G ON	5*	
MEAS	ENA 3		VEL	0.03		GPS		
NAV								
SV SEL	4 FLTR		RR GPC			STAT	P	1 σ DES
RNG	25.721		RNG	25.610		1		75 31
\dot{R}	- 21.19		\dot{R}	- 20.80		2*		75 32
θ	25.76		EL	- 0.4		3		75 33
Y	+ 0.08		AZ	- 0.8		SV TRANSFER		
\dot{Y}	+ 0.1	\oplus P		+ 0.8		FLTR	MINUS PROP	
NODE	2:54:00	\oplus R		+ 0.1		POS		4.99
FILTER								
S TRK	12	RR 13*	COAS	14		VEL		5.72
STAT			X	- 3.4		FLTR	TO PROP	8
FLTR UPDATE	15	ORB	Y	+ 4.4		PROP	TO FLTR	9
COVAR REINIT	16					ORB	TO TGT	10
EDIT OVRD								
RES ID	RATIO	ACPT	REJ			TGT	TO ORB	11
RNG	+ 0.09	0.2	807	0		AUT	INH	FOR
\dot{R}	+ 0.02	0.0	807	0		17*	18	19
V/EL / Y	+ 0.02	0.0	807	0		20*	21	22
H/AZ / X	+ 0.01	0.0	807	0		23*	24	25
GPS P	+ 0.19	0.4				42	43 *	44
V	+ 0.26	0.3						

Range



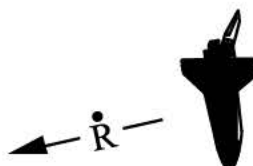
Range (in kilofeet) is the distance between the ORBITER and the TARGET as measured along the line-of-sight from the ORBITER to the TARGET.

2021/033 /			REL	NAV	1 005 / 02 : 07 : 37
RNDZ	NAV	ENA	1*	SV UPDATE	000 / 00 : 00 : 00
KU ANT		ENA	2*	POS	Avg G ON
MEAS		ENA	3	VEL	5*
NAV			GPS		
SV SEL	4	FLTR	RR	GPC	STAT P 1 σ DES
RNG	25.721		RNG	25.610	1 75 31
R	-	21.19	R	-	2 * 75 32
θ	25.76		EL	-	3 75 33
Y	+ 0.08		AZ	- 0.4	SV TRANSFER
Ẏ	+ 0.1		ΦP	+ 0.8	FLTR MINUS PROP
NODE	2:54:00		ΦR	+ 0.1	POS 4.99
FILTER					
S TRK	12	RR 13*	COAS	14	VEL 5.72
STAT			X	- 3.4	FLTR TO PROP 8
FLTR UPDATE	15	ORB	Y	+ 4.4	PROP TO FLTR 9
COVAR REINIT	16		TGT	TO TGT 10	ORB TO TGT 10
				TO ORB 11	TGT TO ORB 11
EDIT OVRD					
RNG	+ 0.09	0.2	807	0	AUT 17* 18 19
R	+ 0.02	0.0	807	0	INH 20* 21 22
V/EL/Y	+ 0.02	0.0	807	0	FOR 23* 24 25
H/AZ/X	+ 0.01	0.0	807	0	
GPS P	+ 0.19	0.4			42 43* 44
V	+ 0.26	0.3			

Range Rate



Negative Range Rate
(Range Decreases)

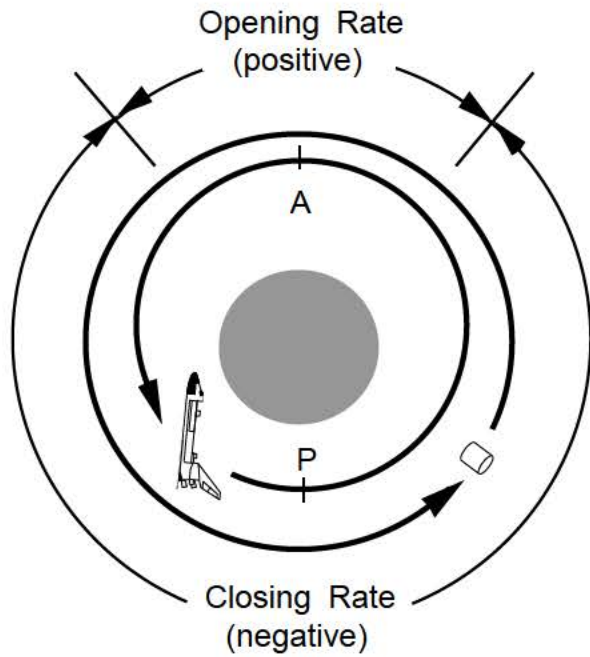


Positive Range Rate
(Range Increases)

Range rate (in feet/second) is the ORBITER velocity relative to the TARGET measured along the line-of-sight to the TARGET.

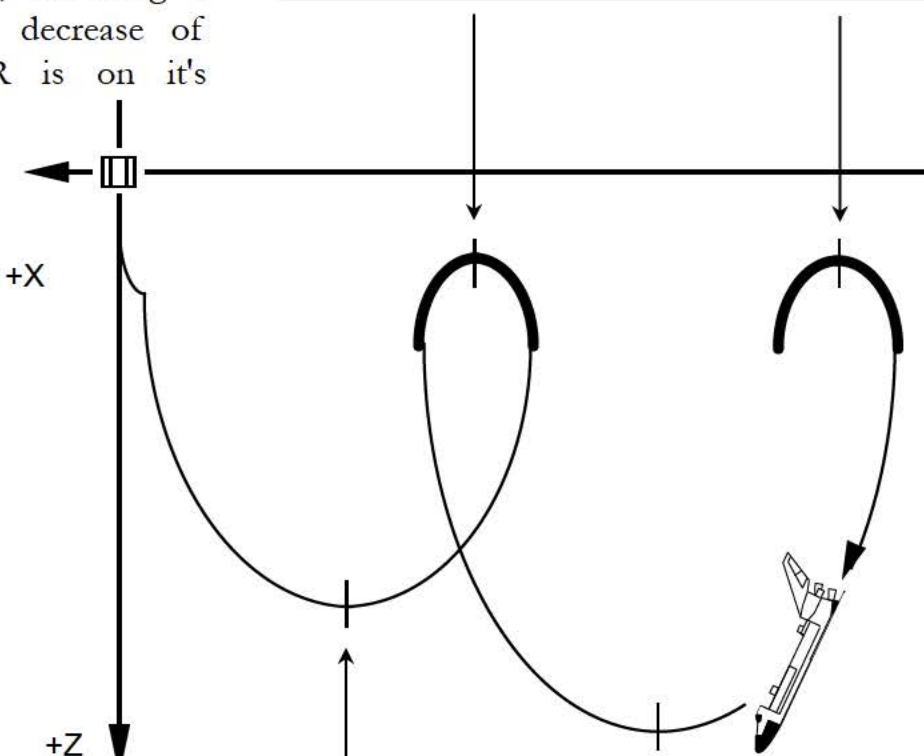
2021/033 /	REL NAV	1 005 / 02 : 07 : 37
RNDZ NAV ENA 1*	SV UPDATE	000 / 00 : 00 : 00
KU ANT ENA 2*	POS 0 . 0 2	Avg G ON 5*
MEAS ENA 3	VEL 0 . 0 3	GPS
NAV		STAT P 1 σ DES
SV SEL 4 FLTR	RR GPC	1 75 31
RNG 25 . 721	RNG 25 . 610	2* 75 32
\dot{R} - 21 . 19	\dot{R} - 20 . 80	3 75 33
θ 25 . 76	EL - 0 . 4	SV TRANSFER
Y + 0 . 08	AZ - 0 . 8	FLTR MINUS PROP
\dot{Y} + 0 . 1	ω_P + 0 . 8	POS 4 . 99
NODE 2 : 54 : 00	ω_R + 0 . 1	VEL 5 . 72
FILTER		FLTR TO PROP 8
S TRK 12 RR 13*	COAS 14	PROP TO FLTR 9
STAT	X - 3 . 4	ORB TO TGT 10
FLTR UPDATE 15	ORB Y + 4 . 4	TGT TO ORB 11
COVAR REINIT 16		EDIT OVRD
RESID	RATIO ACPT REJ	AUT INH FOR
RNG + 0 . 09	0 . 2 807 0	17* 18 19
\dot{R} + 0 . 02	0 . 0 807 0	20* 21 22
V / EL / Y + 0 . 02	0 . 0 807 0	23* 24 25
H / AZ / X + 0 . 01	0 . 0 807 0	
GPS P + 0 . 19	0 . 4	42 43 * 44
V + 0 . 26	0 . 3	

Range rate varies as the magnitude of the ORBITER's velocity varies (since the TARGET's velocity is constant in magnitude, assuming a circular TARGET orbit). Polarity and the increase or decrease of range rate is an indication of where the ORBITER is on its rendezvous profile.



Inertial Space

Relative Apogee (A) - Maximum Opening Rate

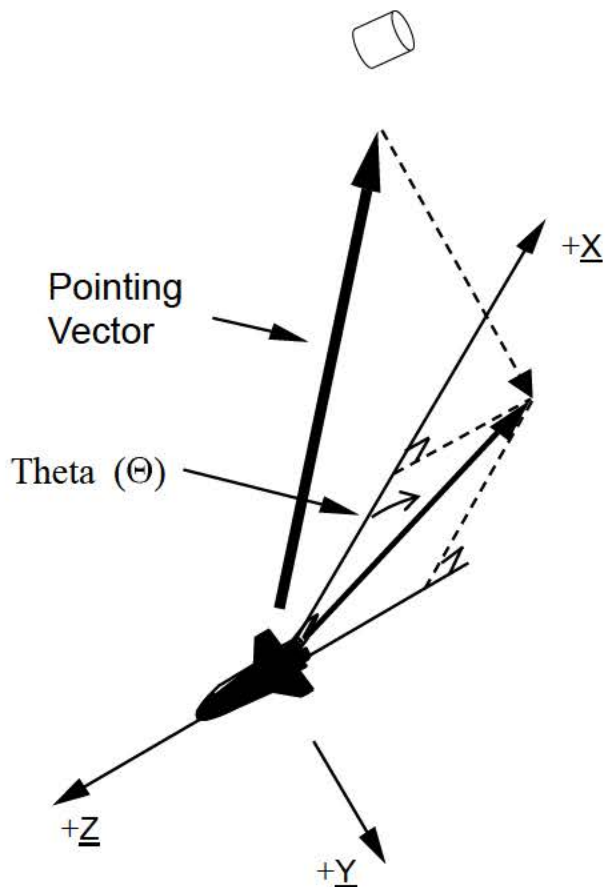


Relative Perigee (P) - Maximum Closing Rate

— Closing Rate (negative)
— Opening Rate (positive)

LVLH Space

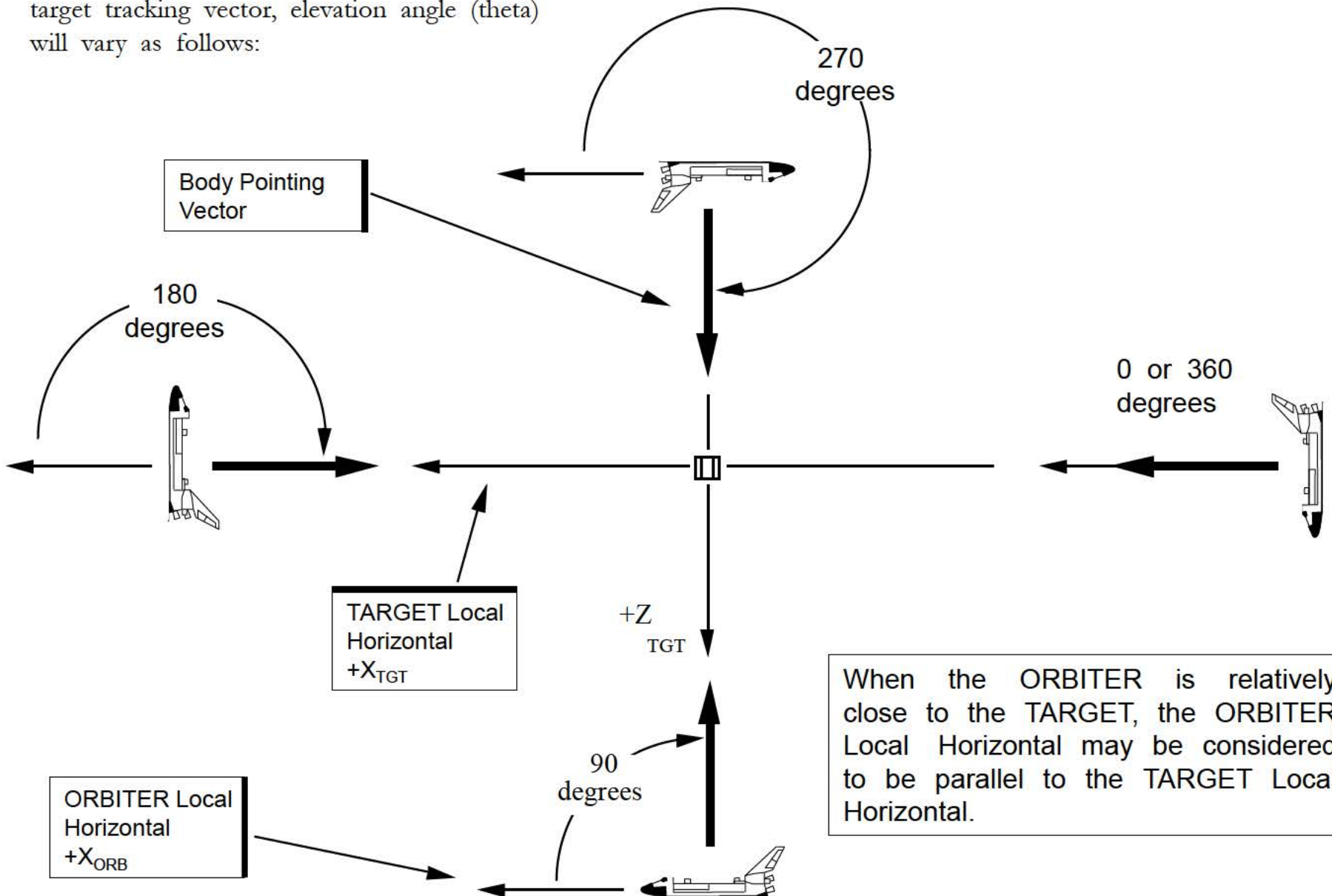
Elevation Angle (Theta)



Angle (in degrees) from the LVLH X axis to the projection of the Universal Pointing defined body pointing vector into the orbital plane of the ORBITER. This angle is computed in an ORBITER centered LVLH frame.

2021/033 /	REL NAV	1 005 / 02 : 07 : 37
RNDZ NAV ENA 1*	SV UPDATE	000 / 00 : 00 : 00
KU ANT ENA 2*	POS 0 . 02	AVG G ON 5 *
MEAS ENA 3	VEL 0 . 03	
	NAV	GPS
SV SEL 4 FLTR	RR GPC	STAT P 1σ DES
RNG 25 . 721	RNG 25 . 610	1 75 31
Ŕ - 21 . 19	Ŕ - 20 . 80	2 * 75 32
θ 25 . 76	EL - 0 . 4	3 75 33
Y + 0 . 08	AZ - 0 . 8	
Ŷ + 0 . 1	OP + 0 . 8	
NODE 2 : 54 : 00	oR + 0 . 1	
	FILTER	SV TRANSFER
S TRK 12 RR 13 *	COAS 14	FLTR MINUS PROP
STAT	X - 3 . 4	POS 4 . 99
FLTR UPDATE 15 ORB	Y + 4 . 4	VEL 5 . 72
COVAR REINIT 16		FLTR TO PROP 8
	RESID RATIO ACPY REJ	PROP TO FLTR 9
RNG + 0 . 09	0 . 2 807 0	ORB TO TGT 10
Ŕ + 0 . 02	0 . 0 807 0	TGT TO ORB 11
V / EL / Y + 0 . 02	0 . 0 807 0	
H / AZ / X + 0 . 01	0 . 0 807 0	
GPS P + 0 . 19	0 . 4	EDIT OVRD
V + 0 . 26	0 . 3	AUT INH FOR

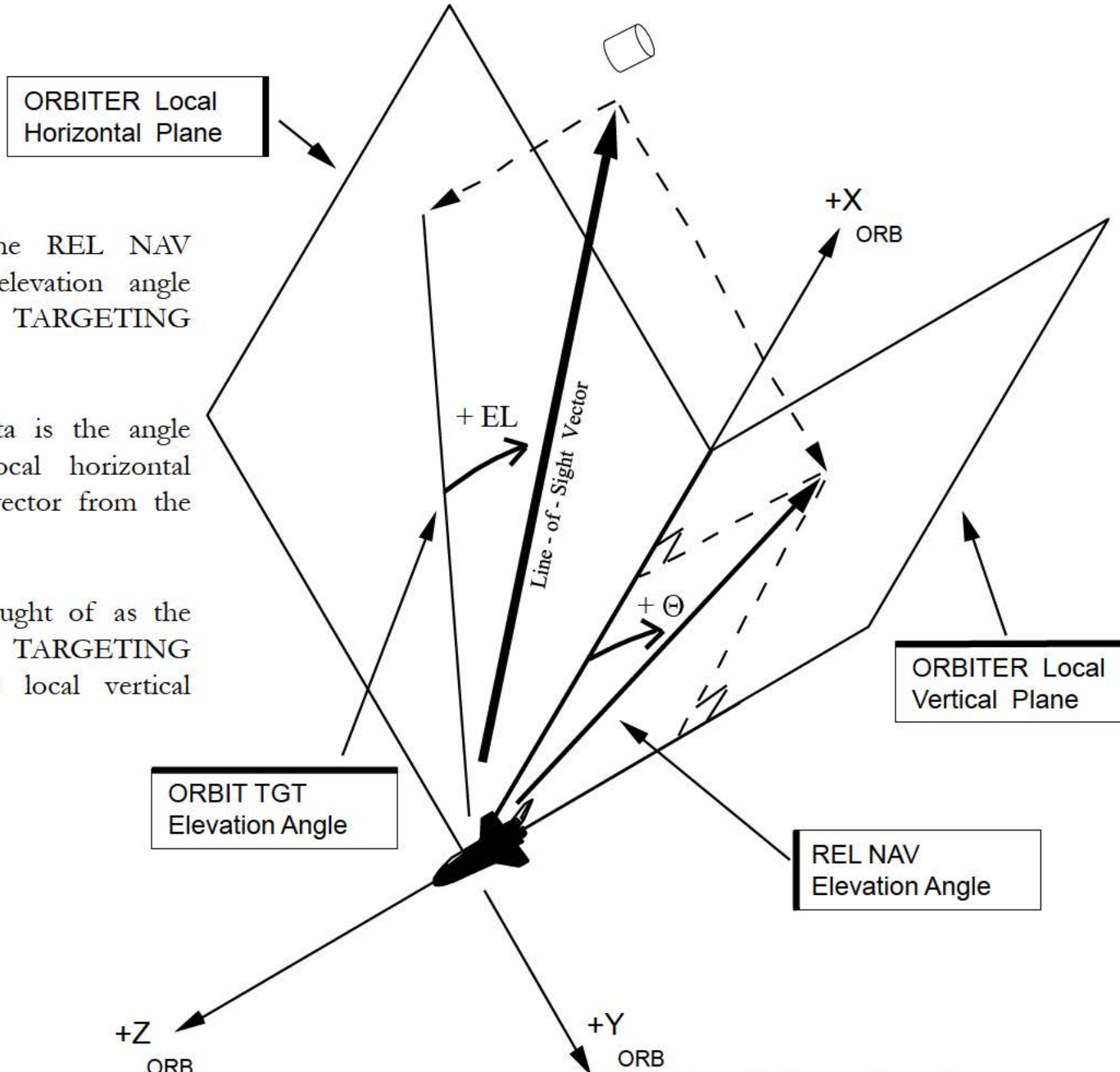
If the -Z orbiter body axis is selected as the target tracking vector, elevation angle (theta) will vary as follows:



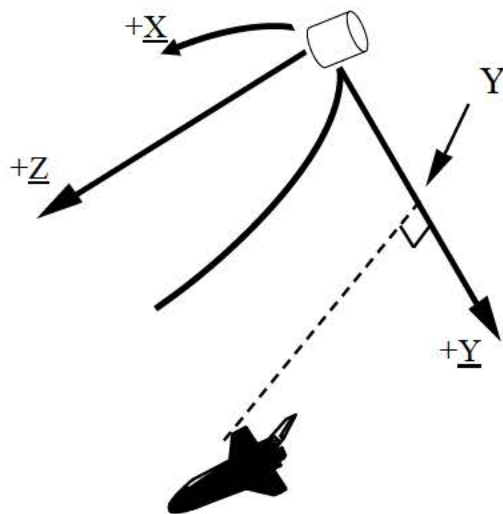
The elevation angle on the REL NAV display is not the same elevation angle used on the ORBIT TARGETING display.

ORBIT TARGETING's theta is the angle between the ORBITER local horizontal plane and the line-of-sight vector from the ORBITER to the TARGET.

REL NAV theta can be thought of as the projection of the ORBIT TARGETING theta into the ORBITER's local vertical plane.



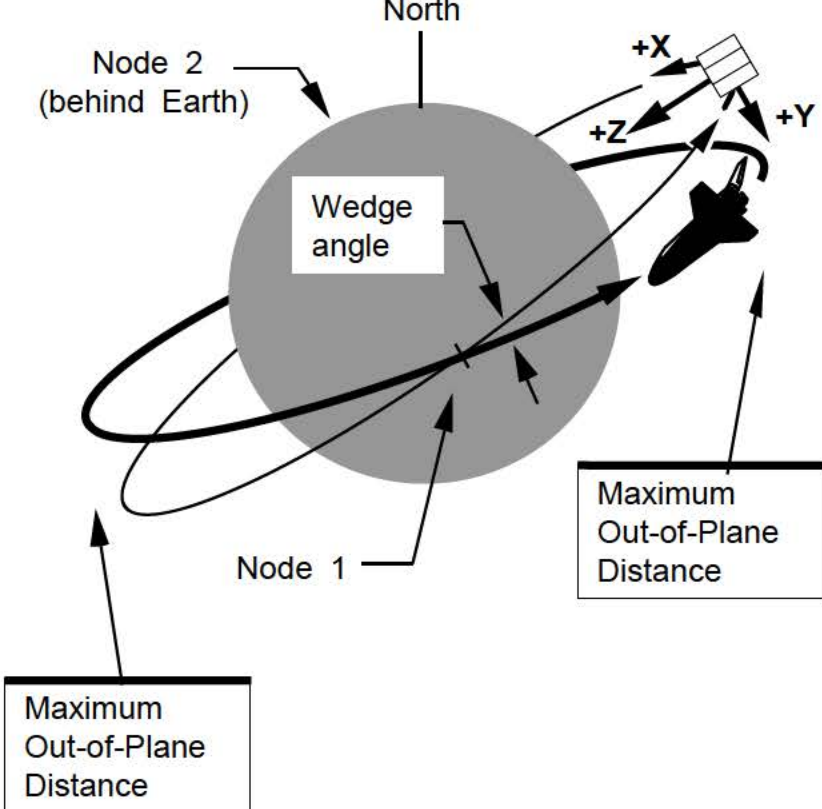
Out-of-Plane Position (Y)



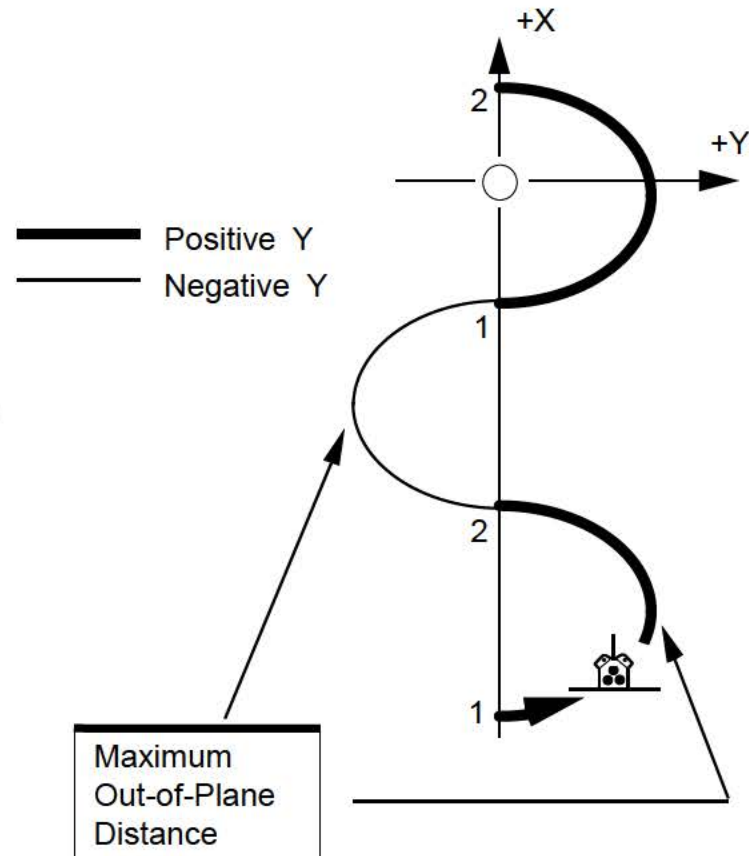
Out-of-plane position (in kilofeet) is the distance from the ORBITER to the orbital plane of the TARGET.

2021/033 /	REL NAV	1 005 / 02 : 07 : 37
RNDZ NAV ENA 1*	SV UPDATE	000 / 00 : 00 : 00
KU ANT ENA 2*	POS 0.02	Avg G ON 5*
MEAS ENA 3	VEL 0.03	
NAV		GPS
SV SEL 4 FLTR	RR GPC	STAT P 1 σ DES
RNG 25.721	RNG 25.610	1 75 31
\dot{R} - 21.19	\dot{R} - 20.80	2* 75 32
θ 25.76	EL - 0.4	3 75 33
Y + 0.08	AZ - 0.8	
\dot{Y} + 0.1	ω P + 0.8	SV TRANSFER
NODE 2:54:00	ω R + 0.1	FLTR MINUS PROP
<hr/>		
FILTER		
S TRK 12	RR 13*	COAS 14
STAT		X - 3.4
FLTR UPDATE 15	ORB	Y + 4.4
COVAR REINIT 16		
RESID	RATIO	EDIT OVRD
RNG + 0.09	0.2	AUT 17* 18 19
\dot{R} + 0.02	0.0	INH 20* 21 22
V/EL/Y + 0.02	0.0	FOR 23* 24 25
H/AZ/X + 0.01	0.0	
GPS P + 0.19	0.4	42 43* 44
V + 0.26	0.3	

Y position is the same as the LVLH Y position. Orbiter out-of-plane motion appears to be sinusoidal due to the wedge angle (difference in inclination) between the orbiter and target orbits.

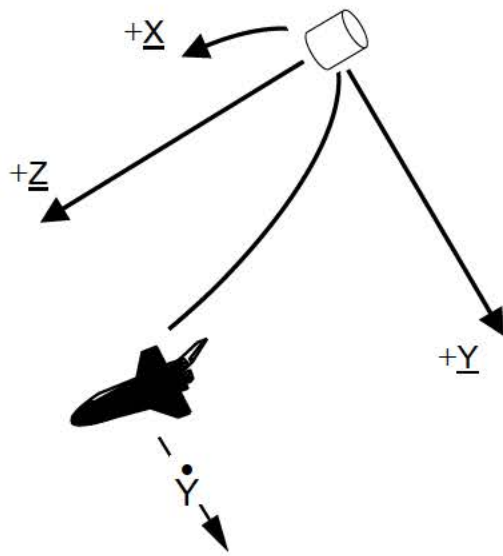


Inertial Space



LVLH Space

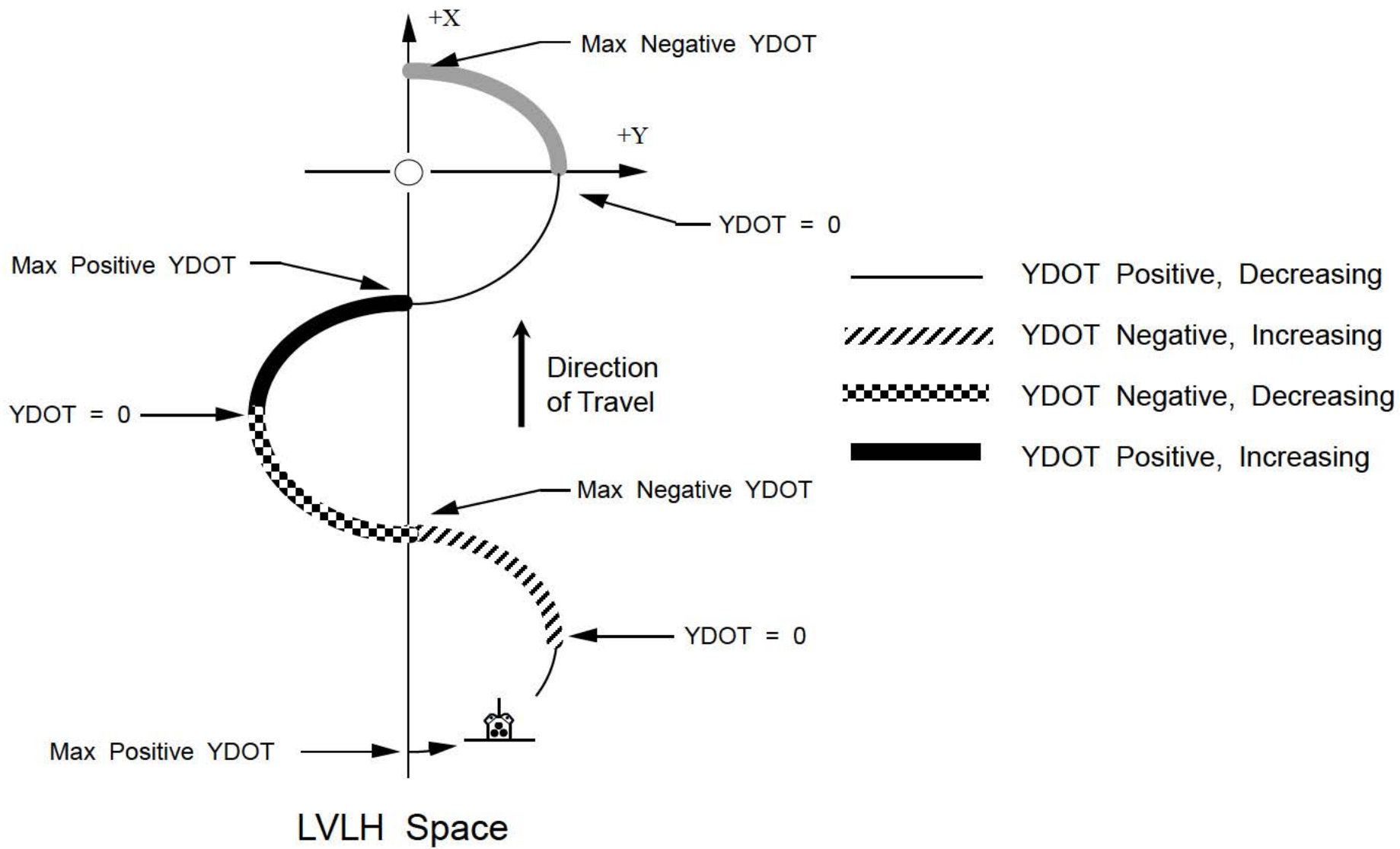
Out-of-Plane Velocity (Y DOT)



Out-of-plane velocity (in feet/second) is the rate at which the ORBITER approaches or moves away from the orbital plane of the TARGET.

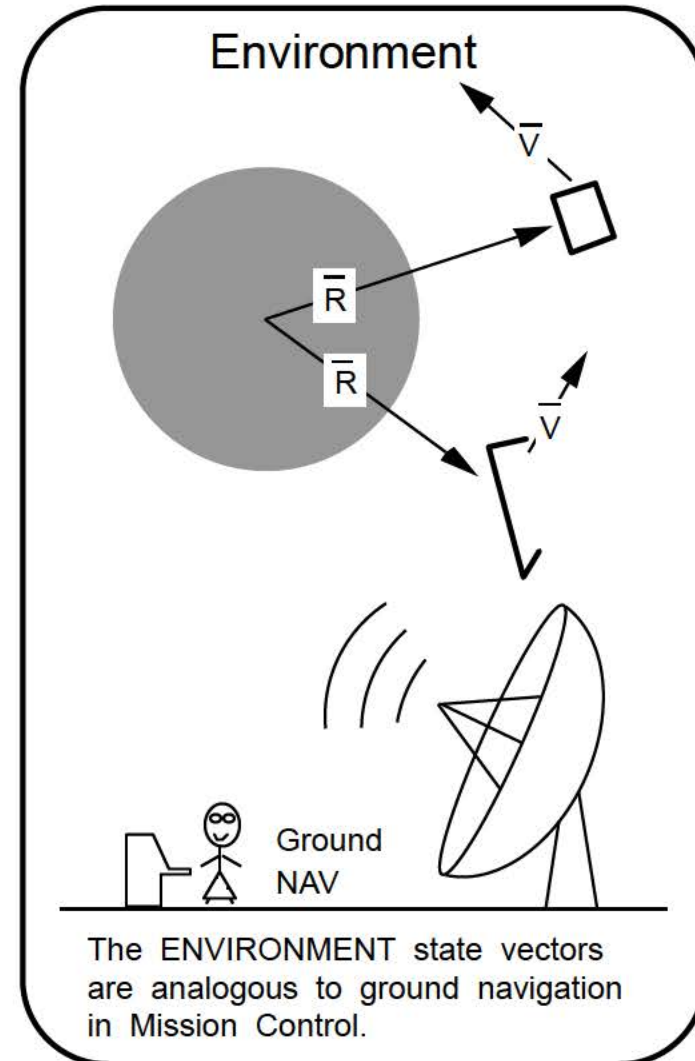
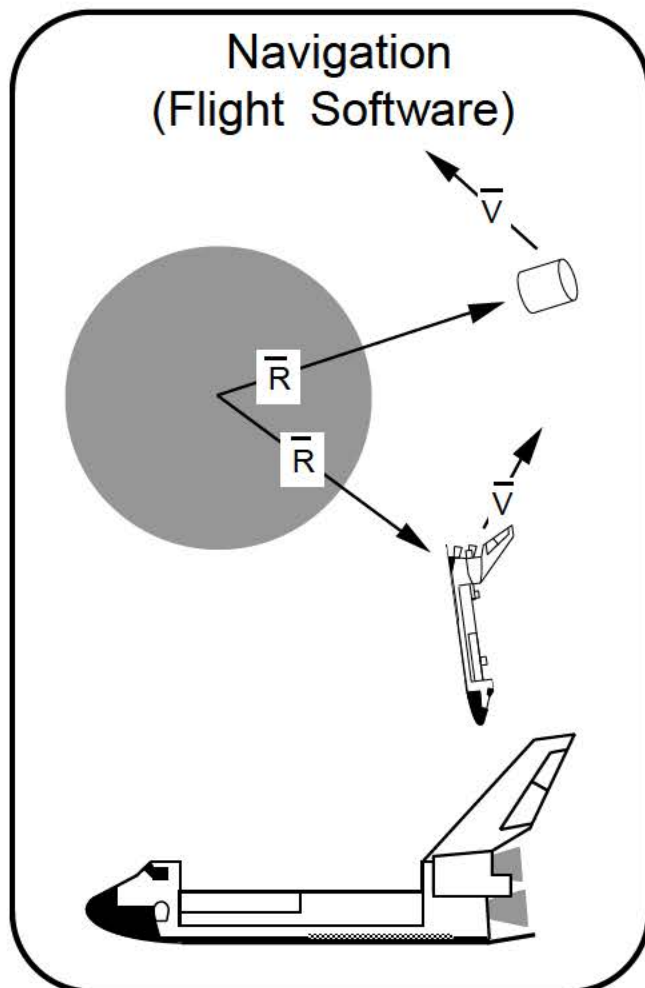
2021 / 033 /	REL	NAV	1 005 / 02 :07 :37
RNDZ NAV ENA 1*	SV UPDATE		000 / 00 :00 :00
KU ANT ENA 2*	POS 0 .02	Avg G ON	5*
MEAS ENA 3	VEL 0 .03	GPS	
	NAV	STAT P 1 σ DES	
SV SEL 4 FLTR	RR GPC	1 75 31	
RNG 25.721	RNG 25.610	2* 75 32	
\dot{R} - 21.19	\dot{R} - 20.80	3 75 33	
θ 25.76	EL - 0 .4	SV TRANSFER	
Y + 0 .08	AZ - 0 .8	FLTR MINUS PROP	
\dot{Y} + 0 .1	\circ P + 0 .8	POS 4 .99	
NODE 2 :54 :00	\circ R + 0 .1	VEL 5 .72	
	FILTER	FLTR TO PROP 8	
S TRK 12	RR 13*	PROP TO FLTR 9	
STAT	COAS 14	ORB TO TGT 10	
FLTR UPDATE 15	X - 3 .4	TGT TO ORB 11	
COVAR REINIT 16	Y + 4 .4	EDIT OVRD	
	RESID RATIO ACPT REJ	AUT INH FOR	
RNG + 0 .09	0 .2 807 0	17* 18 19	
\dot{R} + 0 .02	0 .0 807 0	20* 21 22	
V / EL / Y + 0 .02	0 .0 807 0	23* 24 25	
H / AZ / X + 0 .01	0 .0 807 0		
GPS P + 0 .19	0 .4	42 43* 44	
V + 0 .26	0 .3		

YDOT is the same as YDOT LVLH. YDOT is a maximum when the ORBITER crosses the TARGET'S orbital plane (a node). It is zero at the maximum out-of-plane position.

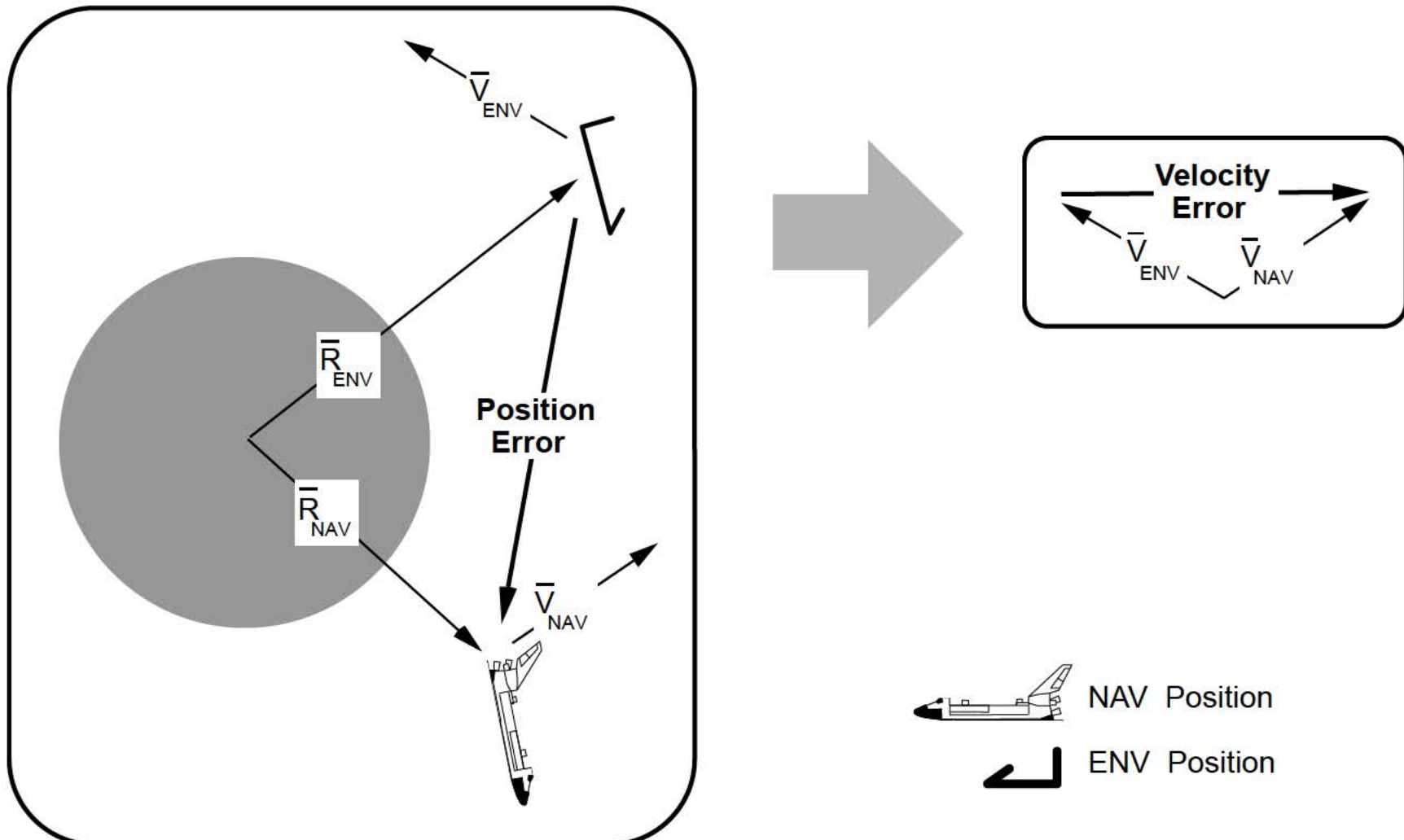


9.9 Inertial State Vector Errors In UVW Coordinates

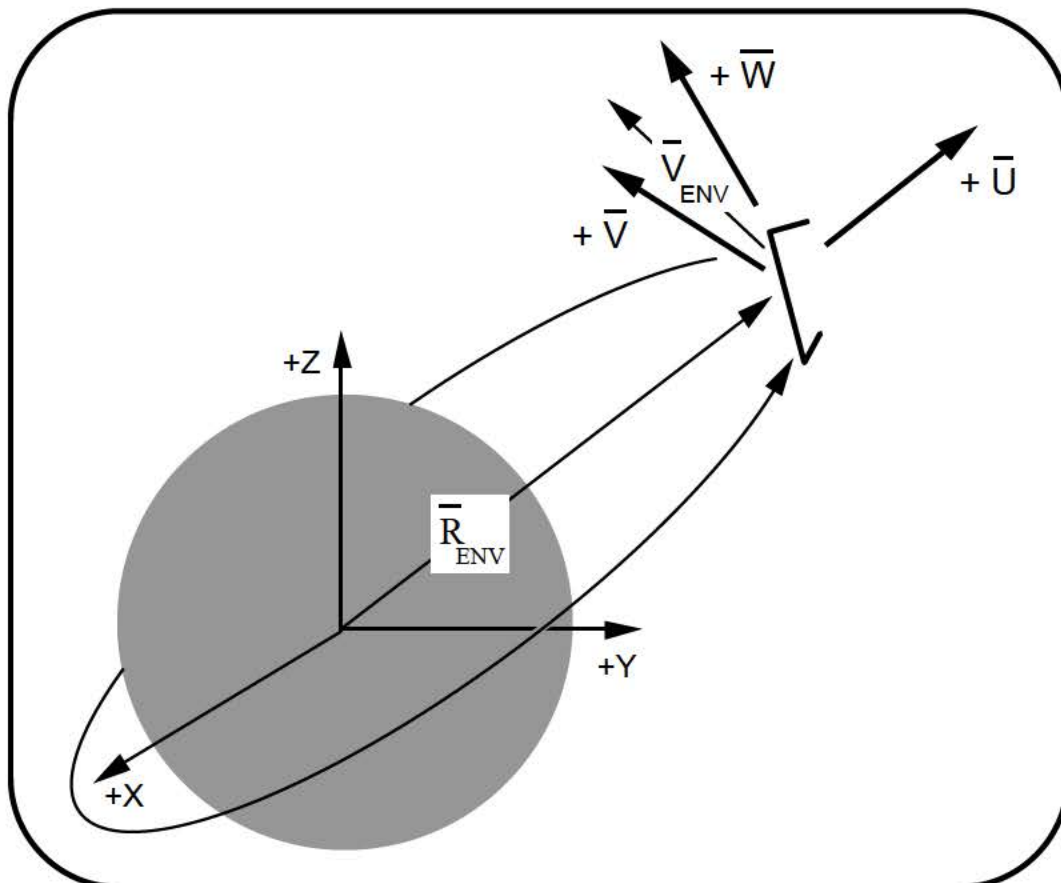
The FSW (NAV) maintains ORBITER and TARGET state vectors. These can be thought of as being the “estimated” state vectors. A simulator (environment) also maintains ORBITER and TARGET state vectors using more accurate (and time consuming) algorithms than the FSW. Environment values are considered to be the “real world” or “correct” values.



The difference between the NAV and Environment (ENV) position vectors at a given time is called the “inertial position error.” The difference in velocity is “inertial velocity error.”



Position and velocity errors can be viewed in the M50 coordinate frame. Since this frame is hard to visualize, another frame, called UVW, is used. UVW is centered on the ENV position.



+ \bar{U} is parallel to the position vector and positive away from the Earth. It can be thought of as the local vertical.

$$+ \bar{U} = \text{Unit}(\bar{R}_{\text{ENV}})$$

+ \bar{W} is along the angular momentum vector (pointing in a northerly direction).

$$+ \bar{W} = \text{Unit}(\bar{R}_{\text{ENV}} \times \bar{V}_{\text{ENV}})$$

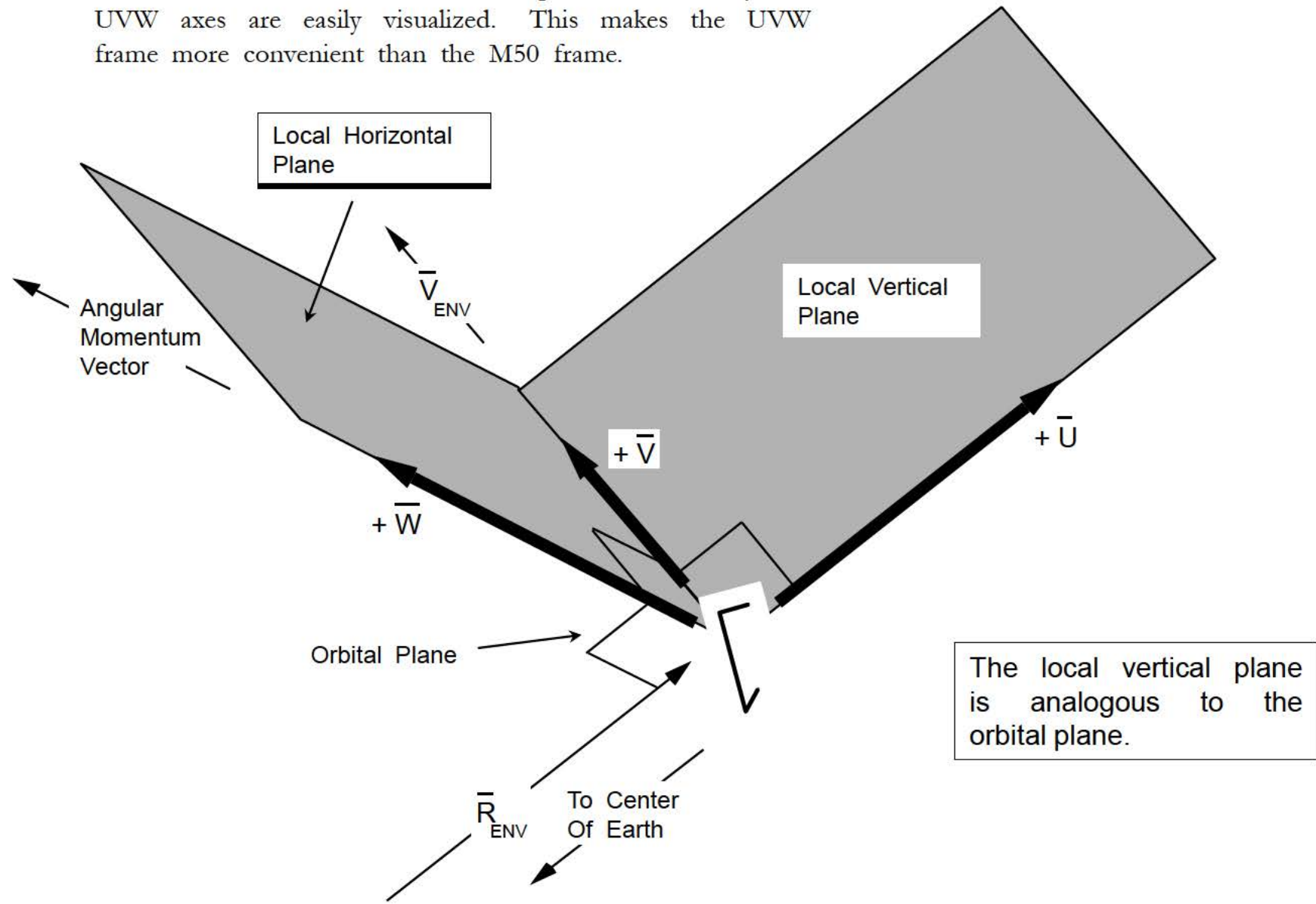
+ \bar{V} completes the right-handed system. It points in the down-range direction.

$$+ \bar{V} = \bar{W} \times \bar{U}$$

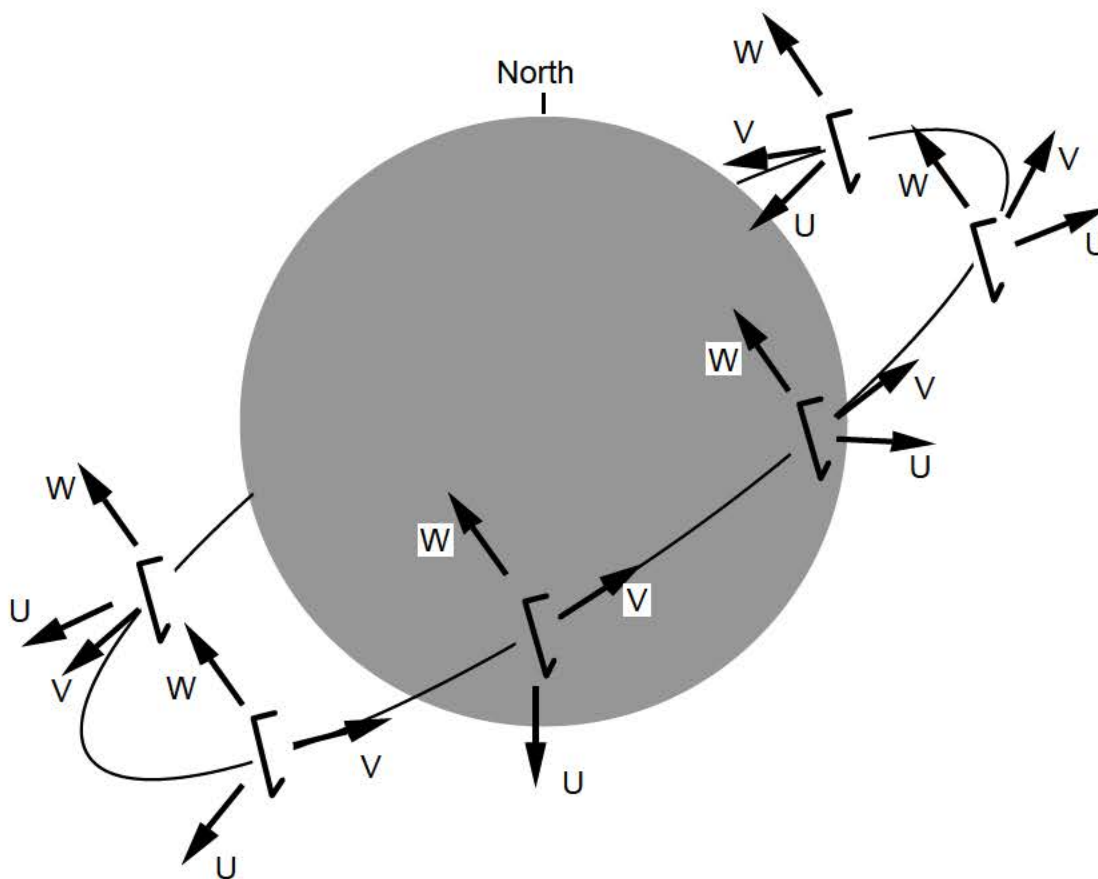
If the orbit is circular, the velocity vector and + \bar{V} will be parallel.

$$\bar{V}_{\text{ENV}} \parallel + \bar{V}$$

Local horizontal and local vertical planes defined by the UVW axes are easily visualized. This makes the UVW frame more convenient than the M50 frame.

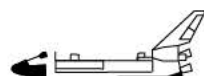
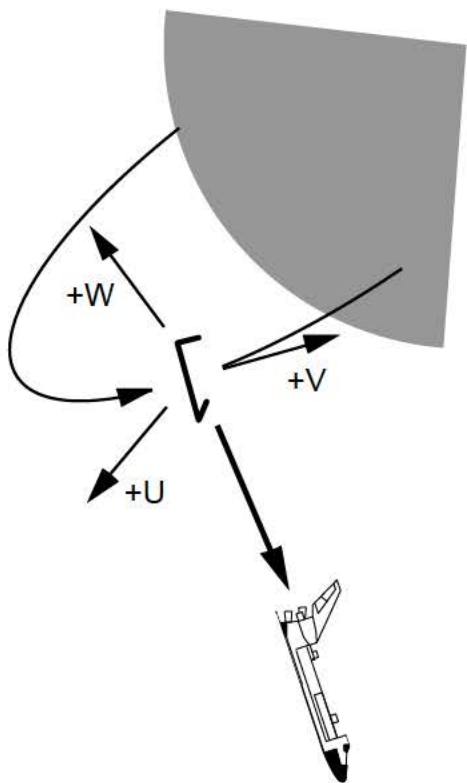


A different UVW frame is defined for each environment state vector. Note that the W axis does not change in orientation (unless two different orbital planes are being compared).



Position error is broken down into components along each UVW axis.

1. Position Error

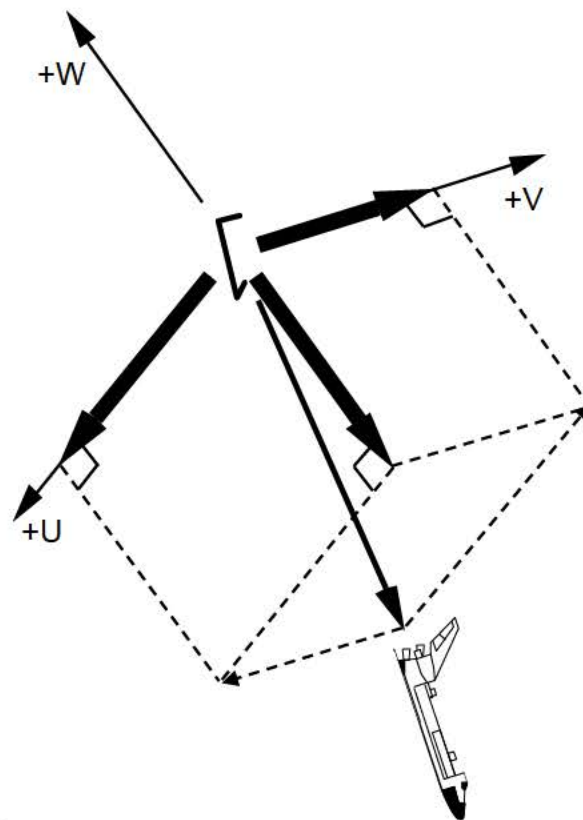


NAV Position



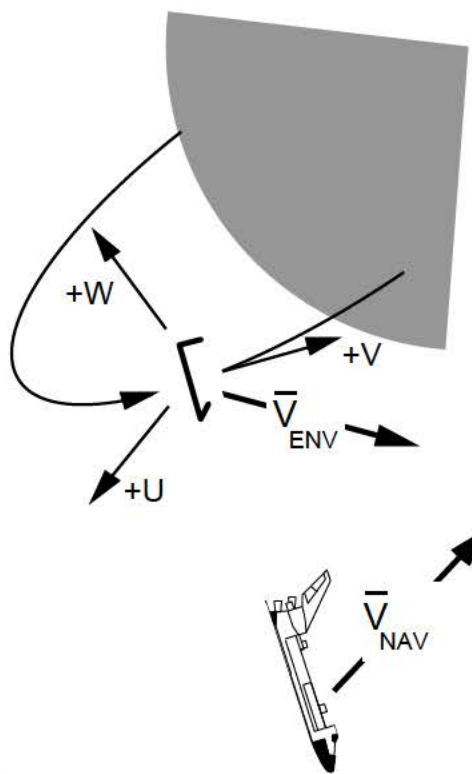
ENV Position

2. Position Error Components In UVW

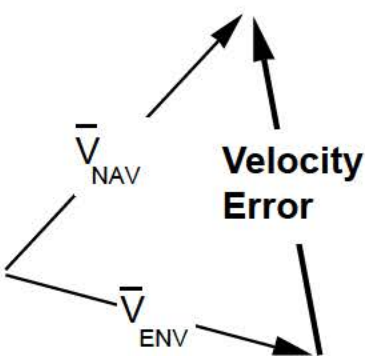


Velocity error is also broken down into UVW components.

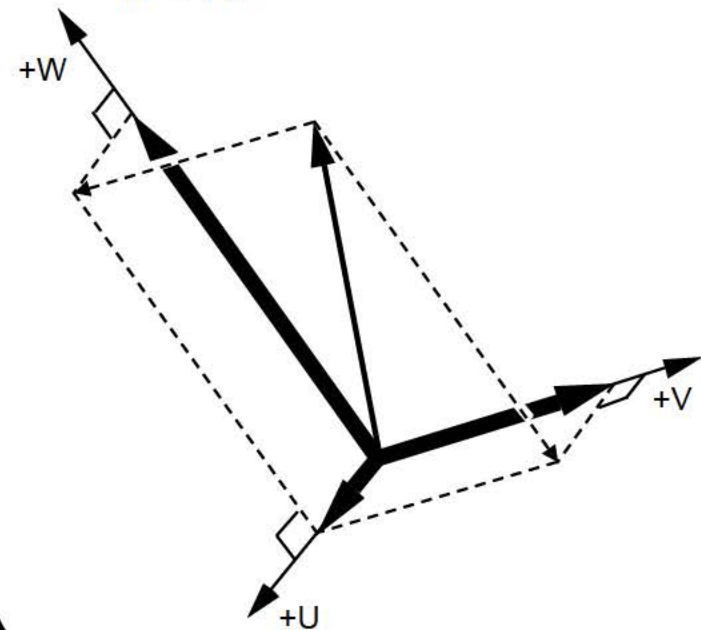
1. ENV and NAV Velocity



2. Inertial Velocity Error

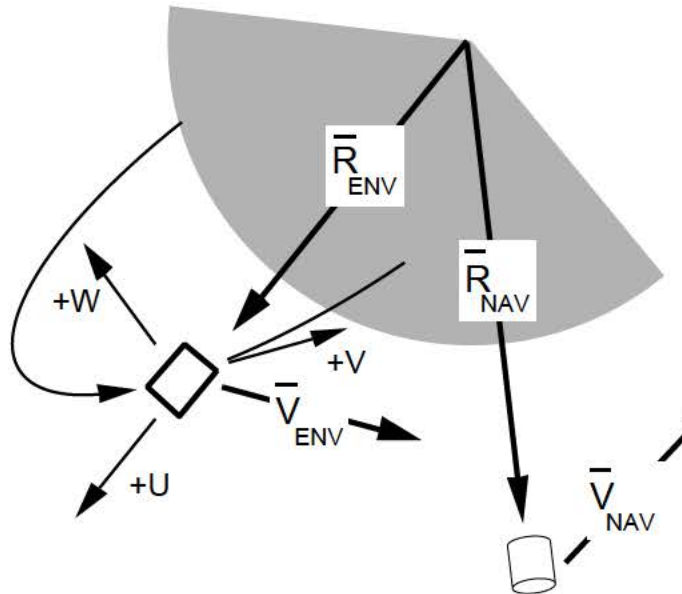


3. Velocity Error Components In UVW

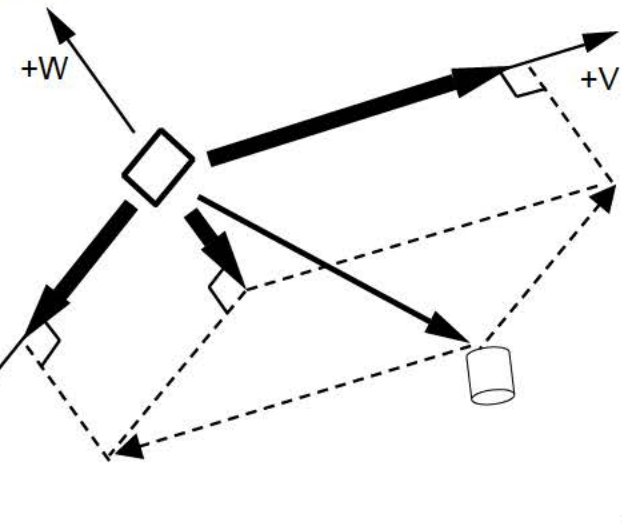


Inertial TARGET position and velocity errors can also be resolved into UVW components.

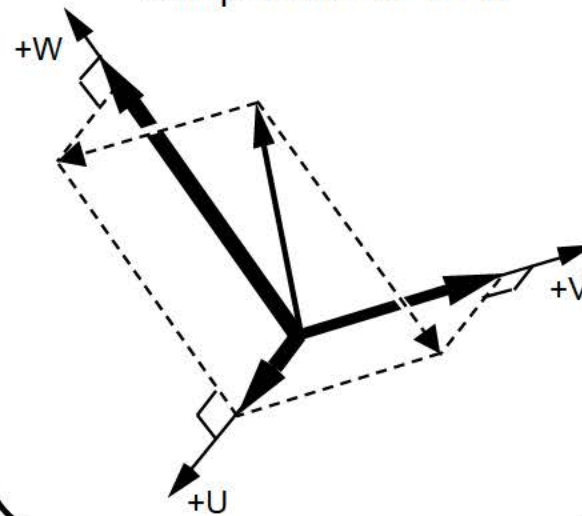
1. TARGET ENV and NAV State Vectors



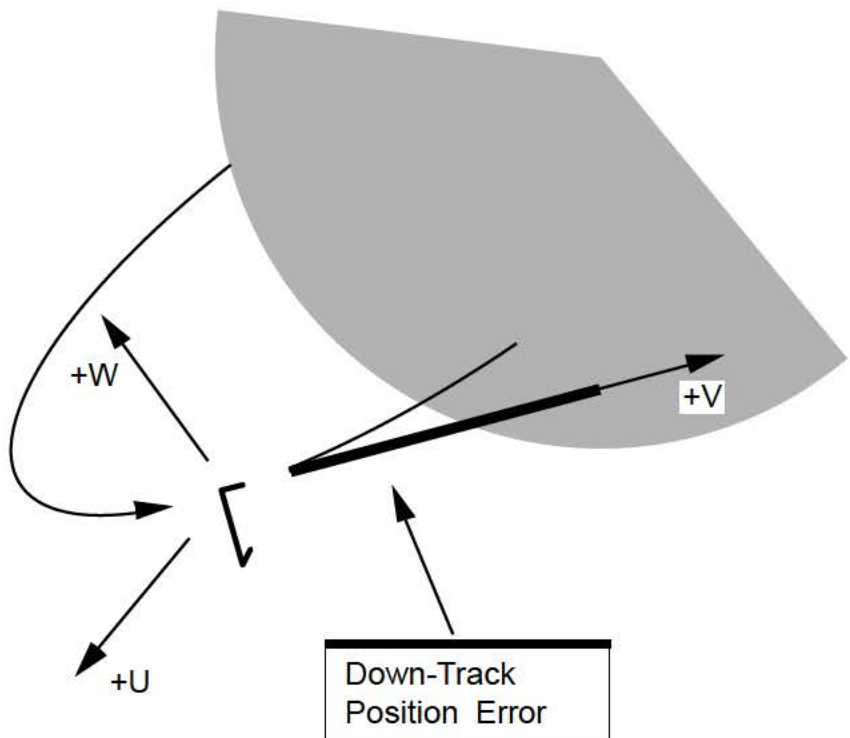
2. TARGET Position Error Components In UVW



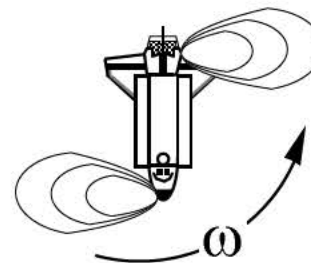
3. TARGET Velocity Error Components In UVW



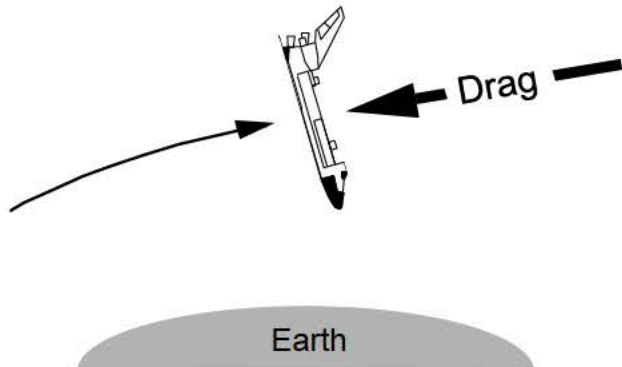
During flight, most position error is in down-track. Radial position error will tend to propagate into down-track position error.



Down-track position error is
Primarily caused by:



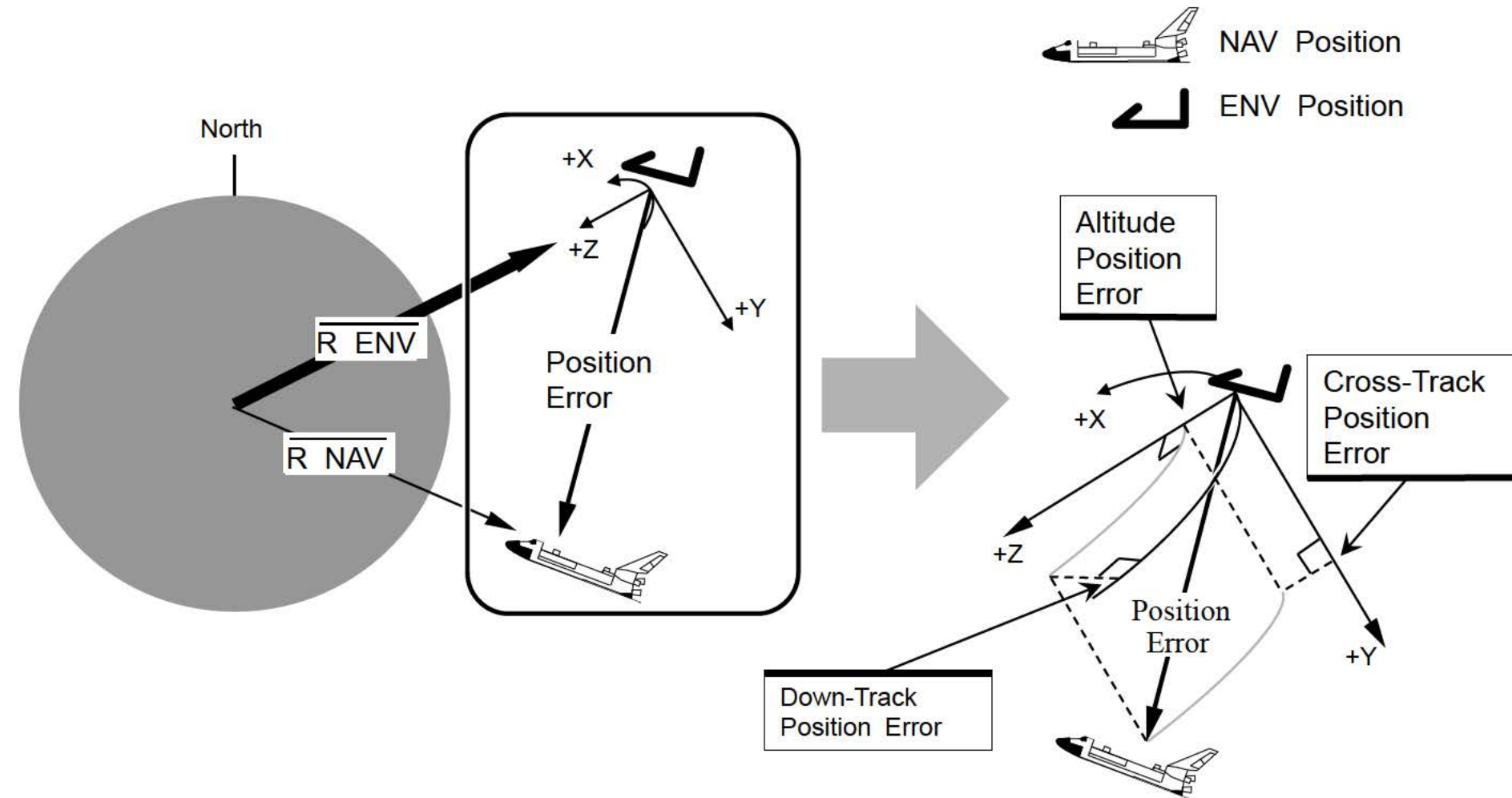
1. Attitude maneuvers produce some in-plane ΔV (in radial as well as down-track).



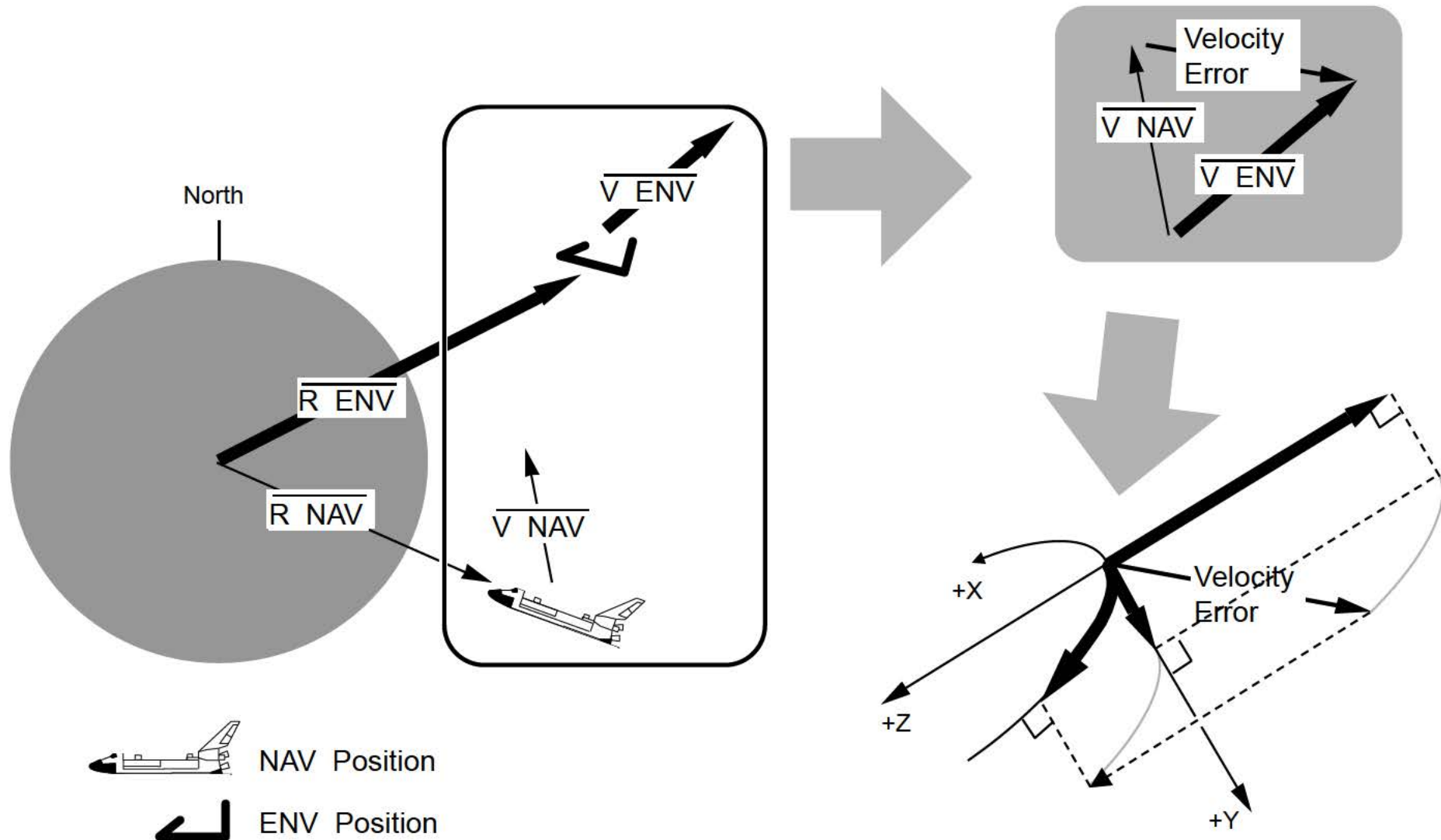
2. Errors in modeling atmospheric drag.

9.10 Inertial State Vector Errors In LVLH Coordinates

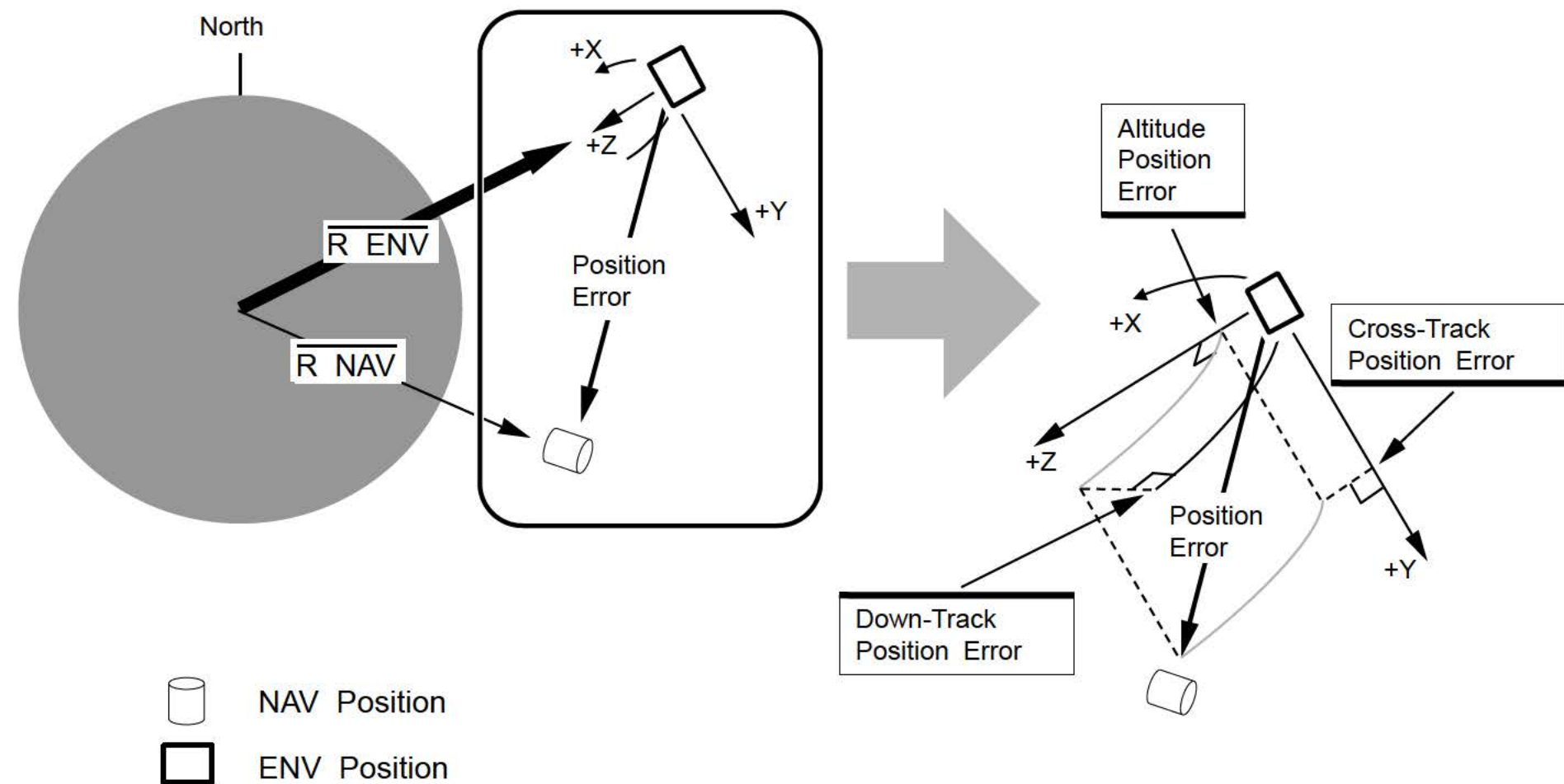
Inertial state errors are usually plotted in the UVW frame. However, the LVLH frame may also be used. A comparison of the NAV (estimated) and ENV (actual) state vectors for the ORBITER can be made.



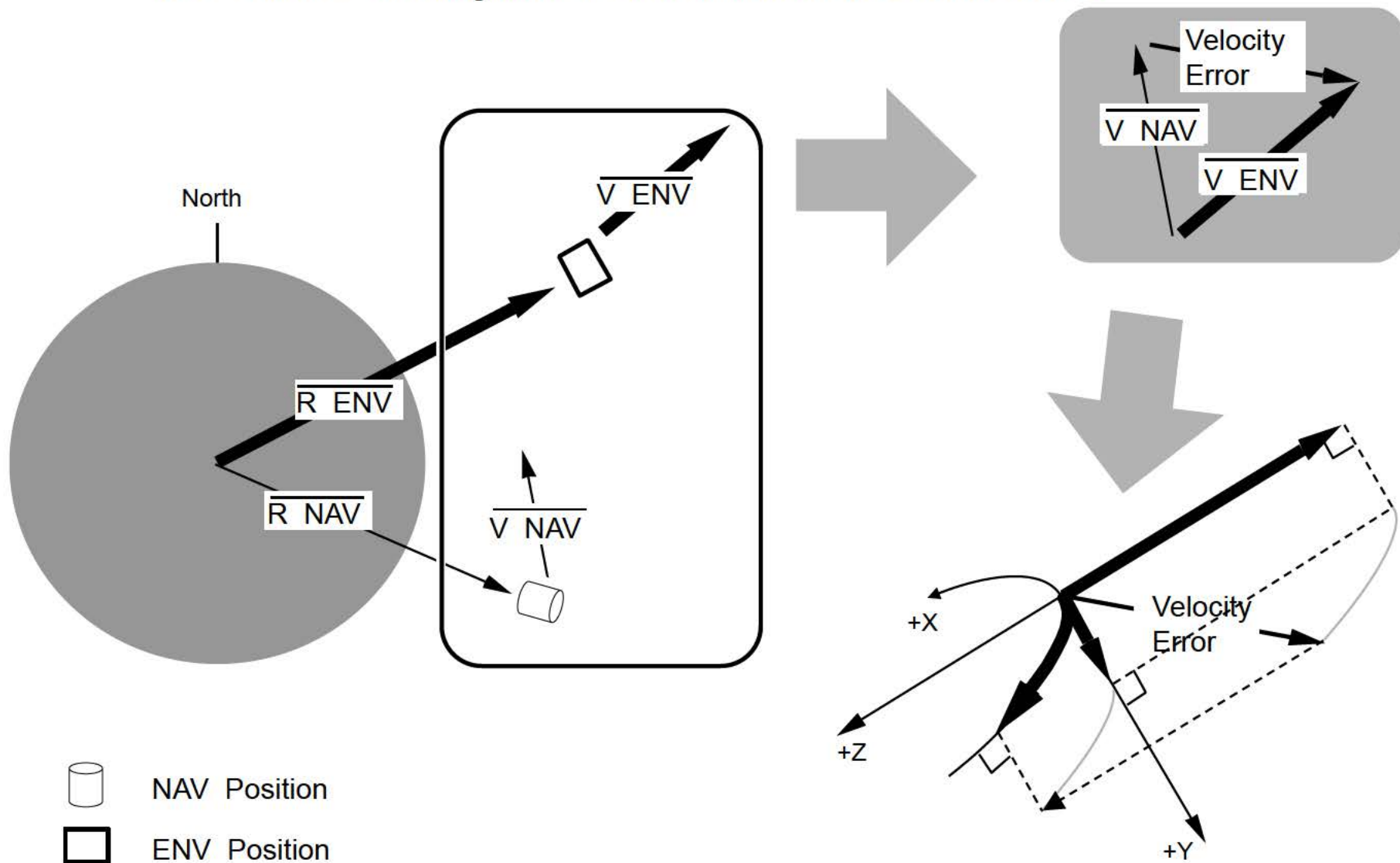
ORBITER inertial velocity errors can be determined by subtracting the NAV and ENV velocities. The components are then rotated into ENV centered LVLH.



Inertial position errors for the TARGET may also be viewed in LVLH.
 For this case, the frame is centered on the TARGET ENV position.



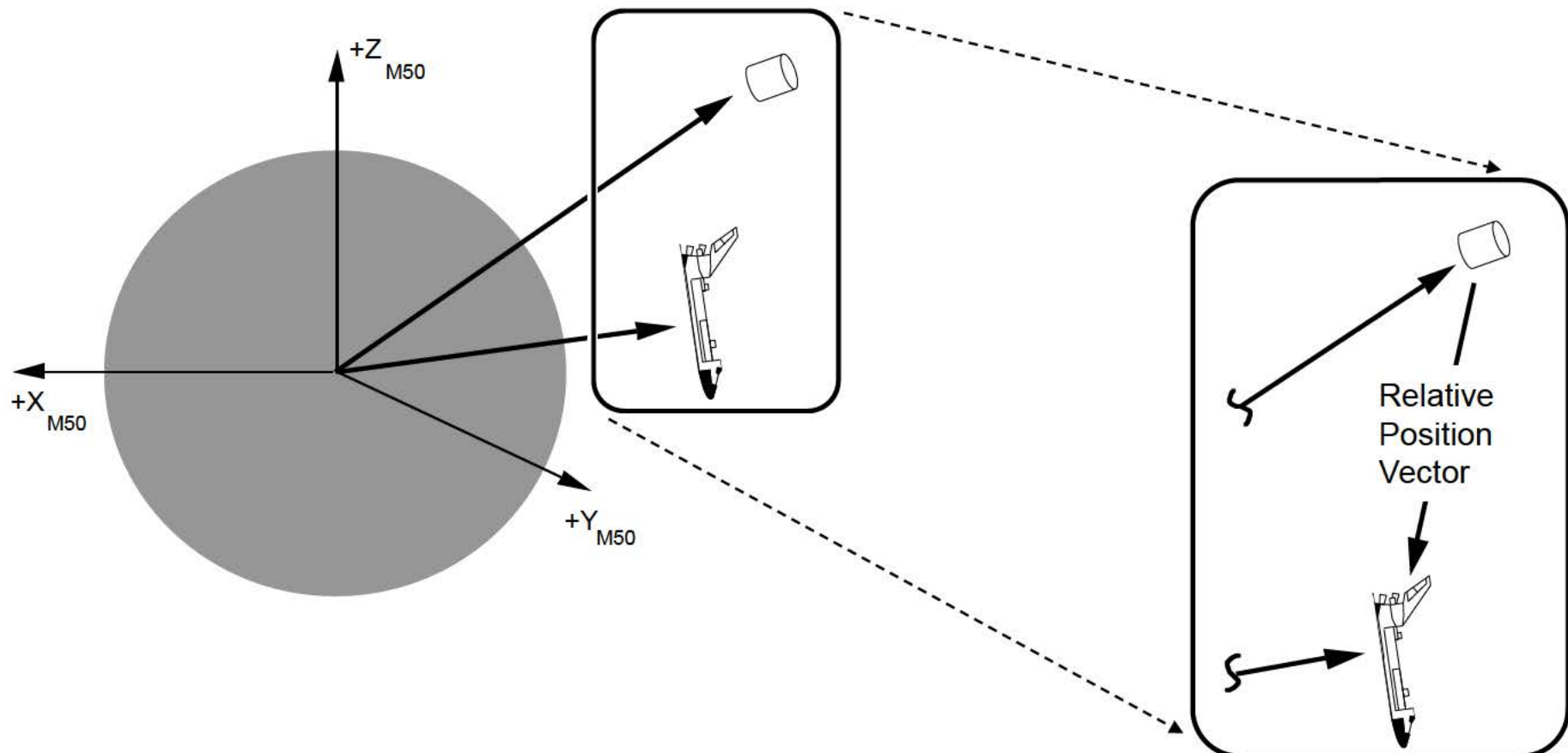
TARGET inertial velocity errors can be determined by subtracting the NAV and ENV velocities. The components are then rotated into ENV centered LVLH.



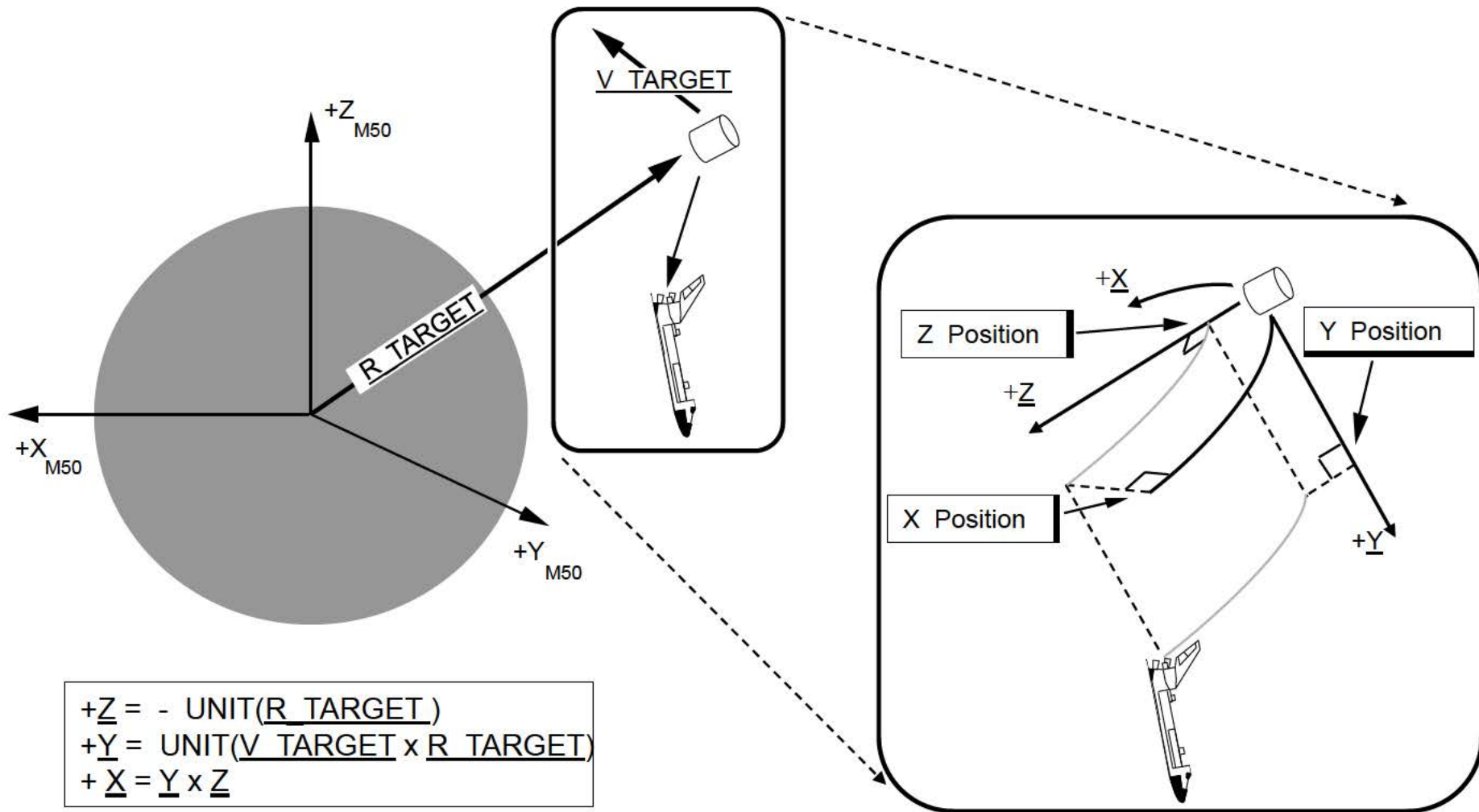
9.11 Relative State Vector Errors In LVLH Coordinates

Since relative motion is plotted in the LVLH frame, it is convenient to plot relative state errors in LVLH as well.

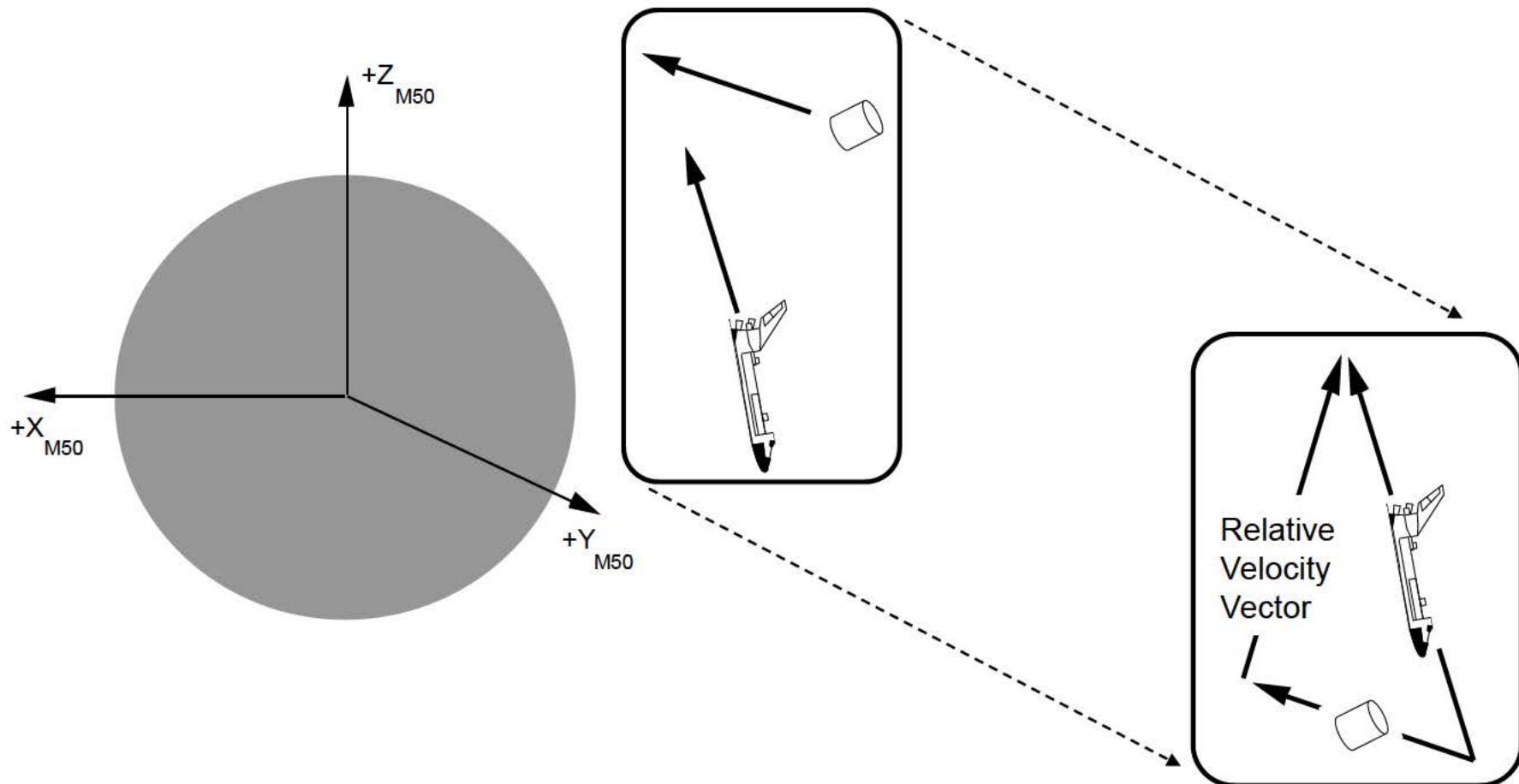
The position of the ORBITER with respect to the TARGET is defined by the relative position vector. This vector may be found by subtracting the TARGET and ORBITER position vectors.



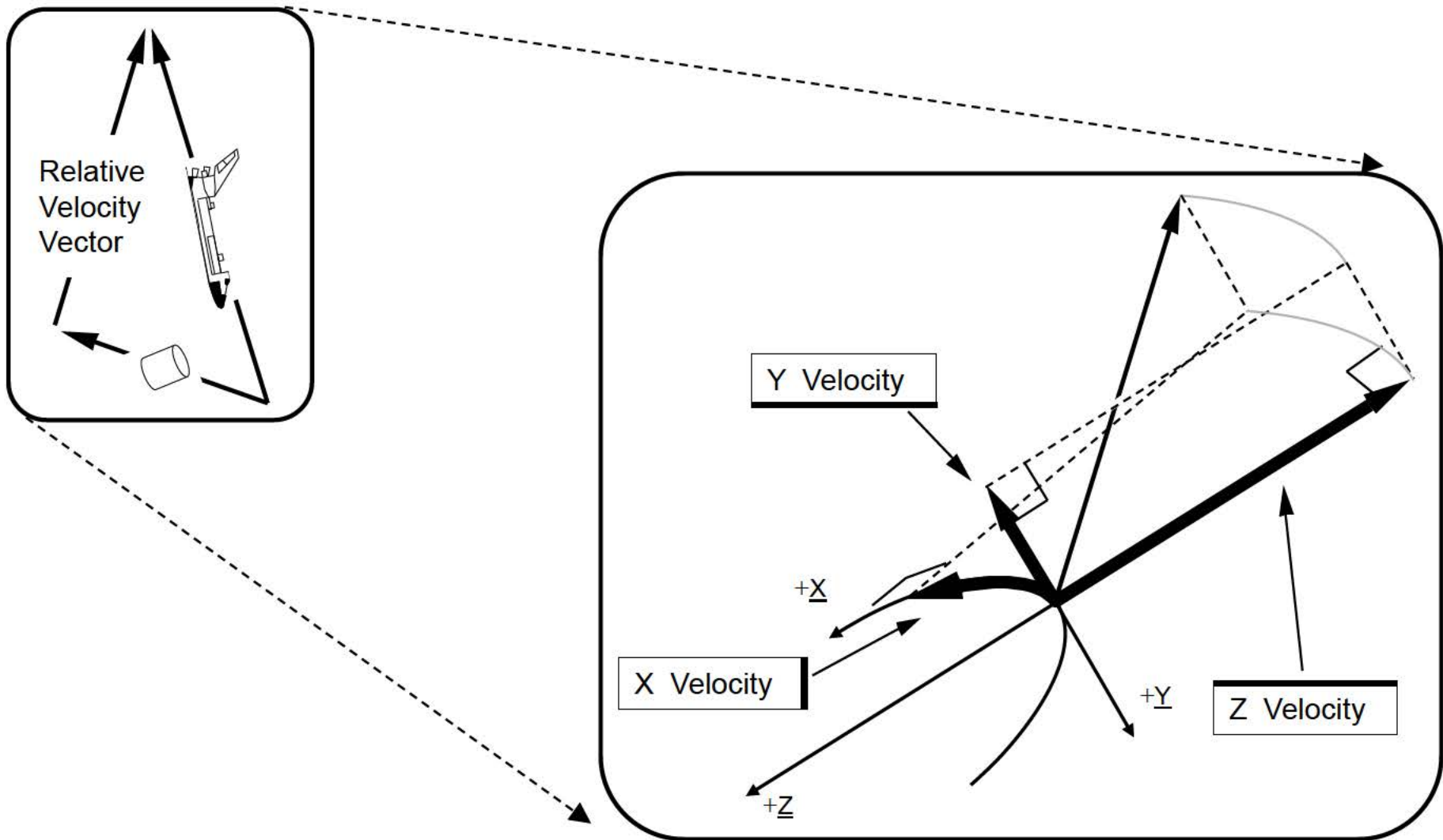
It is more convenient to view the relative position vector in a TARGET centered frame (such as LVLH) than in the M50 frame. The LVLH axes are defined by the TARGET position and velocity vectors. A rotation matrix (based on the axes) rotates the M50 components of the relative position vector into the LVLH frame.



The ORBITER's velocity with respect to the TARGET can be computed by subtracting the ORBITER and TARGET inertial velocity vectors.

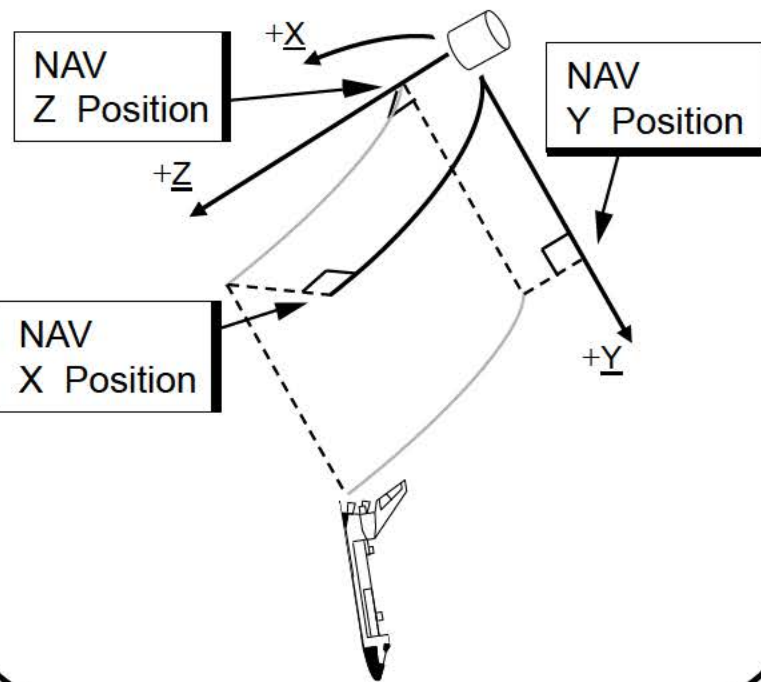


The relative velocity vector is then rotated into the LVLH frame.

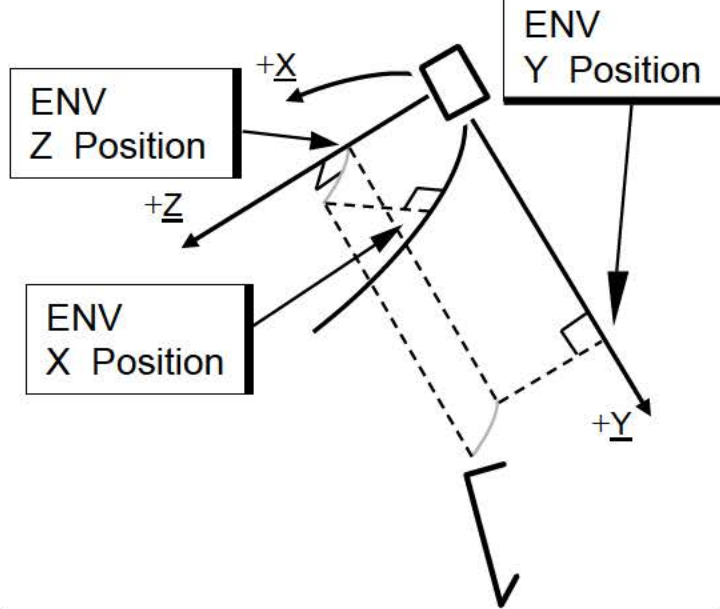


An ORBITER relative position may be computed from both the NAV (estimated) and environment (actual) state vectors.

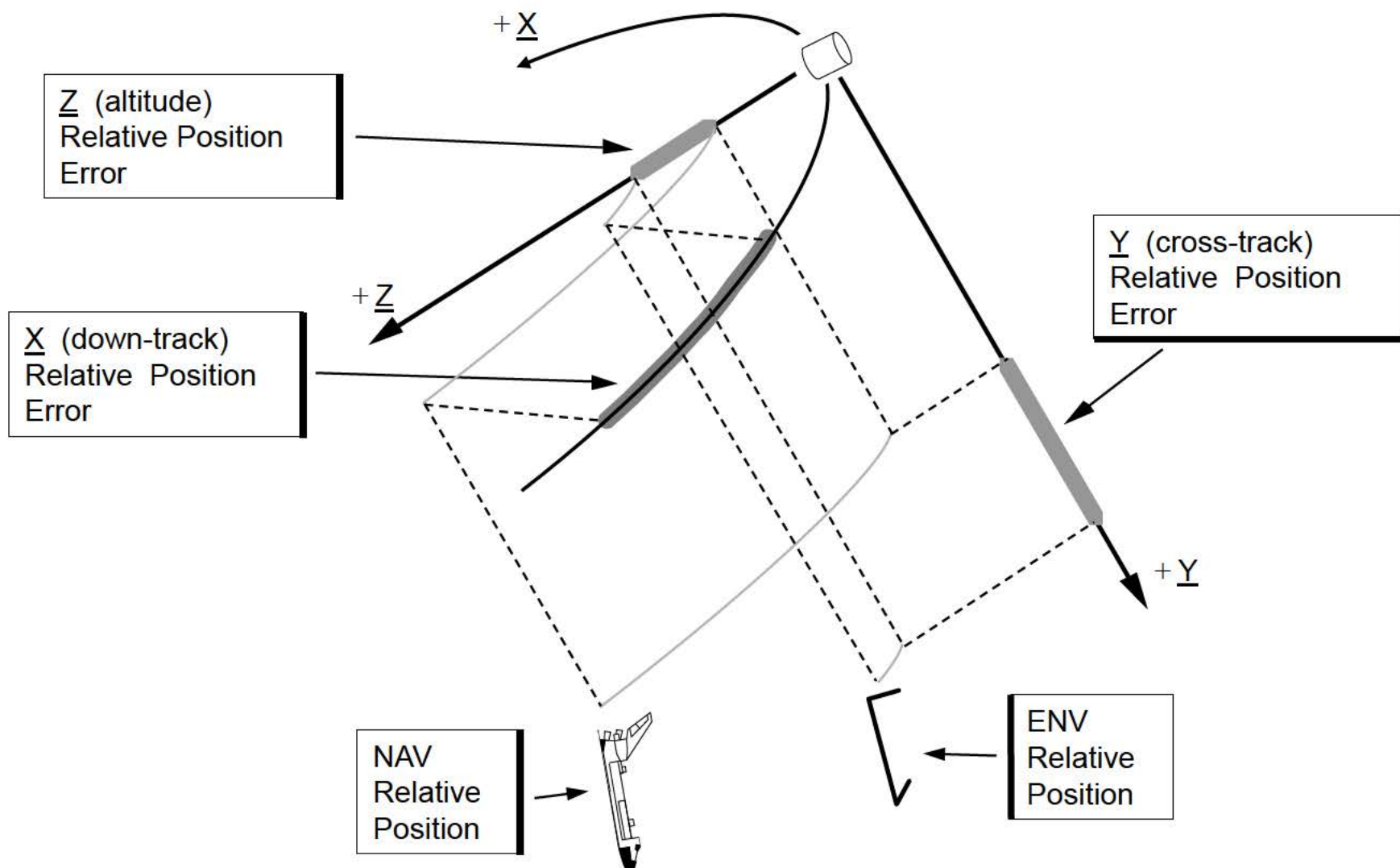
NAV Relative Position



Environment Relative Position

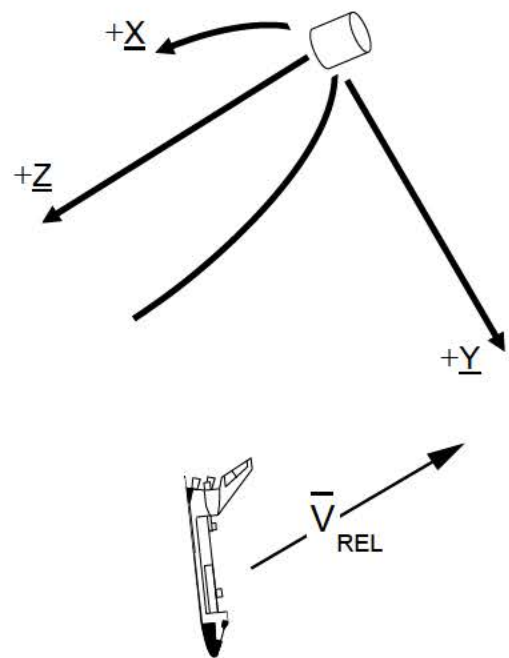


The difference between the two relative positions is the relative position error. Relative position error can be broken down into three components, one along each LVLH axis.

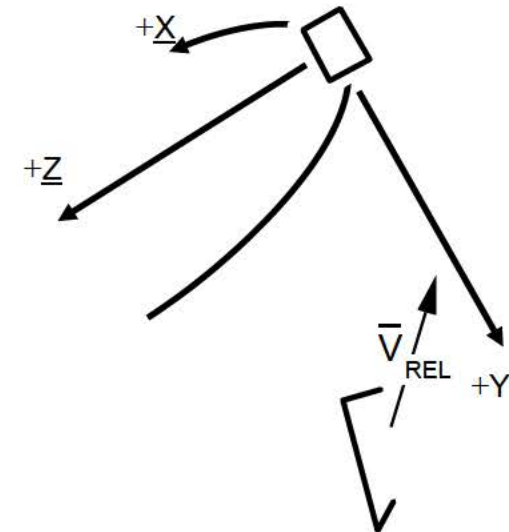


Relative velocities may also be computed from the ORBITER and TARGET states maintained by NAV and the environment (ENV). The difference between the NAV and ENV relative velocities is the relative velocity error.

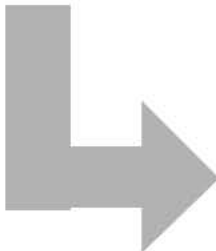
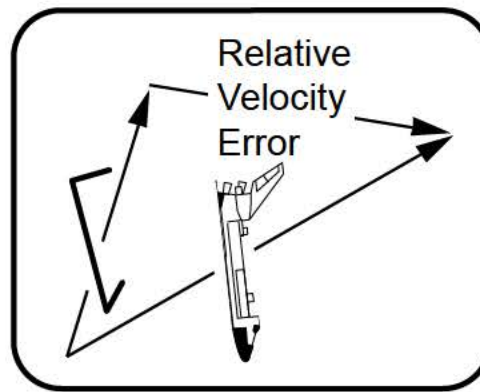
NAV Relative Velocity



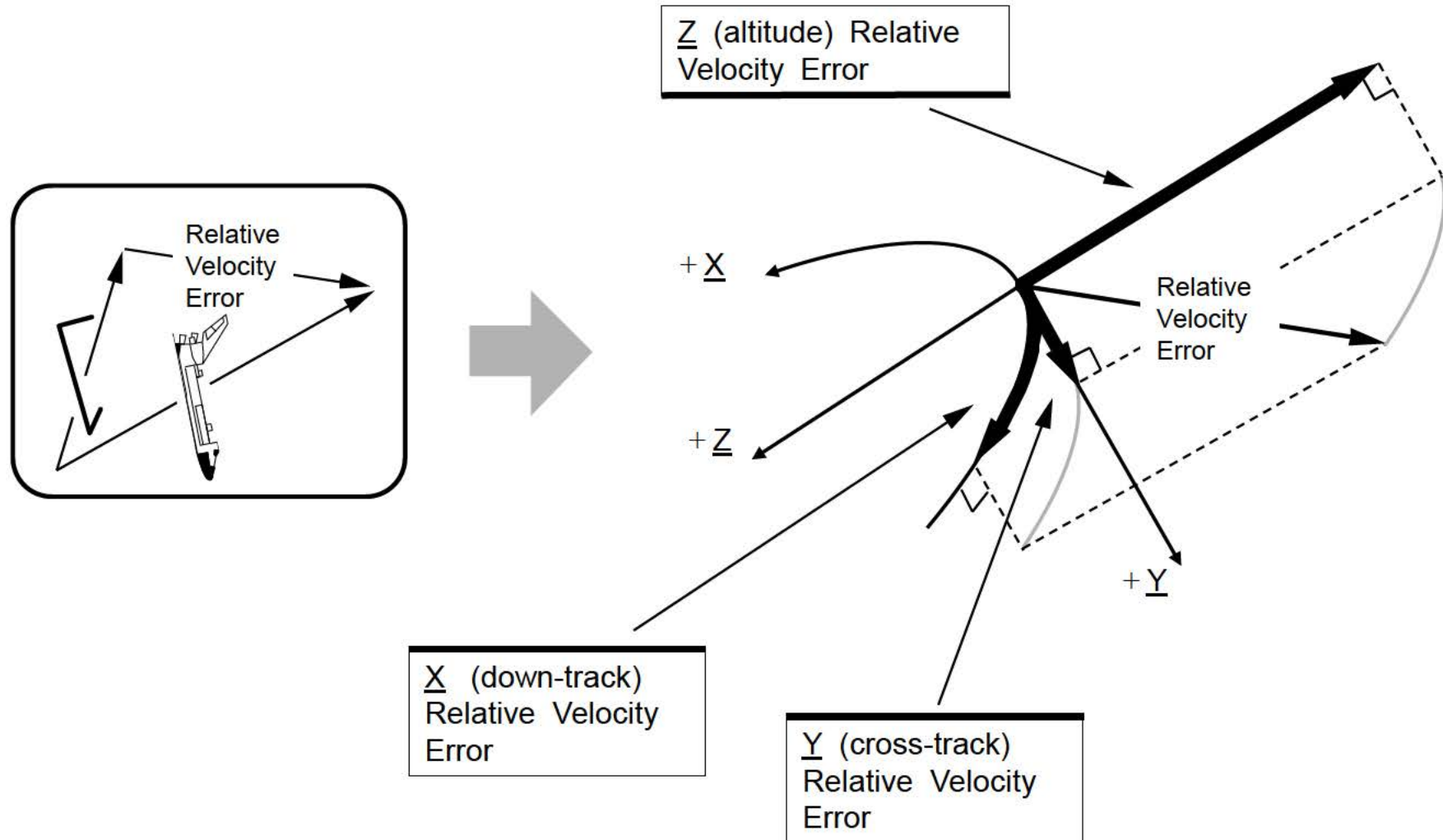
Environment Relative Velocity



Relative
Velocity
Error



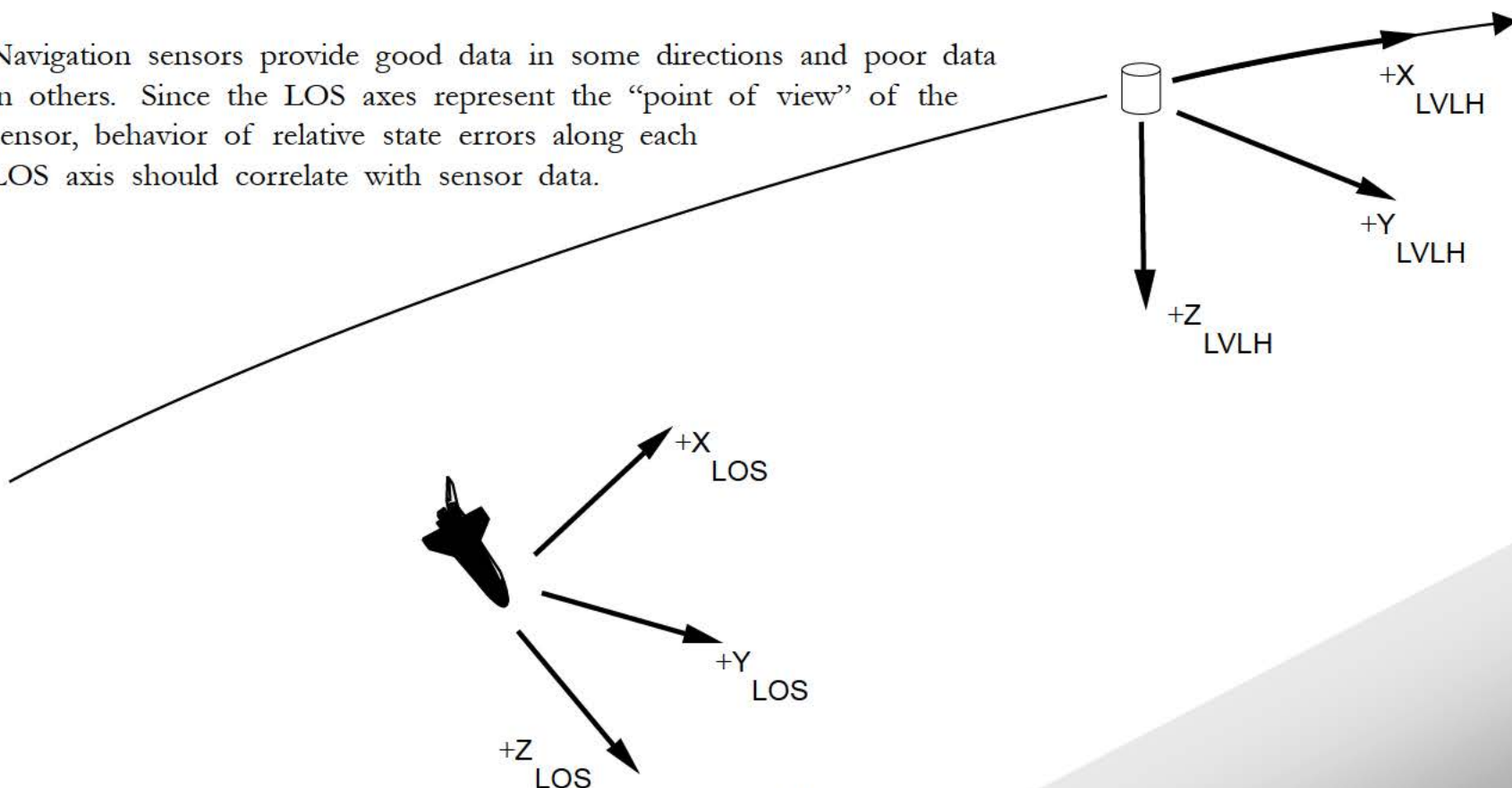
The relative velocity error is usually broken down into components along each LVLH axis.



9.12 Relative State Vector Errors In Line-of-Sight (LOS) Coordinates

LOS is an alternate frame for viewing relative state errors. It is useful since it allows errors to be viewed from the viewpoint of the navigation sensor. The X LOS axis is directed along the line of sight from the ORBITER to the TARGET. Z LOS is normal to X and can be thought of as being roughly parallel to the orbital plane of the TARGET. Y LOS is normal to X and Z. The LOS axes rotate as the ORBITER moves through LVLH space and as the ORBITER's position relative to the TARGET changes. LOS axes are not always parallel to the LVLH axes. LOS can be thought of as a "tilted LVLH."

Navigation sensors provide good data in some directions and poor data in others. Since the LOS axes represent the "point of view" of the sensor, behavior of relative state errors along each LOS axis should correlate with sensor data.

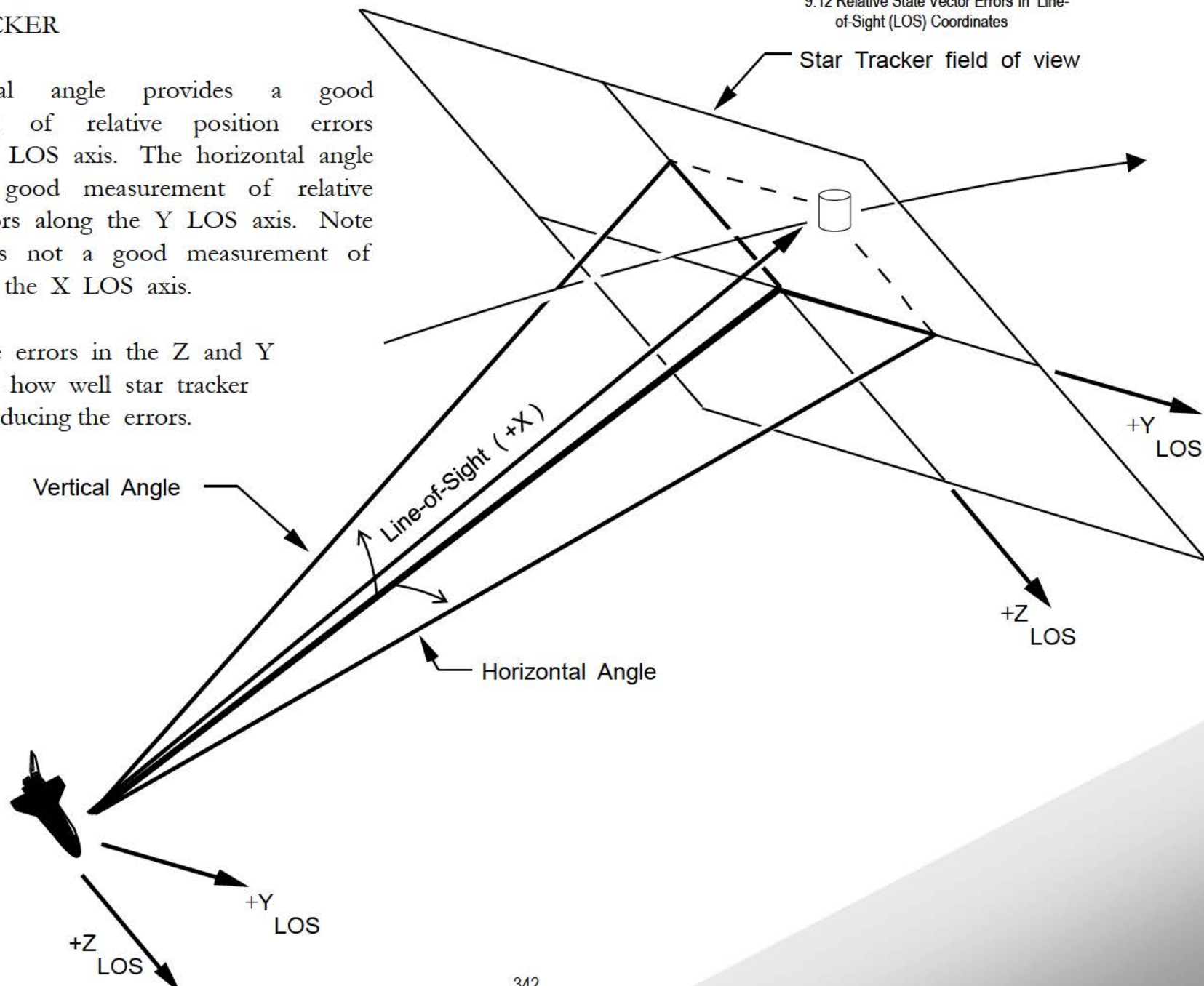


STAR TRACKER

The vertical angle provides a good measurement of relative position errors along the Z LOS axis. The horizontal angle provides a good measurement of relative position errors along the Y LOS axis. Note that there is not a good measurement of errors along the X LOS axis.

Relative state errors in the Z and Y axes indicate how well star tracker marks are reducing the errors.

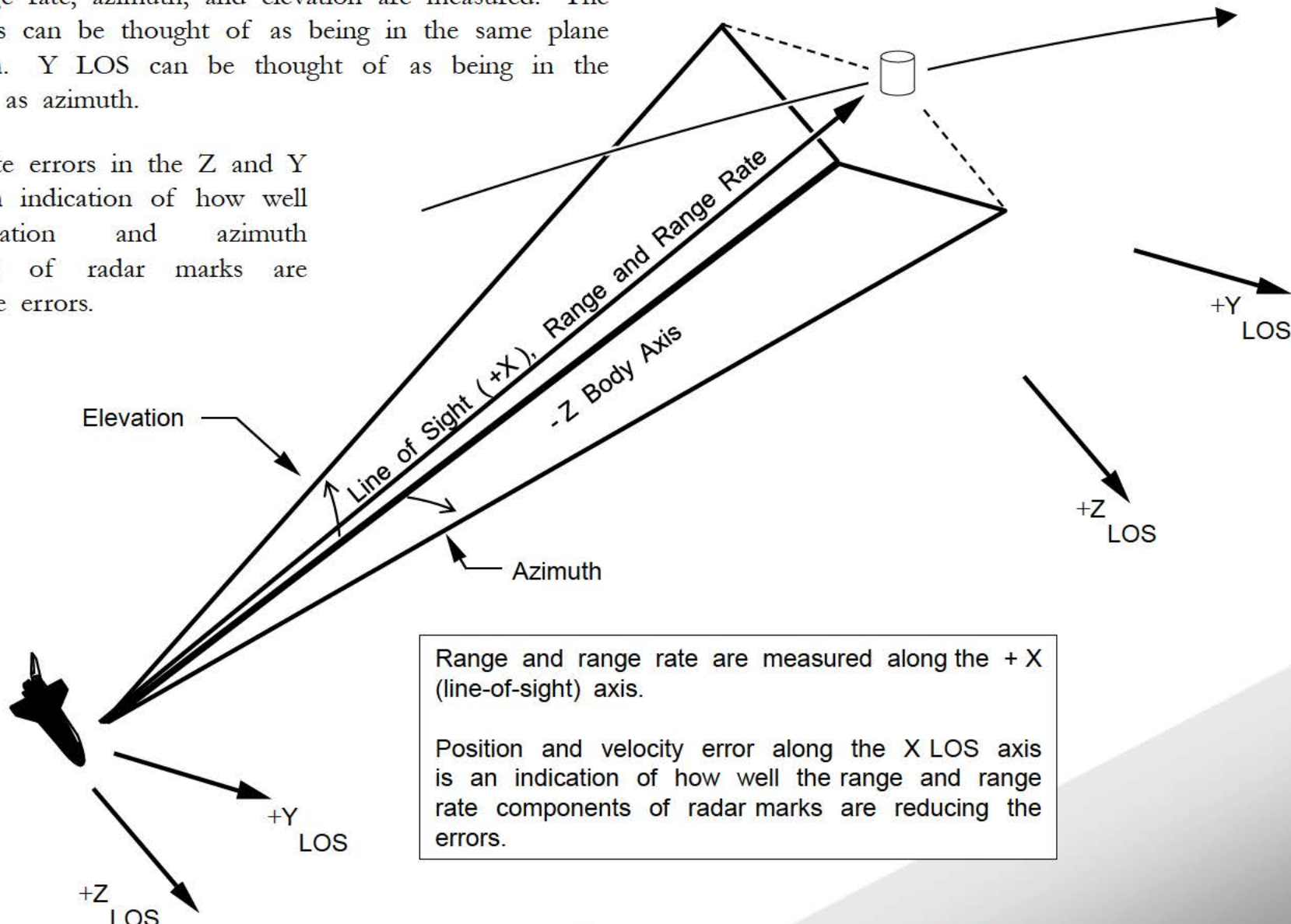
9.12 Relative State Vector Errors In Line-of-Sight (LOS) Coordinates



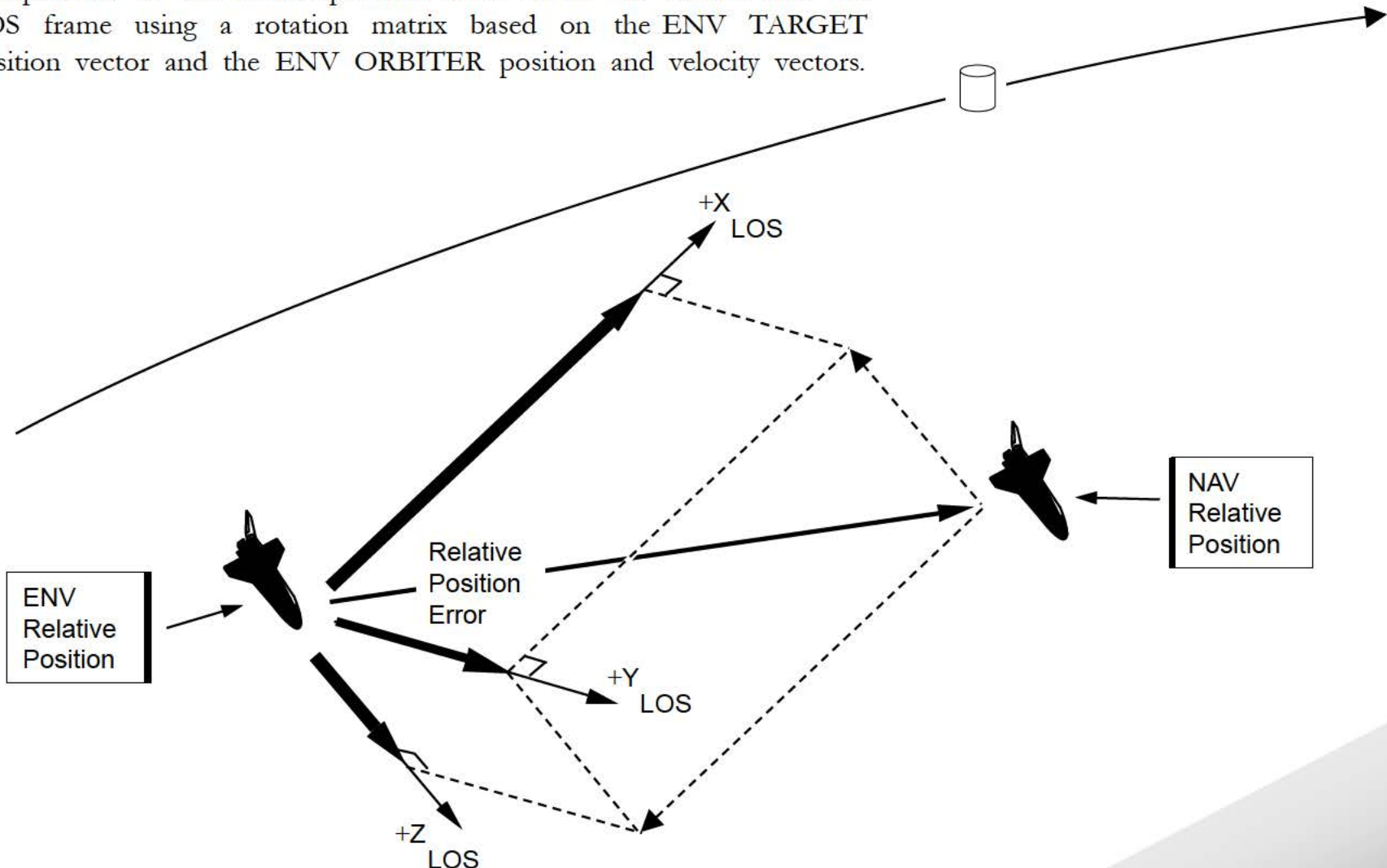
RADAR

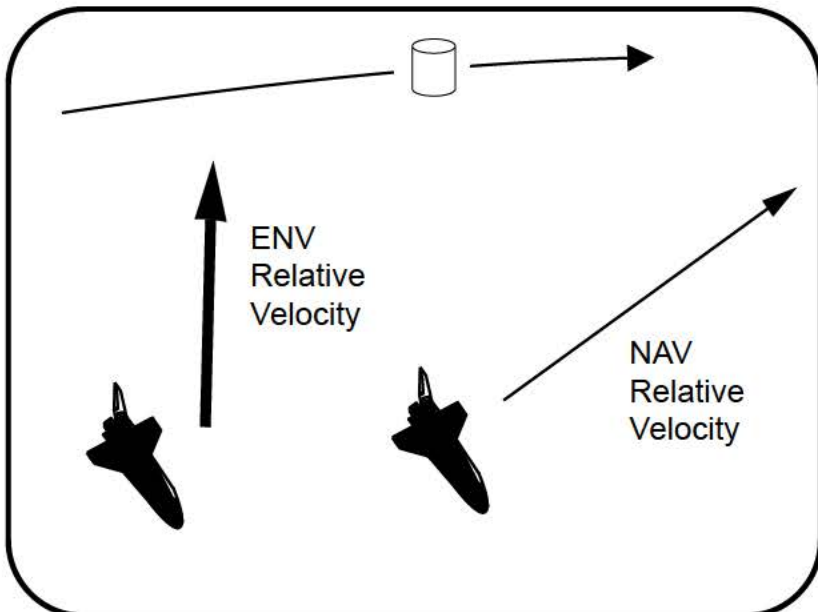
Range, range rate, azimuth, and elevation are measured. The Z LOS axis can be thought of as being in the same plane as elevation. Y LOS can be thought of as being in the same plane as azimuth.

Relative state errors in the Z and Y axes are an indication of how well the elevation and azimuth components of radar marks are reducing the errors.

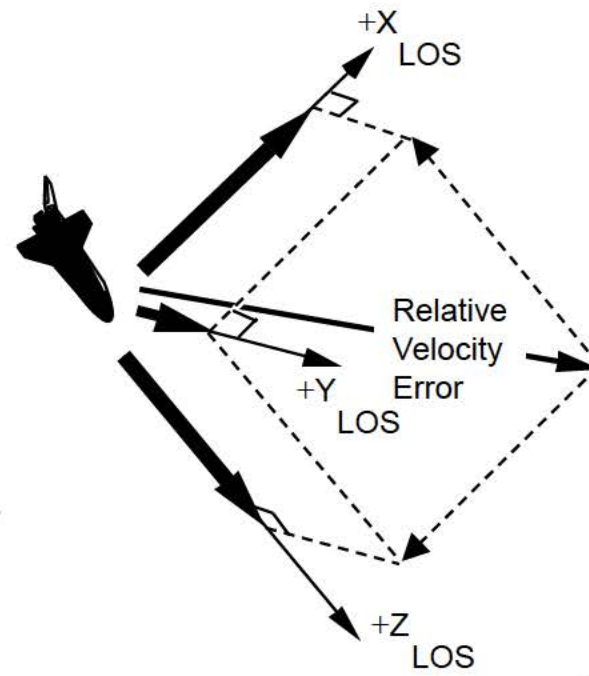
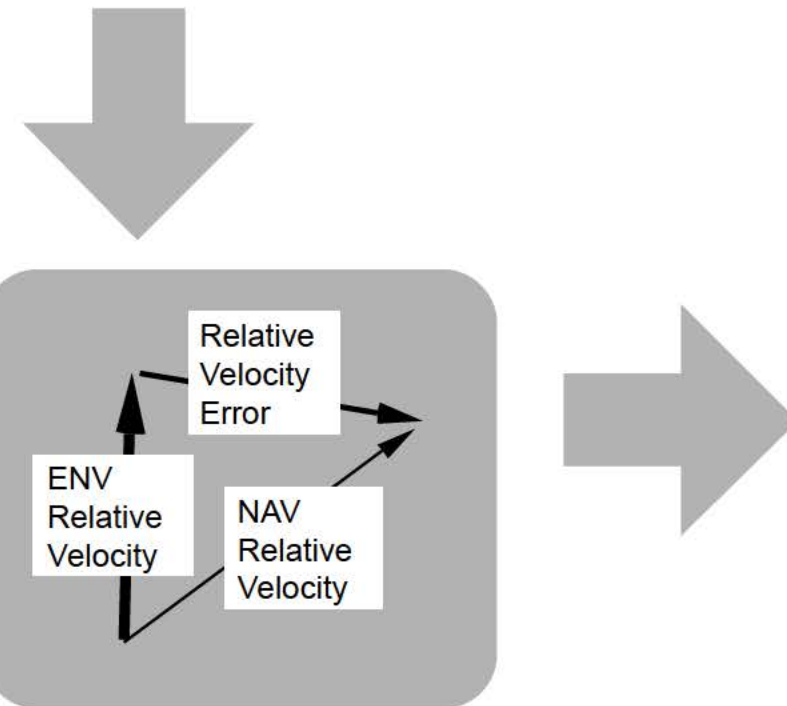


The LOS frame is centered on the ORBITER ENV position. Components of the relative position error vector are rotated into the LOS frame using a rotation matrix based on the ENV TARGET position vector and the ENV ORBITER position and velocity vectors.





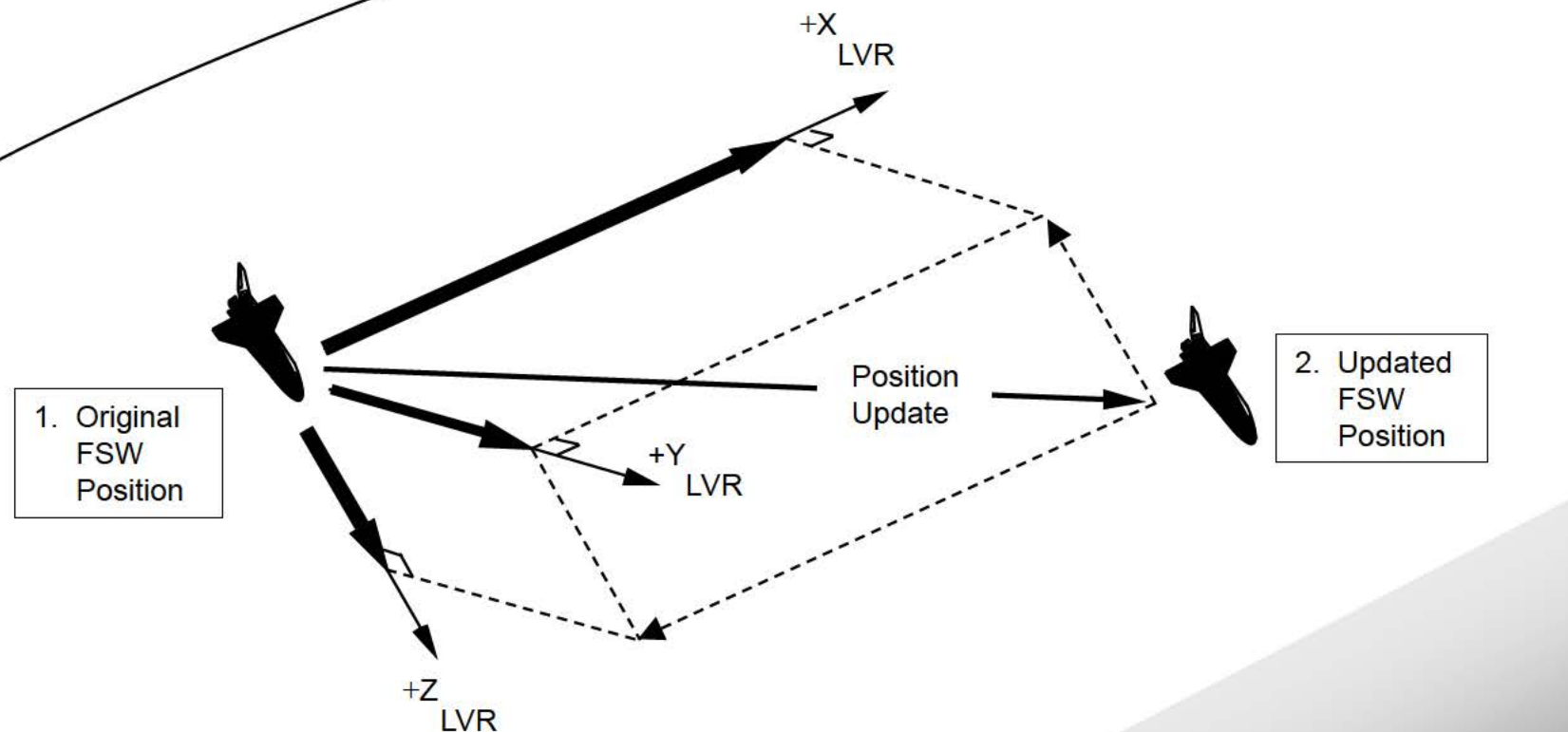
Relative velocity error may also be rotated into the LOS frame.



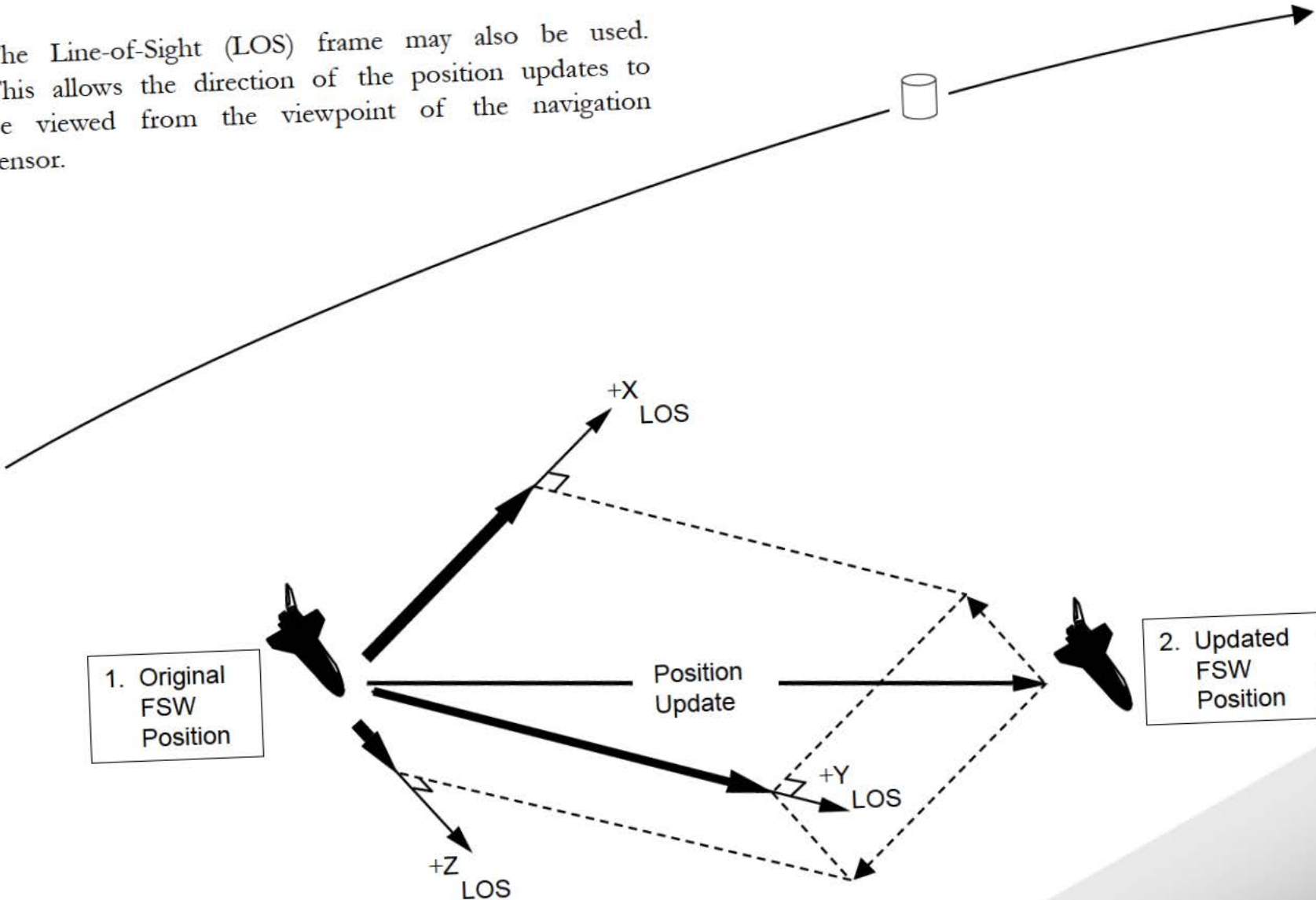
9.13 Position Updates In LVR and LOS Coordinates

For convenience, the position update can be rotated into a rotating Local Vertical Rectilinear (LVR) (or rectilinear LVLH) frame. This allows the analyst to “see” in which direction the updates are taking the ORBITER.

The LVR frame used is most often based on the ORBITER state vector. Note that the LVR X axis is straight, not curved.



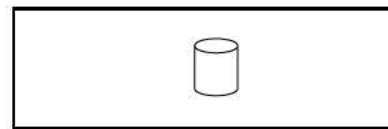
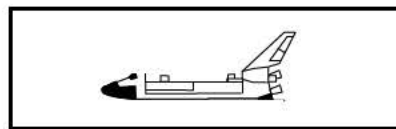
The Line-of-Sight (LOS) frame may also be used. This allows the direction of the position updates to be viewed from the viewpoint of the navigation sensor.



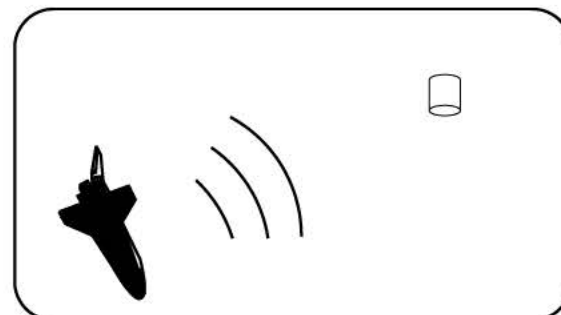
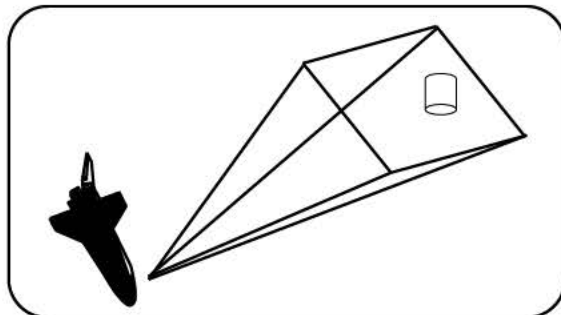
9.14 State Vector Management

State vector management is an integral part of the rendezvous navigation process. Activities performed during rendezvous effect both of these state vectors, which in turn impact users of ORBITER and TARGET states in the Flight Software. In addition, sudden changes will be seen in data derived from downlisted state vectors. It is important to understand the state vector management process in order to properly interpret changes in parameters on on-board displays and plotted output from simulations such as SAIL or SPF.

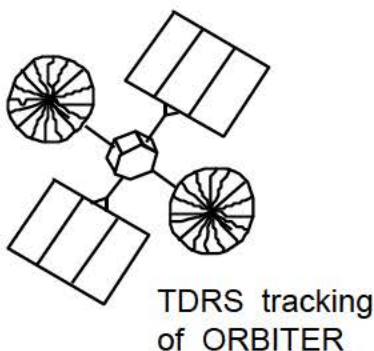
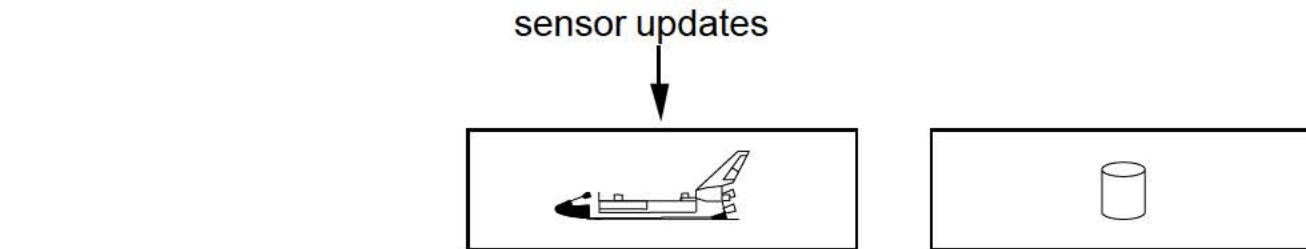
Navigation maintains an estimate of ORBITER and TARGET position and velocity in M50 (inertial) coordinates. In this section, state vectors will be represented by appropriately labeled boxes:



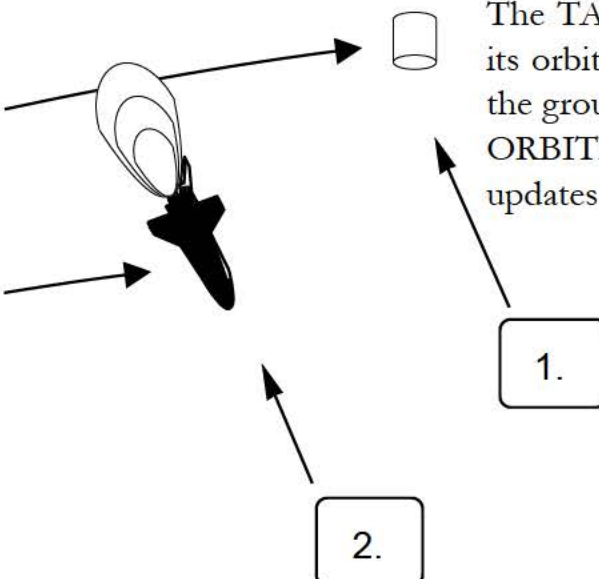
In rendezvous, a star tracker and radar are used to measure the position and velocity of the ORBITER with respect to the TARGET.



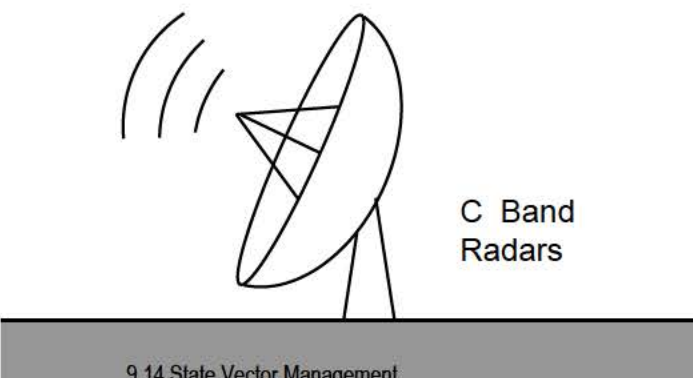
Data derived from the measurements is used to adjust the ORBITER state vector.



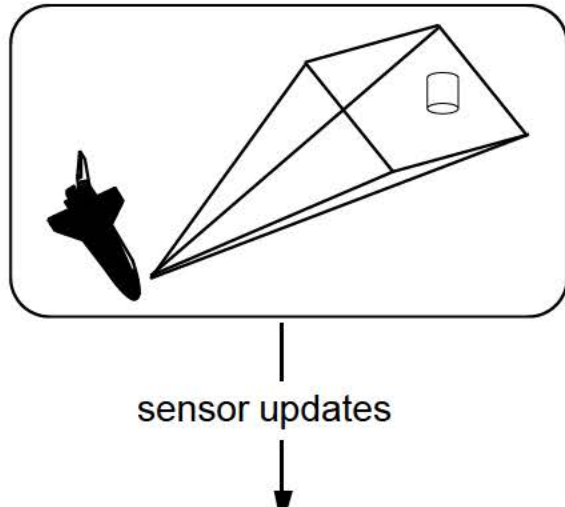
During both the ground and on-board targeted phases of rendezvous, the ORBITER is tracked by radars and the Tracking and Data Relay Satellite (TDRS). The TARGET is only tracked by radar. Prior to the initialization of rendezvous navigation, the MCC uplinks the latest orbiter and target states computed from radar and TDRS Tracking. In the future it is possible that the GPS Ground Filter (see chapter 9.20) could be used to supply ORBITER and SPACE STATION state vectors for initializing rendezvous navigation.



The TARGET (1.) typically does not do any maneuvering or venting which may change its orbit. The ORBITER (2.) executes maneuvers that change its orbit. For this reason, the ground tracking estimate of TARGET position and velocity is more accurate than the ORBITER estimate of position and velocity. This is why onboard sensor measurement updates are applied to the ORBITER state.



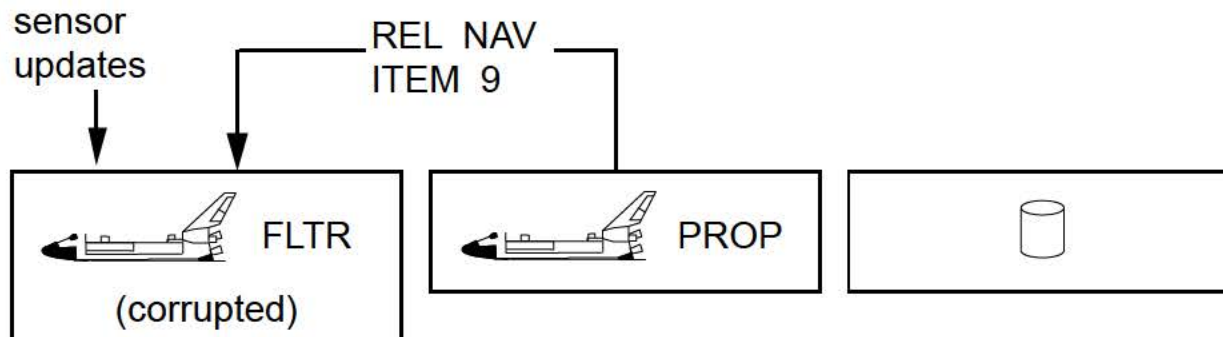
C Band
Radars

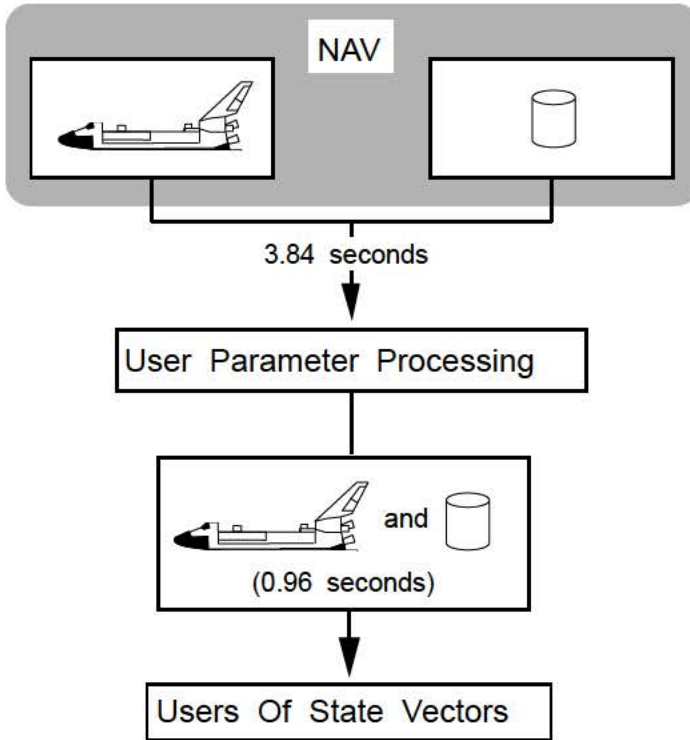


The application of sensor updates to the ORBITER state creates the possibility of bad updates corrupting the state vector. Although the Kalman filter tries to protect the ORBITER state from bad updates, the ORBITER state could still become corrupted.

To help protect against this, a back-up ORBITER state is also maintained by NAV. This state, known as the “PROP” state, is not updated by sensor data. The state that is updated is known as the “FLTR” state.

If the ORBITER FLTR state does become bad, it can be thrown out and replaced with the good ORBITER PROP state (PROP TO FLTR transfer, ITEM 9 on REL NAV). Maintaining a “clean” back-up state also ensures that a good ORBITER state will always be available for a contingency deorbit.





If rendezvous navigation is enabled (ITEM 1, REL NAV), the TARGET state is also sent to UPP. Every 3.84 seconds, NAV sends UPP new ORBITER and TARGET (if rendezvous) state vectors.

Various users of ORBITER and TARGET state vectors exist within the FSW. These users of NAV data need the state vectors at a rate higher than the NAV propagation rate of 3.84 seconds. A special set of code exists called User Parameter Processing (UPP), which supplies the ORBITER state vector to users at a rate of 0.96 seconds.

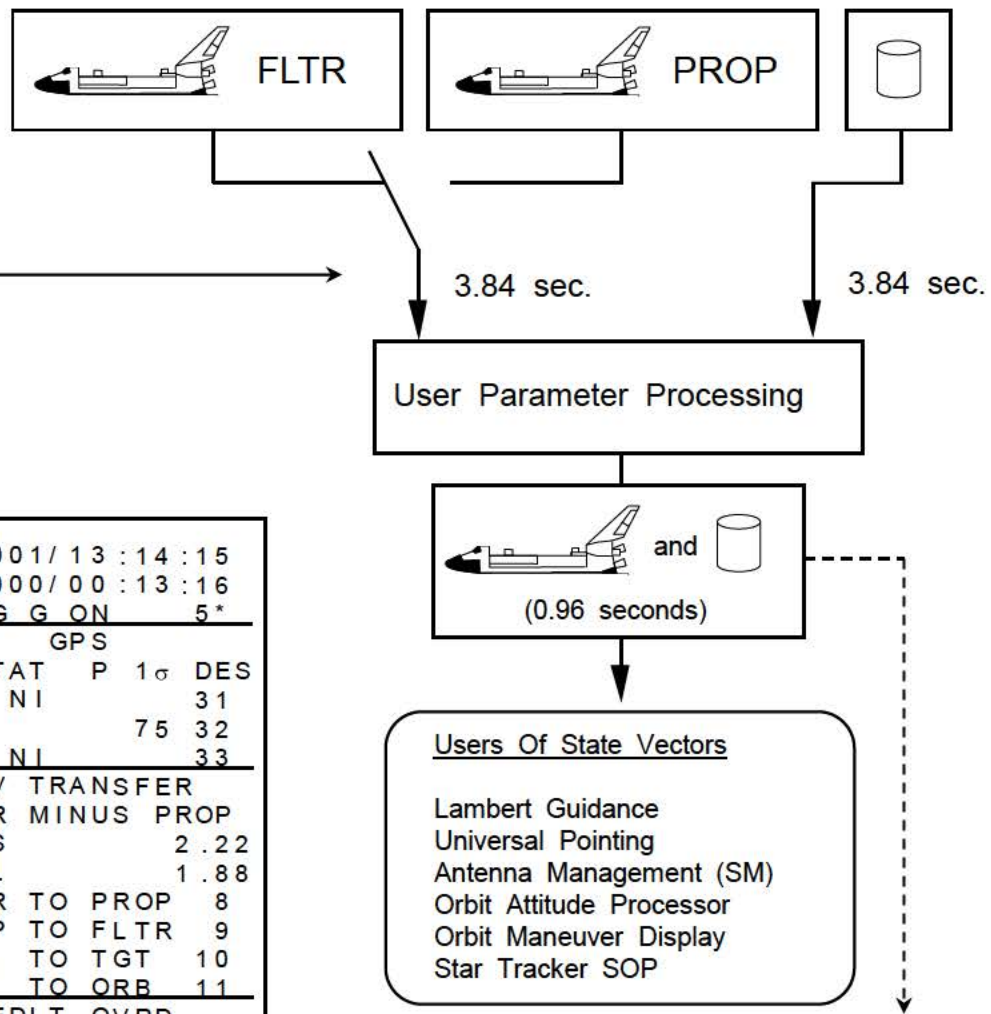
2021 / 033 /			REL NAV	1 005 / 02 :07 :37		
RNDZ	NAV	ENA 1*	SV UPDATE	000 / 00 :00 :00	AVG G ON	5*
KU ANT	ENA 2*		POS 0.02		GPS	
MEAS	ENA 3		VEL 0.03		STAT P 1 σ DES	
		NAV			1 75 31	
SV SEL	4 FLTR		RR GPC		2* 75 32	
RNG	25.721	RNG	25.610		3 75 33	
R	- 21.19	R	- 20.80			
θ	25.76	EL	- 0.4			
Y	+ 0.08	AZ	- 0.8			
Ẏ	+ 0.1	ωP	+ 0.8			
NODE	2:54:00	ωR	+ 0.1			
FILTER						
S TRK	12	RR 13*	COAS 14			
STAT			X - 3.4			
FLTR UPDATE	15	ORB	Y + 4.4			
COVAR REINIT	16					
					EDIT OVRD	
	RES ID	RATIO	ACPT	REJ	AUT	INH FOR
RNG	+ 0.09	0.2	807	0	17*	18 19
R	+ 0.02	0.0	807	0	20*	21 22
V/EL/Y	+ 0.02	0.0	807	0	23*	24 25
H/AZ/X	+ 0.01	0.0	807	0		
GPS P	+ 0.19	0.4			42	43* 44
V	+ 0.26	0.3				

ITEM 4 on REL NAV enables the crew to decide which ORBITER state (FLTR or PROP) is sent to UPP.

2021/033/				REL NAV
RNDZ	NAV	ENA 1*	SV UPDATE	1 001/13:14:15
KU ANT	ENA 2	POS	0.06	000/00:13:16
MEAS	ENA 3	VEL	0.03	Avg G ON 5*
NAV				
SV SEL	4 FLTR	RR ATRK		GPS
RNG	235.395	RNG	0.000↓	STAT P 1σ DES
R	- 29.55	R	0.00↓	1 NI 31
θ	2.81	EL	0.0↓	2↓ 75 32
Y	+ 0.13	AZ	0.0↓	3 NI 33
Ẏ	+ 0.9	ωP	0.0↓	
NODE	13:56:00	ωR	0.0↓	
FILTER				
S TRK	12*	RR	13	COAS 14
STAT				X + 1.6
FLTR UPDATE	15	ORB		Y - 0.8
COVAR REINIT	16			
RESID	RATIO	ACPT	REJ	EDIT OVRD
RNG	0.00	0.0	0	AUT INH FOR
R	0.00	0.0	0	17 18* 19
V/ EL / Y	0.00	0.0	11	20 21* 22
H/ AZ / X	0.00	0.0	11	23* 24 25
GPS P +	2.41	3.6↓		42 43* 44
V +	1.78	1.2↓		

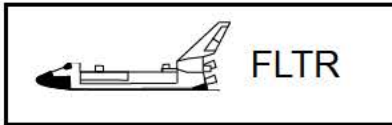
ITEM 4 EXEC

1 001/13:14:15
000/00:13:16
Avg G ON 5*
GPS
STAT P 1σ DES
1 NI 31
2↓ 75 32
3 NI 33
SV TRANSFER
FLTR MINUS PROP
POS 2.22
VEL 1.88
FLTR TO PROP 8
PROP TO FLTR 9
ORB TO TGT 10
TGT TO ORB 11

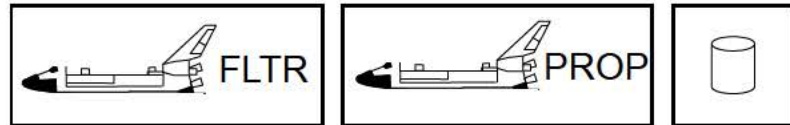


ORBITER and TARGET states provided by UPP are often used to compute parameters such as relative position and velocity in simulations. The selection of PROP or FLTR, and the execution of state vector error uplinks will show up in this data, usually as abrupt changes.

Prior to the initialization of rendezvous navigation, only the ORBITER FLTR state is propagated.

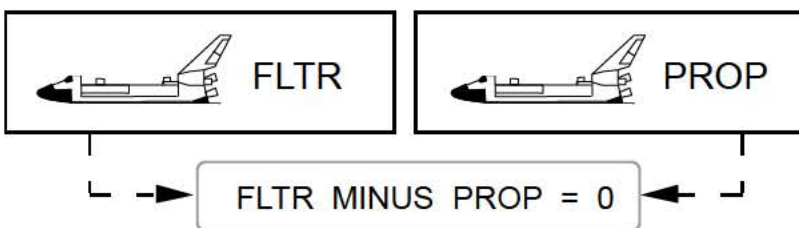


After the TARGET state is uplinked, rendezvous navigation is enabled (ITEM 1, REL NAV). NAV will begin to propagate the TARGET and ORBITER PROP state vectors, in addition to the ORBITER FLTR state.



At this time the FLTR and PROP states are equal (FLTR MINUS PROP differences on REL NAV are zero).

2021/033/	REL NAV	1 001/13:01:09
RNDZ NAV ENA 1*	SV UPDATE	000/00:00:00
KU ANT ENA 2	POS 0.00	Avg G ON 5*
MEAS ENA 3	VEL 0.00	
NAV		GPS
SV SEL 4 PROP	RR ATRK	STAT P 1σ DES
RNG 246.287	RNG 0.000↓	1 NI 31
ꝝ + 1.31	ꝝ 0.00↓	2* 75 32
θ 239.14	EL 0.0↓	3 NI 33
Y - 0.16	AZ 0.0↓	
ꝝ + 0.4	ꝝ P 0.0↓	SV TRANSFER
NODE 13:07:29	ꝝ R 0.0↓	FLTR MINUS PROP
		POS 0.00
		VEL 0.00
FILTER		FLTR TO PROP 8
S TRK 12*	RR 13 COAS 14	PROP TO FLTR 9
STAT X		ORB TO TGT 10
FLTR UPDATE 15 ORB Y		TGT TO ORB 11
COVAR REINIT 16		EDIT OVRD
RESID	RATIO ACPT REJ	AUT INH FOR
RNG 0.00	0.0 0 0	17 18* 19
R 0.00	0.0 0 0	20 21* 22
V/ EL / Y 0.00	0.0 0 0	23 24* 25
H/ AZ / X 0.00	0.0 0 0	
GPS P + 0.19	0.4	42 43* 44
V + 0.27	0.3	
ITEM 1 EXEC		

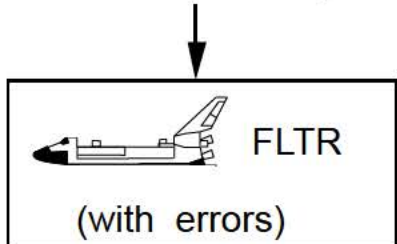


At the start of a simulation, state vector errors are uplinked to the TARGET and ORBITER states. The ORBITER FLTR state always receives the uplink (making FLTR MINUS PROP difference on REL NAV non-zero).

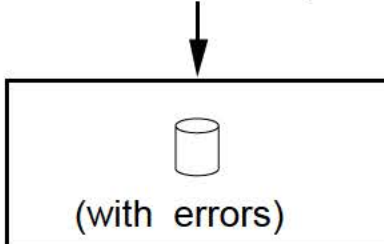
Placing errors in the states makes it easier to confirm that rendezvous navigation is improving the ORBITER FLTR state vector via sensor measurements.

2021/033/	REL NAV	1 001/13:08:54
RNDZ NAV ENA 1*	SV UPDATE	000/00:18:37
KU ANT ENA 2	POS 0.00	AVG G ON 5*
MEAS ENA 3	VEL 0.00	GPS
	NAV	STAT P 1 σ DES
SV SEL 4 PROP	RR ATRK	1 NI 31
RNG 243.302	RNG 0.000↓	2↓ 75 32
\dot{R} - 15.35	\dot{R} 0.00↓	3 NI 33
θ 270.51	EL 0.0↓	SV TRANSFER
Y - 0.06	AZ 0.0↓	FLTR MINUS PROP
\dot{Y} + 0.6	ω_P 0.0↓	POS 2.01
NODE 13:13:24	ω_R 0.0↓	VEL 0.97
	FILTER	FLTR TO PROP 8
S TRK 12*	RR 13 COAS 14	PROP TO FLTR 9
STAT	X	ORB TO TGT 10
FLTR UPDATE 15	ORB Y	TGT TO ORB 11
COVAR REINIT 16		EDIT OVRD
RES ID	RATIO ACPT REJ	AUT INH FOR
RNG 0.00	0.0 0 0	17 18* 19
R 0.00	0.0 0 0	20 21* 22
V/ EL/ Y 0.00	0.0 0 0	23 24* 25
H/ AZ/ X 0.00	0.0 0 0	
GPS P + 2.25	4.0↓	42 43* 44
V + 0.82	0.7	

ORBITER error uplink



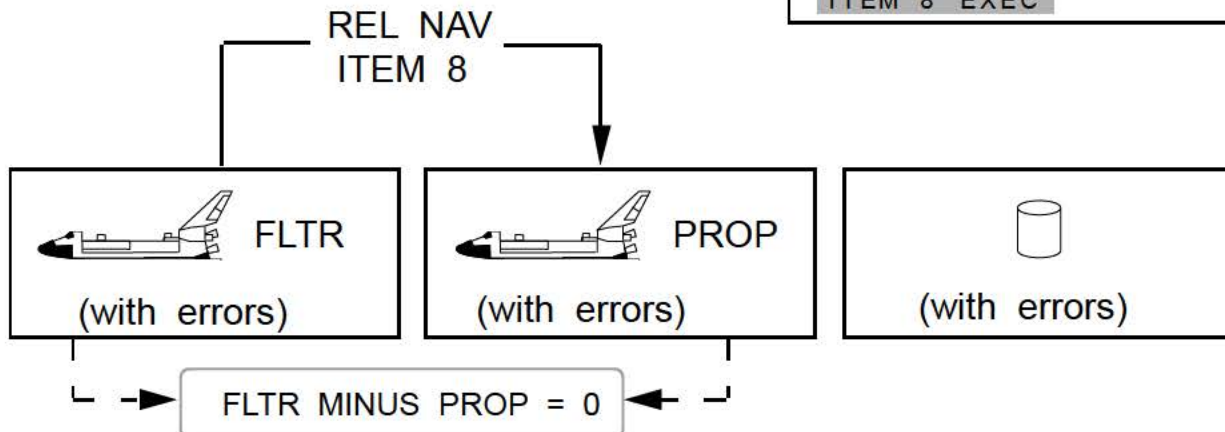
TARGET error uplink



L → FLTR MINUS PROP > 0 ← R

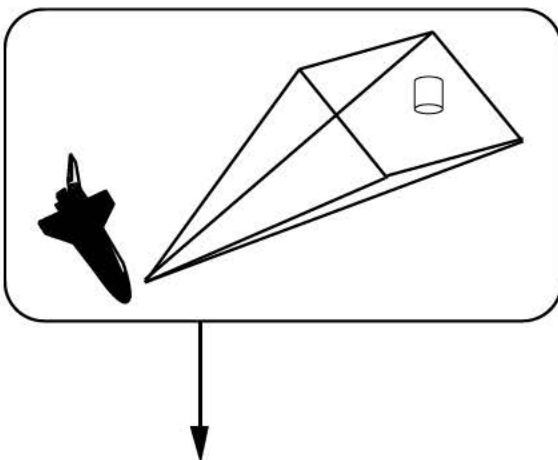
An ITEM 8 (FILT TO PROP, REL NAV) is then performed to replace the error-free PROP state with the FLTR state containing state errors. After the ITEM 8, the difference between the FLTR and PROP position and velocity will again be zero.

All three states now have the uplinked state errors.

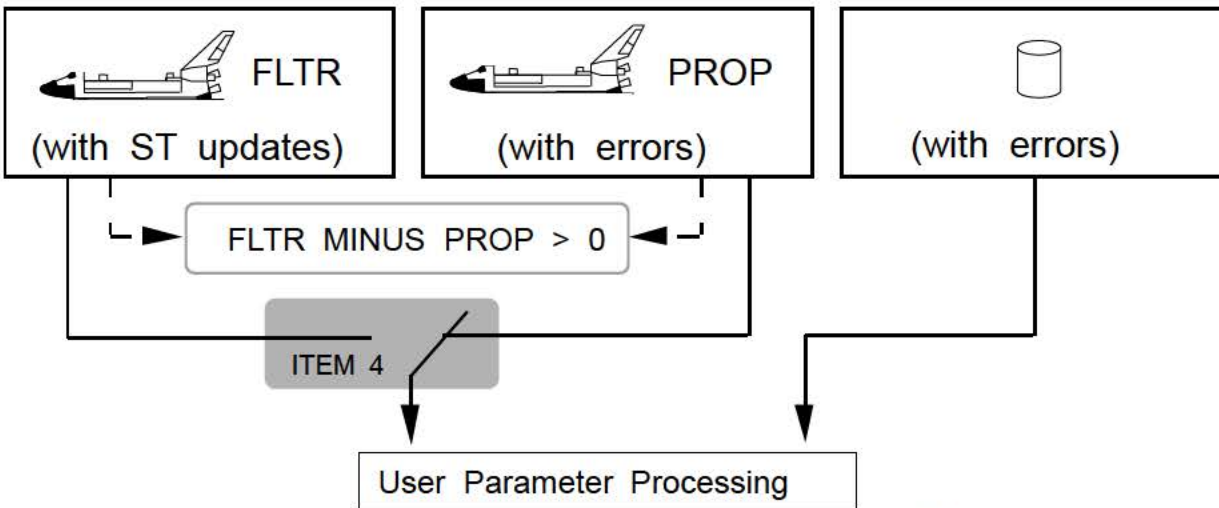


2021/033/	REL NAV	1 001/13:09:02
RNDZ NAV ENA 1*	SV UPDATE	000/00:18:29
KU ANT ENA 2	POS 0.00	AVG G ON 5*
MEAS ENA 3	VEL 0.00	GPS
NAV		STAT P 1σ DES
SV SEL 4 PROP	RR ATRK	1 NI 31
RNG 241.423	RNG 0.000↓	2↓ 75 32
R - 16.05	R 0.00↓	3 NI 33
θ 271.35	EL 0.0↓	SV TRANSFER
Y - 2.12	AZ 0.0↓	FLTR MINUS PROP
Ŷ + 1.3	ωP 0.0↓	POS 0.00
NODE 13:26:21	ωR 0.0↓	VEL 0.00
FILTER		
S TRK 12*	RR 13 COAS 14	FLTR TO PROP 8
STAT	X	PROP TO FLTR 9
FLTR UPDATE 15	ORB Y	ORB TO TGT 10
COVAR REINIT 16		TGT TO ORB 11
RES ID	RATIO ACPT REJ	EDIT OVRD
RNG 0.00	0.0 0 0	AUT 17 18* 19
R 0.00	0.0 0 0	20 21* 22
V/ EL/ Y 0.00	0.0 0 0	23 24* 25
H/ AZ/ X 0.00	0.0 0 0	
GPS P + 2.25	4.0↓	42 43* 44
V + 0.84	0.7	
ITEM 8 EXEC		

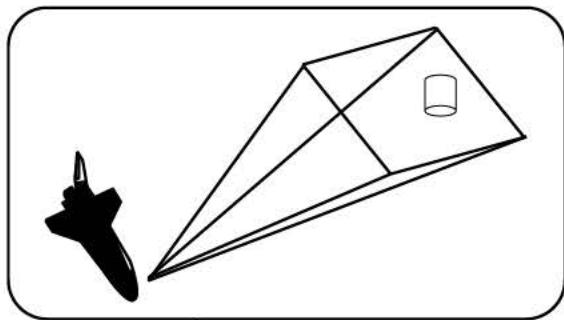
At the start of the star tracker pass, the PROP state is selected. FLTR MINUS PROP will increase as marks are incorporated into the FLTR state.



2021/033/	REL NAV	1 001/13:13:10
RNDZ NAV ENA 1*	SV UPDATE	000/00:14:21
KU ANT ENA 2	POS 0.02	Avg G ON 5*
MEAS ENA 3	VEL 0.05	
NAV		
SV SEL 4 PROP	RR ATRK	
RNG 236.060	RNG 0.000↓	
Ŕ - 27.19	Ŕ 0.00↓	
θ 4.22	EL 0.0↓	
Y - 1.79	AZ 0.0↓	
Ŷ + 2.0	OP 0.0↓	
NODE 13:26:21	OR 0.0↓	
FILTER		
S TRK 12*	RR 13 COAS 14	
STAT X +3.4		
FLTR UPDATE 15 ORB Y -0.9		
COVAR REINIT 16		
RESID RATIO ACPT REJ		
RNG 0.00 0.0 0 0		
R 0.00 0.0 0 0		
V/ EL / Y +0.01 0.0 3 0		
H/ AZ / X 0.00 0.0 3 0		
GPS P + 2.35 3.8↓ 42 43*		
V + 1.57 1.0 44		
EDIT OVRD		
AUT INH FOR		
17 18* 19		
20 21* 22		
23* 24 25		

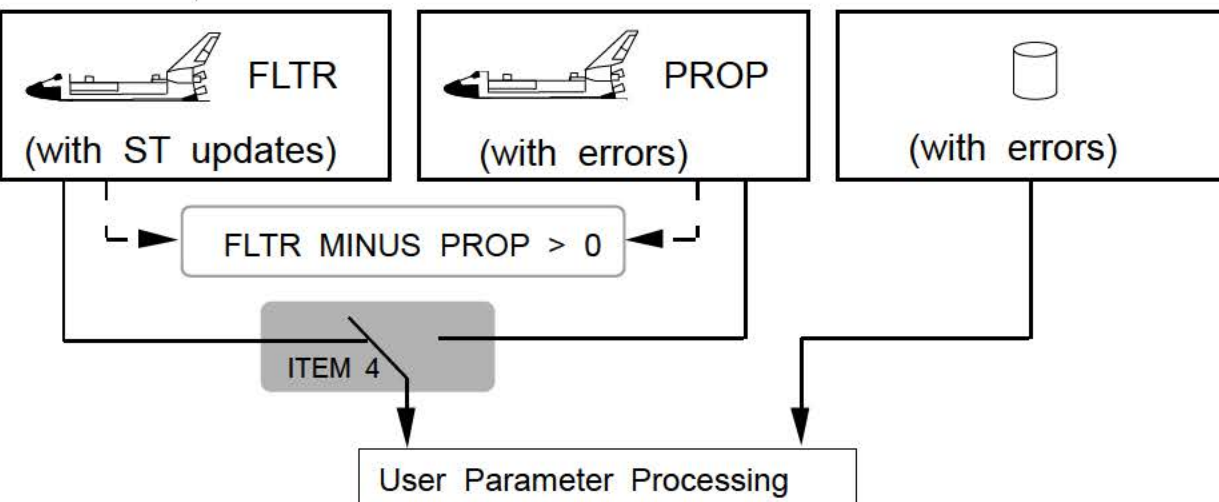


Once 9 marks have been incorporated and the position updates are less than 1,000 feet, the FLTR state is selected.



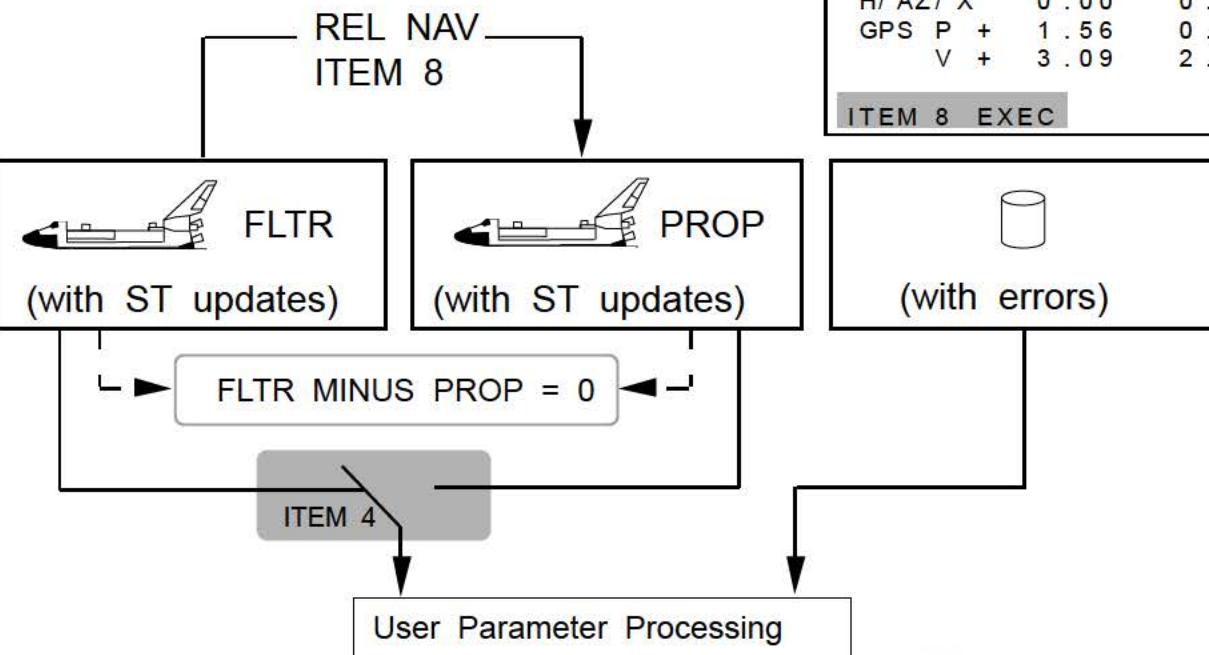
2021/033/	REL NAV	1 001/13:14:15
RNDZ NAV ENA 1*	SV UPDATE	000/00:13:16
KU ANT ENA 2	POS 0.06	Avg G ON 5*
MEAS ENA 3	VEL 0.03	
NAV		GPS
SV SEL 4 FLTR	RR ATRK	STAT P 1 σ DES
RNG 235.395	RNG 0.000↓	1 NI 31
R - 29.55	R 0.00↓	2↓ 75 32
θ 2.81	EL 0.0↓	3 NI 33
Y + 0.13	AZ 0.0↓	SV TRANSFER
Y + 0.9	ωP 0.0↓	FLTR MINUS PROP
NODE 13:56:00	ωR 0.0↓	POS 2.22
		VEL 1.88
FILTER		FLTR TO PROP 8
S TRK 12*	RR 13 COAS 14	PROP TO FLTR 9
STAT	X +1.6	ORB TO TGT 10
FLTR UPDATE 15 ORB	Y -0.8	TGT TO ORB 11
COVAR RE INIT 16		EDIT OV RD
RESID RATIO ACPT REJ		
RNG 0.00 0.0 0 0		AUT 17 18* 19
R 0.00 0.0 0 0		V 20 21* 22
V/ EL/ Y 0.00 0.0 11 0		23* 24 25
H/ AZ/ X 0.00 0.0 11 0		42 43* 44
GPS P + 2.41 3.6↓		
V + 1.78 1.2↓		

ITEM 4 EXEC

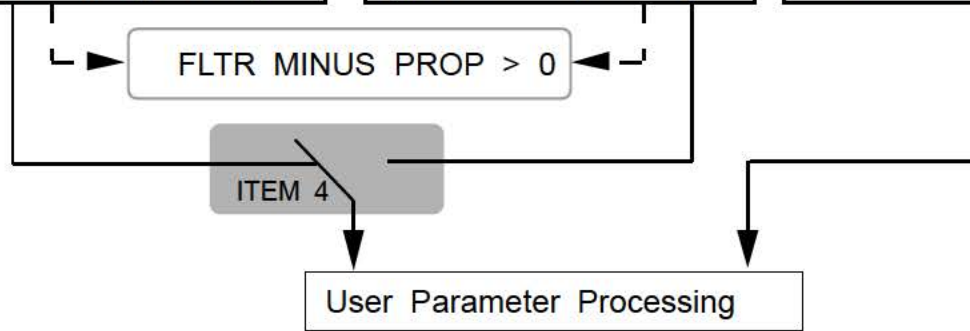
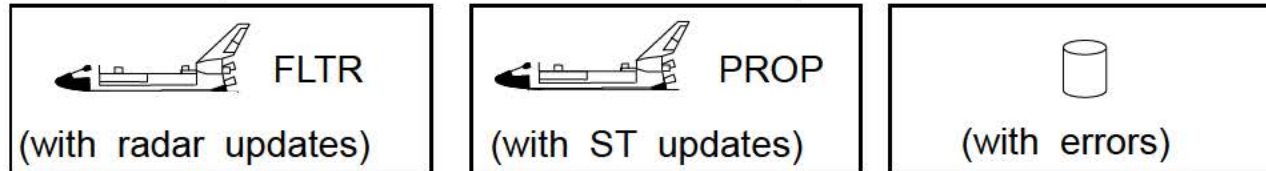
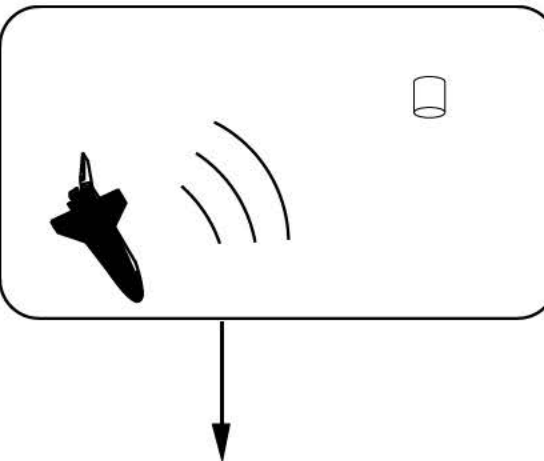


2021/033/	REL NAV	1 001/13:30:32
RNDZ NAV ENA 1*	SV UPDATE	000/00:54:41
KU ANT ENA 2	POS 0.00	Avg G ON 5*
MEAS ENA 3	VEL 0.00	
	NAV	GPS
SV SEL 4 FLTR	RR ATRK	STAT P 1 σ DES
RNG 185.923	RNG 0.000↓	1 NI 31
R - 69.20	R 0.00↓	2↓ 75 32
θ 10.49	EL 0.0↓	3 NI 33
Y + 0.22	AZ 0.0↓	
Y - 0.4	ω P 0.0↓	
NODE 13:37:18	ω R 0.0↓	
	FILTER	SV TRANSFER
S TRK 12	RR 13*	FLTR MINUS PROP
STAT	COAS 14	POS 0.00
FLTR UPDATE 15	ORB Y	VEL 0.00
COVAR REINIT 16		FLTR TO PROP 8
		PROP TO FLTR 9
RES ID	RATIO ACPT REJ	ORB TO TGT 10
RNG 0.00	0.0 0 0	TGT TO ORB 11
R 0.00	0.0 0 0	
V/ EL/ Y 0.00	0.0 0 0	
H/ AZ/ X 0.00	0.0 0 0	
GPS P + 1.56	0.4	EDIT OVRD
V + 3.09	2.4↓	17 18* 19
		20 21* 22
		23 24* 25
		42 43* 44
	ITEM 8 EXEC	

Prior to the initiation of radar marks, the PROP state (containing the uplinked state errors for the ORBITER) is replaced by the updated FLTR state.

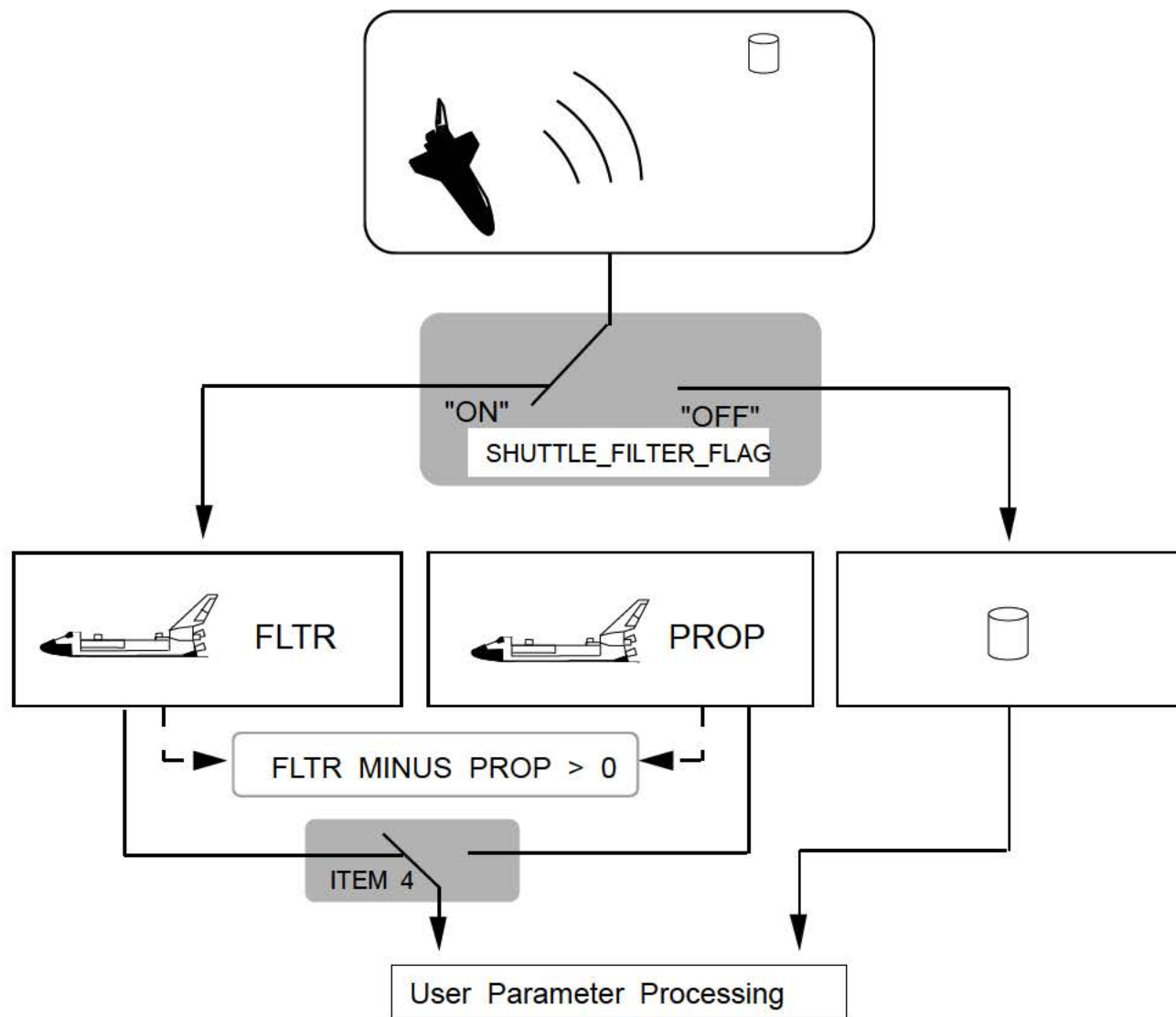


The following configuration is maintained throughout the rest of the rendezvous run. FLTR MINUS PROP will continue to increase.

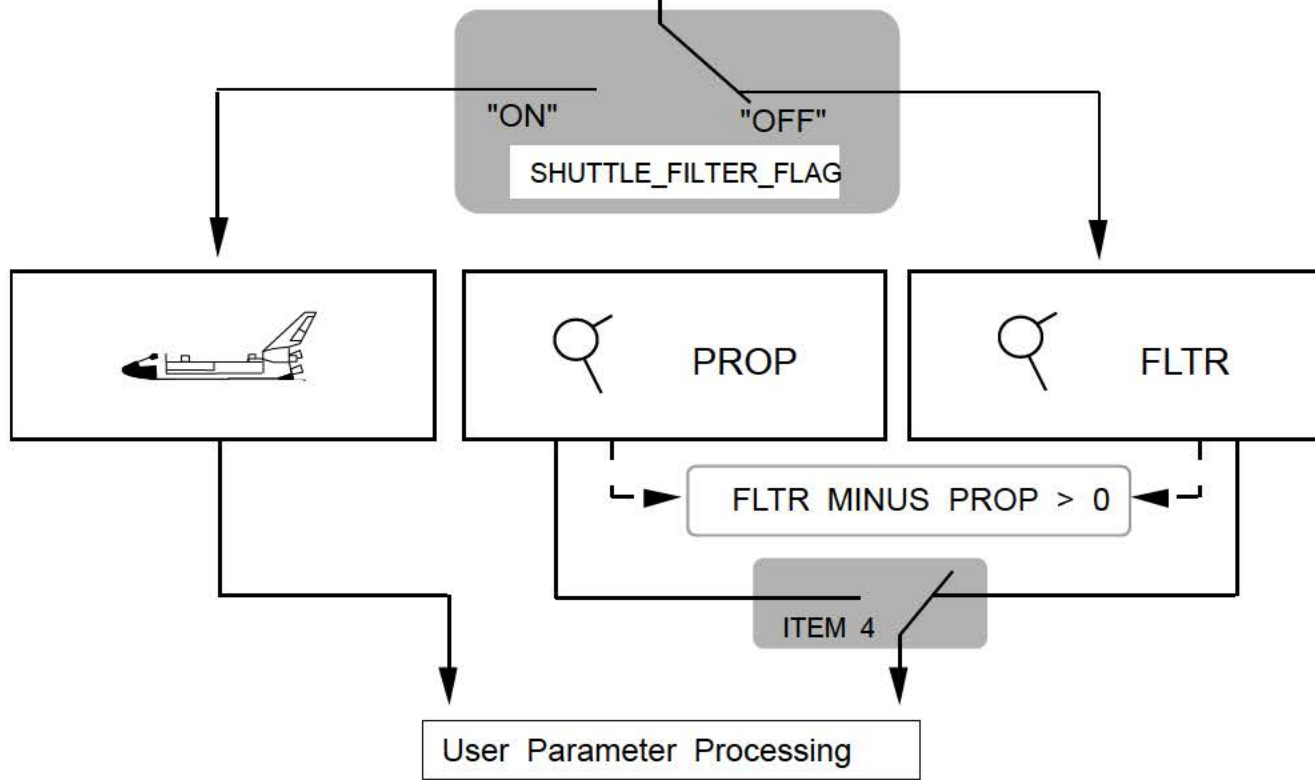
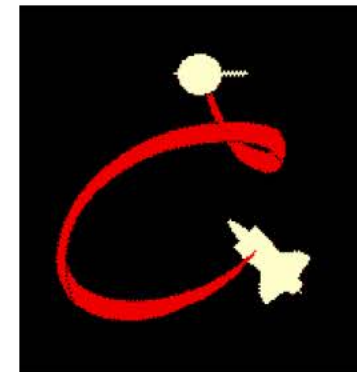
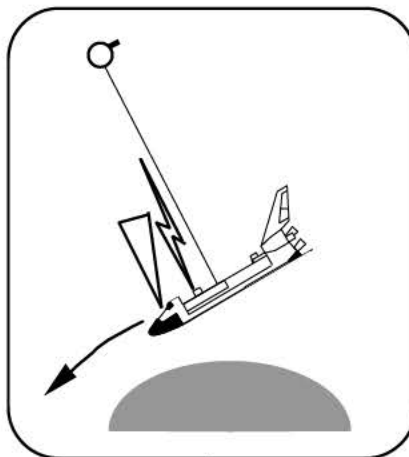


2021 / 033 /	REL NAV	1 001 / 15 :35 :38
RNDZ NAV ENA 1*	SV UPDATE	000 / 00 :00 :56
KU ANT ENA 2*	POS 0 .0 1	AVG G ON 5*
MEAS ENA 3	VEL 0 .0 1	
	NAV	GPS
SV SEL 4 FLTR	RR ATRK	STAT P 1 σ DES
RNG 5 .0 51	RNG 5 .0 40	1 NI 31
R - 7 .71	R - 7 .45	2↓ 75 32
θ 55 .95	EL + 0 .7	3 NI 33
Y - 0 .04	AZ + 0 .8	
Y + 0 .1	OP + 0 .7	
NODE 15 :43 :24	ORB - 0 .0	
	FILTER	SV TRANSFER
S TRK 12	RR 13*	FLTR MINUS PROP
STAT	X	POS 2 .55
FLTR UPDATE 15	ORB Y	VEL 2 .61
COVAR REINIT 16		FLTR TO PROP 8
		PROP TO FLTR 9
RES ID RATIO ACPT REJ		ORB TO TGT 10
RNG + 0 .04 0 .1 367 0		TGT TO ORB 11
R - 0 .16 0 .0 367 0		
V/ EL/ Y - 0 .06 0 .0 345 0		
H/ AZ/ X - 0 .02 0 .0 345 0		
GPS P + 38 .11↓ 4 .4↓		EDIT OVRD
V + 39 .19↓ 3 .3↓		AUT INH FOR
		17* 18 19
		20* 21 22
		23* 24 25
		42 43* 44

Which state is updated by sensor measurements is selectable (either ORBITER or TARGET). The ILOAD "SHUTTLE_FILTER_FLAG" determines if the FLTR state is an ORBITER or TARGET state. Normally the flag is set to "ON," and FLTR is the shuttle state. **ITEM 15 on the REL NAV display can be used to change the flag, as long as relative navigation (ITEM 1) is not enabled.**



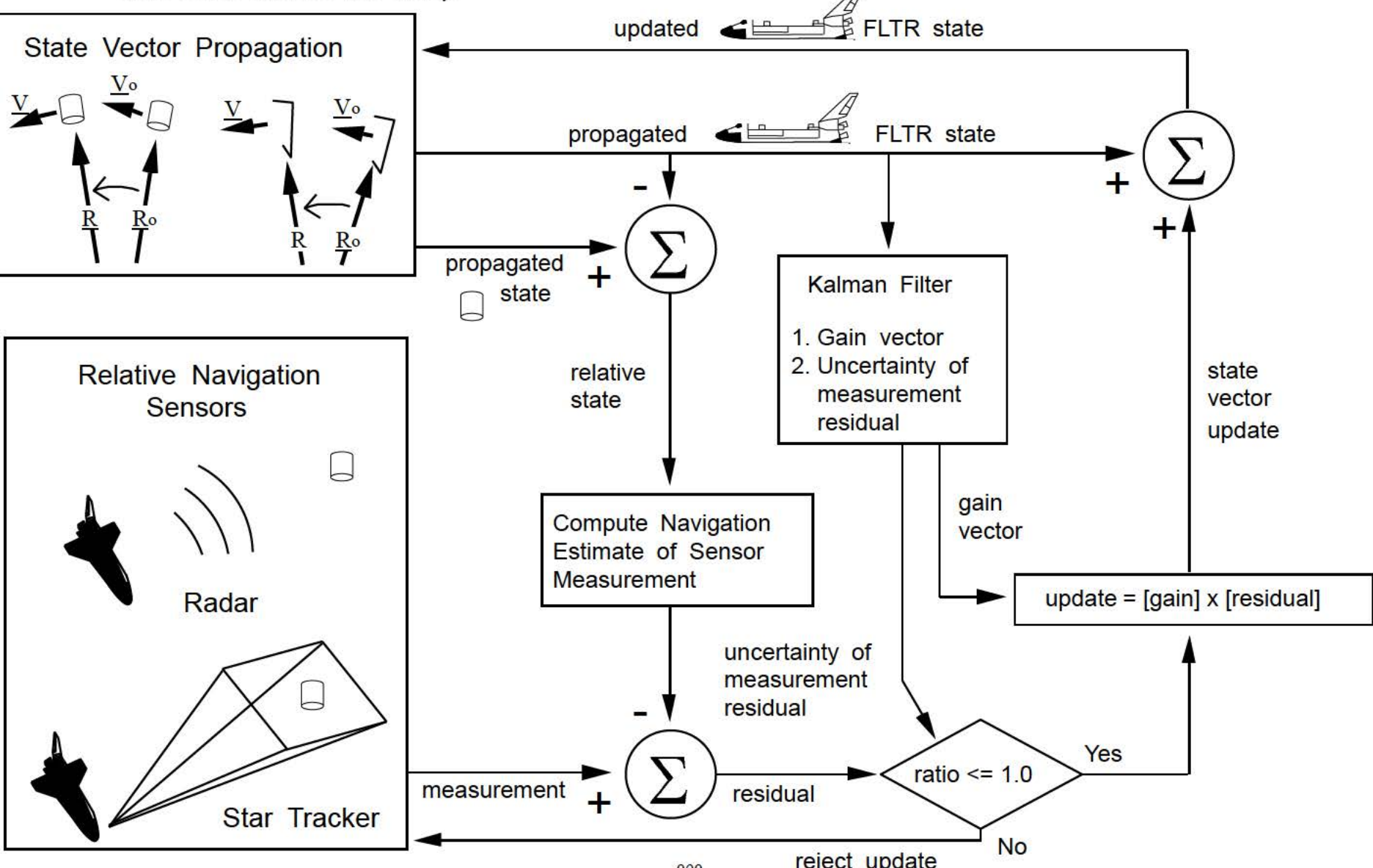
As of this writing, the only time a TARGET state was designated as the "FLTR" state was for STS - 46 and STS - 75 in support of the Tethered Satellite System (TSS).



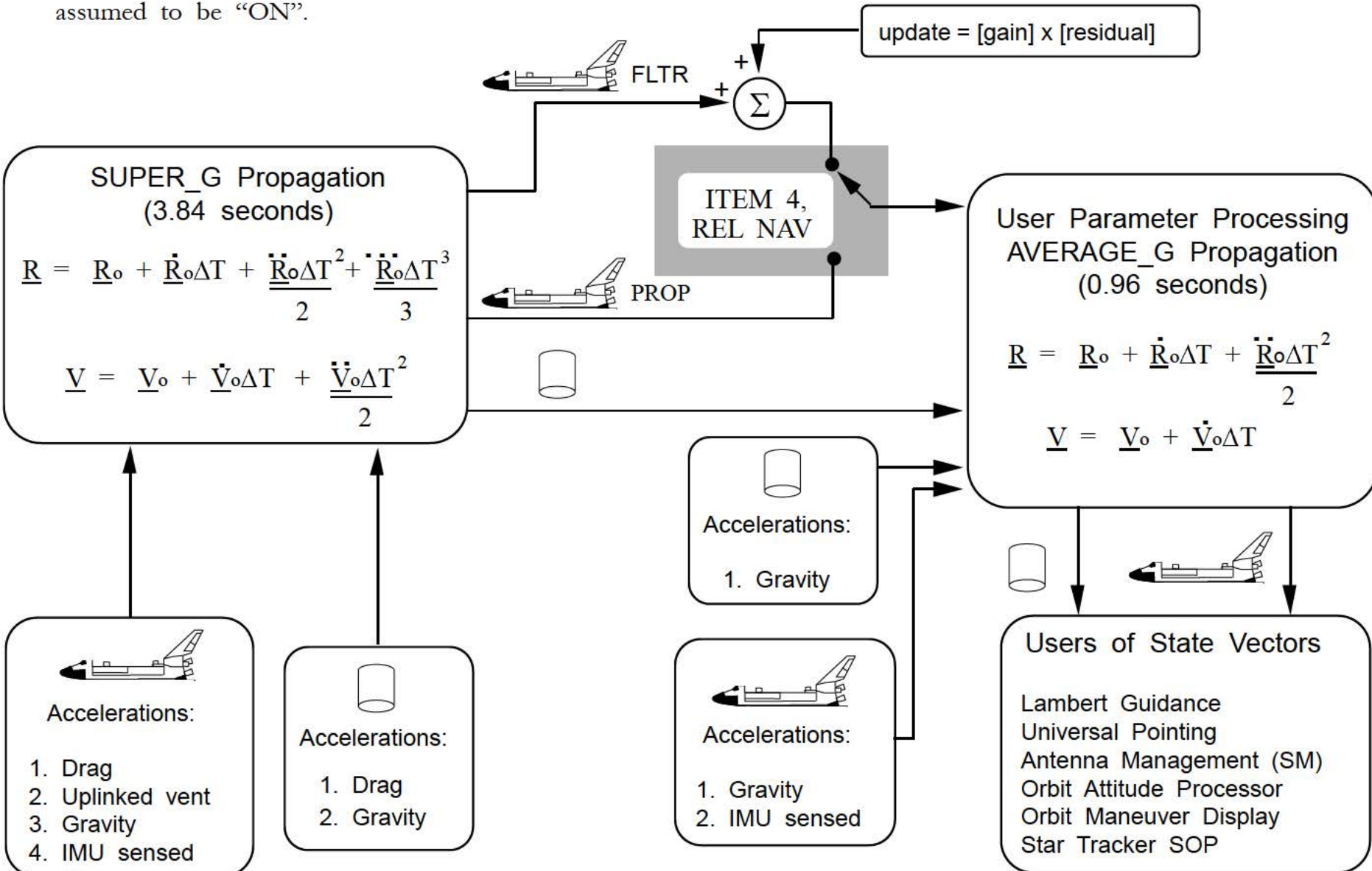
In the Rendezvous Flight Data File and on the REL NAV display, the state updated by sensor data is referred to as the “FLTR” state. However, in the FSW and the On-Orbit NAV FSSR, the term “FILT” is used in variable names for position and velocity.

9.15 Rendezvous Navigation Summary

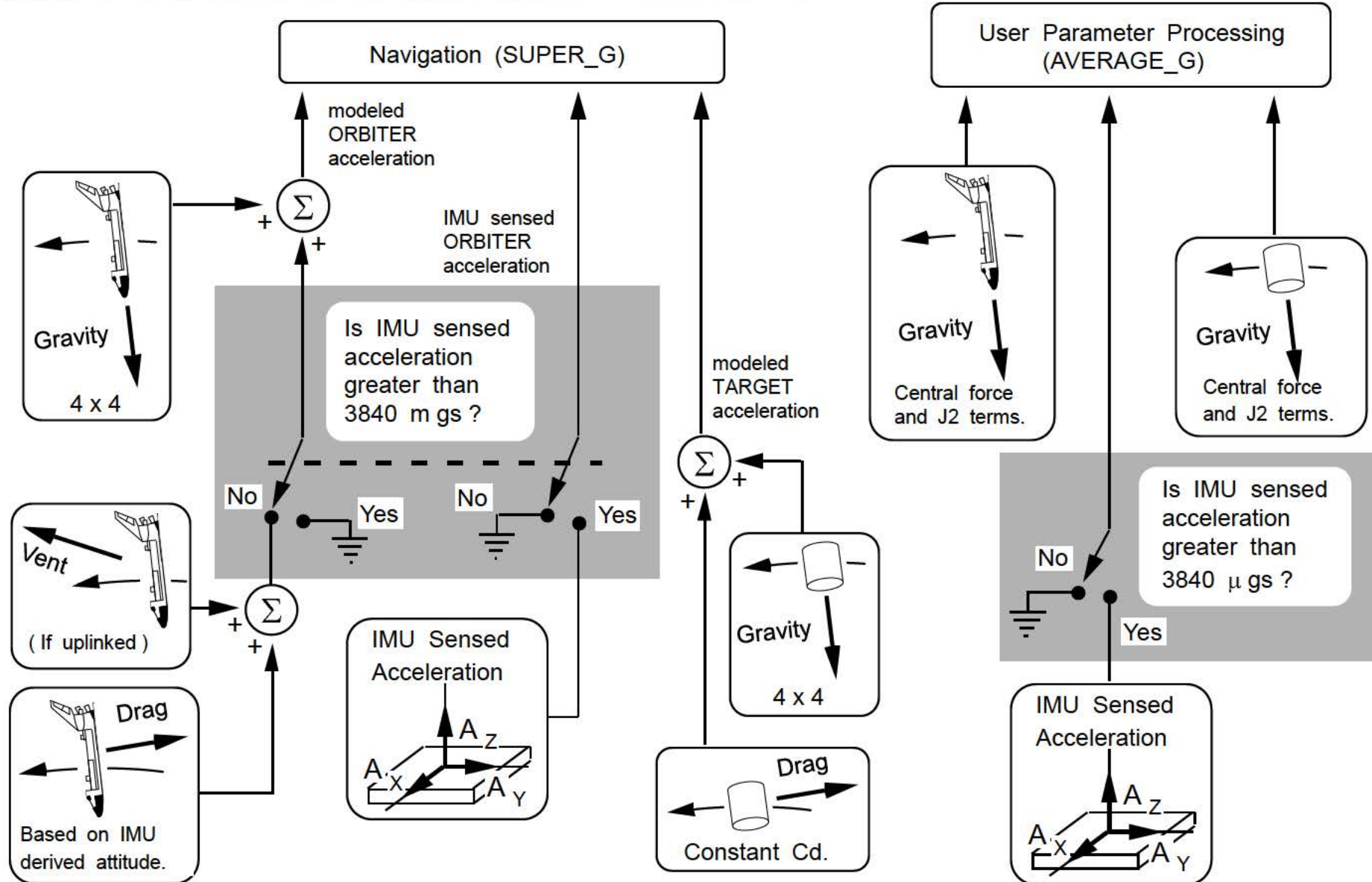
This is a highly simplified representation of the rendezvous navigation process. Some features have been omitted for clarity.



This is a highly simplified representation of the state vector propagation process. Some features have been omitted for clarity. An acceleration summary may be found on the next page. SHUTTLE_FILTER_FLAG is assumed to be "ON".



This is a highly simplified representation of the acceleration computation process. Some features have been omitted for clarity. If ΔV over an RCS maneuver < 0.06 ft/sec, sensed acceleration for SUPER_G is adjusted to "take out" acceleration incorporated into propagation during maneuver. SHUTTLE_FILTER_FLAG is assumed to be "ON."



9.16 GPS

The Shuttle Program certified the 5 channel Collins Miniaturized Airborne GPS Receiver/Shuttle (MAGR/S) for TACAN replacement. In addition to use during entry, GPS state vectors may also be incorporated into navigation while on-orbit.

***Discovery* and *Atlantis* are equipped with one GPS receiver. *Endeavour* is the only orbiter with three GPS receivers and no TACANs.**

Section 9.17 will discuss the difference between differential and relative GPS, and why the current implementation of GPS on the Shuttle cannot be used for relative navigation (**or relative sensor replacement**) during rendezvous.

Section 9.18 details the GPS Resynch function, which can be used while performing relative navigation with the rendezvous radar and the star trackers.



9.17 Differential and Relative GPS

Two techniques can be used to improve the position and velocity solution determined by a GPS receiver, Differential GPS (DGPS) and relative GPS. The two are often confused.

In the simplest form of DGPS, a ground station, with very accurately known clock and position, broadcasts pseudorange corrections for each visible satellite. These corrections are picked up by a GPS receiver on a vehicle and used to correct the pseudoranges of the satellites tracked by that receiver.

Differential GPS has many uses, the most relevant to the shuttle program being precision landing (possible MLS replacement). To support precision landings, an all in view receiver with Receiver Autonomous Integrity Monitoring (RAIM) and carrier phase measurements would be needed.

Relative GPS involves two GPS receivers, neither of which has a position, velocity and time (PVT) solution that are as accurate as the PVT for a differential ground station, but whose errors are correlated. Relative GPS could be used during rendezvous. This application would require two identical, all in view receivers, one on the shuttle and the other on the target (such as space station). GPS measurements from the target would be transmitted to the shuttle. Since raw Y code measurements are classified, both receivers would have to be unkeyed (tracking C/A code with SA effects).

A Kalman filter on the orbiter would process GPS measurements from both vehicles for those satellites that both receivers are obtaining measurements from. This permits common (“correlated”) errors (such as SA, uncompensated ionospheric effects, ephemeris, satellite clock errors) to be canceled.

Processing of “uncommon” measurements will degrade accuracy. To get accurate enough velocities for rendezvous, carrier phase measurements should be obtained and processed by the filter. An upper limit on the range of relative GPS use would probably be in the 10s of kilometers, before some common errors (such as iono, ephemeris) no longer cancel. Both relative and inertial states could be very accurately estimated by this filter.

Due to multipath and antenna obscuration, relative GPS may not provide accurate enough velocities to support proximity operations and docking. The use of pseudolites on station could overcome this problem, but would require significant hardware modifications to the space station.

Relative GPS technology is not mature enough to support shuttle rendezvous, and is currently not an option for shuttle as a replacement for relative sensors (star trackers, Ku band radar). The radar antenna is also used for TDRS communications, and the star trackers are used for IMU alignments. Relative GPS requires “cooperative vehicles” (common GPS receiver and a RF link).

The five channel MAGR/S is not the type of receiver that should be used to support either differential GPS for landings, or relative GPS for rendezvous and proximity operations.

The shuttle must be able to rendezvous with targets that are not equipped with relative GPS (such as the Hubble Space Telescope). The current relative navigation system on the shuttle results in very accurate relative states. Rendezvous can be accomplished with less accurate inertial states, if the relative state between the vehicles is accurate.

9.18 GPS Resynch

When the MIT Instrumentation Lab (now Draper) was developing the rendezvous Kalman filter for Apollo, it was found that the most optimum filter for rendezvous would update the state vectors of both the active vehicle and the target. This would reduce the inertial relative state errors as well as the inertial state errors on each vehicle at the same time.

However, since the Apollo computers (LEM and CSM) did not have enough memory for a Kalman filter that could filter both vehicle states at the same time (resolve both CSM and LEM inertial errors). It was found, however, that acceptable results could be obtained with a sub-optimal filter, which only updated one vehicle's state vector. In other words, one could rendezvous if you had an accurate relative state, but large inertial errors. Furthermore, they wanted to use the same Kalman filter code for both rendezvous and cis-lunar navigation (taking marks on stars and the earth with a sextant). This could be done if only one vehicle state was to be filtered.

The original shuttle rendezvous navigation filter design in the mid 1970s was optimal, with a 19 state filter. The additional 6 states would allow updating of both the orbiter and target vectors at the same time. However, due to memory limitations in the AP-101B, a sub-optimal filter (13 state) was used. In the sub-optimal filter, only the mean squared relative error is reduced. The non-filtered state is assumed to be perfect, and the covariance matrix represents the inertial relative state error, not the inertial error of the filtered state. The filter updates one vehicle's state vector in order to drive the difference (residual) between the measured relative state parameters and the navigation estimate of those parameters to zero. The result of this is that the inertial state vector errors on the filtered state change to eventually match the inertial state vector errors on the non-filtered state.

This aspect of the orbiter's rendezvous navigation filter is well known, and is observed in SPF Level 8 Testing and SAIL. The sub-optimal filter is “good enough” for rendezvous, as has been demonstrated by Apollo and shuttle rendezvous missions. However, having inertial errors on the navigated orbiter and target state vectors can lead to errors in targeting and burn guidance. A sub-optimal filter will not solve for relative error as well as an optimal filter. The real test of Kalman filter performance is not relative error, but error in the Lambert targeting solutions.

The reason Draper included the resynch in CR 91051K was to “make up” for the sub-optimal implementation of the filter. The GPS/AP-101S data fusion experiment conducted during STS-69 by Dr. Russell Carpenter (then of the JSC Engineering Directorate, now with Goddard) and Dr. Robert Bishop (University of Texas at Austin) was also an attempt to compensate for the sub-optimal nature of the rendezvous filter.

The Kalman filter works to achieve a good relative state. If SHUTTLE_FILTER_FLAG is ON, whatever inertial errors are on the target will become the inertial errors on the orbiter, since the orbiter state is being updated. Historically, SHUTTLE_FILTER_FLAG has always been ON, since ground tracking gives us a target state (it is doing little or no thrusting) that is more accurate than the ground tracking orbiter state (orbiter is thrusting).

If the target has high inertial errors, the orbiter inertial errors should increase as sensor marks are taken. For a star tracker pass, out-of-plane and altitude inertial errors of the two vehicles will start to match, while downtrack errors should still differ. During a radar pass, angles, range rate and range marks will result in inertial errors matching in all three directions.

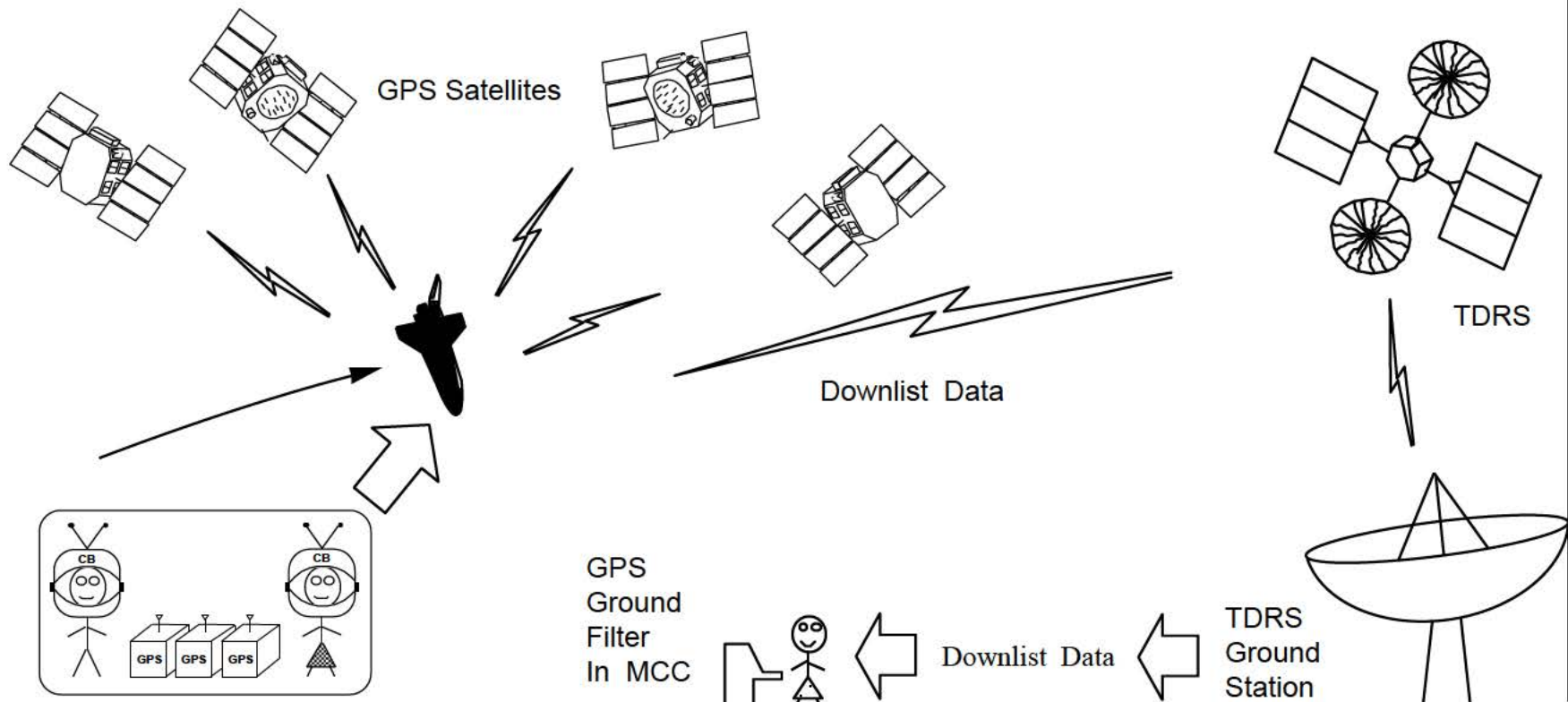
When Pete Kachmar designed the GPS Resynch logic, he intended for SHUTTLE_FILTER_FLAG to be OFF (filter the target state). GPS would be used to maintain an accurate shuttle inertial state, and the target state would be filtered to put the small shuttle inertial errors on the target. This would result in a good relative state and good inertial states. GPS Resynch allows the shuttle inertial error to be kept small while preserving the good relative state that the filter has been working to achieve.

Since the Resynch is performed in inertial space, it is transparent to the relative sensor residuals.

Spacecraft Trajectory Analysis and Mission Planning Simulation (STAMPS) rendezvous runs performed by USA Flight Design have shown that the use of GPS Resynch during nominal rendezvous does not improve propellant use enough to warrant use of it. However, GPS Resynch may be of value during long term station keeping when the use of Relative Navigation is required.

9.19 GPS Ground Filter

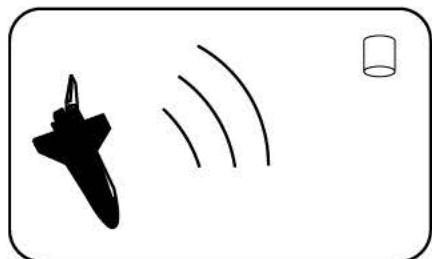
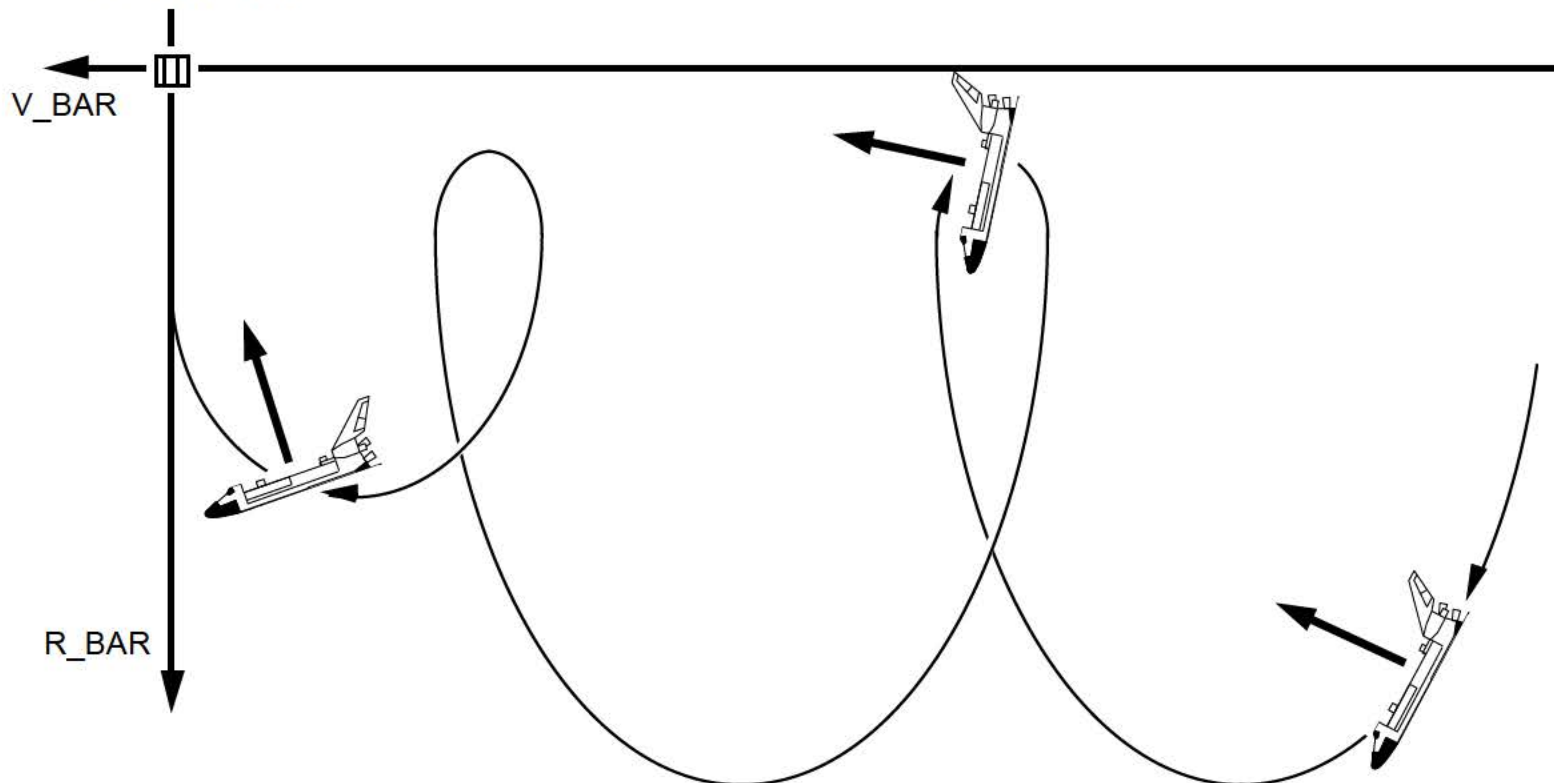
The MAGR on the shuttle contains a Kalman filter and navigation algorithms that were designed to support “terrestrial” users (planes, helicopters, missiles). Furthermore, the MAGR Kalman filter was tuned so that it could be placed on a variety of platforms without having to be retuned. The tuning assumes “worst case” IMU performance and a poor MAGR clock. While the MAGR states are far more accurate than TACAN based navigation, they are not accurate enough to support orbit determination and maneuver planning. A GPS ground filter, called the Spacecraft Position, Optimal Tracking (SPOT) program, was developed to obtain more accurate estimates of spacecraft position and velocity. SPOT will filter MAGR position and velocity, using the MAGR Figure of Merit, high order Earth gravity, lunar and solar perturbations and atmospheric drag model data as inputs. The GPS Ground Filter will first be used to support ISS state determination. For shuttle, MAGR states filtered by SPOT could be used to supplement the current orbit determination scheme, which uses TDRS (S Band) and ground radar (C Band) tracking.



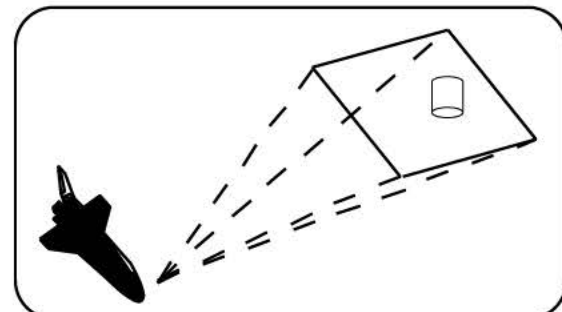
This page intentionally left blank.

10.0 FLIGHT CONTROL DURING ON-BOARD TARGETED PHASE

While coasting during the on-board targeted phase, the flight control system uses Relative Navigation (REL NAV) and Universal Pointing (UNIV PTG) to point the -Z body axis at the TARGET.

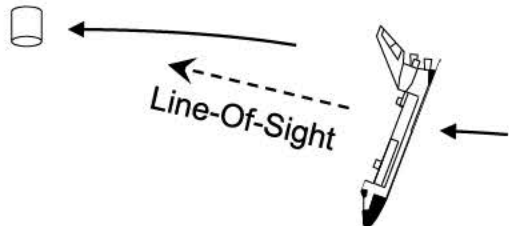


The -Z body axis is pointed at the TARGET since the radar and -Z star tracker "see" in that direction.



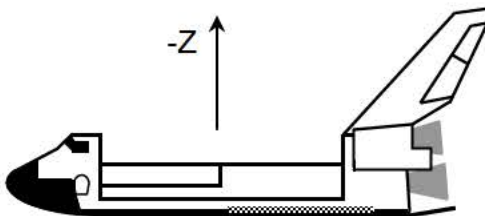
10.1 Target ID and - Z Body Axis

Target ID



Target ID = 1 corresponds to an orbiting body (TARGET) and requires REL NAV to be enabled. ORBITER and TARGET state vectors are used to compute a line-of-sight vector.

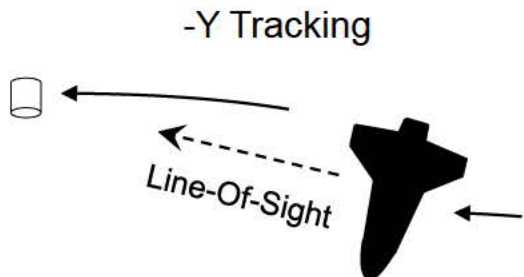
-Z Body Axis



The -Z body axis corresponds to Body Vector 3 on the Universal Pointing display.

2011 / /		UNIV PTG	1 004 / 23 : 53 : 00
CUR MNVR COMPL		23 : 53 : 20	000 / 00 : 20 : 54
1 START TIME		<u>_0 / 00 : 00 : 00</u>	
MNVR	OPTION	START	CUR FUT
5 R	<u>--0 .00</u>	TRK	RBST 25
6 P	<u>0 .00</u>	ROT	CNCL 26
7 Y	<u>0 .00</u>	CNCL	DURATION 27
			<u>_0 : 00 : 00 .00</u>
TRK / ROT OPTIONS		ATT MON	
8 TGT ID <u>_1</u>		22 MON AXIS 1 +X	
9 RA	<u>--0 .000</u>	ERR TOT	23*
10 DEC	<u>--0 .000</u>	ERR DAP	24
11 LAT	<u>--0 .000</u>	ROLL	YAW
12 LON	<u>--0 .000</u>	CUR	212 .39 6 .41 4 .09
13 ALT	<u>----0 .0</u>	REQD	212 .44 10 .53 6 .70
14 BODY VECT 3		ERR	+ 0 .43 - 4 .86 + 0 .00
		RATE	- 0 .001 - 0 .169 - 0 .002
15 P	<u>-90 .00</u>		
16 Y	<u>0 .00</u>		
17 OM			
ITEM 19 EXEC			

10.2 -Y Star Tracker and Rendezvous

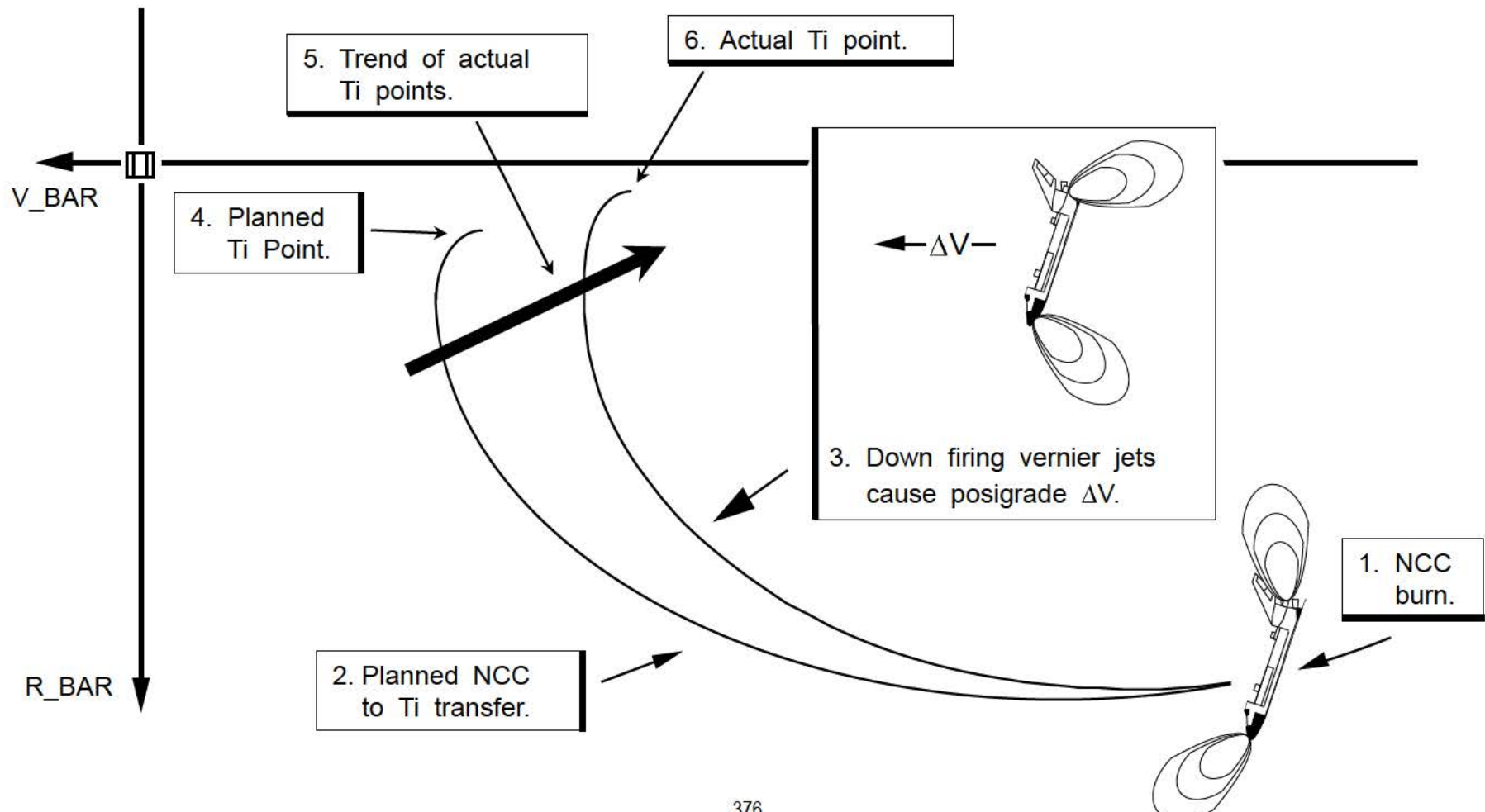


In the event of a -Z star tracker problem, the -Y tracker may be used. The choice of attitude is intended to keep the maneuver from and back to the -Z target track attitude as close to pure roll as possible. After a -Y star tracker pass, -Z tracking will be resumed to facilitate radar operation or manual piloting during proximity operations.

2011 / /	UNIV PTG	1 001 / 15 :18 :40
CUR MNVR COMPL	15 :18 :40	000 / 00 :24 :41
1 START TIME	_ _0 / 00 :00 :00	
		CUR FUT
MNVR OPTION	START MNVR	18
5 R _ _0 . 00	TRK	19 *
6 P _ _0 . 00	ROT	20
7 Y _ _0 . 00	CNCL	21
		RBST 25
		CNCL 26
		DURATION 27
		_ _0 : 00 : 00 . 00
TRK / ROT OPTIONS	ATT MON	
8 TGT ID _ _1	22 MON AXIS	1 +X
	ERR TOT	23*
	ERR DAP	24
9 RA _ _0 . 000	ROLL	PITCH YAW
10 DEC _ _0 . 000	CUR	133 . 52 128 . 58 341 . 57
11 LAT _ _0 . 000	REQD	134 . 69 128 . 02 340 . 19
12 LON _ _0 . 000	ERR	+ 1 . 35 - 0 . 62 + 1 . 35
13 ALT _ _0 . 0	RATE	- 0 . 013 - 0 . 056 + 0 . 067
14 BODY VECT 4		
15 P _ _0 . 00		
16 Y _ _280 . 57		
17 OM _ _90 . 00		
ITEM 19 EXEC		

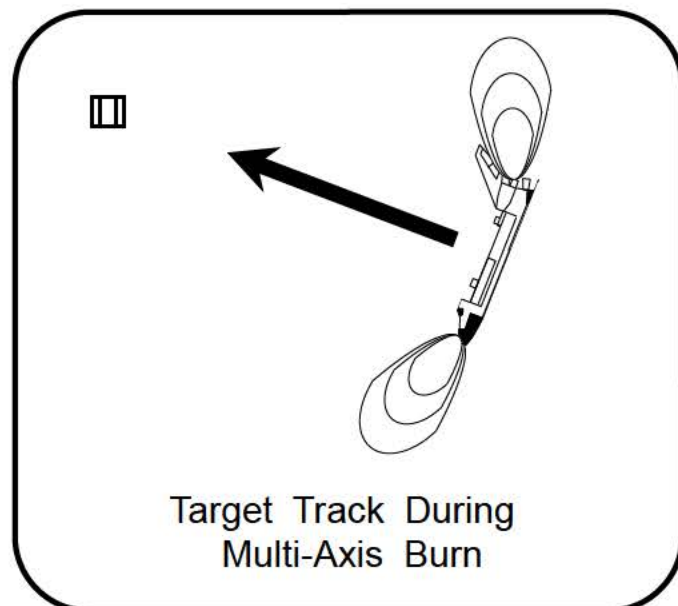
10.3 Ti Burn Position Miss Due to Vernier Jets

Vernier jets are used to maintain proper attitude during target track (Major Mode 201) periods. These jets produce translational as well as rotational acceleration. The effect of the translational acceleration (often referred to as 6 degree-of-freedom, or 6 DOF, effects) often manifests in the actual position of the Ti burn.



10.4 Flight Control During Burns

If the DV for a burn is less than 4.0 ft/sec, the ORBITER remains in target track during the burn. The burn is performed manually via THC commands one axis at a time (also called axis-by-axis), using the primary RCS jets. This is called a “multi-axis” burn.

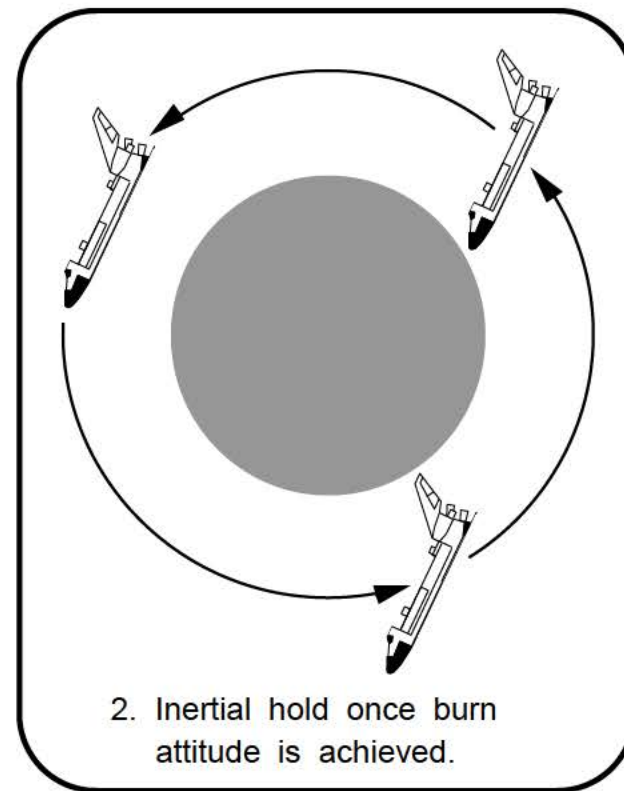
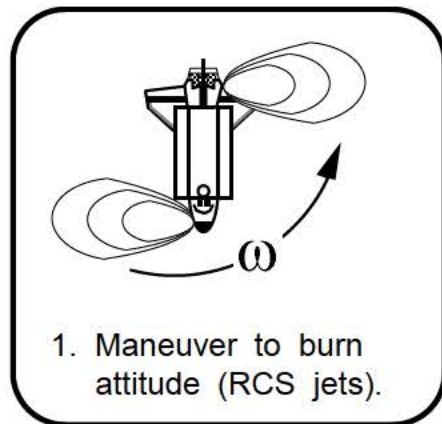


If the ΔV for a burn is greater than 4.0 ft/sec, the ORBITER is maneuvered to the burn attitude. Once the burn attitude is achieved, an inertial attitude hold is initiated.

If the ΔV is from 4 to 6 ft/sec, the burn is done manually via THC commands. Due to the maneuver to attitude, the 4 +X primary RCS jets do most of the firing. This is called a “+X burn.”

For ΔV from 6 to 12 ft/sec, one OMS engine is used. If ΔV is greater than 12 ft/sec, both OMS engines are fired. Sometimes burns greater than 12 ft/sec will be fired with one OMS engine to keep the number of engine starts low.

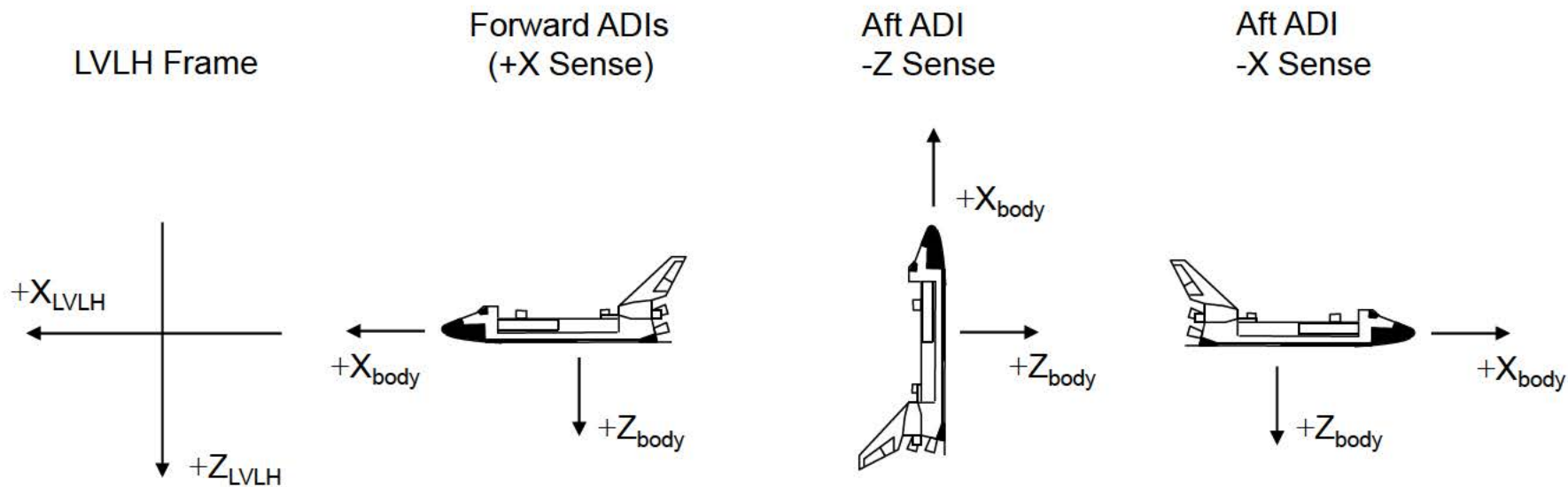
These are referred to as “single” and “dual” OMS burns.



10.5 0/0/0 LVLH Attitudes

Orbiter attitudes are frequently expressed in the LVLH frame, using a pitch, yaw, and roll Euler angle sequence. In order to visualize the attitude, one must know how the Orbiter is oriented with respect to LVLH when pitch, yaw and roll are all zero.

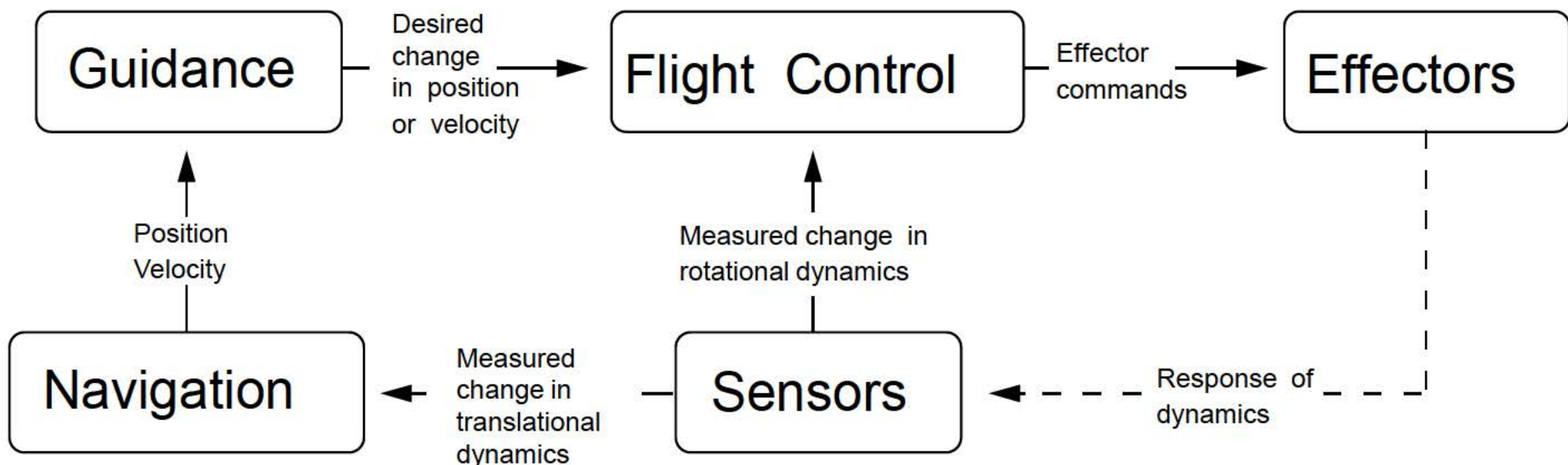
Illustrated below is the LVLH 0/0/0 attitude for each sense of the Attitude Director Indicators (ADI) in the cockpit. The body axes are shown for each. Both the LVLH Y axis and the Y body axis are into the page.



This page intentionally left blank.

11.0 INTEGRATED GN&C DURING RENDEZVOUS

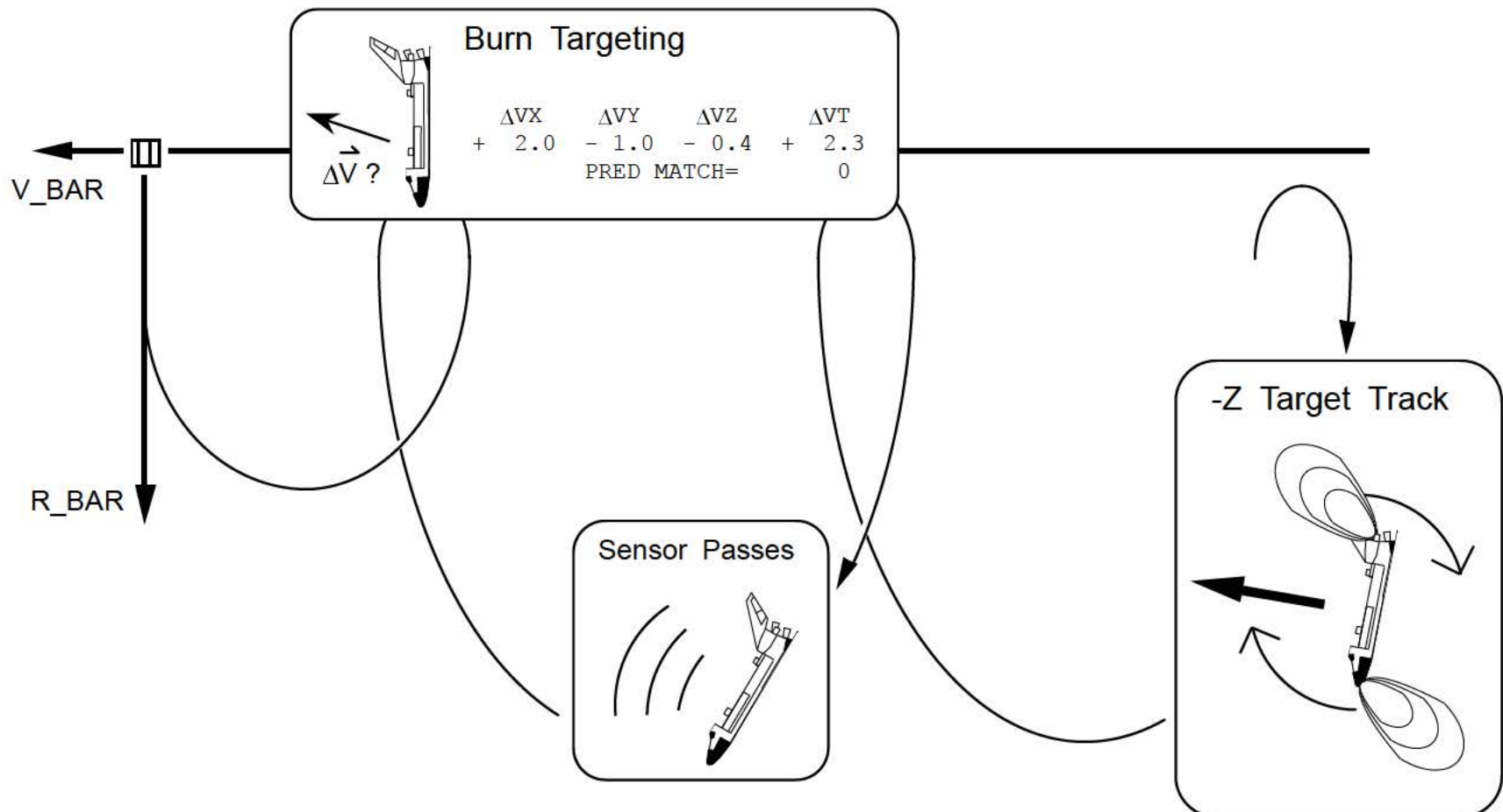
Navigation, guidance, flight control, sensors, and effectors (such as gimbaled engines and attitude control jets) in space vehicles work together to control vehicle motion so that mission objectives may be attained. A simple GN&C system is shown below.



Sensors, such as an Inertial Measurement Unit (or IMU), detect changes in vehicle velocity and orientation. Acceleration is used by the navigation system to determine current position and velocity. Guidance uses position and velocity in conjunction with some desired vehicle position and/or velocity at a future time to determine the ΔV vector. Flight control uses the ΔV from guidance and the measured change in rotational dynamics to compute steering commands for the effectors. The effectors in turn change the translational and rotational dynamics of the vehicle.

11.1 Integrated GN&C During Orbit Coast

Between burns, while the GPC is in Major Mode 201 (orbit coast), activities performed by the crew (burn targeting, -Z target tracking, and sensor passes) require that the different parts of the GN&C, sensor, and effector system communicate with each other. The GN&C system deals with two areas of vehicle dynamics in Major Mode 201, translational (burn targeting) and rotational (-Z target track). Sensor passes improve navigation's estimate of ORBITER (or TARGET) translational dynamics and are facilitated by the -Z target track.

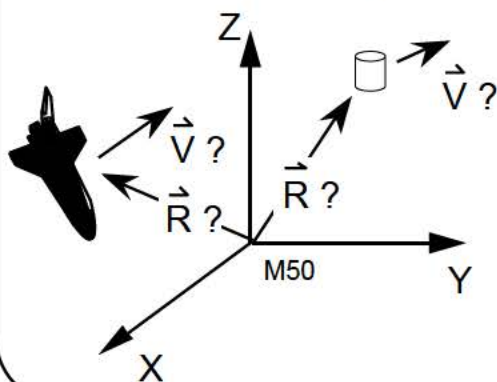


It is easier to understand the integrated GN&C process if the translational and rotational functions are considered separately. The role of these systems is best understood in terms of a question that each works to answer. Below are the “questions” concerning translation.

Navigation

Where is the ORBITER ?
How fast is it moving ?

Where is the TARGET ?
How fast is it moving ?



Orbit Targeting (Lambert)

How should the ORBITER change its dynamics (ΔV) to achieve a desired position at a given time ?

ΔV ?	ΔV_X	ΔV_Y	ΔV_Z	ΔV_T
	+ 2.0	- 1.0	- 0.4	+ 2.3
	PRED MATCH=			0

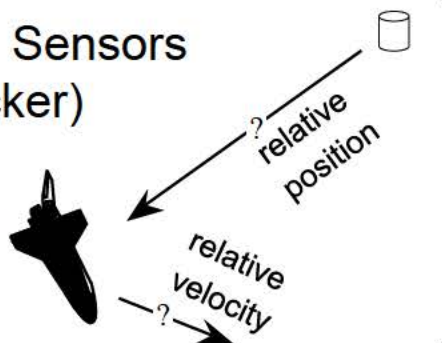
Flight Control

How should the ORBITER use its effectors to achieve this ΔV ?



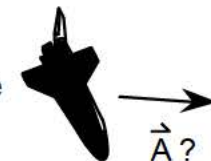
Relative Navigation Sensors (radar, star tracker)

What is the ORBITER's position and velocity relative to the TARGET ?

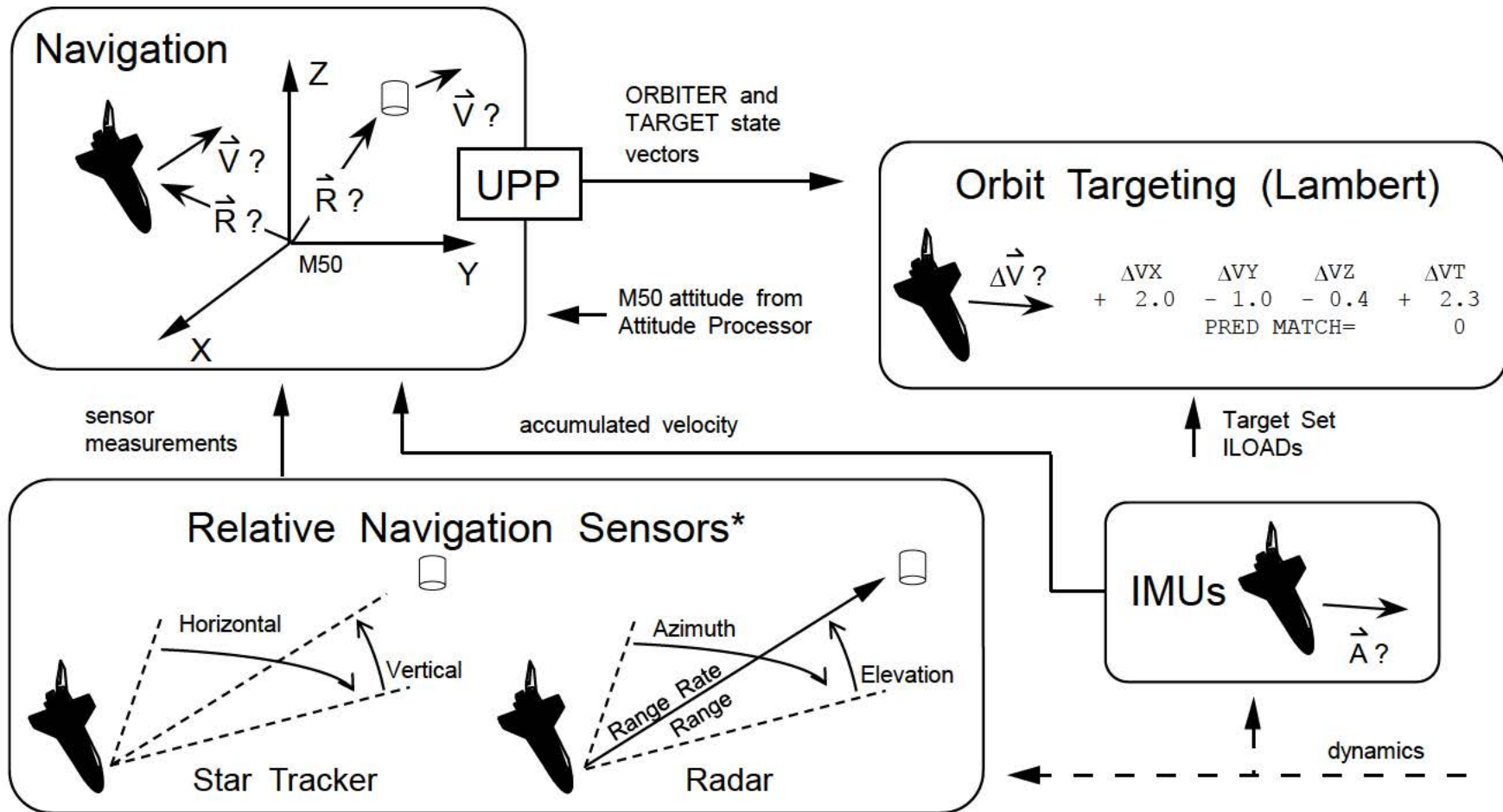


IMUs

How is the ORBITER accelerating ?



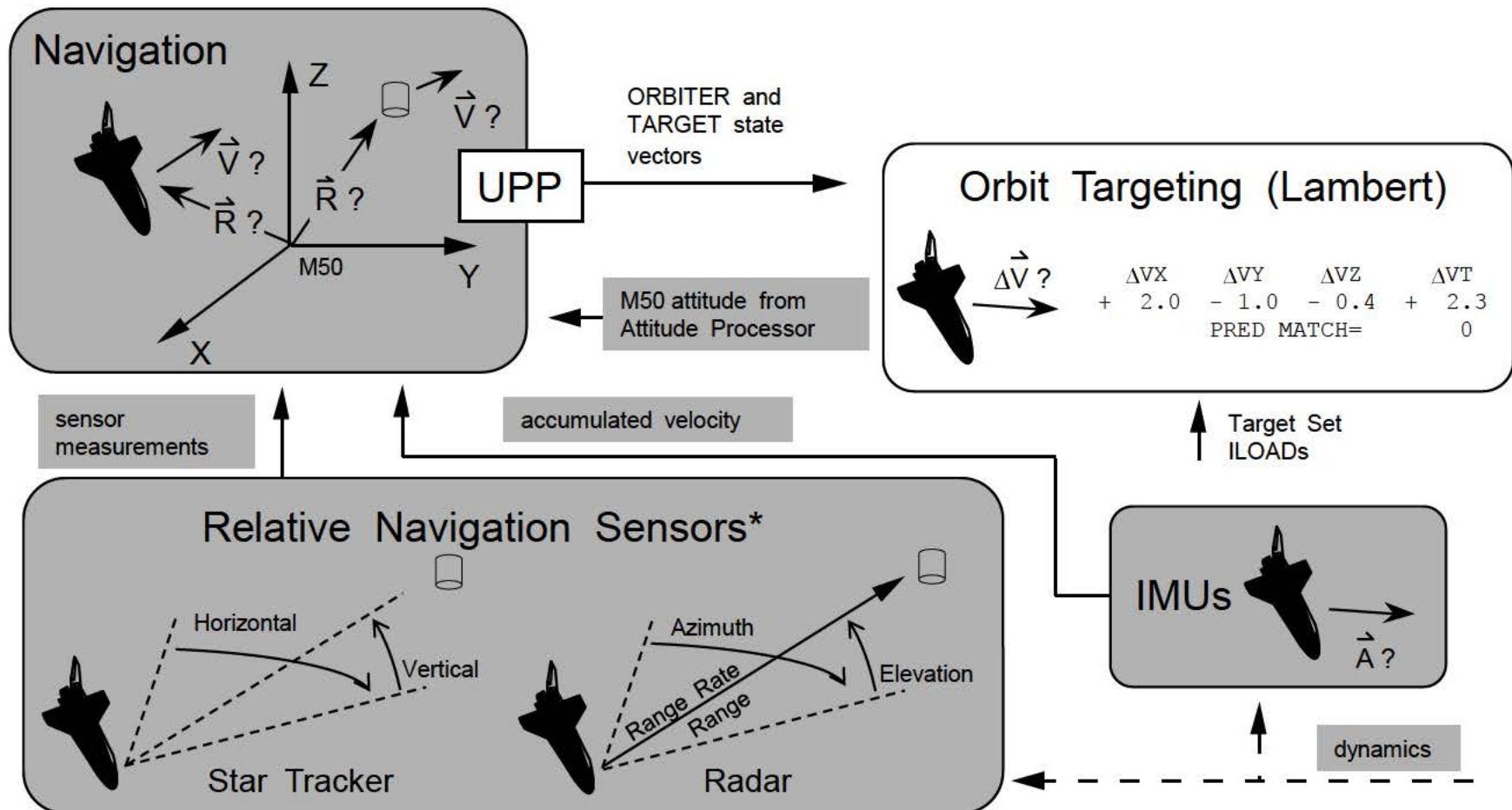
This is a highly simplified chart illustrating the interfaces concerning translational dynamics. Only those interfaces which are critical to developing an understanding of integrated GN&C are shown. The following two pages describe the interfaces.



*The Crew Optical Alignment Sight is not shown for simplicity.

Accelerometers in the IMUs detect translational acceleration. The sensed acceleration is accumulated in terms of a velocity count. Navigation uses the accumulated velocity, along with radar and/or star tracker measurements of ORBITER translational dynamics relative to the TARGET, to compute ORBITER position and velocity in the M50 frame. ORBITER M50 attitude from the Attitude Processor is also used by navigation to compute the ORBITER state.

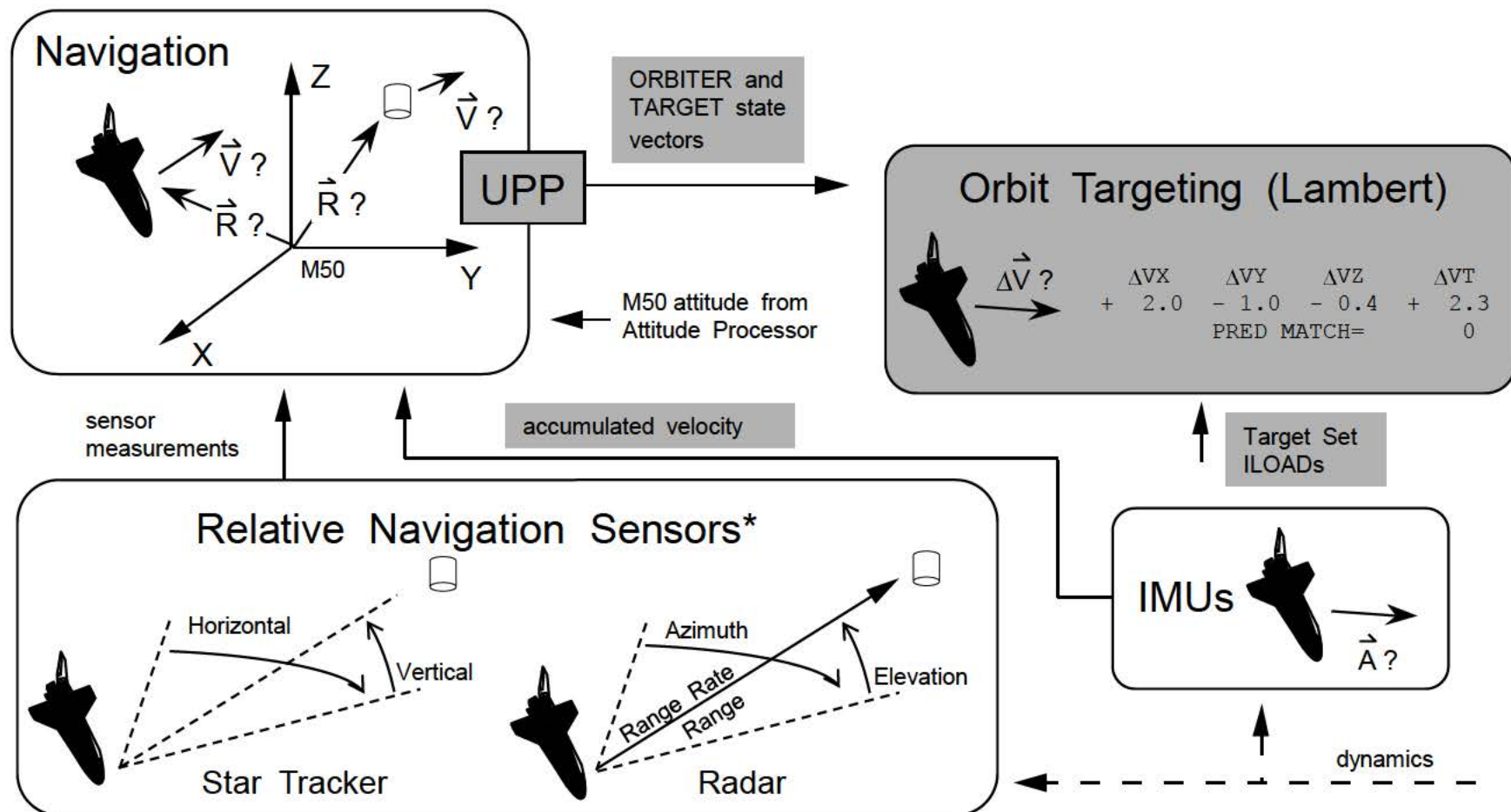
IMU data is never used to compute the TARGET state, but radar, star tracker or Crew Optical Alignment Sight (COAS) data may be used.



*The Crew Optical Alignment Sight is not shown for simplicity.

User Parameter Processing sends ORBITER and TARGET state vectors to Orbit Targeting, which uses them in computing burns. It is important to note that the ΔV computed by Orbit Targeting is not acted upon by the Flight Control system while in MM 201.

The target set ILOADs are also used by Orbit Targeting.



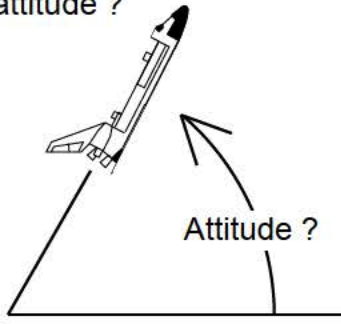
*The Crew Optical Alignment Sight is not shown for simplicity.

A similar set of questions may be formulated concerning the manipulation of the ORBITER's rotational dynamics (attitude, rotational rate) so that the -Z body axis remains pointed at the TARGET.

The Attitude Processor is officially considered to be a part of Flight Control, but is shown separately for clarity.

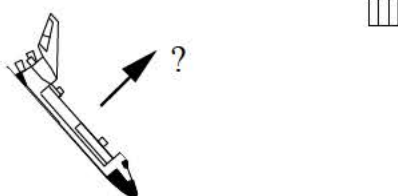
Attitude Processor

What is the ORBITER'S attitude ?



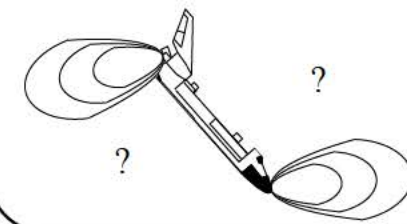
Universal Pointing

What attitude should the ORBITER have so that the -Z body axis is pointed at the TARGET ?



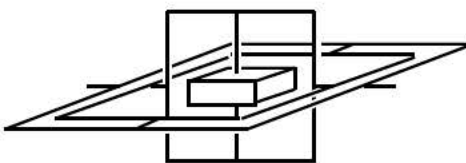
Flight Control

How should ORBITER effectors be used to get to that attitude ?



IMUs

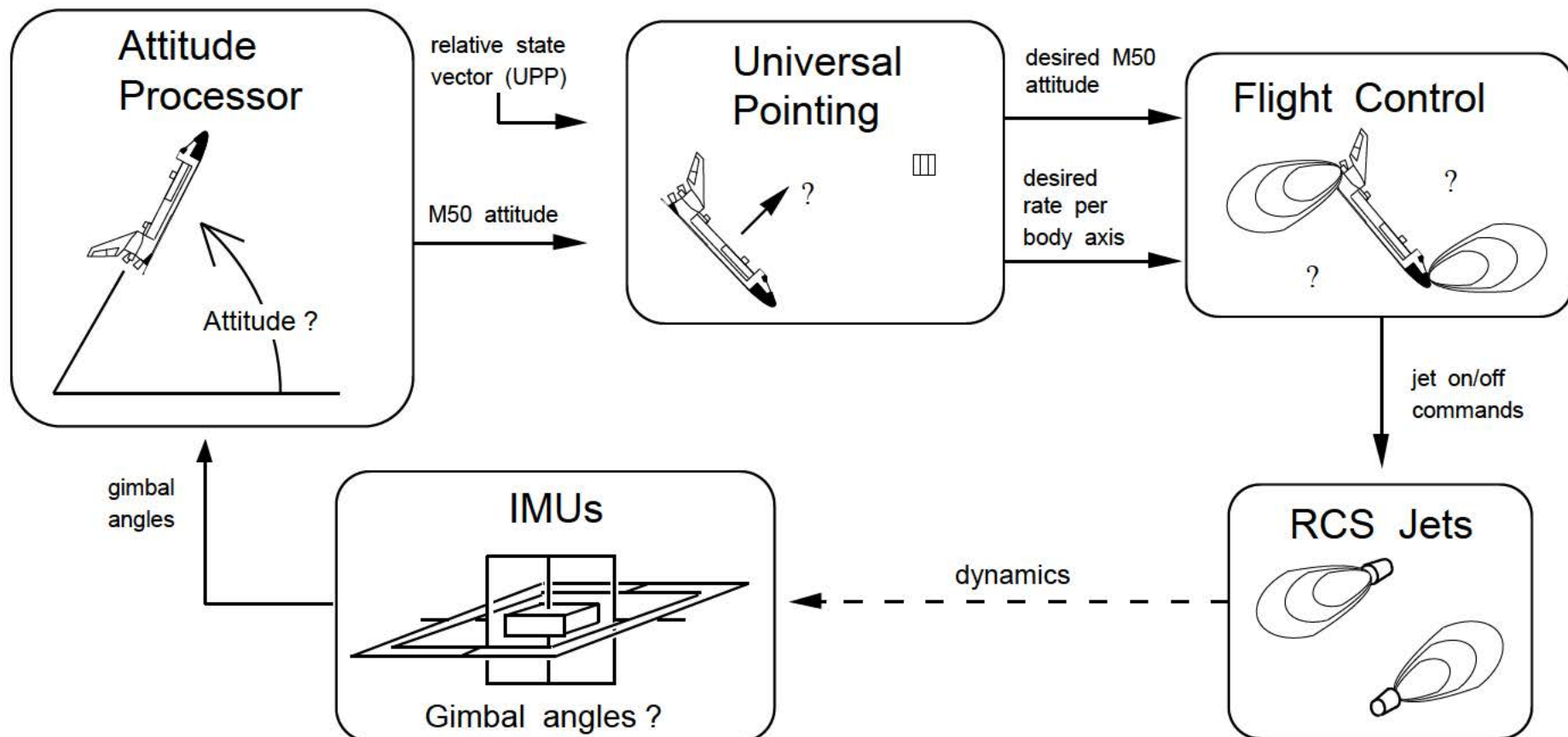
How should the IMU platform be rotated to maintain a constant orientation?



This is a highly simplified chart illustrating the interfaces concerning rotational dynamics. Only those interfaces which are critical to developing an understanding of integrated GN&C are shown.

The function of the Attitude Processor is analogous to that performed by navigation for translational dynamics. Universal Pointing can be thought of as being “rotational guidance.”

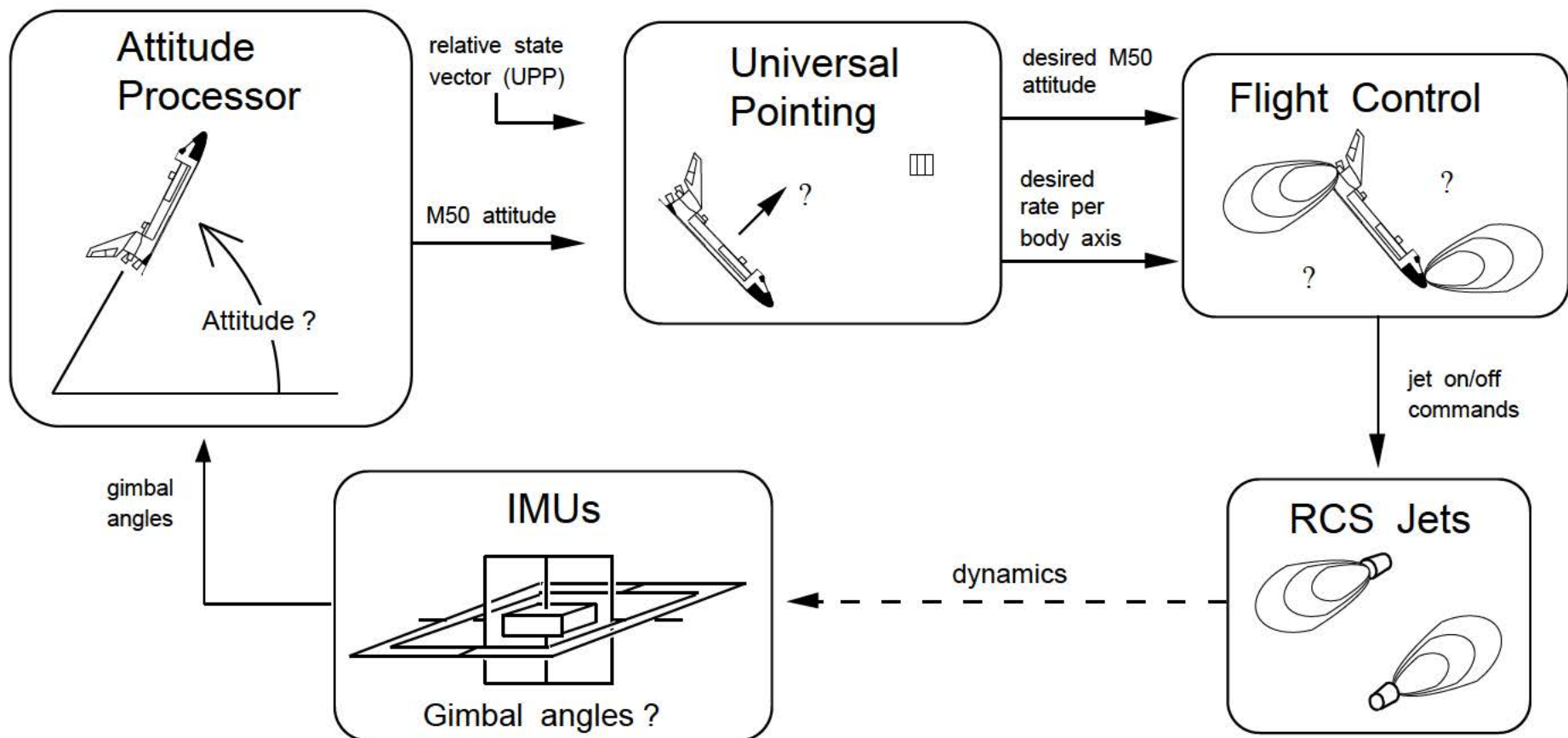
The next page describes the interfaces.



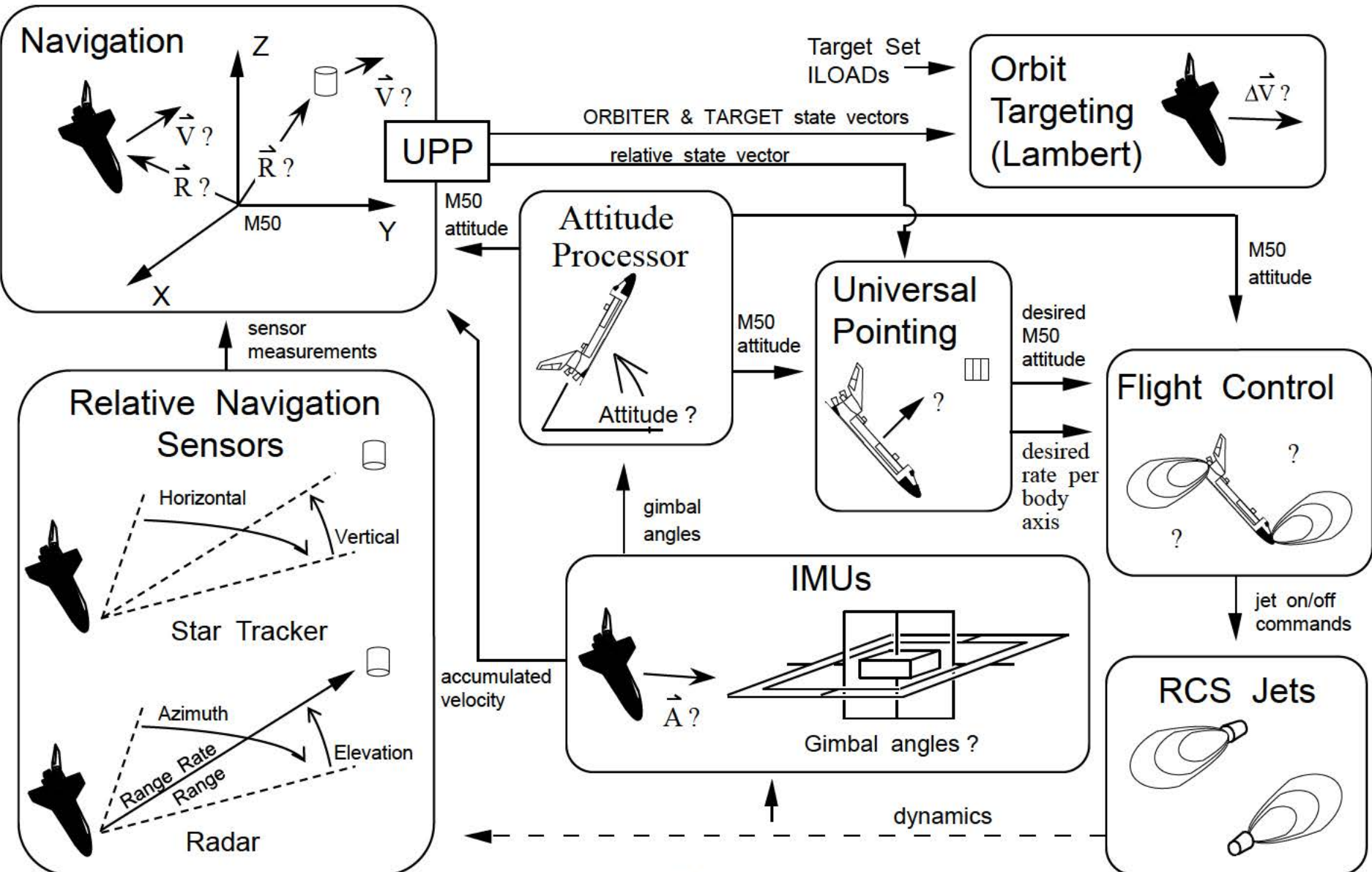
Each IMU platform is mounted on a set of 4 gimbals. This enables the platform to be rotated so that it maintains a constant inertial orientation. The IMUs measure the ORBITER attitude with respect to the IMU platform (gimbal angles). From the gimbal angles, the Attitude Processor determines the ORBITER M50 attitude. Inputs to Universal Pointing include the current attitude and the ORBITER's position and velocity relative to the TARGET (from UPP). These are used to compute the desired attitude and how fast the ORBITER should rotate in each body axis.

Flight Control selects and fires RCS jets so that the desired attitude and body rates are maintained.

The impact of jet firings on the rotational dynamics is then sensed by the IMUs.

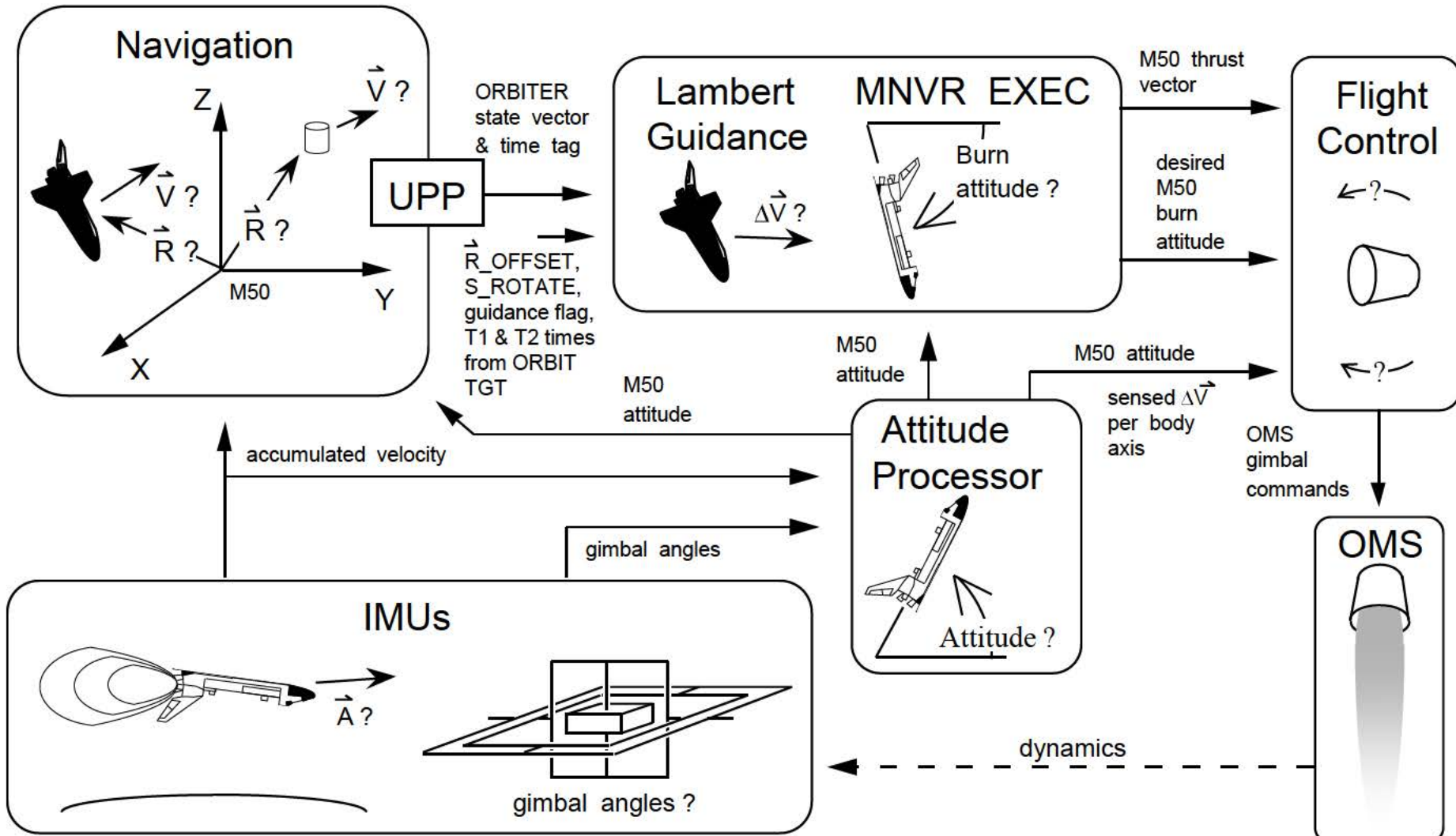


Below is a highly simplified diagram of the integrated GN&C, sensors, and effectors for both translation and rotation in Major Mode 201.

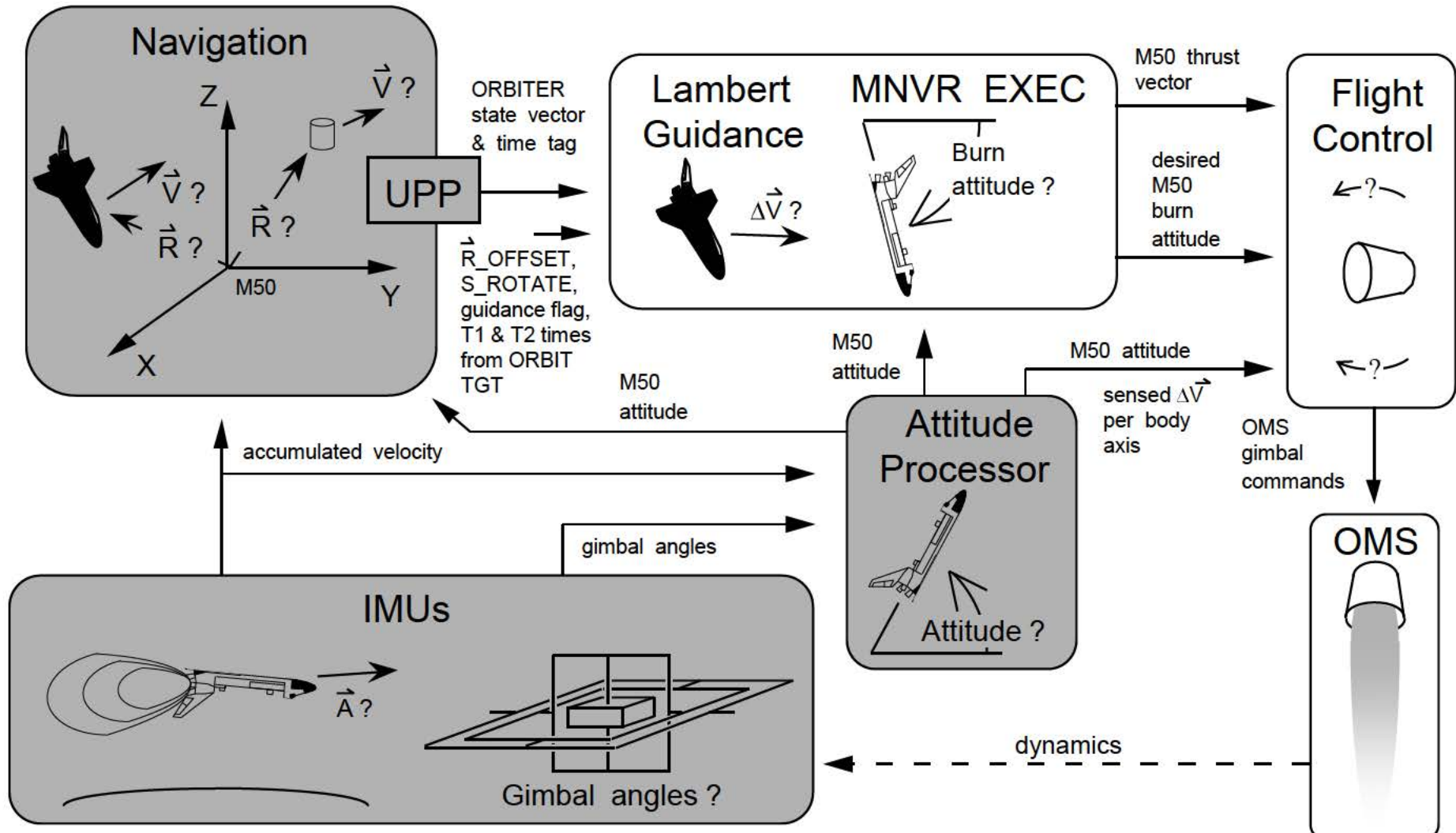


11.2 Integrated GN&C For OMS Burns

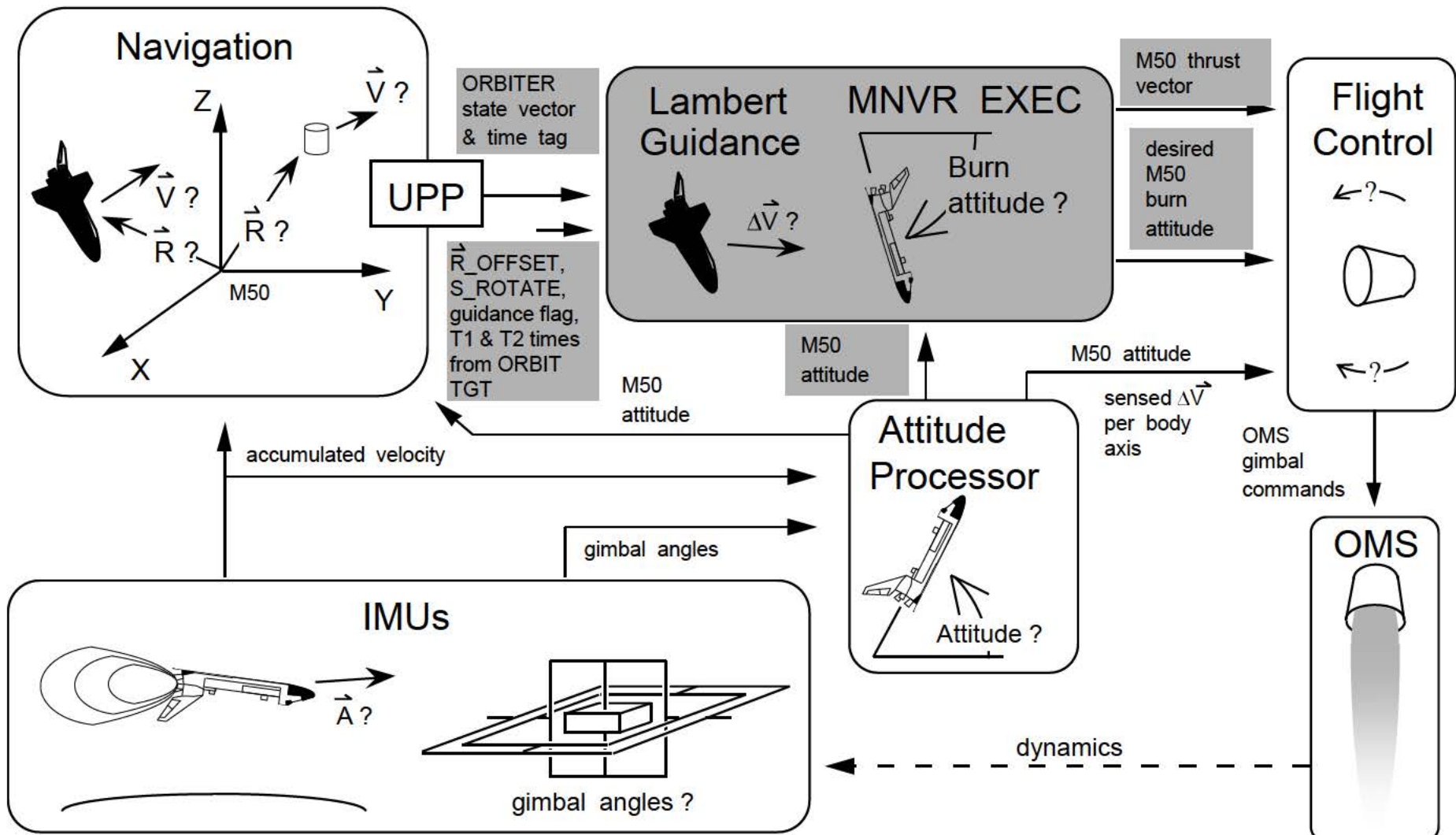
This is a highly simplified diagram for integrated GN&C during Lambert guided OMS burns. Ti is normally the only Lambert guided burn executed with the OMS (although on some profiles, Ti may be low enough to be executed with RCS). Only those interfaces which are critical to developing an understanding of integrated GN&C are shown. Only one OMS engine is shown for clarity. The following three pages describe the interfaces.



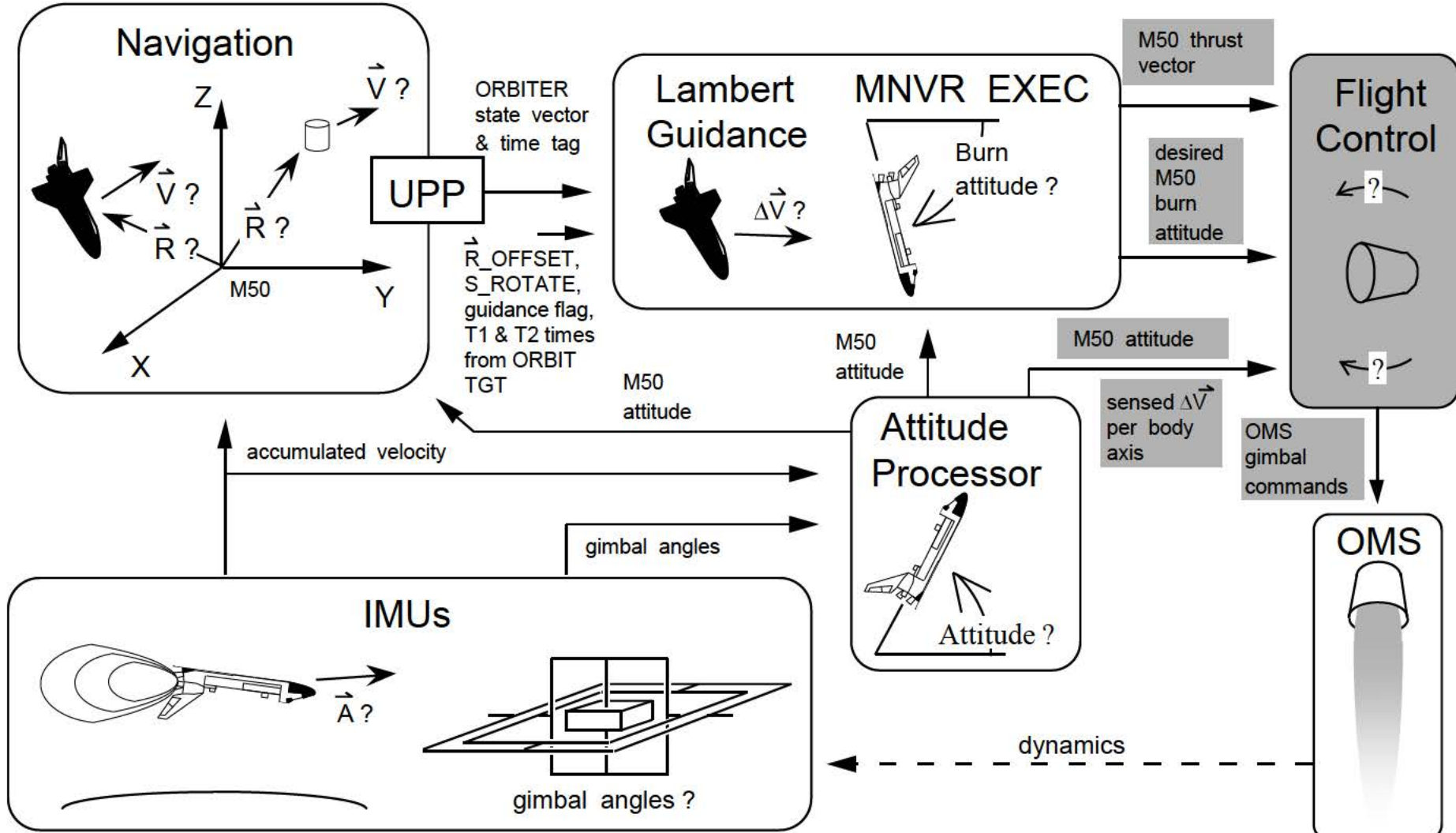
The roles played by the Attitude Processor, the IMUs and Navigation are the same as during orbit coast. Relative navigation sensor data is not normally incorporated during Major Mode 202, and the -Z target track is not performed.



Inputs to Lambert guidance consist of the current ORBITER state vector from navigation and the desired M50 final position (**R_OFFSET**) at the end of the transfer, the 180 degree singularity region protection flag (**S_ROTATE**), the guidance flag, T1 TIG and the time of arrival at the T2 point. The **R_OFFSET** vector is obtained from targeting computations performed in Major Mode 201 via the ORBIT TGT display. Processing associated with the Maneuver Execute (MNVR EXEC) display uses the ΔV from Lambert and the current attitude from the attitude processor to determine the M50 thrust unit vector and desired burn attitude.

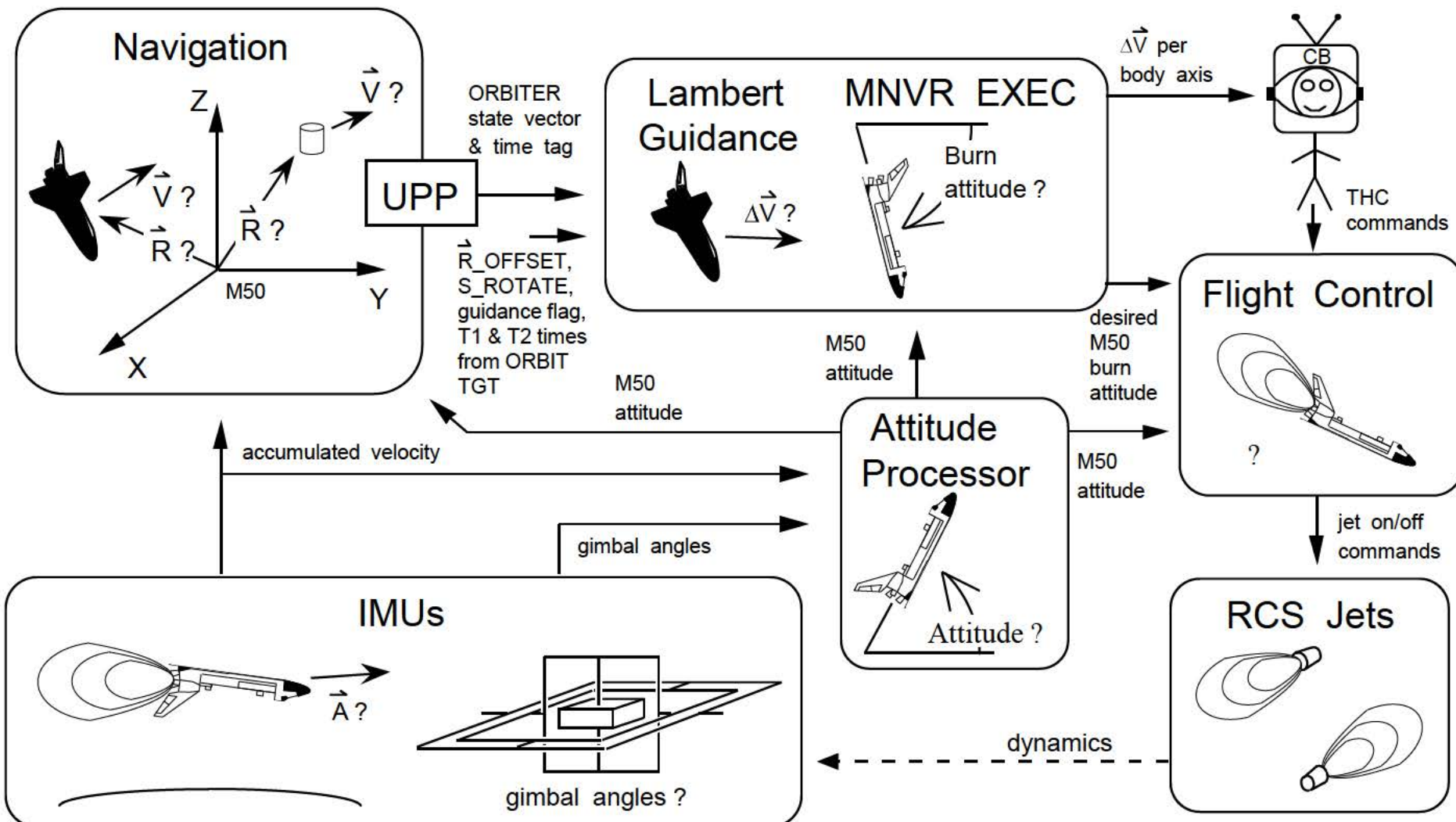


Prior to the OMS burn, Flight Control maneuvers the ORBITER to the desired burn attitude computed by guidance. One OMS engine is used if the pre-burn ΔV is between 6 and 12 ft/sec, and both OMS engines are used for pre-burn ΔV s greater than 12 ft/sec. Flight control uses the M50 thrust unit vector and desired burn attitude from guidance, along with the current attitude and sensed ΔV per body axis from the Attitude Processor to determine gimbal commands for the OMS engine(s).

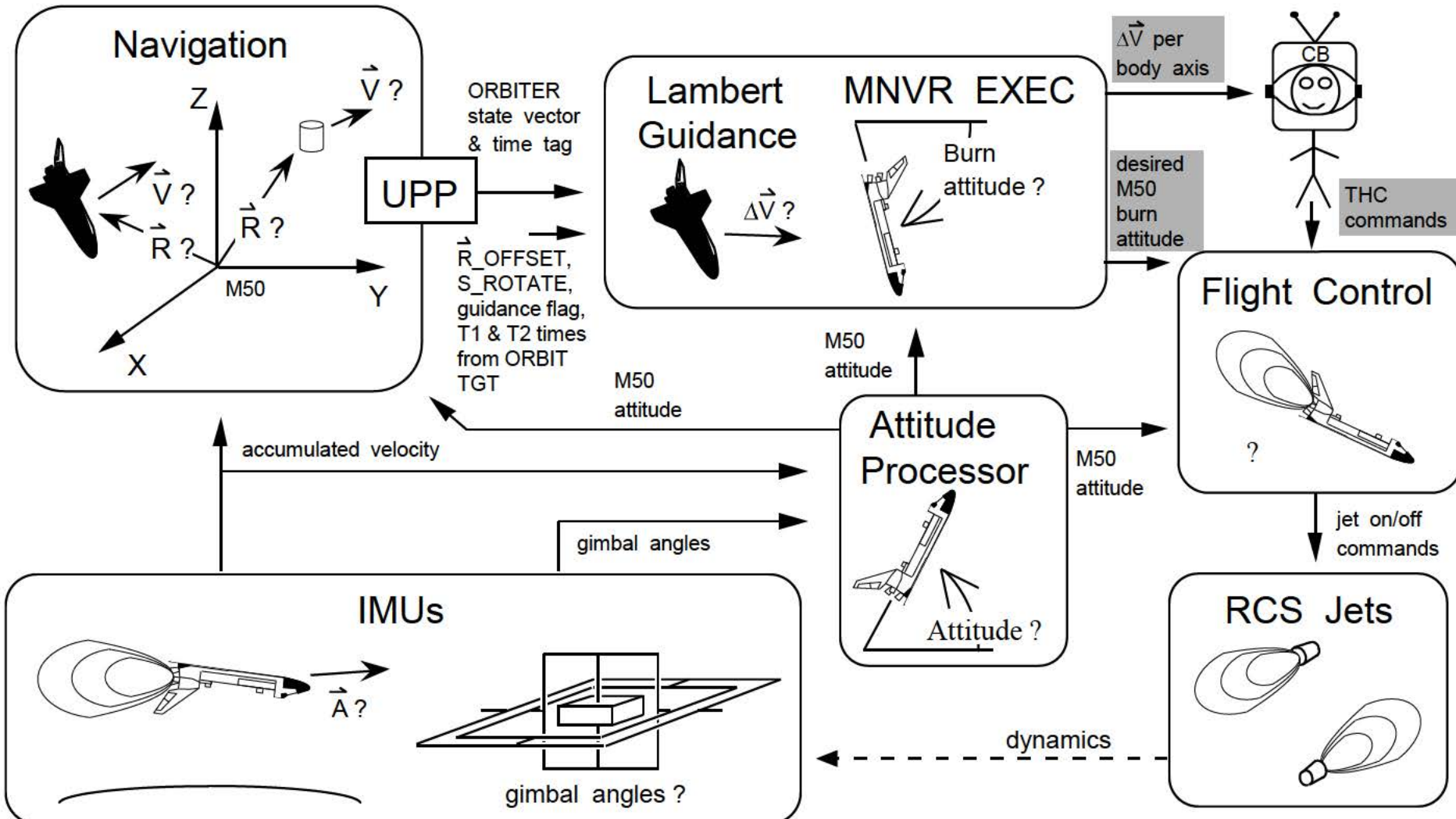


11.3 Integrated GN&C During +X RCS Burns

The 4 +X primary RCS jets are used for ΔV s between 4 and 6 ft/sec. This is a highly simplified diagram for integrated GN&C during Lambert guided +X RCS burns. Only those interfaces which are critical to developing an understanding of integrated GN&C are shown. The following page describes the interfaces.

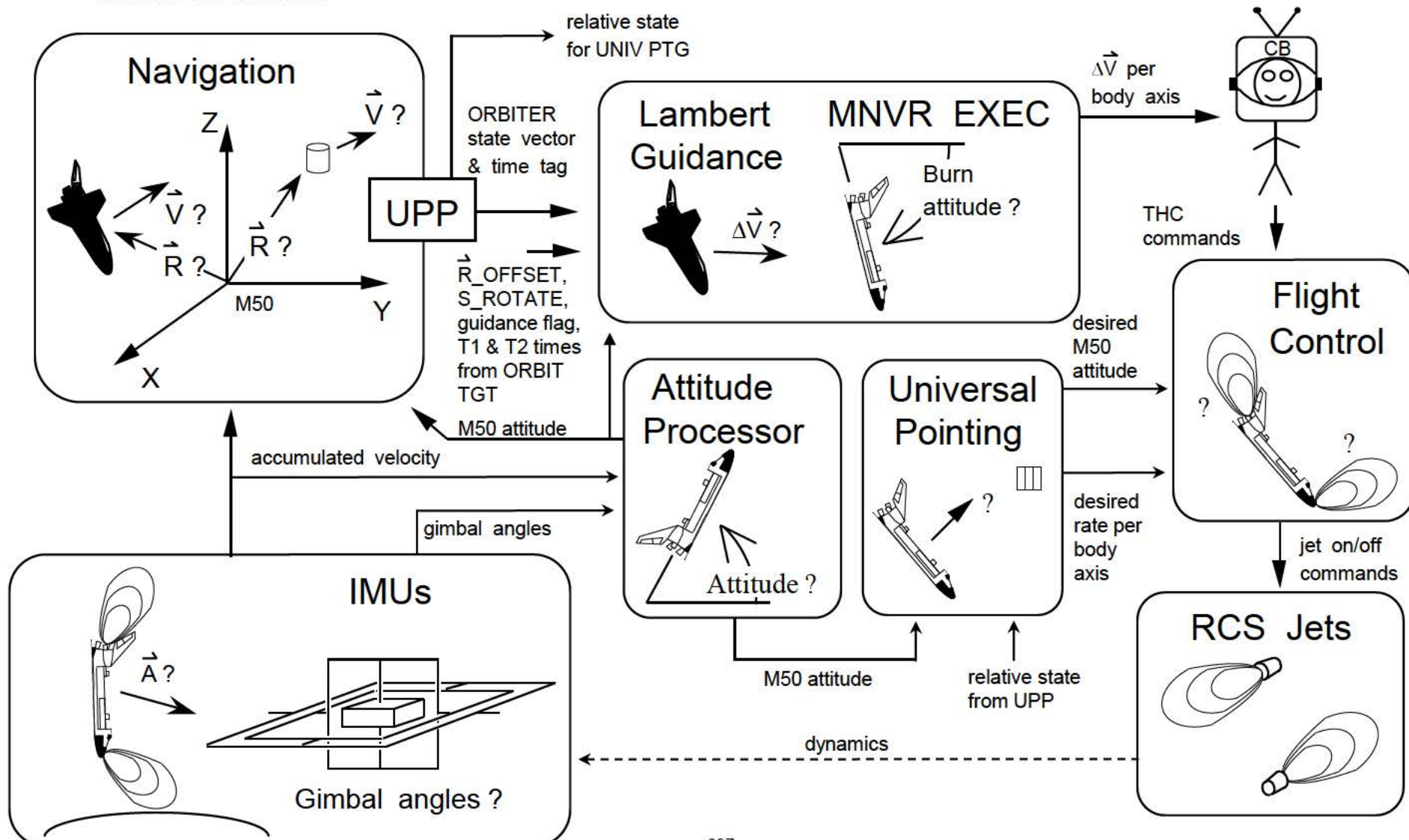


The functions of Navigation, the IMUs, UPP, and guidance are the same as for Lambert guided OMS burns. The sensed ΔV per body axis from the Attitude Processor and the M50 thrust vector from guidance are not used by Flight Control for RCS burns. Prior to the burn, Flight Control maneuvers the ORBITER to the desired burn attitude. Translational Hand Controller (THC) commands are issued by an astronaut based on the remaining ΔV shown on the MNVR EXEC display. Flight control maintains the burn attitude with the primary RCS jets.

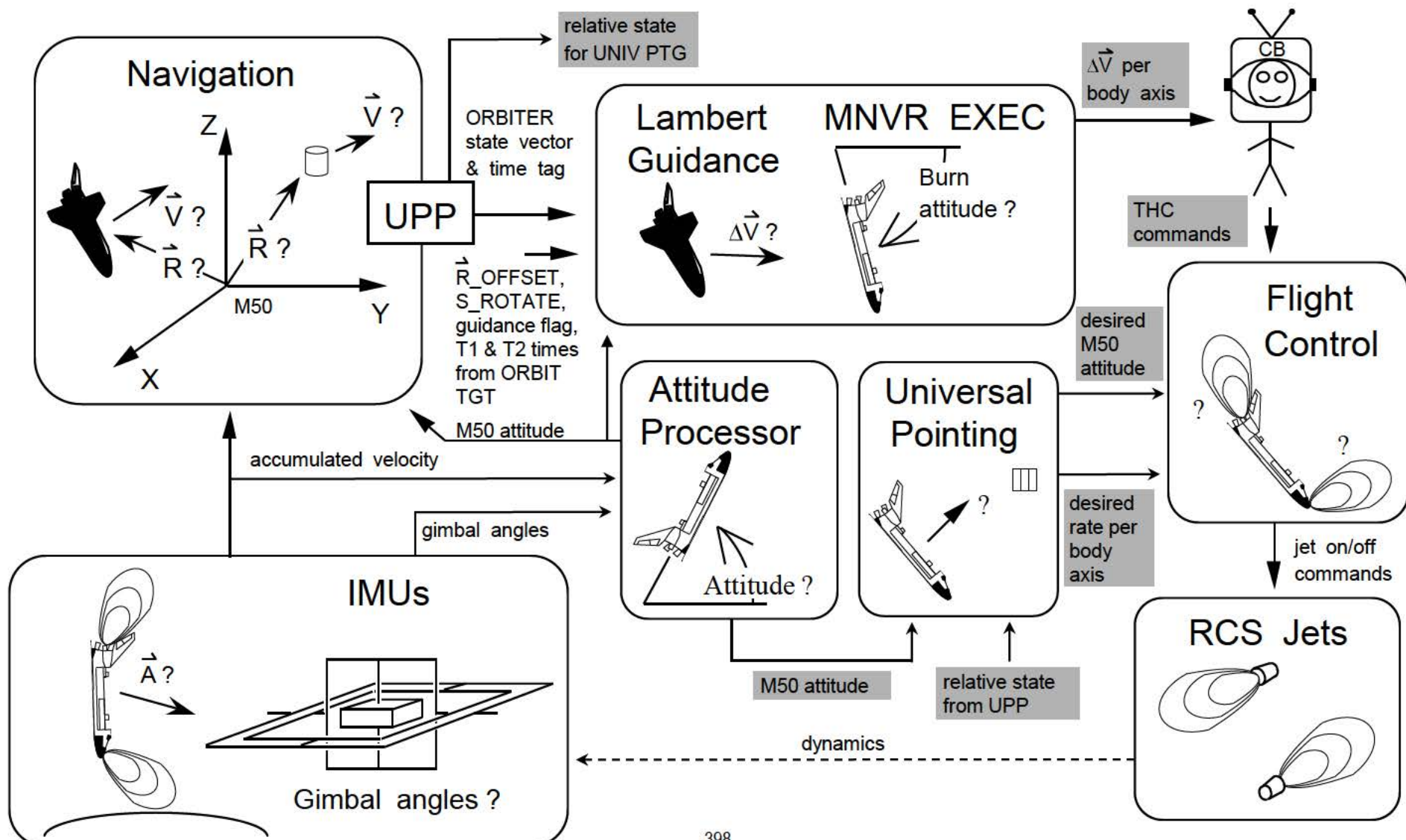


11.4 Integrated GN&C During Multi-Axis RCS Burns

If the pre-burn ΔV is less than 4 ft/sec, a maneuver to the burn attitude is not performed, and the ORBITER remains in target track. This is a highly simplified diagram for integrated GN&C during a Lambert guided “multi-axis” RCS burn. Only those interfaces which are critical to developing an understanding of integrated GN&C are shown. The following page describes the interfaces.



Although guidance computes a desired burn attitude, it is not used since the ORBITER remains in target track. Universal Pointing computes the desired M50 attitude and desired rate per body axis for Flight Control. These computations use the M50 attitude from the Attitude Processor and the relative state from User Parameter Processing (UPP). The astronaut issues jet commands by observing the ΔV on the MNVR EXEC display and making the appropriate deflections of the THC.



12.0 GLOSSARY

BSOR	Baseline Stable Orbit Rendezvous
CCTV	Closed Circuit Television
CIRC	Circularization Burn
Cmnds	Commands
COAS	Crew Optical Alignment Sight
C1	Vertical velocity axis intercept of line relating vertical and horizontal velocity components for PEG 4 burns.
C2	Slope of line relating vertical and horizontal velocity components for PEG 4 burns.
D	Desired
DAP	Digital Auto Pilot
DH	Delta or Differential Height. See also ΔH .
DT	Delta Time (Transfer Time)
DV	Delta Velocity. See also ΔV .
deg	Degrees
EL	Elevation Angle
EL_ANG	Elevation Angle
EL_TOL	Elevation Angle Tolerance
ENV	Environment
ET	External Tank
FDO	Flight Dynamics Officer
FLIT	Filtered State Vector
FLTR	Filtered State Vector
FSW	Flight Software
GN&C	Guidance, Navigation and Control
H	Angular Momentum Vector
HHL	Hand Held Laser
HT	Altitude above the surface of the Earth of the PEG 4 target point.

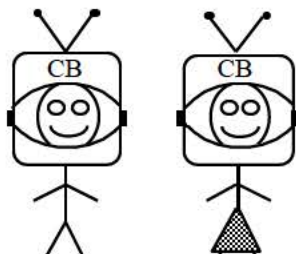
i	Inclination Angle or Initial
ILOAD	Initialization Load
IMU	Inertial Measurement Unit
ISS	International Space Station
<u>IY</u>	Unit Vector Normal to the Trajectory Plane, = - Unit(<u>R</u> x <u>V</u>)
KFT	Kilofeet
KSC	Kennedy Space Center
LAMB	Lambert
Level 8	Testing of Shuttle Flight Software after it has been customized for a specific mission.
LOS	Line-of-Sight Coordinate System
LVC	Local Vertical Curvilinear Coordinate System
LVLH	Local Vertical Local Horizontal Curvilinear Coordinate System
LVR	Local Vertical Rectilinear Coordinate System
MC-1	Mid-Course Correction Burn 1
MC-2	Mid-Course Correction Burn 2
MC-3	Mid-Course Correction Burn 3
MC-4	Mid-Course Correction Burn 4
MECO	Main Engine Cut-Off (SSMEs)
MET	Mission Elapsed Time
MNVR EXEC	Maneuver Execute Display
M50	Mean of 1950 Inertial Coordinate System
NAV	Navigation
NC	Phasing (or catch-up) Burn
NCC	Corrective Combination Burn
NH	Height Adjustment Burn
N. M.	Nautical Miles
NPC	Plane Change Burn
NSR	Coelliptic Burn (Slow Rate)

OMS	Orbital Maneuvering System
ONOM1	Level 8 Nominal On-Orbit Test Case (non-rendezvous)
ORBT	Optimized R-Bar Targeting Rendezvous
ORB	ORBITER
ORBIT TGT	Orbit Targeted Display
PASS	Primary Avionics Software System
PEG	Powered Explicit Guidance
PEG 1	Guidance algorithm for second stage ascent and Trans-Atlantic abort.
PEG 4	Guidance algorithm for OMS-1, OMS-2, and deorbit burns.
PROP	Propagated State Vector (no updates from rendezvous navigation sensors)
quat.	Quaternion
<u>R</u>	Position Vector
R_BAR	LVLH Z axis, positive from TARGET to center of Earth.
RCS	Reaction Control System
REL NAV	Relative Navigation Display
RNDC	Level 8 rendezvous coldstart test case
RND1	Level 8 rendezvous test case spanning second star tracker pass to pre-Ti
RPM	Rbar Pitch Maneuver
RPOP	Rendezvous and Proximity Operations Program
RR	Rendezvous Radar
RSOC	Rockwell Space Operations Company
R_TOL	Tolerance used to test for convergence of Lambert guidance
SSME	Space Shuttle Main Engine
SM	Systems Management
SOP	Subsystem Operating Program
SPOT	Spacecraft Position, Optimal Tracking
SRB	Solid Rocket Booster
TCS	Trajectory Control Sensor
TDRS	Tracking and Data Relay Satellite

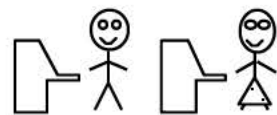
TGT	TARGET
THC	Translational Hand Controller
Ti	Transition Initiation Burn
TIG	Time of Ignition
TPS	Thermal Protection System
TSS	Tethered Satellite System
T1	Initial point (where burn is conducted) in two-point rendezvous transfer maneuver
T2	Target point in two-point rendezvous transfer maneuver
UNIV PTG	Universal Pointing Display
UPP	User Parameter Processing
UVW	Environment state-centered coordinate system
<u>V</u>	Velocity Vector
<u>V_BAR</u>	LVLH X axis, positive along TARGET velocity vector, curved to form arc of circle with radius equal to magnitude of TARGET position vector
Vh	Horizontal component of desired velocity to be achieved by a PEG 4 targeted burn
Vv	Vertical component of desired velocity to be achieved by a PEG 4 targeted burn
ΔH	Delta Height. See also "DH."
ΔV	Delta Velocity. See also "DV."
γ	Flight Path Angle
Φ	Phase Angle
Θ	Elevation angle on REL NAV display
ΘT	Angle from KSC to the PEG 4 target point (OMS-1 and OMS-2 only)
ω	Omega, Rotational Rate
Ω	Longitude of descending node
	Location of Disney World



Second stage ascent guidance (PEG 1) target point (MECO), OMS-2 (PEG 4) target point, or T2 point (Lambert).



Fire breathing members of the Astronaut Corps.



Mission Control personnel.

This page intentionally left blank.

13.0 BIBLIOGRAPHY

The bibliography includes JSC documents, NASA documents, conference papers, and journal articles that are part of the rendezvous canon. All may be located through the Building 45 Technical Library.

13.1 JSC Documents

Bernhardt, S. and Heilman, W., "On-Orbit Translation Maneuver Models Workbook," JSC-20747, Mission Operations Directorate (Flight Design and Dynamics Division), August 31, 1985.

Goodman, John L., and Wiuff, Kelli S., "Space Shuttle Rendezvous and Proximity Operations Experience Report," JSC-49626, Flight Design and Dynamics Division, Mission Operations Directorate, NASA JSC, February 2003.

Goodman, John L., "Space Shuttle Lambert Targeting," JSC-49708, Flight Design and Dynamics Division, NASA JSC, May 2003.

Goodman, John L., "Space Shuttle Lambert Cyclic Guidance," JSC-49709, Flight Design and Dynamics Division, NASA JSC, May 2003.

Goodman, John L., "STS-49 Lambert Targeting Anomaly and Aftermath," JSC-49710, Flight Design and Dynamics Division, NASA JSC, May 2003.

Goodman, John L., "History of Space Shuttle Rendezvous," JSC-63400, Flight Design and Dynamics Division, NASA JSC, 2006.

Kirkpatrick, James C., "The Theory of the Potential Applied to Orbit Prediction," JSC Internal Note No. 76-FM-9, JSC-10936, Mission Planning and Analysis Division, NASA JSC, February 20, 1976.

Lardas, M. N., "Equations of Relative Motion Workbook," JSC - 20746, Mission Operations Directorate (Flight Design and Dynamics Division), October 1, 1985.

Lear, William M., "Some Self-Starting Integrators For $x_{dot} = f(x,t)$," JSC Internal Note No. 75-FM-2, JSC-09334, Mission Planning and Analysis Division, NASA JSC, January 27, 1975.

Meissen, Thomas J., "Space Shuttle Lambert Guidance Improvement, SCR 92843/93009 OI-32," JSC-49830, Flight Design and Dynamics Division, NASA JSC, October 2006..

Semar, Cary, "Pines Method For Circular and Elliptical Orbits," JSC-10924, Mission Planning and Analysis Division, NASA JSC, February 1976.

Spencer, Jose L., "Use of a Nonsingular Potential," JSC Internal Note No. 75-FM-29, JSC-09661, Mission Planning and Analysis Division, NASA JSC, May 27, 1975.

Uzzell, Bobby R., "Elliptic Lambert For Space Shuttle On-Board Software," JSC-14905, 79-FM-17 Rev. 1, Mission Planning And Analysis Division, NASA Johnson Space Center, July, 1979.

"Parametric Study of Predictor Accuracy Impact On OFT Rendezvous Targeting," Internal Note No. 76-FM-112, JSC-11814, Mission Planning and Analysis Division, NASA JSC, December 9, 1976.

13.2 NASA Publications

Evans, Bernard W., et. al., "Summary Of Rendezvous Operations," Gemini Summary Conference, NASA SP-138, NASA Manned Spacecraft Center, Houston Texas, February 1-2, 1967.

"Gemini Midprogram Conference," NASA SP-121, NASA Manned Spacecraft Center, Houston, Texas, February 23-25, 1966.

Goodman, J. L., "GPS Lessons Learned From The ISS, Space Shuttle and X-38," NASA Contractor Report NASA/CR-2005-213693, NASA Johnson Space Center, November 2005. See the NASA JSC Technical Reports server at <http://ston.jsc.nasa.gov/collections/TRS/>

Goodman, J. L. Lessons Learned From Seven Space Shuttle Missions, NASA Contractor Report NASA/CR-2007-213697, NASA Johnson Space Center, January 2007. See the NASA Technical Reports server at <http://ntrs.nasa.gov/>, or the Johnson Technical Reports server at <http://ston.jsc.nasa.gov/collections/TRS/>.

Lancaster, E. R., and R. C. Blanchard, "A Unified Form Of Lambert's Theorem," NASA TN D-5386, NASA Goddard Spaceflight Center, September, 1969.

13.3 Conference and Journal Papers

Adamo, D. R., "Contingency ISS Rendezvous Recovery Planning By Houston And Moscow Control Centers," Astrodynamics 1999, Advances in the Astronautical Sciences, Vol. 103, Part III, Univelt, San Diego, CA, 1999.

Adamo, D. R., "ISS Rendezvous Phasing Considerations Pertaining to Optimal STS-114/LF1 Launch Opportunities," AIAA Guidance, Navigation, and Control Conference, AIAA, Reston, VA, 2005.

Adamo, D. R., "A Meaningful Relative Motion Coordinate System For Generic Use," 2005 AAS/AIAA Astrodynamics Specialist Conference, Advances in the Astronautical Sciences, Univelt, San Diego, CA, 2005.

Alexander, R. N., and Chiu, P. B., "Space Shuttle On-Orbit Proximity Operations," Proceedings of the 20th Aerospace Sciences Meeting, AIAA, Reston, VA, 1982.

Battin, R. H., An Introduction To The Mathematics And Methods Of Astrodynamics, Revised Edition, AIAA, Reston, VA, 1999.

Bigonesse, R., and Summa, W. R., "Unmanned Orbiter Undocking: Method for Disposal of a Damaged Space Shuttle Orbiter," Spaceflight Mechanics 2006, Advances In The Astronautical Sciences, Univelt, Inc., San Diego, CA, 2006.

Brazzel, J., Clark, F., and Spehar, P., "RPOP Enhancements to Support the Space Shuttle R-Bar Pitch Maneuver for Tile Inspection," AIAA Guidance, Navigation, and Control Conference, AIAA, Reston, VA, 2005.

Carson, D. E., "SPARTAN Project Overview," Proceedings of the First Annual NRO-OSL/CSFC-ATS Rideshare Conference, National Reconnaissance Office, Chantilly, VA, 1999.

Clark, F., Spehar, P., Hinkel, H., and Brazzel, J., "Laser-Based Relative Navigation and Guidance for Space Shuttle Proximity Operations," Guidance and Control 2003, Advances in the Astronautical Sciences, Vol. 113, Univelt, San Diego, CA, 2003.

Clohessy, W. H., and R. S. Wiltshire, "Terminal Guidance System For Satellite Rendezvous," *Journal of the Aerospace Sciences*, Volume 27, Number 9, September 1960, pages 653-659.

Collins, D. J., "Flight Operations For Shuttle Rendezvous Navigation and Targeting," *Proceedings of the IEEE PLANS '84 – Position Location and Navigation Symposium*, IEEE, New York, NY, 1984, pp. 106-112.

Crippen, R. L., and Hauck, F. H., "Orbiter Operations In Close Proximity To Free-Flying Satellites Or Formation Flying In Space," *Proceedings of the 27th Symposium of the Society of Experimental Test Pilots*, Society of Experimental Test Pilots, Lancaster, CA, 1983, pp. 314-334.

Dagen, J. D., "Structural Integration of the Space Shuttle and the Mir Space Station," *Spaceflight Mechanics 1996, Advances in the Astronautical Sciences*, Vol. 93, Part I, Univelt, San Diego, CA, 1996, pp. 461-471.

Dreger, F., et al., "Eureca: The Flight Dynamics of the Retrieval," *ESA Bulletin*, No. 76, Nov. 1993, pp. 92-99.

Gavin, R. T., "Development Of A Cooperative Operational Rendezvous Plan For Eureca And Other Maneuvering Shuttle Payloads," *Proceedings of the 38th Congress of the International Astronautical Federation*, International Astronautical Federation, Paris, France, 1987.

Gibson, R. L., and Precourt, C. J., "The First Space Shuttle to Mir Docking Mission," *Proceedings of the 39th Symposium of the Society of Experimental Test Pilots*, Society of Experimental Test Pilots, Lancaster, CA, 1995, pp. 386-419.

Goodman, J. L., "Space Shuttle Navigation in the GPS Era," *Proceedings of the Institute of Navigation National Technical Meeting*, Institute of Navigation, Fairfax, VA, 2001.

Goodman, J. L., "History of Space Shuttle Rendezvous and Proximity Operations," *AIAA Journal of Spacecraft and Rockets*, Vol. 43, No. 5, Sept.-Oct. 2006.

Goodman, J. L., Brazzel, J. P., and Chart, Ph.D., D. A., "Challenges of Orion Rendezvous Development," AIAA Guidance, Navigation, and Control Conference, AIAA, Reston, VA, 2007.

Goodman, J. L., and Walker, S. R., "Hubble Servicing Challenges Drive Innovation of Shuttle Rendezvous Techniques," 32nd Annual AAS Guidance And Control Conference, Guidance and Control 2009, Advances in the Astronautical Sciences, Univelt, San Diego, CA, 2009.

Goodman, J. L., and Brazzel, J. P., "Rendezvous Integration Complexities of NASA Human Flight Vehicles," 32nd Annual AAS Guidance And Control Conference, Guidance and Control 2009, Advances in the Astronautical Sciences, Univelt, San Diego, CA, 2009.

Hale, N. W., and Conte, B. A., "Considerations in Rendezvous Launch Window Management," 53rd International Astronautical Congress, International Astronautical Federation, Paris, France, 2002.

Hall, R., et al., "Flight Control Overview Of STS-88, The First Space Station Assembly Flight," Astrodynamics 1999, Advances in the Astronautical Sciences, Vol. 103, Part II, Univelt, San Diego, CA, 1999, pp. 1063-1081.

Hauck, F. H., and Gardner, D. A., "Space Salvage – A Report On Shuttle Mission STS 51-A," Proceedings of the 29th Symposium of the Society of Experimental Test Pilots, Society of Experimental Test Pilots, Lancaster, CA, 1985, pp. 236-261.

Jackson, M., Zimpfer, D., and Lepanto, J., "Identification of Shuttle/Mir Structural Dynamics For Notch Filter Tuning," Spaceflight Mechanics 1996, Advances in the Astronautical Sciences, Vol. 93, Part I, Univelt, San Diego, CA, 1996, pp. 493-509.

Jezewski, D. J., "A Survey of Rendezvous Trajectory Planning (Paper AAS 91-505)," McDonnell Douglas Space Systems Company, Presented at AAS/AIAA Astrodynamics Specialist Conference, Durango, Colorado, August 19 - 22, 1991.

Jones, R., "Architecture In Mission Integration, Choreographing Constraints," 30th International Conference on Environmental Systems, Society of Automotive Engineers, Warrendale, PA, 2000.

Kachmar, P., "Apollo and Space Shuttle On-Board Navigation Systems: Application of Kalman Filtering Techniques," 58th Annual Meeting of the Institute of Navigation and CIGTF Guidance Test Symposium, Institute of Navigation, Fairfax, VA, 2002.

Lancaster, E. R., Blanchard, R. C. and Devaney, R. A., "A Note On Lambert's Theorem," Journal Of Spacecraft And Rockets, American Institute Of Aeronautics And Astronautics, Volume 3 (9), September, 1966, pages 1436-1438.

Lee, S., et al., "Hubble Space Telescope Servicing Mission 3A Rendezvous Operations," Guidance and Control 2001, Advances in the Astronautical Sciences, Vol. 107, Univelt, San Diego, CA, 2001, pp. 615-633.

Logan, B. A., "Shuttle Payload Deployment and Retrieval System," AIAA Guidance and Control Conference, AIAA, Reston, VA, 1982.

McQuillan, W. F., et al., "Rendezvous Radar For Space Shuttle Orbiter," Proceedings of the International Telemetering Conference, International Foundation for Telemetering, 1974, pp. 447-465.

Machula, M., "Orbiter Repair Maneuver Contingency Separation Methods and Analysis," AIAA Guidance, Navigation, and Control Conference, AIAA, Reston, VA, 2005.

Muller, E. S., and Kachmar, P. M., "A New Approach To On-Board Navigation," Navigation: Journal of the Institute of Navigation, Vol. 18, No. 4, Winter 1971-1972, pp. 369-385.

Nakano, M. M., and Williams, R. L., "Space Shuttle On-Orbit Flight Control System," Proceedings of the AIAA Guidance and Control Conference, AIAA, Reston, VA, 1982.

Oberg, J. E., "Control Of RCS Plume Effects During Proximity Operations On STS Missions," Proceedings of the AIAA Shuttle Environment And Operations Meeting, AIAA, Reston, VA, 1983, pp. 68-71.

Pearson, D. J., "Shuttle Rendezvous and Proximity Operations," Proceedings of the CNES International Symposium on Space Dynamics, Centre National d'Etudes Spatiales, Paris, France, 1989, pp. 833-851.

Pearson, D. J., "The Glideslope Approach," Orbital Mechanics and Mission Design – Advances in the Astronautical Sciences, Vol. 69, Univelt, San Diego, CA, 1989.

Rochelle, W. C., Reid, E. A., Carl, T. L., Smith, R. N., and Lumpkin III, F. E., "Thermal Analysis For Orbiter And ISS Plume Impingement On International Space Station," 35th AIAA Thermophysics Conference, AIAA, Reston, VA, 2001.

Sampaio, C. E., "A Lighting and Visibility Evaluation of the Shuttle/Mir Docking Target," Proceedings of the 39th Human Factors and Ergonomics Society Annual Meeting, Human Factors and Ergonomics Society, Santa Monica, CA, 1995, pp. 45-49.

Smith, F. E., Campbell, M. E., Blucker, T. J., Manry, C. E., and Saulietis, I., "Shuttle Orbiter Stellar-Inertial Reference System," AIAA Journal Of Guidance And Control, Vol. 6, No. 6, 1983, pp. 424-431.

Walker, S., LoPresti, J., Schrock, M., and Hall, R., "Space Shuttle Rbar Pitch Maneuver for Thermal Protection System Inspection Overview," AIAA Guidance, Navigation, and Control Conference, AIAA, Reston, VA, 2005.

Wattenbach, R., and Moritz, K., "Astronomical Shuttle Pallet Satellite (ASTRO-SPAS)," Acta Astronautica, Vol. 40, No. 10, May, 1997, pp. 723-732.

Wylie, A. D., and deVezin, H. G., "Onboard Rendezvous Navigation For The Space Shuttle," Navigation: Journal of the Institute of Navigation, Vol. 32, No. 3, Fall 1985, pp. 197-220.

Zimpfer, D., and Spehar, P., "STS-71 Shuttle/Mir GNC Mission Overview," Spaceflight Mechanics 1996, Advances In The Astronautical Sciences, Vol. 93, Part I, Univelt, San Diego, CA, 1996, pp. 441-460.

Zimpfer, D., et al., "Shuttle Stability and Control for the STS-71 Shuttle/Mir Mated Configuration," Spaceflight Mechanics 1996, Advances in the Astronautical Sciences, Vol. 93, Part I, Univelt, San Diego, CA, 1996, pp. 473-492.

This page intentionally left blank.

14.0 Background On This Document

The following charts were created in 2000 to provide the rationale behind the creation and use of this manual.

Background On Introduction To Rendezvous GN&C

John L. Goodman
United Space Alliance

Supporting

Flight Design And Dynamics Division
Mission Operations Directorate
NASA Johnson Space Center
Houston, Texas

John L. Goodman
July 7, 2000



In Use Since February, 1993

- Written in 1991-1992 to train engineers in rendezvous concepts using graphics.
- Originally written for Flight Software Verification, but quickly adopted by other organizations.
- Used within Flight Design And Dynamics Division (for both civil servants and contractors).
 - USA Flight Design Orbit and Navigation.
 - Rendezvous GPOs, Orbit FDOs.
 - USA Flight Software
- Provided to crews by Rendezvous/Proximity Operations Training Group as supplementary reading.
 - Target audience of book is engineers, rather than the crew.
 - Does not replace any existing crew training documents.
- Used by Boeing Reusable Space Systems/Huntington Beach.
- Recently used to educate JPL Mars Sample Return personnel on Shuttle rendezvous.
- Tends to get passed around JSC, making it difficult to track exactly how many other organizations have used it.

John L. Goodman
July 7, 2000



Document Developed To Train FSW Verification Personnel

- Rendezvous training materials available circa 1986-1991 were difficult to use for training entry level engineers to perform verification of Shuttle Flight Software.
 - Many aspects of rendezvous profiles, guidance, navigation and control were not covered.
 - Existing materials did not tie the “components” of rendezvous together to give the trainee the big picture.
 - Difficult to bring management personnel not familiar with Mission Operations and trajectories up to speed on rendezvous.
- Development began in mid 1991 within the RSOC Level 8 Testing group.
 - Emphasized building a “visual rendezvous vocabulary.”
 - Creating pictures required a thorough understanding of rendezvous design and Flight Software algorithms, necessitating authorship by an engineer, rather than OMNIPLAN graphic artists.
 - Flight Design and Crew Training reviewed the draft in 1992.
 - Final draft submitted to STSOC document process, subjected to OMNIPLAN review.
 - Published as STSOC-TM-001498 in February, 1993. 250 pages

By 1999, An Updated Version Was Needed

- May, 1999, author asked by Rendezvous GPOs and Orbit Flight Design if book could be updated to reflect the new ORBT rendezvous profile.
 - Work began in the Fall of 1999.
 - Book moved from MacDraw™ to PowerPoint™.
 - 117 pages of new material added.
 - Graphics cleanup.
 - ORBT updates.
 - More realistic looking crew displays.
 - Lambert and External ΔV Guidance.
 - Targeting alarms and crew display illegal entries.
 - Rendezvous profile development (Gemini through Shuttle ORBT).
 - Kalman filter measurement partials.
 - On-Orbit (non-rendezvous) processing of Global Positioning System vectors.
 - Reviewed by USA Orbit Flight Design and Crew Training.
 - New edition informally published on February 9, 2000. Corrected new edition published on May 17, 2000.
 - First edition was available only as a hardcopy, new edition available in PDF format from Rendezvous Crew Training web site on USA Intranet.
-

John L. Goodman
July 7, 2000



Introduction To Space Shuttle Rendezvous Guidance, Navigation, and Control
Fourth Edition
JSC-49686, November 2009

NASA JSC

CB / Antonelli, Dominic
CB / Ferguson, Chris
CB / Hobaugh, Charles
CB / Nyberg, Karen
CB / Zamka, George
DA7 / Barnett, Gail
DA8 / Ceccacci, Anthony J.
DA8 / Horlacher, Gary
DS62 / Gruber, David
DM3 / Dunham, Scott
DM32 / González, Edward
DM34 / Machula, Mike
DM34 / Spehar, Jeannette
DM34 / Walker, Steve
EG2 / Cryan, Scott
EG2 / Gonzalez, Rodolfo
EG5 / Bryant, Lee E.
EG5 / Merriam, Bob
EG6 / Brazzel, Jack
EG6 / Crain, Dr. Tim
EG6 / D'Souza, Dr. Chris
EG6 / Hanak, Dr. Chad
EG6 / Hart, Jeremy
EG6 / Hinkel, Heather
EG6 / Merkle, Scott
EG6 / Mitchell, Jennifer
EG6 / Ruiz, Jose
EG6 / Weeks, Dr. Michael
EV151 / Murray, Scott
IS23 / STI Center (Caballero, Laurie) (4)
NC / Miller, Todd

NASA KSC

NE-A2 / Menendez, Alfred

Pouch Mail

United Space Alliance-Houston
USH-480A / Dannemiller, David
USH-483L / Orbit Library
USH-483L / Gilmore, Deidre
USH-484T / Fox, Alan
USH-484T / Frank, Jorge
USH-485L / Navigation Library
USH-485L / Zimmerman, Patrick
USH-634G / White, David
USH-634L / Nolan, Sean
USH-634L / Roberts, Larry
USH-634L / Smith, Dr. Gary R.
USH-636L / White, Terry
USH-636X / Butler, Dennis
USH-806A / Goodman, John (3)

Boeing-Houston

HB5-41 / Vaughn, Michael E.
HM5-10 / Benishek, Lowell
HM5-40 / Clark, Terry